Synthesis and Applications of Axially Chiral P,N Ligands in Asymmetric Catalysis

James Barker B.Sc.

UCD Student Number: 13334931

This thesis is submitted to University College Dublin in fulfilment of the requirements for the degree of Doctor of Philosophy

Centre for Synthesis and Chemical Biology

School of Chemistry

University College Dublin

National University of Ireland

Supervisor: Prof. Patrick J. Guiry MRIA

Head of School: Assoc. Prof. Michael Casey

2021

Ollscoil na hÉireann
National University of Ireland

CSCB
Centre for Synthesis & Chemical Biology

Table of Contents

Statement of Original Authorship

I hereby certify that the submitted work is my own work, was completed while registered as a candidate for the degree of Doctor of Philosophy, and I have not obtained a degree elsewhere on the basis of the research presented in this submitted work.

James Barker

21 December 2021

Acknowledgments

I have received a great deal of support and encouragement, which helped me throughout the course of my PhD programme.

I would first like to thank my supervisor, Professor Pat Guiry, whose expertise, and guidance during my PhD were of the utmost value to me. The skills I developed under your supervision over the past four years are something I do not take for granted and are tools I look forward to utilising into my future. The time and effort you focussed towards securing funding for me to completing my PhD programme is something I will be eternally grateful for.

I would like to acknowledge both past and present Guiry group members for their role in helping me complete my PhD. Earlier group members, you all took time from your busy schedules to help me hone my lab skills and begin my research journey. For that I am extremely grateful. Thank you to the wider group, for making the lab a great place to be for the duration of my time there (both inside and outside of the lab!). You all provided stimulating discussions and fun distractions in equal measure to make the lab environment a welcoming one. I would also like to especially thank Dr. Balaji Rokade, who's day-to-day guidance and thought-provoking conversations were key in helping me complete my PhD.

I would like to acknowledge and thank the technical staff in UCD for their assistance in my studies, with specific mention to Dr. Yannick Ortin and Dr. Jimmy Muldoon. Your willingness to help and accommodate me during my PhD programme is something that deserves mentioning.

Lastly, I would like to thank my family and friends for their unwavering and constant support throughout my PhD. You were always there for me, even on the days when not everything went to plan. Your love and support provided me with the energy and drive to complete my PhD and is something I will recognise for the rest of my life.

Abstract

The development of tools used to access enantiomerically pure compounds is a task with particular relevance to the pharmaceutical industry and the greater area of modern medicine. As such, it garners great attention in the form of research from both academic and industrial settings alike. A synopsis of the synthetic tools available to perform asymmetric synthesis is described, outlining the advantages and limitations of each.

Work towards accessing novel imidazoline-based axially chiral P,N ligands and the synthesis of centrally chiral P,N ligands is presented. The synthesis of axially chiral P,N ligands previously reported by the Guiry is described, alongside investigations into a modular synthetic pathway for accessing novel imidazoline-based axially chiral P,N ligands. Numerous methodologies towards functionalising naphthalene systems are discussed, including a new undescribed palladium-catalysed C-H halogenation of naphthoic acid. A new route towards synthesising centrally chiral imidazoline-based P,N ligands employing established Cu-catalysed C-P bond formation chemistry is also presented. Four reported centrally chiral P,N ligands were synthesised over the novel three-step route, in yields ranging from 36 to 48%.

Asymmetric A3 (aldehyde, amine, alkyne) couplings are well-studied reactions, involving the condensation of an aldehyde and amine before attack of an alkynyl nucleophile on the electrophilic imine/iminium ion. In this thesis, work is described towards accessing a protocol for an asymmetric A3 coupling system with dynamic kinetic resolution. Racemic chiral aldehydes were employed in asymmetric A3 coupling reactions with the intention of producing products with two contiguous stereocentres as a single diastereomer, with theoretical yields up to 100%. An initial substrate scope to synthesise eight different products was performed, before a subsequent investigation into the role of catalyst identity, catalyst loading, reaction temperature, and additives had on the diastereoselecitivity of the reaction. To date,

poor yields persist regarding α-aryl aldehydes and poor diastereoselectivities regarding α-aliphatic aldehydes have been observed. Preliminary work towards accessing enantiopure aldehydes is also described.

Finally, a novel protocol for the heteroatom-directed borylation of hetereoaryl-alkenes is described. Four P,N ligands were tested in the reaction, before extensive optimisation regarding catalyst identity, solvent identity, base identity, temperature, alcohol additive and boron source equivalents. The asymmetric Cu-catalysed system furnished borylated intermediates, which were subsequently oxidised to the corresponding novel alcohols for characterisation purposes. The system boasts short reaction times of one hour, with yields up to 88% and enantioselectivities up to 76% ee reported in a substrate scope containing twelve heteroaryl-substituted products. The enantioenriched organoboron intermediates contain a versatile synthetic handle that is amenable to further synthetic transformations.

Symbols and Abbreviations

δ	chemical shift
%	per cent
Å MS	Angstrom
$[M + H]^+$	protonated molecular ion
9-BBN	9-borabicyclo(3.3.1)nonane
BINAP	2,2'-bis(diphenylphosphino)-1,1'-binaphthyl
Bn	benzyl
Boc	*tert*-butoxycarbonyl
Boc_2O	di-*tert*-butyl decarbonate
Br	broad
BSA	*N*,*O*-bis(trimethylsilyl)acetamide
Bz	benzoyl
Cat.	catalytic
CH_2Cl_2	dichloromethane
COD	cyclooctadiene
d	doublet
DABCO	1,4-diazabicyclo[2.2.2]octane
Dba	dibenzylideneacetone
DCE	1,2-dichloroethane
Dd	doublet of doublets
Ddd	doublet of doublet of doublets
DDQ	2,3-dichloro-5,6-dicyano-1,4-benzoquinone
de	diastereomeric excess
DIPT	diisopropyl tartrate
DKR	dynamic kinetic resolution
DMAP	dimethylaminopyridine
DME	dimethoxyethane
DMEDA	*N*,*N*'-dimethylethylenediamine
DMF	dimethylformamide

dppe	1,2-bis(diphenylphosphino)ethane
dppf	1,1'-bis(diphenylphosphino)ferrocene
DyKat	dynamic kinetic asymmetric transformation
ee	enantiomeric excess
Ent	enantiomer
Equiv.	equivalents
ESI-MS	electrospray ionisation mass spectrometry
Et_2O	diethyl ether
EtOAc	ethyl acetate
FDH	formate dehydrogenase
h	hours
H_2O_2	hydrogen peroxide
HCl	hydrochloric acid
HRMS	high resolution mass spectrometry
Hz	Hertz
*i*Pr	*iso*-propyl
IUPAC	international union of pure and applied chemistry
J	coupling constant (in Hz)
k	reaction rate
LTMP	lithium tetramethylpiperidide
m	meta
M	molar
Me	methyl
mg	milligrams
Min	minutes
mL	millilitre
MS	molecular sieves
MTBE	methyl *tert*-butyl ether
n/a	not available
NAD	nicotinamide adenine dinucleotide
Nap	naphthyl
NBS	*N*-bromosuccinimide

*n*BuLi	normal butyllithium
NIS	*N*-iodosuccinimide
NMR	nuclear magnetic resonance
o	ortho
OTf	trifluoromethanesulfonate
p	para
p-TsOH	*para*-toluenesulfonic acid
ph	phenyl
PKR	parallel kinetic resolution
ppm	parts per million
P_x	product (subscript denotes stereocentre config.)
PyBim	pyridyl bis(imidazoline)
PyBox	pyridyl bis(oxazolines)
R_f	retention factor
Rt	room temperature
rxn	reaction
sat.	saturated
*sec*BuLi	secondary butyllithium
SFC	supercritical fluid chromatography
SM_x	starting material (subscript denotes stereocentre config.)
S_NAr	nucleophilic aromatic substitution
soln.	solution
t	triplet
TBAF	tetrabutylammonium fluoride
TBHP	*tert*-butyl hydroperoxide
^tBu	*tert*-butyl
Temp	temperature
Tf_2O	trifluoromethanesulfonic anhydride
THF	tetrahydrofuran
TLC	thin layer chromatography
TMEDA	*N*,*N*,*N*',*N*'-tetramethylethylenediamine
TMS	trimethlysilyl

UHPLC	ultra high performance liquid chromatography
UPC^2	ultra performance convergence chromatography
UV	ultraviolet
v/*v*	volume per volume

Chapter 1: Introduction

Chirality

A molecule is deemed to be chiral if it is unable to be superimposed on its mirror image. Molecules that can be superimposed on their mirror image are termed achiral and an example of this is cyanohydrin **1** (**Scheme 1**). Cyanohydrin can be formed though the nucleophilic attack of a cyanide anion on acetone. The cyanide anion can attack acetone on the front face or back face and in doing so it will form either **1**-**a** or **1**-**b**. However, by simply rotating **1**-**a** by 180°, it will become superimposable on **1**-**b** and as such **1**-**a** and **1**-**b** are the same molecule.

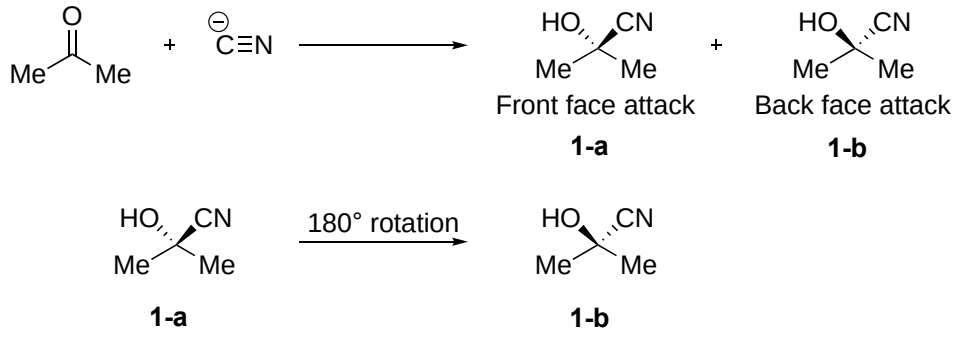

Scheme 1**: Attack of cyano group on acetone to form cyanohydrin **1

Compounds containing the same atoms and connectivity but differing in the spatial arrangement of their atoms are termed stereoisomers. The two main types of stereoisomers are enantiomers and diastereomers, the characterisation of which depends on the number of absolute configurations of the stereochemical elements present in the compound. Enantiomers are direct mirror image of each other, where every stereochemical element in one enantiomer has the opposite configuration in the other enantiomer. Diastereomers are compounds that not related to each other by reflection, *i.e.* they have one or more different stereochemical element configurations relative to each other, but crucially they are not the direct opposite configuration of each other. More simply put, diastereomers are stereoisomers that are not enantiomers.

Enantiomers have the same physical and chemical properties when they are in an achiral environment, but they can have vastly different properties in a chiral environment. This is particularly important in the pharmaceutical industry when synthesising medicines for human or animal consumption. A key example being carvedilol (a high blood pressure medication), where the (*R*)-enantiomer is preferentially metabolised *in vivo*, leading to a highly diminished half-life when compared to the (*S*)-enantiomer (5 hours v 11 hours).[1] The (*R*)- and (*S*)-enantiomers also exhibit different biological *in vivo*, where only the (*R*)-enantiomer can block α_1-adrenoceptor blocking activity.[1] In contrast, diastereomers possess different chemical and physical properties, irrespective of their environment.

Drugs react with enzymes and receptors in the body, which themselves consist of proteins.[2] Proteins are comprised of one or more long chains of amino acid residues. In nature, amino acids occur only as one enantiomer, (*S*), with the exception of cysteine which exists naturally as the (*R*)-enantiomer (**Figure 1**). The origin of this stereochemistry in nature is a topic that is still currently under investigation, however a few noteworthy hypotheses have been proposed, namely by Blackmond.[3,4]

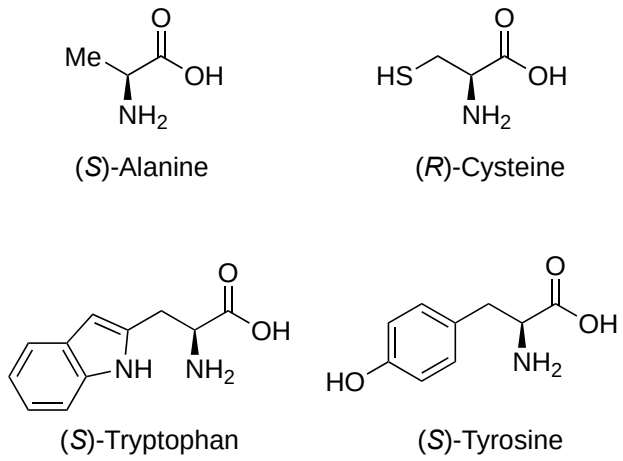

***Figure 1**: Selection of naturally occurring amino acids*

The human body is a chiral environment due to the presence of chiral amino acids that make up the receptors and enzymes present in the body. Therefore, two enantiomers of a drug can react with these receptors in vastly different ways. For example, only one enantiomer of a drug may fit in the desired receptor or chiral pocket of an enzyme to give the desired effect. In the best case scenario, this means that only 50% of the racemic mixture of a drug will deliver the desired therapeutic effect. In more sinister cases however, the other enantiomer will not Just be unreactive but instead can have serious undesired side effects.

An unfortunate example of this was observed in the drug Thalidomide which was synthesised as a racemate – meaning that the two enantiomers of the drug were synthesised and the drug was sold as a 50/50 mixture of enantiomers (**Figure 2**). The (*R*)-enantiomer had the desired sedative effects, however the (*S*)-enantiomer was teratogenic (an agent that disrupts the development of a fetus).[5] As a result of Thalidomide being sold as a mixture of enantiomers, numerous children whose mothers took Thalidomide were born with severe birth defects.[5] This event led to changes in the regulation and sale of medicines containing stereocentres, where both enantiomers had to be individually tested to ensure all side effects were documented before the drug would be allowed to enter the market.[6]

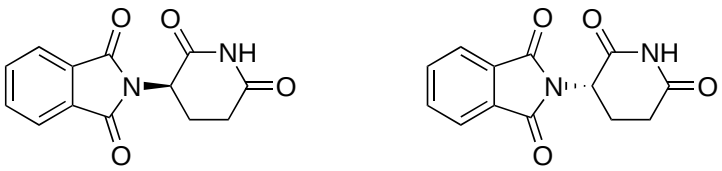

(*R*)-Thalidomide (*S*)-Thalidomide

***Figure 2**: Enantiomers of morning sickness drug Thalidomide*

There are many types of chirality in chemistry including central/point, axial, and planar chirality. Each type has slightly different rules towards the assignment of their chirality. The different types of chirality arise due to different structural elements within the compounds, which will be outlined in this section.

Central Chirality

Central chirality most often occurs in carbon atoms, where four different substituents bonded to it. These carbon atoms are termed chiral or stereogenic centres. Central chirality is not limited to *J*ust carbon atoms, and is a characteristic present in other atoms such as phosphorus, sulfur and nitrogen. Stereoinversion can occur rapidly at nitrogen if the lone pair is available (not involved in resonance) and if inversion will not cause strain *via* unfavourable bond angles *e.g* a nitrogen atom in a ring system.[7]

Central chirality is assigned *via* the Cahn-Ingold-Prelog rules as stipulated by IUPAC.[8] The first step in assigning the stereochemistry is to assign priorities to the atoms on the stereogenic centre based on their atomic number (**Figure 3**). The lowest priority atom is placed in the plane behind the observer. If the priority of the atoms decreases in a clockwise manner, it is assigned as (*R*) (rectus) and if they decrease in a counter clockwise manner it is assigned as (*S*) (sinister) – the Latin for right and left, respectively.

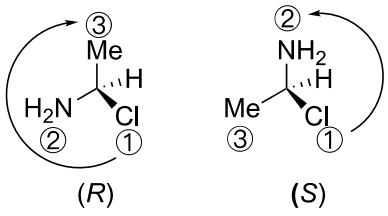

***Figure 3**: Assignment of central chirality*

Axial Chirality

Axial chirality exists when there is restricted rotation about a bond, which results in a set of substituents being held in a spatial arrangement that is not superimposable on its mirror image. The most common instance of axial chirality occurs when there is restricted rotation about an aryl-aryl bond. The chiral ligand BINAP shall be considered as an example of an axially chiral compound (**Figure 4**). The two naphthalene rings in BINAP sit perpendicular to each other in order to minimise the steric strain in the compound that would otherwise exist if these rings eclipsed. The steric strain is so large that these rings were found to only eclipse after being heated to 491 °C.[9] At this elevated temperature the molecules have sufficient energy to overcome this barrier and they can interconvert between the (*S*)- and (*R*)-enantiomers.

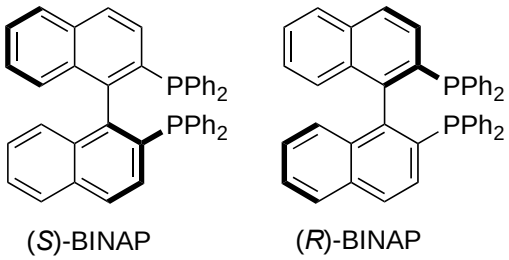

***Figure 4**: Axially chiral ligand BINAP*

Assigning axial chirality is similar to that of assigning central chirality. The observer looks down the axis of chirality, and assigns the priorities of the groups by atomic number. There is one extra caveat in assigning axial chirality, being that the near substituents with respect to the observer are given higher priority over the two further substituents (**Figure 5**). A chiral axis of (R_a) is assigned if the priority of substituents two to three proceeds in a clockwise manner and if the priority proceeds counter clockwise then a chiral axis of (S_a) is assigned (where subscript a denotes the chirality is axial).

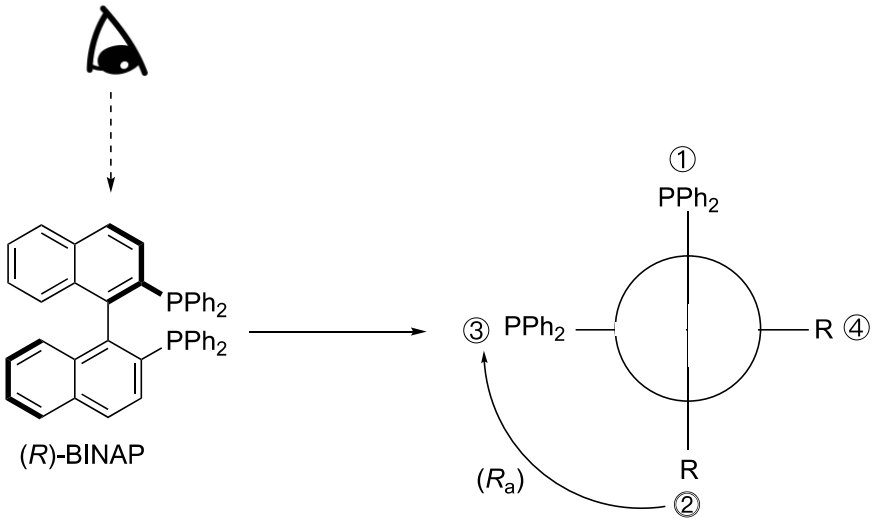

***Figure 5**: Assignment of Axial Chirality*

Planar Chirality

Planar chirality is defined by IUPAC as the stereoisomerism that results from the arrangement of out-of-plane groups with respect to a plane.[8] A classic example is a 1,2-disubstituted ferrocene ring, where a stereogenic plane exists that results in a form of stereoisomerism (**Figure 6**). The two isomers of the ferrocene compound **2** possess planar chirality, which is assigned as per the rules for central chirality. If R^1 is higher in priority than R^2 in the example below, the left configuration of compound **2** would be (S_p) and the right configuration of compound **2** would be (R_p) (where subscript p denotes planar chirality).

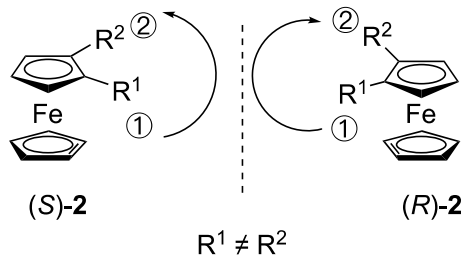

***Figure 6**: Non-superimposable planar chiral ferrocene enantiomers*

Enantiopure Compounds

As mentioned earlier in this chapter, accessing optically pure compounds is of utmost importance for use as pharmaceuticals. A flow chart outlining various ways available to chemists towards accessing optically pure compounds is given below (**Figure 7**).

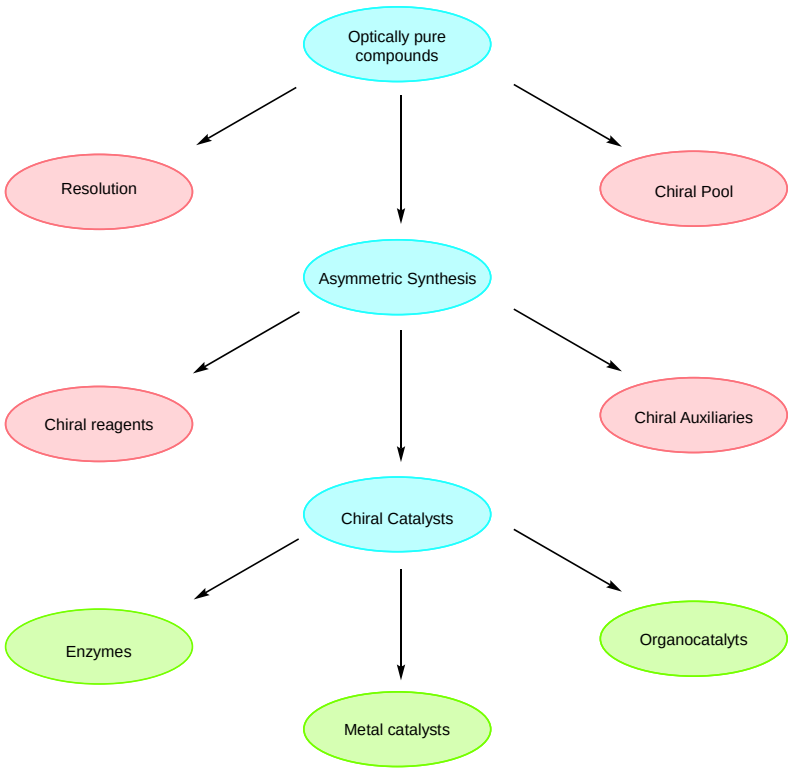

***Figure 7**: Flow chart of methods available towards accessing optically pure compounds*

Resolution

Resolution of racemic mixtures is the first way in which chemists can access optically pure compounds. This often involves synthesising a compound as a racemic mixture which is then treated with a resolving agent (often a chiral salt) to form diastereomeric complexes. The resolution of the chiral ligand BINAP, which is complexed with a chiral palladium salt, is a typical example (**Scheme 2**). The diastereomeric complexes will have different chemical/physical properties which can be separated by either recrystallisation or column chromatography. The chiral resolving agent can then be removed, leaving the optically pure compound.

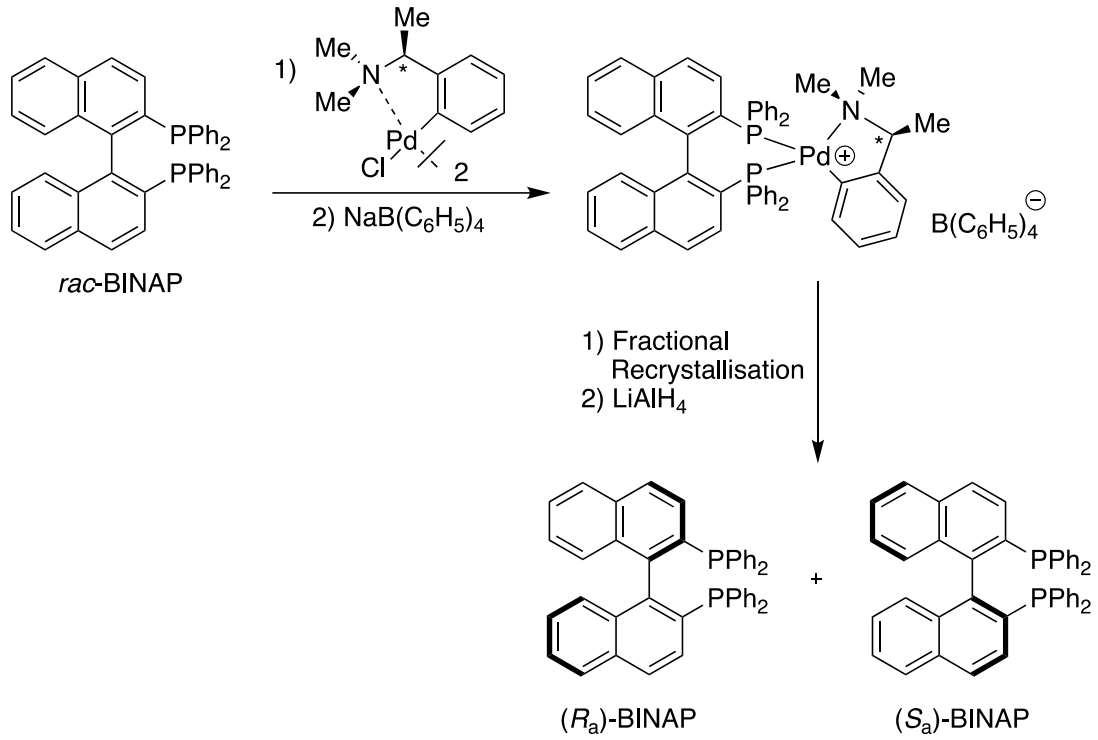

Scheme 2: *Resolution of a mixture of enantiomers of BINAP*

Chiral Pool

Many compounds that exist naturally do so in an optically pure form. Examples of such compounds includes natural sugars glucose, amino acids such as L-valine and terpenoids such as carvone (**Figure 8**). These naturally occurring optically pure compounds can be isolated and used in chemical syntheses as a way of introducing stereochemistry into a compound, bypassing the need for stereospecific reactions.

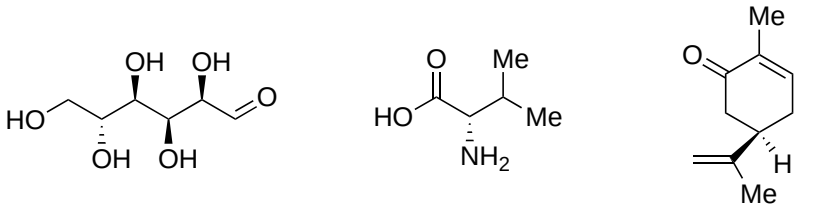

D-Glucose L-Valine (*R*)-Carvone

***Figure 8**: Commonly used molecules in the chiral pool*

Asymmetric Synthesis

There are drawbacks to using either resolution or the chiral pool as a way of accessing optically pure compounds. In the case of classical resolution, the maximum yield of a specific stereoisomer is limited to 50% when isolating one of two enantiomers from a racemic mixture. In the case of the chiral pool there is the obvious limitation in what compounds occur naturally. High cost can often be associated with chiral pool compounds, depending on quantity and demand.

Asymmetric synthesis aims to overcome these issues by synthesising compounds with a bias towards forming one stereoisomer preferentially. The common methodologies used in asymmetric synthesis will now be outlined below.

Chiral Reagents

The first tool available to a chemist is the use of chiral reagents in chemical syntheses in order to form an enantioenriched product. These chiral reagents react with a prochiral substrate to form a diastereomeric transition state, which biases the formation of a particular enantiomer of product.[10] Noyori reported the use of BINAL, an axially chiral reagent derived from the treatment of BINOL with $LiAlH_4$, for the asymmetric reduction of aryl ketones (**Scheme 3**).[11] Lithium coordination to the carbonyl of the substrate and alkoxy group on BINAL was proposed to guide the substrate towards the catalyst, with the larger R group facing away from the catalyst to minimise steric clash. Hydride attack on the prochiral face of the carbonyl furnishes the reduced products with enantioselectivities of >99% ee and yields of up to 75% reported.

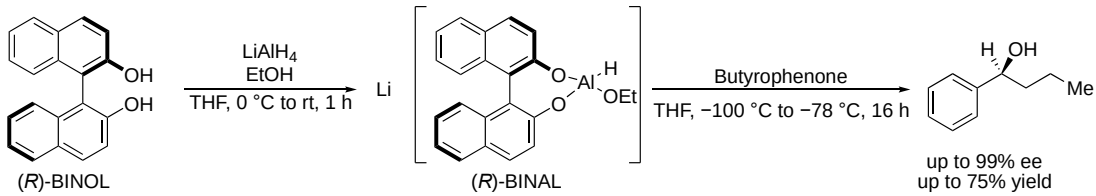

***Scheme 3**: Reduction of aryl ketones using BINAL*[11]

Chiral Auxiliaries

Chiral auxiliaries are temporary units that are incorporated into a molecule to provide stereochemical information for an asymmetric transformation, before subsequently being removed. A number of chiral auxiliaries exist as tools for asymmetric synthesis. A popular family of recyclable chiral auxiliaries are oxazolidinones, first reported by Evans in 1981.[12] Oxazolidinones can be readily synthesised from the corresponding optically pure amino alcohol and either phosgene or diethyl carbonate. They were first employed as chiral auxiliaries for carboxylic acid substrates, in highly enantioselective aldol condensations *via* the respective lithium or boron enolates. The stereochemical information on the chiral oxazolidinones auxiliaries led to aldol type products being formed with

diastereooselectivities of up to >99% de reported (**Scheme 4**).

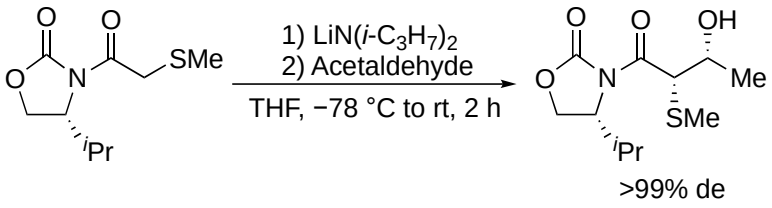

***Scheme 4**: Evans' oxazolidinone auxiliaries for asymmetric aldol reactions*[12]

There are a variety of options for the cleavage of the resulting aldol products, depending on the functionality required for the remainder of the synthesis. A few of these cleaved products and the reagents required are highlighted below, which helps to illustrate the synthetic utility of these chiral auxiliaries in chemical syntheses (**Scheme 5**).

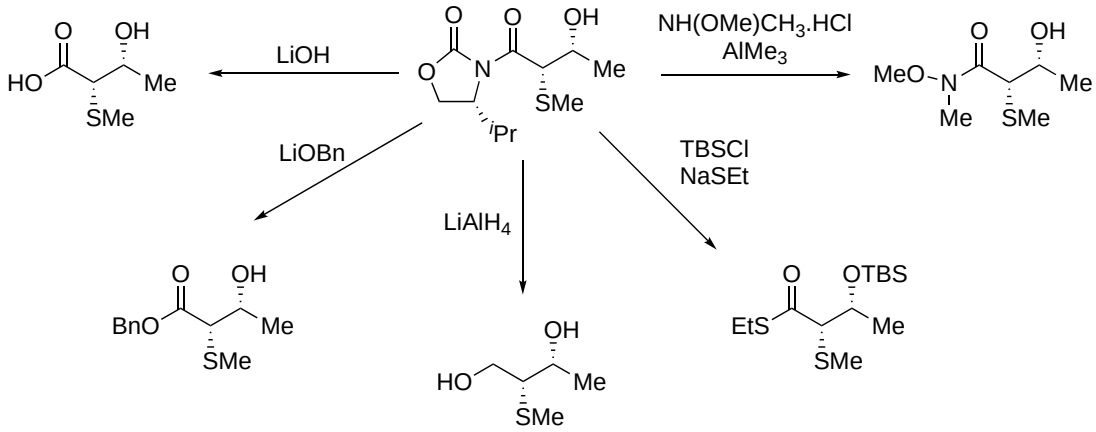

***Scheme 5**: Conditions for the cleavage of Evans' auxiliaries from the asymmetric aldol products*

Chiral Catalysts

Chiral catalysts represent in principle the most efficient way of introducing stereochemical information into substrates. At its most basic form, a chiral catalyst is a reagent that accelerates a chemical process, resulting in the formation of a chiral product without itself being consumed. Two numbers are often cited when analysing a catalyst in terms its efficiency, namely turnover number and turnover frequency. Turnover number is defined as the moles of reactant consumed/moles of catalyst and turnover frequency is defined as turnover number/unit time (e.g. 200 per sec).[13]

Enzymes

Enzymes are proteins produced by living organisms that catalyse biological processes in vivo and chemical reactions *ex vivo*. For a chemical example, Kula reported the use of leucine dehydrogenase and phenylalanine dehydrogenase in the asymmetric reductive amination of α-keto acids to form the corresponding optically pure synthetic L-amino acids (**Scheme 6**).[14] Enantioselectivities of 99% ee and yields of up to 86% were reported and are shown for the respective products.

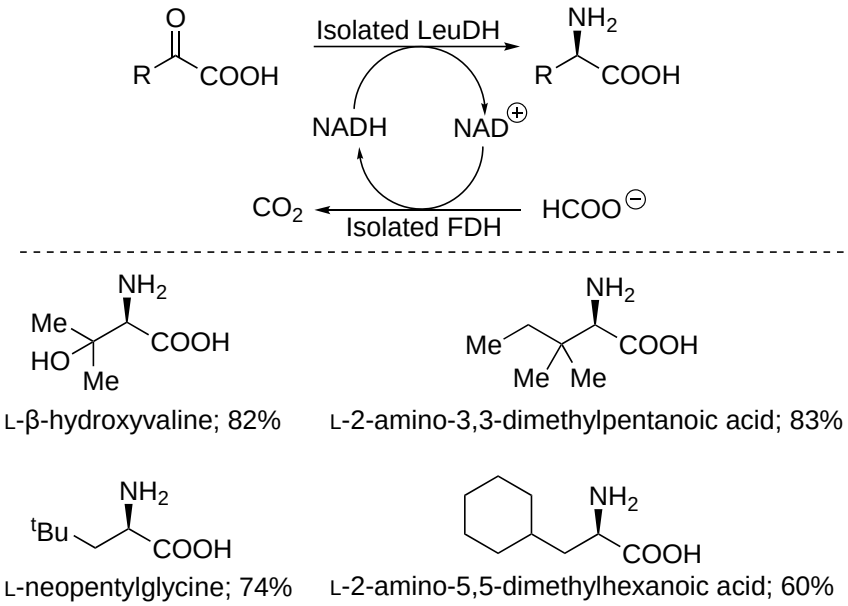

***Scheme 6**: Enzyme-catalysed reductive amination of α-keto acids*[14]

Organocatalysis

Organocatalysis refers to the use of catalysts consisting of carbon, hydrogen and other non-metallic elements.[15] They boast several advantages including the lack of metal waste and often operate under mild reaction conditions.[16] Organocatalysts have seen use in many asymmetric reactions including those with enamine iminium ion substrates or mediate reactions through hydrogen-bonding and counter-ion.[17] In 2021, Ben*J*amin List and David MacMillan were awarded the Nobel Prize in chemistry "*for the development of asymmetric organocatalysis*". The chair of the Nobel Committee for Chemistry, *J*ohan Åqvist, described their work establishing the field of

organocatalysis per the following quote:

"This concept for catalysis is as simple as it is ingenious, and the fact is that many people have wondered why we didn't think of it earlier"

An influential publication in the field of organocatalysis came from MacMillan in 2007, describing a protocol for the enantioselective α-allylation of aldehydes (**Scheme 7**).[18] They used an amine catalyst **3**, which would condense onto the aldehyde substrate to form an iminium ion. Subsequent tautomerisation to the enamine followed by single electron oxidation mediated by ceric ammonium nitrate (CAN) yielded the radical cation which would readily undergo enantiospecific attack by the allylsilane SOMO (singly occupied molecular orbital) nucleophile. Hydrolysis yielded the substituted aldehydic product and releases the amine catalyst. Yields of up to 88% and enantioselectivities up to 95% ee were reported.

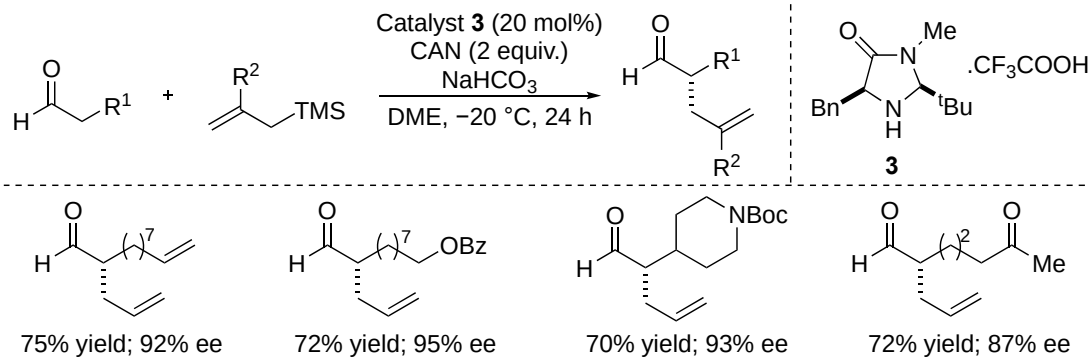

***Scheme 7**: Organocatalytic system for α-allylation of aldehydes reported by MacMillan*

Another important class of organocatalysts are cinchona-derived phase transfer catalysts.[19] An example of a reaction they catalyse is the enantioselective epoxidation of alkenes, which was reported in 2017 by Shibata, using the cinchona catalyst **4** (**Scheme 8**).[20] The system employed methylhydrazine under aerobic conditions to produce hydrogen peroxide *in situ* in high purity, as the system furnished products of type **5** in lower yields when reagent grade hydrogen peroxide was used. A range of aryl rings bearing synthetically useful handles such as chlorine, bromine, and nitro groups were well tolerated. Enantioselectivities up to 99% ee and diastereoselectivities up to 90% de being reported for a range of substrates.

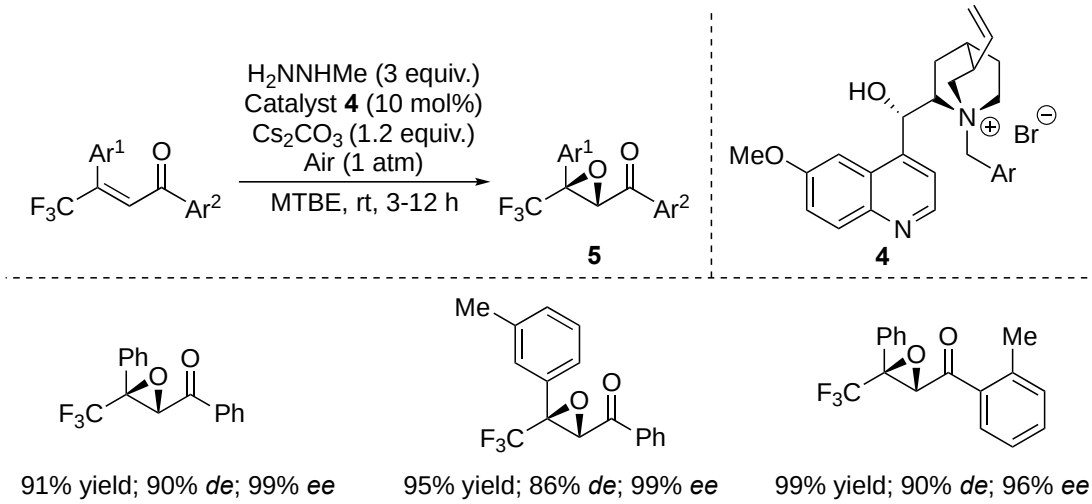

***Scheme 8**: Cinchona-derived phase transfer catalyst for the enantioselective epoxidation of alkenes*

Transition Metal Catalysis

Transition metal catalysis represents possibly the most developed area of asymmetric catalysis in organic chemistry.[21,22,23] The asymmetry in these transition metal-catalysed reactions arises from the use of chiral ligands, which coordinate to the transition metal. These chiral ligands serve two purposes:

1) They alter the steric environment around the metal and bias the approach of substrates to the metal centre;[24]
2) They can alter the electronic properties of the metal.[25]

Chiral ligands can possess central, axial or planar chirality as a means of inducing stereochemistry into the products of the reactions they catalyse. The chiral information attempts to limit the number of ways in which the substrate can approach the ligand-metal complex through steric or non-covalent interactions. Once the substrate has approached the chiral ligand-metal complex in the most energetically favourable way, the metal can then interact with the substrate in order to catalyse either bond formation or cleavage, leading to enantioenriched product formation.

Centrally Chiral Ligands

There are a huge number of chiral ligands in the scientific literature, and as such the subsequent discussion with provide a very limited overview. Bis(oxazoline) ligands of type **6** and PyBox ligands of type **7** represent versatile classes of easily synthesised centrally chiral ligands that are used extensively in asymmetric catalysis (**Scheme 9**).[26] Bidentate and tridentate nitrogen-based ligands respectively, they are both readily synthesised from the corresponding amino alcohol and either malononitrile or 2,6-pyridinedicarboxylic acid, respectively.[27]

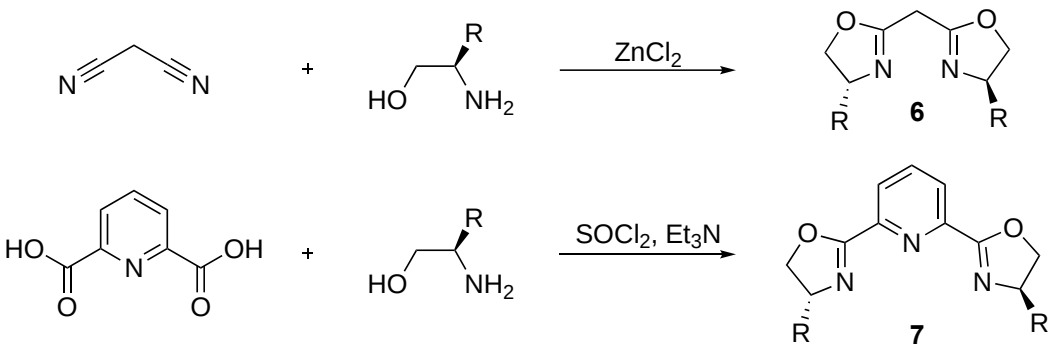

***Scheme 9**: Synthesis of bis(oxazoline) and PyBox ligands from the corresponding amino alcohol*

Singh reported the enantioselective one-pot formation of propargylamines using a copper catalyst and PyBox ligand **8** (**Scheme 10**).[28] These A3 coupling (aldehyde, amine, alkyne) reactions are atom efficient protocols for accessing chiral propargylamines. The reaction involves the condensation of the aldehyde and amine to form an imine, before interception by a copper acetylide nucleophile.

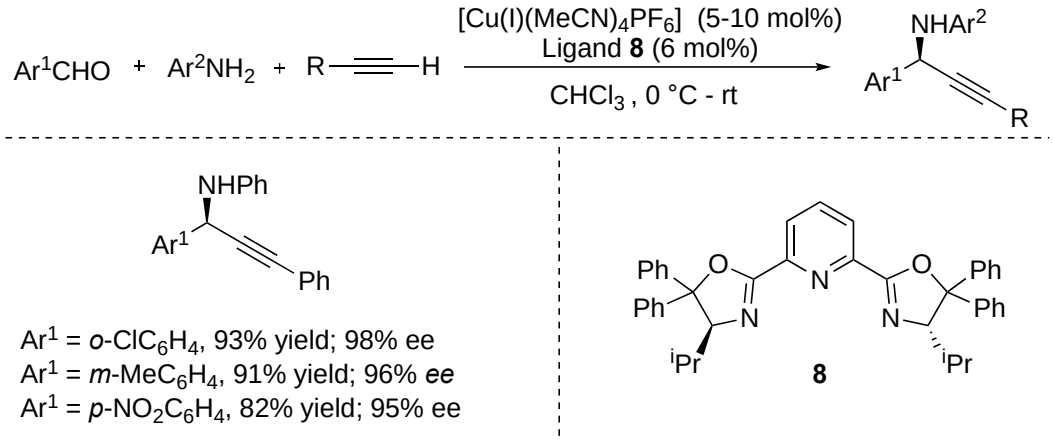

***Scheme 10**: PyBox ligand used in the catalytic asymmetric formation of propargylamines*[28]

In their publication, Singh also proposed a transition state to explain the stereochemistry of the resulting propargylamine products (**Figure 9**). Favourable C-H - π and π-π interactions between the aryl rings on the substrate and ligand, coupled with the centrally chiral *iso*-propyl groups on the ligands, leads to attack on the *si*-face of the imine by the copper acetylide nucleophile.

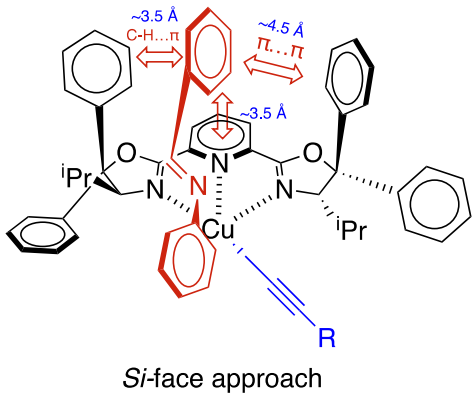

***Figure 9**: Proposed transition state in Cu-Pybox-mediated A3 coupling reaction*[28]

Phosphino-oxazoline (PHOX) ligands are another notable class of centrally chiral ligands. PHOX ligands are C_1 symmetric bidentate P,N ligands which can be synthesised from scaffolds such as 2-bromobenzonic acid (**Scheme 11**). As seen previously with the PyBox ligands, the oxazoline moiety can be synthesised from the parent acid and amino alcohol, when treated with thionyl chloride and triethylamine.[29] Many methodologies for the subsequent installation of the diarylphosphine moiety have been developed, with the Cu-catalysed

phosphinylation reported by Buchwald seeing extensive use.[30] One of the most successful PHOX ligands is the (*S*)-^{t}Bu-PHOX ligand, derived from the non-natural amino acid (*S*)-*tert*-leucine.

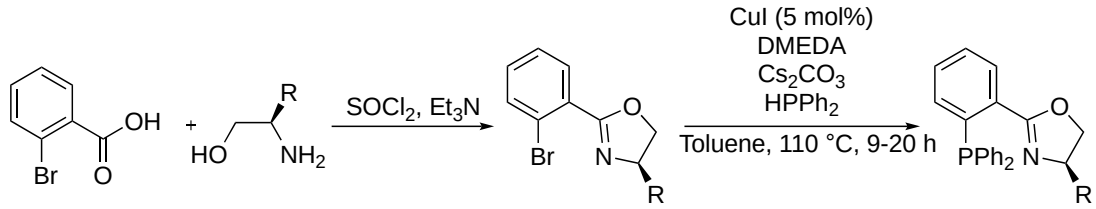

***Scheme 11**: General protocol towards accessing PHOX ligands*

PHOX ligands have been employed in a wide variety of reactions including hydrogenations, allylic alkylations and asymmetric intermolecular Heck reactions.[31,26] A PHOX ligand was the ligand of choice in decarboxylative asymmetric protonation reactions reported by Guiry in 2017 (**Scheme 12**).[32] The system employed a palladium catalyst and α-aryl-allyl β-keto esters as substrates for the synthesis of tertiary α-aryl 1-indanones. The protocol was found to be enantiodivergent depending on which proton source was used in the reaction. Meldrum's acid furnished (*S*)-tertiary α-aryl 1-indanones while formic acid furnished the corresponding (*R*)-enantiomers. Enantioselectivities up to 94% ee and yields up to 98% were reported, with variation on the indanone aryl ring R^1 and variation of the aryl R^2 group being well tolerated in the protocol.

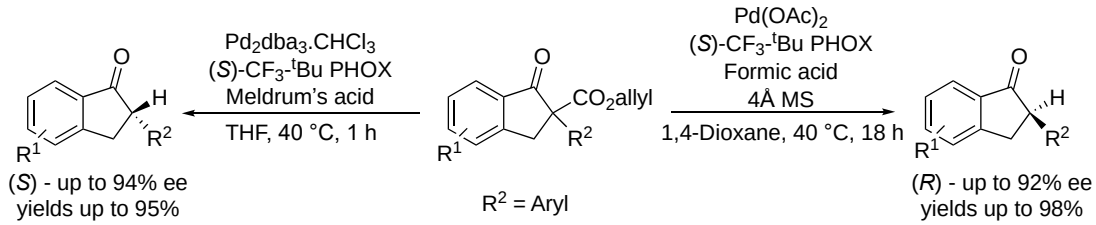

***Scheme 12**: Pd-catalysed enantioselective asymmetric protonation with CF_3-(S)-t-Bu PHOX*

Planar Chiral Ligands

Planar chiral ligands are another class of chiral ligands that are ubiquitous in the literature for use in transition metal-catalysed asymmetric transformations.[33,34,35] The most common form of these ligands are 1,2 or 1,1'-disubstituted ferrocene based ligands. Ferrocene has a number of advantages that make it a good backbone as a chiral ligand:[36,37]

1) It is easily derivatised due to the partial negative charge that is carried on the cyclopentadienyl rings, specifically with respect to electrophilic substitution reactions;
2) The partial negative charge on the cyclopentadienyl rings of ferrocene enhances the ligands donor quality;
3) Ferrocene is cheap, thermally stable and tolerant of oxygen and moisture.

Feringa reported the use of one such chiral ligand, JosiPhos, in the Cu-catalysed enantioselective conjugate addition of Grignard reagents to acyclic enones (**Scheme 13**).[38] This report overcame the previous limitations, where enantioselectivities for acyclic enone substrates rarely exceeded 90% *ee*.[39,40] Aliphatic β-substituted ketones are common subunits in biologically active molecules and are important building blocks in natural product syntheses, which motivated the Feringa group to develop tools towards their access.

Grignard reagents are known to form the organocuprate species in the presence of a copper catalyst. The organocuprate is a softer nucleophile compared to the Grignard reagent and will add to the β-position of the enone to form the Cu(III) species, which will reductively eliminate to form a carbon-carbon bond and regenerate the Cu(I) catalyst.[32] The chiral JosiPhos ligand was crucial towards achieving high enantioselectivities with the troubling acyclic enone substrates.

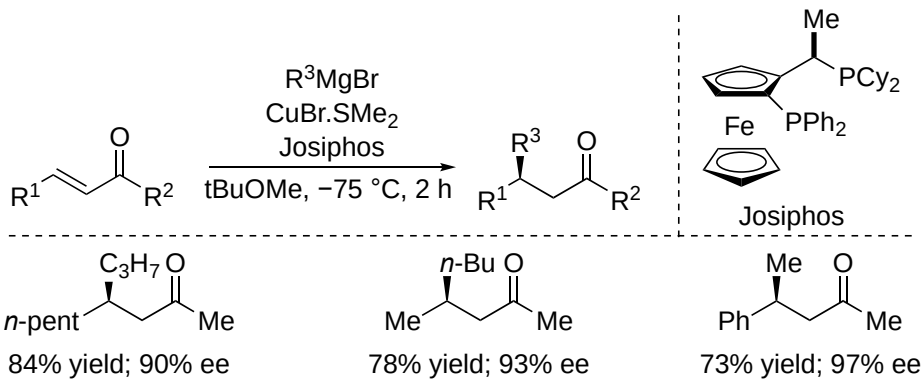

***Scheme 13**:Cu-catalysed enantioselective conJugate addition of Grignard reagents to acyclic enones using chiral ferrocene ligand Josiphos*[32]

Axially Chiral Ligands

Axially chiral ligands are chiral scaffolds that exist as enantiomers or diastereomers due to the presence of restricted rotation about a bond in the compound. They see extensive use in the field of asymmetric catalysis.[41,42,43] Rh(I)-BINAP complexes are a good example of transition metal catalysts used in asymmetric synthesis. Noyori reported a Rh(I)-BINAP asymmetric hydrogenation protocol in the original publication describing the synthesis and resolution of the BINAP ligand, where it was applied in the asymmetric hydrogenation of α-(acylamino)acrylic acids.[44] Noyori later extended the use of the BINAP ligand in asymmetric hydrogenation reactions, by using a Ru(II)-BINAP complex **9** in the synthesis of (*S*)-Naproxen, a key non-steroidal anti-inflammatory drug (**Scheme 14**).[45]

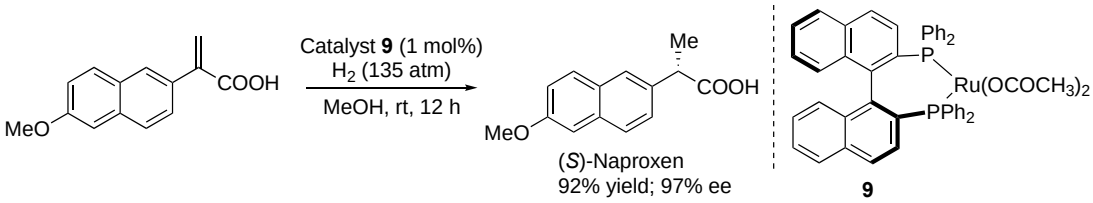

***Scheme 14**: Ru(II)-BINAP system for asymmetric hydrogenation*

Ru(II)-BINAP complexes see use industrially also, namely as a key step in the synthesis of (–)-menthol (**Scheme 15**).[46] Lithium diisopropyl amide is added to myrcene to afford compound **10**, which is isomerised asymmetrically with a Ru-BINAP catalyst with an enantioselectivity of 98% ee. Hydrolysis of **11** to the aldehyde, an intramolecular ene reaction followed by hydrogenation gives the (–)-menthol product. The process described below is used to synthesise over 1000 tons/year of (–)-menthol annually.[46]

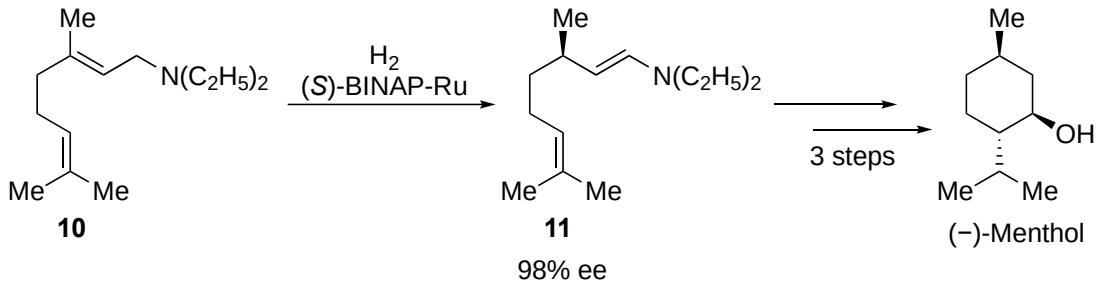

***Scheme 15**: Takasago synthesis of (–)-menthol where a Ru-BINAP complex is used in the key isomerisation step*[46]

Conclusion

Despite the existence of many distinct and well-researched strategies for conducting asymmetric synthesis, there remains persistent need to further develop the tools and methodologies available to chemists. The most attractive of these include the development of ligands for use in asymmetric catalysis. The small loadings of these ligands used in reactions and the benefit of such ligands being successfully applied in mechanistically different reactions warrants the continued effort towards their access. Axially chiral P,N ligands represent a major class of chiral ligands that see continued use and development in research, a collection of which are shown below (**Scheme 16**).

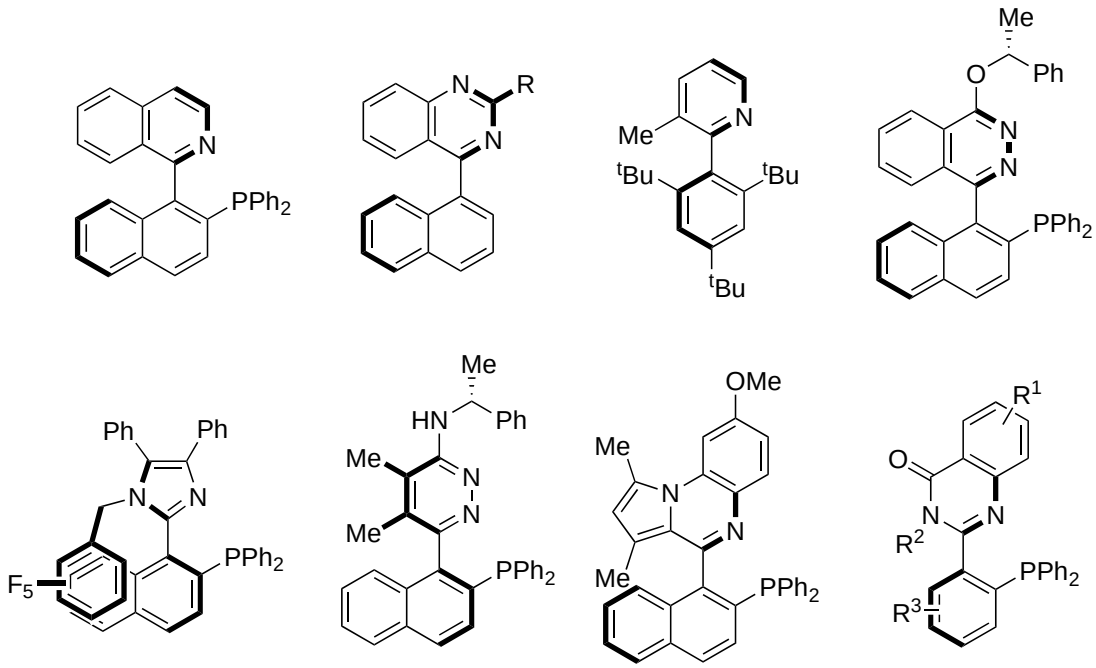

***Scheme 16**: A selection of axially chiral P,N ligands employed in asymmetric catalysis*

The aim of this research project was to apply existing P,N ligand scaffolds, developed within in the Guiry group, in novel asymmetric transformations to understand the utility of such scaffolds. Further to this, there was an aim to devise a route towards synthesising novel imidazoline-based axially chiral P,N ligands of type **12** and type **13** (**Scheme 17**). The effect of varying the centrally chiral R^1 group on asymmetric induction and the effect of R^2 on the barrier to rotation about the chiral axis of the proposed ligands was to be investigated.

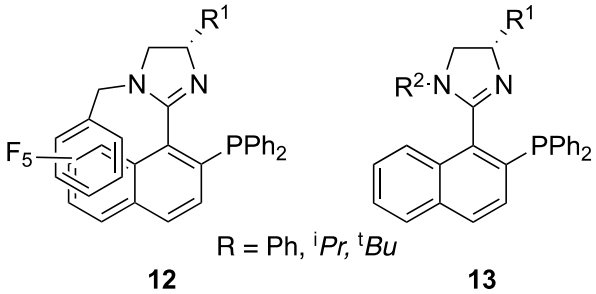

R = Ph, ^{i}Pr, ^{t}Bu

12 **13**

***Scheme 17**: Novel imidazoline-based P,N ligands*

References

(1) Levêque, D.; Becker, G.; Bilger, K.; Natarajan-Amé, S. *Clin. Pharmacokinet.* **2020**, *59* (7), 849–856.

(2) Hall, J.; Guyton, A. *Guyton and Hall Textbook of Medical Physiology*, 13th Editi.; Elsevier, 2016.

(3) Blackmond, D. G. *Cold Spring Harb. Perspect. Biol.* **2010**, *2* (5), 1–17.

(4) Hawbaker, N. A.; Blackmond, D. G. *Nat. Chem.* **2019**, *11* (10), 957–962.

(5) Teo, S. K.; Colburn, W. A.; Tracewell, W. G.; Kook, K. A.; Stirling, D. I.; Jaworsky, M. S.; Scheffler, M. A.; Thomas, S. D.; Laskin, O. L. *Clin. Pharmacokinet.* **2004**, *43* (5), 311–327.

(6) Strong, M. *Food Drug Law* J. **1999**, *54* (3), 463–487.

(7) Lehn, J. M. In *Dynamic Stereochemistry*; Springer-Verlag: Berlin/Heidelberg, 1870; pp 311–377.

(8) MOSS, G. P. *Pure Appl. Chem* **1996**, *68* (12), 2193–2222.

(9) Sanz García, J.; Lepetit, C.; Canac, Y.; Chauvin, R.; Boggio-Pasqua, M. *Chem. - An Asian J.* **2014**, *9* (2), 462–465.

(10) Brunel, J. M. *Chem. Rev.* **2005**, *105* (3), 857–897.

(11) Noyori, R.; Tomino, I.; Tanimoto, Y. *J. Am. Chem. Soc.* **1979**, *101* (11), 3129–3131.

(12) Evans, D. A.; Bartroli, J.; Shih, T. L. *J. Am. Chem. Soc.* **1981**, *103* (8), 2127–2129.

(13) Bligaard, T.; Bullock, R. M.; Campbell, C. T.; Chen, J. G.; Gates, B. C.; Gorte, R. J.; Jones, C. W.; Jones, W. D.; Kitchin, J. R.; Scott, S. L. *ACS Catal.* **2016**, *6* (4), 2590–2602.

(14) Krix, G.; Bommarius, A. S.; Drauz, K.; Kottenhahn, M.; Schwarm, M.; Kula, M. R. *J. Biotechnol.* **1997**, *53* (1), 29–39.

(15) List, B. *Chem. Rev.* **2007**, *107* (12), 5413–5415.

(16) Oliveira, V. da G.; Cardoso, M. F. D. C.; Forezi, L. da S. M. *Catalysts* **2018**, *8* (12).

(17) MacMillan, D. W. C. *Nature* **2008**, *455* (7211), 304–308.

(18) Beeson, T. D.; Mastracchio, A.; Hong, J.-B.; Ashton, K.; MacMillan, D. W. C. *Science* **2007**, *316* (1), 582–585.

(19) Jew, S. S.; Park, H. G. *Chem. Commun.* **2009**, No. 46, 7090–7103.

(20) Kawai, H.; Okusu, S.; Yuan, Z.; Tokunaga, E.; Yamano, A.; Shiro, M.; Shibata, N. *Angew. Chem. Int. Ed.* **2013**, *52* (8), 2221–2225.

(21) Beaumier, E. P.; Pearce, A. J.; See, X. Y.; Tonks, I. A. *Nat. Rev. Chem.* **2019**, *3* (1), 15–34.

(22) Fanourakis, A.; Docherty, P. J.; Chuentragool, P.; Phipps, R. *J. ACS Catal.* **2020**, *10* (18), 10672–10714.

(23) Trowbridge, A.; Walton, S. M.; Gaunt, M. *J. Chem. Rev.* **2020**, *120* (5), 2613–2692.

(24) Helmchen, G.; Pfaltz, A. *Acc. Chem. Res.* **2000**, *33* (6), 336–345.

(25) Akermark, B.; Krakenberger, B.; Hansson, S.; Vitagliano, A. *Organometallics* **1987**, *6* (3), 620–628.

(26) Hargaden, G. C.; Guiry, P. J. *Chem. Rev.* **2009**, *109* (6), 2505–2550.

(27) Corey, E. J.; Imai, N.; Zhang, H. Y. *J. Am. Chem. Soc.* **1991**, *113* (2), 728–729.

(28) Bisai, A.; Singh, V. K. *Org. Lett.* **2006**, *8* (11), 2405–2408.

(29) Tani, K.; Behenna, D. C.; McFadden, R. M.; Stoltz, B. M. *Org. Lett.* **2007**, *9* (13), 2529–2531.

(30) Gelman, D.; Jiang, L.; Buchwald, S. L. *Org. Lett.* **2003**, *5* (13), 2315–2318.

(31) McManus, H. A.; Guiry, P. *J. Chem. Rev.* **2004**, *104*, *4152-4202*

(32) Kingston, C.; Guiry, P. J. *J. Org. Chem.* **2017**, *82* (7), 3806–3819.

(33) Cunningham, L.; Benson, A.; Guiry, P. J. *Org. Biomol. Chem.* **2020**, *18* (46), 9329–9370.

(34) Hassan, Z.; Spuling, E.; Knoll, D. M.; Lahann, J.; Bräse, S. *Chem. Soc. Rev.* **2018**, *47* (18), 6947–6963.

(35) Deng, W. P.; You, S. L.; Hou, X. L.; Dai, L. X.; Yu, Y. H.; Xia, W.; Sun, *J. J. Am. Chem. Soc.* **2001**, *123* (27), 6508–6519.

(36) Astruc, D. *Eur. J. Inorg. Chem.* **2017**, *2017* (1), 6–29.

(37) De Souza, A. C.; Pires, A. T. N.; Soldi, V. *J. Therm. Anal. Calorim.* **2002**, *70* (2), 405–414.

(38) López, F.; Harutyunyan, S. R.; Minnaard, A. J.; Feringa, B. L. *J. Am. Chem. Soc.* **2004**, *126* (40), 12784–12785.

(39) Pichota, A.; Pregosin, P. S.; Valentini, M.; Wörle, M.; Seebach, D. *Angew. Chem.*

Int. Ed. **2000**, *39* (1), 153–156.

(40) Kanai, M.; Nakagawa, Y.; Tomioka, K. *Tetrahedron* **1999**, *55* (13), 3843–3854.

(41) Rokade, B. V.; Guiry, P. J. *ACS Catal.* **2018**, *8* (1), 624–643.

(42) Li, Y. M.; Kwong, F. Y.; Yu, W. Y.; Chan, A. S. C. *Coord. Chem. Rev.* **2007**, *251* (17–20), 2119–2144.

(43) Yurino, T.; Ohkuma, T. In *Atropisomerism and Axial Chirality*; WORLD SCIENTIFIC (EUROPE), 2019; pp 149–247.

(44) Miyashita, A.; Yasuda, A.; Takaya, H.; Toriumi, K.; Ito, T.; Souchi, T.; Noyori, R. *J. Am. Chem. Soc.* **1980**, *102* (27), 7932–7934.

(45) Ohta, T.; Takaya, H.; Kitamura, M.; Nagai, K.; Noyori, R. *J. Org. Chem.* **1987**, *52* (14), 3174–3176.

(46) Akutagawa, S. *Appl. Catal. A, Gen.* **1995**, *128* (2), 171–207.

Chapter 2: Synthesis of P,N Ligands

Introduction

Beneficial Properties of P,N Ligands

As outlined in the introductory chapter of this thesis, asymmetric catalysis through the use of chiral ligands complexed to transition metals represents a substantial field in organic chemistry.[1,2,3,4,5,6] Transition metals with a diverse range of electronic properties are available to chemists for use in catalysis and as such, there is an inherent drive towards synthesising chiral ligands to use in tandem with these metals. Chiral ligands offer a way of harnessing the power of such metals and utilising them to their full potential in asymmetric synthesis to make valuable compounds such as active pharmaceutical compounds.

P,N ligands represent one such class of ligands available to chemists for use in tandem with transition metals in asymmetric catalysis. P,N ligands are privileged chiral ligands, a term coined by Jacobsen used to describe ligands that can be used in a variety of mechanistically different reactions.[7] Chiral ligands in general have two major roles in catalytic reactions;

1) They provide steric information when bound to a transition metal. They limit the number of ways in which a substrate can favourably approach a metal with respect to sterics and in doing so impart stereochemical information into the product being formed;

2) They can modulate the electronic properties of the given metal centre.

To further develop the second point in particular in the context of P,N ligands, they offer a unique advantage over other privileged chiral ligands such as P,P ligands. The presence of two distinct donor atoms in P,N ligands allows for greater modulation of the electronic properties of the metal during key phases in a given catalytic cycle (**Figure 10**).[8] The phosphorus atom can help stabilise the metal centre in its electron rich low oxidation state *via* π-backbonding.[9] The phosphorus donor is often triaryl in nature in P,N ligands, which allows for further tuning of the electronic and steric properties at P, through electron-donating or electron-withdrawing groups on the aryl rings. The presence of a second electronically different donor atom in the form of nitrogen allows the ligands to stabilise the metal in ways in which phosphorus is unable to due to its electronically soft nature. More specifically, nitrogen can help stabilise the metal when it is electron-deficient after oxidative addition reactions through its σ-donating properties.

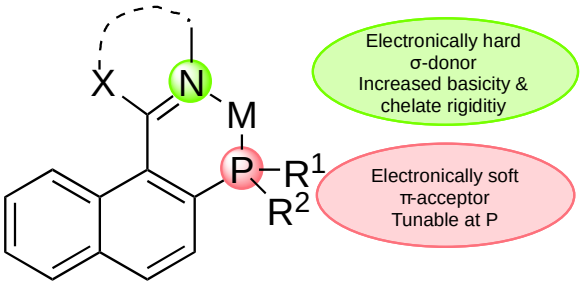

***Figure 10**: Electronic properties of P,N ligands*[10]

Synthesis and Application of Axially P,N Ligands

The first axially chiral P,N ligand was reported by Brown and co-workers in 1992 (**Scheme 18**).[11] The lithiated phosphine oxide **1** was treated with Cu bromide dimethylsulfide to form intermediate **2**. Cuprate **2** was then reacted with 1-iodo-isoquinoline under reflux conditions to give the biaryl phosphine oxide **3**, which was subsequently reduced with trichlorosilane. The P,N ligand **4** was complexed with chiral palladium salts to form diastereomers, which could readily be separated by recrystallisation. Unfortunately, it was found that **4** readily racemises about its chiral axis at ambient temperatures within minutes. The energy barrier for its rotation was calculated to be 93 K*J* mol^{-1}. This excluded the use of **4** as a potential ligand for asymmetric catalysis.

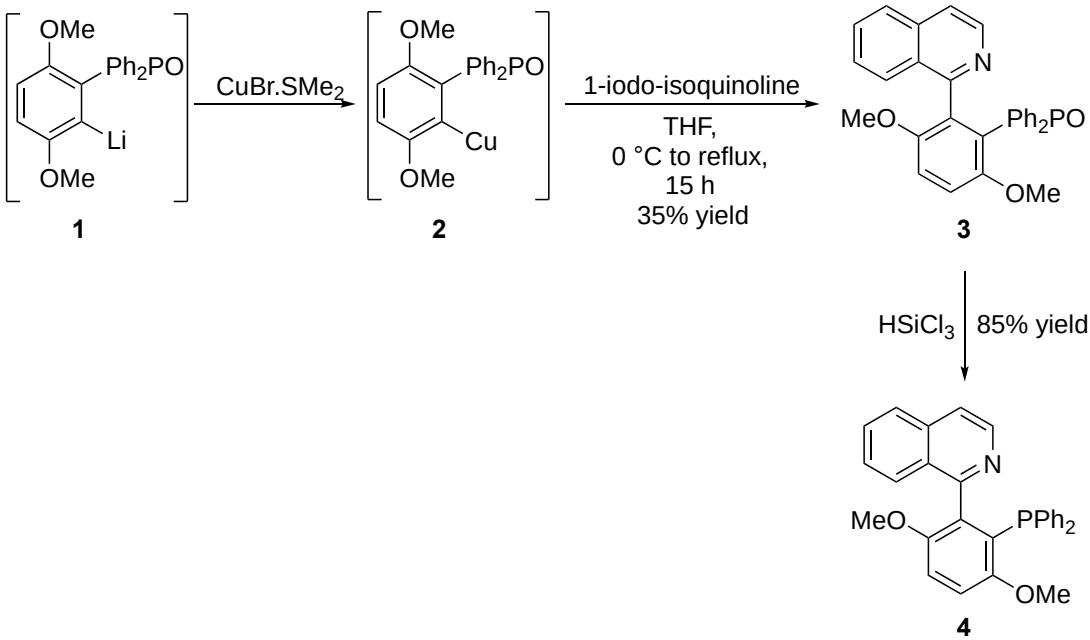

***Scheme 18**: First reported synthesis of an axially chiral P,N ligand*

In 1993, Brown and co-workers subsequently reported the synthesis of a second axially chiral P,N ligand, Quinap **5** (**Scheme 19**).[12] The naphthalene core in the ligand was incorporated to overcome the racemisation problems encountered with the previously reported ligand **4** (**Scheme 18**). Quinap **5** was accessed as a racemate in five steps starting from boronic acid **6** and 1-chloroisoquinoline (**Scheme 19**). Boronic

acid **6** was synthesised from the Grignard reagent derived from 1-bromo-2-methoxynaphthalene and trimethoxyborane, and then coupled with 1-chloroisoquinoline *via* Pd catalysis to yield the corresponding biaryl in a 78% yield. A boron tribromide-mediated demethylation of the aryl methoxy group yielded the free hydroxy group, which was subsequently reacted with trifluoromethanesulfonic anhydride to form triflate **7**. A Pd-catalysed phosphorylation yielded the phosphine oxide **8**, which was then reduced with trichlorosilane to furnish a racemic mixture of the atropisomeric ligand **5** in a 35% yield across five steps.

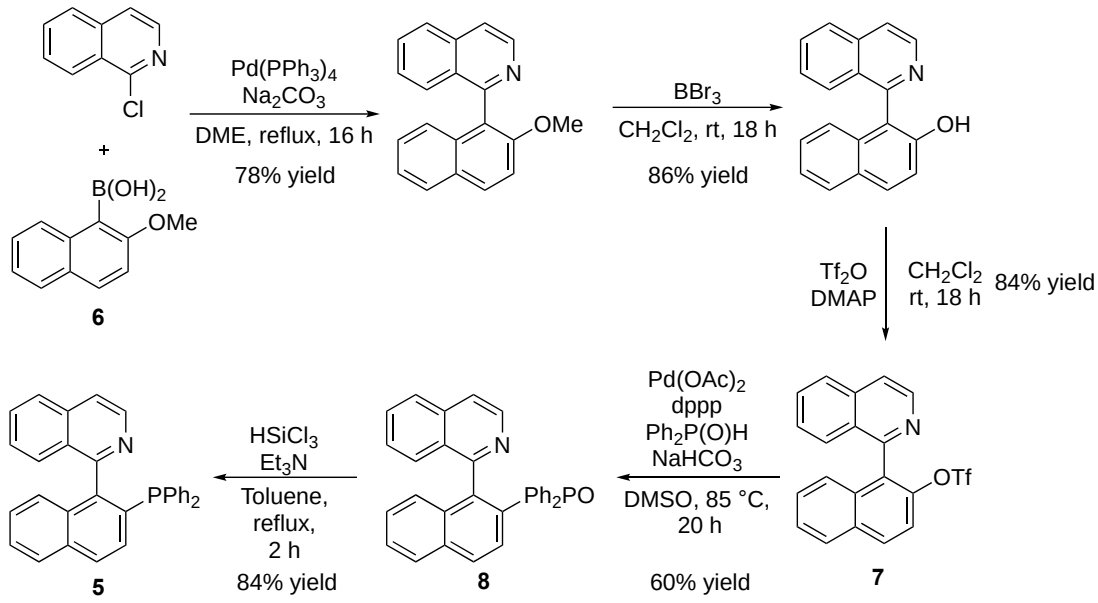

***Scheme 19**: Synthesis of Quinap by Brown and co-workers*

Once the racemic mixture of the Quinap ligand was accessed, it needed to be resolved into its respective enantiomers before it could be applied in asymmetric catalysis. Following the precedent in the literature for the resolution of other axially chiral ligands such as BINAP, Brown employed the chiral palladium salt **9** as resolving agent (**Scheme 20**).[13] The two enantiomers of Quinap co-ordinate to the chiral palladium salt **9** to form the diastereomers **10** and *dia*-**10**, respectively. The two diastereomers could be separated based on their differing solubilities, where **10** could be accessed *via* recrystallisation from $CHCl_3$ and *dia*-**10** could be accessed *via* recrystallisation from butanone/diethyl ether.[12] The free ligands were then accessed from the palladium salts *via* ligand exchange with 1,2-bis(diphenylphosphino)ethane

(dppe) in CH_2Cl_2. The ligand was reported to not racemise "appreciably" on heating at 65 °C for 24 h in solution. The use of these chiral palladium salts for the resolution of Quinap makes it very expensive commercially (Sigma Aldrich: €548/250mg).

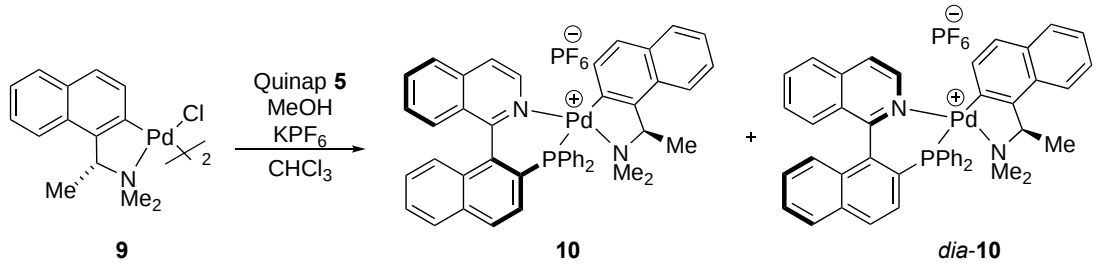

***Scheme 20**: Resolution of Quinap via chiral palladium salts*[12]

In a subsequent publication, Brown and co-workers reported the use of the newly developed Quinap ligand in the asymmetric Rh-catalysed hydroboration of vinylarenes (**Scheme 21**).[14] Interestingly, they reported that lowering the reaction temperature did not enhance the enantioselectivity of the reaction but did reduce the chemoselectivity of the reaction with respect to the formation of branched/linear products. The reaction was also reported to be insensitive to solvent and as such no improvement on the initial enantioselectivity with THF was observed in the optimisation process.

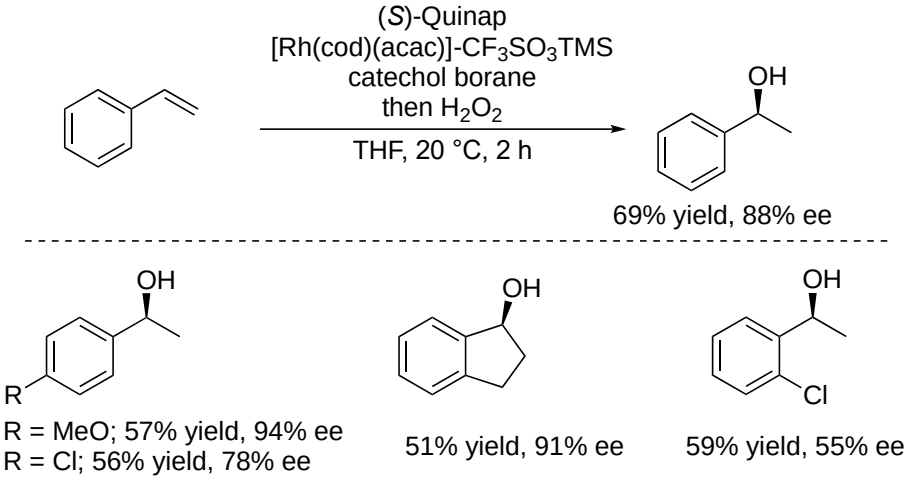

***Scheme 21**: Application of Quinap in the catalytic asymmetric hydroboration of vinylarenes*

A significant advancement in the field of axially chiral P,N ligands occurred in 2004, when Carreira and co-workers reported the synthesis of the novel axially chiral P,N ligand Pinap (**Scheme 22**).[3] The major development for the field was that the Pinap ligand contained a covalently bound centrally chiral element in the form of either (*R*)-phenylethanol or (*R*)-α-phenylethylamine. The incorporation of the centrally chiral element meant that the ligand would readily exist as diastereomers, which would allow for the separation of the diastereomers of ligand *via* column chromatography. This eliminated the need for the expensive chiral palladium salts that were used up to this point as a method for resolving axially chiral P,N ligands (**Scheme 20**).

An aluminium trichloride-mediated Friedel-Crafts arylation between dichlorophthalazine and 2-naphthol formed the corresponding biaryl **11** in a 77% yield. Triflation of **11** to from aryl-triflate **12** proceeded smoothly in a 93% yield and was followed by an S_NAr reaction with (*R*)-α-phenylethylamine or (*R*)-α-phenylethanol to give the racemic ligand precursor of type 13 in a 91% and 93% yield respectively. A Ni-catalysed phosphinylation furnished the novel ligand Pinap in a 53% yield across four steps.

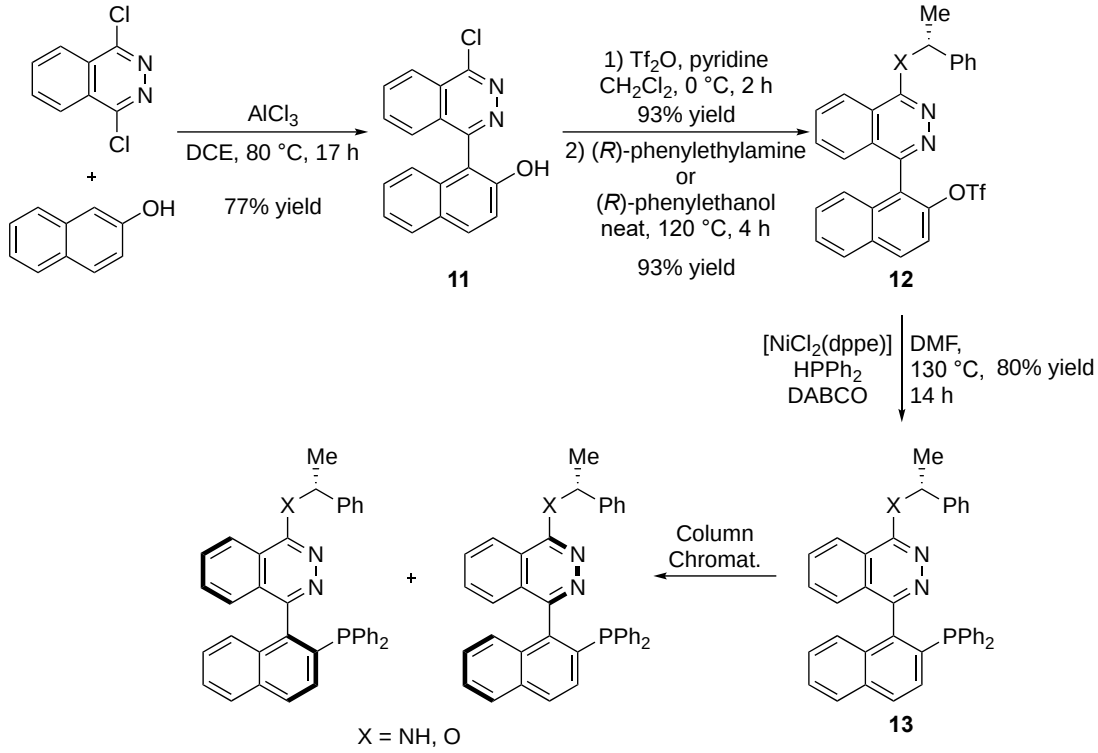

***Scheme 22**: Synthesis of novel axially chiral P,N ligand Pinap reported by Carreira*[3]

In order to demonstrate the synthetic utility of the novel Pinap ligands, Carreira applied them in a variety of asymmetric catalytic reactions (**Scheme 23**).[3] In the asymmetric Rh-catalysed hydroboration reactions of vinylarenes, Pinap performed broadly on par with Quinap (**Scheme 21**). Sterically hindered substrates such as *o*-tolyl were well tolerated, with a yield of 81% and ee of 91% reported. Pinap was also successfully applied in the asymmetric Ag-catalysed azomethine ylide cycloaddition reaction to form products of type **14**, with high yields and enantioselectivities observed with a modest catalyst loading of 3 mol%. Finally, the utility of Pinap in asymmetric A3 couplings was demonstrated, with the highest enantioselectivities (>99% ee) for the reaction at the time being reported.

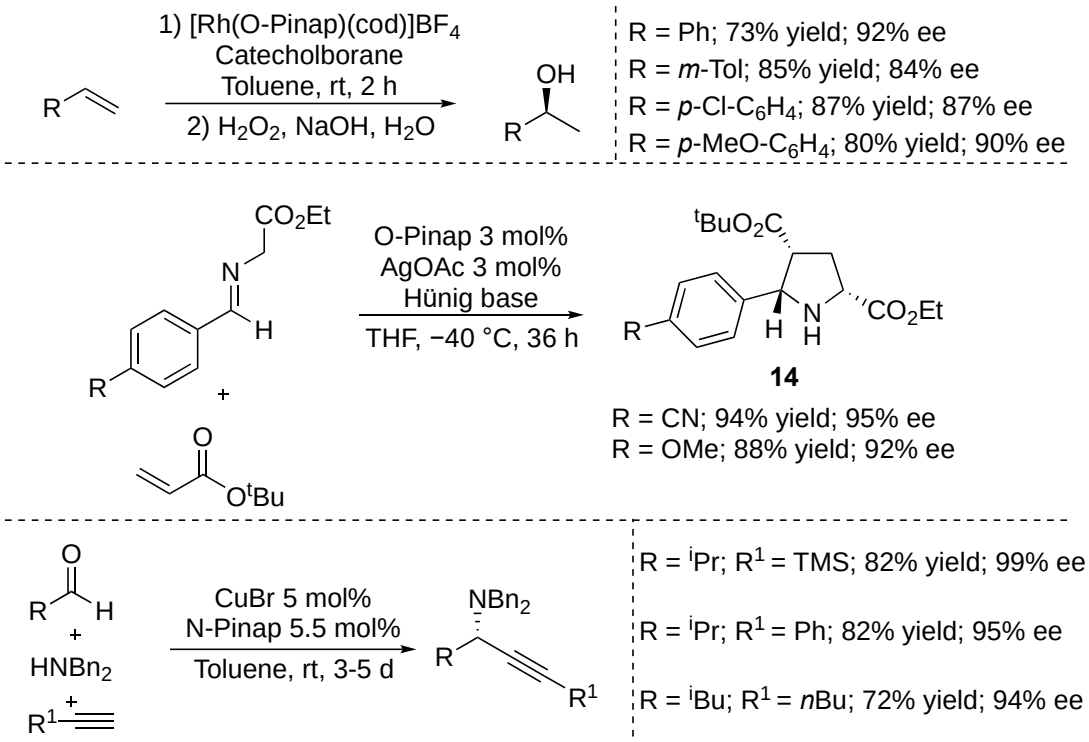

***Scheme 23**: Application of Pinap in a selection of asymmetric catalytic reactions*

Later in 2006, Guiry reported the synthesis of the novel axially chiral P,N Quinazox ligands.[15] The first step in the synthesis of the ligand was to synthesise the required coupling partner **15** (**Scheme 24**). Commercial anthranilamide **16** and the easily synthesised acid chloride **17** were reacted in the presence of triethylamine to form amide **18**. The amide **18** was telescoped to the next step, where it was treated with NaOH under reflux in ethanol to furnish quinazolinol **19** in a 96% yield. Treatment of quinazolinol **19** with phosphoryl chloride formed the coupling partner **15** in an overall 92% yield across three steps.

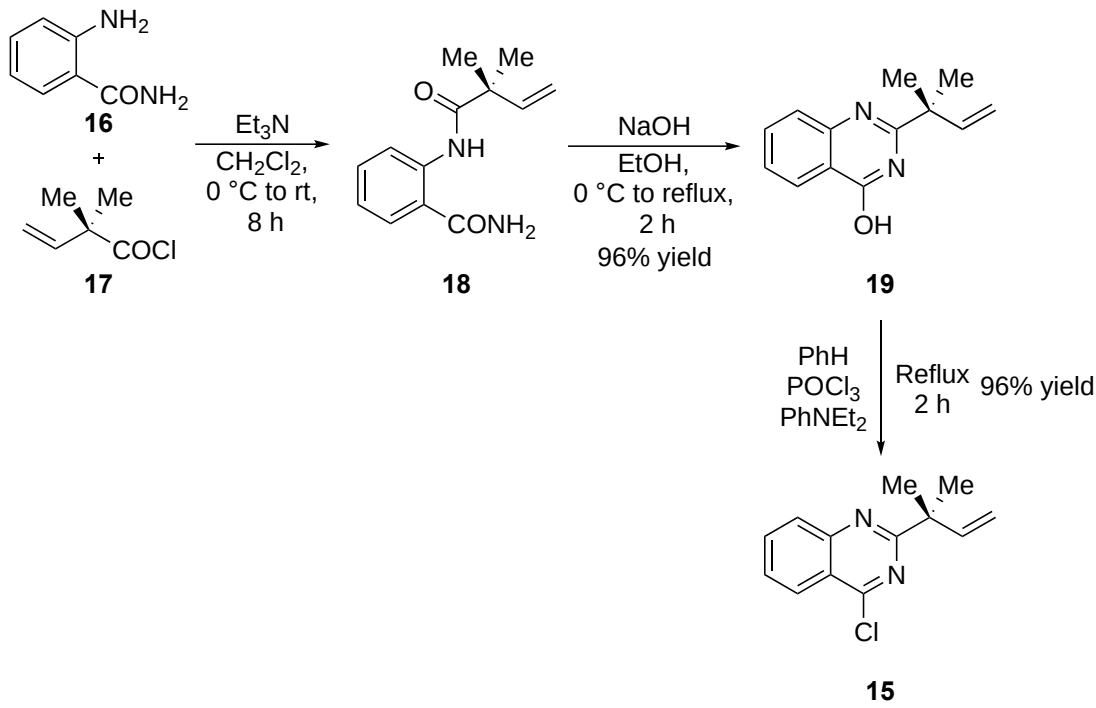

***Scheme 24**: Synthesis of coupling partner required for the synthesis of Quinazox*

Coupling partner **15** was then reacted with boronic acid **20** in a Suzuki-Miyaura coupling to give biaryl **21** in a 97% yield (**Scheme 25**). The terminal alkene in **21** was subjected to osmium tetroxide-mediated dihydroxylation, followed by oxidative cleavage with periodic acid to give aldehyde **22** in a 96% yield over two steps. Formation of the corresponding oxime from aldehyde **22** and hydroxylamine proceeded well, and was subsequently dehydrated with acetic anhydride to give nitrile **23** in a 95% yield over two steps. An $AlBr_3$/NaI-mediated demethylation of the naphthalene methoxy group furnished the free hydroxy group, which was triflated on treatment with trifluoromethanesulfonic anhydride and DMAP to give triflate **24**. A Ni-catalysed phosphinylation gave the triarylphosphine **25** in an 80% yield.

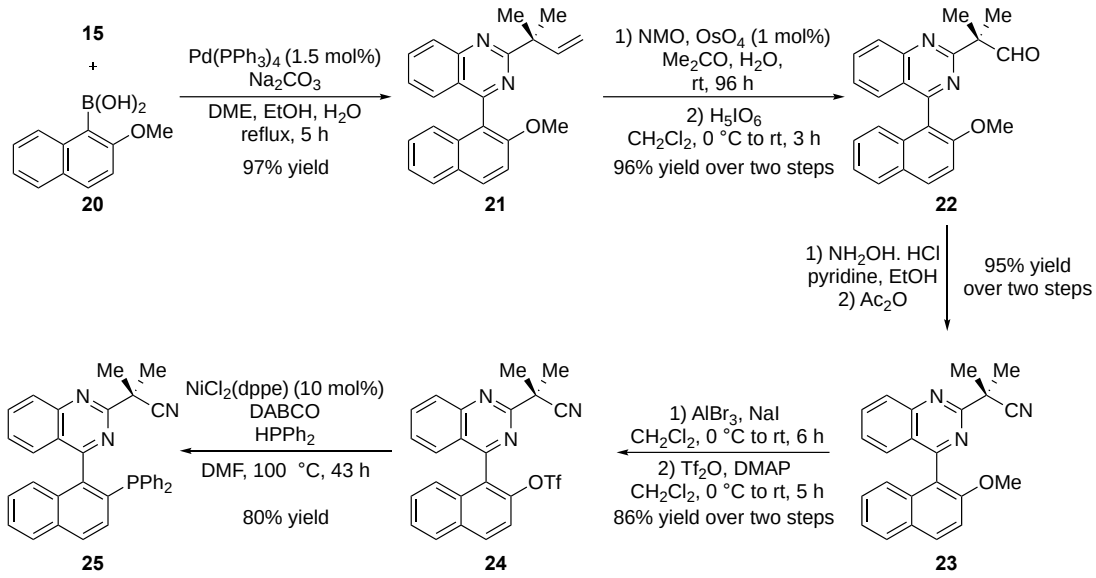

***Scheme 25**: Synthesis of Quinazox ligand precursor reported by Guiry in 2006*[15]

The final steps towards the novel axially P,N Quinazox ligands was to take nitrile **25** and the appropriate amino alcohols to form the oxazoline moiety (**Scheme 26**). The Quinazox ligands were synthesised through the heating of nitrile **25** in chlorotoluene under sealed tube conditions, in the presence of both $Cd(OAc)_2$ and an amino alcohol. The final ligands were separated into the respective diastereomers by column chromatography and were applied in Pd-catalysed asymmetric allylic alkylations as a demonstration of their synthetic utility (**Scheme 26**). Yields of >95% and enantioselectivities up to 81% ee were reported for the Quinazox ligand in this Pd-catalysed reaction.

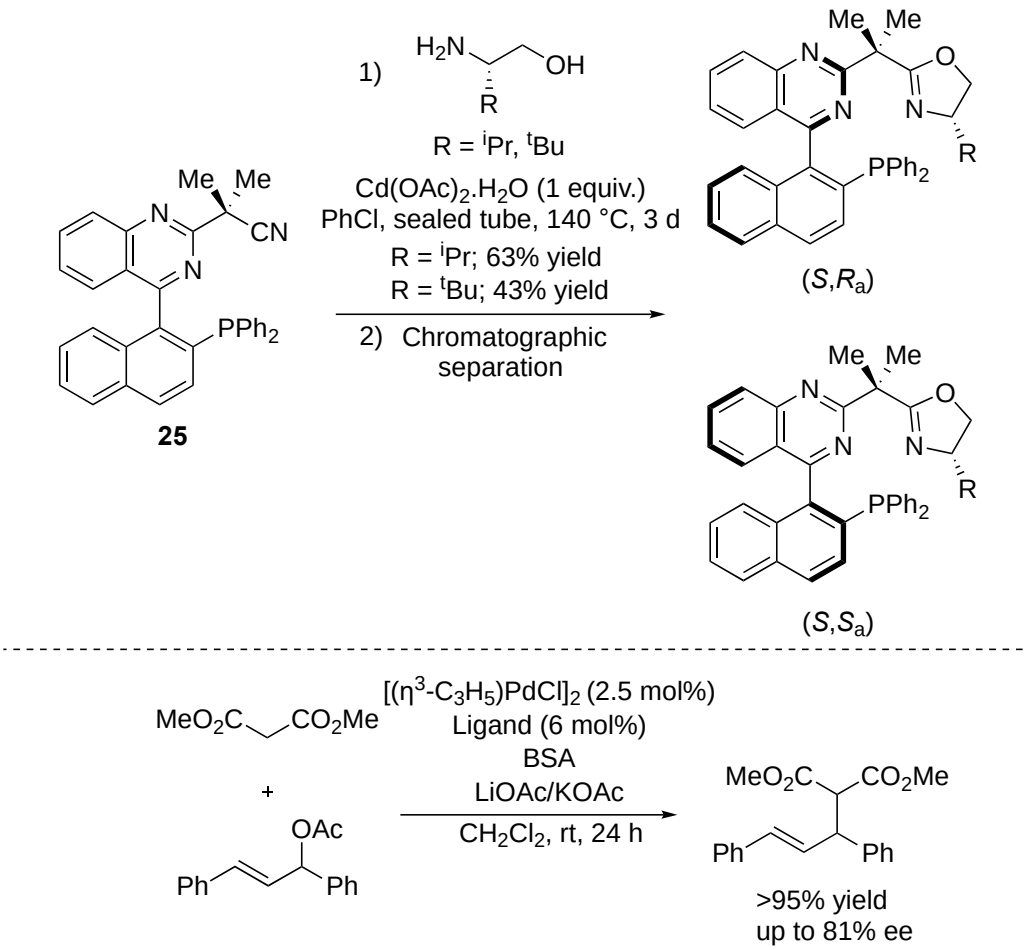

***Scheme 26**: Installation of oxazoline moiety to complete the synthesis of Quinazox ligands and its subsequent application in Pd-catalysed asymmetric allylic alkylation*

In 2017, Guiry reported the synthesis of the UCDPhim ligand (**Scheme 27**).[16] The ligand design exploited the strategy used previously in the literature where the ligand contained both central and axial chirality.[3] The ligand readily exists as diastereomers that can be separated by column chromatography or fractional crystallisation. The key design element of the ligand is the incorporation of a pendant electron-deficient pentafluorobenzyl group, which had previously been reported by Aponick in the synthesis of the related imidazole based ligand in 2013.[17] The pentafluorobenzyl group has been shown to π-π stack with the electron rich naphthalene core *via* X-ray analysis of the crystal structure, where such π-π stacking inhibits epimerisation of the compound about the chiral axis.

The first step of the synthesis involves the NBS-mediated cyclisation of 2-methoxy-1-naphthaldehyde and (1*S*,2*S*)-diphenylethylenediamine to furnish the corresponding imidazoline **26** in an 80% yield (**Scheme 27**). Deprotonation with sodium hydride and subsequent alkylation with pentafluorobenzyl bromide yielded the functionalised imidazoline **27** in a 1:1 diastereomeric ratio in a 76% yield. Demethylation with BBr_3 in heptane and functionalisation of the crude naphthol with triflic anhydride installed the triflate handle for the planned cross coupling in a 63% yield over two steps. A Ni-catalysed cross-coupling between triflate **28** and diphenylphosphine gave the target ligand in a 3:1 diastereomeric ratio after purification by column chromatography. The diastereomerically pure ligand was accessed *via* fractional crystallisation from diethyl ether. The ligand showed proficiency in A3 coupling reactions with yields and ees up to 99% reported.[16,18] The key limitation of this ligand is the epimerisation of the ligand about its chiral axis at temperatures above 40 °C, which excludes its application in asymmetric catalysis above room temperature, such as the protocol reported by Guiry in 2019 for the construction of quaternary stereocentres *via* Pd-catalysed decarboxylative propargylation.[19]

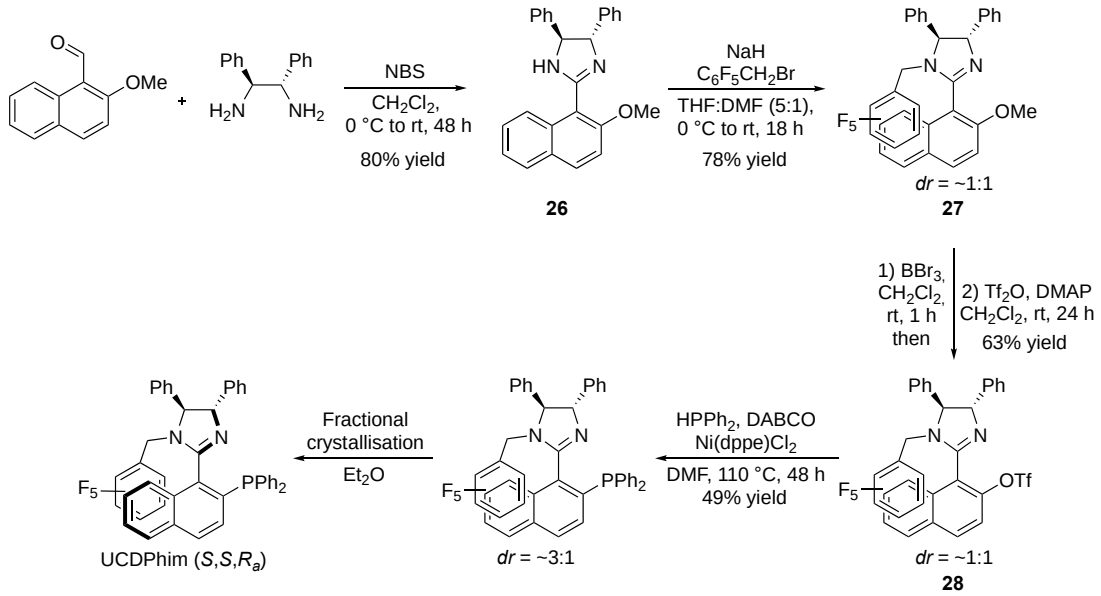

***Scheme 27**: Synthesis of UCDPhim reported by Guiry in 2017*[16]

More recently in 2021, the Jiang group reported the syntheses of two novel families of axially chiral P,N ligands.[20,21] The first report detailed the enantioselective construction of axially chiral quinoxaline-based heterobiaryls through the use of a chirality transfer strategy (**Scheme 28**). 2-Pyrrolylanilines were reacted with aryl aldehydes in the presence of a chiral phosphoric acid to furnish the corresponding the chiral precursors **29**. The desired quinoxaline-based heterobiaryls were readily accessed from the precursors of type **30** *via* CH-NH oxidation mediated by MnO_2 or *tert*-butyl hydroperoxide.

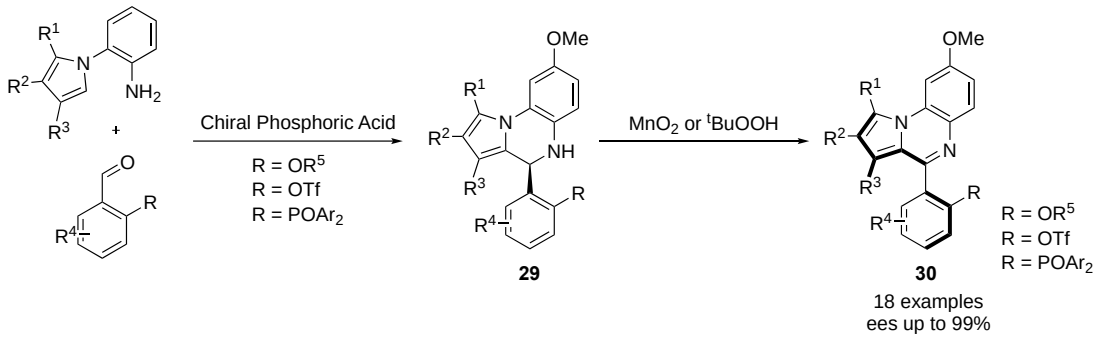

***Scheme 28**: Enantioselective of quinoxaline-based heterobiaryls via chirality transfer strategy*[20]

To demonstrate the utility of the ligands, *J*iang applied them in selected examples of transition-metal catalysis (**Scheme 29**). The Quinoxalinap ligand **31** was employed in an enantioselective Cu-catalysed addition of quinoline and phenylacetylene in order to benchmark the performance of the ligand compared to established P,N ligands. In dichloromethane, Quinoxalinap **31** formed the desired dihydroquinoline in a 65% yield and 88% ee. In direct comparison, StackPhos formed the same product in a 74% yield and 98% ee. Jiang also applied the Quinoxalinap ligands in Ag-catalysed [3+2] annulation reactions, with ees up to 90% being reported.[20]

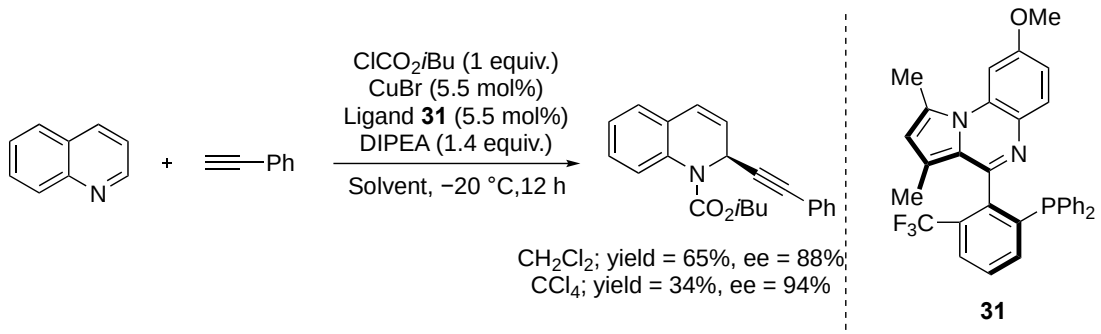

Scheme 29**: Enantioselective Cu-catalysed addition of quinoline and phenylacetylene using Quinoxalinap **31

Later in 2021, Jiang reported the enantioselective construction of axially chiral quinazolinones *via* chirality exchange or phase transfer catalysis (**Scheme 30**).[21] Substituted 2-amino-benzamides were reacted with aryl aldehydes in the presence of chiral phosphoric acid **32**, before oxidation with 2,3-dichloro-5,6-dicyano-1,4-benzoquinone (DDQ) to give the desired methoxyarylquinazolinones of type **33**. Twenty nine products were prepared using this methodology, in yields up to 91% and ees up to 94%. Unfortunately, the Pd-catalysed phosphorylation of compounds of type **33** proved unsuccessful due to the racemisation of the five-membered palladacycle intermediate at high temperatures.

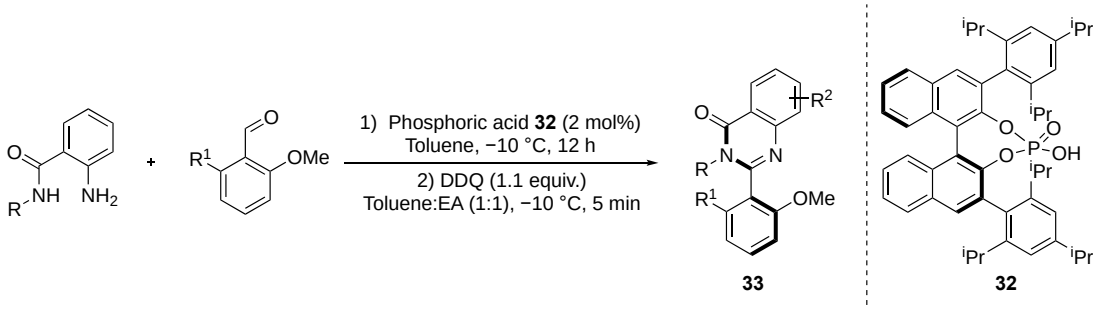

***Scheme 30**: Enantioselective construction of axially chiral quinazolinones via chirality transfer*[21]

In the same publication, Jiang described the successful protocol for accessing the desired Quinazolinonap ligands of type **34** (**Scheme 31**). The revised approached utilised substrates of type **35**, which contained the phosphorus moiety prior to establishing the chiral axis. The cinchona alkaloid-derived quaternary ammonium bromide **36** facilitated the chiral benzylation of **35**. The desired P,N ligands were then accessed *via* trichlorosilane-promoted reduction of the phosphine oxide. These two publications reported by Jiang presented new libraries of P,N ligands for application in asymmetric transition-metal catalysis.

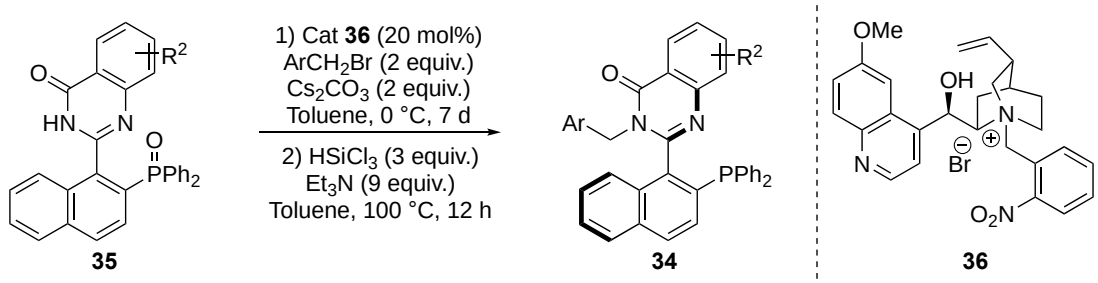

***Scheme 31**: Enantioselective construction of Quinazolinonaps via asymmetric phase-transfer catalysis*

The four successfully synthesised ligands were applied in the same enantioselective Cu-catalysed addition of quinoline and phenylacetylene (**Scheme 32**).[21] Moderate yields and enantioselectivities were reported for the ligands described. Further applications of these ligands developed by Jiang are currently underway at the time of writing this thesis.

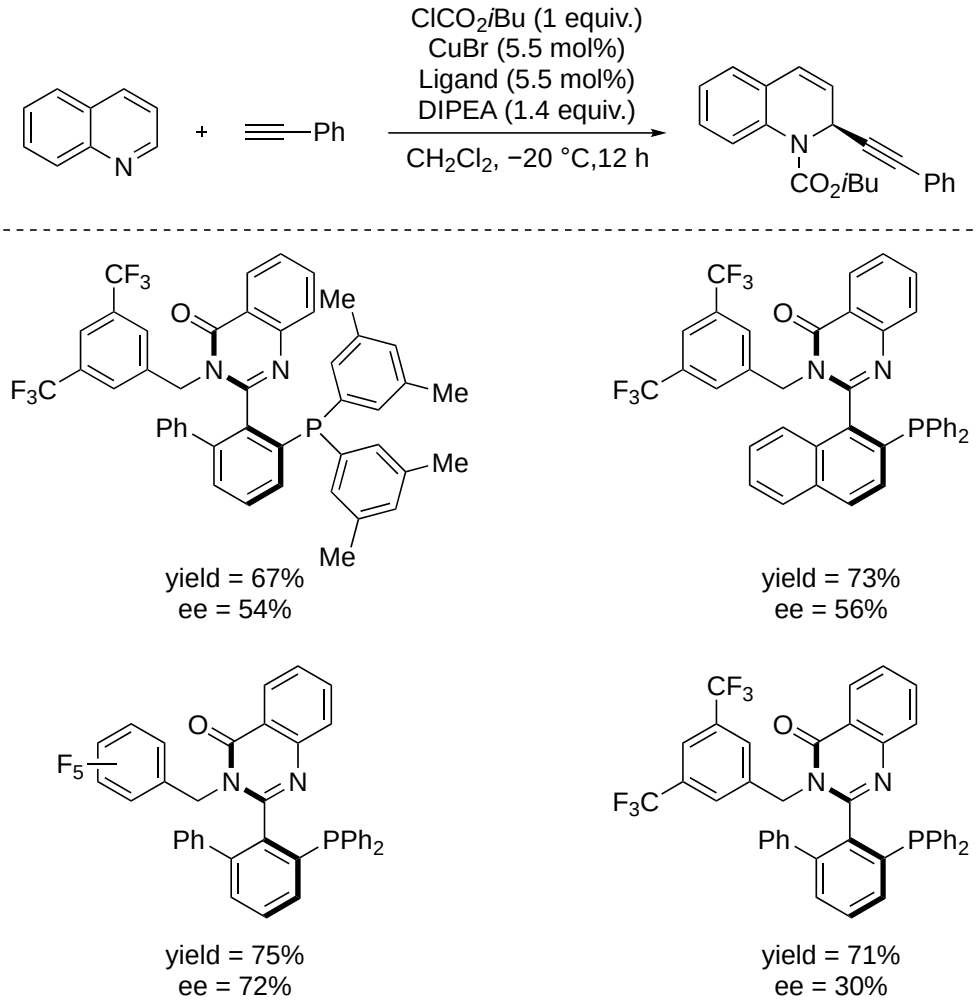

***Scheme 32**: Enantioselective Cu-catalysed addition of quinoline and phenylacetylene using novel Quinazolinonaps*

In 2021, Ma described the synthesis of the novel Pyrinap ligands **37** and **38**.[22] A Suzuki cross-coupling of 3,6-dichloro-4,5-dimethylpyridazine and the corresponding boronate yielded the product biaryl compound **39** in a 58% yield. The subsequent amination with (*R*)-1-phenylethylamine and biaryl **39** formed the desired product **40** in a 83% yield. Deprotection and triflation furnished the desired cross-coupling precursor **41** in a 90% yield. A Ni-catalysed C-P bond formation successfully installed the diphenylphoshine moiety, before separation of the epimers by column chromatography on silica gel in the yields given in **Scheme 33**. The ligands were applied in asymmetric A3 coupling reactions, with the naphthyl-substituted ligand proving to offer the best enantioselectivities in their substrate scope.

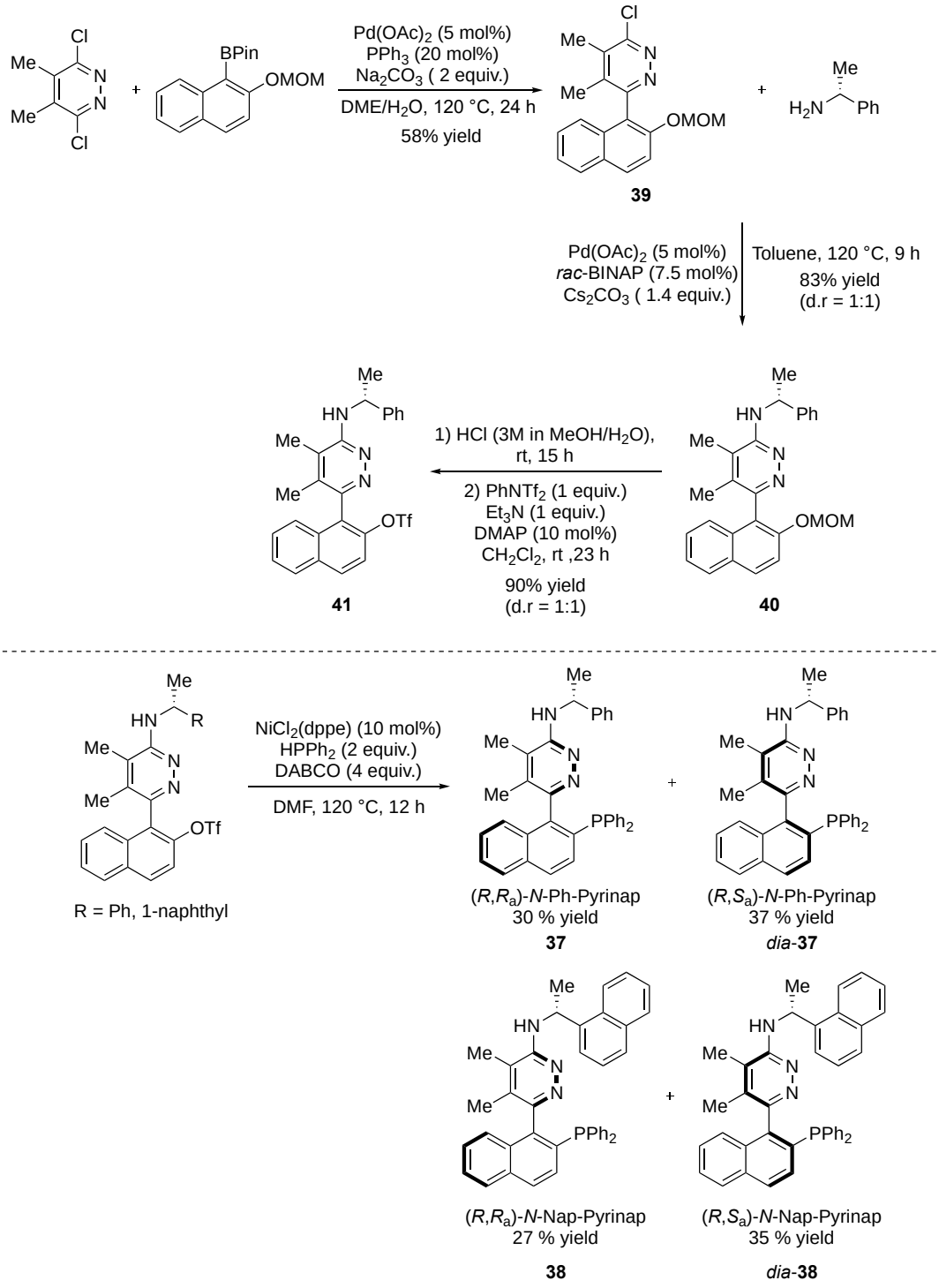

***Scheme 33**: Synthesis of Pyrinap ligands reported by Ma in 2021*[22]

Project Aim

The aim of this research project was synthesise the existing UCDPhim ligand (**Figure 11**), reported by Guiry in 2017, and to apply it in novel asymmetric transformations to further our understanding of its utility in asymmetric transformations.[16]

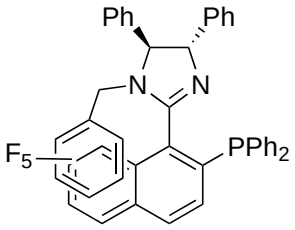

***Figure 11**: UCDPhim ligand reported by Guiry in 2017*

Further to this, there was an aim to devise a route towards synthesising novel imidazoline-based axially-chiral P,N ligands of type **42** and type **43** (**Scheme 17**). The effect of varying the centrally chiral R^1 group on asymmetric induction and the effect of R^2 on the barrier to rotation about the chiral axis of the proposed ligands was to be investigated. The UCDPhim epimerises about its chiral axis at 40 °C, which excludes it use in asymmetric catalysis above room temperature. The proposed ligands of type **43** were hoped to have a more stable chiral axis, which would expand the catalysis that these imidazoline-based axially chiral P,N ligands could be applied to.

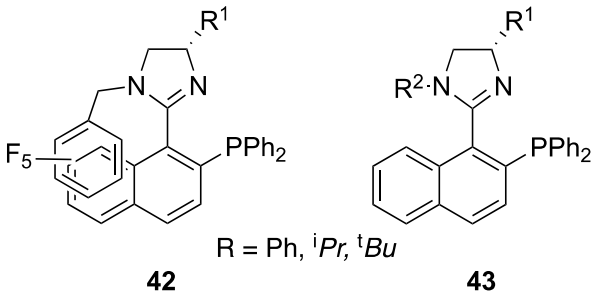

***Scheme 34**: Novel imidazoline-based P,N ligands*

Results and Discussion

UCDPhim Synthesis

2-Methoxy-1-naphthlaldehyde Route Towards UCDPhim

The present study began with the replication of the UCDPhim synthesis reported by Guiry in 2017 (**Scheme 36**).[16] The first step of this synthesis was the condensation reaction of 2-methoxy-1-naphthaldehyde and (1*S*, 2*S*)-(–)-1,2,-diphenylethylenediamine, which forms an aminal intermediate. This aminal is subsequently oxidised *via* the addition of NBS to furnish the imidazoline **26**, which was isolated in an 37% yield. A characteristic singlet peak at δ 4.92 ppm in the ^{1}H NMR spectrum for the two benzylic imidazoline protons showed the formation of the imidazoline ring. A notable side product **44** was formed in the reaction, which was isolated. It was suspected that **44** was formed through the oxidation of unreacted diamine by NBS. Impurity **44** was isolated in a 27% yield when the diamine was reacted with NBS in a test reaction during this current research project (**Scheme 35**).

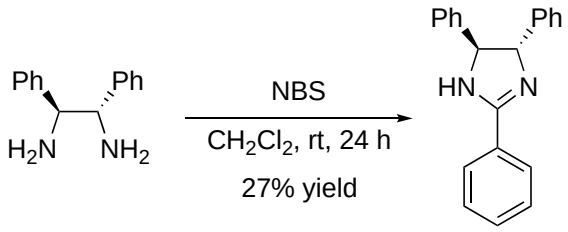

44

***Scheme 35**: Side-product formation via NBS-mediated oxidation of diphenylethylenediamine*

It is worth noting that the quality of NBS is of utmost importance, due to its propensity to degrade to succinimide in the presence of light. NBS was freshly recrystallised from water for each reaction and was stored under high vacuum for 24 h prior to use. This helped to lower the presence of residual water from the recrystallisation step, which readily hydrolyses the aminal intermediate back to the starting aldehyde and diamine.

Numerous repetitions (~15) of the reaction have been conducted, with similar yields obtained in each case. Analysis of the reaction mixture by TLC prior to NBS addition showed the presence of unreacted aldehyde after 24 h in each case. Extension of the time for 48 h before addition of NBS did not lead to complete consumption of the aldehyde starting material.

Treatment of imidazoline **26** with sodium hydride before dropwise addition of a pentafluorobenzyl bromide solution in THF furnished the functionalised imidazoline **27** in a 61% yield. Characteristic fluorine peaks at δ -141.6 ppm, δ -142.5 ppm, δ -155.7 ppm, δ -156.0 ppm, δ -162.9 ppm and δ -163.3 ppm showed that the atropdiastereomeric mixture of pentfluorobenzylated compound had been formed in an approximation 1:1 diastereomeric ratio. TLC analysis of the reaction mixture in each case showed the presence of the starting material and a di-benzylated imidazoline side product. The full consumption of imidazoline **26** was not observed through extension of the reaction time to 48 h.

A bromine tribromide-mediated demethylation of the aryl methoxy group in **27** afforded an intermediate naphthol. Management of the pH of the aqueous phase (pH ~7) proved crucial in order to maximise yields in this step, as the naphthol hydroxy group was required in the neutral state in order to ensure it would preferentially enter the organic phase upon extraction with dichloromethane during the aqueous work up. The crude ^{1}H NMR spectrum of the naphthol was quite messy and previous work in the group towards its isolation proved challenging. As such, the crude naphthol was telescoped to the next step.

Treatment of the crude naphthol with trifluoromethanesulfonic anhydride and DMAP gave the triflate functionalised imidazoline **28**, which was isolated in a 67% yield across two steps. Two new peaks in the ^{19}F NMR spectrum at δ -73.7 and δ -73.8 ppm were consistent for the aryl triflate group in the diastereomeric mixture of the reported compound in an approximate 1:1 diastereomeric ratio.

The final step of the synthesis was installation of the diphenylphosphine group. A Ni-catalysed cross coupling was used,[23] *via* the triflate handle on the naphthalene ring. The coupling proceeded well, with the mixture of UCDPhim atropdiastereomers isolated in a 59% yield in an approximate 3:1 diastereomeric ratio. Successful phosphinylation was identified by the presence of the two new peaks in the ^{31}P NMR spectrum at δ -11.6 ppm δ -12.2 ppm, again consistent with reported chemical shifts for the UCDPhim ligand.

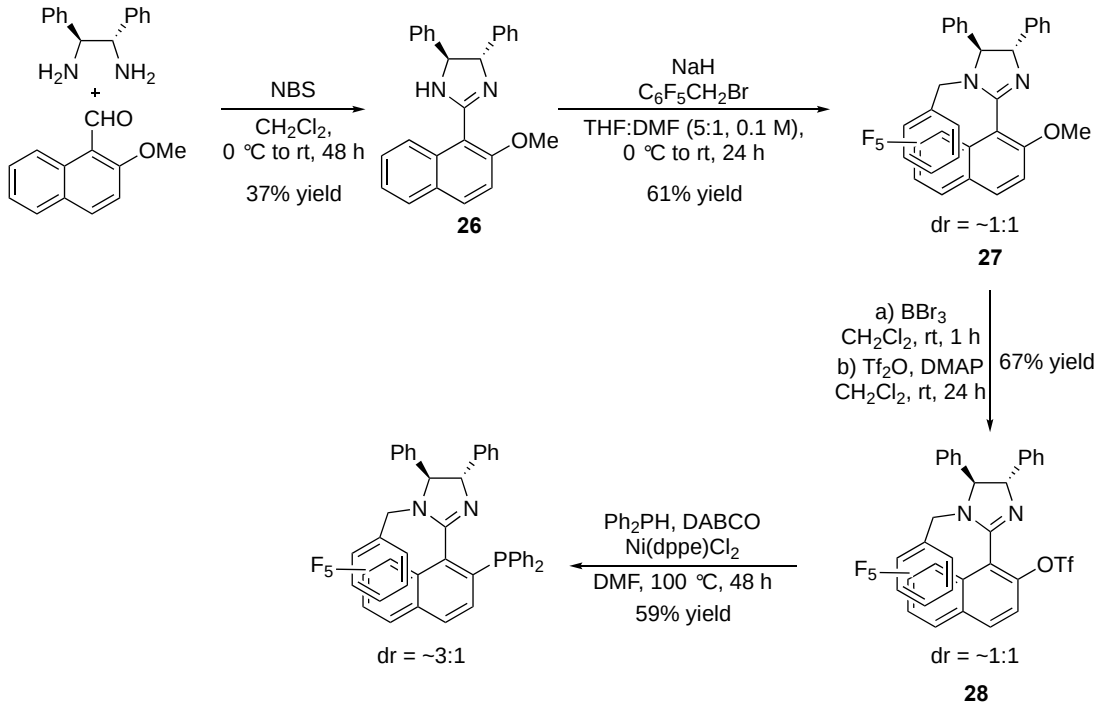

***Scheme 36**: Replication of reported UCDPhim route in this current study*

In the original report by Guiry in 2017,[16] the mixture of atropdiastereomeric ligands was purified *via* fractional crystallisation (**Scheme 37**). Attempts towards isolation of the pure atropdiastereomers by column chromatography proved unsuccessful at that time. Fractional crystallisation of the mixture of atropdiastereomers resulted in the isolation of the optically pure (*S*,*S*,R_a) atropdiastereomer as a white solid, where the absolute stereochemical configuration was confirmed by X-ray analysis. Isolation of pure (*S*,*S*,S_a) epimer of UCDPhim from the mother liquor was not possible as the mother liquor contained epimers in a 3:1 ratio.

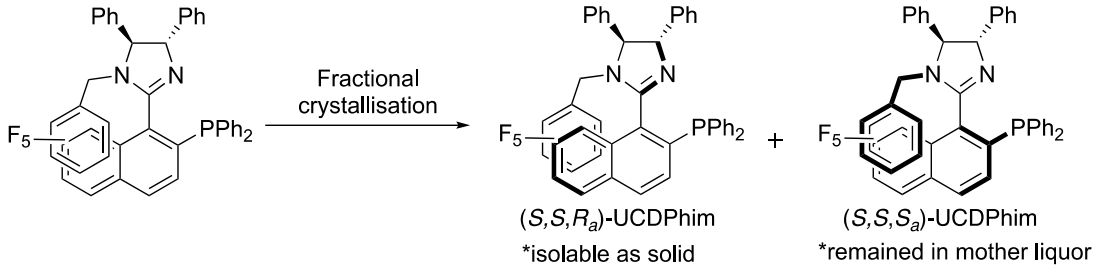

***Scheme 37**: Previously reported method for accessing UCDPhim (S,S,R$_a$)*[16]

In the current study, the mixture of atropdiastereomers were subjected to a variety column conditions, before finding suitable conditions for their separation (**Scheme 38**). A CH_2Cl_2/Et_2O system with a very gradual increase in Et_2O from 2 to 5% on a 14 cm silica gel column allowed for the isolation of both atropdiastereomers of the UCDPhim ligand. Despite a significant difference in R_f values (0.5 and 0.3 in 5% Et_2O/CH_2Cl_2) between the two atropdiastereomers, an appreciable amount of co-elution/epimerisation was observed. This was reflected in the difference between the yield of the phosphinylation step and corresponding isolated yields of the two atropdiastereomers of UCDPhim (**Scheme 38**). Decreasing the column length, in order to minimise band broadening on separation, led to more co-elution.

Isolation *via* column chromatography removes the possibility of product loss to the mother liquor compared to when fractional crystallisation is employed as a method of isolation. However, co-elution of both atropdiastereomers during column chromatography is also an issue when it is employed as the method for accessing optically pure ligand.

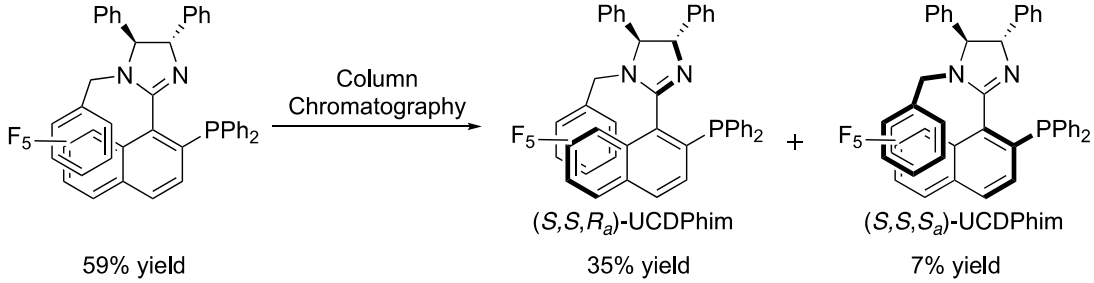

***Scheme 38**: Successful isolation of UCDPhim (S,S,S$_a$) in the current study*

The ^{1}H NMR spectra of the two UCDPhim atropdiastereomers in **Figure 12** and **Figure 13** show that the chemical shifts of some protons in the aromatic region of the ^{1}H NMR spectra are quite different, and may be caused by the lack of π-stacking in the minor atropdiastereomer. Evidence of π-stacking in the major diastereomer was found *via* X-ray analysis in the original publication by Guiry in 2017. Attempts towards growing a crystal of the minor atropdiastereomer (*S*,*S*,*S*$_a$) for X-ray analysis were unsuccessful, including attempts at 0 °C.

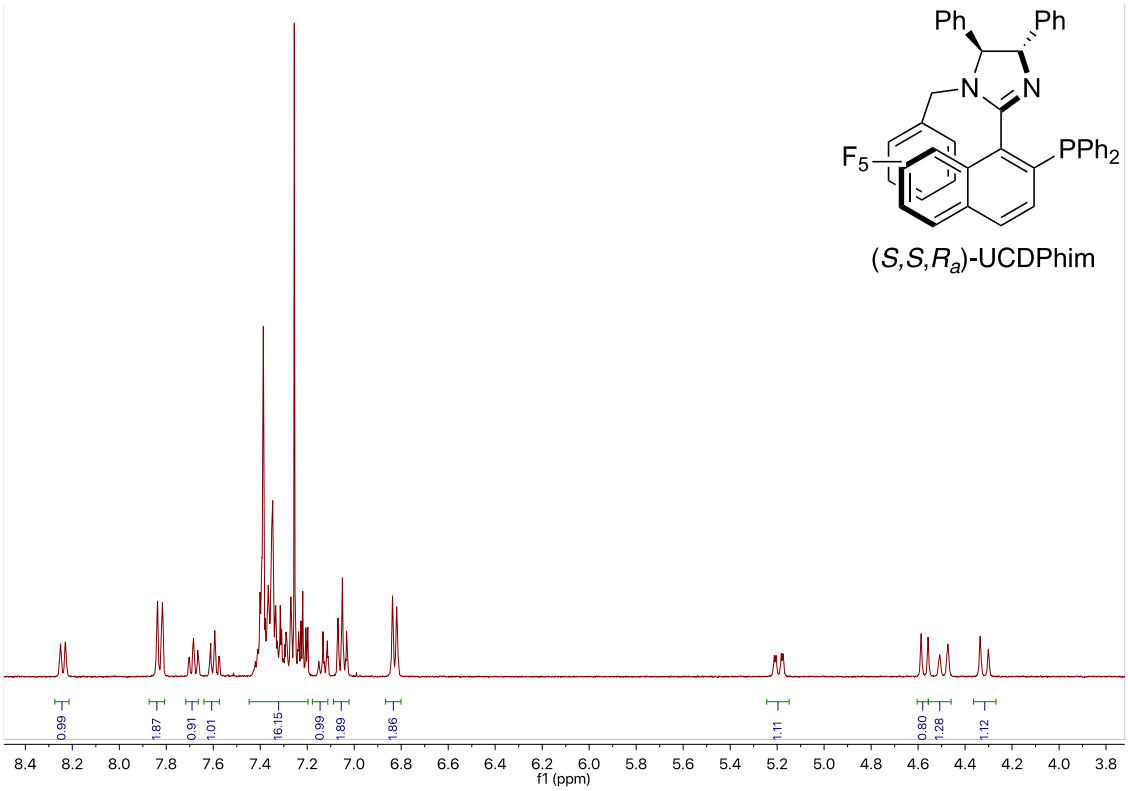

***Figure 12**: [1]H NMR of the major UCDPhim atropdiastereomer (S,S,R_a)*

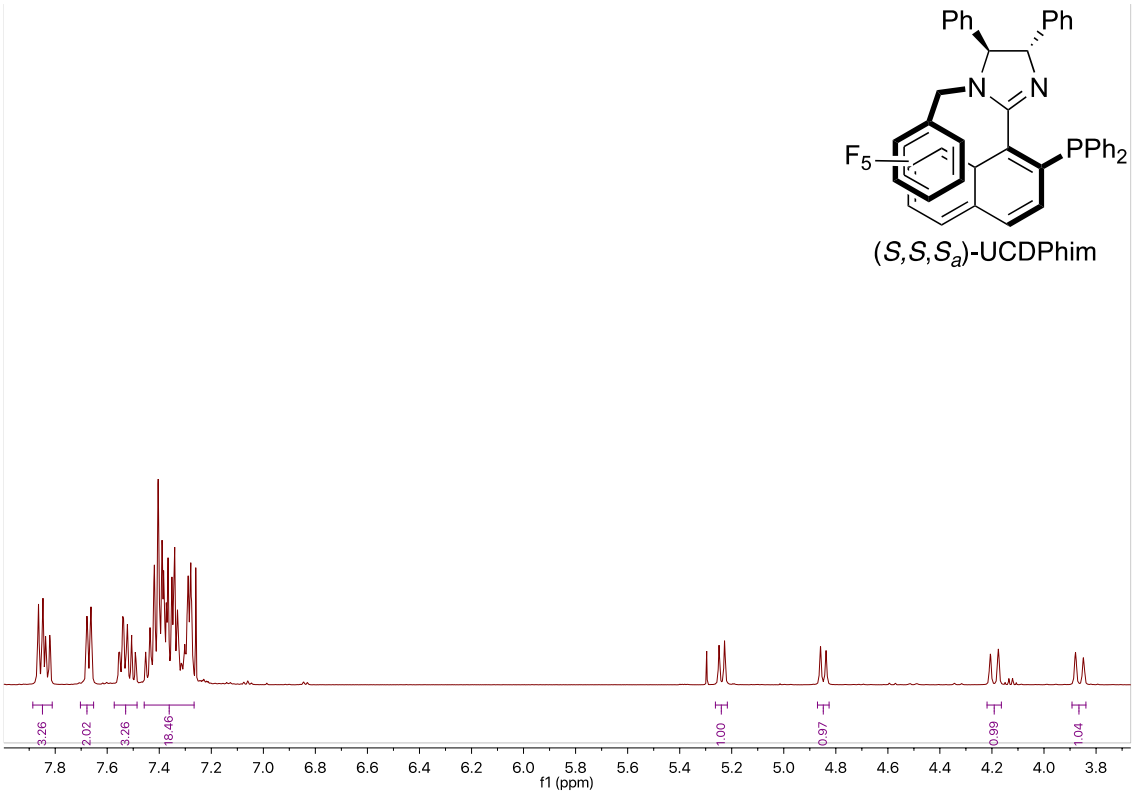

***Figure 13**: [1]H NMR of the minor atropdiastereomer of UCDPhim (S,S,S_a)*

A consistent issue arose during the synthesis of UCDPhim, which occurred while attempting to install the pentafluorobenzyl moiety to form imidazoline **26**, thus limited its access (**Scheme 39**). The sodium hydride-mediated deprotonation facilitated the installation of the pentafluorobenzyl group on the non co-ordinating nitrogen as expected, but unfortunately the imidazoline would then attack a second equivalent of pentafluorobenzyl bromide at the co-ordinating nitrogen to furnish **45**. The difficulty in isolating a pure sample of the di-benzylated product prevented the accurate reporting of a yield for this side reaction.

Despite making a dilute solution of pentafluorobenzyl bromide in THF and adding it dropwise over 30 minutes, the issue of dibenzylated persisted. Later work involving analogues lacking the aryl methoxy group showed no problems with dibenzylation 51and suggested that the aryl methoxy group may act as a directing group towards benzylation at the co-ordinating nitrogen of the imidazoline ring. A ^{19}F NMR spectrum of the dibenzylated salt, **Figure 14**, shows the presence of ten fluorine atoms (and is consistent with the fully characterised compound previously reported within our group). The three small peaks in the ^{19}F NMR spectrum in **Figure 14** correspond to the literature chemical shifts of the mono-benzylated product of starting material **26**.[16]

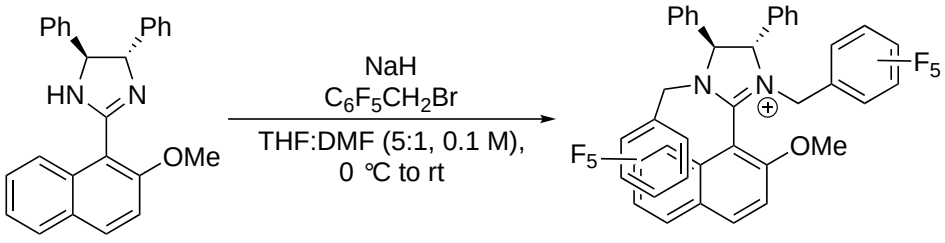

26 **45**

***Scheme 39**: Dibenzylation of imidazoline **26** during the synthesis of UCDPhim*

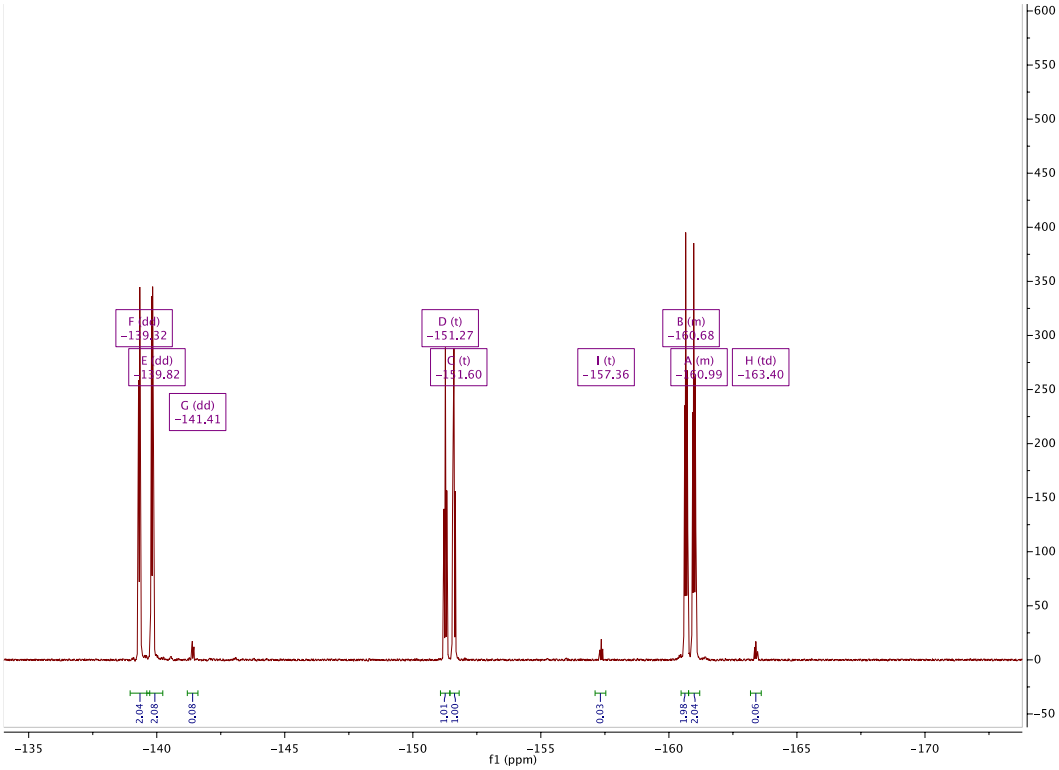

Figure 14**: [19]F NMR spectrum of the 52ebenzylatio salt **45

The de-benzylation of the quaternary ammonium centre was attempted using a protocol reported by Wakisaka (**Scheme 41**),[24] who used thiophenol for this transformation. It is proposed that thiophenol would attack the benzylic CH_2 group to form the corresponding thioether and tertiary amine. Unfortunately, this methodology did not furnish the desired de-benzylated tertiary amine and further procedures for this transformation were not investigated.

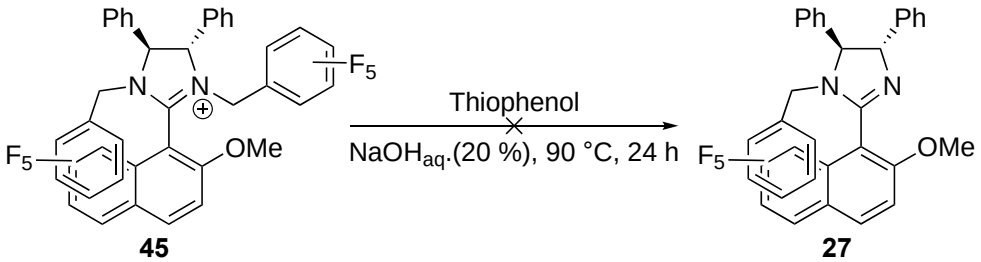

45 **27**

***Scheme 40**: Attempted de-benzylation of quaternary ammonium salt **45** with thiophenol*

β-Tetralone Route Towards UCDPhim

Inconsistencies in accessing UCDPhim through the 2-methoxy-1-naphthaldehyde route caused by the issue of 53dibenzylation of imidazoline **26** led to the use of another approach for accessing UCDPhim (**Scheme 41**). This approach was devised by a past group member, Dr. Alex Doran, and provided an alternative route in the present study for accessing the UCDPhim ligand.

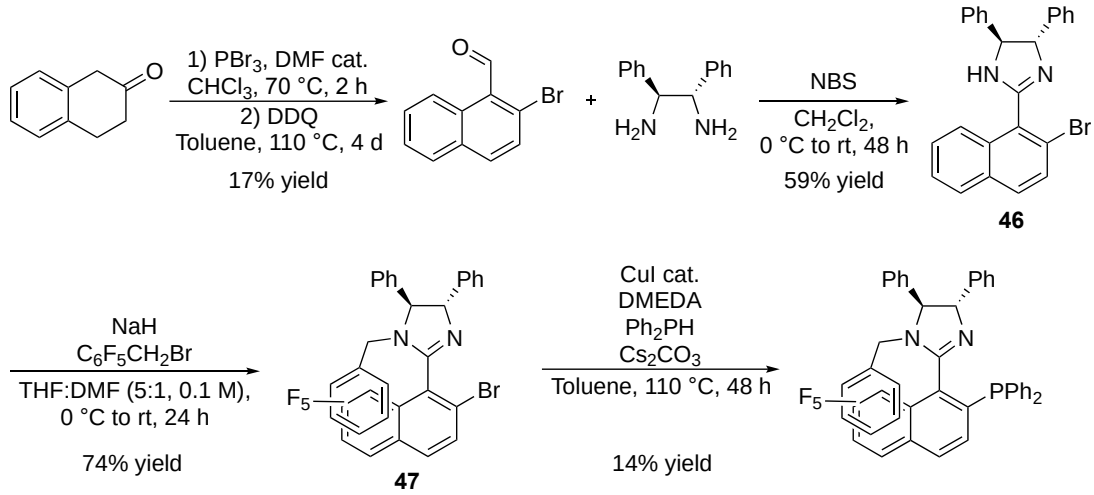

***Scheme 41**: β-tetralone route for accessing UCDPhim conducted in this present study*

Commercially available β-tetralone (25 g, €191; sigma Aldrich) provides the starting point for the route. A Vilsmeier-Haack type formylation-bromination of β-tetralone,[25] followed by a DDQ (2,3-dichloro-5,6-dicyano-1,4-benzoquinone)-mediated oxidation, furnished 2-bromo-1-naphthaldehyde in a 17% yield. A characteristic singlet at δ 10.8 ppm in the ^{1}H NMR spectrum was diagnostic for the aldehyde functional group and was consistent with the literature for the known compound.[26]

In the present study it was not possible to replicate the higher yielding results obtained previously in the group. The yields reported in **Scheme 24** were the best yields reproduced by my hands in the present study. An impurity inseparable (highlighted by the black arrows in the NMR spectrum below) by column chromatography was also present, which did not match any reagent used in the reaction or the other possible regioisomer of 2-bromo-1-naphthaldehyde (3-bromo-2-naphthaldehyde), which is also known in the literature (**Figure 15**).[27]

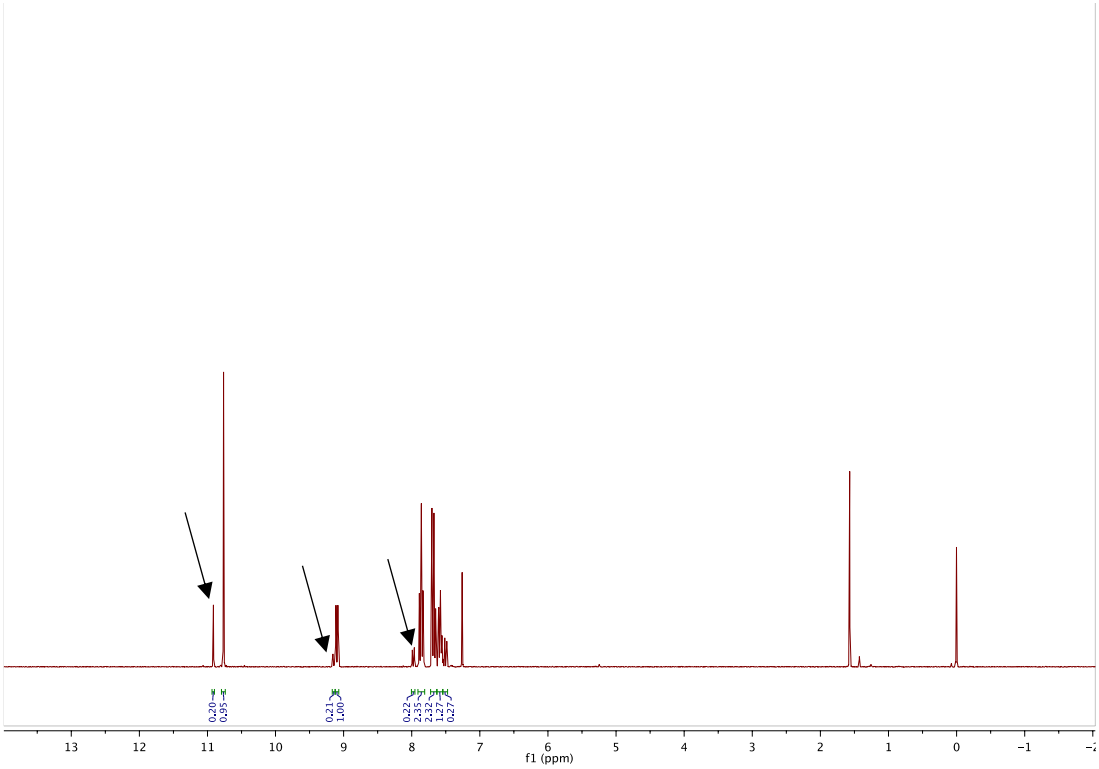

***Figure 15**: Inseparable impurity in 2-bromo-1-naphthaldehyde synthesis from β-tetralone*

The condensation between 2-bromo-1-naphthaldehyde and (1*S*, 2*S*)-(–)-1,2,-diphenylethylenediamine and oxidation by NBS proceeded well with an isolated yield of 59% achieved (compared to 37% *via* the 2-methoxy-1-naphthaldehyde route; **Scheme 37**). As with the previous imidazoline **26** (**Scheme 36**), the formation of imidazoline **46** (**Scheme 41**) was confirmed by the presence of the two benzylic imidazoline protons which appeared at δ 5.02 ppm in the ^{1}H NMR spectrum.

The pentafluorobenzylation of imidazoline **46** proceeded smoothly, with an isolated yield of 79% (compared to 61% as a one-off result from multiple repetitions *via* the 2-methoxy-1-naphthaldehyde route; **Scheme 37**). No dibenzylation occurred with the 2-bromo analogue in this route, when using identical reaction conditions to the 2-methoxy analogue. The formation of the imidazoline **47** was confirmed by comparison with the fully characterised data for **47** within the Guiry group.

The final step towards accessing UCDPhim *via* the route described in **Scheme 41** was the Cu-catalysed phosphinylation of aryl-bromide **47**. These conditions were reported by Buchwald in 2003 and were successfully able to convert aryl bromide **47** to the target ligand.[28] However, the yield for the C-P bond forming step was a disappointing 14%. This was in spite of careful exclusion of water from the reaction mixture through the use of flame-dried glassware, anhydrous and degassed toluene and oven-dried caesium carbonate. The presence of the two peaks in the ^{31}P NMR spectrum was due to the atropdiastereomeric nature of the product and was consistent with the reported data.[16]

Towards Accessing New Chiral Ligands With Variation in the Imidazoline Backbone

Diamine Condensations

The main goal of this research project was to synthesise novel axially chiral P,N imidazoline-based ligands of type **42** (**Scheme 42**). The obvious starting point to achieve this goal would be to use the appropriate chiral diamine using the established methodology in the group in order to vary the centrally chiral element on the imidazoline backbone.

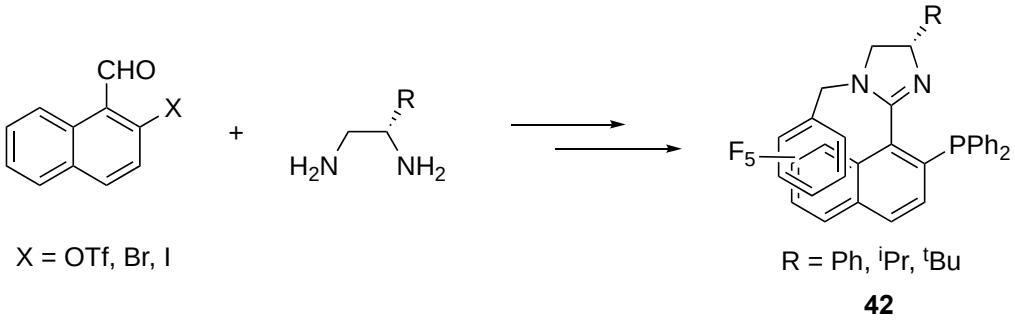

Scheme 42**: Proposed route via chiral diamines towards novel Phim ligands of type **42

The *tert*-butyl substituted chiral diamine was previously synthesised in the group by Dr. Rokade from L-*tert*-leucine, where the corresponding methyl ester was synthesised (**Scheme 43**).[29] The methyl ester of L-*tert*-leucine was stirred with ammonium hydroxide to furnish the corresponding amide, which was then reduced to the diamine using lithium aluminium hydride.[30,31] At this point I would like to thank Dr. Rokade for the use of his diamine material for these test reactions.

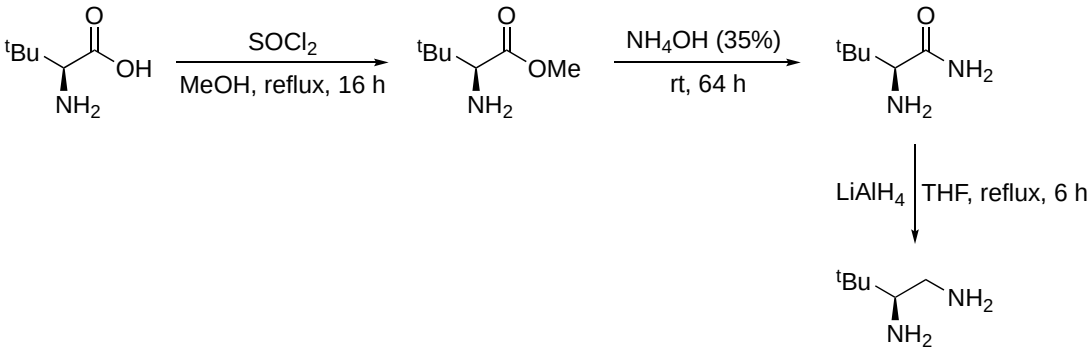

***Scheme 43**: Synthesis of L-tert-leucine-derived diamine*

Test reactions between (*S*,*S*)-3,3-dimethylbutane-1,2-diamine **48** and 2-bromo-naphthaldehyde were conducted (**Scheme 44**), in order to test the viability of the established diamine route towards accessing imidazolines with variation at the backbone. Chiral diamine **48** is an amorphous wax that has very poor solubility in most solvents, including CH_2Cl_2 and MeOH. The conditions used in the synthesis of UCDPhim were unsuccessful when diamine **48** was used to prepare imidazoline **49**. DMF was found to partially solubilise diamine **48** and was used as a method of adding it to the reaction, but it did not help form **49**. The use of additives (4Å MS and $MgSO_4$) to sequester water to aid condensation did not lead to product formation. Increased reaction temperatures and irradiation in the microwave for 3 h at 60 °C before oxidation with NBS for 48 h did not form the desired product. Crude NMR spectra and TLC analysis showed the majority of the reaction mixture consisted of the aldehyde starting material.

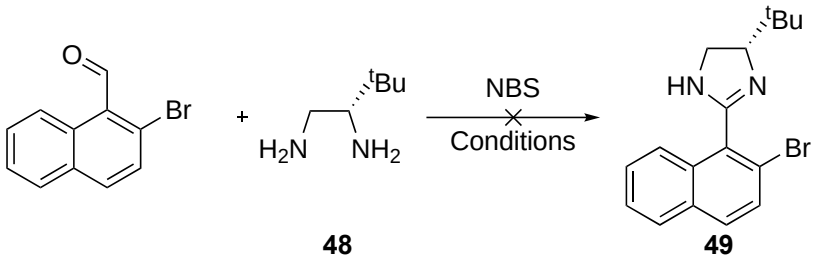

48 **49**

Scheme 44**: Attempted condensation of aliphatic diamine **48** and aldehyde **49

The over-alkylation problem found in the 2-methoxynaphthaldehyde route (**Scheme 39**) and the low yielding formation of 2-bromonaphthaldehyde from the expensive commercially available β-tetralone (**Scheme 41**), prompted an investigation towards another suitable starting material. Work previously conducted in the group by Dr. Alex Doran showed that the 2-iodonaphthalene-derived compound **50,** accessed *via* an aromatic Finkelstein reaction (**Scheme 45**), was superior in the final phosphinylation reaction. Particularly, the iodine handle in **50** was required in order to cross couple other phosphorus-containing moieties such as dicyclohexylphosphine. It was concluded that future in the work in this area in the group would be best served by using the iodine handle for cross coupling. Dr. Doran also used 2-iodo-1-naphthaldehyde to synthesise imidazoline **50** (**Scheme 45**), which

was useful as the NMR spectroscopic data and other characterisation data was available.

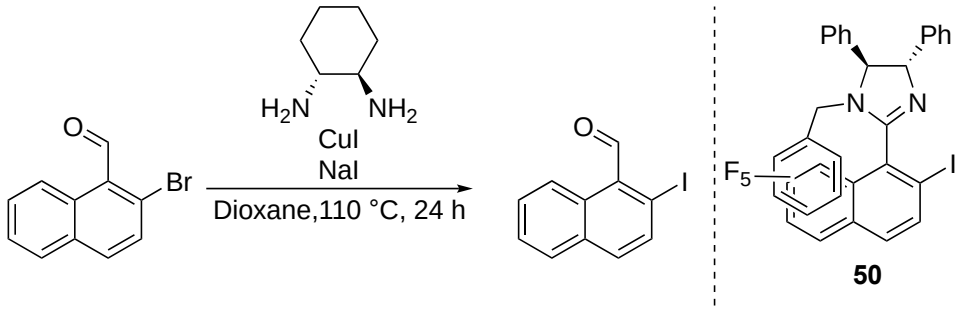

***Scheme 45**: Previous group work on the aromatic Finkelstein of 2-bromo-1-naphthaldehyde*

Pd-catalysed C-H Activation of Imidazoline Scaffold

An investigation into the possibility of a Pd-catalysed C-H activation system for substrate **51** was undertaken for the installation of an iodine handle for the subsequent phosphine cross-coupling (**Scheme 46**). The advantage of this reaction would be that the starting material for the synthesis would be the readily available and commercially cheap 1-naphthaldehyde.

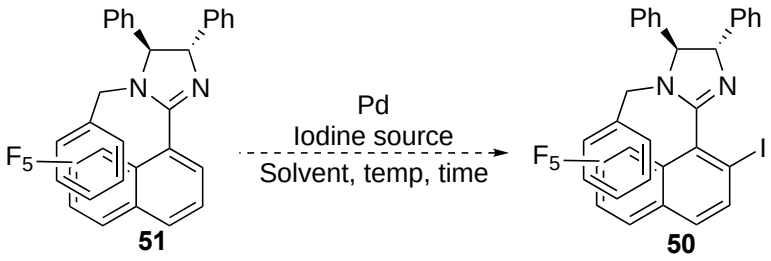

Scheme 46**: Proposed Pd catalysed C-H activation iodination of imidazoline **51

Therefore, the first step was the synthesis of the required imidazoline substrate **51** (**Scheme 47**). The condensation between (1*S*,2*S*)-(–)-1,2,-diphenylethylenediamine and 1-naphthaldehyde, followed by oxidation by NBS, proceeded moderately well with an isolated yield of 39%.

The pentafluorobenzylation of imidazoline **52** (**Scheme 47**) occurred without any over-alkylation and in similar yields to the brominated imidazoline **46** (**Scheme 41**). This observation was consistent with the hypothesis that the 2-methoxy group in compound **26** (**Scheme 39**) is a contributing factor towards its over-alkylation.

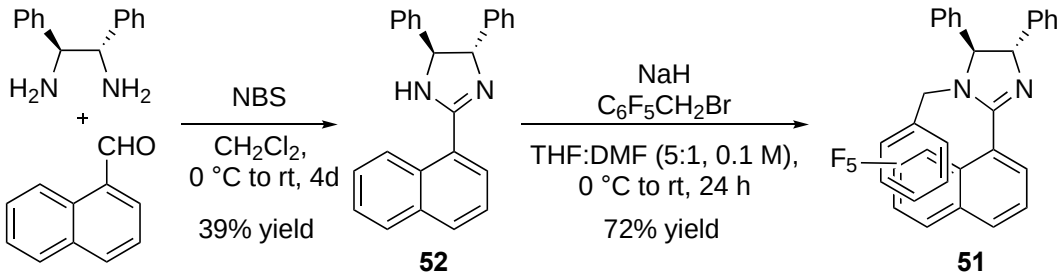

***Scheme 47**: Synthesis of imidazoline **51** as a test substrate for Pd catalysed C-H activation*

With the imidazoline **51** (**Scheme 48**) in hand, a selection of Pd-catalysed C-H activated iodination protocols were screened. The results of these reactions are summarised below. The crude ^{1}H NMR spectra could be directly compared with the verified ^{1}H NMR data of **50**, which had been previously synthesised in the group as per **Scheme 45**. A diagnostically useful doublet in the ^{1}H NMR spectrum at 8.12 ppm for iodinated imidazoline **50** was used as a means of analysing the reaction in conjunction with TLC of the authentic sample (previously synthesised by Dr. Alex Doran).

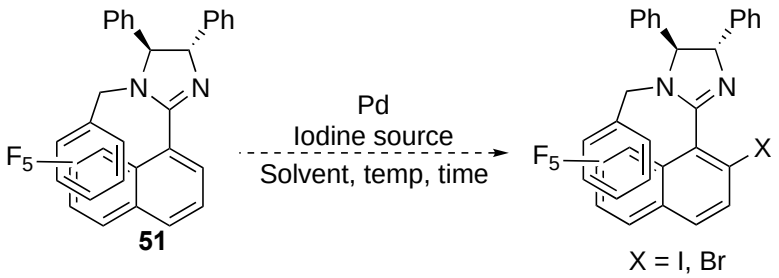

***Scheme 48**: Pd-catalysed C-H halogenation test reaction*

Entry	Pd Source (10-20 mol%)	Halogen Source	Solvent	Temp[a]	Time	Additive	Result
1	**$Pd(OAc)_2$**	**NIS**	**MeCN**	**100 °C**	**4 d**	**-**	**Mess**
2	**$Pd(OAc)_2$**	**I_2**	**MeCN**	**100 °C**	**4 d**	**PIDA**	**S.M only**
3	**$Pd(OAc)_2$**	**NBS**	**MeCN**	**100 °C**	**4 d**	**-**	**Mess**
4	**$Pd(OAc)_2$**	**NIS**	**MeCN**	**130 °C, microwave**	**1 h**	**-**	**S.M only**
5	**$Pd(OAc)_2$**	**NIS**	**DCE**	**100 °C**	**24 h**	***p*TSA**	**S.M only**
6	**$Pd(OAc)_2$**	**NIS**	**DMF**	**120 °C**	**24 h**	**-**	**S.M only**
7	**$Pd(OAc)_2$**	**NIS**	**DMSO**	**120 °C**	**24 h**	**-**	**S.M only**
8	**$PdCl_2$**	**NIS**	**Acetic acid**	**100 °C**	**3 d**	**PPh_3**	**S.M only**
9	**$Pd(OAc)_2$**	**NIS**	**Toluene**	**110 °C**	**3 d**	**PivOH**	**S.M only**
10	**$Pd(OAc)_2$**	**NIS**	**DCE**	**90 °C**	**24 h**	**$Ag(CF_3CO_2)$**	**S.M only**
11	**$Pd(OAc)_2$**	**NIS**	**DCE**	**110 °C**	**24 h**	**$Ag(CF_3CO_2)$**	**S.M only**

***Table 1**: Screen of Pd-catalysed C-H halogenation reaction conditions; [a]conditions are thermal in Schlenk flask unless otherwise stated.*

Entries 1 and **2** were the most prevalent conditions in the literature for Pd-catalysed C-H activation iodination reactions.[32.33,34] Unfortunately, none of the conditions yielded the target compound in the present study.

An increase in reaction temperature to 130 °C and the use of NBS (**entry 3**) did not furnish the corresponding bromo analogue of **50**. This protocol was inspired through a similar system reported by Sanford**.**[32]

The use of a microwave for heating the reaction (**entry 4**) also had no positive effect on the formation of the desired product **50**, with only starting material being present on analysis by ^{1}H NMR spectroscopy.

A solvent change to dichloroethane and the use of an acid additive (*p*-toluenesulfonic acid) as reported by Dabiri did not lead to the formation of product (**entry 5**).[35] The Dabiri group found success in this system for the iodination of benzoxazinones and quinazolinones, and noted that acid additives can help stabilise the Pd^{II}/Pd^{IV} cycle. Similar methods for Pd-catalysed C-H halogenation reactions in DCE with *p*-TSA are known in the literature.[33,36] Unfortunately, the protocol was incompatible with substrate **51**.

Entries 6 and **7** focussed on the changing of solvent, analogous to the Pd-catalysed C-H halogenation protocol reported by Fürstner.[37] However, in this system only the starting material **51** was present in the crude ^{1}H NMR spectrum.

The literature is dominated by examples of $Pd(OAc)_2$ as the palladium catalyst of choice for these transformations. Despite this clear preference for this catalyst choice, Peng reported a system that successfully employed $PdCl_2$ as a catalyst, where they used triphenylphosphine as an additive.[38] This change of catalyst had no positive influence on the formation of the desired product **50** (**entry 8**). The protocol also used acetic acid as the solvent, based on the literature precedent that Brønsted acids can stabilise the Pd^{II}/Pd^{IV} cycle.[38] However, no iodinated product was observed under these reaction conditions.

Entry **9** was a set of conditions reported for the *ortho*-halogenation of 2-substituted 1,2,3-triazoles.[39] These conditions closely mimicked the model substrate, with a five-membered nitrogen ring directing halogenation to the 2-position of the ad*J*acent phenyl ring. This reaction was unsuccessful and did not yield the target compound.

The final entry (**entry 10**) used silver trifluoroacetate as an additive, a known additive for Pd-catalysed C-H functionalisations, [40] whose role is unclear (but is thought to aid in C-H bond cleavage).[41] This presence of silver trifluoroacetate did not aid formation of the desired product **50**.

Although certain acid additives and Pd sources led to increase yields in the substrates of the cited literature above, most systems would yield at least some of the desired halogenated product throughout the optimisation process. The lack of product formation for **50** in any of the attempted protocols led to further investigations being halted.

The conditions from entry **5** (**Table 1**) were also applied to imidazoline **52** to probe whether the iodinated imidazoline **53** would be formed (**Scheme 49**).[35] It was hoped that lack of the pentafluorobenzyl group would aid the transformation as it increases the electron density at the nitrogen atom directing the C-H activation. However, as with the other cases for substrate **51**, the C-H iodination of imidazoline was unsuccessful.

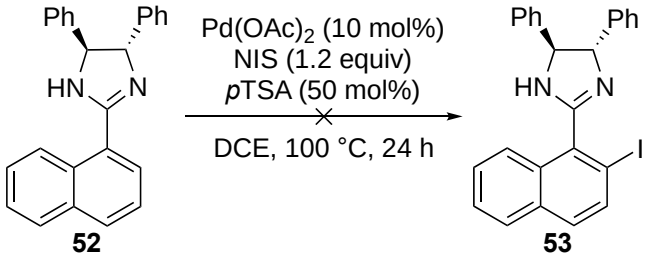

Scheme 49**: Attempted Pd-catalysed C-H iodination of imidazoline **52

In 2002, Yu reported a Cu(II)-catalysed system for the functionalisation of aryl C-H bonds.[37] The protocol was applied to many transformations by the Yu group including iodinations, chlorinations, cyanations, aminations and thioether formations. This system was applied to imidazolines **51** and **52** in order to probe the reactivity towards iodination (**Scheme 50**). In the case of the alkylated imidazoline **51**, only starting material was present in the ^{1}H NMR spectrum. Imidazoline **52** was consumed in the reaction when analysed by TLC but no clean product could be isolated by column chromatography.

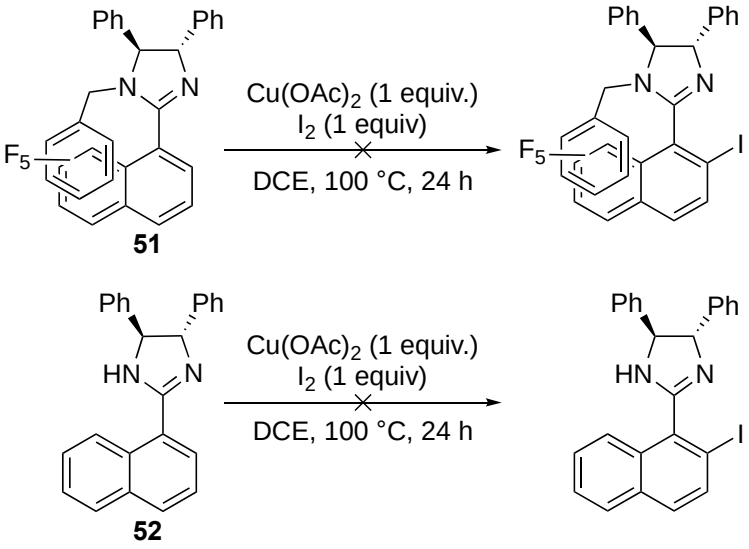

***Scheme 50**: Attempted Cu(II) protocol for aryl C-H functionalisation*

C-H Lithiation Attempts Towards Imidazoline-Based Axially Chiral P,N Ligands

Late stage installation of a synthetic handle on the imidazoline scaffolds for C-P bond formation had been unsuccessful at this stage in the present study. A further look into the literature led to another approach that had seen success in synthesising imidazoline-based P,N ligands. In 2002, Pfaltz reported the synthesis and application of centrally chiral phosphino-imidazoline ligands.[42] Pfaltz exploited the directing effect of the co-ordinating nitrogen in the imidazoline ring and lack of any acidic protons in imidazolines of type **54** to utilise a lithiation methodology. Pfaltz used *sec*-butyllithium to selectively lithiate the 2-position on the phenyl-ring of the ligand scaffold, before quenching with a variety of chlorodiarylphosphines to furnish novel P,N ligands of type **55**. These ligands were synthesised in poor to good yields, and were applied in enantioselective Ir-catalysed hydrogenations.[42]

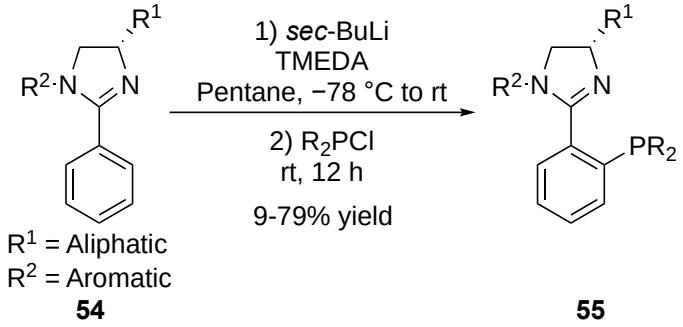

***Scheme 51**: Lithiation strategy for phosphine moiety installation reported by Pfaltz*[42]

The route developed by Pfaltz was adapted in the present study to see if it would be a viable template for accessing axially chiral imidazoline-based P,N ligands. Commercially available 1-naphthoic acid was treated with oxalyl chloride to generate the acid chloride *in situ* before the addition of L-valinol to furnish amide **56**. L-Valinol was chosen in this instance as a cost saving measure compared to L-*tert*-leucinol, until the route was proven to be successful. Amide **56** was then used to furnish imidazolines **57**, **58**, and **59**, with various R groups on the non-coordinating nitrogen. This was achieved by heating amide **56** under reflux neat in thionyl chloride followed by introduction of the appropriate nucleophile. The non-functionalised imidazoline

58 was successfully synthesised using a 7N NH_3 solution of MeOH, which opens the route towards accessing imidazolines synthesised from both nucleophiles and electrophiles. The yield for imidazoline **58** was moderate at 44%, with some competitive formation of the corresponding oxazoline being observed for the first time, which may have been caused by the presence of water in the 7N NH_3 MeOH solution. Mesityl-substituted imidazoline **59** was synthesised in an 81% yield as another possible substrate to test in the lithiation protocol.

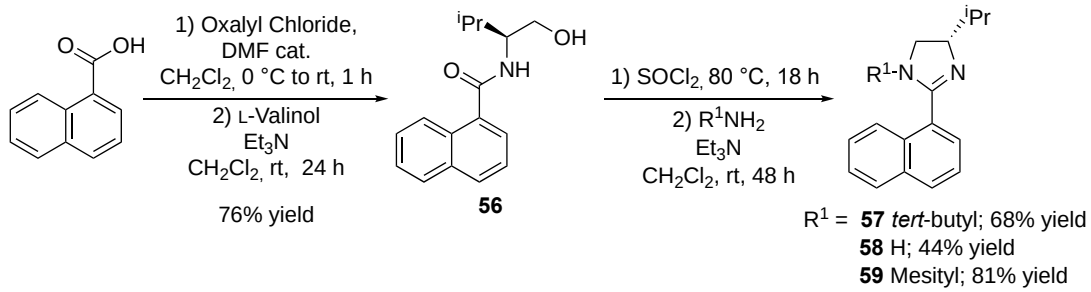

***Scheme 52**: Synthesis of imidazolines from 1-naphthoic acid for lithiation investigation*

Various lithiation conditions were probed using the imidazolines **57** and **59** (**Table 2**). All solvents were dried over 4Å molecular sieves for 48 hours prior to their use in the lithiation reactions. Freshly distilled TMEDA and new reagent bottles of the alkyllithiums were also used. The reactions were conducted in flame-dried Schlenk flasks under N_2.

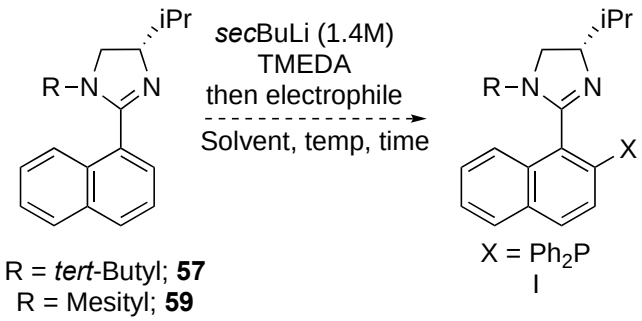

R = *tert*-Butyl; **57**
R = Mesityl; **59**

X = Ph_2P
I

Entry	R	*sec*BuLi (equiv.)	TMEDA (equiv.)	Electrophile (equiv.)	Solvent	Temp (°C)	Result
1	**^{t}Bu**	**3**	**3**	**Ph_2PCl (4.3)**	**Pentane**	**-78 to 0 to rt**	**S.M**
2	**^{t}Bu**	**3**	**3**	**Ph_2PCl (3.5)**	**Pentane**	**-78 to 0 to rt**	**S.M**
3	**^{t}Bu**	**3**	**3**	**Ph_2PCl (3.5)**	**THF**	**-78 to 0 to rt**	**S.M**
4	**^{t}Bu**	**3**	**3**	**Ph_2PCl, (3.5)**	**Et_2O**	**-78 to 0 to rt**	**S.M**
5	**^{t}Bu**	**3**	**3**	**I_2 (1.2)**	**Pentane**	**-78 to rt**	**S.M**
6	**Mesityl**	**1.1**	**1.1**	**Ph_2PCl (1.5)**	**Pentane**	**78 to 0 to rt**	**S.M**
7	**Mesityl**	**3.3**	**3.3**	**Ph_2PCl (4.6)**	**Pentane**	**-78 to rt**	**S.M**

Table 2**: Screening for lithiation conditions for imidazolines **57** and **59

The first set of conditions (**entry 1**) attempted were those used successfully by Pfaltz in his reported synthesis of centrally chiral P,N ligands (**Scheme 51**).[43] Unfortunately, only starting material was observed in the crude ^{1}H NMR spectrum and no triarylphosphine peak at approximately δ –15 to –10 ppm was observed in the ^{31}P NMR spectrum. Analysis by TLC also showed no compounds of expected polarity for the target compound being present (triarylphosphine-substituted imidazolines are significantly less polar compared to the starting materials). A reduction in the excess of chlorodiphenylphosphine used (**entry 2**) did not aid product formation. A change to other common solvents used in lithiations (**entry 3, entry 4**) did not lead to the formation of the target compound.

The electrophile was changed from chlorodiphenylphosphine to iodine (**entry 5**) to probe if the 2-position on the naphthalene ring was being lithiated. Iodine was chosen as the resulting iodine-bearing carbon would show up unambiguously at approximately δ 90 ppm in the ^{13}C NMR spectrum, an area that was free of any other peaks in the ^{13}C NMR spectrum of the starting material. For this test, the reaction was allowed to warm from –78 °C to rt following the addition of the alkyllithium reagent to allow sufficient time at elevated temperatures for formation of the desired aryllithium species. Unfortunately, no aryl-iodine bond was observed in the ^{13}C NMR spectrum.

The substrate was changed from ^{t}Bu-substituted imidazoline **57** to mesityl substituted imidazoline **59**. Mesityl-imidazoline **59** is a solid and as such simplified the addition of the substrate to the Schlenk flask in order to maintain inert conditions, compared to ^{t}Bu-imidazoline **57** which is an amorphous wax. The use of mesityl-imidazoline **59** with reduced amounts of *sec*-BuLi and TMEDA (**entry 6**) did not help form the target compound. Mesityl-imidazoline **59** was stirred at rt for 2 h in the presence of *sec*-BuLi prior to electrophile introduction (**entry 7**), however, that did not yield the target compound.

C-H Magnesiation Attempt Towards Imidazoline-Based Axially Chiral P,N Ligands

The lithiation protocol described by Pfaltz and other variations proving incompatible with our substrates, we looked towards other strategies. In 2006 Knochel reported a system for the magnesiation of aromatics and heteroaromatics using mixed Mg/Li amides (**Scheme 53**).[44] The addition of LiCl to the Grignard reagents was found to improve their reactivity in previous Br/Mg exchange reactions and as such was used in the preparation of mixed amide **60**. In their report, they used mixed amide **60** with 2-phenylpyridine **61** in THF at elevated temperatures to form the magnesiated intermediate **62**. This intermediate was then quenched with a solution of iodine to furnish the iodinated compound **63** in an 80% yield.

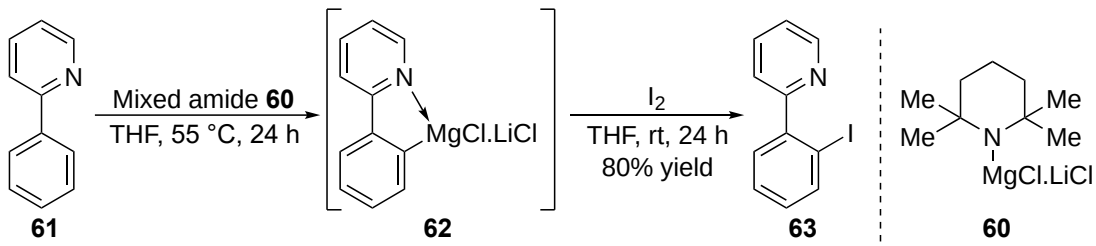

Scheme 53**: Selective heteroatom-directed magnesiation of 2-phenylpyridine using mixed amide **60

With this precedent observed in the literature, it was applied towards the attempted magnesiation of the imidazoline scaffold **59** as a means of selectively installing a diphenylphosphine group (**Scheme 54**). It was hoped that the higher temperature of the reaction would form the desired magnesiated-intermediate **62**, as the use of alkyllithium reagents at room temperature had already proved to be unsuccessful with imidazolines **57** and **59** in the present study (**Table 2**). Unfortunately, no peak in the corresponding triarylphosphine region was observed (δ –5 to –20 ppm upon analysis of the crude ^{31}P NMR spectrum. The mass of the crude material recovered was approximately equal to the starting material used and as such no appreciable degradation of the starting material was observed under the reaction conditions.

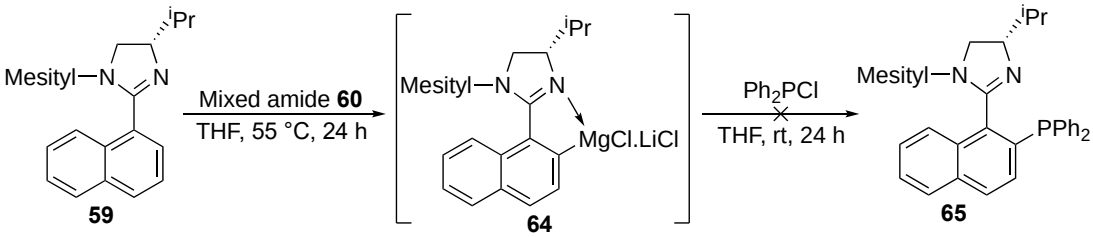

***Scheme 54**: Attempted magnesiation of imidazoline **59** using mixed Mg/Li amide reported by Knochel*[44]

Accessing 2-Iodo-1-Naphthaldehyde

To date, C-H activation work and lithiation/magnesiation strategies proved unsuccessful for the installation of synthetic handles or phosphine groups on the described imidazoline scaffolds. The lack of promising results with the imidazoline scaffolds prompted attention to be shifted towards naphthalene compounds with handles for C-P bond formation. More specifically, synthetically useful amounts of iodinated naphthalene derivatives were required. With this in mind, we proceeded to try to reproduce the few reported methods in the literature for accessing 2-iodo-1-naphthaldehyde.

In 2014, Bräse reported a selective *ortho*-halogenation of [2.2]paracyclophane and its derivatives using a Pd-catalysed C-H activation protocol.[40] In the present study, we adapted the protocol to suit the synthesis of our imidazoline scaffold (**Scheme 55**). The first step involved a condensation reaction between 1-naphthaldehyde and methoxyamine hydrochloride, which formed oxime ether **66** in a 89% yield after purification by silica plug. Imine **66** was then subjected to the Pd C-H activation conditions, with N-iodosuccinimide as the electrophilic iodine source. Previous work in the group by Dr. Vivek Kumar using the same protocol on a formylated [2.2]paracyclophane substrate showed that separation of the analogous starting material/product of the Pd C-H iodination step was not possible *via* column chromatography. As such, crude product **67** was telescoped to the deprotection step using *p*-TSA and formaldehyde. This deprotection step proved difficult, with trace amounts of crude product **68** isolated after two rounds of the deprotection procedure. The difficulty in isolating material in meaningful quantities and trouble in

hydrolysing the protecting group led to further optimisation of this route not being considered.

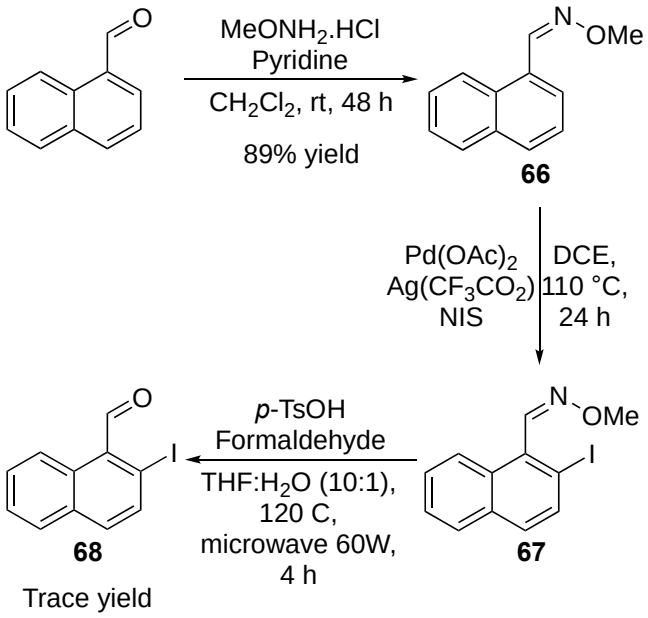

***Scheme 55**: Pd-catalysed C-H iodination of 1-naphthaldehyde using O-methyloxmine as a directing group*[40]

Another strategy towards the C-H iodination of aryl aldehydes was reported by Barbasiewicz in 2014 (**Scheme 56**).[45] This methodology involved the selective *ortho*-lithiation of 1-naphthaldehyde using *n*-BuLi and *N*,*N*,*N*'-trimethylethylenediamine as a directing group. The Barbasiewicz group reported a 40% yield for this transformation but in our hands the best result obtained was a 10% isolated yield of **68**, with the diagnostic peak being the aryl-iodine bond with the characteristic shift at δ 105.3 ppm in the ^{13}C NMR spectrum. The reaction was repeated multiple times, with extension in reaction times both in the lithiation step to form intermediate **69** and in reaction times after the addition of the iodine solution in THF. Unfortunately, these modifications did not improve the poor yields observed for this reaction. Different bottles of *n*-BuLi did not help with the formation of **68** either, suggesting that the alkyllithium reagent was not the cause of the poor yields. As with other lithiations in this study, the anhydrous THF was taken from our Grubbs solvent still and was dried over 4Å molecular sieves for 48 h prior to use. The consistently poor yields excluded this procedure as a viable way of accessing the necessary starting

material for ligand synthesis.

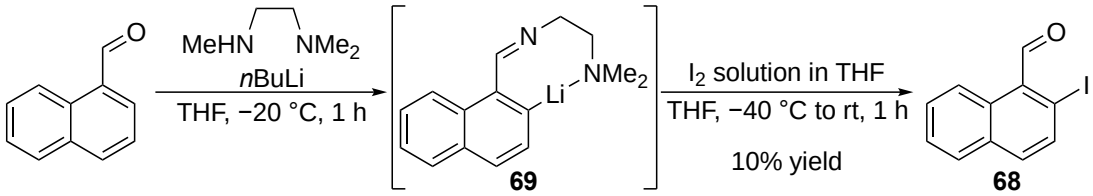

***Scheme 56**: Lithiation protocol with N,N,N'-trimethylethylenediamine as a direction group for C-H iodination*

Route Re-evaluation Towards Naphthoic Acid Derivatives

In this research project and in previous work in the Guiry group, accessing imidazoline scaffolds for ligand synthesis has been achieved through condensation reactions of either 2-methoxy-1-naphthaldehyde (**Scheme 36**) or 2-bromo-1-naphthaldehyde (**Scheme 41**) and (1*S*,2*S*)-(−)1,2-diphenylethylenediamine. This furnishes the corresponding imidazoline with a free N-H which can be functionalised by electrophiles following deprotonation with a suitable base such as sodium hydride. The current routes (**Scheme 36** and **Scheme 41**) have a few limitations:

1) The commercially available 2-methoxy-1-naphthladehyde leads to over-alkylation of the imidazoline on treatment with an electrophile (**Scheme 39**);
2) The imidazoline can only be functionalised by electrophiles through deprotonation of the N-H nitrogen on the imidazoline ring;
3) Accessing other 2-halogenated aldehydes has proved difficult or low yielding;
4) Requires use of aryl diamines for the condensation reaction and thus limits variation of imidazoline backbone.

Based on these limitations ,it was desirable to find a route that would allow for more flexibility towards accessing analogues of UCDPhim and other novel ligands in synthetically useful quantities.

In 2012, Overman reported the synthesis of palladacyclic imidazoline-naphthalene complexes (**Scheme 57**).[46] The route involved using 1-cyanonaphthalene, where the nitrile group facilitated the selective lithiation of the 2-position on the naphthalene ring with lithium tetramethylpiperidine. This was quenched with iodine to allow for the installation of iodine on the 2-position of the naphthalene ring. Hydrolysis of the nitrile group yielded the primary aryl-amide. The generation of nitrious acid *in situ* from sodium nitrite and sulfuric acid was reported to hydrolyse the amide to 2-iodo-1-naphthoic acid in a 65% yield across three steps.

A variety of amides were synthesised by Overman from the synthesis 2-iodo-naphthoic acid, through the use of oxalyl chloride which generated the corresponding acid chloride. The acid chloride was then treated with various amino alcohols to furnish amides of type **70** in yields from 82-93%. The key step involved treatment of the amides with thionyl chloride which formed a chloroalkylimidoyl chloride *in situ*. These were reacted with substituted primary amines or ammonia to synthesise imidazolines of type **71** in yields from 43-76%. Overman treated these imidazolines with $Pd_2.dba_3$ and sodium acetylacetonate to furnish the desired palladacyclic compounds for his study.

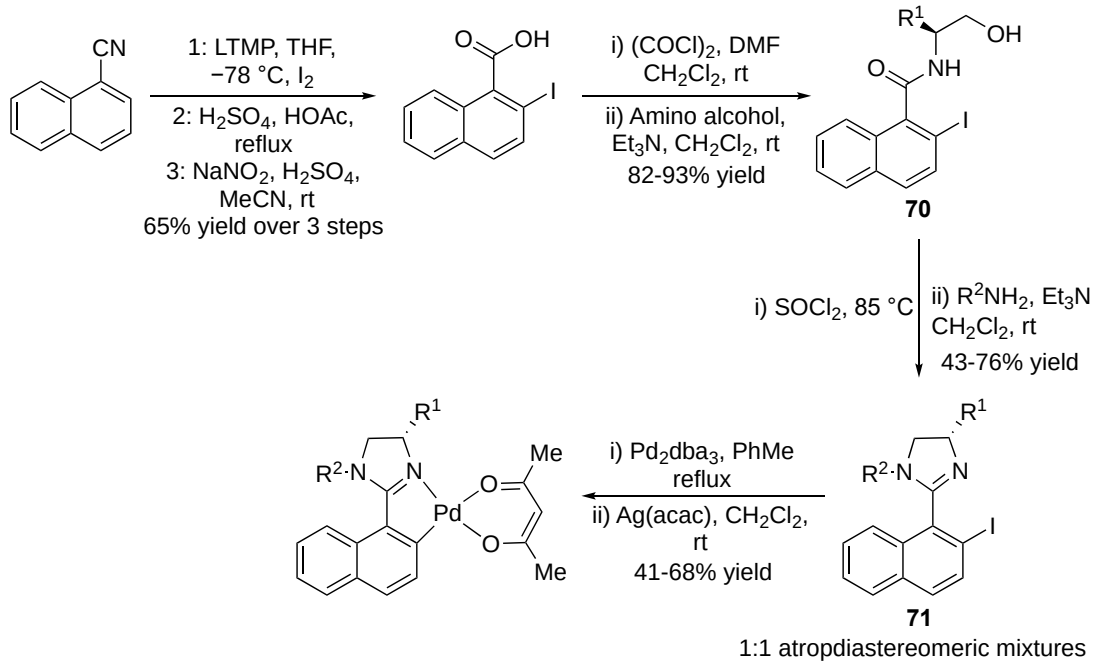

***Scheme 57**: Synthesis of palladcycle imidazoline-naphthalene complexes for enantioselective catalysis by Overman in 2012*[46]

The route devised by Overman was a source of inspiration for the work in this current research project, as imidazolines of type **71** (**Scheme 57**) could be subjected to a Cu-catalysed phosphinylation to access novel axially chiral imidazoline-based P,N ligands. Importantly, the route readily allows for variation on the imidazoline backbone through the appropriate choice of amino alcohol and also allows for the synthesis of imidazolines derived from both nucleophiles and electrophiles (treatment with ammonia would give the N-H imidazoline, which could be deprotonated and treated with an electrophile). This would offer the possibility of exploring different R groups on the non-co-ordinating nitrogen of the imidazoline ring with the aim of increasing the barrier of rotation about the imidazoline-naphthalene biaryl bond.

Accessing 2-Iodo-1-Naphthoic Acid

The first step in the present study was to replicate the protocol outlined by Overman to access 2-iodo-naphthoic acid (**Scheme 58**).[46] The lithiation of 1-cyanonaphthalene proceeded smoothly by using the described procedure with lithium 2,2,6,6-tetramethylpiperidine and its subsequent quench with a solution of iodine. 2-Iodo-1-cyanonaphthalene was accessed on a 5 g scale after purification by recrystallisation from hot chloroform and pentane anti-solvent. Hydrolysis of the nitrile to 2-iodo-1-naphthamide proceeded smoothly, with an isolated yield of 57% after purification by recrystallisation from hot acetonitrile. The final hydrolysis of 2-iodo-1-naphthamide proved problematic. None of the desired 2-iodo-1-naphthoic acid was isolated from the work-up, despite following the method described by Overman and adjusting the aqueous phase to pH 1 before extraction with the organic solvent. The reaction was conducted in the dark and the reaction vessel was covered in aluminium foil to protect the light-sensitive sodium nitrite. Repetition of the amide hydrolysis in triplicate did not yield the desired acid.

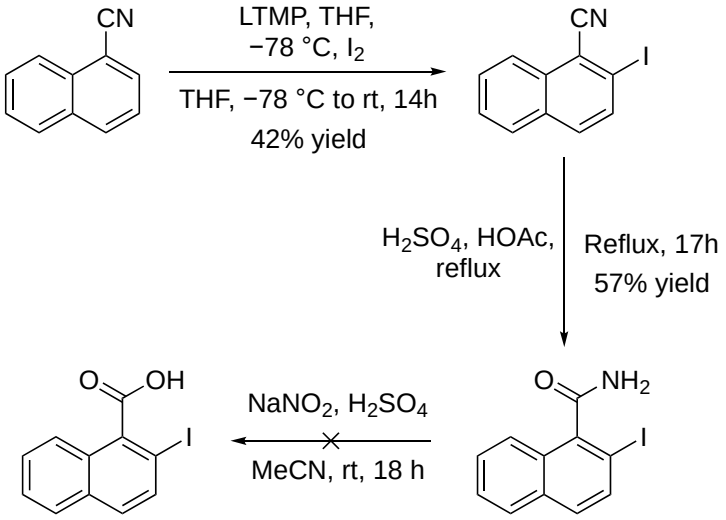

***Scheme 58**: Attempted replication of Overman's 2-iodo-naphthoic acid protocol*

A previous group member had success in replicating a Pd-catalysed C-H iodination procedure reported by Yu in 2008 in order to access halogen-substituted benzoic acids.[47] The conditions outlined by Yu were applied in the present study for the iodination of 1-naphthoic acid (**Scheme 59**). TLC analysis showed complete consumption of the 1-naphthoic acid starting material but the loss of product on work-up was troublesome. The reaction was repeated approximately ten times, with an isolated yield of 34% being the highest obtained for **72** . This was achieved after much optimisation of the work-up procedure. Loading the reaction mixture directly onto a silica column and directly purifying it proved to be the most consistent method for isolating the product. The key diagnostic peak in the ^{13}C NMR spectrum was at δ 90.7 ppm, which is indicative of an aryl-iodine C-I bond. To the best of our knowledge, there are no known examples of a Pd-catalysed C-H halogenation of 1-naphthoic acid in the literature. Despite the low yields, this single step methodology proved more attractive than the three step route described by Overman and also avoids the use of harmful nitric acid. In addition, it was the only methodology to date that furnished the product in appreciable quantities.

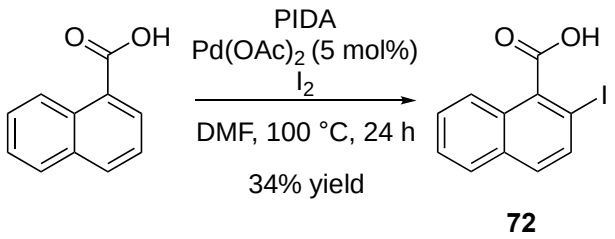

72

***Scheme 59**: Pd-catalysed C-H iodination of 1-naphthoic acid*

The trace amount of 2-iodo-1-naphthaldehyde **68** synthesised *via* the lithiation protocol described in **Scheme 56** was oxidised to the corresponding acid (**Scheme 60**). This was done in order to confirm the identity of 2-iodo-1-naphthoic acid synthesised *via* the Pd-catalysed C-H activation protocol (**Scheme 59**), as there is only one example in the literature for the preparation of the acid that reports NMR spectral data.[48] The oxidation reaction only afforded trace amounts of the target acid **72** due to the poor solubility of **68** in the reaction solvent. However, the ^{1}H NMR spectroscopic data of **72** derived from the oxidation of aldehyde **68** was consistent with the ^{1}H NMR spectroscopic data for the 2-iodo-1-naphthoic acid **72** derived from the Pd-catalysed C-H iodination described in **Scheme 59**.

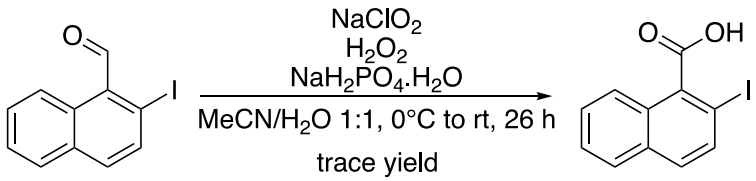

68 **72**

Scheme 60**: Oxidation of 2-iodo-1-naphthaldehyde derived from lithiation strategy in **Scheme 56

Fortunately, a suitable crystal of 2-iodo-1-naphthoic acid prepared by Pd-catalysed C-H activation was grown for X-ray analysis (**Figure 16**). This confirmed that the Pd-catalysed C-H activation protocol described by Yu could be extended to naphthoic acid derivatives. More importantly, only one product was observed in the ^{1}H NMR spectra of the compound and we could therefore confirm that no competitive iodination of the 8-position of the naphthalene ring had occurred upon analysis of the X-ray crystal structure. This was necessary as there is currently only one reported set of NMR data for 2-iodo-1-naphthaldehyde in the literature from the Mortier group in 2005.[48] The lack of iodination in the 8-position is consistent with theory in the literature, citing that substituents other than hydrogen in the 1 and 8-position in a naphthalene ring will have a considerable steric interaction due to the shorted distance between the non-bonded *peri*-carbons of 2.4-2.5 Å (compared to the typical non-bonded carbon-carbon distances of ~3 Å in the rest of the molecule).[49]

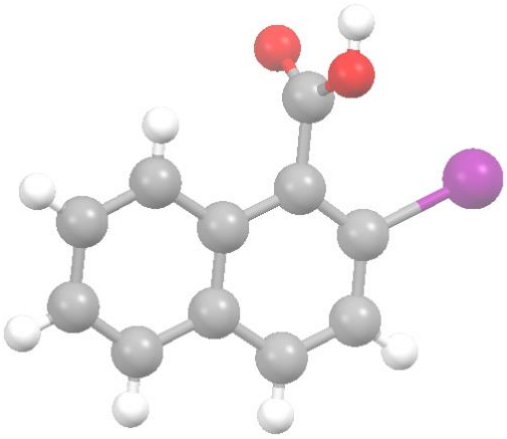

***Figure 16**: X-ray structure of 2-iodo-1-naphthoic acid prepared via direct Pd-catalysed C-H activation*

While investigations into accessing 2-iodo-1-naphthoic acid were underway, a concurrent test reaction was performed to probe the compatibility of phenylglycinol with the Overman route. Phenylglycinol-derived amide **73** was subjected to the Overman cyclisation conditions before treatment with *tert*-butyl amine as a nucleophile in an attempt to furnish imidazoline **74** (**Scheme 61**). Here we discovered a limitation of the route, where aryl substitution on the amide precursor led to the exclusive formation of the nitrile product **75**. Amide **73** was dehydrated under reflux conditions with thionyl chloride to yield the corresponding literature known nitrile

75.[50]

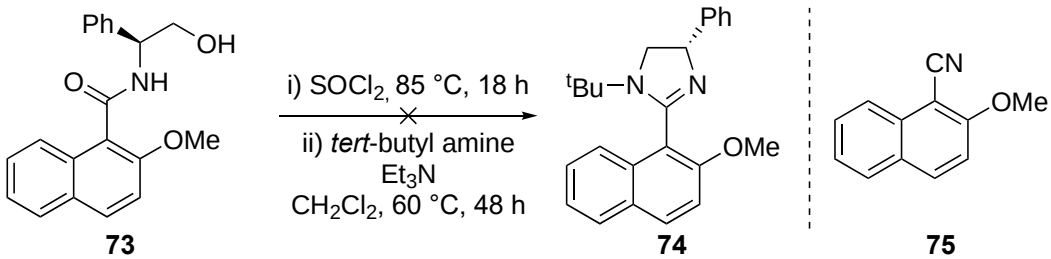

73 **74** **75**

Scheme 61**: Attempted imidazoline formation from phenylglycinol-derived amide **73

Based on this observation, it was decided that accessing the *tert*-butyl-substituted amide would be the most promising substituent, as it has been consistently shown to be the best aliphatic substituent in terms of asymmetric induction in the analogous PHOX ligands.[51,52,53,54] L-*tert*-Leucinol was therefore readily synthesised from L-*tert*-leucine *via* a sodium borohydride/iodine system in a 72% yield (**Scheme 62**).[55]

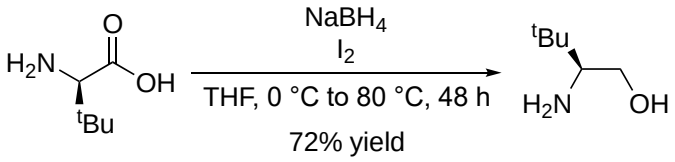

***Scheme 62**: Reduction of (L)-tert-leucine using sodium borohydride/iodine*[55]

Ligand Synthesis Using 2-Iodo-1-Naphthoic Acid

Synthesis of Key Amide Intermediate

The Pd-catalysed C-H iodination of 1-naphthoic acid afforded the iodinated product in a 34% yield (**Scheme 63**). Amide **76** was synthesised in one step from iodo-acid **72** through the use of oxalyl chloride, which generated the corresponding acid chloride *in situ* (**Scheme 63**). Removal of the excess oxalyl chloride *in vacuo* before treatment with L-tert-leucinol and triethylamine in CH_2Cl_2 formed the target amide in a 59% yield after purification by column chromatography.

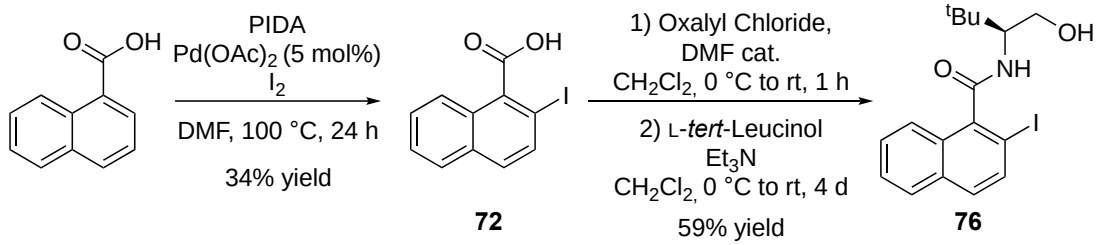

***Scheme 63**: Pd-catalysed C-H activation of 1-naphthoic acid and subsequent amide formation*

At this point a range of nucleophiles were chosen in order to synthesise a range of imidazolines bearing different groups at N. The commercially available 2,4,6-trimethylaniline, *p*-anisidine, *tert*-butyl amine, and ammonia were chosen. Aryl amines were chosen as they were substituents previously incompatible *via* the route devised by Guiry for UCDPhim in 2017.[16]

A *tert*-butyl substituted imidazoline was highly desired due to a literature example published by Yan in 2019 (**Scheme 64**), which described the synthesis of axially chiral naphthyl-C2-indoles.[56] The racemisation between **77** and *ent*-**77** was studied by heating **77** at reflux in toluene at 110 °C. Only 0.6% erosion in the enantiopurity of **77** was observed after heating **77** for 165 h at 110 °C. Therefore, it was hoped that a similar imidazoline based system bearing a *tert*-butyl group on the imidazoline nitrogen may have a more stable chiral axis. This could open the possibility of synthesising a novel axially chiral imidazoline-based P,N ligand that was amenable to

high temperature catalysis. A notable example of such catalysis was reported by Guiry in 2019, which employed the axially chiral ligand Pinap at 130 °C in Pd-catalysed decarboxylative asymmetric propargylation.[19] A contributing factor limiting the ees in the reaction was the epimerisation of the free Pinap ligand about its chiral axis at elevated temperatures.

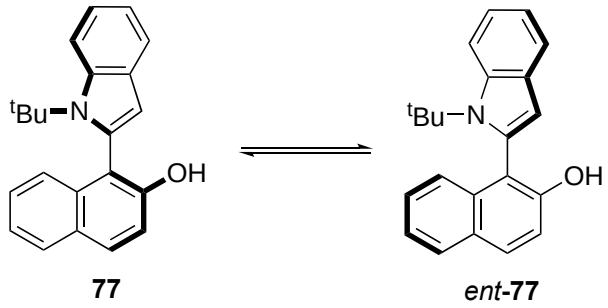

***Scheme 64**: Racemisation test of axially chiral naphthyl-C2-indoles conducted by Yan*[21]

In addition, *tert*-butyl carbamate and pentafluorobenzyl amine were also chosen as nucleophiles for synthesising imidazolines. *Tert*-butyl carbamate was synthesised by treating di-*tert*-butyl dicarbonate **78** with a 35% (*w*/*v*) ammonium hydroxide solution in ethanol at room temperature (**Scheme 65**). The target carbamate **79** was accessed in a 65% yield after purification by recrystallisation.

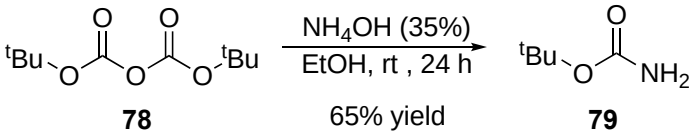

Scheme 65**: Synthesis of boc-amine **79** from ammonium hydroxide and di-tert-butyl decarbonate **78

Pentafluorobenzyl amine **80** was synthesised over two steps as per Gabriel's synthesis (**Scheme 66**). Commercially available potassium phthalimide **81** was suspended in DMF and to which pentafluorobenzyl bromide was added. After 24 h, the reaction mixture was poured into H_2O and cooled to 4 °C which facilitated precipitation of the N-alkylphthalimide in a 90% yield. Compound **82** was then heated at reflux in MeOH as per the Ing-Manske procedure, furnishing the target amine **80** in 68% yield upon purification by column chromatography.[57] It is worth noting that vigorous stirring is required to avoid solidification of the reaction mixture as the

reaction progresses, due to the formation of the phthalylhydrazide precipitate.

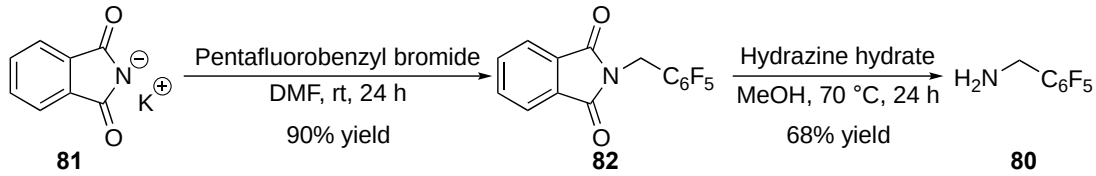

***Scheme 66**: Synthesis of pentafluorobenzyl amine*

Synthesis of C-P Bond Formation Precursors

The planned range of imidazoline ligand precursors were synthesised in yields from 39% to 99% (**Scheme 67**). Purification of the products proved difficult, with varying quantities of triethylamine required to avoid degradation of the products on silica. The unfunctionalized NH imidazoline was synthesised from 7N NH_3 solution in methanol, as a proof of concept that further analogues could be synthesised from electrophiles as per the procedure reported by Guiry in 2017.[16]

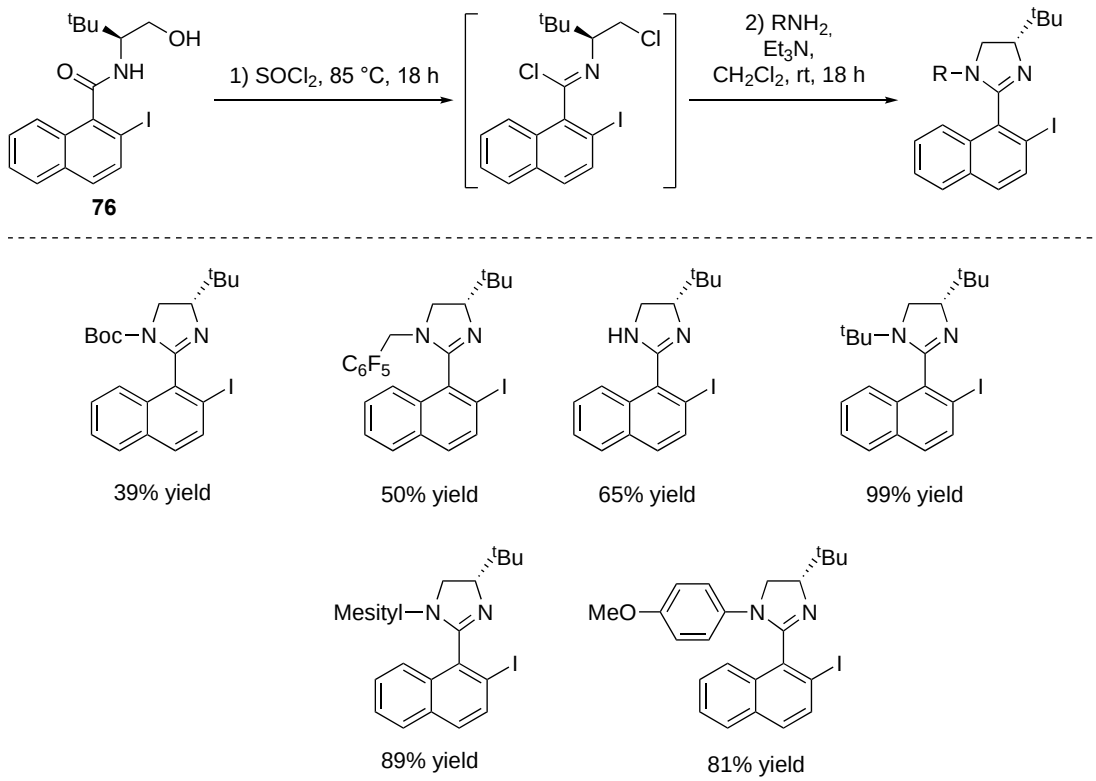

Scheme 67**: Synthesis of ligand precursors from amide **76

The unfunctionalised imidazoline **83** (**Figure 17**) was isolated during the purification process of Boc-substituted ligand precursor, although it was unclear if the Boc group was removed during the basic aqueous work-up conditions or during purification on silica gel.

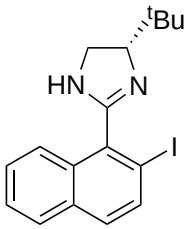

83

***Figure 17**: Imidazoline **83** isolated via column chromatography from the reaction for the formation of Boc-substituted imidazoline*

Attempted Transition-Metal Catalysed C-P Bond Formation

Disappointingly, the final Cu-catalysed C-P bond formation step did not proceed with any of the substrates prepared (**Scheme 68**). In all cases, a complex mixture of products was instead observed. The reduced C-H product was isolated in varying yields for the 2,4,6-trimethylaniline-, *p*-anisidine- and *tert*-butyl-substituted imidazolines. This result was particularly disappointing as aryl-iodine bonds are consistently reported as the most reactive coupling partners in the literature for C-P bond forming reactions.[58,59,60,61,62] These results with the synthetic handle most likely to yield the desired product based on literature precedent prompted other methodologies to be explored to the successful installation of a C-P bond.

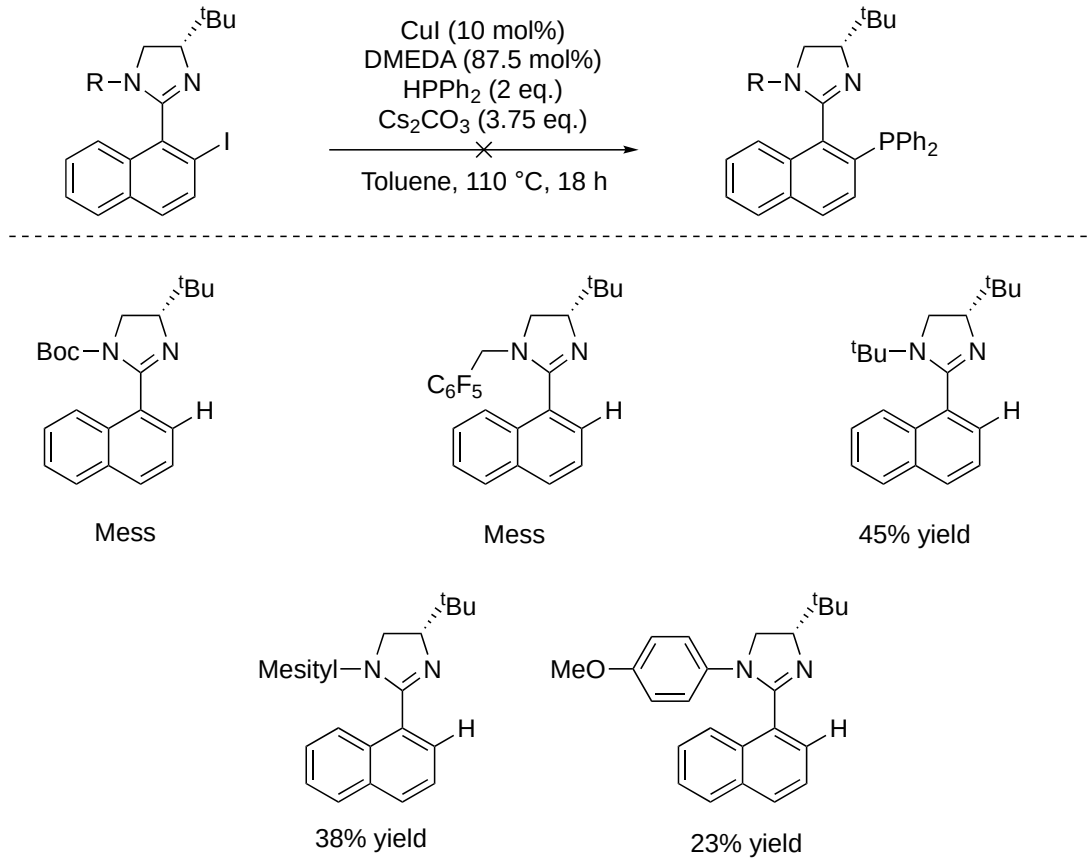

Scheme 68: *Unsuccessful Cu-catalysed C-P bond formation of iodinated imidazoline ligand precursors*

Milder Pd-catalysed conditions for the formation of triarylphosphines were reported by Wang in 2016.[63] The protocol involved the use of acylphosphine **84**, which was synthesised in the current study (**Scheme 69**). Wang described the use of acylphosphine **84** in the synthesis of triarylphosphines from the corresponding aryl-iodides, with yields from 52-95% reported.

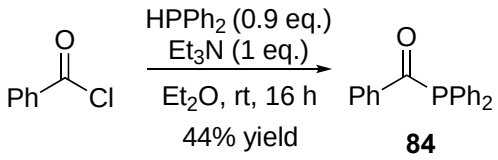

Scheme 69: *Synthesis of acylphosphine reagent for Pd-catalysed C-P bond formation*

The mesityl-substituted imidazoline **85** was reacted under the conditions described by Wang (**Scheme 70**). As with the previous attempted C-P bond forming reactions, the reaction did not proceed cleanly. The only isolable product from the reaction was the reduced product, which was isolated in a 38% yield. The *tert*-butyl-substituted

imidazoline was also reacted under these conditions but no product was observed. The reported more reactive nature of acylphosphine reagent **84** and lower reaction temperature were hoped to promote C-P bond formation, but disappointingly only the reduced product of the mesityl-substituted imidazoline **85** was isolated.

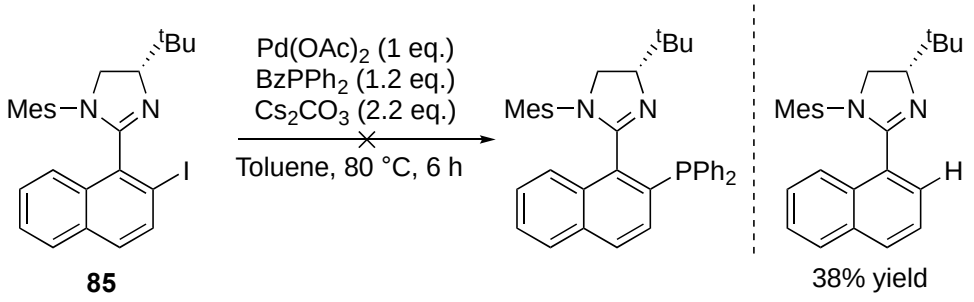

***Scheme 70**: Attempted phosphinylation using acylphosphine substrate reported by Wang.* [63]

Herzon reported a mild Pd-catalysed P-arylation of secondary phosphine oxide protocol in 2012, which was adapted in the present study (**Scheme 71**).[64] The protocol uses small Pd catalyst loadings of 0.5 mol% and yields the corresponding triarylphosphine oxides in 34-94% yields after Just 2 h. The authors credit the large bite angle (108°) of the Xantphos ligand as a potential reason for the high reactivity of the system, as it would promote the oxidative addition of the aryl iodide precursors. The conditions were adapted for the test reaction using substrate **86** in the present study, with higher catalyst loadings and a longer reaction time used. The only observable peak in the ^{31}P NMR spectrum corresponded to the diphenylphosphine oxide starting material, and the aryl-iodine bond of the imidazoline starting material **86** was observed in the ^{13}C NMR spectrum.

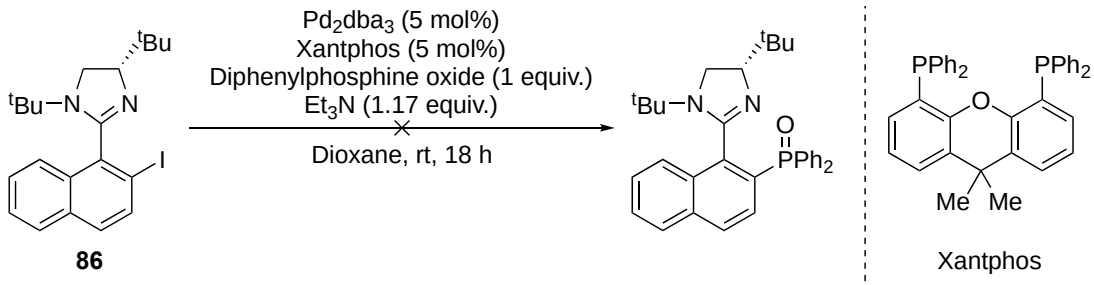

Scheme 71**: Unsuccessful conditions for the synthesis of triarylphosphine oxide product from substrate **86

Attempted Lithium-Halogen Exchange Reactions

The attempted transition metal-catalysed C-P bond forming reactions proved unsuccessful to date in the present study, so attention turned to a lithium-halogen exchange strategy. Lithium-halogen exchange reactions have proved a viable method in the literature for installing phosphine moieties into sterically hindered binaphthalene halogenated arene scaffolds, even phosphine moieties bearing *ortho*-substitution on its corresponding aryl groups.[65,66,67] The *tert*-butyl- and mesityl-substituted imidazoline substrates were subjected to lithium-halogen exchange protocols (**Table 3**). Unfortunately, none of the conditions probed in the study yielded any of the desired product upon examination of the crude products by ^{31}P NMR spectroscopy. The reduced product was isolated in the case of one test reaction (**entry 7**, **Table 3**). In each case, a variety of spots were observed when the reaction mixture was analysed by TLC. Two test reaction were conducted with the mesityl-substituted imidazoline, where the reactions were quenched with isopropanol and water respectively with the aim of isolating a clean sample of the reduced product. In these test reactions, multiple spots were visible on TLC analysis. Isolation of these side products by column chromatography proved unsuccessful.

It was worth noting that after workup by celite filtration and concentration *in vacuo*, an insoluble precipitate was formed upon addition of deuterated chloroform for NMR analysis. This insoluble precipitate required filtration prior to NMR analysis. The presence of this precipitate and multiple spots *via* TLC analysis suggested the imidazoline scaffolds were unstable under lithium-halogen exchange conditions. This observation was also made by another other group member, Dr. Vivek Kumar, conducting similar reactions on imidazoline-based scaffolds with the aim of synthesising imidazoline-[2.2]paracyclophane based ligands.

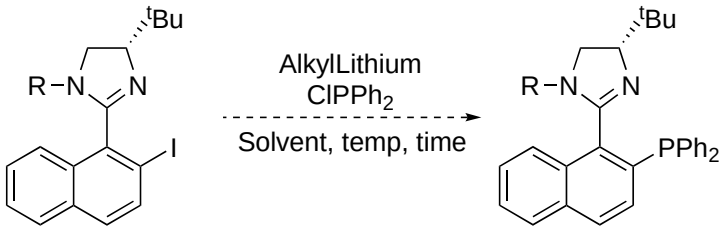

***Table 3**:Lithium-halogen exchange conditions for phosphine installation*

Entry	R Group	Solvent	Temp.	RLi	$ClPPh_2$ (equiv.)	Time[a]	Result
1	***t*Bu**	**Et_2O**	**0 °C**	***n*-BuLi (3 equiv.)**	**3.5**	**2h to 18 h**	**Mess**
2[b]	***t*Bu**	**THF**	**-78 °C**	***n*-BuLi (3 equiv.)**	**3.5**	**1 h to rt**	**Mess**
3	***t*Bu**	**THF**	**-88 °C**	***n*-BuLi (2 equiv.)**	**1**	**30 min to 1h**	**Mess**
4	**Mesityl**	**THF**	**-88 °C**	***n*-BuLi (2 equiv.)**	**1**	**30 min to 1h**	**Mess**
5	**Mesityl**	**THF**	**-96 °C**	***t*-BuLi (2 equiv.)**	**2.5**	**10 min to 2 h**	**No PAr_3**
6	**Mesityl**	**THF**	**-90°C**	***n*-BuLi (5 equiv.)**	**6**	**10 min to 2 h**	**Mess**
7	**Mesityl**	**THF**	**-78 °C**	***t*-BuLi (3 equiv.)**	**3.5**	**10 min to 2h**	**54% isolated reduced product**

[a]First time length denotes duration of lithiation-halogenation exchange, second time length denotes time stirred in presence of chlorodiphenylphosphine; [b]Reaction was performed with TMEDA (1.2 equiv.)

Installation of C-P Bond Prior to Cyclisation

The unsuccessful strategies to date in the present study, utilising the iodinated imidazoline ligand precursors, caused the order of the route to be evaluated. The difficulty in the previous strategy was the installation of the phosphorus moiety as the last step of the synthesis. A different approach was considered, where the C-P bond would be formed earlier with amide **76** (**Scheme 72**). Installation of a diphenylphosphine oxide moiety was chosen due to the inherent stability of the functional group. There was concern that oxidation of the triarylphosphine product might occur during the rest of the synthesis if a diphenylphosphine group was installed before the thionyl chloride-mediated cyclisation step. A stoichiometric Cu-mediated cross coupling between amide **76** and diphenylphosphine oxide proceeded smoothly, with the target compound **87** isolated in a 68% yield. This positive result proved the 2-iodonaphthalene system bearing substitution in the 1-position was compatible with C-P bond reactions by my hands. Disappointingly, the subsequent cyclisation did not lead to the formation of the desired imidazoline **88** and instead, oxazoline **89** was isolated in a 23% yield.

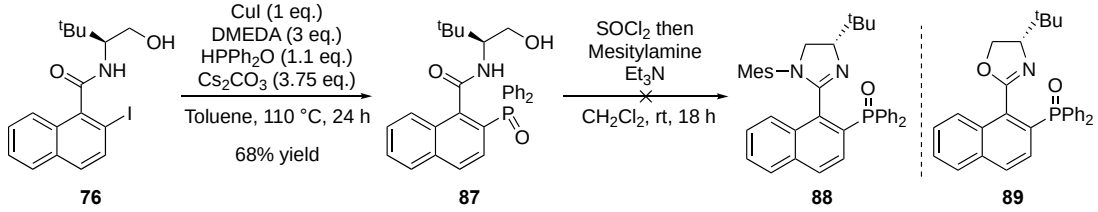

***Scheme 72**: Revised synthetic approach towards accessing novel axially chiral imidazoline-based P,N ligands*

Synthesis of Known P,N Ligands *Via* a Novel Route

The difficulty in accessing axially chiral imidazoline-based P,N ligand resulted in the exploration towards a novel route for the centrally-chiral P,N ligands (**Scheme 73**). The reported route for accessing these ligands involves the use of benzoic acid and relies on using the imidazoline core for the directed selective lithiation of the 2-position of the bottom phenyl ring.[68] The reported lithiation step in the protocol by Pfaltz suffers from poor yields (~40%) and requires the handling of sensitive *s*-BuLi at –78 °C.

In the present study, we proposed an alteration to the protocol by using 2-bromo-benzoic acid as the commercially available starting material of the synthesis. Treatment of 2-bromobenzoic acid with oxalyl chloride and a catalytic amount of DMF generated the acid chloride *in situ*, which was reacted with L-*tert*-leucinol to give amide **90** in a 77% yield (**Scheme 73**). Amide **90** was refluxed in thionyl chloride before being concentrated *in vacuo* and reacted with a primary amine nucleophile in dichloromethane. The phenyl-, *p*-methoxyphenyl- and *p*-trifluoromethylphenyl-substituted imidazolines were isolated in 81%, 83% and 73% yields, respectively. Crucially, these novel compounds contained the necessary synthetic handle required for the proposed Cu-catalysed C-P bonding forming reaction.[58] To our delight, the three imidazoline bromides were compatible with the Cu-catalysed protocol first reported by Buchwald.[28] The corresponding P,N ligands were isolated in 65-84% yields in short reaction times of 2-5 h on a half gram scale. The higher yields and avoidance of preparing discrete anionic intermediates makes the amended route described in this work more attractive. The facile isolation of these P,N ligands suggested there were no issues with the reagents or synthetic operation of the previous experiments with the axially chiral ligand precursors .

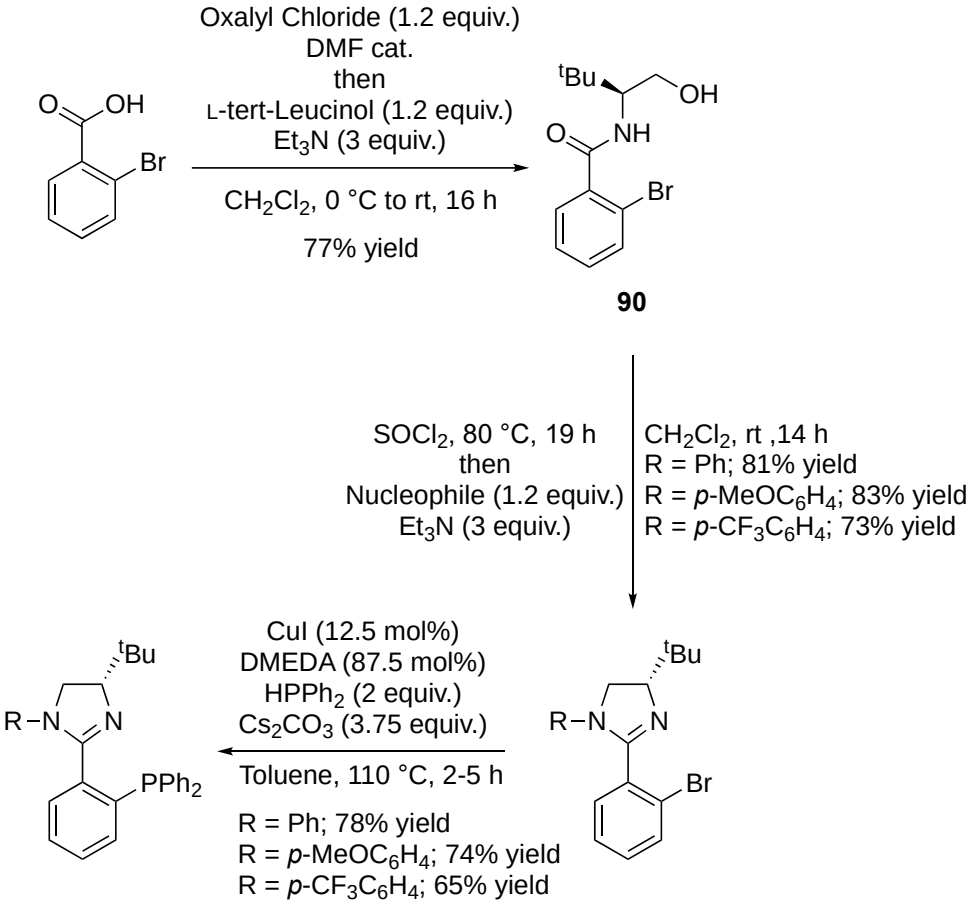

***Scheme 73**: Novel route towards accessing centrally chiral imidazoline-based P,N ligands*

The previously reported synthesis of *tert*-butyl PHOX was also conducted in the present study (**Scheme 74**).[69] Amide **90** was treated with *p*-toluenesulfonyl chloride at reflux in dichloromethane for 14 h before the addition of water and reflux for a further 2 h (**Scheme 74**). This furnished the oxazoline bromide in an 67% yield after purification. The same described Cu-catalysed C-P bond formation conditions were applied to oxazoline **91** and resulted in the formation of *tert*-butyl PHOX **92** in an 84% yield after 18 h.

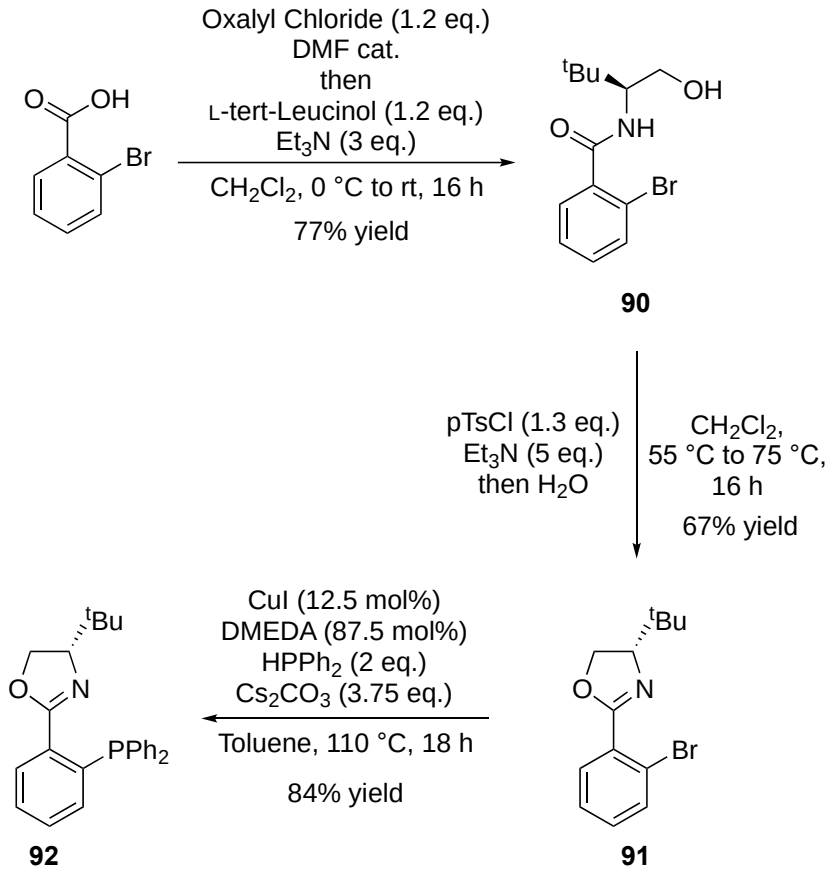

***Scheme 74**: Synthesis of ^{t}Bu-PHOX in the present study*[69]

Conclusions and Future Work

The synthesis of novel imidazoline-based axially chiral P,N ligands presented many challenges throughout this project. The lack of suitable commercially available starting materials represented a significant challenge towards beginning work on accessing new ligands. 2-Methoxynaphthalene derivatives remain unattractive due to the observed dibenzylation issues that significantly hindered access towards UCDPhim *via* the established route by my hands. Halogenated naphthalene derivatives remain the preferred synthetic handle for future work in this area.

Accessing halogenated-naphthalene or imidazoline compounds, which are the necessary intermediates required for the synthesis of novel axially chiral imidazoline—based P,N ligands, proved consistently challenging. Reported methods were irreproducible or low yielding and unsustainable towards accessing sufficient quantities required for the optimisation of a new ligand route. The optimisation of an unreported Pd-catalysed C-H activation halogenation strategy for naphthoic acid derivatives eventually yielded the necessary starting material. However, more work is required to improve the ease of accessing the product from the reaction mixture, due to the high-boiling point and water soluble nature of the DMF solvent.

The cyclisation step of the key iodinated amide proceeded smoothly after becoming familiar with air sensitive nature of the reaction and handling of the key chloroalkylimidoyl chloride intermediate. Aromatic and aliphatic primary amines proved to be equally compatible, including highly sterically hindered nucleophiles such as *tert*-butylamine. The resulting imidazolines required significant amounts of triethylamine (1-10% *v*/*v*) in the column chromatography solvent in order to limit their degradation on silica. Similar compounds in the literature have been reported to have similar issues with decomposition on silica.[46]

The installation of the carbon-phosphorus bond form the iodo-imidazoline ligand precursors proved unsuccessful *via* Cu-catalysed phosphinylation, Pd-catalysed phosphinylation, Cu-mediated phosphorylation, Pd-catalysed phosphorylation, and lithium-halogenation exchange reactions with a variety of alkyllithium sources. The changed route allowed for the successful installation of a C-P bond in the iodo-amide substrate, but the subsequent cyclisation yielded the corresponding oxazoline product.

Three centrally chiral imidazoline-based P,N ligands were synthesised in good yields of 36-48% yields across three steps. Gratifyingly, the C-P bond forming step occurred in good yields in short reaction times. The replication of the reported synthesis of *tert*-butyl PHOX also proceeded well in a 43% yield over three step.

The facile C-P bond formation in the centrally chiral imidazoline scaffolds suggested that the increased sterics in the axially chiral substrates was a key factor in the problematic C-P bond forming reactions for those substrates. It may be the case that a dichotomy exists, where the increased steric requirements for a more stable chiral axis in imidazoline-based axially chiral P,N ligands hinders the incorporation of phosphorus moieties into the compounds.

In terms of future work, work is on-going within the Guiry group exploring the synthesis of quaternary pyridyl salt analogues of UCDPhim (**Figure 18**). It is hoped that the formally positively charged quaternary pyridyl salt will have a stronger non-covalent interaction with the electron rich naphthalene core, which may lead to a more stable chiral axis in the compound.

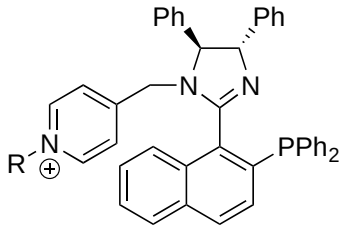

***Figure 18**: Quaternary pyridyl salt analogue of UCDPhim ligand*

Work is also on going in the group, investigating the potential for established imidazoline-based axially chiral P,N ligands through the use of aliphatic linker chains of varying length. It is hoped through the judicious choice of chain length that the free-rotation of the imidazoline-phenyl ring bond will be hindered in order to establish a stable chiral axis.

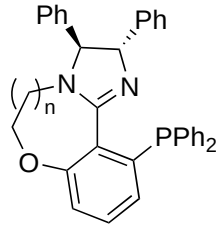

***Figure 19**: Investigations into imidazoline-based axially chiral P,N ligands with aliphatic linker chains*

In recent years, tools for synthesising other axially chiral scaffolds, including indole- and quinolone-based compounds with ligand **93** *via* organocatalysis and central to axial chirality strategies, have been developed.[70,71,72] These newer strategies allow for the stereospecific access of axially chiral heteroaryl compounds without the need for in-built resolution centres or expensive chiral salts (**Scheme 75**).

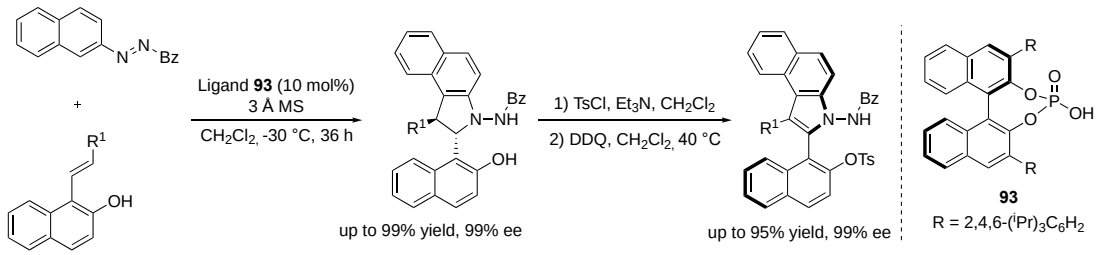

***Scheme 75**: Example of central to axial chirality transfer synthesis in the literature*[73]

The reported methodology by Zhou was also used towards accessing a monodentate phosphorus based ligand for asymmetric catalysis, **Scheme 75**.[73] The established chemistry by Zhou is repeated to furnish the triflated centrally chiral compound **94**, **Scheme 76**. It is proposed that a NBS-mediated oxidation of **94** would yield product **95**, which could be then reacted under the same Ni-catalysed C-P bond forming conditions used within the group.[16] This could furnish novel axially chiral P,N ligands with structures similar to the original aim of this current project. The maintenance of the centrally chiral group in the compound would allow for similar resolution of diastereomeric product **96**, in the event that epimerisation about the chiral axis occurred during the elevated temperatures for the proposed C-P bond forming steps.

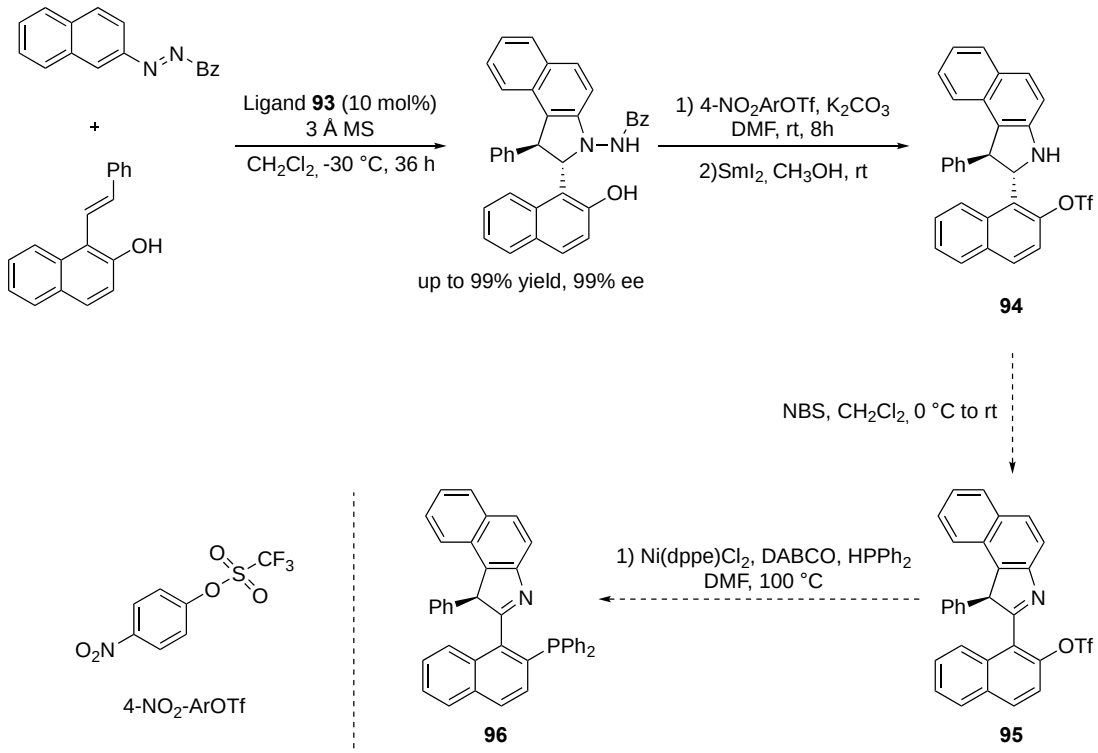

***Scheme 76**: Proposed route towards novel axially chiral P,N ligand*

Experimental

All chemicals were purchased from Sigma-Aldrich, Acros, or Fluorochem unless otherwise stated. Anhydrous solvents were obtained from a Puresol Grubbs solvent system unless otherwise stated. All the solvents were reagent grade and were used as received. Toluene and dimethylformamide (DMF) were dried and degassed using standard protocols. *N*-Bromosuccinimide (NBS) was recrystallised from water using standard protocols. Column chromatography was performed on Davilsil LC60A 40-63 micron silica gel. Thin-layer chromatography (TLC) was performed on aluminium-backed sheets purchased from Merck pre-coated with silica 60 F254. All reactions were performed under an atmosphere of N_2 and in flame-dried glassware unless otherwise stated. The Varian 300 MHz, 400 MHz and 500 MHz NMR instruments were used for the recording of ^{1}H NMR, ^{13}C NMR, ^{19}F NMR and ^{31}P NMR spectra. Deuterated chloroform was used as the solvent for recording NMR spectra unless otherwise state, the chemical shifts (δ) are given in parts per million and the coupling constants (*J*) are given in absolute values expressed in Hz. HRMS were measured on a Micromass/Water LCT mass spectrometer. Infrared spectra were recorded on a FT-IR spectrometer and are reported in terms of wavenumbers (*v*max) with units of reciprocal centimetres (cm^{-1}). Supercritical fluid chromatography (SFC) was performed on a Waters Acquity UPC2 ® instrument with Chiralpak ® IA3, IB3, IC3 and ID3 columns. Optical rotation measurements were recorded using a Schmidt-Haensch Unipol L2000 polarimeter at 589 nm and are quoted in units of deg dm^{-1} cm^3 g^{-1} (concentration c is given in g/100 mL).

(4*S*,5*S*)-2,4,5-Triphenyl-4,5-dihydro-1*H*-imidazole **44**[74]

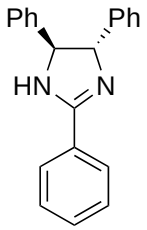

(1*S*,2*S*)-(–)-1,2-Diphenyethylenediamine (213 mg, 1.00 mmol, 1 equiv.) was added to a flame-dried 50 mL Schlenk flask. CH_2Cl_2 (10 mL) was added followed by freshly recrystallised N-bromosuccinimide (267 mg, 1.50 mmol, 1.5 equiv.). The reaction was stirred at rt for 24 h. The reaction was quenched with a saturated solution of sodium thiosulfate solution (150 mL) and CH_2Cl_2 (100 mL) was added. The organic phase was separated and was washed with H_2O (4 x 150 mL). The organic phase was dried with magnesium sulfate, was filtered and was concentrated *in vacuo*. The crude product was purified by flash column chromatography (10% to 60% EtOAc/cyclohexane) to yield the title compound as a white solid (83 mg, 27% yield). $\mathbf{R_f}$ = 0.3 (60% EtOAc/cyclohexane);**^{1}H NMR** (400 MHz, $CDCl_3$) δ 7.97 – 7.87 (m, 2H), 7.53 – 7.39 (m, 4H), 7.37 – 7.21 (m, 11H), 4.88 (s, 2H); **^{13}C NMR** (101 MHz, $CDCl_3$) δ 163.2, 143.6, 131.1, 130.2, 128.8, 128.7, 127.6, 127.5, 126.7. All characterisation data are in agreement with reported literature data.

(4*S*,5*S*)-2-(2-Methoxynaphthalen-1-yl)-4,5-diphenyl-4,5-dihydro-1*H*-imidazole **26**[17]

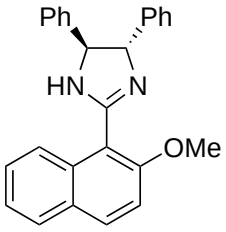

2-Methoxy-1-naphthaldehyde (1.86 g, 10 mmol, 1 equiv.) was added to a flame-dried 3 neck round-bottomed flask. CH_2Cl_2 (110 mL, 0.1 M) was cooled to 0 °C and (1*S*,2*S*)-(–)-1,2-diphenyethylenediamine (2.18 g, 10.5 mmol, 1.05 equiv.) was added. The

reaction mixture was allowed to warm to room temperature and was stirred for 24 h. The reaction was cooled to 0 °C and freshly recrystallised NBS (2.14 g, 12.0 mmol, 1.2 equiv.) was added. The reaction was allowed to stir at room temperature for 21 h. The reaction mixture was quenched with sat. aq. sodium thiosulfate solution, washed with water (5 x 100 mL), extracted with excess CH_2Cl_2 (3 x 100 mL). The organics were combined, washed with brine (100 mL), dried with magnesium sulfate and concentrated *in vacuo* to give a gummy oil which was purified by flash column chromatography (60% EtOAc/cyclohexane to 5% MeOH/$CHCl_3$) to give the title compound as a yellow solid (1.46 g, 37%).**R_f** = 0.45 (10% $CHCl_3$/MeOH); **^{1}H NMR** (300 MHz, DMSO-d6) δ 8.12 (d, *J* = 9.1 Hz, 1H), 8.05 – 8.00 (m, 1H), 7.96 (d, *J* = 8.2 Hz, 1H), 7.64 – 7.25 (m, 13H), 4.96 (s, 2H), 4.03 (s, 3H). All characterisation data are in agreement with reported literature data.

(4*S*,5*S*)-2-(2-Methoxynaphthalen-1-yl)-1-[(perfluorophenyl)methyl)]-4,5-diphenyl-4,5-dihydro-1*H*-imidazole **27**[17]

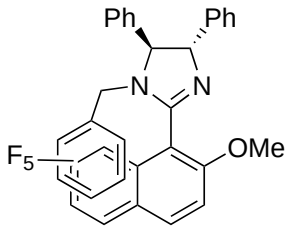

(4*S*,5*S*)-2-(2-Methoxynaphthalen-1-yl)-1-((perfluorophenyl)methyl)-4,5-diphenyl-4,5-dihydro-1*H*-imidazole (1.46 g, 3.86 mmol, 1.0 equiv.) was dissolved in DMF (6.5 mL) and then THF (32 mL) was added (THF:DMF, 5:1, 0.1 M). The reaction mixture was cooled to 0 °C and sodium hydride (314 mg 60% dispersion in mineral oil, 7.85 mmol, 2 equiv.) was added. The reaction was stirred at 0 °C for 30 min and then 2,3,4,5,6-pentafluorobenzyl bromide (1.07 g, 4.1 mmol, 1.05 equiv.) in THF (5 mL) was added dropwise. The reaction was allowed to warm to room temperature and was stirred for 21 h. The reaction was cooled to 0 °C and was quenched slowly with water (40 mL) until no evolution of gas was observed. THF was removed under

reduced pressure. The reaction mixture was then dissolved in EtOAc (50 mL) and was washed with water (4 x 100 mL). The organics were combined, washed with brine (50 mL), dried with magnesium sulfate and concentrated *in vacuo* to give a crude product which was purified using flash column chromatography (30% EtOAc/cyclohexane to 60% EtOAc/cyclohexane) to give compound the title compound as a yellow solid in a 1:1 atropdiastereomeric ratio (1.33 g, 62%). $\mathbf{R_f}$ = 0.50 (100% EtOAc); **^{1}H NMR** (300 MHz, $CDCl_3$) δ 8.06 (d, *J* = 8.5 Hz, 1H), 7.95 (dd, *J* = 9.1, 4.1 Hz, 2H), 7.87 –7.77 (m, 3H), 7.62 (m, 1H), 7.56 – 7.21 (m, 22H), 5.32 – 5.20 (m, 2H), 4.76 (d, *J* = 7.9 Hz, 1H), 4.48 (d, *J* = 10.2 Hz, 1H), 4.33 – 4.19 (m, 2H), 4.20 – 3.99 (m, 5H); **^{19}F NMR** (282 MHz, $CDCl_3$) δ -141.58 (dd, *J* = 22.6, 8.4 Hz), -142.45 (dd, *J* = 22.6, 8.4 Hz), -155.68 (t, *J* = 20.8 Hz), -156.00 (t, *J* = 20.8 Hz), -162.91 (td), -163.34 (td). All characterisation data are in agreement with reported literature data.

1-((4*S*,5*S*)-1-((Perfluorophenyl)methyl)-4,5-diphenyl-4,5-dihydro-1*H*-imidazol-2-yl)naphthalen-2-ol[17]

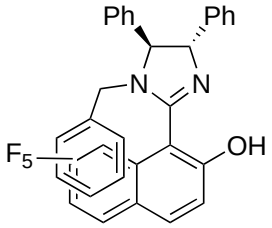

1-((4*S*,5*S*)-1-((Perfluorophenyl)methyl)-4,5-diphenyl-4,5-dihydro-1*H*-imidazol-2-yl)naphthalen-2-ol (1.01 g, 1.81 mmol, 1.0 equiv.) was dissolved in CH_2Cl_2 (36 mL, 0.05 M) and was cooled to 0 °C. Boron tribromide (9.0 mL, 1.0 M in heptane, 9 mmol, 5 equiv.) was added in a dropwise fashion. The reaction mixture was allowed to warm to room temperature and was stirred until completion of the reaction (14 h). The reaction mixture was then cooled to 0 °C and the pH was ad*J*usted to ~7 with 1 M NaOH solution (12 mL). The phases were separated and the aqueous phase was extracted with excess CH_2Cl_2 (3 x 50 mL). The organics were combined, washed with brine (100 mL), dried with magnesium sulfate. The reaction mixture was

concentrated *in vacuo* to afford the phenol as a brown solid in a quantitative yield. The crude product was used in the next reaction without purification.

1-((4*S*,5*S*)-1-((Perfluorophenyl)methyl)-4,5-diphenyl-4,5-dihydro-1*H*-imidazol-2-yl)naphthalen-2-yl trifluoromethanesulfonate **28**[17]

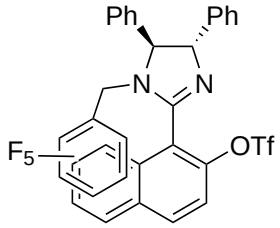

The crude naphthol (0.98 g, 1.81 mmol, 1.0 equiv.) was suspended in CH_2Cl_2 (18 mL, 0.1 M). 4-Dimethylaminopyridine (0.89 g, 7.23 mmol, 4 equiv.) was added and the reaction was stirred for 10 min. Triflic anhydride (2.80 mL, 1.0 M in CH_2Cl_2, 2.8 mmol, 1.5 equiv.) was added in a dropwise fashion. The reaction was allowed to warm to room temperature and was stirred for 24 h. The reaction was then re-cooled to 0 °C and the pH was adJusted to ~7 with 1 M HCl solution. The phases were separated and the aqueous phase was extracted with extra portions of CH_2Cl_2 (3 x 30 mL). The organics were combined, washed with brine (100 mL), dried with magnesium sulfate. The organic layers were filtered and concentrated *in vacuo* to afford a solid which was purified by flash column chromatography (10% to 30% EtOAc/cyclohexane) to give compound the title compound as a white solid (1.06 g, 94%). $\mathbf{R_f}$ = 0.75 (50% EtOAc/cyclohexane); **^{1}H NMR** (300 MHz, $CDCl_3$) δ 8.29 (d, *J* = 8.4 Hz, 1H), 8.11 – 7.92 (m, 5H), 7.79 (ddd, *J* = 8.4, 6.9, 1.3 Hz, 1H), 7.72 – 7.53 (m, 5H), 7.44 – 7.21 (m, 20H), 5.29 (t, *J* = 11.8 Hz, 2H), 4.70 (d, *J* = 10.7 Hz, 1H), 4.55 (d, *J* = 11.8 Hz, 1H), 4.26 – 43.99 (m, 4H); **^{19}F NMR** (282 MHz, $CDCl_3$) δ -73.75, -73.79, -141.18 (dd, *J* = 22.4, 8.4 Hz), -141.85 (dd, *J* = 22.4, 8.4 Hz), - 154.69 (t, *J* = 20.8 Hz), -154.93 (t, *J* = 20.8 Hz), -162.38 – -162.60 (m), -162.86 (td, *J* = 22.4, 8.4 Hz). All characterisation data are in agreement with reported literature data.

(4S,5S)-2-(2-(Diphenylphosphaneyl)naphthalen-1-yl)-1-((perfluorophenyl)methyl)-4,5-diphenyl-4,5-dihydro-1*H*-imidazole[17]

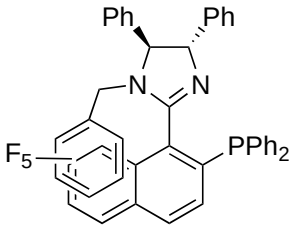

A flamed-dried Schlenk flask (25 mL) was charged with $NiCl_2$(dppe) (61 mg, 0.16 mmol, 0.10 equiv.). Anhydrous and degassed DMF (4 mL) and diphenylphosphine (0.15 mL, 1.2 mmol, 0.75 equiv.) were added and the solution was stirred at 100 °C for 30 min. A solution of (4S,5S)-2-(2-(Diphenylphosphaneyl)naphthalen-1-yl)-1-((perfluorophenyl)methyl)-4,5-diphenyl-4,5-dihydro-1*H*-imidazole (767 mg, 1.16 mmol, 1 equiv.) in DMF (4 mL) was added and the reaction mixture was stirred at 100 °C for an additional hour. A second portion of diphenylphosphine (0.15 mL, 1.2 mol, 0.75 equiv.) was added and the reaction mixture was then stirred for 68 h. CH_2Cl_2 (20 mL) was added and the reaction mixture was filtered through Celite®. The organics were washed with water (200 mL x 4), followed by brine (20 mL) and then was dried with magnesium sulfate. The organics were filtered and the volatiles were removed under reduced pressure to afford a white solid product (491 mg, 59%) in a ~3:1 atropdiastereomeric ratio. $\mathbf{R_f}$ = 0.70 (50% EtOAc/cyclohexane).

Separation of atropdiastereomers of (4*S*,5*S*)-2-(2-(Diphenylphosphaneyl)naphthalen-1-yl)-1-((perfluorophenyl)methyl)-4,5-diphenyl-4,5-dihydro-1*H*-imidazole (UCDPhim)

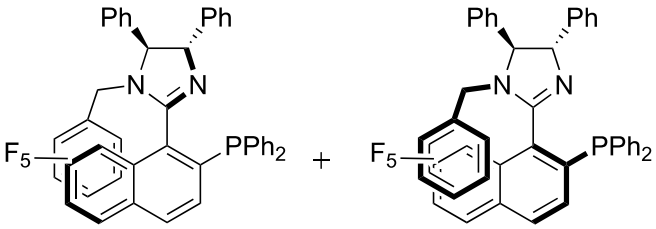

(S,S,R_a)-UCDPhim (S,S,S_a)-UCDPhim

The crude product (491 mg, ~3:1 atropdiastereomeric ratio) was loaded on a flash chromatography column (30 cm length x 4 cm width). The column was performed with a very gradual increase in gradient (3% Et_2O/CH_2Cl_2 to 5% Et_2O/CH_2Cl_2 to 8% Et_2O/CH_2Cl_2). This afforded both atropisomers of the UCDPhim ligand with some co-elution of atropisomers being unavoidable.

(*S*,*S*,*Ra*)-UCDPhim (290 mg) $\mathbf{R_f}$ = 0.52 (5% Et_2O/CH_2Cl_2); **^{1}H NMR** (400 MHz, $CDCl_3$) δ 8.24 (d, *J* = 8.4 Hz, 1H), 7.83 (dd, *J* = 8.4, 1.9 Hz, 2H), 7.69 (ddd, *J* = 8.2, 6.8, 1.3 Hz, 1H), 7.60 (ddd, *J* = 8.2, 6.8, 1.3 Hz, 1H), 7.44 – 7.20 (m, 16H), 7.17 – 7.11 (m, 1H), 7.09 – 7.02 (m, 2H), 6.86 – 6.81 (m, 2H), 5.20 (dd, *J* = 11.9, 3.0 Hz, 1H), 4.58 (d, *J* = 11.9 Hz, 1H), 4.50 (d, *J* = 14.0 Hz, 1H), 4.32 (d, *J* = 14.0 Hz, 1H); **^{31}P NMR** (162 MHz, $CDCl_3$) δ -11.60; **^{19}F NMR** (376 MHz, $CDCl_3$) δ -140.70 (dd, *J* = 22.7, 8.0 Hz), -155.89 (t, *J* = 20.8 Hz), -163.37 (td, *J* = 22.1, 8.2Hz). All characterisation data are in agreement with reported literature data.

(*S*,*S*,*Sa*)-UCDPhim (40 mg) $\mathbf{R_f}$ = 0.32 (5% Et_2O/CH_2Cl_2);**^{1}H NMR** (500 MHz, $CDCl_3$) δ 7.89– 7.81 (m, 3H), 7.67 (d, *J* = 7.5 Hz, 2H), 7.57 – 7.49 (m, 3H), 7.46 – 7.27 (m, 18H), 5.24 (d, *J* = 10.6 Hz, 1H), 4.85 (d, *J* = 10.6 Hz, 1H), 4.19 (d, *J* = 15.3 Hz, 1H), 3.89 – 3.84 (m, 1H); **^{13}C NMR** (126 MHz, $CDCl_3$) δ 162.0, 161.9, 143.5, 141.3, 136.9, 136.9, 136.8, 136.1, 135.9, 134.9, 134.8, 134.1, 133.9, 133.5, 133.4, 133.3, 131.6, 131.5, 129.9, 129.7, 128.9, 128.7, 128.7, 128.6, 128.5, 128.4, 128.3, 128.3, 128.1, 128.0, 127.1, 127.0, 126.9, 126.7, 125.2, 79.6, 75.7, 36.6; **^{31}P NMR** (121 MHz, $CDCl_3$) δ -12.20; **^{19}F**

NMR (282 MHz, $CDCl_3$) δ -141.09 (m), -155.42 (t), -162.67 (td, *J* = 29.2 Hz); **HRMS**: (ESI-TOF) calculated for $C_{44}H_{30}F_5N_2P$ [M + H]+713.2145, found 713.2131 All characterisation data are in agreement with reported literature data.

2-Bromo-1-naphthaldehyde[75]

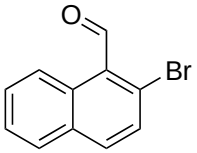

A flame-dried three-neck round-bottomed flask was charged with chloroform (100 mL) and phosphorus tribromide (8.90 mL, 104.13 mmol, 2.5 equiv.). The reaction was cooled to 0 °C and DMF (8.75 mL, 113.47 mmol, 3 equiv.) was added. 2-Tetralone (5.0 mL, 37.83 mmol, 1 equiv.) as a solution in chloroform (100 mL) was subsequently added and the reaction was refluxed at 70 °C until the starting material was consumed (1.5 h by TLC). The reaction was quenched with saturated sodium bicarbonate solution (100 mL) – ***caution – gas evolution.*** The phases were separated and the aqueous was extracted with CH_2Cl_2 (4 x 100 mL). The combined organics were dried with magnesium sulfate, filtered and concentrated *in vacuo*. The crude reaction mixture was used without purification.

The reaction mixture was dissolved in toluene (265 mL) was transferred to a flame-dried three-neck 500 mL round-bottomed flask. 2,3-Dichloro-5,6-dicyano-*p*-benzonquinone (8.60 g, 37.94 mmol, 1 equiv.) was added and the reaction was refluxed at 110 °C for 3 d. The reaction mixture was filtered through Celite® with CH_2Cl_2 to give the crude product. The product was purified using column chromatography (5% EtOAc/cyclohexane) to give the title compound (1.51 g, 17%) as a yellow solid. **^{1}H NMR** (300 MHz, $CDCl_3$) δ 10.76 (s, 1H), 9.16 – 9.07 (m, 1H), 7.90 – 7.86 (m, 2H), 7.74 – 7.48 (m, 3H). All characterisation data are in agreement with reported literature data.

(4*S*,5*S*)-2-(2-Bromonaphthalen-1-yl)-4,5-diphenyl-4,5-dihydro-1*H*-imidazole **46**

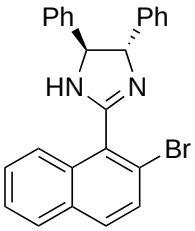

2-Bromo-naphthaldehyde (2.40 g, 10.2 mmol, 1 equiv.) was added to a flame-dried 250 mL three-neck round-bottomed flask. CH_2Cl_2 (110 mL) was added and the reaction was cooled to 0 °C. (1*S*,2*S*)-(–)-1,2-Diphenyethylenediamine (2.27 g, 10.71 mmol, 1.05 equiv.) was added and the reaction was allowed to warm to rt. The reaction was stirred for 24 h at rt. The reaction was cooled to 0 °C and freshly recrystallised N-bromosuccinimide (2.18 g, 12.24 mmol ,1.2 equiv.) was added. The reaction was allowed to warm to rt and was stirred for 24 h. The reaction was quenched with sat. aq. sodium thiosulfate solution (300 mL). The phases were separated and the organic phase was washed with H_2O (3 x 200 mL) followed by brine (200 mL). The organic phase was dried with magnesium sulfate, filtered and concentrated *in vacuo* to afford the crude product was a brown solid. The product was purified by column chromatography (30% to 60% EtOAc/cyclohexane) to afford the title compounds as a white solid product (2.13g, 53%). $\mathbf{R_f}$ = 0.6 (60% EtOAc/cyclohexane); **^{1}H NMR** (500 MHz, $CDCl_3$) δ 8.25 – 8.20 (m, 1H), 7.88 – 7.83 (m, 1H), 7.79 (d, *J* = 8.7 Hz, 1H), 7.67 (d, *J* = 8.7 Hz, 1H), 7.65 – 7.60 (m, 1H), 7.58 – 7.51 (m, 1H), 7.47 – 7.36 (m, 8H), 7.36 – 7.30 (m, 2H), 5.46 – 4.99 (m, 2H); **^{13}C NMR** (126 MHz, $CDCl_3$) δ 161.9, 160.6, 142.9, 142.7, 132.7, 132.5, 132.0, 131.8, 130.9, 130.7, 130.4, 129.5, 128.7, 128.6, 128.1, 128.1, 127.9, 127.9, 127.6, 127.5, 127.0, 126.9, 126.8, 126.7, 126.6, 126.6, 125.4, 125.3, 120.2, 77.2. All characterisation data are in agreement with reported data within the Guiry group.

(4S,5S)-2-(2-Bromonaphthalen-1-yl)-1-((perfluorophenyl)methyl)-4,5-diphenyl-4,5-dihydro-1*H*-imidazole **47**

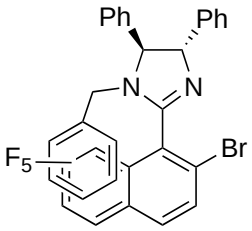

Imidazoline **46** (1.91 g, 4.46 mmol, 1 equiv.) was added to a 250 mL flame-dried three-neck round-bottomed flask. DMF (7.5 mL) and THF (40 mL) were added and the reaction was cooled to 0 °C. Sodium hydride (540 mg, 60% dispersion in mineral oil, 13.5 mmol, 3.02 equiv.) was added and the reaction mixture was stirred for 30 min. Pentafluorobenzyl bromide (1.38 g, 0.80 mL, 5.35 mmol ,1.2 equiv.) in THF (8 mL) was added dropwise while the reaction was maintained at 0 °C. The reaction was allowed to warm to rt and was stirred for 48 h. The reaction was quenched with H_2O (15 mL) at 0 °C. The THF in the reaction mixture was removed *in vacuo*. The reaction mixture was dissolved in EtOAc (200 mL), was washed with H_2O (4 x 200 mL) followed by brine (150 mL). The combined organics were dried with magnesium sulfate, filtered and concentrated *in vacuo* to afford the crude product was a white solid. The product was purified by column chromatography (20% EtOAc/cyclohexane) to afford the product as a (1.6 g, 59%) white solid. $\mathbf{R_f}$ = 0.23 (20% EtOAc/cyclohexane); **^{1}H NMR** (400 MHz, $CDCl_3$) δ 8.14 (d, *J* = 8.7 Hz, 1H), 7.92 – 7.79 (m, 5H), 7.76 – 7.67 (m, 3H), 7.63 – 7.45 (m, 5H), 7.43 – 7.21 (m, 18H), 5.40 – 5.35 (m, 0.7H), 5.30 – 5.25 (m, 1.3H), 4.80 – 4.75 (m, 0.7H), 4.57 – 4.51 (m, 1.3H), 4.32 – 4.23 (m, 1.3H), 4.20 – 4.10 (m, 2H), 4.06 – 3.96 (m, 0.7H); **^{19}F NMR** (376 MHz, $CDCl_3$) δ -141.24 (m), -141.60 (m), -154.94 – -155.30 (m), -155.50 (m), -162.41 – -162.84 (m), -162.90 – -163.33 (m). All characterisation data are in agreement with reported data within the Guiry group.

(4*S*,5*S*)-2-(Naphthalen-1-yl)-4,5-diphenyl-4,5-dihydro-1*H*-imidazole **52**

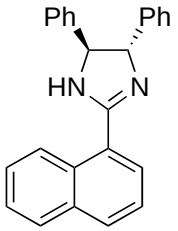

A 250 mL three-neck round-bottomed flask was flame-dried and CH_2Cl_2 (100 mL) was added. 1-Naphthaldehyde (1. 56 g, 1.38 mL, 10 mmol, 1 equiv.) was added and the flask was cooled to 0 °C. (1*S*,2*S*)-(–)-1,2-diphenyethylenediamine (2.30 g, 12 mmol, 1.2equiv.) was added and the reaction was stirred at 0 °C for 1 h. The reaction was allowed to warm to rt and was stirred for a further 24 h. The reaction was cooled to 0 °C and freshly recrystallised N-bromosuccinimide (2.10 g, 12 mmol, 1.2 equiv.) was added. The reaction was allowed to warm to rt and was stirred for 3 d. The reaction was quenched with sat. aq. sodium thiosulfate solution (200 mL) and the phases were separated. The organic phase was washed with H_2O (4 x 200 mL), brine (200 mL) and was dried using magnesium sulfate. The organic phase was then filtered and concentrated *in vacuo* to give a crude solid. The crude product was purified using column chromatography (30% EtOAc/cyclohexane to 50% EtOAc/cyclohexane) to give the title compound (1.35 g, 39%). was a white solid. **Melting point**: 203 – 206 °C; $\mathbf{R_f}$ = 0.5 (50% EtOAc/cyclohexane); **^{1}H NMR** (400 MHz, DMSO-d_6) δ 9.08 – 8.98 (m, 1H), 8.06 (d, *J* = 8.4 Hz, 1H), 8.03 – 7.95 (m, 2H), 7.84 (s, 1H), 7.64 – 7.53 (m, 3H), 7.44 – 7.26 (m, 9H), 4.84 (s, 2H); **^{13}C NMR** (101 MHz, DMSO-d_6) δ 163.2, 144.3, 133.4, 130.7, 130.4, 128.7, 128.3, 128.3, 127.3, 127.2, 126.8, 126.5, 126.3, 126.2, 125.1; **IR** ν(cm^{-1}): 3056, 3026, 2915, 1510, 1254, 693, 531; **$[\alpha]^{20}$D** = -29.53 (c = 0.1, $CHCl_3$); **HRMS**: (ESI-TOF) calculated for $C_{25}H_{21}N_2$ $[M + H]^+$ 349.1699, found 349.1703.

(4*S*,5*S*)-2-(Naphthalen-1-yl)-1-((perfluorophenyl)methyl)-4,5-diphenyl-4,5-dihydro-

(4*S*,5*S*)-2-(naphthalen-1-yl)-1-((perfluorophenyl)methyl)-4,5-diphenyl-4,5-dihydro-1*H*-imidazole 51

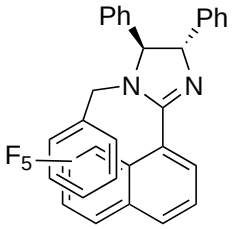

(4*S*,5*S*)-2-(Naphthalen-1-yl)-4,5-diphenyl-4,5-dihydro-1H-imidazole (0.93 g, 2.68 mmol, 1 equiv.) was added to a flame-dried 100 mL three neck round-bottomed flask and was dissolved in DMF (4.5 mL) followed by THF (22.5 mL) and the flask was then cooled to 0 °C. Sodium hydride (322 mg, 60% dispersion in mineral oil, 8.04 mmol, 3 equiv.) was added and the reaction was stirred for 30 min. 2,3,4,5-pentafluorobenzyl bromide (0.73 g, 0.425 mL, 2.81 mmol, 1.05 equiv.) was dissolved in THF (6 mL) and was added dropwise to the reaction at 0 °C. The reaction was allowed to warm to rt and was stirred for 16 h. The reaction was cooled to 0 °C, was quenched with H_2O (10 mL) and the THF was removed *in vacuo*. EtOAc (100 mL) was added and the solution was transferred to a separatory funnel. The organics were washed with H_2O (4 x 100 mL), brine (100 mL) and were dried with magnesium sulfate. The organics were filtered and concentrated *in vacuo*. The crude product was purified using column chromatography (20% to 30% EtOAc/cyclohexane) to give the title compound (1.02 g, 72%) as a white solid; **Melting point**: 67 – 69 °C; $\mathbf{R_f}$ = 0.5 (30% EtOAc/cyclohexane); **^{1}H NMR** (400 MHz, $CDCl_3$) δ 8.30 (d, *J* = 8.4 Hz, 1H), 7.98 (d, *J* = 8.3 Hz, 1H), 7.93 (d, *J* = 8.3 Hz, 1H), 7.87 (d, *J* = 7.0 Hz, 1H), 7.73 – 7.52 (m, 3H), 7.46 – 7.20 (m, 10H), 5.26 – 5.19 (m, 1H), 4.44 (s, 1H), 4.29 – 4.08 (m, 2H); **^{13}C NMR** (101 MHz, $CDCl_3$) δ 164.7, 155.9, 146.2, 143.7, 143.2, 141.1, 138.1, 135.6, 133.5, 131.0, 130.3, 128.70, 128.65, 128.5, 128.0, 127.4, 127.11, 127.08, 126.6, 126.4, 125.2, 125.0, 109.9, 79.0, 75.8, 38.9;**^{19}F NMR** (376 MHz, $CDCl_3$) δ -139.89 – -142.63 (m), -153.43 – -155.70 (m), -161.23 – -163.52 (m); **IR** ν(cm^{-1}): 3030, 2867, 1507, 964, 923, 671; **$[\alpha]^{20}$D** = +65.92 (c = 1, $CHCl_3$); **HRMS**: (ESI-TOF) calculated for $C_{32}H_{21}F_5N_2$ $[M + H]^+$ 528.1619, found 528.1618.=

(*S*)-*N*-(1-Hydroxy-3-methylbutan-2-yl)-1-naphthamide **56**

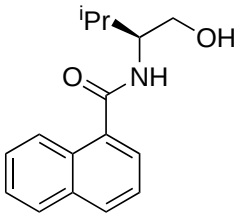

1-Naphthoic acid (3.0 g, 17.43 mmol, 1 equiv.) was added to a flame-dried 100 mL Schlenk flask and CH_2Cl_2 (50 mL) was added. Oxalyl chloride (9.0 mL, 106.4 mmol, 6.1 equiv.) and DMF (0.1 mL) were added and the reaction was stirred until homogenous (1 h) - ***caution - gas evolution***. The reaction was concentrated *in vacuo* using an in-line trap.

CH_2Cl_2 (75 mL) was added to a 500 mL flame-dried three necked-flask. L-Valinol (2.15 g, 20.9 mmol, 1.2 equiv.) and Et_3N (4.0 mL, 28.7 mmol, 1.6 equiv.) were added. The crude acid chloride was added to the three-necked flask in CH_2Cl_2 (2 x 20 mL) at rt and was stirred at rt for 18 h. The reaction mixture was washed with 1M HCl (2 x 200 mL) followed by 1M NaOH (2 x 200 mL). The organic phase was dried with magnesium sulfate, filtered and concentrated *in vacuo*. The crude solid was purified using column chromatography (40% to 60% EtOAc/pentane) to give the title compound as a white solid (3.40 g , 75% yield). **Melting point**: 120 – 122 °C; $\mathbf{R_f}$ = 0.24 in 40% EtOAc/pentane; **^{1}H NMR** (400 MHz, $CDCl_3$) δ 8.32 – 8.19 (m, 1H), 7.91 – 7.77 (m, 2H), 7.58 – 7.45 (m, 3H), 7.36 (dd, *J* = 8.2, 7.1 Hz, 1H), 6.33 (d, *J* = 8.8 Hz, 1H), 4.03 – 3.95 (m, 1H), 3.82 – 3.67 (m, 2H), 3.08 (s, 1H), 1.94 (h, *J* = 6.9 Hz, 1H), 1.02 – 0.96 (m, 6H); **^{13}C NMR** (101 MHz, $CDCl_3$) δ 170.7, 134.7, 133.7, 130.6, 130.2, 128.4, 127.3, 126.5, 125.5, 124.9, 124.8, 63.9, 57.6, 29.2, 19.7, 19.1; **IR** ν(cm^{-1}): 3463, 3329, 3047, 2961, 1625, 1610, 1298. **$[\alpha]^{20}D$** = -22.04 (c = 1, $CHCl_3$); **HRMS**: (ESI-TOF) calculated for $C_{16}H_{19}NO_2$ $[M + H]^+$ 258.1489, found 258.1490.

(*S*)-1-(*tert*-Butyl)-4-isopropyl-2-(naphthalen-1-yl)-4,5-dihydro-1*H*-imidazole **57**

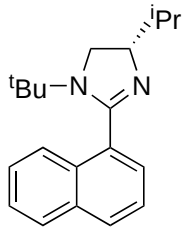

(*S*)-*N*-(1-hydroxy-3-methylbutan-2-yl)-1-naphthamide (1.33 g, 5.18 mmol, 1 equiv.) was added to a flame-dried 25 mL Schlenk flask. Thionyl chloride (2.0 mL, 27.4 mmol, 5.3 equiv.) was added and the reaction was heated at 80 °C for 18 h - ***caution - gas evolution***. Anhydrous toluene (1 mL) was added and the reaction was concentrated *in vacuo* using an in-line trap. The crude chloroalkylimidoyl chloride was dissolved in CH_2Cl_2 (13 mL) and Et_3N (2.16 mL, 15.5 mmol, 3 equiv.) was added. A solution of *tert*-butylamine (0.66 mL, 6.28 mmol, 1.21 equiv.) in CH_2Cl_2 (5 mL) was added and was stirred at rt for 14 h. 2M NaOH (25 mL) was added and the reaction was stirred vigorously for 30 min. The phases were separated and the aqueous phase was extracted with CH_2Cl_2 (3 x 30 mL). The organic phases were combined, dried with magnesium sulfate, was filtered and concentrated *in vacuo*. The crude product was purified using column chromatography (19:2:1, pentane/Et_3N/EtOAc) to yield the title compound as a brown oil (1.05 g, 68% yield). **Melting point**: 74 – 77 °C; $\mathbf{R_f}$ = 0.33 (17:2:1, pentane/Et_3N/EtOAc); **^{1}H NMR** (400 MHz, $CDCl_3$) δ 8.00 – 7.93 (m, 1H), 7.83 – 7.74 (m, 2H), 7.50 – 7.38 (m, 4H), 3.96 – 3.84 (m, 1H), 3.74 – 3.65 (m, 1H), 3.49 – 3.24 (m, 1H), 1.97 – 1.83 (m, 1H), 1.09 – 1.02 (m, 6H), 0.96 (m, 9H); **^{13}C NMR** (101 MHz, $CDCl_3$) δ 164.1, 163.8, 134.0, 133.7, 133.3, 133.2, 132.3, 131.8, 128.8, 128.7, 128.0, 127.8, 126.6, 126.3, 126.2, 126.1, 126.0, 125.9, 125.9, 124.8, 124.8, 69.3, 69.3, 54.6, 54.4, 50.8, 50.6, 33.6, 33.4, 29.2, 28.9, 28.88, 19.2, 19.1, 18.8, 18.4; **IR** ν(cm^{-1}): 3043, 2958, 2872, 1603, 1528, 1506, 1356**. [α]^{20}D** = 0.38 (c = 0.1, $CHCl_3$); **HRMS**: (ESI-TOF) calculated for $C_{20}H_{26}N_2$ $[M + H]^+$ 295.2169, found 295.2177.

(*S*)-4-Isopropyl-2-(naphthalen-1-yl)-4,5-dihydro-1*H*-imidazole **58**

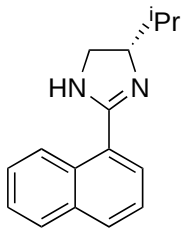

(*S*)-*N*-(1-Hydroxy-3-methylbutan-2-yl)-1-naphthamide (133 mg, 0.518 mmol, 1 equiv.) was added to flame-dried 10 mL Schlenk flask. Thionyl chloride (1.0 mL, 13.7 mmol, 26.4 equiv.) was added and the reaction was heated to 80 °C for 18 h - ***caution - gas evolution***. Anhydrous toluene (1 mL) was added and the reaction was concentrated *in vacuo* using an in-line trap. The crude chloroalkylimidoyl chloride was dissolved in CH_2Cl_2 (2 mL) and was stirred at rt. 7N NH_3 in MeOH (68 μL, 3.11 mmol, 6 equiv.) was added and the reaction was stirred at rt for 3 d. CH_2Cl_2 (2 mL) and 2M NaOH (5 mL) were added and the reaction was stirred vigorously for 30 min. The phases were separated and the aqueous was extracted with CH_2Cl_2 (3 x 3mL). The organic phases were combined, dried with magnesium sulfate, was filtered and concentrated *in vacuo*. The crude product was purified by column chromatography (20% EtOAc/cyclohexane with 1% Et_3N) to yield the title compound as a while solid (54 mg, 44% yield). **Melting point**: 153 – 155 °C.; $\mathbf{R_f}$ = 0.35 in 20% EtOAc/cyclohexane with 1% Et_3N); **^{1}H NMR** (400 MHz, $CDCl_3$) δ 8.31 (d, *J* = 8.2, 1H), 7.94 – 7.85 (m, 2H), 7.67 – 7.42 (m, 4H), 6.23 – 6.13 (m, 1H), 4.32 – 4.23 (m, 1H), 3.93 – 3.76 (m, 2H), 2.10 – 1.96 (m, 1H), 1.07 (m, 6H); **^{13}C NMR** (101 MHz, $CDCl_3$) δ 169.5, 134.6, 133.8, 130.8, 130.2, 128.4, 127.3, 126.6, 125.5, 125.0, 124.9, 55.6, 46.9, 29.6, 19.5, 19.2;**IR** ν(cm^{-1}): 3264, 2960, 1635, 1620, 1535, 768. **$[\alpha]^{20}D$** = -25.41 (c = 0.1, $CHCl_3$); **HRMS**: (ESI-TOF) calculated for $C_{16}H_{19}N_2$ $[M + H]^+$ 239.1543, found 239.1543.

(*S*)-4-Isopropyl-1-mesityl-2-(naphthalen-1-yl)-4,5-dihydro-1*H*-imidazole **59**

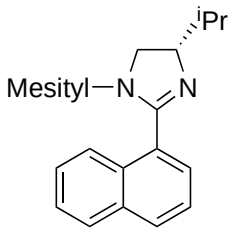

S)-*N*-(1-Hydroxy-3-methylbutan-2-yl)-1-naphthamide (500 mg, 1.40 mmol, 1 equiv.) was added to flame-dried 50 mL Schlenk flask. Thionyl chloride (2.0 mL, 27.4 mmol, 19.6 equiv.) was added and the reaction was heated to 80 °C for 18 h - ***caution - gas evolution***. Anhydrous toluene (2 mL) was added and the reaction was concentrated *in vacuo* using an in-line trap. The crude chloroalkylimidoyl chloride was dissolved in CH_2Cl_2 (7 mL) and was stirred at rt. Et_3N (0.80 mL, 5.82 mmol, 4.1 equiv.) was added, followed by 2,4,6-trimethylaniline (0.33 mL, 2.33 mmol, 1.66 equiv.) and the reaction was stirred at rt for 3 d. 2M NaOH (20 mL) were added and the reaction was stirred vigorously for 30 min. The phases were separated and the aqueous layer was extracted with CH_2Cl_2 (3 x 30 mL). The organic phases were combined, dried with magnesium sulfate, was filtered and concentrated *in vacuo*. The crude product was purified by column chromatography (5% EtOAc/cyclohexane with 1% Et_3N) to yield the title compound as a while solid (374 mg, 81% yield. **N.B** Product is hydroscopic and will take on water to form gum in air. $\mathbf{R_f}$ = 0.11 in 20% EtOAc/cyclohexane; **Melting point**: 65 – 68 °C; **^{1}H NMR** (400 MHz, $CDCl_3$) δ 8.84 (d, *J* = 8.5, 1H), 7.78 – 7.68 (m, 2H), 7.57 – 7.52 (m, 1H), 7.48 – 7.42 (m, 1H), 7.22 – 7.13 (m, 2H), 6.75(s, 1H), 6.66 (s, 1H), 4.36 – 4.27 (m, 1H), 3.88 – 3.81 (m, 1H), 3.52 (t, *J* = 9.5 Hz, 1H), 2.33 – 2.07 (m, 10H), 1.20 (d, *J* = 6.7 Hz, 3H), 1.10 (d, *J* = 6.7 Hz, 3H); **^{13}C NMR** (101 MHz, $CDCl_3$) δ 162.6, 136.8, 136.8, 136.5, 136.4, 134.0, 131.5, 129.8, 129.5, 129.5, 129.4, 128.3, 128.2, 126.8, 126.6, 125.8, 124.2, 71.8, 53.8, 33.8, 20.9, 19.7, 18.6, 18.5, 18.5, 18.5; **IR** ν(cm^{-1}): 3046, 2954, 2920, 2867, 1624, 1585, 775; **[α]^{20}D** = 5.96 (c = 0.1, $CHCl_3$); **HRMS**: (ESI-TOF) calculated for $C_{25}H_{28}N_2$ $[M + H]^+$ 357.2325, found 357.2325.

2-Iodo-1-naphthonitirile[84]

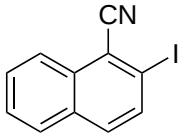

2,2,6,6-Tetramethylpiperidine (7.28 mL, 43.16 mmol, 1.05 equiv.) was added to a flame-dried 500 mL three-necked flask. Anhydrous THF (150 mL) was added and the reaction was cooled to 0 °C. *n*-BuLi (17.3 mL, 43.16 mmol, 2.5 M in hexanes, 1.05 equiv.) was added dropwise and the reaction was stirred for 1 h. The reaction was furthered cooled to -78 °C and 1-cyanonaphthalene (6.23 g, 41.03 mmol, 1 equiv.) was dissolved in anhydrous THF (12 mL) in a dropwise manner. Iodine (10.96 g, 43.16 mmol, 1.05 equiv.) in anhydrous THF (120 mL) was added and stirred for 2 h at -78 °C before warming to rt. The reaction was stirred at rt for 14 h.

The reaction was quenched with H_2O (100 mL) at 0 °C. The reaction mixture was extracted with EtOAc (3 x 150 mL). The combined organic phases were washed with a saturated sodium thiosulfate solution (2 x 100 mL), followed by 1 M HCl (150 mL) and brine (300 mL). The combined organic phases were dried using sodium sulfate, were filtered and concentrated *in vacuo*. The crude organic residue was recrystallised using hot chloroform with pentane as an anti-solvent. The pure product precipitated from solution and was isolated using vacuum filtration as a tan solid (4.89 g, 42% yield).**^{1}H NMR** (400 MHz, $CDCl_3$) δ 8.24 – 8.19 (m, 1H), 7.92 – 7.85 (m, 2H), 7.75 (dd, *J* = 8.8, 0.8 Hz, 1H), 7.71 – 7.60 (m, 2H); **^{13}C NMR** (101 MHz, $CDCl_3$) δ 135.2, 134.6, 133.7, 131.8, 129.6, 128.8, 128.0, 125.4, 118.7, 118.4, 100.3. All characterisation data are in agreement with reported literature data.

2-Iodo-1-naphthamide[46]

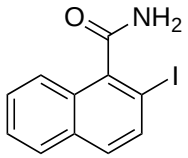

2-Iodo-1-naphthonitirile (4.89 g, 17.52 mmol, 1 equiv.) was added to H_2O (60 mL) and glacial acetic acid (120 mL) was added. The reaction was cooled to 0 °C and concentrated H_2SO_4 (100 mL) was added slowly. The reaction temperature was monitored and was not allowed to exceed 55 °C during H_2SO_4 addition. The reaction was subsequently refluxed at 120 °C for 17 h. The reaction was quenched by pouring the reaction mixture into an ice solution (300 mL). The combined aqueous phases were extracted using EtOAc (3 x 150 mL). The organic phases were combined and washed with 3 M NaOH (3 x 150 mL), dried using magnesium sulfate, were filtered and concentrated *in vacuo*. Toluene (300 mL) was added to the crude reaction paste before concentrating *in vacuo* (azeotrope for acetic acid). This was repeated in triplicate. The concentrated reaction mixture was then recrystallised from hot acetonitrile. The tan product was isolated *via* vacuum filtrated (2.99 g, 57% yield). **^{1}H NMR** (400 MHz, $CDCl_3$) δ 8.02 – 7.90 (m, 1H), 7.89 – 7.77 (m, 2H), 7.63 – 7.49 (m, 3H), 6.18 (s, 1H), 5.87 (s, 1H); **^{13}C NMR** (101 MHz, $CDCl_3$) δ 171.3, 140.4, 135.4, 132.53, 130.9, 130.6, 128.3, 128.0, 127.1, 125.3, 90.6 All characterisation data are in agreement with reported literature data.

(*E*)-1-Naphthaldehyde O-methyl oxime **66**[40, 76]

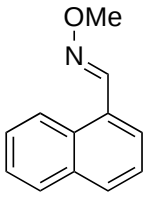

Methoxyamine hydrochloride (2.03 g, 24.36 mmol, 1.2 equiv.) was suspended in CH_2Cl_2 (60 mL) and pyridine anhydrous (6.45 g, 6.6 mL, 81.6 mmol, 4 equiv.) was added. 1-Naphthaldehyde (3.17 g, 2.78 mL, 20.32 mmol, 1 equiv.) was subsequently added and the reaction was stirred at rt for 48 h. The volatiles were removed *in vacuo*

and the crude product was filtered through a silica plug (50% EtOAc/cyclohexane) to give the title compounds as a brown oil (3.33 g, 88%). **^{1}H NMR** (500 MHz, $CDCl_3$) δ 8.72 (s, 1H), 8.53 (dq, *J* = 8.5, 0.9 Hz, 1H), 7.87 (dd, *J* = 8.5, 1.2 Hz, 2H), 7.76 (dt, *J* = 7.1, 0.9 Hz, 1H), 7.61 – 7.45 (m, 3H), 4.07 (s, 3H). All characterisation data are in agreement with reported literature data.

2-Iodo-1-naphthaldehyde[45]

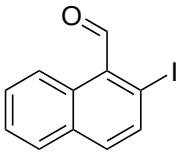

N,*N*,*N*'-Trimethylethylenediamine (1.25 mL, 9.8 mmol, 1.09 equiv.) was dissolved in THF (24 mL) and was cooled to –30 °C. *n*-BuLi (3.80 mL, 2.5 M, 9.5 mmol, 0.97 equiv.) was added and the solution was stirred for 15 min. 1-Naphthaldehyde (1.22 mL, 8.96 mmol, 1 equiv.) was dissolved in THF (6 mL) and was added dropwise to the amine solution. The reaction was stirred for 40 min. *n*-BuLi (11.0 mL, 2.5 M, 27.5 mmol, 3.07 equiv.) was added and the reaction was stirred at –30 °C for 16 h. Iodine (13.70 g, 53.9 mmol, 6 equiv.) was dissolved in THF (6 mL) and was added dropwise to the reaction mixture. The reaction was allowed to warm to rt and was stirred for 20 min. The reaction mixture was poured into HCl solution (120 mL, 1/3 *v*/*v* HCl/H_2O). The phases were separated and the aqueous was extracted with EtOAc (3 x 70 mL). The combined organics were washed with sat. aq. sodium thiosulfate solution (2 x 120 mL). The organic phases were dried with magnesium sulfate, were filtered and concentrated *in vacuo*. The crude product was purified using column chromatography (33% toluene/cyclohexane) to give the title compound as a yellow solid (0.255 g, 10% yield). **R_f** = 0.40 (33% toluene/cyclohexane); **^{1}H NMR** (500 MHz, $CDCl_3$) δ 10.42 (s, 1H), 9.04 (d, *J* = 8.7 Hz, 1H), 7.98 (d, *J* = 8.7 Hz, 1H), 7.86 – 7.81 (m, 1H), 7.65 (m, 2H), 7.61 – 7.57 (m, 1H). All characterisation data are in agreement with reported literature data.

2-Iodo-1-naphthoic acid[48]

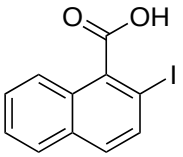

Sodium phosphate monobasic monohydrate (141 mg, 1.02 mmol, 0.24 equiv.) was dissolved in H_2O (2.0 mL). H_2O_2 (0.52 mL, 30% w/v in H_2O, 5.1 mmol, 1.2 equiv.) was added and the reaction was cooled to 0 °C. Acetonitrile (5 mL) and 2-iodo-naphthaldehyde (1.20 g, 4.25 mmol, 1 equiv.) were added. Sodium chlorite (600 mg, 6.63 mmol, 1.56 equiv.) was dissolved in H_2O (5 mL) and was added dropwise to the reaction. Acetonitrile (10 mL) was added, followed by a second portion of H_2O_2 (0.52 mL, 30% *w*/*w* in H_2O, 5.1 mmol, 1.2 equiv.). The reaction was stirred at rt for 24 h. An additional portion of sodium chlorite (600 mg, 6.63 mmol, 1.56 equiv.) and H_2O_2 (0.52 mL, 30% *w*/*w* in H_2O, 5.1 mmol, 1.2 equiv.) were added until the reaction the aldehyde was consumed by TLC. Sodium sulfite (0.75 g) was added to quench the reaction. The pH was ad*J*usted to 9 with 1M NaOH and was extracted with CH_2Cl_2 (3 x 50 mL). The aqueous was then ad*J*usted to pH 1 with concentrated HCl and was then extracted with EtOAc (3 x 100 mL). The combined organic phases were dried with magnesium sulfate, were filtered and concentrated *in vacuo* to give trace product of 2-iodo-naphthoic acid as a tan solid.**^{1}H NMR** (500 MHz, DMSO-d_6) δ 8.01 – 7.96 (m, 1H), 7.89 (d, *J* = 8.6 Hz, 1H), 7.78 – 7.74 (m, 2H), 7.62 (tt, *J* = 6.9, 5.2 Hz, 2H); **^{13}C NMR** (126 MHz, DMSO- d_6) δ 170.3, 140.0, 135.4, 132.2, 130.6, 130.2, 128.8, 128.4, 127.4, 124.9, 91.0. All characterisation data are in agreement with reported literature data.

2-Iodo-1-naphthoic acid[48] (See previous page for another synthesis)

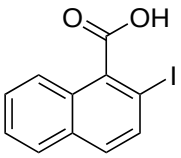

1-Naphthoic acid (2.00 g, 11.61 mmol, 1 equiv.), $Pd(OAc)_2$ (127 mg, 0.58 mmol, 5 mol%), (diacetoxyiodo)benzene (3.74 g, 11.61 mol, 1 equiv.), iodine (2.95 g, 11.61 mol, 1 equiv.) were added to a 250 mL three-neck round-bottomed flask under air atmosphere. DMF (58 mL, 0.2 M) was added and the reaction was heated at 110 °C for 24 h under an air atmosphere. The reaction was concentrated *in vacuo* in a fumehood and was directly purified by column chromatography (10 to 40% EtOAc/cyclohexane) to isolate the target compound as a tan coloured solid (1.27 g, 34%). $\mathbf{R_f}$ = 0.2 in 50% EtOAc/cyclohexane; **^{1}H NMR** (500 MHz, $CDCl_3$) δ 7.97 – 7.94 (m, 1H), 7.89 – 7.84 (m, 2H), 7.65 – 7.62 (m, 1H), 7.61 – 7.55 (m, 2H); **^{13}C NMR** (126 MHz, $CDCl_3$) δ 172.6, 136.9, 135.3, 132.2, 131.1, 130.7, 128.3, 128.0, 127.1, 124.7, 90.7. All characterisation data are in agreement with reported literature data.

2-Methoxy-1-naphthoic acid[82]

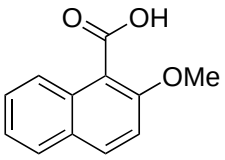

2-Methoxy-1-naphthaldehyde (5.58 g, 30 mmol, 1 equiv.) was added a 500 mL round bottomed flask containing *tert*-butanol:H_2O (66 mL, 1.2:1 *v*/*v*) at 30 °C. 2-Methyl-2-butene (21 mL, 198 mmol, 6.6 equiv.), sodium chlorite (4.38 g, 39 mmol, 1.3 equiv.) and sodium dihydrogen phosphate monohydrate (5.34 g, 38.7 mmo, 1.3 equiv.) were added -***caution - gas evolution***. The reaction was stirred at 30 °C for 2 d. The reaction was concentrated *in vacuo* in a fumehood using a rotary evaporator. H_2O (120 mL) was added and the reaction was washed with cyclohexane (3 x 120 mL). The aqueous

phase was acidified with 1M HCl (50 mL) to pH 1 and was extracted with Et_2O (3 x 300 mL). The combined organics were concentrated *in vacuo*. The crude reaction mixture was suspended in 2M NaOH (100 mL) and was extracted with CH_2Cl_2 (3 x 100 mL) to remove the remaining unreacted aldehyde starting material. The aqueous phase was acidified with conc. HCl (50 mL) and was extracted with Et_2O (3 x 200 mL). The combined organics were dried with magnesium sulfate, were filtered and concentrated *in vacuo* to furnish the pure target compound as a white solid (4.7 g, 77% yield). **^{1}H NMR** (500 MHz, $CDCl_3$) δ 8.44 (dd, *J* = 8.6, 1.1 Hz, 1H), 7.98 (d, *J* = 9.1 Hz, 1H), 7.84 – 7.80 (m, 1H), 7.58 (ddd, *J* = 8.6, 6.8, 1.1 Hz, 1H), 7.43 (ddd, *J* = 8.0, 6.8, 1.1 Hz, 1H), 7.33 (d, *J* = 9.1 Hz, 1H), 4.09 (s, 3H); **^{13}C NMR** (126 MHz, $CDCl_3$) δ 169.9, 155.9, 133.6, 131.7, 129.0, 128.4, 128.2, 124.8, 124.6, 115.7, 114.7, 112.8, 57.2. All characterisation data are in agreement with reported literature data.

(*S*)-*N*-(2-Hydroxy-1-phenylethyl)-2-methoxy-1-naphthamide **73**

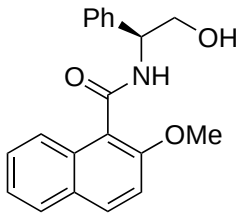

2-Methoxy-1-naphthoic acid (2.0 g, 9.89 mmol, 1 equiv.) was added to a flame-dried 100 mL Schlenk flask and CH_2Cl_2 (17 mL) was added. Oxalyl chloride (3.0 mL, 35.4 mmol, 3.6 equiv.) and DMF (0.1 mL) were added and the reaction was stirred at rt until the reaction mixture was homogenous (2 h) - ***caution - gas evolution***. The reaction was concentrated *in vacuo* using an in-line trap.

In a separate flame-dried 250 mL Schlenk flask, CH_2Cl_2 (50 mL) and (L)-phenylglycinol (1.63 g, 11. 87 mmol, 1.2 equiv.) were added. Et_3N (4.1 mL, 29.67 mmol, 3 equiv.) was then added. The crude acid chloride was added to the reaction mixture in CH_2Cl_2 (7 mL x 2) and was stirred at rt for 18 h. The reaction mixture was diluted with CH_2Cl_2 (100 mL), was washed with 1M HCl (2 x 100 mL) and 1M NaOH (2 x 100 mL). The

organic phase was separated, dried with magnesium sulfate, was filtered and concentrated *in vacuo*. The crude product was purified *via* recrystallisation from hot $CHCl_3$ to yield the target compound as a white solid (2.74 g, 86% yield). **Melting point**: 121 – 124 °C; **^{1}H NMR** (500 MHz, $CDCl_3$) δ 7.95 (d, *J* = 8.6 Hz, 1H), 7.90 – 7.86 (m, 1H), 7.79 – 7.76 (m, 1H), 7.50 – 7.46 (m, 1H), 7.44 – 7.41 (m, 2H), 7.40 – 7.35 (m, 3H), 7.34 – 7.29 (m, 1H), 7.28 – 7.25 (m, 2H), 6.66 (d, *J* = 7.6 Hz, 1H), 5.47 – 5.43 (m, 1H), 4.09 – 3.97 (m, 2H), 3.96 (s, 3H), 2.76 – 2.71 (m, 1H);**^{13}C NMR** (126 MHz, $CDCl_3$) δ 167.8, 153.5, 138.8, 131.5, 131.5, 128.8, 128.8, 128.0, 127.9, 127.7, 126.9, 124.4, 124.3, 120.1, 115.7, 112.9, 66.7, 56.8, 56.7, 56.2; **IR** ν(cm^{-1}): 3285, 3003, 1626, 1296, 1249, 748; **[α]^{20}D** = +16.10 (c = 1, $CHCl_3$); **HRMS**: (ESI-TOF) calculated for $C_{20}H_{19}NNaO_3$ [M + Na] 344.1257, found 344.1258.

2-Methoxy-1-naphthonitrile **75** [50]

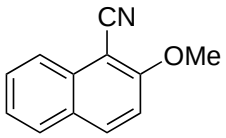

The title compound was isolated as the main product when phenylglycinol derived amide as used as a substrate for imidazoline formation (**Scheme 61**).**^{1}H NMR** (400 MHz, $CDCl_3$) δ 8.09 (dd, *J* = 8.4, 0.9 Hz, 1H), 8.03 (d, *J* = 9.2 Hz, 1H), 7.85 – 7.80 (m, 1H), 7.64 (ddd, *J* = 8.4, 6.9, 1.3 Hz, 1H), 7.47 – 7.42 (m, 1H), 7.29 – 7.25 (m, 1H), 4.07 (s, 3H); **^{13}C NMR** (101 MHz, $CDCl_3$) δ 161.6, 135.0, 133.6, 129.2, 128.5, 128.0, 125.1, 124.1, 115.7, 112.0, 95.3, 56.6. All characterisation data are in agreement with reported literature data.

(*S*)-*tert*-Leucinol[77]

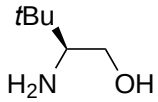

A flame-dried 500 mL three-neck round-bottomed flask was charged with $NaBH_4$ (4.31 g, 114 mmol, 2.4 equiv.). THF (140 mL) was added, followed by (*S*)-*tert*-leucine (6.23 g, 47.5 mmol, 1 equiv.) and the reaction was cooled to 0 °C. An iodine solution (12.05 g, 47.5 mmol, 1 equiv.) in THF (37.5 mL) was added slowly and the solution was allowed to stir at 0 °C until colourless. The ice bath was then removed and the solution was refluxed at 80 °C for 48 h. The reaction was then cooled to 0 °C and methanol (300 mL) was added (solution turned colourless from white). The solvent was then removed in *vacuo* to yield a white paste. This paste was dissolved in 20% aqueous KOH (75 mL) and was stirred at rt for 4 h, before being extracted with CH_2Cl_2 (3 x 50 mL). The organic phases were combined, dried with magnesium sulfate and were concentrated in *vacuo* to furnish (*S*)-*tert*-leucinol as a colourless waxy solid (4.03 g, 72%). **^{1}H NMR** (300 MHz, $CDCl_3$) δ 3.70 (dd, *J* = 10.2, 3.8 Hz, 1H), 3.22 (t, *J* = 10.2 Hz, 1H), 2.51 (dd, *J* = 10.2, 3.8 Hz, 1H), 0.89 (s, 9H) All characterisation data are in agreement with reported literature data.

(*S*)-*N*-(1-Hydroxy-3,3-dimethylbutan-2-yl)-2-iodo-1-naphthamide **76** [46]

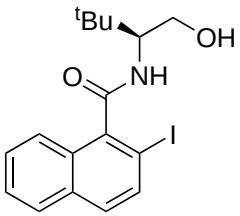

2-Iodo-naphthoic acid (2.06 g, 7.05 mmol, 1 equiv.) was added to a 100 mL flame-dried Schlenk flask. CH_2Cl_2 (35 mL) was added followed by oxalyl chloride (2.40 g, 1.6 mL, 8.35 mmol, 1.18 equiv.). The reaction was cooled to 0 °C and DMF (0.10 mL, catalytic) was added. The reaction was allowed to warm to rt and was stirred until

the solution became homogenous (1 h). The reaction mixture was concentrated *in vacuo* using an inline trap.

In a separate 250 mL flame-dried Schlenk flask, CH_2Cl_2 (50 mL) was added, followed by (*S*)-tert-leucinol (1.17 g, 1.3 mL, 10.58 mmol, 1.5 equiv.) and triethylamine (2.18 g, 3.0 mL, 21.5 mmol, 3.05 equiv.). The Schlenk flask was then cooled to 0 °C. The acid chloride was suspended in CH_2Cl_2 (16 mL) and was added to the (*S*)-tert-leucinol solution at 0 °C. The reaction was allowed warm to rt and was stirred for 4 d. The reaction was diluted with CH_2Cl_2 (50 mL), was washed with 1M HCl (2 x 80 mL) followed by 1M NaOH (2 x 80 mL) and brine (150 mL). The combined organics were dried with magnesium sulfate, were filtered and concentrated *in vacuo* to afford the crude product. The crude product was purified using column chromatography (30% EtOAc/cyclohexane) to give the title compound as a white solid (1.65 g, 59%). $\mathbf{R_f}$ = 0.15 (30% EtOAc/cyclohexane); **^{1}H NMR** (500 MHz, $CDCl_3$) δ 7.99 (s, 1H), 7.83 – 7.78 (m, 2H), 7.58 – 7.50 (m, 3H), 6.10 – 6.02 (m, 1H), 4.20 – 4.14 (m, 1H), 4.09 – 4.03 (m, 1H), 3.76 (s, 1H), 2.58 – 2.52 (m, 1H), 1.07 (s, 9H); **^{13}C NMR** (126 MHz, $CDCl_3$) δ 170.7, 141.3, 135.3, 132.6, 131.4, 130.5, 128.3, 128.0, 127.1, 125.4, 91.3, 63.5, 60.6, 60.5, 33.9, 27.5. All characterisation data are in agreement with reportedliterature data.

tert-Butyl carbamate **79**[78, 79]

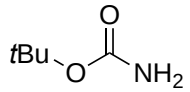

Di-*tert*-butyl dicarbonate (2.0 g, 10 mmol, 1 equiv.) was dissolved in EtOH (20 mL) and was stirred vigorously. Ammonium hydroxide (2.5 ml, 35% NH_3 in H_2O, 51 mmol, 5.1 equiv.) was added and the reaction was stirred for 24 h. The EtOH was removed *in vacuo* to give a white solid. The product was purified by recrystallisation in boiling pentane to give a white solid (1.17 g, 65%) which was isolated by vacuum filtration.**^{1}H NMR** (300 MHz, $CDCl_3$) δ 4.62 (s, 2H), 1.46 – 1.41 (m, 9H). All characterisation data are in agreement with reported literature data.

2-((Perfluorophenyl)methyl)isoindoline-1,3-dione **82**[80]

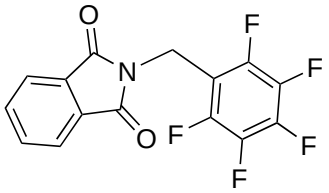

Phthalimide potassium salt (2.20 g, 11.6 mmol, 1 equiv.) was added to a flame-dried 100 mL Schlenk flask. DMF (18 mL) was added followed by pentafluorobenzyl bromide (3.12 g, 1.8 mL, 11.9 mmol, 1.03 equiv.). The reaction was stirred at room temperature for 24 h. The reaction mixture was poured into a beaker containing water (600 mL) and was allowed to sit for 2 h, before being cooled to 4 °C for 30 min to facilitate precipitation. The resulting white solid was filtered and dried *in vacuo*. Compound **82** was isolated as a white solid (3.43 g, 82%).**^{1}H NMR** (300 MHz, $CDCl_3$) δ 7.85 – 7.80 (m, 2H), 7.75 –7.70 (m, 2H), 4.94 (m, 2H);**^{19}F NMR** (282 MHz, $CDCl_3$) δ -141.67 – -141.80 (m), -154.05 – -154.20 (m), -161.64 – -161.88 (m).All characterisation data are in agreement with reported literature data.

(Perfluorophenyl)methanamine **80**[81]

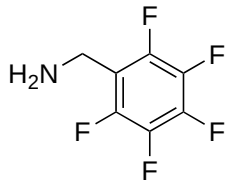

2-((Perfluorophenyl)methyl)isoindoline-1,3-dione (1.0 g, 3.05 mmol, 1 equiv.) was added to a flame-dried 50 mL Schlenk flask. MeOH (10 mL) was added and the solution was stirred vigorously. Hydrazine hydrate (0.46 mL, 9.15 mmol, 3 equiv.) was added and the reaction was refluxed at 70 °C for h. The reaction mixture was poured into a beaker containing 1M HCl (20 mL) and was filtered. 2M NaOH (50 mL) was added to the filtrate and the filtrate was then extracted with Et_2O (3 x 100 mL). The combined organics were dried with magnesium sulfate, were filtered and

concentrated *in vacuo*. The crude product was purified using silica gel column chromatography 20% to 30% EtOAc (with 0.5% Et_3N)/cyclohexane to give the title compound as a colourless oil (312 mg, 52%). **R_f** = 0.17 (30% EtOAc (with 0.5% Et_3N)/cyclohexane); **^{1}H NMR** (400 MHz, $CDCl_3$) δ 3.95 (s, 2H), 1.50 (s, 2H); **^{13}C NMR** (101 MHz, $CDCl_3$) δ 146.11, 143.68, 141.57, 138.87 (d, *J* = 36.0 Hz), 136.18, 116.21, 33.86;**^{19}F NMR** (376 MHz, $CDCl_3$) δ -145.46 – -145.80 (m), -156.42 (t, *J* = 20.6 Hz), -162.11 – -162.45 (m). All characterisation data are in agreement with reported literature data.

tert-Butyl (*S*)-4-(*tert*-butyl)-2-(2-iodonaphthalen-1-yl)-4,5-dihydro-1H-imidazole-1 carboxylate

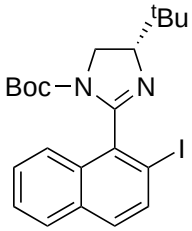

(*S*)-*N*-(1-Hydroxy-3,3-dimethylbutan-2-yl)-2-iodo-1-naphthamide (692 mg, 1.74 mmol, 1 equiv.) was added to a flame-dried 10 mL Schlenk flask. Thionyl chloride (2.0 mL, 27.4 mmol 27.4 equiv.) was added and the reaction was refluxed at 85 °C for 24 h. The reaction was cooled to rt and toluene (2 mL) was added (azeotrope). The volatiles were removed *in vacuo* using an inline trap.

In a flame-dried sealed tube, *tert*-butyl carbamate (500 mg, 4.27 mmol, 2.45 equiv.) was added and dissolved in CH_2Cl_2 (2 mL). Triethylamine (2.06 g, 1.5 mL, 20.4 mmol, 4.8 equiv.) was then added. The crude chloroalkylimidoyl chloride was suspended in CH_2Cl_2 (5 mL) and was added to the *tert*-butyl carbamate solution. The tube was then sealed and heated to 60 °C for 48 h. The reaction was diluted with CH_2Cl_2 (50 mL) and 2M NaOH was added (20 mL) followed by vigorous stirring for 30 min. The phases were separated and the aqueous was extracted with EtOAc (3 x 50 mL). The combined organics were dried with $MgSO_4$, were filtered and concentrated *in vacuo*.

The crude product was purified with column chromatography (5% to 10% EtOAc/cyclohexane) to give the title compound as a white solid (325 mg, 39%). **Melting point**: 92 – 94 °C; $\mathbf{R_f}$ = 0.10 (10% EtOAc/cyclohexane with 1% Et_3N); **^{1}H NMR** (500 MHz, $CDCl_3$) δ 7.84 – 7.75 (m, 2H), 7.73 – 7.64 (m, 1H), 7.54 (d, *J* = 8.7 Hz, 1H), 7.52 – 7.44 (m, 2H), 4.17 – 4.08 (m, 1H), 4.07 – 4.01 (m 1H), 3.90 – 3.79 (m, 1H), 1.14 – 1.08 (m, 9H), 0.91 – 0.75 (m, 9H); **^{13}C NMR** (126 MHz, $CDCl_3$) δ 157.4, 149.9, 149.8, 137.2, 135.3, 134.93, 134.8, 133.1, 132.6, 132.34, 132.27, 130.8, 129.8, 129.7, 128.0, 127.9, 127.6, 127.3, 127.2, 126.5, 126.4, 125.3, 125.1, 95.5, 94.5, 81.2, 74.7, 74.6, 47.9, 47.5, 34.4, 34.2, 27.33, 27.27, 26.8, 26.3.;**IR** ν(cm^{-1}): 3055, 1699, 1577, 1475, 1423, 1237, 675; **[α]^{20}D** = -48.58 (c = 0.1, $CHCl_3$); **HRMS**: (ESI-TOF) calculated for $C_{22}H_{27}IN_2O_2$ $[M + H]^+$ 479.1190, found 479.1184.

(*S*)-4-(*tert*-Butyl)-2-(2-iodonaphthalen-1-yl)-1-((perfluorophenyl)methyl)-4,5-dihydro-1H-imidazole

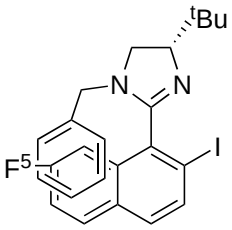

(*S*)-*N*-(1-Hydroxy-3,3-dimethylbutan-2-yl)-2-iodo-1-naphthamide (416 mg, 1.05 mmol, 1 equiv.) was added to a flame-dried 10 mL Schlenk flask. Thionyl chloride (2.0 mL, 27.4 mmol 26 equiv.) was added and the reaction was refluxed at 85 °C for 24 h. The reaction was cooled to rt and toluene (2 mL) was added (azeotrope). The volatiles were removed *in vacuo* using an inline trap.

In a flame-dried sealed tube, CH_2Cl_2 (3 mL) and 1-(perfluorophenyl)methanamine (227 mg, 1.15 mmol, 1.1 equiv.) were added. Triethylamine (0.50 mL, 3.46 mmol, 3 equiv.) was then added. The crude chloroalkylimidoyl chloride was suspended in CH_2Cl_2 (2 x 1 mL) and was added to the 1-(perfluorophenyl)methanamine solution. The tube was then sealed and heated to 60 °C for 48 h. The reaction was diluted with CH_2Cl_2 (40 mL) and 2M NaOH was added (30 mL) followed by vigorous stirring for 30

min. The phases were separated and the aqueous was extracted with EtOAc (3 x 50 mL). The combined organics were dried with magnesium sulfate, were filtered and concentrated *in vacuo*. The crude product was purified with column chromatography (20% Et_2O/cyclohexane with 1% Et_3N) to give the title compound as a white solid (295 mg, 50% yield). **Melting point**: 146 – 148 °C; $\mathbf{R_f}$ = 0.1 in 20% Et_2O/cyclohexane with 1% Et_3N; **^{1}H NMR** (500 MHz, $CDCl_3$) δ 7.89 – 7.84 (m, 1H), 7.83 – 7.79 (m, 0.5H), 7.80 – 7.75 (m, 0.5H), 7.74 – 7.68 (m, 1H), 7.62 – 7.56 (m, 1H), 7.55 – 7.42 (m, 2H), 4.26 – 4.20 (m, 0.5H), 4.20 – 4.10 (m, 1.5H), 4.08 – 3.99 (m, 1H), 3.67 – 3.55 (m, 1H), 3.51 – 3.45 (m, 0.5H), 3.33 – 3.27 (m, 0.5H), 1.12 – 1.05 (m, 9H); **^{13}C NMR** (126 MHz, $CDCl_3$) δ 163.7, 163.4, 146.1, 144.1, 141.6, 139.6, 138.1, 138.0, 136.1, 135.4, 134.9, 134.5, 134.2, 133.0, 132.6, 132.4, 130.7, 130.6, 130.4, 128.2, 128.1, 127.7, 127.3, 127.2, 126.9, 126.8, 126.6, 125.6, 125.1, 111.0, 97.0, 96.2, 75.5, 52.8, 52.1, 39.0, 38.5, 27.1, 26.5.; **^{19}F NMR** (376 MHz, $CDCl_3$) δ -142.15 (dd, *J* = 22.6, 8.4 Hz), -142.48 (dd, *J* = 22.4, 8.5 Hz), -154.76 (t, *J* = 20.8 Hz), -154.96 (t, *J* = 20.8 Hz), -161.84 – -162.20 (m);**IR** ν(cm^{-1}): 2949, 2864, 1656, 1563, 1519, 1042; **[α]^{20}D** = -41.71 (c = 0.1, $CHCl_3$); **HRMS**: (ESI-TOF) calculated for $C_{24}H_{20}F_5IN_2$ $[M + H]^+$ 559.0664, found 559.0664

(*S*)-1,4-Di-*tert*-butyl-2-(2-iodonaphthalen-1-yl)-4,5-dihydro-1*H*-imidazole **86**

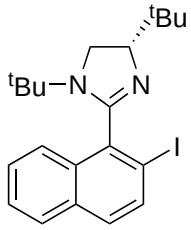

(*S*)-N-(1-Hydroxy-3,3-dimethylbutan-2-yl)-2-iodo-1-naphthamide (1.0 g, 2.52 mmol, 1 equiv.) was added to a 100 mL flame-dried Schlenk flask. Thionyl chloride (4.0 mL, 54.8 mmol, 22 equiv.) was added, and the reaction was heated at 75 °C for 19 h. Anhydrous toluene (4 mL) was added, and the reaction was concentrated in *vacuo* using an in-line trap. CH_2Cl_2 (6.5 mL) was added to the crude chloroalkylimidoyl chloride. *tert*-Butylamine (0.66 mL, 6.3 mmol, 2.5 equiv.) in CH_2Cl_2 (2.5 mL) was added to the reaction mixture, followed by triethylamine (1.05 mL, 7.53 mmol, 3

equiv.). The reaction was stirred at rt for 18 h. 2M NaOH (20 mL) was then added, and the reaction was stirred vigorously for 20 min. The phases were separated, and the aqueous phase was extracted with CH_2Cl_2 (3 x 20 mL). The combined organic phases were dried with magnesium sulfate, filtered, and concentrated in *vacuo* to yield the crude product. The crude mixture was purified *via* column chromatography (18:1:1, cyclohexane:EtOAc:Et_3N) to give the pure product as a brown wax (1.08 g, 99% yield). **Melting point**: 105 – 107 °C; $\mathbf{R_f}$ = 0.27 in 18:1:1 (cyclohexane:EtOAc:Et_3N); **^{1}H NMR** (400 MHz, $CDCl_3$) δ 7.94 – 7.87 (m, 1H), 7.84 – 7.71 (m, 2H), 7.51 – 7.43 (m, 3H), 3.95 (t, *J* = 11.6 Hz, 1H), 3.73 – 3.64 (m, 1H), 3.55 – 3.48 (m, 1H), 1.10 – 1.01 (m, 18H); **^{13}C NMR** (101 MHz, $CDCl_3$) δ 163.0, 162.9, 139.2, 139.2, 135.9, 135.7, 134.0, 132.8, 132.7, 132.5, 129.7, 129.7, 128.1, 127.9, 127.1, 126.9, 126.9, 126.8, 126.5, 126.5, 98.3, 96.1, 73.6, 73.6, 54.7, 54.6, 48.8, 48.7, 34.8, 34.3, 29.5, 29.2, 27.2, 26.7; **IR** ν(cm^{-1}): 3054, 2946, 2860, 1755, 1594, 747; **[α]^{20}D** = +0.42 (c = 0.5, $CHCl_3$); **HRMS**: (ESI-TOF) calculated for $C_{21}H_{27}IN_2$ $[M + H]^+$ 435.1292, found 435.1296.

(*S*)-1,4-Di-*tert*-butyl-2-(naphthalen-1-yl)-4,5-dihydro-1*H*-imidazole

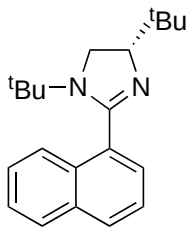

The title compound was isolated as the reduced product in CuI phosphinylations as an amorphous wax.**^{1}H NMR** (400 MHz, $CDCl_3$) δ 8.06 – 7.94 (m, 1H), 7.84 – 7.74 (m, 2H), 7.53 – 7.39 (m, 4H), 3.94 – 3.84 (m, 1H), 3.64 (ddd, *J* = 10.8, 9.6, 6.3 Hz, 1H), 3.55 – 3.48 (m, 0.5H), 3.43 – 3.35 (m, 0.5H), 1.08 – 1.01 (m, 9H), 1.00 – 0.94 (m, 9H); **^{13}C NMR** (101 MHz, $CDCl_3$) δ 164.0, 163.9, 134.3, 133.9, 133.5, 133.3, 132.5, 131.9, 128.8, 128.7, 128.1, 127.9, 127.0, 126.5, 126.5, 126.2, 126.1, 126.1, 126.0, 125.9, 124.9, 73.3, 72.8, 54.7, 54.5, 49.3, 49.2, 34.6, 34.19, 29.4, 28.94, 28.94, 26.5, 26.3; **IR** ν(cm^{-1}): 3047, 2952, 2864, 1604, 1590, 776. **[α]^{20}D** = +2.19 (c = 0.2, $CHCl_3$); **HRMS**: (ESI-TOF) calculated for $C_{21}H_{28}N_2$ $[M + H]^+$ 309.2333, found 309.2333.

(*S*)-4-(*tert*-Butyl)-2-(2-iodonaphthalen-1-yl)-4,5-dihydro-1*H*-imidazole **83**

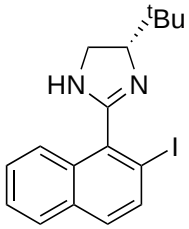

(*S*)-N-(1-Hydroxy-3,3-dimethylbutan-2-yl)-2-iodo-1-naphthamide (100 mg, 0.25 mmol, 1 equiv.) was added to a 10 mL flame-dried Schlenk flask. Thionyl chloride (1 mL, 13.7 mmol, 54.8 equiv.) was added and the reaction was heated at 75 °C for 19 h. Toluene (1 mL) was added and the reaction was concentrated in *vacuo* using an in-line trap. CH_2Cl_2 (1 mL) was added to the crude chloroalkylimidoyl chloride. 7N NH_3 in MeOH (66 µL, 0.462 mmol, 1.8 equiv.) was added to the reaction mixture and was stirred at rt for 18 h. 2M NaOH (2 mL) was then added and the reaction was stirred vigorously for 20 min. The phases were separated and the aqueous phase was extracted with CH_2Cl_2 (3 x 2 mL). The combined organic phases were dried with magnesium sulfate, filtered and concentrated in *vacuo* to yield the crude product. The crude mixture was purified *via* column chromatography (10% EtOAc/cyclohexane) to yield the title compound as a white solid (61 mg, 65% yield). **Melting point**: 191 – 193 °C; $\mathbf{R_f}$ = 0.15 in 10% EtOAc/cyclohexane; **^{1}H NMR** (400 MHz, $CDCl_3$) δ 8.03 (s, 1H), 7.90 – 7.74 (m, 2H), 7.65 – 7.43 (m, 3H), 6.01 (d, *J* = 9.5 Hz, 1H), 4.48 – 4.40 (m, 1H), 4.03 (dd, *J* = 11.8, 3.6 Hz, 1H), 3.71 (s, 1H), 1.14 (s, 9H); **^{13}C NMR** (101 MHz, $CDCl_3$) δ 169.5, 141.1, 135.6, 132.6, 131.4, 130.5, 128.2, 127.8, 127.1, 125.7, 91.1, 58.3, 45.3, 35.6, 27.7; **IR** ν(cm^{-1}): 3236, 3066, 2991, 1636, 1553, 782; **$[\alpha]^{20}$D** = +4.57 (c = 0.1, $CHCl_3$); **HRMS**: (ESI-TOF) calculated for $C_{17}H_{19}IN_2$ $[M + H]^+$ 379.0666, found 379.0668.

(*S*)-4-(*tert*-Butyl)-2-(2-iodonaphthalen-1-yl)-1-mesityl-4,5-dihydro-1*H*-imidazole **85**

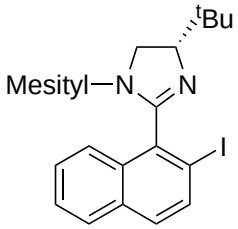

(*S*)-*N*-(1-Hydroxy-3,3-dimethylbutan-2-yl)-2-iodo-1-naphthamide (500 mg, 1.26 mmol, 1 equiv.) was added to flame-dried 25 mL Schlenk flask. Thionyl chloride (3 mL, 41.10 mmol, 32.6 equiv.) was added the reaction heated at 80 °C in the sealed Schlenk flask for 16 h. Anhydrous toluene (4 mL) was added and the reaction was concentrated *in vacuo* using an inline trap. CH_2Cl_2 (5.35 mL) was added to reaction. The reaction was stirred at rt and 2,4,6-trimethylaniline (0.25 mL, 1.77 mmol, 1.4 equiv.) was added. Triethylamine (0.44 mL, 3.21 mmol, 2.54 equiv.) was subsequently added and the reaction was stirred at rt for 18 h. 2 M NaOH (6 mL) was added and the reaction was stirred vigorously at rt for 30 min. The phases were separated and the aqueous phase was extracted with CH_2Cl_2 (50 mL x 3). The organic phases were combined, dried with sodium sulfate, were filtered and concentrated *in vacuo*. The crude product was purified using flash column chromatography (cyclohexane:EtOAc:Et_3N, 18:1:1) to yield the title compound as a white foamy solid (0.561 g, 89% yield). **Melting point**: 73 – 75 °C; $\mathbf{R_f}$ = 0.27 in 18:1:1 (cyclohexane:EtOAc:Et_3N); **^{1}H NMR** (400 MHz, $CDCl_3$) δ 8.27 – 8.08 (m, 1H), 7.84 – 7.67 (m, 1H), 7.66 – 7.53 (m, 1H), 7.45 – 7.27 (m, 3H), 6.72 – 6.45 (m, 2H), 4.41 – 4.30 (m, 1H), 3.89 – 3.82 (m, 1H), 3.81 – 3.74 (m, 1H), 3.70 – 3.63 (m, 1H), 2.50 – 1.87 (m, 9H), 1.25 – 1.13 (m, 9H); **^{13}C NMR** (101 MHz, $CDCl_3$) δ 162.6, 162.2, 137.05, 137.03, 136.5, 136.4, 136.34, 136.29, 136.22, 136.19, 134.82, 134.80, 134.6, 134.3, 132.9, 132.7, 132.5, 132.3, 130.2, 130.1, 129.5, 129.3, 129.26, 129.17, 127.9, 127.7, 127.2, 126.6, 126.3, 126.1, 125.8, 97.6, 97.4, 75.9, 75.6, 53.7, 53.4, 34.5, 34.0, 27.4, 27.0, 21.8, 21.5, 20.72, 20.67, 20.1, 19.5; **IR** ν(cm^{-1}): 2948, 2861, 1668, 1598, 1560, 778; **$[\alpha]^{20}$D** = +1.14 (c = 0.1, $CHCl_3$); **HRMS**: (ESI-TOF) calculated for $C_{26}H_{29}IN_2$ $[M + H]^+$ 497.1448, found 497.1448.

(*S*)-4-(*tert*-Butyl)-1-mesityl-2-(naphthalen-1-yl)-4,5-dihydro-1*H*-imidazole

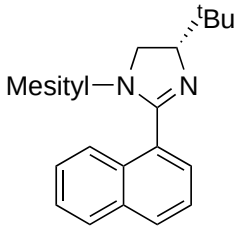

The title compound was isolated as the reduced product in CuI phosphinylations as a colourless amorphous wax. $\mathbf{R_f}$ = 0.4 in 10% EtOAc/cyclohexane; **^{1}H NMR** (400 MHz, $CDCl_3$) δ 8.89 – 8.82 (m, 1H), 7.76 (d, *J* = 8.1, 1H), 7.72 – 7.66 (m, 1H), 7.57 – 7.50 (m, 1H), 7.48 – 7.42 (m, 1H), 7.21 – 7.12 (m, 2H), 6.80 (s 1H), 6.61 (s, 1H), 4.24 (t, *J* = 11.4 Hz, 1H), 3.82 (dd, *J* = 11.4, 9.4 Hz, 1H), 3.54 (dd, *J* = 11.5, 9.4 Hz, 1H), 2.39 (s, 3H), 2.14 (s, 3H), 1.98 (s, 3H), 1.17 (s, 9H); **^{13}C NMR** (101 MHz, $CDCl_3$) δ 162.7, 136.8, 136.5, 136.2, 134.0, 131.5, 129.7, 129.7, 129.6, 129.4, 128.4, 128.3, 126.9, 126.8, 126.5, 125.8, 124.3, 75.8, 52.9, 34.5, 26.9, 20.9, 18.6, 18.5; **IR** ν(cm^{-1}): 3046, 2950, 1624, 1608, 1569, 774. **[α]^{20}D** = +8.49 (c = 0.18, $CHCl_3$); **HRMS**: (ESI-TOF) calculated for $C_{26}H_{30}N_2$ $[M + H]^+$ 371.2482, found 371.2483.

(*S*)-4-(*tert*-Butyl)-2-(2-iodonaphthalen-1-yl)-1-(4-methoxyphenyl)-4,5-dihydro-1*H*-imidazole

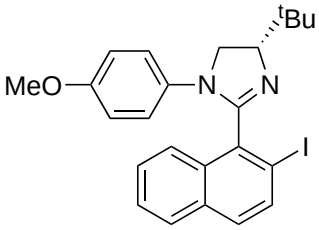

(*S*)-*N*-(1-Hydroxy-3,3-dimethylbutan-2-yl)-2-iodo-1-naphthamide (300 mg, 0.78 mmol, 1 equiv.) was added to a 25 mL flame-dried Schlenk flask. Thionyl chloride (2 mL, 27.04 mmol, 34.6 equiv.) was added and the reaction was heated at 75 °C for 5 h. Anhydrous toluene (2 mL) was added and the reaction was concentrated in *vacuo* using an in-line trap. CH_2Cl_2 (3.75 mL) was added to the crude alkylimidoyl chloride.

p-Anisidine (115mg, 0.94 mmol, 1.2 equiv.) was added to the reaction mixture, followed by triethylamine (0.43 mL, 3.08 mmol, 3 .95 equiv.). The reaction was stirred at rt for 17 h. 2M NaOH (5 mL) was then added, and the reaction was stirred vigorously for 20 min at rt. The phases were separated, and the aqueous phase was extracted with CH_2Cl_2 (3 x 10 mL). The combined organic phases was dried with magnesium sulfate, filtered, and concentrated in *vacuo* to give the crude product. The crude mixture was purified *via* column chromatography to afford the pure product as a brown wax (306 mg, 81% yield). $\mathbf{R_f}$ = 0.30 in 18:1:1 cyclohexane:EtOAc:Et_3N; **^{1}H NMR** (400 MHz, $CDCl_3$) δ 8.09 – 8.01 (m, 1H), 7.97 – 7.88 (m, 0.5H), 7.82 – 7.73 (m, 1.5H), 7.69 (d, *J* = 8.7 Hz, 1H), 7.58 – 7.43 (m, 3H), 6.72 – 6.63 (m, 1H), 6.60 – 6.47 (m, 3H), 4.25 – 4.15 (m, 1H), 4.14 – 3.96 (m, 1H), 3.93 – 3.83 (m, 1H), 3.64 – 3.59 (m, 3H), 1.18 – 1.12 (m, 9H); **^{13}C NMR** (101 MHz, $CDCl_3$) δ 161.1, 161.0, 155.5, 155.3, 135.7, 135.4, 135.4, 135.3, 133.9, 133.7, 133.6, 132.9, 132.5, 132.4, 130.3, 128.2, 128.1, 127.7, 127.4, 126.7, 126.5, 125.9, 125.6, 121.5, 121.0, 113.8, 113.7, 97.2, 96.3, 74.59, 74.56, 55.2, 55.2, 52.8, 52.6, 34.2, 34.1, 27.1, 26.5; **IR** ν(cm^{-1}): 3053, 2950, 2863, 2191, 1608, 1280; **[α]^{20}D** = -8.30(c = 0.75, $CHCl_3$); **HRMS**: (ESI-TOF) calculated for $C_{24}H_{25}IN_2O$ $[M + H]^+$ 485.1084, found 485.1090.

(*S*)-4-(*tert*-Butyl)-1-(4-methoxyphenyl)-2-(naphthalen-1-yl)-4,5-dihydro-1*H*-imidazole

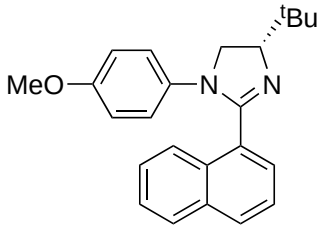

The title compound was isolated as the reduced product in CuI phosphinylations as an amorphous wax.**^{1}H NMR** (500 MHz, $CDCl_3$) δ 8.29 – 8.21 (m, 1H), 7.84 – 7.77 (m, 2H), 7.53 (d, *J* = 7.1, 1H), 7.50 – 7.41 (m, 2H), 7.40 – 7.35 (m, 1H), 6.70 – 6.63 (m, 2H), 6.56 – 6.49 (m, 2H), 4.16 – 4.07 (m, 2H), 3.77 (t, *J* = 6.8 Hz, 1H), 3.62 (s, 3H), 1.10 (s, 9H); **^{13}C NMR** (126 MHz, $CDCl_3$) δ 161.2, 155.6, 135.6, 133.6, 131.2, 129.7, 129.6, 128.2, 127.7, 126.5, 125.9, 125.7, 125.0, 123.2, 113.9, 74.4, 55.2, 54.4, 34.3, 26.2; **IR**

ν(cm^{-1}): 3045, 2950, 2864, 2309, 1609, 1573; **[α]^{20}D** = +4.58 (c = 0.12, $CHCl_3$); **HRMS**: (ESI-TOF) calculated for $C_{24}H_{26}N_2O$ $[M + H]^+$ 359.2118, found 359.2119.

(Diphenylphosphaneyl)(phenyl)methanone **84**[63]

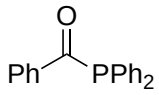

Anhydrous Et_2O (10 mL) was added to a flame-dried Schlenk flask under N_2, followed by benzoyl chloride (0.38 mL, 3.3 mmol, 1 equiv.) at rt. Triethylamine (0.46 mL, 3.3 mmol, 1equiv.) was added, followed by diphenylphosphine (0.52 mL, 3 mmol, 0.9 equiv.) in a dropwise fashion. The reaction was stirred at rt for 16 h. H_2O (14 mL) was added and the reaction mixture was transferred to a separatory funnel. The reaction mixture was extracted with CH_2Cl_2 (2 x 20 mL), was dried with Na_2SO_4, filtered and concentrated *in vacuo* to afford the crude product. The product was purified by recrystallisation from hot MeOH and was cooled under a flow on N_2 to limit oxidation of the product. The product was isolated by vacuum filtration as a bright yellow solid (386 mg, 44% yield).**^{1}H NMR** (300 MHz, Chloroform-*d*) δ 8.02 – 7.96 (m, 2H), 7.47 – 7.33 (m, 13H); **^{31}P NMR** (121 MHz, Chloroform-*d*) δ 13.50. All characterisation data are in agreement with reported literature data.

(*S*)-2-(diphenylphosphoryl)-*N*-(1-hydroxy-3,3-dimethylbutan-2-yl)-1-naphthamide **87**

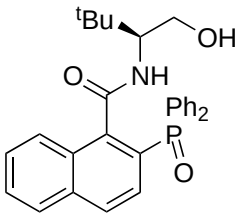

CuI (95 mg, 0.5 mmol, 1 equiv.) was added to a flame-dried 25 mL Schlenk flask. Anhydrous and degassed toluene (2.5 mL) was added, followed by DMEDA (0.16 mL,

1.5 mmol, 3 equiv.) and diphenylphosphine oxide (112.2 mg, 0.55 mmol, 1.1 equiv.). The reaction was stirred at rt for 30 min. (*S*)-*N*-(1-Hydroxy-3,3-dimethylbutan-2-yl)-2-iodo-1-naphthamide (198.5 mg, 0.5 mmol, 1 equiv.), Cs_2CO_3 (663 mg, 2.035 mmol, 3.7 equiv.) were added to the reaction mixture followed by a further portion of toluene (2.5 mL). The reaction was heated to 110 °C and was stirred for 18 h. The reaction was filtered through a pad of celite and was concentrated *in vacuo*. The crude product was purified by flash column chromatography (2% MeOH/CH_2Cl_2) to yield the product as a white solid (161 mg, 68% yield). **Melting point**: 254 – 255 °C; **R_f** = 0.2 (5% MeOH/CH_2Cl_2); **^{1}H NMR** (600 MHz, $CDCl_3$) δ 8.32 (dd, *J* = 8.4, 1.4 Hz, 0.5H), 8.18 (dd, *J* = 8.4, 1.4 Hz, 0.5H), 7.94 – 7.91 (m, 0.5H), 7.89 7-.84 (m, 1H), 7.82 – 7.78 (m, 1H), 7.71 – 7.41 (m, 10H), 7.10 – 7.04 (m, 0.5H), 6.20 – 6.12 (m, 1H), 5.76 (s, 0.5H), 4.22 – 4.15 (m, 0.5H), 4.10 – 3.98 (m, 1H), 3.79 – 3.67 (m, 1H), 3.57 – 3.45 (m, 0.5H), 2.48 (s, 0.5H), 1.06 (s, 5H), 0.95 (s, 4H); **^{13}C NMR** (151 MHz, $CDCl_3$) (Phosphorus decoupled) δ 171.10, 167.60, 167.56, 142.73, 142.68, 135.1, 135.0, 135.0, 133.8, 132.73, 132.71, 132.59, 132.57, 132.4, 132.31, 132.30, 132.2, 130.8, 130.3, 129.1, 129.0, 128.9, 128.84, 128.83, 128.76, 128.74, 128.4, 128.21, 128.17, 127.7, 127.6, 127.4, 126.9, 126.7, 125.6, 124.9, 124.8, 63.6, 61.4, 60.4, 60.3, 33.9, 33.8, 27.4, 27.2; **^{31}P NMR** (243 MHz, $CDCl_3$) δ 33.80.; **IR** ν(cm^{-1}): 3423, 3303, 2953, 2865, 1664, 1584; **[α]^{20}D** = +1.09 (c = 1.09, $CHCl_3$); **HRMS**: (ESI-TOF) calculated for $C_{29}H_{30}N_3P$ $[M + H]^+$ 472.2036, found 473.2038.

(*S*)-(1-(4-(*tert*-butyl)-4,5-dihydrooxazol-2-yl)naphthalen-2-yl)diphenylphosphine oxide **89**

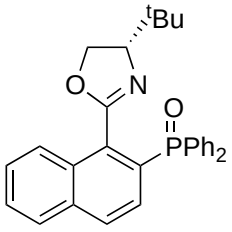

Isolated as a side-product during the attempted imidazoline formation from (*S*)-2-(diphenylphosphoryl)-*N*-(1-hydroxy-3,3-dimethylbutan-2-yl)-1-naphthamide as an amorphous brown wax (78 mg, 23%). **R_f =** 0.15 in 50%EtOAc/cyclohexane**^{1}H NMR** (600 MHz, $CDCl_3$) δ 8.19 – 8.12 (m, 1H), 7.89 – 7.82 (m, 4H), 7.70 – 7.66 (m, 2H), 7.62

– 7.40 (m, 9H), 4.10 – 4.05 (m, 1H), 4.08 – 3.98 (m, 1H), 3.70 – 3.65 (m, 1H), 0.92 (s, 9H). **^{13}C NMR** (151 MHz, $CDCl_3$) (Phosphorus decoupled) δ 161.42, 134.59, 134.57, 133.9, 133.3, 133.2, 133.1, 133.0, 132.6, 132.5, 132.4, 131.98, 131.91, 131.74, 131.72, 131.6, 131.55, 131.53, 130.5, 129.9, 129.5, 129.4, 128.34, 128.30, 128.26, 128.23, 128.1, 127.7, 126.4, 77.2, 68.9, 33.4, 26.4. **^{31}P NMR** (243 MHz, $CDCl_3$) δ 30.16**; IR ν (cm^{-1})**: 3057, 2955, 2902, 2867, 2219, 1664, 1589, 1561, 722; **[a]^{20}** = - 5.81 (c = 0.26, $CHCl_3$); **HRMS**: (ESI-TOF) calculated for $C_{29}H_{28}NO_2PNa$ [M + Na] 476.1750, found 476.1752

(*S)*-2-Bromo-*N*-(1-hydroxy-3,3-dimethylbutan-2-yl)benzamide **90**[85]

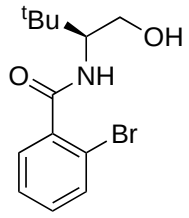

2-Bromobenzoic acid (2.41 g, 12 mmol, 1 equiv.) was added to a flame-dried 250 mL Schlenk flask under N_2. CH_2Cl_2 (60 mL) was added and the flask was cooled to 0 °C. Oxalyl chloride (4.08 g, 2.72 mL, 14.4 mmol, 1.2 equiv.) was added followed by dried DMF (0.1 mL). ***Caution – gas evolution*.** The reaction was allowed to warm to rt and was stirred for 1 h until the reaction mixture was homogenous. The reaction was concentrated in the Schlenk flask using an in-line trap.

In a separate flame-dried 500 mL two-necked round-bottomed flask, was added CH_2Cl_2 (85 mL) and L-*tert*-leucinol (1.68 g, 14.4 mmol, 1.2 equiv.). Et_3N (5 mL, 36 mmol, 3 equiv.) was added and the flask was cooled to 0 °C. CH_2Cl_2 (3 x 10 mL) was added to the crude alkylimidoyl chloride, which was transferred to the two-necked flask *via* a syringe in a dropwise manner. The two-necked reaction flask was allowed to warm to rt and was stirred for 16 h. The reaction mixture was diluted with CH_2Cl_2 (150 mL), was washed with 1M HCl (2 x 200 mL) followed by 1M NaOH (2 x 200 mL) and brine (100 mL). The organic phase was dried over sodium sulfate, was filtered

and concentrated *in vacuo* to afford the crude product. The crude product was purified by column chromatography (20% to 40% acetone/cyclohexane) to yield a white solid (2.76 g, 77% yield). $\mathbf{R_f}$ = 0.2 in 30% acetone/cyclohexane; **^{1}H NMR** (400 MHz, $CDCl_3$) δ 7.56 (dd, *J* = 7.9, 1.3 Hz, 1H), 7.53 -7.48 (m, 1H), 7.35 – 7.29 (m, 1H), 7.29 – 7.22 (m, 1H), 6.34 (d, *J* = 9.4 Hz, 1H), 4.03 (ddd, *J* = 9.4, 7.4, 3.6 Hz, 1H), 3.90 (dd, *J* = 11.4, 3.6 Hz, 1H), 3.64 (dd, *J* = 11.4, 7.4 Hz, 1H), 2.83 (s, br, 1H), 1.02 (s, 9H);**^{13}C NMR** (101 MHz, $CDCl_3$) δ 168.7, 138.1, 133.3, 131.2, 129.6, 127.5, 119.1, 62.6, 60.1, 27.1, 26.9; **HRMS**: (ESI-TOF) calculated for $C_{13}H_{18}BrNO_2$ $[M + H]^+$ 300.0597, found 300.0597. All characterisation data are in agreement with reported literature data.

(*R*)-2-(2-Bromophenyl)-4-(*tert*-butyl)-4,5-dihydrooxazole **91**[85]

(*S)*-2-Bromo-*N*-(1-hydroxy-3,3-dimethylbutan-2-yl)benzamide (250 mg, 0.83 mmol, 1 equiv.) was added to a flame-dried sealed tubed under N_2. *p*-Toluenesulfonyl chloride (206 mg, 1.08 mmol, 1.3 equiv.) and Et_3N (0.58 mL, 4.15 mmol, 5 equiv.) were added. The tube was sealed and heated at 55 °C for 14 h. H_2O (1 mL) was added and the reaction was re-sealed and heated at 75 °C for 2 h. The phases were separated, and the organic phases was dried over sodium sulfate. The organic phase was filtered and concentrated *in vacuo* to yield the crude product. The product was purified by column chromatography (5% EtOAc/cyclohexane) to afford the product as a white solid (156 mg, 67% yield). **^{1}H NMR** (400 MHz, $CDCl_3$) δ 7.70 – 7.58 (m, 2H), 7.31 (td, *J* = 7.5, 1.3 Hz, 1H), 7.25 (td, *J* = 7.7, 1.9 Hz, 1H), 4.36 (dd, *J* = 10.2, 8.6 Hz, 1H), 4.24 (dd, *J* = 8.7, 8.0 Hz, 1H), 4.09 (dd, *J* = 10.2, 8.0 Hz, 1H), 0.99 (s, 9H); **^{13}C NMR** (101 MHz, $CDCl_3$) δ 162.88, 133.78, 133.77, 131.6, 131.36, 130.34, 130.33, 129.7, 127.2, 127.1, 121.9, 76.8, 69.1, 34.1, 26.1. All characterisation data are in agreement with reported literature data.

(*R*)-4-(*tert*-Butyl)-2-(2-(diphenylphosphaneyl)phenyl)-4,5-dihydrooxazole **92**[85]

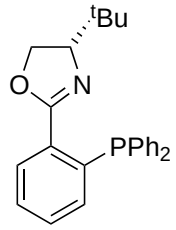

CuI (33 mg, 0.175 mmol, 12.5 mol%) was added to a flame-dried 50 mL Schlenk flask under N_2. Dried and degassed toluene (5.9 mL) was added, followed by DMEDA (0.13 mL, 1.25 mmol, 0.875 equiv.) and diphenylphosphine (0.487 mL, 2.8 mmol, 2 equiv.). The reaction was stirred at rt for 30 min. (*S)*-2-Bromo-*N*-(1-hydroxy-3,3-dimethylbutan-2-yl)benzamide (393 mg, 1.4 mmol, 1 equiv.) was added followed by toluene (5.9 mL). The reaction flask was sealed and refluxed at 110 °C for 18 h. The reaction was filtered through celite with CH_2Cl_2 and was concentrated *in vacuo* to give the crude product. The crude product was purified by column chromatography (3% to 10% Et_2O/pentane) to give the pure product as a white solid (456 mg, 84% yield). $\mathbf{R_f}$ = 0.39 in 5% Et_2O/pentane.; **^{1}H NMR** (400 MHz, $CDCl_3$) δ 7.95 (ddd, *J* = 7.7, 3.7, 1.5 Hz, 1H), 7.39 – 7.21 (m, 12H), 6.89 (ddd, *J* = 7.8, 4.0, 1.3 Hz, 1H), 4.09 (dd, *J* = 10.2, 8.4 Hz, 1H), 3.89 (dd, *J* = 10.2, 8.2 Hz, 1H), 0.75 (s, 9H); **^{13}C NMR** (101 MHz, $CDCl_3$) δ 162.80 (d, *J* = 3 Hz), 138.92 (d, *J* = 25 Hz), 138.68 (d, *J* = 13 Hz), 138.41 (d, *J* = 10 Hz), 134.44 (d, *J* = 21 Hz), 134.02 (d, *J* = 42 Hz), 133.61, 132.09 (d, *J* = 19 Hz), 130.45, 129.95 (d, *J* = 3 Hz), 128.57 (d, *J* = 9 Hz), 128.43 (d, *J* = 6 Hz), 128.34 (d, *J* = 1 Hz), 128.15, 76.84, 68.39, 33.73, 25.88; **^{31}P NMR** (162 MHz, $CDCl_3$) δ -6.00. All characterisation data are in agreement with reported literature data.

(*R*)-2-(2-Bromophenyl)-4-(*tert*-butyl)-1-phenyl-4,5-dihydro-1*H*-imidazole

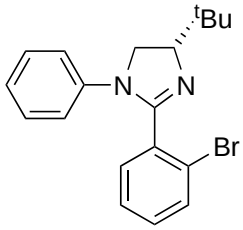

(*S*)-2-Bromo-*N*-(1-hydroxy-3,3-dimethylbutan-2-yl)benzamide (600 mg, 2 mmol, 2 equiv.) was added to a flame-dried Schlenk flask under N_2. Thionyl chloride (2 mL, 27.4 mmol, 13.7 equiv.) was added and the reaction was heated at 80 °C for 19 h. Anhydrous toluene (2 mL) was added and the reaction was concentrated *in vacuo* using an in-line trap. Anhydrous CH_2Cl_2 (2 mL) was added, followed by aniline (0.22 mL, 2.41 mmol, 1.2 equiv.) and Et_3N (0.84 mL, 6.02 mmol, 3 equiv.). The reaction was stirred at rt for 18 h. 2M NaOH (2 mL) was added to the reaction and was stirred vigorously for 30 min. The phases were separated and the aqueous phase was extracted with CH_2Cl_2 (3 x 5 mL). The combined organic phases were dried using sodium sulfate, were filtered and concentrated *in vacuo*. The crude product was purified by column chromatography to give the product as a white solid (575 mg, 81% yield). **Melting point**: 99 – 100 °C; $\mathbf{R_f}$ = 0.36 in 18:4:1 pentane:Et_2O:Et_3N); **^{1}H NMR** (500 MHz, $CDCl_3$) δ 7.49 (dd, *J* = 8.1, 4.0 Hz, 2H), 7.33 (t, *J* = 7.6, 1H), 7.22 (t, *J* = 7.8 Hz, 1H), 7.13 – 7.07 (m, 2H), 6.91 (t, *J* = 7.5 Hz, 1H), 6.72 – 6.65 (m, 2H), 4.10 – 3.96 (m, 2H), 3.83 (t, *J* = 7.4 Hz, 1H), 1.07 (s, 9H); **^{13}C NMR** (126 MHz, CDC_3) δ 159.7, 141.0, 134.3, 133.1, 131.1, 130.8, 128.7, 127.5, 122.5, 122.2, 119.6, 73.9, 52.5, 34.3, 26.2; **IR** ν(cm^{-1}): 3067, 2901, 2860, 1622, 1563, 763; **$[\alpha]^{20}D$** = -5.15 (c = 1.25, $CHCl_3$); **HRMS**: (ESI-TOF) calculated for $C_{19}H_{21}BrN_2$ $[M + H]^+$ 356.0888, found 356.0888.

(*R*)-2-(2-Bromophenyl)-4-(*tert*-butyl)-1-(4-(trifluoromethyl)phenyl)-4,5-dihydro-1*H*-imidazole

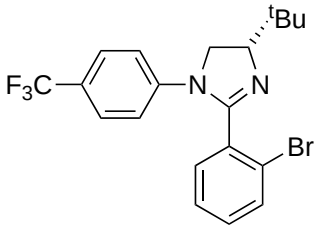

(*S)*-2-Bromo-*N*-(1-hydroxy-3,3-dimethylbutan-2-yl)benzamide (600 mg, 2 mmol, 2 equiv.) was added to a flame-dried Schlenk flask under N_2. Thionyl chloride (2 mL, 27.4 mmol, 13.7 equiv.) was added and the reaction was heated at 80 °C for 19 h. Anhydrous toluene (2 mL) was added and the reaction was concentrated *in vacuo* using an in-line trap. Anhydrous CH_2Cl_2 (2 mL) was added, followed by 4-(trifluoromethyl)aniline (0.30 mL, 2.4 mmol, 1.2 equiv.) and Et_3N (0.84 mL, 6.02 mmol, 3 equiv.). The reaction was stirred at rt for 18 h. 2M NaOH (2 mL) was added to the reaction and was stirred vigorously for 30 min. The phases were separated and the aqueous phase was extracted with CH_2Cl_2 (3 x 5 mL). The combined organic phases were dried using sodium sulfate, filtered and concentrated *in vacuo*. The crude product was purified by column chromatography to afford the title compound as a colourless wax (621 mg, 73% yield) **Melting point**: 90 – 92 °C; $\mathbf{R_f}$ = 0.26 in 18:4:1 Pentane:Et_2O:Et_3N);**^{1}H NMR** (400 MHz, $CDCl_3$) δ 7.51 (td, *J* = 7.5, 1.5 Hz, 2H), 7.42 – 7.25 (m, 4H), 6.69 – 6.59 (m, 2H), 4.11 – 3.94 (m, 2H), 3.83 (t, *J* = 8.5 Hz, 1H), 1.05 (s, 9H); **^{13}C NMR** (101 MHz, $CDCl_3$) δ 158.7, 143.7, 134.0, 133.4, 131.3, 131.0, 128.0, 126.1 (q, *J* = 3.8 Hz), 125.7, 123.7, 123.3 (d, *J* = 32.2 Hz), 122.1, 117.8, 117.8, 74.0, 52.0, 34.3, 26.2; **^{19}F NMR** (376 MHz, $CDCl_3$) δ -61.85; **IR** ν(cm^{-1}): 3047, 2968, 2931, 1609, 1522, 778; **[α]^{20}D** = -5.42 (c = 1.02, $CHCl_3$); **HRMS**: (ESI-TOF) calculated for $C_{20}H_{20}BrF_3N_2$ $[M + H]^+$ 425.0835, found 425.0836.

(*R*)-2-(2-Bromophenyl)-4-(*tert*-butyl)-1-(4-methoxyphenyl)-4,5-dihydro-1*H*-imidazole

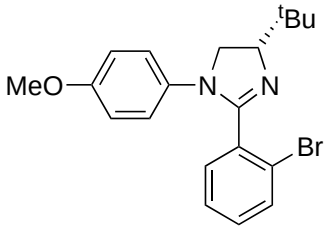

(*S)*-2-Bromo-*N*-(1-hydroxy-3,3-dimethylbutan-2-yl)benzamide (600 mg, 2 mmol, 2 equiv.) was added to a flame-dried Schlenk flask under N_2. Thionyl chloride (2 mL, 27.4 mmol, 13.7 equiv.) was added and the reaction was heated at 80 °C for 19 h. Anhydrous toluene (2 mL) was added and the reaction was concentrated *in vacuo* using an in-line trap. Anhydrous CH_2Cl_2 (2 mL) was added, followed by *p*-anisidine (296 mg, 2.4 mmol, 1.2 equiv.) and Et_3N (0.84 mL, 6.02 mmol, 3 equiv.). The reaction was stirred at rt for 18 h. 2M NaOH (2 mL) was added to the reaction and was stirred vigorously for 30 min. The phases were separated and the aqueous phase was extracted with CH_2Cl_2 (3 x 5 mL). The combined organic phases were dried using sodium sulfate, was filtered and concentrated *in vacuo*. The crude product was purified by column chromatography to yield the product as a colourless wax (639 mg, 83% yield). **Melting point**: 104 – 106 °C; $\mathbf{R_f}$ = 0.26 in 14:5:1 pentane:Et_2O:Et_3N);**^{1}H NMR** (400 MHz, $CDCl_3$) δ 7.48 – 7.40 (m, 2H), 7.29 – 7.22 (m, 1H), 7.17 – 7.12 (m, 1H), 6.74 – 6.67 (m, 2H), 6.67 – 6.59 (m, 2H), 4.05 – 3.92 (m, 2H), 3.76 – 3.69 (m, 1H), 3.66 (s, 3H), 1.08 – 0.99 (m, 9H);**^{13}C NMR** (101 MHz, $CDCl_3$) δ 160.5, 155.7, 134.6, 134.0, 132.9, 131.1, 130.5, 127.2, 122.7, 122.1 113.9, 74.1, 55.3, 53.5, 34.2, 26.12; **IR** ν(cm^{-1}): 3067, 2949, 2863, 1612, 1559, 769; **$[\alpha]^{20}D$** = -1.77 (c = 0.1, $CHCl_3$); **HRMS**: (ESI-TOF) calculated for $C_{20}H_{23}BrN_2O$ $[M + H]^+$ 387.1067, found 387.1071.

(*R*)-4-(*tert*-Butyl)-2-(2-(diphenylphosphaneyl)phenyl)-1-(4-methoxyphenyl)-4,5-dihydro-1*H*-imidazole[68]

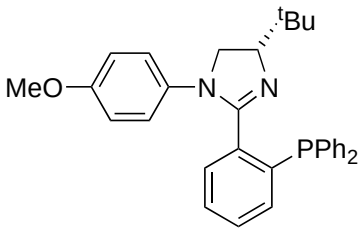

CuI (33 mg, 0.175 mmol, 12.5 mol%) was added to a flame-dried Schlenk flask under N_2. Anhydrous and degassed toluene (5.91 mL) was added, followed by DMEDA (0.13 mL, 1.225 mol, 0.875 equiv.) and diphenylphosphine (0.487 mL, 2.8 mmol, 2 equiv.). The reaction was stirred at rt for 30 min. (*R*)-2-(2-Bromophenyl)-4-(*tert*-butyl)-1-(4-methoxyphenyl)-4,5-dihydro-1*H*-imidazole (543 mg, 1.40 mmol, 1 equiv.) was added, followed by oven-dried Cs_2CO_3 (1.71 g, 5.25 mmol, 3.75 equiv.) and anhydrous/degassed toluene (5.91 mL). The Schlenk flask was sealed and heated at 110 °C for 5 h. The reaction was filtered through Celite with CH_2Cl_2 and was concentrated *in vacuo* to furnish the crude product. The crude product was purified by column chromatography to give the title compound as a white foamy solid (510 mg, 74% yield). $\mathbf{R_f}$ = 0.48 in 14:5:1 pentane/Et_2O/Et_3N; **^{1}H NMR** (400 MHz, $CDCl_3$) δ 7.57 - 7.52 (m, 1H), 7.33 (t, *J* = 7.5 Hz, 1H), 7.28 – 7.16 (m, 7H), 7.13 – 7.06 (m, 2H), 7.00 – 6.93 (m, 3H), 6.74 – 6.67 (m, 2H), 6.62 – 6.54 (m, 2H), 3.92 – 3.84 (m, 2H), 3.74 – 3.64 (m, 4H), 0.90 (s, 9H); **^{13}C NMR** (101 MHz, $CDCl_3$ δ 161.8 (d, *J* = 3 Hz), 155.6, 139.3, 138.9, 138.2, 138.1, 137.2, 137.1, 136.5, 136.4, 135.5 (d, *J* = 1 Hz), 135.2 (d, *J* = 2 Hz), 133.6 (d, *J* = 8 Hz), 133.4 (d, *J* = 8 Hz), 129.8 (d, *J* = 7 Hz), 129.3 (d, *J* = 17 Hz), 128.3 (d, *J* = 2 Hz), 128.2 (d, *J* = 2 Hz), 128.2, 123.2 (d, *J* = 1.8 Hz), 113.9, 74.6, 55.5, 54.0, 34.0, 26.4; **^{31}P NMR** (162 MHz, $CDCl_3$) δ -12.66.

All characterisation data are in agreement with reported literature data.

(*R*)-4-(*tert*-Butyl)-2-(2-(diphenylphosphaneyl)phenyl)-1-phenyl-4,5-dihydro-1*H*-imidazole[68]

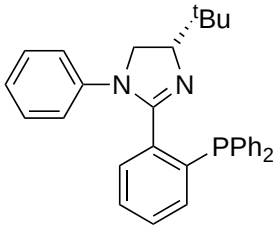

CuI (33 mg, 0.175 mmol, 12.5 mol%) was added to a flame-dried Schlenk flask under N_2. Anhydrous and degassed toluene (5.91 mL) was added, followed by DMEDA (0.13 mL, 1.225 mol, 0.875 equiv.) and diphenylphosphine (0.487 mL, 2.8 mmol, 2 equiv.). The reaction was stirred at rt for 30 min. (*R*)-2-(2-Bromophenyl)-4-(*tert*-butyl)-1-phenyl-4,5-dihydro-1*H*-imidazole (500 mg, 1.40 mmol, 1 equiv.) was added, followed by oven-dried Cs_2CO_3 (1.71 g, 5.25 mmol, 3.75 equiv.) and anhydrous/degassed toluene (5.91 mL). The Schlenk flask was sealed and heated at 110 °C for 5 h. The reaction was filtered through Celite with CH_2Cl_2 and was concentrated *in vacuo* to furnish the crude product. The crude product was purified by column chromatography to afford the title compound as a white foamy solid (495 mg, 78% yield). $\mathbf{R_f}$ = 0.30 in 20:2:1 pentane/Et_2O/Et_3N; **^{1}H NMR** (400 MHz, $CDCl_3$) δ 7.60 – 7.55 (m, 1H), 7.37 (t, *J* = 7.5, 1H), 7.31 – 7.15 (m, 7H), 7.06 (td, *J* = 7.6, 2.1 Hz, 4H), 7.01 – 6.95 (m, 1H), 6.89 (dtd, *J* = 11.5, 7.5, 1.3 Hz, 3H), 6.73 – 6.64 (m, 2H), 3.93 – 3.76 (m, 3H), 0.88 (s, 9H); **^{13}C NMR** (101 MHz, $CDCl_3$) δ 160.8 (d, *J* = 3 Hz), 141.7 (d, *J* = 2 Hz), 139.1, 138.8, 137.8, 137.6, 136.9, 136.8, 136.5, 136.3, 135.0 (d, *J* = 2 Hz), 133.5 (d, *J* = 6 Hz), 133.3 (d, *J* = 6 Hz), 129.6 (d, *J* = 7 Hz), 129.4 (d, *J* = 15 Hz), 128.5, 128.2 (d, *J* = 7Hz), 122.0, 120.3 (d, *J* = 2 Hz), 74.2, 52.8, 33.8, 26.2; **^{31}P NMR** (162 MHz, $CDCl_3$) δ -12.55. All characterisation data are in agreement with reported literature data.

(*R*)-4-(*tert*-Butyl)-2-(2-(diphenylphosphaneyl)phenyl)-1-(4-(trifluoromethyl)phenyl)-4,5-dihydro-1*H*-imidazole[68]

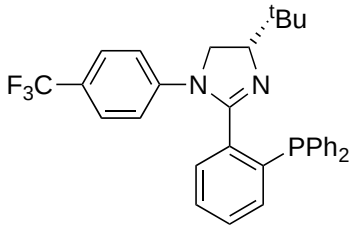

CuI (33 mg, 0.175 mmol, 12.5 mol%) was added to a flame-dried Schlenk flask under N_2. Anhydrous and degassed toluene (5.91 mL) was added, followed by DMEDA (0.13 mL, 1.225 mol, 0.875 equiv.) and diphenylphosphine (0.487 mL, 2.8 mmol, 2 equiv.). The reaction was stirred at rt for 30 min. (*R*)-2-(2-Bromophenyl)-4-(*tert*-butyl)-1-phenyl-4,5-dihydro-1*H*-imidazole (500 mg, 1.40 mmol, 1 equiv.) was added, followed by oven-dried Cs_2CO_3 (1.71 g, 5.25 mmol, 3.75 equiv.) and anhydrous/degassed toluene (5.91 mL). The Schlenk flask was sealed and heated at 110 °C for 5 h. The reaction was filtered through Celite with CH_2Cl_2 and was concentrated *in vacuo* to furnish the crude product. The crude product was purified by column chromatography to yield the title compound as a white foamy solid (483 mg, 65% yield). $\mathbf{R_f}$ = 0.7 in 20:2:1 pentane/Et_2O/Et_3N; **^{1}H NMR** (400 MHz, $CDCl_3$) δ 7.64 (ddd, *J* = 7.6, 3.8, 1.4 Hz, 1H), 7.46 (td, *J* = 7.6, 1.3 Hz, 1H), 7.35 (td, *J* = 7.6, 1.5 Hz, 1H), 7.30 – 7.14 (m, 9H), 7.07 – 6.96 (m, 3H), 6.83 (td, *J* = 7.9, 1.5 Hz, 2H), 6.63 (d, *J* = 8.4 Hz, 2H), 3.98 – 3.79 (m, 3H), 0.91 (s, 9H); **^{13}C NMR** (101 MHz, $CDCl_3$) δ 160.1 (d, *J* = 4.0 Hz), 144.3, 138.9, 138.6, 137.0, 136.9, 136.44, 136.39, 136.28, 136.26, 135.4 (d, *J* = 2 Hz), 133.5 (d, *J* = 8 Hz), 133.3 (d, *J* = 9 Hz), 130.0 (d, *J* = 19 Hz), 129.6 (d, *J* = 7 Hz), 128.5 (d, *J* = 6 Hz), 128.4 (d, *J* = 7 Hz), 125.8 (q, *J* = 4 Hz), 123.8 – 122.4 (m), 120.8, 120.5, 118.7, 74.3, 52.3, 34.0, 26.3;**^{19}F NMR** (376 MHz, $CDCl_3$) δ -61.73; **^{31}P NMR** (162 MHz, $CDCl_3$) δ -13.01. All characterisation data are in agreement with reported literature data.

References

(1) McManus, H. A.; Guiry, P. J. *Chem. Rev.* **2004;** *104,* 4154-4202

(2) Fernández, E.; Guiry, P. J.; Connole, K. P. T.; Brown, J. M. *J. Org. Chem.* **2014**, *79* (12), 5391–5400.

(3) Knöpfel, T. F.; Aschwanden, P.; Ichikawa, T.; Watanabe, T.; Carreira, E. M. *Angew. Chemie - Int. Ed.* **2004**, *43* (44), 5971–5973.

(4) Dai, L. X.; Tu, T.; You, S. L.; Deng, W. P.; Hou, X. L. *Acc. Chem. Res.* **2003**, *36* (9), 659–667.

(5) Akutagawa, S. *Appl. Catal. A, Gen.* **1995**, *128* (2), 171–207.

(6) Schettini, R.; Sala, G. Della. *Catalysts* **2021**, *11* (3), 1–3.

(7) Zhou, Q.-L. *Privileged Chiral Ligand and Catalysts*; *Wiley-VCH, Wienheim, Germany, 2011.*

(8) Akermark, B.; Krakenberger, B.; Hansson, S.; Vitagliano, A. *Organometallics* **1987**, *6* (3), 620–628.

(9) Orpen, A. G.; Connelly, N. G. *Organometallics* **1990**, *9* (4), 1206–1210.

(10) Rokade, B. V.; Guiry, P. J. *ACS Catal.* **2018**, *8* (1), 624–643.

(11) Alcock, N.; Brown, J.; Pearson, M.; Woodward, S. **1992**, *3* (1), 17–20.

(12) Alcock, N. W.; Brown, J. M.; Hulmes, D. I. *Tetrahedron: Asymmetry* **1993**, *4* (4), 743–756.

(13) Brown, J. M.; Woodward, S. J. *Org. Chem.* **1991**, *56* (24), 6803–6809.

(14) Miyashita, A.; Yasuda, A.; Takaya, H.; Toriumi, K.; Ito, T.; Souchi, T.; Noyori, R. *J. Am. Chem. Soc.* **1980**, *102* (27), 7932–7934.

(15) Brown, J. M.; Hulmes, D.; Layzell, T. P. *J. Chem. Soc. , Chem. Commun.* **1993**, 1673–1674.

(16) Fekner, T.; Bunz, H. M.; Guiry, P. J. *Org. Lett.* **2006**, *8* (22), 3–6.

(17) Rokade, B. V.; Guiry, P. J. *ACS Catal.* **2017**, *7* (4), 2334–2338.

(18) Cardoso, F. S. P.; Abboud, K. A.; Aponick, A. *J. Am. Chem. Soc.* **2013**, *135* (39), 14548–14551.

(19) Rokade, B. V.; Guiry, P. J. *J. Org. Chem.* **2019**, *84* (9), 5763–5772.

(20) O'Broin, C. Q.; Guiry, P. J. *Org. Lett.* **2019**, *21* (14), 5402–5406.

(21) Gao, Z.; Wang, F.; Qian, J.; Yang, H.; Xia, C.; Zhang, J.; Jiang, G. *Org. Lett.* **2021**, *23* (4), 1181–1187.

(22) Gao, Z.; Qian, J.; Yang, H.; Zhang, J.; Jiang, G. *Org. Lett.* **2021**, *23* (5), 1731–1737.

(23) Cai, D.; Payack, J. F.; Bender, D. R.; Hughes, D. L.; Verhoeven, T. R.; Reider, P. J. *J. Org. Chem.* **1994**, *59* (23), 7180–7181.

(24) Kametani, T.; Kigasawa, K.; Hiiragi, M.; Wagatsuma, N.; Wakisaka, K. *Tetrahedron Lett.* **1969**, *10* (8), 635–638.

(25) Paul, S.; Samanta, S.; Ray, J. K. *Tetrahedron Lett.* **2010**, *51* (42), 5604–5608.

(26) Li, D.; Zhao, B.; LaVoie, E. J. *J. Org. Chem.* **2000**, *65* (9), 2802–2805.

(27) Wood, T. K.; Piers, W. E.; Keay, B. A.; Parvez, M. *Chem. - A Eur. J.* **2010**, *16* (40), 12199–12206.

(28) Gelman, D.; Jiang, L.; Buchwald, S. L. *Org. Lett.* **2003**, *5* (13), 2315–2318.

(29) Moir, M.; Lane, S.; Lai, F.; Connor, M.; Hibbs, D. E.; Kassiou, M. *Eur. J. Med. Chem.* **2019**, *180*, 291–309.

(30) Tsukano, C.; Yokouchi, S.; Girard, A. L.; Kuribayashi, T.; Sakamoto, S.; Enomoto, T.; Takemoto, Y. *Org. Biomol. Chem.* **2012**, *10* (30), 6074–6086.

(31) Malkov, A. V.; Gouriou, L.; Lloyd-Jones, G. C.; Starý, I.; Langer, V.; Spoor, P.; Vinader, V.; Kočovský, P. *Chem. - A Eur. J.* **2006**, *12* (26), 6910–6929.

(32) Kalyani, D.; Dick, A. R.; Anani, W. Q.; Sanford, M. S. *Org. Lett.* **2006**, *8* (12), 2523–2526.

(33) John, A.; Nicholas, K. M. *J. Org. Chem.* **2012**, *77* (13), 5600–5605.

(34) Sun, X.; Sun, Y.; Zhang, C.; Rao, Y. *Chem. Commun.* **2014**, *50* (10), 1262–1264.

(35) Dabiri, M.; FaraJinia Lehi, N.; Kazemi Movahed, S.; Khavasi, H. R. *Org. Biomol. Chem.* **2017**, *15* (29), 6264–6268.

(36) Du, B.; Jiang, X.; Sun, P. *J. Org. Chem.* **2013**, *78* (6), 2786–2791.

(37) Chen, X.; Hao, X. S.; Goodhue, C. E.; Yu, J. Q. *J. Am. Chem. Soc.* **2006**, *128* (21), 6790–6791.

(38) Hu, L.; Xu, H.; Yang, Q.; Deng, Z.; Yu, C. Y.; Peng, Y. J. *Organomet. Chem.* **2017**, *843*, 20–25.

(39) Tian, Q.; Chen, X.; Liu, W.; Wang, Z.; Shi, S.; Kuang, C. *Org. Biomol. Chem.* **2013**, *11* (45), 7830–7833.

(40) Kramer, J. J. P.; Yildiz, C.; Nieger, M.; Bräse, S. *European J. Org. Chem.* **2014**, *2014* (6), 1287–1295.

(41) Lotz, M. D.; Camasso, N. M.; Canty, A. J.; Sanford, M. S. *Organometallics* **2017**, *36* (1), 165–171.

(42) Menges, F.; Neuburger, M.; Pfaltz, A. *Org. Lett.* **2002**, *4* (26), 4713–4716.

(43) Helmchen, G.; Pfaltz, A. *Acc. Chem. Res.* **2000**, *33* (6), 336–345.

(44) Krasovskiy, A.; Krasovskaya, V.; Knochel, P. *Angew. Chemie - Int. Ed.* **2006**, *45* (18), 2958–2961.

(45) Grudzień, K.; Zukowska, K.; Malińska, M.; Woźniak, K.; Barbasiewicz, M. *Chem. - A Eur.* J. **2014**, *20* (10), 2819–2828.

(46) Cannon, J. S.; Frederich, J. H.; Overman, L. E. *J. Org. Chem.* **2012**, *77* (4), 1939–1951.

(47) Mei, T. S.; Giri, R.; Maugel, N.; Yu, J. Q. *Angew. Chemie - Int. Ed.* **2008**, *47* (28), 5215–5219.

(48) Tilly, D.; Castanet, A. S.; Mortier, J. *Chem. Lett.* **2005**, *34* (3), 446–447.

(49) Balasubramaniyan, V. *Chem. Rev.* **1966**, *66* (6), 567–641.

(50) Hayrapetyan, D.; Rit, R. K.; Kratz, M.; Tschulik, K.; Gooßen, L. J. *Chem. - A Eur. J.* **2018**, *24* (44), 11288–11291.

(51) Eichelmann, H.; Gais, H. J. *Tetrahedron: Asymmetry* **1995**, *6* (3), 643–646.

(52) Wiese, B.; Helmchen, G. *Tetrahedron Lett.* **1998**, *39* (32), 5727–5730.

(53) Roseblade, S. J.; Pfaltz, A. *Acc. Chem. Res.* **2007**, *40* (12), 1402–1411.

(54) Ripa, L.; Hallberg, A. *J. Org. Chem.* **1997**, *62* (3), 596–602.

(55) Kanth, J. V. B.; Periasamy, M. *J. Org. Chem.* **1991**, *56* (20), 5964–5965.

(56) Peng, L.; Li, K.; Xie, C.; Li, S.; Xu, D.; Qin, W.; Yan, H. *Angew. Chemie - Int. Ed.* **2019**, *58* (48), 17199–17204.

(57) Ing, H. R.; Manske, R. H. F. J. *Chem. Soc.* **1926**, *129* (6), 2348–2351.

(58) Gelman, D.; Jiang, L.; Buchwald, S. L. *Org. Lett.* **2003**, *5* (13), 2315–2318.

(59) Alayrac, C.; Gaumont, A.-C. In *Copper-Mediated Cross-Coupling Reactions*; John Wiley & Sons, Inc.: Hoboken, NJ, USA, 2013; Vol. 18, pp 93–111.

(60) Allen, D. Van; Venkataraman, D. *J. Org. Chem.* **2003**, *68* (11), 4590–4593.

(61) Klapars, A.; Buchwald, S. L. *J. Am. Chem. Soc.* **2002**, *124* (50), 14844–14845.

(62) Woźnicki, P.; Stankevič, M. *European J. Org. Chem.* **2021**, *2021* (24), 3484–

3491.

(63) Yu, R.; Chen, X.; Wang, Z. *Tetrahedron Lett.* **2016**, *57* (30), 3404–3406.

(64) Bloomfield, A. J.; Herzon, S. B. *Org. Lett.* **2012**, *14* (17), 4370–4373.

(65) Mešková, M.; Putala, M. *Tetrahedron Lett.* **2011**, *52* (41), 5379–5383.

(66) Hoshi, T.; Sasaki, K.; Sato, S.; Ishii, Y.; Suzuki, T.; Hagiwara, H. *Org. Lett.* **2011**, *13* (5), 932–935.

(67) Hoshi, T.; Hayakawa, T.; Suzuki, T.; Hagiwara, H. *J. Org. Chem.* **2005**, *70* (22), 9085–9087.

(68) Nanchen, S.; Pfaltz, A. *Chem. - A Eur. J.* **2006**, *12* (17), 4550–4558.

(69) Tani, K.; Behenna, D. C.; McFadden, R. M.; Stoltz, B. M. *Org. Lett.* **2007**, *9* (13), 2529–2531.

(70) Li, T. Z.; Liu, S. J.; Tan, W.; Shi, F. *Chem. - A Eur. J.* **2020**, *26* (68), 15779–15792.

(71) Wang, J.; Chen, M. W.; Ji, Y.; Hu, S. B.; Zhou, Y. G. *J. Am. Chem. Soc.* **2016**, *138* (33), 10413–10416.

(72) Wang, Y. Bin; Tan, B. *Acc. Chem. Res.* **2018**, *51* (2), 534–547.

(73) Hu, Y. L.; Wang, Z.; Yang, H.; Chen, J.; Wu, Z. B.; Lei, Y.; Zhou, L. *Chem. Sci.* **2019**, *10* (28), 6777–6784.

(74) Murai, K.; Fukushima, S.; Hayashi, S.; Takahara, Y.; FuJioka, H. *Org. Lett.* **2010**, *12* (5), 964–966.

(75) Wu, F.; Zhu, S. *Org. Lett.* **2019**, *21* (5), 1488–1492.

(76) Yu, Z.; Zhang, Y.; Tang, J.; Zhang, L.; Liu, Q.; Li, Q.; Gao, G.; You, J. *ACS Catal.* **2020**, *10* (1), 203–209.

(77) Pezzetta, C.; Bonifazi, D.; Davidson, R. W. M. *Org. Lett.* **2019**, *21* (22), 8957–8961.

(78) Best, D.; KuJawa, S.; Lam, H. W. *J. Am. Chem. Soc.* **2012**, *134* (44), 18193–18196.

(79) Tsuzuki, Y.; Chiba, K.; Mizuno, K.; Tomita, K.; Suzuki, K. *Tetrahedron Asymmetry* **2001**, *12* (21), 2989–2997.

(80) Doyon, J. B.; Jain, A. *Org. Lett.* **1999**, *1* (2), 183–185.

(81) Liu, C.; Liu, Q.; Huang, A. *Chem. Commun.* **2016**, *52* (16), 3400–3402.

(82) Ahmed, A.; Bragg, R. A.; Clayden, J.; Lai, L. W.; McCarthy, C.; Pink, J. H.; Westlund, N.; Yasin, S. A. *Tetrahedron* **1998**, *54* (43), 13277–13294.

(83) McManus, *J*. B.; Nicewicz, D. A. *J. Am. Chem. Soc.* **2017**, *139* (8), 2880–2883.

(84) Fraser, R. R.; Savard, S. *Can. J. Chem.* **1986**, *64* (3), 621–625.

(85) Behenna, D. C.; Mohr, J. T.; Sherden, N. H.; Marinescu, S. C.; Harned, A. M.; Tani, K.; Seto, M.; Ma, S.; Novák, Z.; Krout, M. R.; McFadden, R. M.; Roizen, J. L.; Enquist, J. A.; White, D. E.; Levine, S. R.; Petrova, K. V.; Iwashita, A.; Virgil, S. C.; Stoltz, B. M. *Chem. - A Eur. J.* **2011**, *17* (50), 14199–14223.

Chapter 3: Towards a Dynamic Kinetic Resolution System for A3 Coupling Reactions

Introduction

Propargylamines

Proparglyamine are valuable synthetic moieties found in a wide variety of biologically active compounds. Traditionally propargylamines were synthesised through the exploitation of the relatively high acidity of the terminal alkyne proton (pKa ~26),[1] where strong bases like *n*-BuLi led to the formation of metal acetylide nucleophiles, which are then reacted with imines or iminium ions (**Scheme 77**).[2,3] The stoichiometric nature of this approach coupled with the sensitivity to moisture and lack of stereocontrol makes it an unattractive methodology for furnishing propargylamines. Furthermore, carbanion addition to *N*-alkyl aldimines requires the use of Lewis acids in order to activate the aldimine substrates.[4]

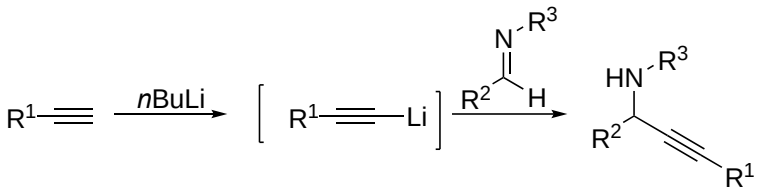

***Scheme 77**: Stoichiometric approach to propargylamines*[5]

An A3 coupling reaction is a multi-component reaction between an aldehyde, an amine and an alkyne that furnishes a propargylamine product. The first report of an A3 (aldehyde, amine, alkyne) coupling reaction was in 1998, when Dax reported the solid-phase synthesis of propargylamines *via* a three component coupling of an aldehyde, secondary amine and alkyne in the presence of two equivalents of CuCl.[6] Later in the same year, Dyatkin reported a similar solid-phase system but used only catalytic loadings of CuCl (**Scheme 78**).[7]

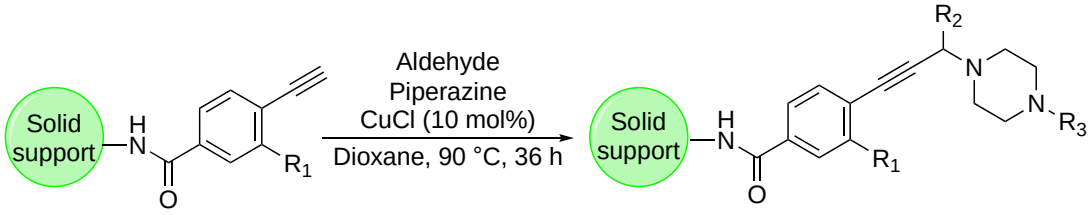

***Scheme 78:** First reported catalytic formation of propargylamines, reported by Dyatkin*[7]

The racemic catalytic direct addition of TMS-acetylene to aldimines was subsequently reported by Carreira in 2001 (**Scheme 79**).[8] The system used an iridium catalyst that was commercially available and air-stable, and notably, the protocol could be used in the absence of solvent. The system provided a highly atom-economical protocol which would readily proceed at room temperature, with yields of up to 85% reported.

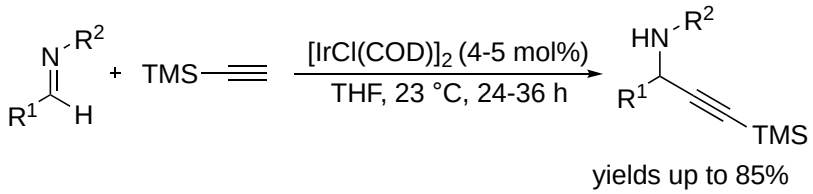

Scheme 79: *Catalytic direct addition of TMS-acetylene to aldimines*[8]

In 2002, Li reported a CuBr-$RuCl_3$ system for the synthesis of *N*-arylpropargylamines in water and solvent free conditions (**Scheme 80**).[9] Li noted that a number of Cu(I) salts showed catalytic activities including but not limited to CuCl, CuBr, CuI and CuO. Li's findings were the first reported case of the direct addition of acetylene to various imines under water/solvent free conditions, *via* C-H activation towards the generation of propargylamines.[9]

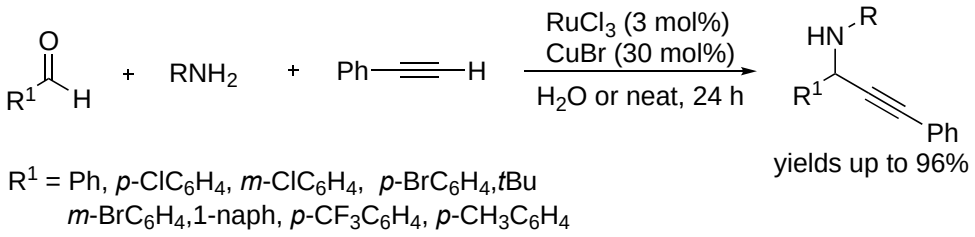

Scheme 80*: Solvent free/water compatible A3 coupling reaction*

Li also reported the first Ag-catalysed A3 coupling reaction (**Scheme 81**).[10] A reverse in the general trend of reactivity with respect to aldehydes was observed, where aliphatic aldehyde substrates showed higher reactivity compared to aromatic aldehydes.[6,11,12] This represented a significant advance at the time as protocols up until this point had poor reactivity when aliphatic aldehydes were used as substrates.

Importantly, aromatic aldehydes were also compatible with this system, furnishing propargylamine products in moderate to excellent yields (47-95%).

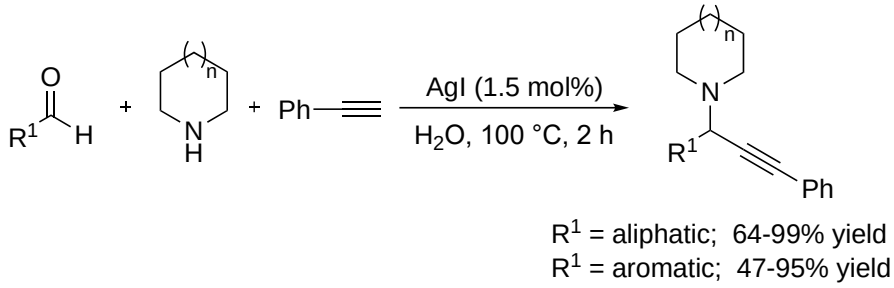

***Scheme 81**: First reported Ag-catalysed A3 coupling reaction*[10]

Enantioselective A3 Coupling Reactions

Before discussing the enantioselective variant of the A3 coupling reaction, an important consideration must be discussed. In the literature, there is a trend regarding the types of ligands that see success in asymmetric A3 coupling reactions. The general trend observed in the literature for asymmetric A3 coupling protocols is related to the choice of amine substrate used. Specifically, higher enantioselectivities for products derived from primary amines substrates tend to be achieved when chiral N,N and N,N,N ligands are used as the source of asymmetric induction (**Scheme 82**).[13] The reaction with primary amine substrates begins with a condensation reaction between the aldehyde (aliphatic or aromatic) and amine to form an imine, which is then attacked by the metal acetylide bearing a chiral ligand to give the propargylamine product in an enantioselective manner (**Scheme 82**). The overwhelming majority of enantioselective A3 couplings with primary amines see the use of the PyBox type ligands.[13] A selection of other nitrogen-based chiral ligands used in asymmetric A3 couplings with primary amine substrates are shown in Scheme 6.

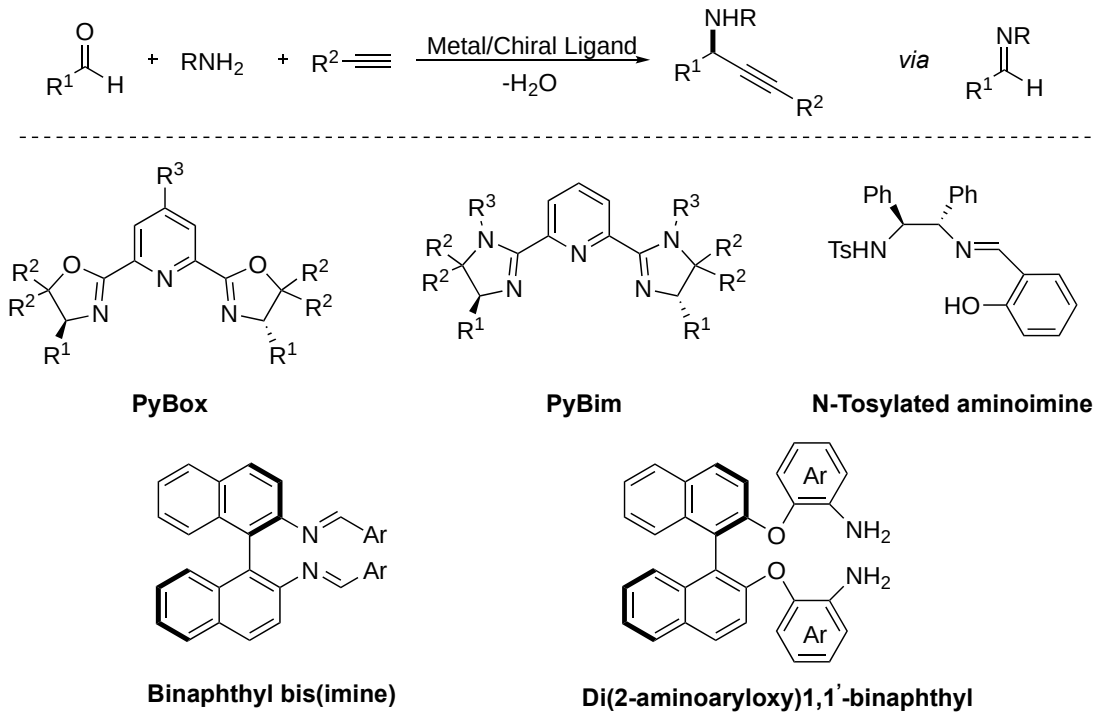

***Scheme 82**: General asymmetric A3 coupling reaction with primary amine substrates*[13]

In contrast, enantioselective A3 coupling reactions employing secondary amines see P,N ligands as the main successful ligand class (**Scheme 83**).[13] Specifically, axially chiral P,N ligands dominate the literature with respect to ligand choice for this substrate class. The most prevalent axially chiral P,N ligands used in asymmetric A3 couplings with secondary amines are shown in Scheme 7.

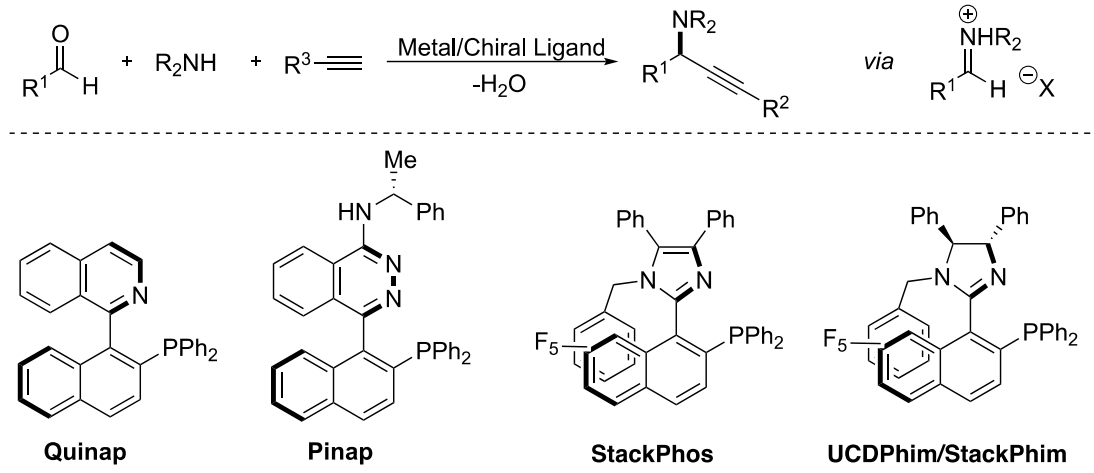

***Scheme 83**: General asymmetric A3 coupling reaction with secondary amine substrates*

The first enantioselective report of an A3 coupling reaction was reported by Li in 2002, using chiral bis(oxazolinyl) ligands **1** with a CuOTf catalyst to furnish propargylamines from phenylacetylene, aniline and a number of aromatic aldehydes (**Scheme 84**).[11] The main disadvantages of this system includes the sluggish reaction times (2-4 d with 10 mol% catalyst) and the low tolerance of the system towards the variation of amines. Enantioselectivities of up to 96% ee were reported in this system.

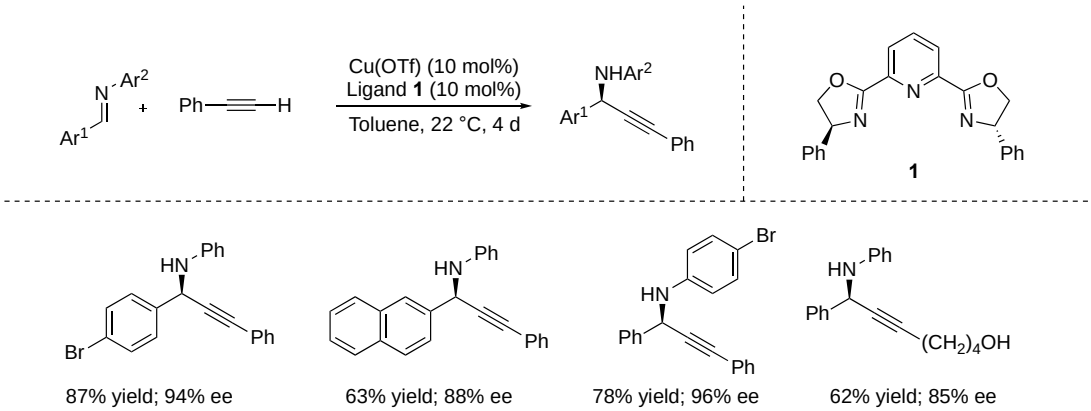

***Scheme 84**: First enantioselective example of A3 coupling[11]*

In 2003, Knochel described the use of the P,N ligand (*R*)-Quinap in A3 couplings of aromatic and aliphatic aldehydes with secondary amines and various alkynes (**Scheme 85**).[14] The generation of iminium ions *in situ* allowed for the extension of the reaction scope to non-enolisable aldehydes, compared to his previous report where enamines where isolated and reacted with with alkynyl nucleophiles[15]. The protocol proved to be successful, with yields up to 99% and ees up to 96% being reported. However, it was hindered by long reaction times of 1-6 d. Importantly, the protocol was amenable to TMS-protected alkynes nucleophiles, which served as valuable products for further functionalisation after desilylation. Knochel used this methodology to successfully synthesise α-aminoalkylpyrimidines, α-aminoalkyl-1,2,3-triazoles and functionalised primary amines.[16,17,18]

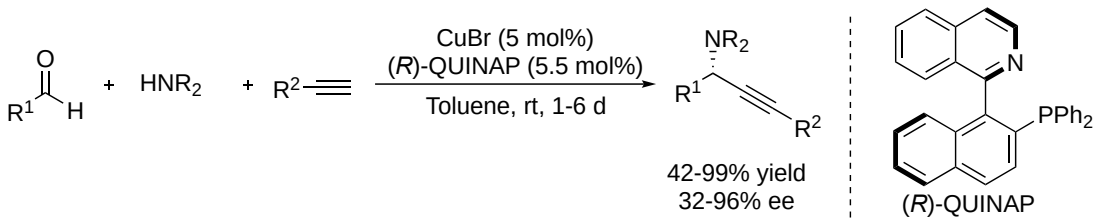

***Scheme 85**: First P,N ligand use in enantioselective A3 coupling reactions*[14]

In the same publication, Knochel also reported that A3 coupling reactions were highly diastereoselective in the absence of a chiral ligand, when chiral aldehydes or amines were used (**Scheme 86**).[14] No enantioselective variants of this protocol were reported by Knochel in this publication or to date.

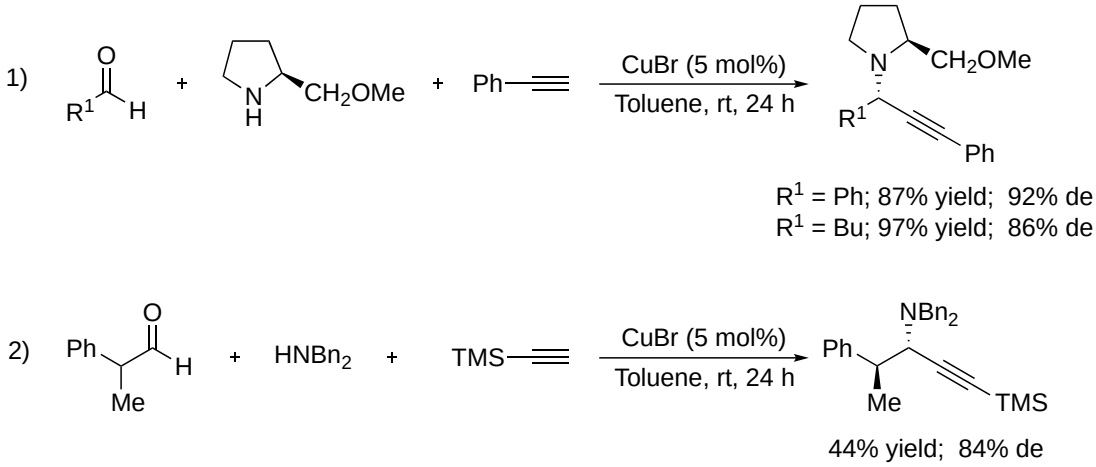

***Scheme 86**: Diastereoselectivity of racemic catalysis using chiral aldehydes/amines*[14]

Knochel observed strong non-linear effects in the enantioselective A3 coupling reaction. In accordance with previous reports in the literature which show Cu/Quinap existing as a dimer in the solid state,[15] Knochel deduced that the non-linear effects in this system were due to the fact that the heterochiral complex [Cu_2Br_2[(*R*)/(*S*)-Quinap]] appeared to react much slower compared to the homochiral complex [[Cu_2Br_2[(*R*)/(*R*)-Quinap]].[14]

From this non-linear effect, Knochel proposed a catalytic cycle for the enantioselective A3 coupling with secondary amines and Quinap as a chiral ligand (**Scheme 87**).[14] The chiral complex dimer coordinates side on with the alkyne to give complex **2**. The attack of the secondary amine on the aldehyde forms an intermediate aminal which coordinates to the Cu *via* the nitrogen lone pair of the aminal to form of complex **3**. Deprotonation of the alkyne and the loss of H_2O gives complex **4**, an end-on copper acetylide with a coordinated iminium ion. The addition of the Cu-acetylide to the iminium ion in the coordination sphere of the chiral Cu(I) complex leads to the enantioselective formation of the propargylamine product **5** and reforms the chiral catalyst.

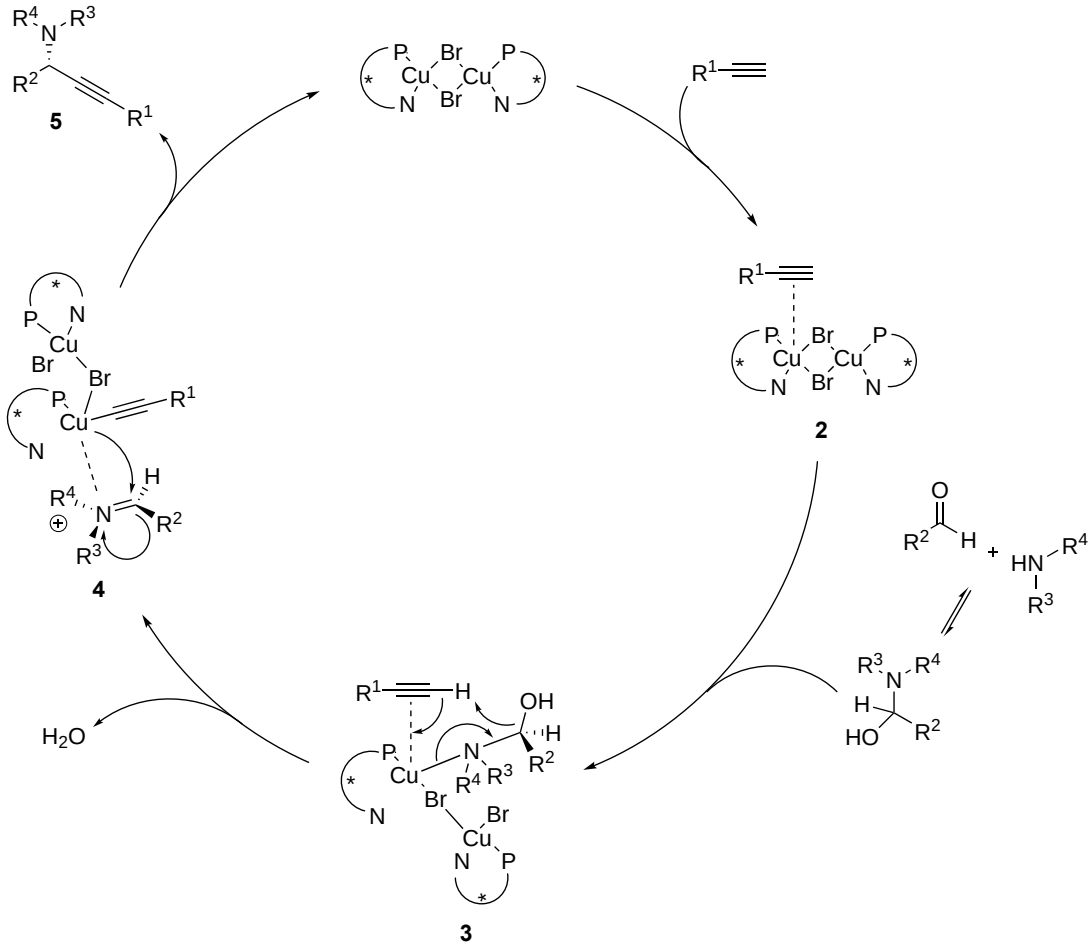

***Scheme 87**: Proposed catalytic cycle for enantioselective A3 coupling with (R)-QUINAP proposed by Knochel[14]*

Application of UCDPhim in Asymmetric A3 Couplings

Guiry reported the synthesis of the imidazoline-based axially chiral P,N ligand UCDPhim and its application in asymmetric A3 coupling reactions in 2017 (**Scheme 88**).[19] A range of aliphatic aldehydes and benzaldehyde were reacted with dibenzylamine and TMS-acetylene/phenylacetylene nucleophiles to furnish propargylamine products. Yields ranged from 23-98% and enantioselectivities from 65-98% ee, with benzaldehyde giving both the lowest yield and enantioselectivity.[19] The TMS groups had to be cleaved before ee determination by chiral UPC^2, which was achieved under standard deprotection conditions with tetra-*N*-butylammonium fluoride.

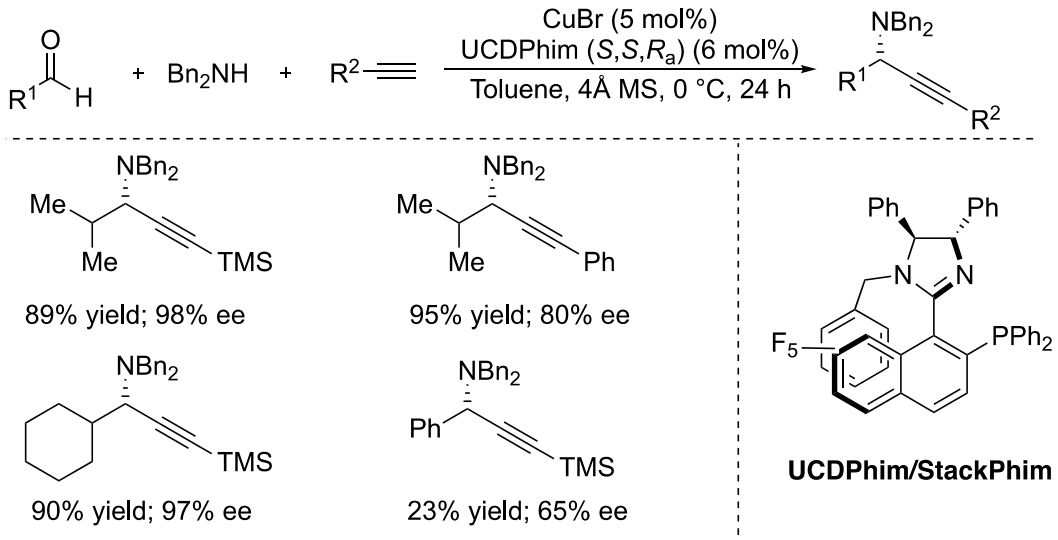

***Scheme 88**: Initial reported application of UCDPhim in asymmetric A^3 couplings*

The substrate scope for asymmetric A3 couplings with UCDPhim was later expanded by Guiry in 2019 (**Scheme 89**).[20] Through careful optimisation, it was found that propargylamine products could be accessed in high enantioselectivities from aryl aldehyde substrates when reacted with various cyclic secondary amines and dimethylpropargyl alcohol **6.** The new substrate combinations allowed for the much cheaper commercially available dimethylpropargyl alcohol to be used instead of TMS-acetylene. The new protocol formed enantioenriched propargylamine products in excellent yields and ees up to 99%. This study showed that the combination of

aldehyde, amine and alkyne need to be precise and synergistic in order to furnish products in good yields and high enantioselectivities. The enantioselectivity was observed to decrease if one suboptimal component, in terms of aldehyde, amine or alkyne, was used in the reaction. Furthermore, once optimal substrate combinations were found, the catalyst loading could be lowered from 5 mol% to 1 mol% while still giving excellent yields and enantioselectivities in short reaction times (24 h).[20] The cheaper dimethylpropargyl alcohol (compared to TMS-acetylene) used throughout this study could be cleaved in excellent yields without erosion of enantiopurity, through treatment with sodium hydride at reflux for 5 h. Again, this left a valuable functional group handle for further functionalisation of the propargylamine product.

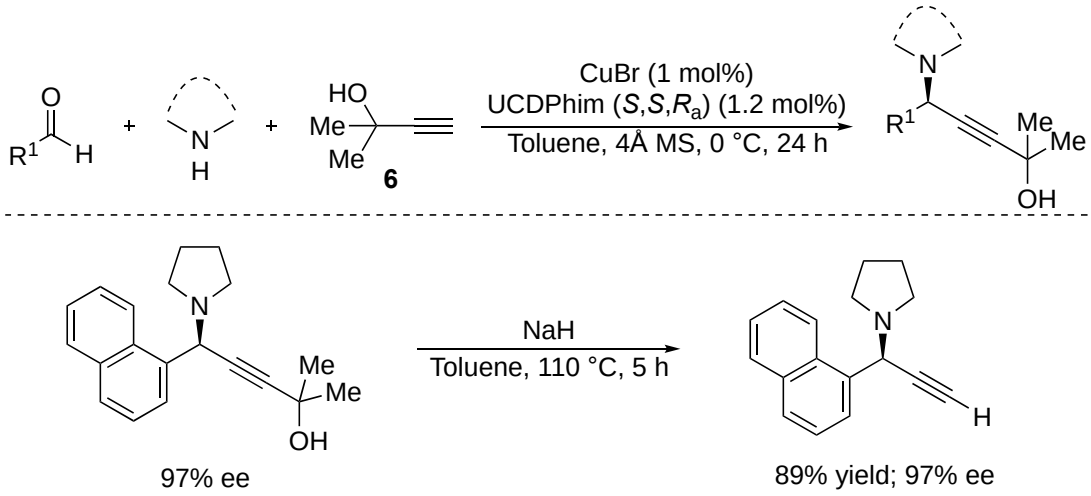

***Scheme 89**: Expanded substrate scope of UCDPhim in asymmetric A³ coupling*

Types of Kinetic Resolution in Asymmetric Synthesis

Kinetic Resolution

The process of kinetic resolution has been summarised schematically (**Scheme 90**). In its simplest terms, kinetic resolution is the reaction of a racemic mixture of two enantiomeric compounds with a chiral reagent to give an enantiomerically enriched compound. The reaction mixture is resolved kinetically as one of the stereoisomers of substrate (SM_R, **Scheme 90**) reacts slower with the catalyst compared with the

other stereoisomer. This slower reaction rate means an appreciable amount of product, P_R, is not formed from SM_R. As a result, product is only formed with the more reactive isomer, SM_S in this example, to form product P_S. This example also serves to highlight the inherent drawback of a kinetic resolution system, i.e. the fact that the maximum possible yield of product is 50%. This is an intrinsic property of kinetic resolution systems as half of the racemic starting material remains unreactive with the chiral reagent/catalyst. In order for a kinetic resolution system to be viable, a selectivity factor (k_{fast}/k_{slow}) of >200 is required between the two enantiomers of starting material (**Scheme 90**).[21]

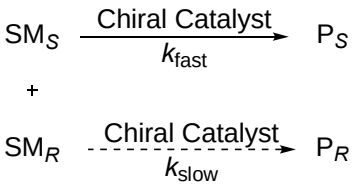

***Scheme 90**: General scheme for asymmetric kinetic resolution*

The most well-known example of kinetic resolution in asymmetric synthesis is the Sharpless epoxidation, developed in 1980 (**Scheme 91**).[22,23,24] The system uses a racemic mixture of an allylic alcohol substrate with a titanium-diisopropyl tartrate catalyst, which selectively reacts with only one enantiomer of the starting material to form the epoxide asymmetrically. The unreactive starting material enantiomer was isolated in a 49% yield and >99% ee and the enantioenriched epoxide was isolated in a 48% yield and 99% ee.

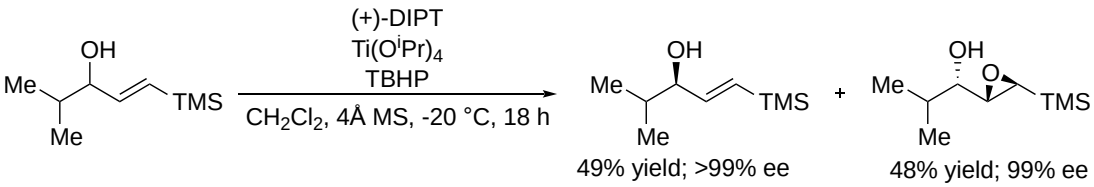

***Scheme 91**: Kinetic resolution of TMS secondary allylic alcohols using Sharpless asymmetric epoxidation[24]*

Parallel Kinetic Resolution

Parallel kinetic resolution (PKR) is a modified version of the kinetic resolution protocol. The premise is largely the same as a kinetic resolution system, except the less reactive starting material isomer reacts to form a different product which removes it from the reaction mixture (**Scheme 92**).[21] Two different products are formed from the two enantiomers of the starting material and as such this circumvents the need for a high selectivity factor that is required for traditional kinetic resolution systems.[21]

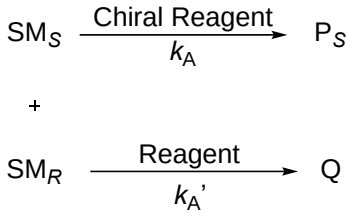

***Scheme 92**: General schematic for parallel kinetic resolution*

The main advantage of a parallel kinetic resolution system is that less erosion of the product ee can occur. As a reaction progresses in a traditional kinetic resolution, the concentration of the less reactive isomer will increase. This is due to the faster reacting starting material isomer being converted into product. This means that there is greater opportunity for the less reactive isomer to react with the catalyst due to an effective increase in its concentration.[21] Therefore a PKR negates the need for low reaction rate of the undesired stereoisomer of starting material as it preferentially converts the undesired isomer into a different product.

An example of a PKR system was reported by Doyle in 1995, for the enantioselective intramolecular cyclopropanation of secondary allylic diazoacetates (**Scheme 93**).[25] The system used a dimeric rhodium catalyst with chiral methoxycarbonyl-2-oxyoxazolidinyl ligands to react with the racemic mixture 2-cycloxene-1-yl-diazoacetate containing (*R*)-**7** and (*S*)-**7**. They found when the (*R*)-enantiomer of the methoxycarbonyl-2-oxyoxazolidinyl ligands were used, they would selectively react with (*R*)-**7** to form the tricyclic cyclopropane **8**. The catalyst would also react with (*S*)-

7 but instead would form the achiral cyclohexanone product **9** *via* an intramolecular hydride abstraction from the allylic C-H α to the oxygen, followed by elimination of the ketene.[25] The (*S*)-enantiomer of catalyst could be used to form the opposite enantiomer of the tricyclicpropane product from the same mixture of racemic 2-cycloxene-1-yl-diazoacetate.

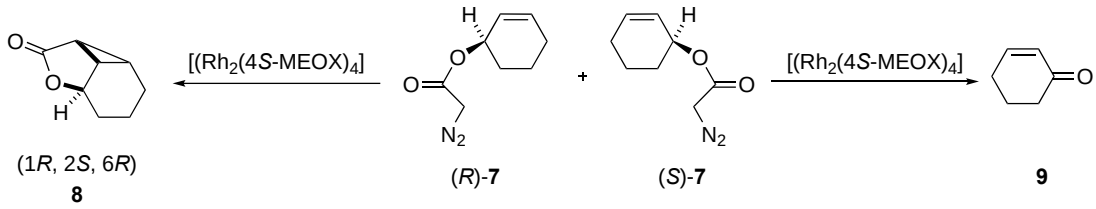

***Scheme 93**: Parallel kinetic resolution system for the enantioselective intramolecular cyclopropanation of allylic diazoacetates[25]*

Dynamic Kinetic Resolution

Dynamic Kinetic Resolution (DKR) is similar to kinetic resolution as a chiral reagent/catalyst reacts with one stereoisomer of starting material preferentially in order to access an enantioenriched product. The key difference in DKR is that the racemic starting material has the ability to interconvert between the two stereoisomers of the starting material, often *via* an deprotonation of an acidic α-proton of a carbonyl species.[26] This is important as the less reactive isomer of starting material, SM_R, can convert to the more reactive isomer of starting material, SM_S (**Scheme 94**). SM_S can subsequently react with the chiral catalyst to form the chiral product P_S. This interconversion overcomes the key problem in KR and PKR systems, where yields are inherently capped at 50%, as the unproductive starting material can interconvert to the productive isomer. For a successful DKR system, the selectivity factor (k_{fast}/k_{slow}) must be >30, with best results achieved when the selectivity factor is >50-100.[26] The rate of interconversion, k_{rac}, must be equal or greater than the rate of converting substrate to product, k_{fast} in this case (**Scheme 94**).[26]

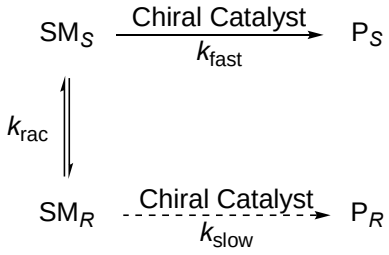

***Scheme 94**: General scheme for a dynamic kinetic resolution system*

A recent example of a DKR system was reported by Dong in 2019 (**Scheme 95**).[27] The system involves using a chiral rhodium catalyst for olefin hydroacylation. The aldehyde (*R*)-**10** undergoes oxidative addition with the chiral Rh catalyst to generate the Rh-acyl-hydride **11**. Subsequent migratory insertion gives the metallocycle **12** which reductively eliminates to give the cyclopentanone product **13**. The unreactive aldehyde (*S*)-**10** reacts with a primary amine catalyst, which facilitates its racemisation to aldehyde (*R*)-**10** *via* an imine-enamine tautomerisation, which is a stereoablative process. This funnels the unreactive isomer (*S*)-**10** to the reactive isomer (*R*)-**10** which results in the formation of the desired product in yields >50%. A control experiment was carried out without the amine catalyst, which facilitates the interconversion of the starting material stereoisomers. While the experiment still yielded the same cyclopentanone product, it did so with lower yields (38%). This showed that the amine is not involved in the formation of lactone product from the reactive (*R*)-**10** isomer. Importantly, the control experiment also showed that the amine catalyst can facilitate the racemisation of the unreactive (*S*)-**10** isomer, as yields of the lactone product exceed 50% when the amine catalyst is present in the reaction.

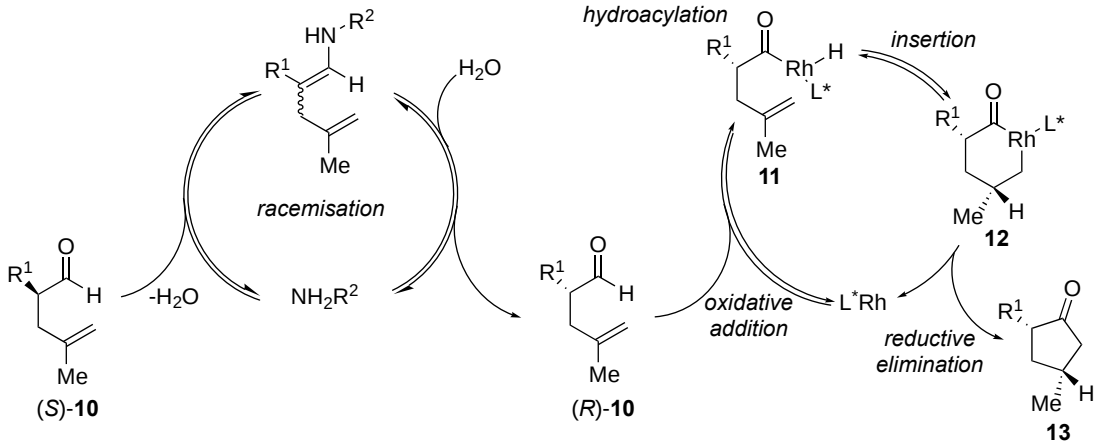

***Scheme 95**: Dynamic kinetic resolution system for enantioselective hydroacylation reported by Dong[27]*

Dynamic Kinetic Asymmetric Transformation

The term Dynamic Kinetic Asymmetric Transformation (DYKAT) was coined by Trost and is summarised in **Scheme 96**.[28,29] DYKAT is similar to DKR but racemisation occurs *via* a chiral substrate-catalyst complex compared to racemisation occurring *via* an achiral intermediate in DKR. The protocol relies on the difference in reactivity between the two diastereomers SM_SCat^* and SM_RCat^* for the resolution of the racemic starting material (SM_SCat^* denotes the starting material-catalyst bound intermediate).

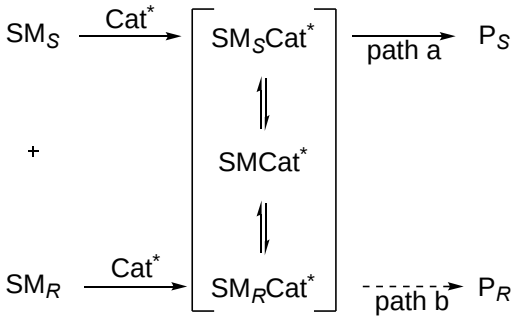

***Scheme 96**: General scheme for dynamic asymmetric transformation*

The first DYKAT system, reported by Trost, is shown below (**Scheme 97**). The protocol employed a racemic mixture of γ-acyloxybutenolides **14** and ent-**14**, which were

reacted with a chiral Pd catalyst.[29] This leads to the formation of two chiral π-allylpalladium η^3 complexes **15** and ent-**15**, which can interconvert *via* an η^1 intermediate **16**. The rate of interconversion between **15** and ent-**15** was increased through the use of a basic additive. They found that one of the diastereomeric complexes reacted with an external nucleophile at a faster rate, giving them a DYKAT protocol for these substrates. This protocol was used a key step for the enantioselective synthesis of (−)-Aflatoxin B.

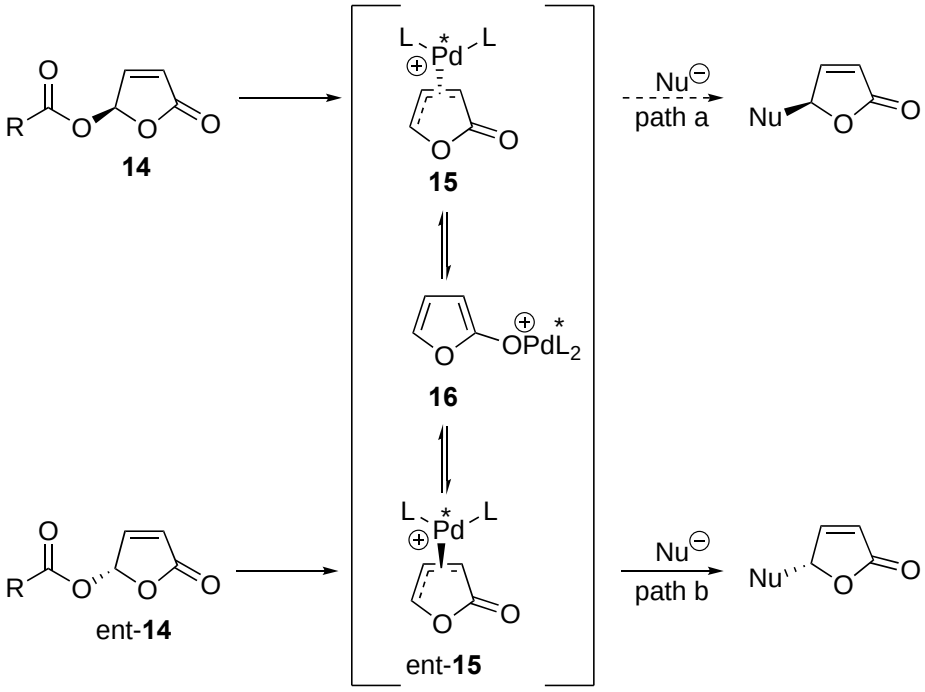

***Scheme 97**: First classification of DYKAT system, report by Trost[29]*

Project Aim

The aim of this project was to establish a protocol for a dynamic kinetic resolution system in an asymmetric A3 coupling reaction using the UCDPhim ligand (**Scheme 98**). The other P,N ligands synthesised in this thesis were not in hand at the time of conducting this project, and as such were not considered in the proposed A3 DKR system. This was based on the one diastereoselective report in the literature by Knochel of a diastereoselective A3 coupling using racemic chiral aldehydes (**Scheme 86**).[14] The system would use chiral racemic aldehydes in asymmetric A3 coupling

reactions with the UCDPhim ligand and a Cu catalyst to furnish propargylamine products of type **17**, containing two contiguous stereocentres as a single diastereomer in yields up to 100%.

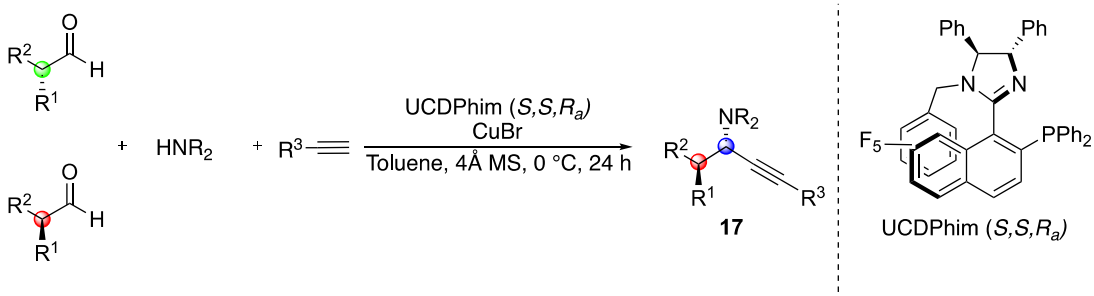

***Scheme 98**: Proposed dynamic kinetic resolution system for A³ coupling reaction with UCDPhim ligand*

The system was proposed to work as per the schematic below (**Scheme 99**), and mirrors the protocol established by Dong in 2019 (**Scheme 95**).[27] The racemic chiral aldehyde starting material would exist as two enantiomers – with the stereocentre configurations depicted by the green and red spheres. The two stereoisomers would react with the secondary amine to form an iminium ion as per a standard A3 coupling reaction. The Cu-UCDPhim catalyst would react with the alkyne to form a copper acetylide, which was hoped to react preferentially with one of the two iminium ion enantiomers. This would lead to the formation of the propargylamine product of type **17**, with two contiguous stereocentres as a single diastereomer, where the red stereocentre is from the starting aldehyde and the blue stereocentre is formed from the stereoselective addition of the alkyne to the iminium ion by the Cu-UCDPhim catalyst.

It was hoped that the mismatch iminium ion isomer (green) would interconvert to the match red iminium ion isomer *via* iminium ion enamine tautomerisation, which is a stereoablative process.

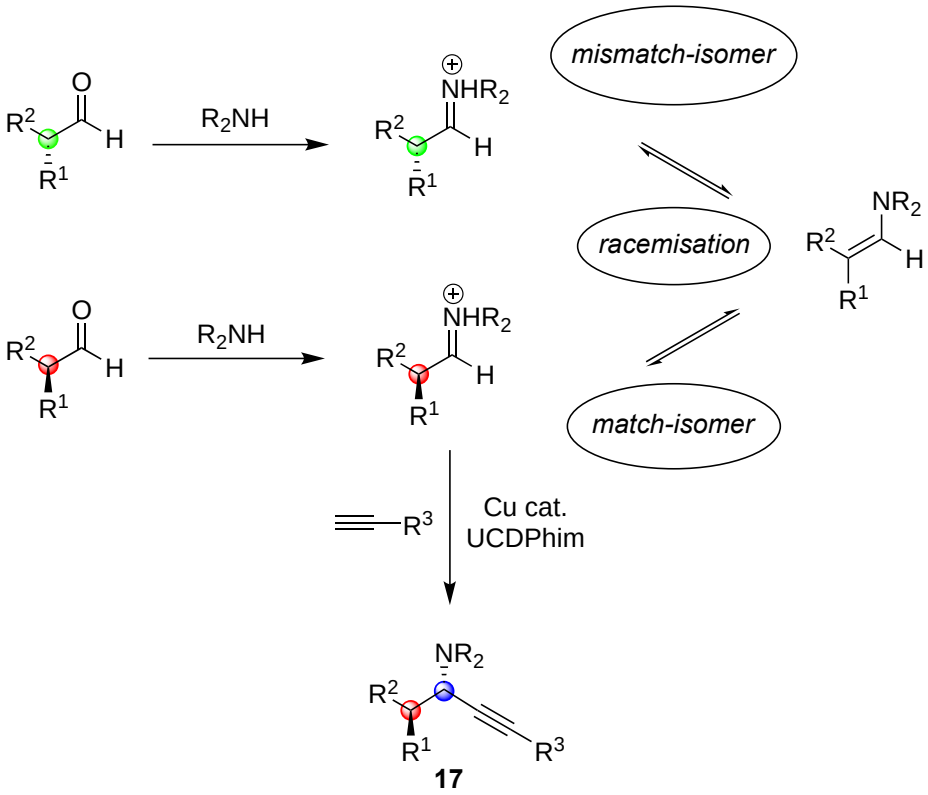

***Scheme 99**: Proposed DKR system for diastereoselective A3 couplings*

Results and Discussion

Initial Substrate Scope

It was decided that a range of A3 coupling products bearing α-chiral centres were to be synthesised using a copper bromide catalyst and the UCDPhim ligand - as reported by Guiry in 2019 (**Scheme 100**).[20] A variety of aliphatic aldehydes with varying chain lengths were used in the synthesis of these products, with products being formed in approximate 1:1 diastereomeric ratio in each case. The alkyne nucleophile was also varied in this initial investigation with TMS-acetylene, dimethylpropargyl alcohol and propargyl alcohol being used. Again, no effect on the diastereoselectivity of the reaction was observed. The only product formed with a degree of diastereoselectivity was product **18** (de 57%), which was formed from 2-phenylpropionaldehyde, TMS-acetylene and dibenzylamine. The innate volatility of TMS-acetylene as a reagent contributed to the disappointingly low yields of the corresponding products derived. Representative ^{1}H and ^{13}C NMR spectra for product

19 are shown after **Scheme 100**, in **Figure 20** and **Figure 21**, respectively. Despite concerted efforts, the four product stereoisomers for the compounds below (**Scheme 100**) were not completely separable by UPC^2 chromatography or by UHPLC.

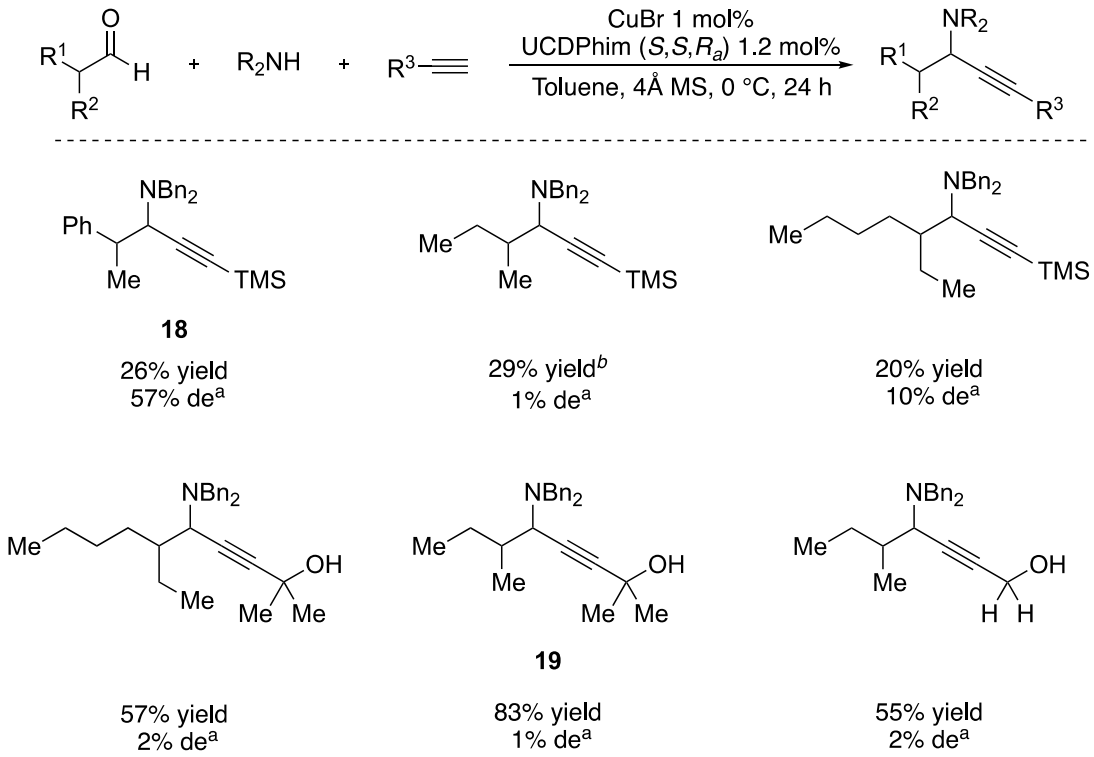

***Scheme 100**: A3 coupling products bearing α-chiral centres for the probing of DKR system, [a]de% determined by ^{1}H NMR, [b]isolated yield calculated after deprotection*

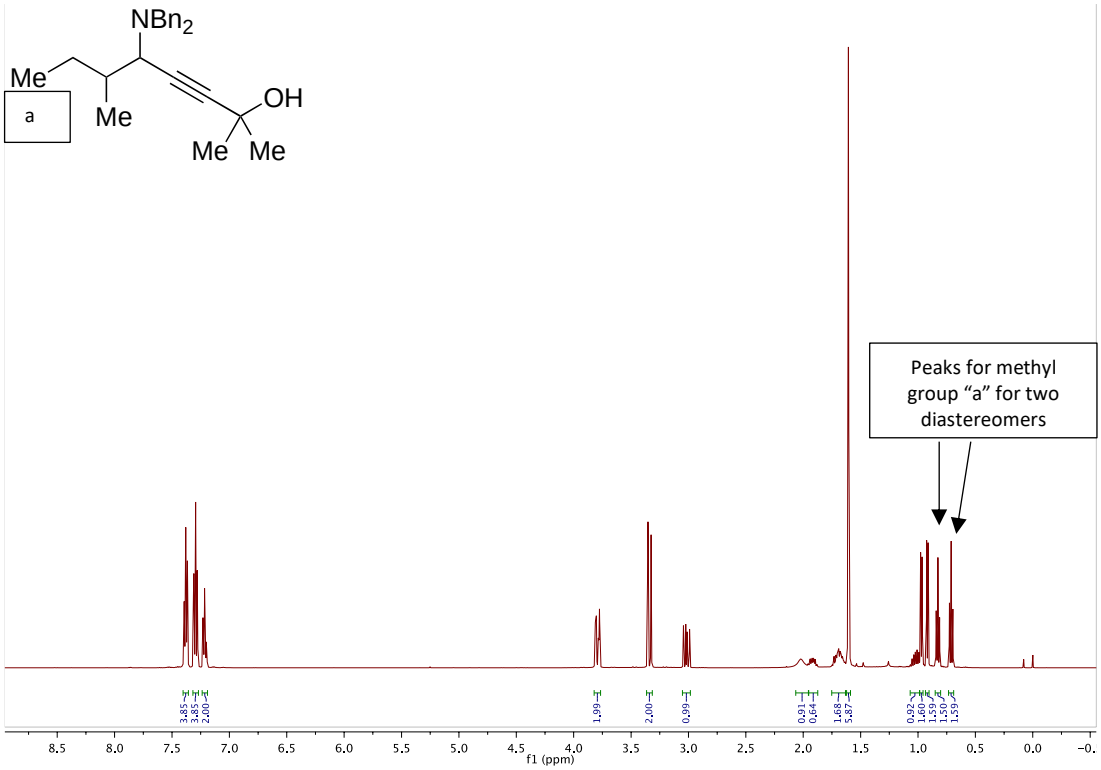

***Figure 20**: [1]H NMR spectrum of product **19** showing presence of two diastereomers*

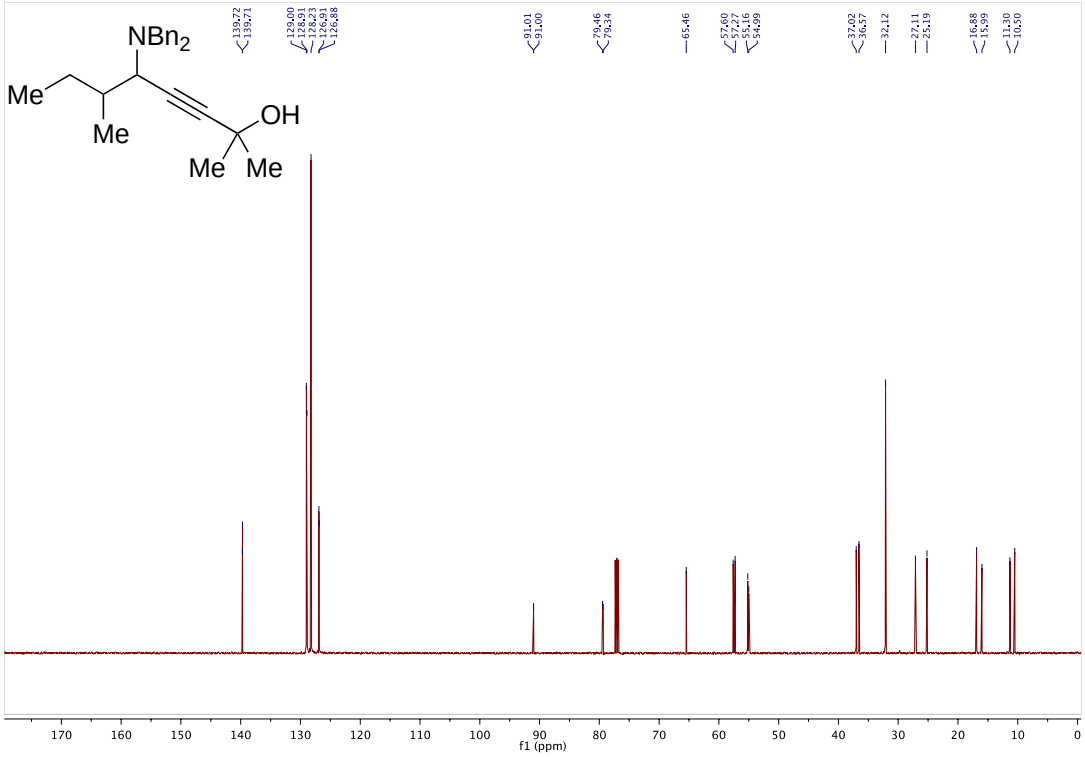

***Figure 21**: [13]C NMR spectrum of product **19** showing presence of two diastereomers*

Reaction Optimisation

Temperature Screen

A temperature screen for the formation of product **20** was performed, the results of which are summarised in **Table 4.** The purpose of this investigation was to probe if lowering the reaction temperature influenced the diastereoselectivity of the test reaction. Unfortunately, no appreciable effect in diastereoselectivity was observed by NMR spectroscopy when the reaction temperature was lowered from rt to −30 °C (**Table 4**). As yield was negatively affected by lowering of the temperature of the reaction (36% to 19%), further lowering of the reaction temperature was not investigated.

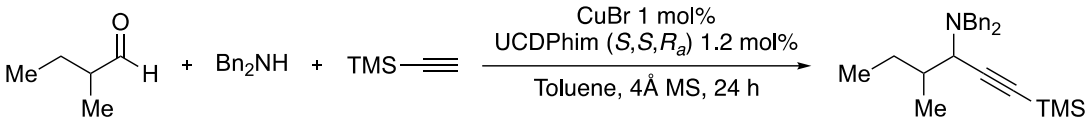

20

Entry	Ligand	Temperature	Yield (%)	De (%)[a]
1	**None**	**rt**	**36**	**7**
2	**UCDPhim (*S*,*S*,*R*a)**	**rt**	**n/a**	**1**
3	**UCDPhim (*S*,*S*,*R*a)**	**0 °C**	**29**	**1**
4	**UCDPhim (*S*,*S*,*R*a)**	**−30 °C**	**19**	**10**

Table 4*: Temperature probe on the diastereoselectivity of the proposed A3 coupling system with DKR, [a]diastereoselectivity determined by [1]H NMR spectroscopy*

Chiral Aliphatic Aldehydes Bearing Increased Steric Bulk

From the initial substrate scope (**Scheme 100**), it appeared that having a large difference in sterics between the two groups on the α-chiral centre was important for the diastereoselectivity of the reaction. However, it was noted that in product **18** where such a large difference exists, the reactivity was greatly diminished. Two aldehyde substrates were synthesised as per **Scheme 101**, in an effort to combine the increased diastereoselectivity of aryl-substituted product **18** with the reactivity observed in products derived from aliphatic aldehydes (**Scheme 100**). Iodobenzene and 2-iodonaphthalene were reacted with methallyl alcohol in a Heck isomerisation reaction to furnish aldehydes **21** and **22** in 23% and 43% yields, respectively. It is worth noting that both aldehydes showed great propensity to undergo oxidation in air, and as such should be stored carefully under nitrogen.

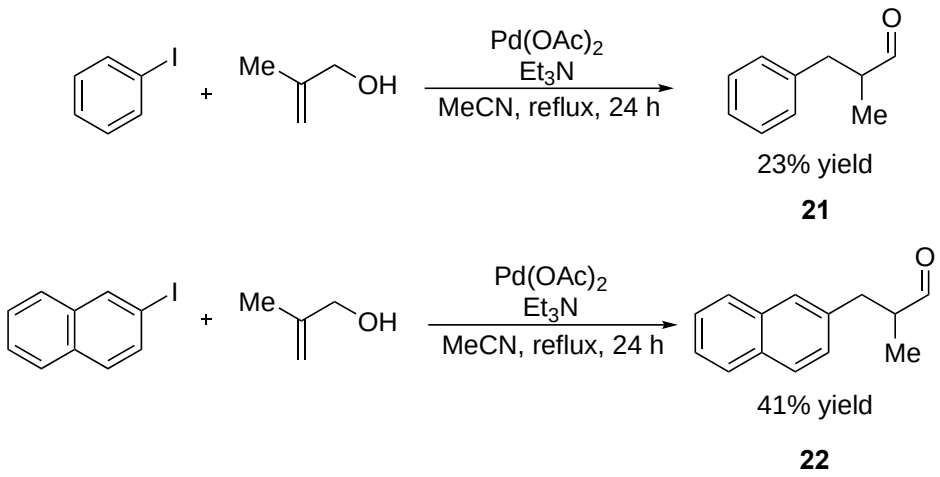

***Scheme 101**: Sterically hindered branched aldehyde substrate synthesis via Heck reaction*

Racemic aldehydes **21** and **22** with then employed in asymmetric A3 coupling reactions to probe their effectiveness in a potential DKR system (**Scheme 102**). Disappointingly, the extra steric bulk of these aliphatic aldehydes did not afford any increase in diastereoselectivity. Gratifyingly, product **23** was separable by chiral SFC and was formed in an 97% ee (**Figure 22** and **Figure 23**). This was evidence that enantioselectivities in a product with an α-chiral centre were similar to the reported ees in traditional A3 coupling reactions using the UCDPhim ligand.[19]

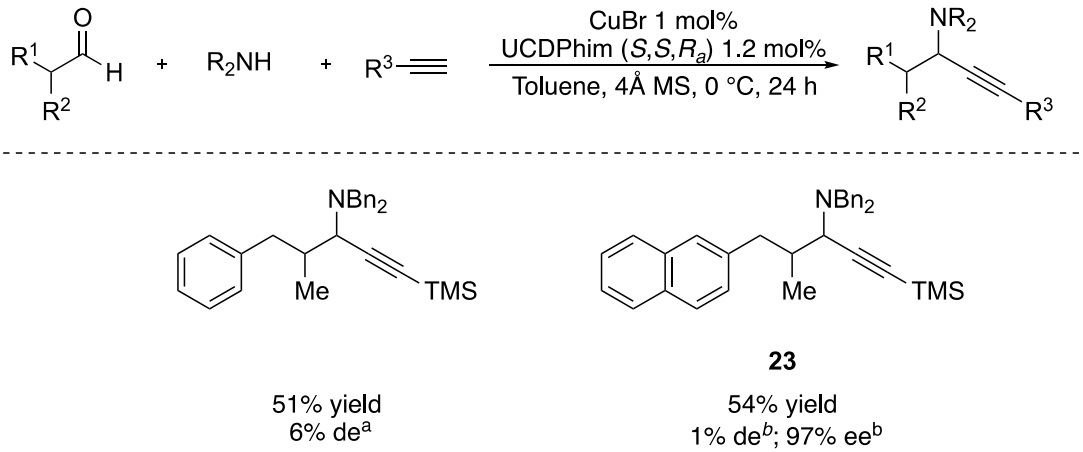

23

51% yield
6% de[a]

54% yield
1% de[b]; 97% ee[b]

***Scheme 102**: A[3] coupling reactions with sterically hindered aliphatic aldehydes, [a]determined by [1]H NMR spectroscopy, [b]determined by chiral UPC[2]*

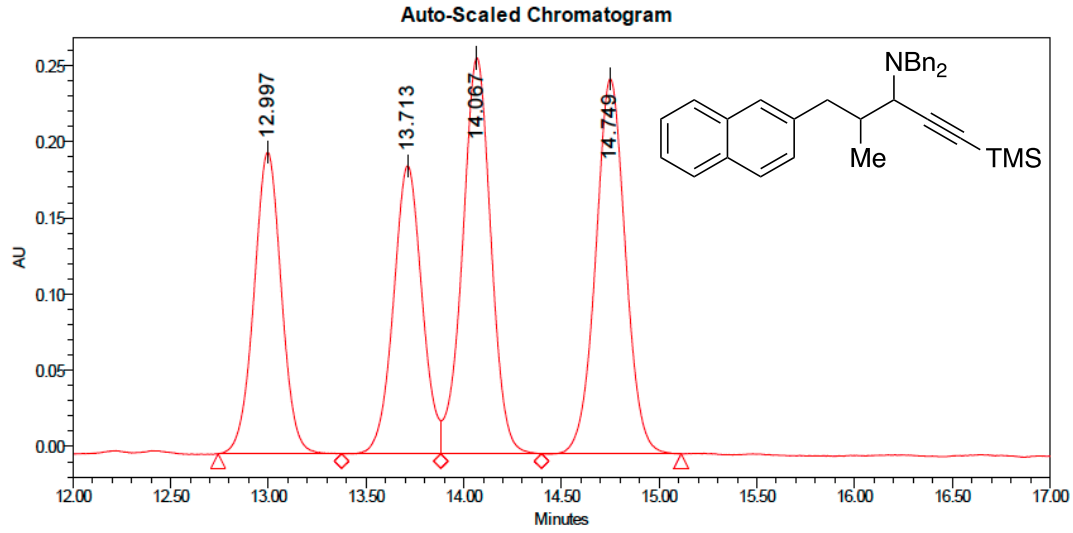

Peak Results

	Name	RT	Area	Height	Amount	Units	% Area
1		12.997	1929588	197775			21.22
2		13.713	1919731	188897			21.11
3		14.067	2634425	259825			28.97
4		14.749	2608710	245974			28.69

Figure 22**: SFC chromatogram of racemic product **23

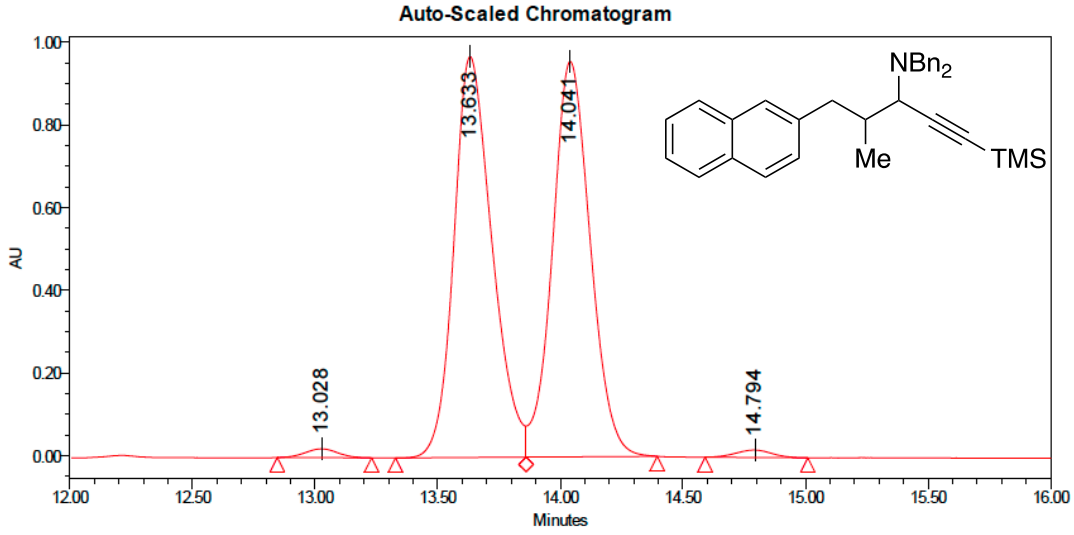

Peak Results

	Name	RT	Area	Height	Amount	Units	% Area
1		13.028	197242	21416			0.93
2		13.633	10492817	970107			49.62
3		14.041	10274727	956431			48.59
4		14.794	183131	18000			0.87

***Figure 23**: SFC chromatogram of enantioenriched product **23** using UCDPhim as chiral ligand*

α-Aryl Product Optimisation

After this investigation, it was decided to focus on product **18** (**Scheme 100**) which has an aryl group attach directly to the α-chiral centre. In the first step of reaction optimisation, different Cu(I) salts commonly used in asymmetric A3 coupling reactions were examined in the A3 DKR system (**Table 5**). The loading of Cu(I) salt and ligand was also increased from 1% to 2% to overcome the low reactivity of the α-aryl aldehyde substrate. The disappointingly low reactivity of the substrate persisted, despite doubling the catalyst loading. Yields remained poor (3-26%) after allowing the reaction to progress for 4 d (**Table 5**). However, a noticeable improvement in diastereoselectivity was observed when CuI was used in the reaction. This increase in diastereoselectivity was unfortunately at the expense of yield when compared to the original conditions with CuBr. A successful DKR protocol would require a high degree of diastereoselectivity in product formation, as such it was decided to use CuI as the catalyst and apply further changes to the system with the aim of increasing reaction yield.

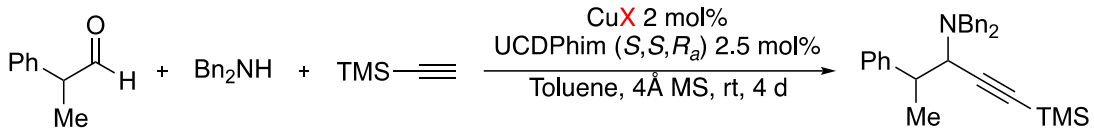

24 **18**

Entry	Copper Salt	Yield (%)[a]	De (%)[b]
1	**CuBr**	**26**	**57**
2	**CuI**	**13**	**84**
3	**CuCl**	**3**	**66**
4	**CuOAc**	**No rxn**	**No rxn**

***Table 5**: Effect of Cu (I) salts on diastereoselectivity, [a]Yields isolated by column chromatography, [b]%de determined by ^{1}H NMR spectroscopy*

Before continuing with further optimisation of the A3 coupling DKR system, an investigation into the presence of ligand acceleration was conducted to determine if the precious UCDPhim ligand was required. This was necessary as each reaction

required 7.1 mg of ligand at 2.5 mol% loading, which was significant due to the challenging nature of accessing the ligand (this will be discussed further in Chapter **3** of this thesis).

The model reaction (**Table 6**) was monitored at a series of time points by ^{1}H NMR spectroscopy with 1,3,5-trimethoxybenzene as an internal standard. The yield of the reaction did not change at any time point when the reaction was performed without chiral ligand (**entry 1**) or in the presence of the chiral UCDPhim ligand (**entry 2**, **Table 6**). The progress of the reaction was investigated in greater detail in **entry 3** and **entry 4** (**Table 6**). Specifically, increasing the catalyst loading to 10 mol% and later using a stoichiometric amount of CuI did not yield the product in a quantitative manner, irrespective of diastereoselectivity.

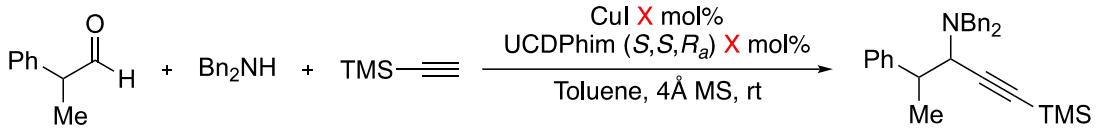

Entry	CuI loading	Ligand loading	Yield (%) (3 h)[a]	Yield (%) (24 h)[a]	Yield (%) (48 h)[a]	Yield (%) (96 h)[a]
1	**2 mol%**	**0 mol%**	**10**	**25**	**25**	**29**
2	**2 mol%**	**3 mol%**	**14**	**23**	**25**	**32**
3	**10 mol%**	**0 mol%**	**n/a**	**52**	**60**	**60**
4	**100 mol%**	**0 mol%**	**n/a**	**69**	**77**	**78**

***Table 6**: Investigation into ligand acceleration with α-aryl aldehyde substrate, [a]% yield determined by ^{1}H NMR spectroscopy with 1,3,5-trimethoxybenzene as an internal standard*

The lack of reactivity of the α-aryl aldehyde substrate was confirmed by the time study conducted above (**Table 6**). We proposed that the iminium ion **25** that would form once dibenzylamine condensed on the α-aryl aldehyde, could subsequently tautomerise to the enamine **26** (**Scheme 103**). The enamine tautomerisation would be possible as the proton on the α-chiral centre is benzylic and therefore relatively acidic. The formation of enamine **26** would be favourable as it would have extended

conjugation with the phenyl ring and would also alleviate the positive charge on nitrogen, both of which would be thermodynamically favourable processes.

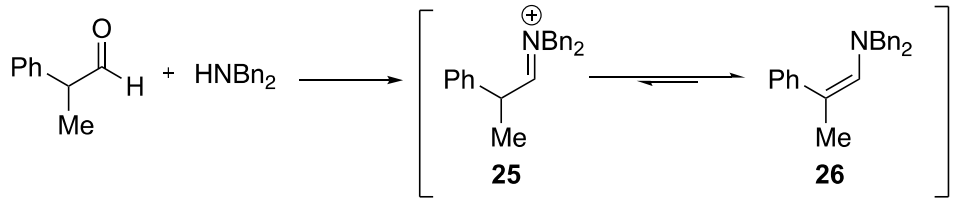

***Scheme 103**: Proposed iminium ion enamine interconversion for α-aryl aldehyde substrate*

With these observations in hand and a proposed hypothesis for the observed lack of reactivity of the α-aryl aldehyde, we decided to conduct a screen of Brønsted acid additives. It was hoped that a Brønsted acid would influence the enamine iminium ion equilibrium towards the formation iminium ion **24** (**Scheme 103**). Brønsted acids with a range of pKa values were screened (**Table 7**), drawing on precedence in the literature where they were employed successfully in other A3 coupling reactions.[30] Unfortunately, all but two cases (**entry 1** and **entry 2**) resulted in no product being formed. In the case of **entries 1** and **2** (**Table 7**), reactivity was hindered by the presence of Brønsted acids compared to the reaction lacking a Brønsted acid, (**entry 2**, **Table 6**).

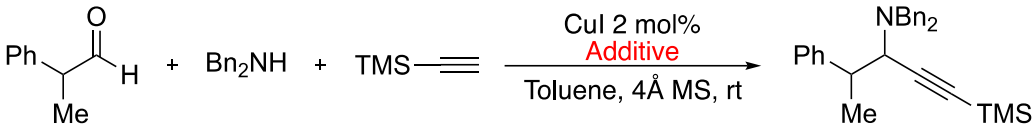

Entry	Additive (1 equiv.)	pKa (H_2O)	Yield (%) (24 h)[a]	Yield (%) (48 h)[a]
1	**Pivalic Acid**	**5.03**	**4**	**6**
2	***p*-TsOH**	**-2.08**	**8**	**9**
3	**Triflic acid**	**-14.7**	**No rxn**	**No rxn**
4	**Formic acid**	**3.75**	**No rxn**	**No rxn**
5	**Trifluoroacetic acid**	**0.23**	**No rxn**	**No rxn**
6	**N-Boc Proline**	**1.99**	**No rxn**	**No rxn**
7	**Benzoic acid**	**4.20**	**No rxn**	**No rxn**

***Table 7**: Brønsted acid screen to promote iminium ion formation, [a]Yields determined by ^1H NMR spectroscopy using 1,3,5-trimethoxybenzene as an internal standard*

A few observations could be made about the scope for a DKR system at this stage in the project:

1) The α-aryl aldehyde substrate **24** had low reactivity, despite increasing catalyst loadings from 1 mol% to 2 mol% (**Table 5**);
2) Changing the Cu(I) source from CuBr to CuI led to an increase in diastereoselectivity (57% to 84% de), however this was at the expense of yield (26% to 13% yield) (**Table 5**);
3) The reaction had no appreciable ligand acceleration and product would not form quantitatively with stoichiometric amounts of CuI at room temperature (**Table 6**);
4) Brønsted acids had no effect on shifting the proposed equilibrium (**Scheme 103**) towards the iminium ion required for product formation (**Table 7**).

Aliphatic Aldehyde Optimisation

Optimisation towards accessing a DKR protocol for α-aryl aldehyde substrates remained unsuccessful in the present study due to the continued poor reactivity towards product formation. As such, efforts were focussed towards optimising an asymmetric A3 coupling DKR protocol for aliphatic aldehyde substrates. This decision was made as aliphatic aldehyde substrates such as **27** had shown greater reactivity towards product formation in the present study (**Scheme 104**).

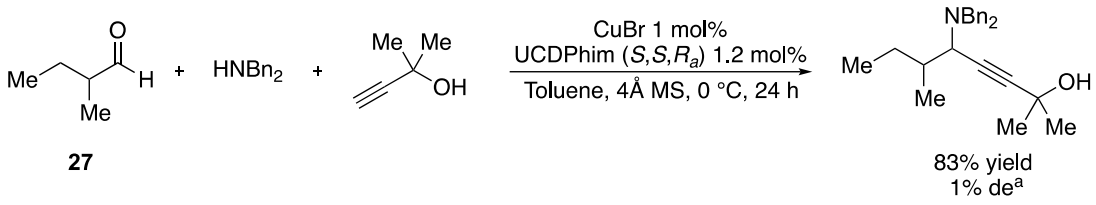

***Scheme 104**: A3 coupling DKR reaction with an aliphatic aldehyde substrate from the initial substrate scope (**Scheme 100**), [a]diastereoselectivity determined by ^{1}H NMR spectroscopy*

The shortcoming for these aliphatic aldehydes was the lack of diastereoselectivity in product formation to date in the present study. It was thought that the presence of

a Lewis acid could increase the rate of iminium ion formation (**Scheme 105**). It was hoped that if a Lewis acid could increase the rate at which the iminium ion **28** was formed, then there would be more time for the desired iminium ion interconversion to occur *via* the enamine **29** (**Scheme 105**). This would be necessary as the stereoablative interconversion of the iminium ion would be required for a successful DKR system.

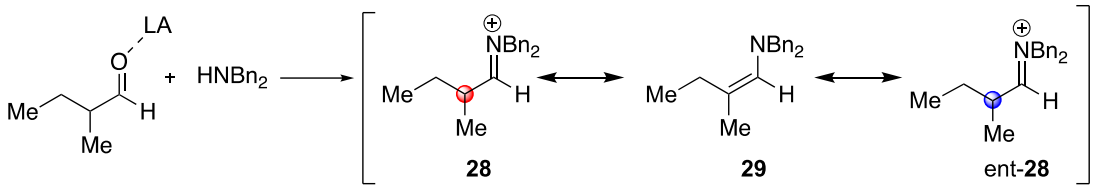

***Scheme 105**: Lewis acid mediated iminium ion formation*

Aliphatic Aldehyde Ligand Acceleration

Test reactions were performed to see if there was ligand acceleration in the case of aliphatic aldehyde substrates (**Table 8**). From this experiment, it was shown that significant ligand acceleration was taking place in the reaction of aliphatic aldehyde **30** with dibenzylamine and TMS-acetylene. This showed that further reaction optimisation with these aliphatic aldehyde substrates would require the use of the UCDPhim ligand.

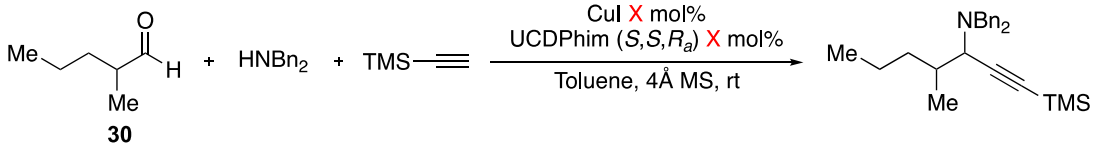

Entry	CuI loading	Ligand loading	Yield (%) (24 h)[a]	Yield (%) (48 h)[a]	de (%)[b]
1	**2 mol%**	**0 mol%**	**37**	**57**	**20**
2	**2 mol%**	**3 mol%**	**92**	**100**	**6**

***Table 8**: Aliphatic aldehyde ligand acceleration test in DKR system, [a]Yields determined by ^{1}H NMR spectroscopy using 1,3,5-trimethoxybenzene as an internal standard, [b]diastereoselectivity determined by ^{1}H NMR spectroscopy*

Aliphatic Aldehyde Lewis Acid Screen

A Lewis acid screen was performed in an attempt to increase the diastereoselectivity of the reaction (**Table 9**). The Lewis acid screen was performed using the same model reaction. Unfortunately, lithium iodide showed no effect (**entry 1**), ceric ammonium nitrate and titanium isopropoxide slowed the reaction with no increase in selectivity (**entries 2 and 5**) and copper (II) triflate and iron (III) chloride stopped product formation (**entries 3 and 5**). There were no promising results in the initial screen of Lewis acids with substrate **30**. Unfortunately, accessing diastereomerically pure UCDPhim ligand became the limiting factor in further optimisation of the DKR protocol.

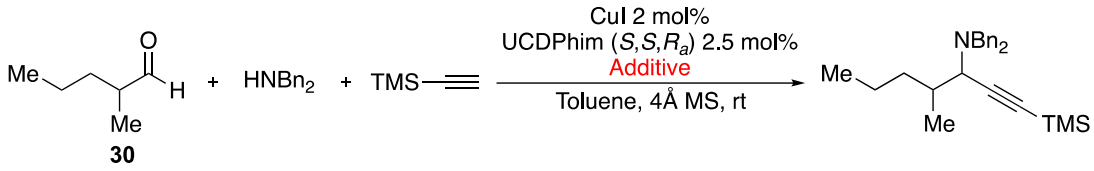

Entry	Additive (1 equiv.)	Yield (%) (24 h)[a]	Yield (%) (48 h)[a]	De (%)[b]
1	**Lithium iodide**	**89**	**100**	**12**
2	**CAN**	**n/a**	**27**	**15**
3	**$Cu(OTf)_2$**	**No rxn**	**No rxn**	**-**
4	**$FeCl_3$**	**No rxn**	**No rxn**	**-**
5	**$Ti(O^iPr)_4$**	**73**	**76**	**9**

***Table 9**: Lewis acid screen for A3 coupling DKR reaction with aliphatic aldehyde substrate **30**, [a]Yields determined by ^1H NMR spectroscopy using 1,3,5-trimethoxybenzene as an internal standard, [b]diastereoselectivity determined by ^1H NMR spectroscopy*

Towards Accessing Sterically Varied Secondary Amines

Attention was next turned towards the amine component of the A3 coupling reaction. As outlined in the introduction of this chapter, P,N ligands typically are more successful in asymmetric A3 couplings with secondary amines substrates. 1-Adamantylamine was chosen as a bulky amine substrate that could potentially influence the diastereoselectivity of the reaction. Methylation of 1-adamantylamine would be required to furnish the required secondary amine that work synergistically with P,N ligands in asymmetric A3 coupling reactions.

The *N*-alkylation of amines is a troublesome reaction that requires careful consideration. Treatment of a primary amine substrate such as 1-adamantylamine with an alkylating agent such as methyl iodide will result in a mixture of products and often over-alkylation at nitrogen *via* the Menshutkin reaction (**Scheme 106**). This is due to the fact the as the nitrogen atom becomes more substituted, it increases in nucleophilicity.

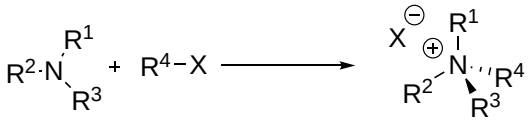

Scheme 106: *Over-alkylation of tertiary amine via Menshutkin reaction*

A common way of overcoming this over-alkylation problem is to use the Eschweiler Clarke reaction (**Scheme 107**). This reaction traditionally is used to give the tertiary amine product without over-alkylating to the quaternary ammonium salt, as it relies on formaldehyde forming an imine with the amine, before formic acid decarboxylates to give a hydride source for the imine reduction to a methyl group. This imine formation can no longer happen once the tertiary amine is formed. Despite using only one equivalent of formaldehyde in this case, only the *N*,*N*-dimethyl-1-adamantylamine product was formed in the present study in a 28% yield.

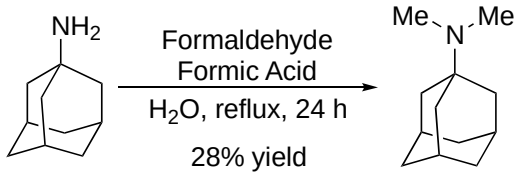

***Scheme 107**: Eschweiler-Clarke reaction for the methylation of 1-adamantylamine*

An alternative strategy was considered, which is outlined below (**Scheme 108**). 1-Adamantylamine was first protected using Boc_2O, which proceeded well with an 87% yield. It was hoped that the presence of the carbamate protecting group would hinder the nucleophilicity of the nitrogen, to stop over-alkylation to the ammonium salt when reacted with methyl iodide. Unfortunately, the alkylation of Boc-protected amine **31** was unsuccessful, with only starting material recovered after reaction with sodium hydride and methyl iodide.

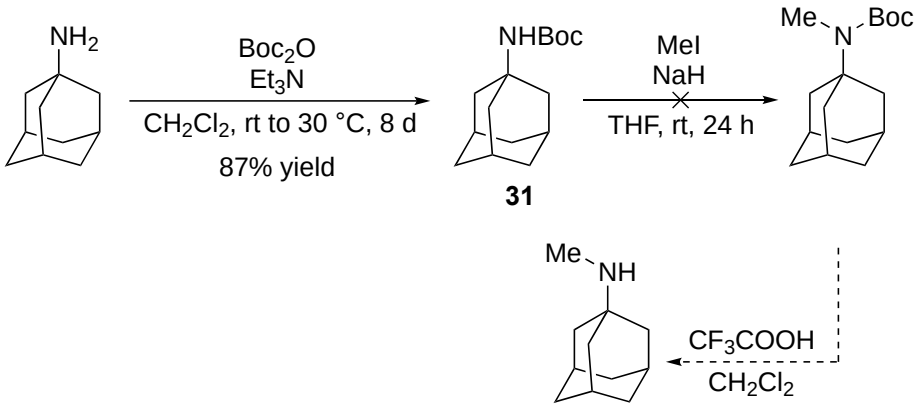

***Scheme 108**: Route towards accessing N-methyl-1-adamantylamine*

Towards Accessing Optically Pure Aliphatic Aldehydes

In order to understand whether racemisation of the α-stereocentre of the aldehyde substrates was occurring, efforts were focussed towards accessing optically pure aldehyde substrates for test reactions. In the literature, the Eames group reported the separation of similar racemic acid chloride substrates *via* the corresponding diastereomers **32** and *dia*-**32**, after reaction with the Evans' auxiliary (**Scheme 109**).[31] These acid chlorides could readily be accessed in two steps from the aldehydes substrates used previously in this study.

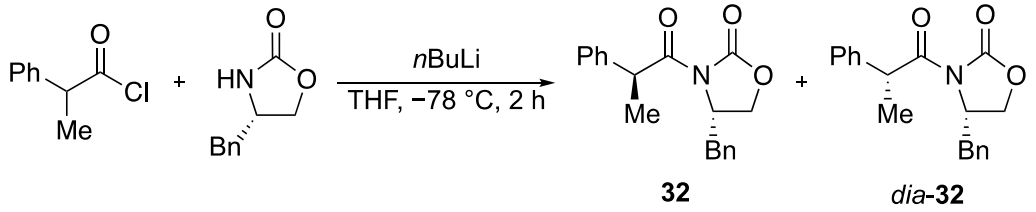

***Scheme 109**: Literature precedent for isolation of α-branched acid chlorides via Evans' auxiliaries* [31]

2-Methyl-pentanal was taken as the model aliphatic substrate and was subjected to a Pinnick oxidation to furnish carboxylic acid **33**, which proceeded well with a 67% yield (**Scheme 110**). The acid chloride **34** was then prepared in an 80% yield from the reaction of carboxylic acid **35** with thionyl chloride and a catalytic amount of dimethylformamide.

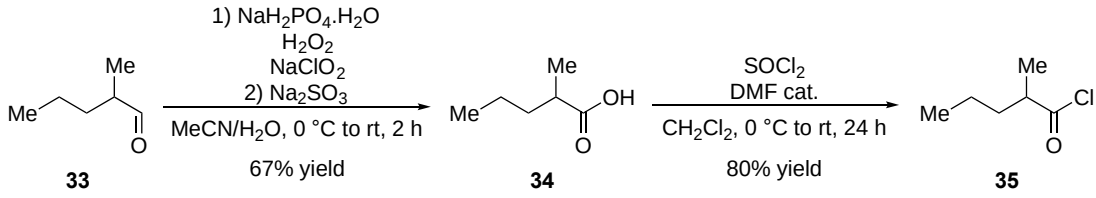

***Scheme 110**: Acid chloride formation from aliphatic aldehyde substrate*

The benzyl-substituted Evans' auxiliary was chosen as the carbamate group, as a chromophore for TLC analysis under UV light was desired after separation of diastereomers through column chromatography. The route for accessing the Evans' auxiliary (**Scheme 111**), shows that (*L*)-phenylalanine was reduced with lithium aluminium hydride to give the corresponding amino alcohol **36** in a 56% yield. The amino alcohol **36** was then reacted with di-*tert*-butyldicarbonate to give the carbamate **37** in an 84% yield. Treatment of carbamate **37** with thionyl chloride and DMF furnished the Evans' auxiliary **38** in a 39% yield after purification by column chromatography.

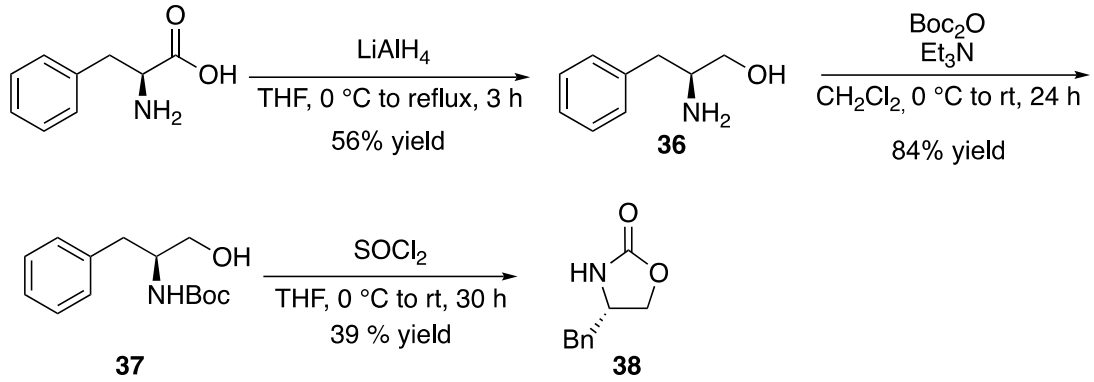

***Scheme 111**: Synthesis of Evan's auxiliary for accessing optically pure aldehyde*

With the acid chloride **35** and Evans' auxiliary **38** in hand, the next step was to react them as per the protocol reported by Eames to access **39** and *dia*-**39**.[31] Unfortunately, the reaction did not proceed smoothly, with six spots appearing on the TLC plate (**Scheme 112**). Purification of the fractions by column chromatography proved extremely difficult, due to the close R_f of the various reaction components under a variety of TLC conditions.

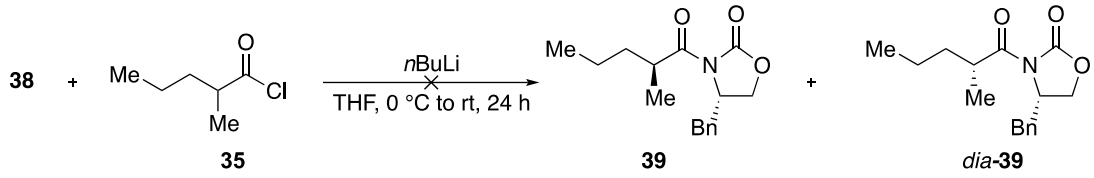

Scheme 112**: Reacting benzyl-substituted Evans' auxiliary with acid chloride **35

The multiple side products formed when attempting to synthesise the diastereomers **39** and *dia*-**39** and the subsequent remaining steps to access the optically pure aldehydes (**Scheme 113**), led to further investigations using this approach being curtailed.

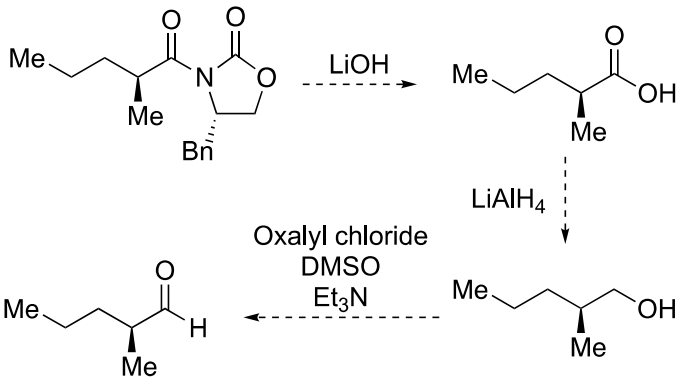

***Scheme 113**: Route for accessing optically pure aldehyde from Evans' auxiliary diastereomer*

The rationale for trying to access an optically pure aldehyde **40** was one of mechanistic relevance. An asymmetric A3 coupling reaction using an optically pure aldehyde and UCDPhim should yield a single diastereomer if no stereoablation of the resulting iminium ion was occurring. This would be the case as the UCDPhim ligand has a literature precedence for formation of the propargylamine stereocentre (blue) with extremely high enantioselectivity (up to 99% ee,[19,20] while the red stereocentre would remain fixed if it was not being scrambled *via* an iminium ion enamine tautomerisation (**Scheme 114**). However, if stereoablation of the optically pure aldehyde was occurring, two diastereomers of product would be formed and would be observable by NMR spectroscopic analysis.

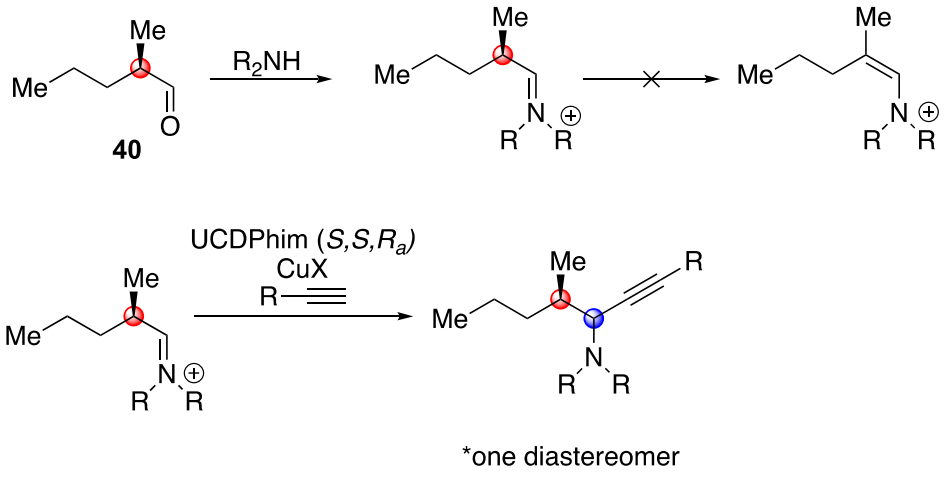

Scheme 114:** Proposed outcome of A3 coupling reaction with optically pure aldehyde **40

Accessing the optically pure aldehyde **40** required to test this rationale proved difficult despite literature precedent.[31] It was decided to use an alternative approach to test for a potential A3 DKR system. As stereoablation is required for this DKR system to work, it was decided that the reactivity of the enamine intermediate would be examined. Enamine **41** was formed *via* the condensation reaction outlined in **Scheme 115**, with a characteristic enamine proton having a chemical shift of 5.38 ppm in the crude ^{1}H NMR spectrum being consistent with the formation of **41**.[32] The enamine was telescoped into the test reaction (**Scheme 116**) for fear of its hydrolysis on silica if purification was attempted.

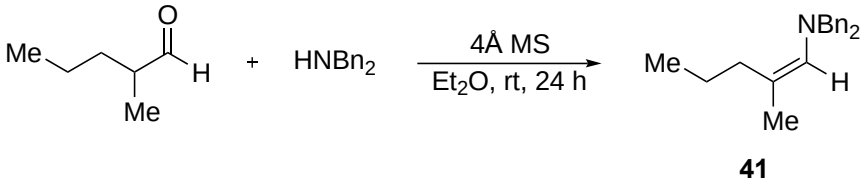

***Scheme 115**: Formation of enamine intermediate **41** required for stereoablation of α-stereocentre in A3 DKR system*

A test reaction was performed (**Scheme 116**) and aliquots of the reaction mixture were taken after time points (24 h, 48 h and 96 h). The aliquots were then concentrated *in vacuo* for NMR spectroscopic analysis. The ^{1}H NMR spectrum of the reaction mixture showed trace formation of the desired product (**Scheme 116**), coupled with competitive enamine hydrolysis to the aliphatic aldehyde starting material (**Scheme 115**).

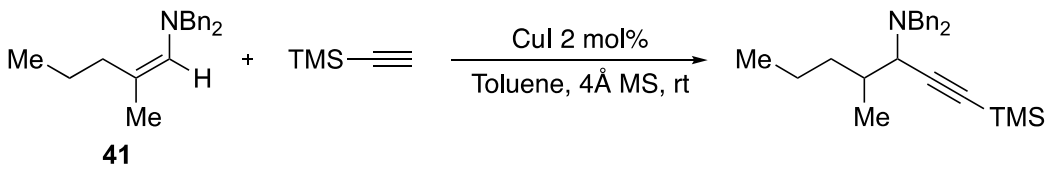

***Scheme 116**: Attempted reaction of enamine **41** with TMS acetylene and CuI to form the propargylamine product*

From this result it was deemed that these aliphatic enamines showed extremely poor reactivity towards A3 couplings. This result halted investigations in the present study as the enamine intermediate necessary for stereoablation appeared to not re-form the required iminium ion electrophile in solution by our hands.

Conclusions and Future Work

The aim of this project was to apply the UCDPhim ligand in asymmetric A3 coupling reactions that contained a dynamic kinetic resolution system (DKR). The difficulty that arose in this proposed system was one of selectivity and reactivity. After the initial substrate scope, α-aryl aldehydes showed promise in terms of diastereoselectivity. This diastereoselectivity was further increased after screening commonly used Cu(I) salts, however this increase in selectivity was at the expense of product formation. Extension of the reaction time to 4 d did not lead to satisfactory yields (3-26%). Further studies showed that there was no ligand acceleration in the reaction of the α-aryl aldehyde, which is a key goal in any asymmetric catalytic process to avoid a competing background racemic reaction.

Brønsted acid additives proved unsuccessful in shifting the enamine iminium ion equilibrium towards favouring propargylamine product formation. Variation of Cu catalyst loadings, up to stoichiometric amounts, would not afford quantitative formation of the α-aryl propargylamine product. This was consistent with the hypothesis that the substrate was being sequestered as the inactive enamine species.

Aliphatic aldehydes proved more reactive in terms of product formation, but they lacked the diastereoselectivity that the α-aryl aldehyde product **18** showed in the initial substrate scope (**Scheme 100**). A Lewis acid screen conducted with the purpose of trying to improve diastereoselectivity *via* longer existence of the iminium ions in solution for tautomerisation, required for stereoablation, did not result in any increase in diastereoselectivity.

Efforts were turned towards accessing secondary amines with "R" groups of different steric bulk, but no progress was made. Replication of literature work was unsuccessful towards accessing optically pure aliphatic aldehydes. Formation of an aliphatic test enamine and its subsequent reaction with a copper acetylide nucleophile showed that these substrates had similar reactivity as their aryl counterparts.

In terms of future work, the next step would be synthesise other P,N ligands with no chiral axis or with sufficiently high rotational barriers so that the system could be tested at higher temperatures (**Scheme 117**). The higher temperature would potentially allow for product formation from the enamine species. However, the higher temperature may have negative impacts on the enantioselectivity and diastereoselectivity of the reaction as it may give the system sufficient energy to negate differences between enantiotopic faces on the iminium ion. Investigations with these ligands and variation of the temperature would be required any before conclusions could be made.

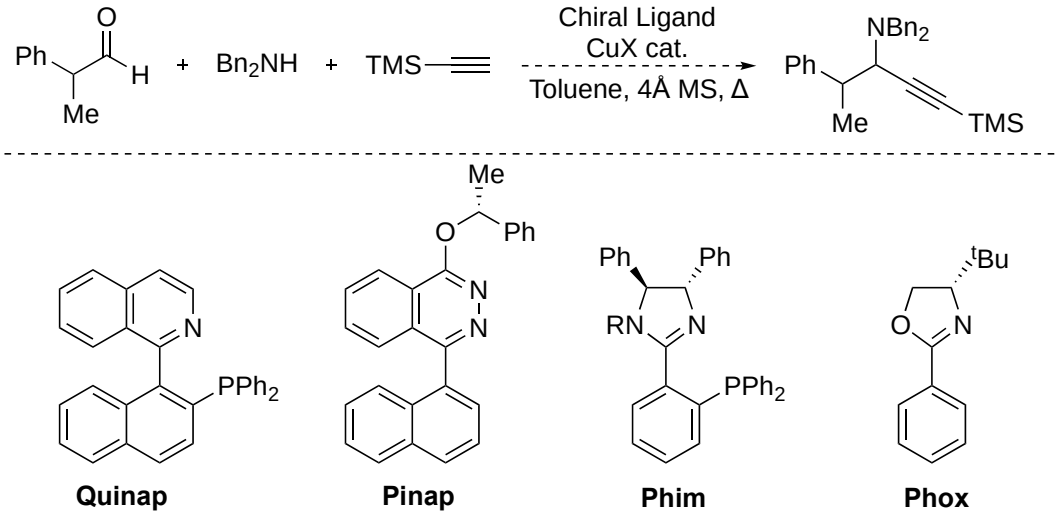

***Scheme 117**: P, N ligands compatible with higher temperatures for A3 DKR system*

Experimental

All chemicals were purchased from Sigma-Aldrich, Acros, or Fluorochem unless otherwise stated. Dry solvents were obtained from a Puresol Grubbs solvent system unless otherwise stated. All of the solvents were reagent grade and were used as received. Toluene and dimethylformamide (DMF) were dried and degassed using standard protocols. N-Bromosuccinimide (NBS) was recrystallised from water using standard protocols. Column chromatography was performed on Davilsil LC60A 40-63 micron silica gel. Thin-layer chromatography (TLC) was performed on Aluminium-backed sheets purchased from Merck pre-coated with silica 60 F254. All reactions were performed under an atmosphere of N_2 and in flame-dried glassware unless otherwise stated. The Varian 300 MHz, 400 MHz and 500 MHz NMR instruments were used for the recording of ^{1}H NMR and ^{13}C NMR spectra. Deuterated chloroform was used as the solvent for recording NMR spectra unless otherwise state, the chemical shifts (δ) are given in parts per million and the coupling constants (*J*) are given in absolute values expressed in Hz. HRMS were measured on a Micromass/Water LCT mass spectrometer. Infrared spectra were recorded on a FT-IR spectrometer and are reported in terms of wavenumbers (*v*max) with units of reciprocal centimetres (cm^{-1}) Supercritical fluid chromatography (SFC) was performed on a Waters Acquity UPC^2 ® instrument with Chiralpak ® IA3, IB3, IC3 and ID3 columns. Optical rotation measurements were recorded using a Schmidt-Haensch Unipol L2000 polarimeter at 589 nm and are quoted in units of deg dm^{-1} cm^3 g^{-1} (concentration c is given in g/100 mL).

General procedure 1 (**GP1**) for the synthesis of asymmetric A3 coupling products

A Schlenk flask (10 mL) was charged with a stir bar, evacuated, and back filled with nitrogen. Aldehyde (0.4 mmol, 1.0 equiv.), (*S*,*S*,R_a)-UCDPhim (1.2 mol%) copper bromide complex (1 mol%) in toluene (1 mL) , amine (0.4 mmol, 1.0 equiv) and alkyne nucleophile (0.48 mmol, 1.2 equiv.) were added. 4Å powdered molecular sieves were added followed by toluene (1 mL) and was stirred at 0 °C for 24 h. EtOAc (5 mL) was added and the reaction mixture was filtered through Celite® on a sintered glass funnel, concentrated *in vacuo* and purified by column chromatography.

General procedure 2 (**GP2**) for the TMS deprotection of TMS-acetylene A3 coupling products

TMS-protected product was dissolved in THF (1 mL) and was cooled to 0 °C. Tetrabutylammonium fluoride (2.0 mL, 1.0 M in THF, 0.5 mmol) was added and the reaction was stirred for 30 min (TLC). The reaction was quenched with H_2O (10 mL), extracted with Et_2O (3 x 10 mL), washed with brine (30 mL) and dried with magnesium sulfate. The organics were filtered and concentrated *in vacuo* to give the crude product which was purified using by column chromatography.

General procedure 3 (**GP3**) for the synthesis of aldehydes from aryl iodides and methyallyl alcohol[33]

$Pd(OAc_2)$ (63 mg, 2 mol %, 0.02 equiv.), Et_3N (2.4 mL, 17.5 mmol, 1.25 equiv.), aryl iodide (14 mmol, 1 equiv.), 2-methy-2-propen-1-ol (1.47 mL, 17.5 mmol, 1.25 equiv.) were solubilised in dry acetonitrile (6.5 mL) . The reaction was heated at reflux for 24 h after which time H_2O (10 mL) was added and the reaction mixture was filtered. The filtrate was transferred to a separatory funnel. Et_2O (30 mL) was added, and the phases were separated. The aqueous phase was further extracted with Et_2O (3 x 30 mL). The organics were combined, washed with brine (100 mL), dried with magnesium sulfate, filtered, and concentrated *in vacuo* giving the crude product. The crude product was purified using flash column chromatography.

N,*N*-Dibenzyl-4-phenyl-1-(trimethylsilyl)pent-1-yn-3-amine **18**[35]

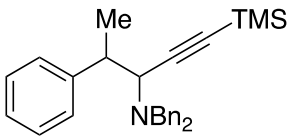

The title compound **18** was synthesised as per general procedure 1 (**GP1**). The product was purified by flash column chromatography (100% cyclohexane) to give a colourless oil (16 mg, 10%) as a mixture of diastereomers in an approximate 1:1 ratio. **R_f** = 0.26 (100% cyclohexane); **^{1}H NMR** (500 MHz, $CDCl_3$) δ 7.45 – 7.40 (m, 1H), 7.33 (t, *J* = 7.5 Hz, 1H), 7.28 – 7.21 (m, 3H), 7.21 – 7.14 (m, 5H), 7.08 – 7.05 (m, 0.3H), 6.97 – 6.91 (m, 3H), 6.90 – 6.86 (m, 1.5H), 3.86 (d, *J* = 13.8 Hz, 0.3H), 3.72 (d, *J* = 13.8 Hz, 1.6H), 3.48 (d, *J* = 10.9 Hz, 0.8H), 3.42 – 3.33 (m, 0.5H), 3.27 (d, *J* = 13.8 Hz, 1.5H), 3.09 – 2.93 (m, 1H), 1.37 – 1.21 (m, 4H), 0.93 – 0.79 (m, 0.5H), 0.28 (s, 7H), 0.08 (s, 2H); **^{13}C NMR** (126 MHz, $CDCl_3$) δ 144.1, 139.6, 139.2, 129.0, 128.9, 128.2, 128.1, 128.0, 127.9, 127.9, 126.9, 126.7, 126.3, 126.1, 103.3, 102.8, 90.6, 59.5, 58.5, 55.1, 54.5, 42.9, 42.7, 21.2, 18.9, 0.4, 0.1; **HRMS**: (ESI-TOF) calculated for $C_{28}H_{33}NSi$ $[M + H]^+$ 412.2455, found 476.2450. All characterisation data are in agreement with reported literature data.

N,*N*-Dibenzyl-4-phenylpent-1-yn-3-amine[35]

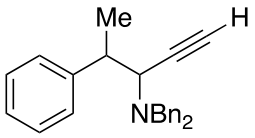

TMS-protected compound **18** (15 mg) was deprotected as per general procedure 2 (**GP2**). The product was purified by flash column chromatography (100% cyclohexane) to give a colourless oil (12 mg, 95%) as a mixture of diastereomers. **R_f** = 0.85 (10% EtOAc/cyclohexane); **^{1}H NMR** (500 MHz, $CDCl_3$) δ 7.46 (dd, *J* = 7.8, 1.4 Hz, 1H), 7.38 – 7.34 (m, 1H), 7.29 (m, 2H), 7.27 – 7.23 (m, 1H), 7.21 – 7.18 (m, 5H), 7.10 – 7.07 (m, 1H), 6.98 – 6.89 (m, 5H), 3.92 (d, *J* = 13.6 Hz, 0.3H), 3.74 (d, *J* = 13.6 Hz,

1.7H), 3.51 – 3.47 (m, 1H), 3.46 – 3.39 (m, 0.5H), 3.32 (d, *J* = 13.6 Hz, 1.7H), 3.13 – 3.11 – 2.99 (m, 1H), 2.46 (d, *J* = 2.2 Hz, 0.71H), 2.18 (d, *J* = 2.2 Hz, 0.15H), 1.35 – 1.32 (m,0.7H), 1.32 -1.29 (m, 2.7H); **^{13}C NMR** (126 MHz, $CDCl_3$)) δ 144.5, 143.9, 139.4, 139.1, 129.0, 128.9, 128.3, 128.2, 128.0*, 127.9*, 127.9*, 127.9, 127.0, 126.8, 126.5, 126.2, 81.0, 80.3, 74.0, 73.8, 58.1, 57.7, 54.9, 54.4, 42.8, 42.8, 21.1, 19.5; **IR** ν(cm^{-1}): 3301, 3062, 2952, 1494, 1453, 1373, 735, 696 *(Peaks with asterisk not fully resolved); **[α]^{20}D** = -38.97 (c = 0.1, $CHCl_3$). All characterisation data are in agreement with reported literature data.

5-(Dibenzylamino)-2,6-dimethyloct-3-yn-2-ol **19**

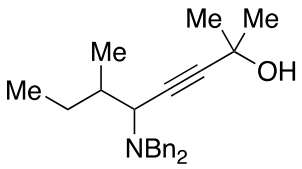

The title compound was synthesised as per general procedure 1 (**GP1**). The product was purified by flash column chromatography (10% EtOAc/cyclohexane) as a brown oil (120 mg, 86%) as a mixture of diastereomers in an approximate 1:1 ratio. **R_f** = 0.18 (10% EtOAc/cyclohexane); **^{1}H NMR** (500 MHz, $CDCl_3$) δ 7.41 – 7.35 (m, 4H), 7.32 – 7.27 (, 4H), 7.24 – 7.19 (m, 2H), 3.79 (dd, *J* = 13.7, 4.0 Hz, 2H), 3.34 (d, *J* = 13.7 Hz, 2H), 3.05 – 2.98 (m, 1H), 2.08 – 1.97 (m, 1H), 1.97 – 1.86 (m, 2H), 1.76 – 1.62 (m, 1H), 1.61 (s, 6H), 1.06 – 0.99 (m, 1H), 0.97 (d, *J* = 6.7 Hz, 1.5H), 0.92 (d, *J* = 6.7 Hz, 1.5H), 0.83 (t, *J* = 7.4 Hz, 1.5H), 0.71 (t, *J* = 7.5 Hz, 1.5H); **^{13}C NMR** (126 MHz, $CDCl_3$)) δ 139.72, 139.71, 129.0, 128.9, 128.2*, 126.9, 126.9, 91.0, 91.0, 79.5, 79.3, 65.5*, 57.6, 57.3, 55.2, 55.0, 37.0, 36.6, 32.1*, 27.1, 25.2, 16.9, 16.0, 11.3, 10.5. *(Peaks with asterisk not fully resolved); **IR** □(cm^{-1}): 3358, 2963, 2930, 1453, 947, 774, 745, 696; **[α]^{20}D** = -159.13 (c = 0.1, $CHCl_3$); **HRMS**: (ESI-TOF) calculated for $C_{24}H_{31}NO$ $[M + H]^+$ 350.2478, found 350.2492.

N,*N*-Dibenzyl-4-methyl-1-(trimethylsilyl)hex-1-yn-3-amine **20**

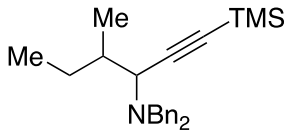

The title compound **20** was synthesised as per general procedure 1 (**GP1**). The product was purified by flash column chromatography (100% cyclohexane) to give a colourless oil (34 mg, 24%) as a mixture of diastereomers in an approximate 1:1 ratio. $\mathbf{R_f}$ = 0.3 (100% cyclohexane); **^{1}H NMR** (400 MHz, $CDCl_3$) δ 7.40 – 7.35 (m, 4H), 7.31 – 7.25 (tm, 4H), 7.23 – 7.18 (m, 2H), 3.77 (dd, *J* = 13.8, 2.3 Hz, 2H), 3.33 (d, *J* = 13.8 Hz, 2H), 3.02 – 2.93 (m, 1H), 1.95 – 1.84 (m, 0.5H), 1.78 – 1.58 (m, 1H), 1.07 – 1.03 – 0.90 (m, 4H), 0.83 (t, *J* = 7.6 Hz, 1.5H), 0.70 (t, *J* = 7.6 Hz, 1.5H), 0.24 – 0.22 (m, 9H); **^{13}C NMR** (101 MHz, $CDCl_3$)) δ 139.8, 139.7, 129.0, 128.9, 128.1*, 126.8, 126.8, 103.9, 103.8, 90.0, 89.9, 58.5, 58.1, 55.1, 54.9, 36.8, 36.3, 27.1, 25.1, 16.8, 15.9, 11.2, 10.4, 0.4* *(Peaks with asterisk not fully resolved); **IR** (cm^{-1}): 2960, 2157, 1248, 838, 696; **HRMS**: (ESI-TOF) calculated for $C_{24}H_{33}NSi$ $[M + H]^+$ 364.2455, found 364.2458.

N,*N*-Dibenzyl-4-methylhex-1-yn-3-amine

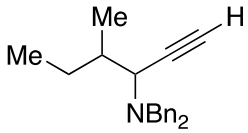

TMS-protected compound (21 mg) was deprotected as per general procedure 2 (**GP2**). The product was purified by flash column chromatography (10% EtOAc/cyclohexane) to give a colourless oil (15 mg, 34%) as a mixture of diastereomers. $\mathbf{R_f}$ = 0.9 (10% EtOAc/ cyclohexane); **^{1}H NMR** (500 MHz, $CDCl_3$) δ 7.43 – 7.37 (m, 4H), 7.34 – 7.28 (m, 4H), 7.25 – 7.21 (m, 2H), 3.82 (dd, *J* = 13.7, 4.0 Hz, 2H), 3.37 (d, *J* = 13.8 Hz, 2H), 3.05 – 2.98 (m, 1H), 2.36 -2.34 (m, 1H), 1.98 – 1.90 (m, 0.5H), 1.82 – 1.66 (m, 0.5H), 1.08 – 0.94 (m, 4H), 0.91 – 0.81 (m, 2.5H), 0.72 (t, *J* = 7.5 Hz, 1.5H); **^{13}C NMR** (126 MHz, $CDCl_3$) δ 139.6, 139.6, 129.0, 128.8, 128.2*, 126.9, 126.85, 81.3, 81.2, 73.3*, 57.50, 57.2, 55.0, 54.8, 36.9, 36.3, 27.0, 25.0, 16.7, 15.8, 11.2,

10.4.*(Peaks with asterisk not fully resolved); **IR** (cm^{-1}): 3302, 302, 2961, 1453, 744, 696; **[α]^{20}D** = -120.51 (c = 0.1, $CHCl_3$); **HRMS**: (ESI-TOF) calculated for $C_{21}H_{25}N$ [M + H]$^+$ 292.206, found 292.2061.

4-(Dibenzylamino)-5-methylhept-2-yn-1-ol

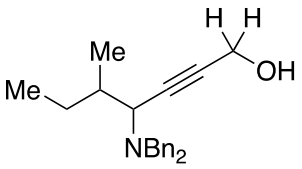

The title compound was synthesised as per general procedure 1 (**GP1**). The product was purified by flash column chromatography (10 to 30% EtOAc/cyclohexane) to give a brown oil (71 mg, 56%) as a mixture of diastereomers in an approximate 1:1 ratio. **R$_f$** = 0.5 (30% EtOAc/cyclohexane); **^{1}H NMR** (500 MHz, $CDCl_3$) δ 7.42 – 7.36 (m, 4H), 7.33 – 7.28 (m, 4H), 7.25 -7.21 (m, 2H), 4.41 (s, 2H), 3.84 – 3.77 (m, 2H), 3.37 (d, *J* = 13.7 Hz, 2H), 3.08 – 3.01 (m, 1H), 1.97 -1.89 (m, 0.5H), 1.78 – 1.65 (m, 1.5H), 1.08 – 0.99 (m, 1H), 0.98 (d, *J* = 6.6 Hz, 1.5H), 0.94 (d, *J* = 6.6 Hz, 1.6H), 0.83 (t, *J* = 7.5 Hz, 1.5H), 0.72 (t, *J* = 7.5 Hz, 1.5H); **^{13}C NMR** (126 MHz, $CDCl_3$) δ 139.6, 139.6, 129.0, 128.8, 128.2*, 126.9, 126.8, 83.9, 83.9, 83.5, 83.4, 57.7, 57.5, 55.1, 54.9, 51.4*, 37.0, 36.5, 27.1, 25.1, 16.9, 15.9, 11.2, 10.4. *(Peaks with asterisk not fully resolved); **IR** (cm^{-1}): 3309, 2961, 1493, 1452, 733, 696; **[α]^{20}D** = 140.42 (c = 0.1, $CHCl_3$); **HRMS**: (ESI-TOF) calculated for $C_{22}H_{27}N$ [M + H]$^+$ 322.2165, found 322.2168.

N,*N*-Dibenzyl-4-ethyl-1-(trimethylsilyl)oct-1-yn-3-amine

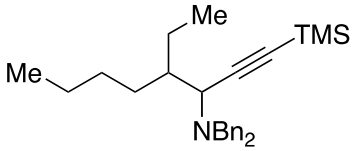

The title compound was synthesised as per general procedure 1 (**GP1**). The product was purified by flash column chromatography (100% cyclohexane as a colourless oil

(32 mg, 20%) as a mixture of diastereomers in an approximate 1:1 ratio. **R_f** = 0.4 (100% cyclohexane); **^{1}H NMR** (500 MHz, $CDCl_3$) δ 7.39 – 7.36 (m, 4H), 7.32 – 7.28 (m, 4H), 7.25 – 7.20 (m, 2H), 3.77 (d, *J* = 13.6 Hz, 2H), 3.32 (d, *J* = 13.6 Hz, 2H), 3.17 – 3.11 (m, 1H), 1.66 – 1.55 (m, 3H), 1.45 – 1.13 (m, 5H), 0.96 – 0.82 (m, 4H), 0.77 (t, *J* = 7.3 Hz, 1.5H), 0.54 (t, *J* = 7.3 Hz, 1.5H), 0.24 (s, 9H); **^{13}C NMR** (126 MHz, $CDCl_3$) δ 139.7, 139.7, 129.1, 129.1, 128.1*, 126.8*, 104.0, 104.0, 90.0, 90.0, 55.9, 55.8, 55.0, 55.0, 40.4, 40.1, 29.3, 28.7, 27.4, 26.6, 23.3, 23.0, 22.8, 20.9, 14.1, 14.0, 10.7, 8.8, 0.4, 0.4. *(Peaks with asterisk not fully resolved); **IR** (cm^{-1}): 3086, 3028, 2157, 1407, 1207, 838, 746, 696; **[α]^{20}D** = -175.95 (c = 0.1, $CHCl_3$); **HRMS**: (ESI-TOF) calculated for $C_{27}H_{39}NSi$ $[M + H]^+$ 406.2925, found 406.2945.

N,*N*-dibenzyl-4-ethyloct-1-yn-3-amine

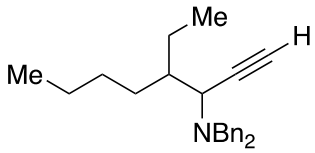

TMS-protected compound (26 mg) was deprotected as per general procedure 2 (**GP2**). The product was purified by flash column chromatography (10% EtOAc/cyclohexane) as a colourless oil (20 mg, 94%) as a mixture of diastereomers in an approximate 1:1 ratio. **R_f** = 0.88 (10% EtOAc/cyclohexane); **^{1}H NMR** (500 MHz, $CDCl_3$) δ 7.41 – 7.37 (m, 4H), 7.34 – 7.28 (m, 4H), 7.27 – 7.20 (m, 2H), 3.81 (d, *J* = 13.5 Hz, 2H), 3.36 (d, *J* = 13.5 Hz, 2H), 3.21 – 3.14 (m, 1H), 2.36 – 2.34 (m, 1H), 1.73 – 1.29 (m, 6H), 1.25 – 1.09 (m, 3H), 1.00 – 0.83 (m, 4H), 0.78 (t, *J* = 7.4 Hz, 1.5H), 0.55 (t, *J* = 7.4 Hz, 1.5H); **^{13}C NMR** (126 MHz, $CDCl_3$) δ 139.6, 139.6, 129.0, 129.0, 128.2*, 126.9*, 81.4, 81.4, 73.3, 73.3, 54.9, 54.9, 54.9*, 54.8*, 40.3, 40.0, 29.1, 28.5, 27.1, 26.6, 23.3, 23.0, 22.6, 20.5, 14.1, 14.0, 10.5, 8.6. *(Peaks with asterisk not fully resolved); **IR** (cm^{-1}): 3304, 2956, 2926, 1494, 1453, 1375, 745, 696; **[α]^{20}D** = -133.72 (c = 0.1, $CHCl_3$); **HRMS**: (ESI-TOF) calculated for $C_{24}H_{31}N$ $[M + H]^+$ 334.2529, found 334.2520.

5-(Dibenzylamino)-6-ethyl-2-methyldec-3-yn-2-ol

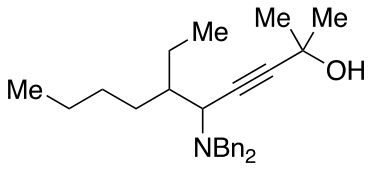

The title compound was synthesised as per general procedure 1 (**GP1**). The product was purified by flash column chromatography (10 to 20% EtOAc/cyclohexane) to give a brown oil (86 mg, 57%) as a mixture of diastereomers in an approximate 1:1 ratio. **R_f** = 0.41 (20% EtOAc/cyclohexane); **^{1}H NMR** (500 MHz, $CDCl_3$) δ 7.39 – 7.35 (m, 4H), 7.32 -7.27 (m, 4H), 7.25 – 7.20 (m, 2H), 3.78 (d, *J* = 13.6 Hz, 2H), 3.32 (d, *J* = 13.6 Hz, 2H), 3.20 – 3.13 (m, 1H), 1.99 (s, 1H), 1.69 – 1.12 (m, 14H), 0.97 – 0.81 (m, 4H), 0.77 (t, *J* = 7.4 Hz, 1.5H), 0.56 (t, *J* = 7.4 Hz, 1.5H); **^{13}C NMR** (126 MHz, $CDCl_3$) δ 139.7, 139.6, 129.1, 129.1, 128.2*, 126.9*, 91.0, 91.0, 79.6, 79.5, 65.5, 55.1, 55.1, 55.0, 54.9, 40.5, 40.3, 32.1, 32.1*, 32.1, 29.3, 28.7, 27.5, 26.7, 23.3, 23.1, 22.8, 20.9, 14.2, 14.0, 10.7, 8.9. *(Peaks with asterisk not fully resolved); **IR** (cm^{-1}): 3360, 3085, 295, 1494, 1453, 943, 746, 696; **[α]^{20}D** = 27.98 (c = 0.1, $CHCl_3$); **HRMS**: (ESI-TOF) calculated for $C_{27}H_{37}NO$ $[M + H]^+$ 392.2948, found 392.2968.

2-Methyl-3-phenylpropanal[34]

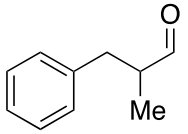

Aldehyde was synthesised as per general procedure 3 (**GP3)** with iodobenzene (1.56 mL, 14 mmol, 1 equiv.). The crude product was purified by flash column chromatography (5% Et_2O/pentane) giving **the title compound** as a colourless oil (837 mg, 41% yield). **R_f** = (0.43 in 5% Et_2O/Pentane); **^{1}H NMR** (400 MHz, $CDCl_3$) δ 9.71 (d, *J* = 1.5 Hz, 1H), 7.31 – 7.13 (m, 5H), 3.08 (dd, *J* = 13.3, 5.6 Hz, 1H), 2.72 – 2.55 (m, 2H), 1.08 (d, *J* = 6.9 Hz, 3H). All characterisation data are in agreement with reported literature data.

2-Methyl-3-(naphthalen-2-yl)propanal **23**

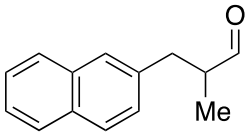

Aldehyde **23** was synthesised as per general procedure 3 (**GP3)** with 2-iodonaphthalene (3.77 g, 14 mmol, 1 equiv.). The crude product was purified by flash column chromatography (5% Et_2O/pentane) to give a colourless oil (0.69 g, 23%). $\mathbf{R_f}$ = (0.24 in 5% Et_2O/Pentane); **^{1}H NMR** (400 MHz, $CDCl_3$) δ 9.78 (s, 1H), 7.89 – 7.80 (m, 3H), 7.66 (d, *J* = 2.1 Hz, 1H), 7.57 – 7.45 (m, 2H), 7.34 (dd, *J* = 8.4, 1.8 Hz, 1H), 3.27 (q, *J* = 9.6 Hz, 1H), 2.84 – 2.73 (m, 2H), 1.14 (d, *J* = 7.5, 3H); **^{13}C NMR** (101 MHz, $CDCl_3$) δ 204.3, 136.5, 133.6, 132.3, 128.2, 127.7, 127.6, 127.5, 127.4, 126.2, 125.6, 47.9, 36.8, 13.3; **IR** n(cm^{-1}): 3052, 1720, 1632, 1599, 6948; **HRMS**: (ESI-TOF) calculated for $C_{14}H_{14}O$ $[M + H]^+$ 198.1045, found 198.1040.

N,*N*-Dibenzyl-4-methyl-5-(naphthalen-2-yl)-1-(trimethylsilyl)pent-1-yn-3-amine **23**

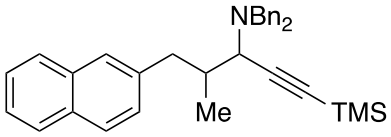

The title compound **23** was synthesised as per general procedure 1 (**GP1**). The product was purified by flash column chromatography (100% cyclohexane) to give a colourless oil (104 mg, 54%) as a mixture of diastereomers in an approximate 1:1 ratio. $\mathbf{R_f}$ = 0.26 (100% cyclohexane); **^{1}H NMR** (500 MHz, $CDCl_3$) δ 7.80 – 7.66 (m, 3H), 7.54 (s, 0.5H), 7.49 – 7.37 (m, 6H), 7.36 – 7.26 (m, 5H), 7.25 – 7.12 (m, 2H), 3.98 – 3.92 (m, 1H), 3.87 -3.82 (m, 1H), 3.73 – 3.66 (m, 0.5H), 3.49 – 3.44 (m, 1H), 3.44 – 3.39 (m, 1H), 3.39 – 3.33 (m, 0.5H), 3.20 – 3.10 (m, 1H), 2.27 – 2.20 (m, 0.5H), 2.17 - 2.05 (m, 1H), 2.04 – 1.95 (m, 0.5H), 0.93 – 0.88 (m, 1.5H), 0.88 – 0.84 (m, 1.5H), 0.32 – 0.28 (m, 4.5H), 0.28 – 0.23 (m, 4.5H);**^{13}C NMR** (126 MHz, $CDCl_3$) δ 139.7, 139.6, 138.9, 138.7, 133.5, 133.5, 132.0, 131.9, 129.1, 128.9, 128.3, 128.2, 128.2, 127.9,

127.8, 127.7, 127.7, 127.6*, 127.4, 127.4*, 127.0, 126.9, 125.8, 125.8, 125.1, 125.0, 103.5, 103.1, 91.1, 90.7, 59.0, 58.8, 55.4, 55.0, 41.2, 39.9, 38.0, 37.5, 17.2, 16.3, 0.5, 0.4. *(Peaks with asterisk not fully resolved); **IR** (cm^{-1}): 3060, 2958, 2156, 1373, 1098, 1009, 839, 736, 696; **[α]^{20}D** = -92.01 (c = 0.1, $CHCl_3$); **HRMS**: (ESI-TOF) calculated for $C_{33}H_{37}NSi$ $[M + H]^+$ 476.2768, found 476.2754.

N,*N*-Dibenzyl-4-methyl-5-(naphthalen-2-yl)pent-1-yn-3-amine

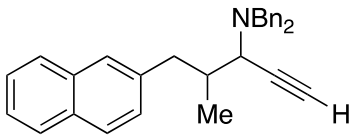

TMS-protected compound (52 mg) was deprotected as per general procedure 2 (**GP2**). The product was purified by flash column chromatography (10% EtOAc/cyclohexane) to give a colourless oil (40 mg, 90%) as a mixture of diastereomers. **R_f** = 0.76 (10 % EtOAc/cyclohexane); **^{1}H NMR** (500 MHz, $CDCl_3$) δ 7.79 – 7.76 (m, 1H), 7.75 – 7.67 (m, 2H), 7.54 (s, 0.5H), 7.50 – 7.46 (m, 2H), 7.45 – 7.37 (m, 4H), 7.36 – 7.26 (m, 5H), 7.24 – 7.19 (m, 1H), 7.14 (d, *J* = 8.5, 0.5H), 3.97 (d, *J* = 13.7 Hz, 1H), 3.87 (d, *J* = 13.7 Hz, 1H), 3.74 – 3.68 (m, 0.5H), 3.49 (d, *J* = 13.7 Hz, 1H), 3.44 (d, *J* = 13.7 Hz, 1H), 3.37 (d, *J* = 12.9, 0.5H), 3.21 – 3.17 (m, 0.5H), 3.17 – 3.13 (m, 0.5H), 2.50 (d, *J* = 2.2, 0.5H), 2.40 (d, *J* = 2.3, 1H), 2.28 – 2.21 (m, 1H), 2.21 – 2.08 (m, 1H), 2.03 – 1.97 (m, 0.5H), 0.91 (d, *J* = 6.3 Hz, 1.5H), 0.88 (d, *J* = 6.6 Hz, 1.5H);**^{13}C NMR** (126 MHz, $CDCl_3$) δ 139.5, 139.4, 138.8, 138.4, 133.5, 133.5, 132.0, 131.9, 129.0, 129.0, 128.4, 128.3, 127.8, 127.8, 127.7, 127.7, 127.6, 127.4*, 127.4, 127.1*, 127.0*, 125.8*, 125.1, 125.1, 81.0, 80.6, 74.3, 73.9, 58.1, 57.9, 55.4, 54.9, 41.1, 39.9, 38.0, 37.5, 17.1, 16.2. *(Peaks with asterisk not fully resolved); **IR** (cm^{-1}): 3329, 3296, 1452, 743, 697; **[α]^{20}D** = 21.63 (c = 0.1, $CHCl_3$); **HRMS**: (ESI-TOF) calculated for $C_{30}H_{29}N$ $[M + H]^+$ 404.2373, found 404.2392.

N,*N*-Dibenzyl-4-methyl-5-phenyl-1-(trimethylsilyl)pent-1-yn-3-amine

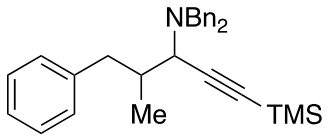

The title compound was synthesised as per general procedure 1 (**GP1**). The product was purified by flash column chromatography (100% cyclohexane) to give a colourless waxy oil (87 mg, 51%) as a mixture of diastereomers in an approximate 1:1 ratio $\mathbf{R_f}$ = 0.26 (100% cyclohexane) **^{1}H NMR** (500 MHz, $CDCl_3$) δ 7.45 – 7.42 (m, 2H), 7.40 – 7.36 (m, 2H), 7.35 – 7.26 (m, 4H), 7.24 – 7.10 (m, 6H), 7.02 – 6.99 (m, 1H), 3.90 (d, *J* = 13.6 Hz, 1H), 3.82 (d, *J* = 13.6 Hz, 1H), 3.57 – 3.52 (m, 0.5H), 3.43 (d, *J* = 13.7 Hz, 1H), 3.38 (d, *J* = 13.7 Hz, 1H), 3.23 – 3.18 (m, 0.5H), 3.13 – 3.06 (m, 1H), 2.03 – 2.05 (m, 1.5H), 1.87 – 1.79 (m, 0.5H), 0.87 (d, *J* = 6.1 Hz, 1.5H), 0.84 (d, *J* = 6.5 Hz, 1.5H), 0.27 (s, 4.5H), 0.24 (s, 4.5H).**^{13}C NMR** (126 MHz, $CDCl_3$) δ 141.3, 141.1, 139.6, 139.6, 129.2, 129.2, 129.0, 128.9, 128.3, 128.2, 128.1, 128.1, 127.0, 126.9, 125.7, 125.6, 103.5, 103.1, 91.0, 90.5, 58.78, 58.7, 55.3, 55.0, 41.1, 39.6, 38.2, 37.5, 17.1, 16.2, 0.4, 0.4. *(Peaks with asterisk not fully resolved). **IR** (cm^{-1}): 3085, 3027, 2157, 1248, 838, 735, 696; **$[\alpha]^{20}$D** = -128.106(c = 0.1, $CHCl_3$); **HRMS**: (ESI-TOF) calculated for $C_{29}H_{35}NSi$ $[M + H]^+$ 426.2612, found 426.2619.

N,*N*-Dibenzyl-4-methyl-5-phenylpent-1-yn-3-amine

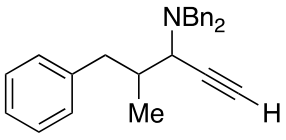

TMS-protected compound (43 mg) was deprotected as per general procedure 2 (**GP2**). The product was purified by flash column chromatography (10% EtOAc/cyclohexane) to give a colourless waxy oil (33 mg, 92%) as a mixture of

diastereomers. **R_f** = 0.9 (10% EtOAc/cyclohexane); **^{1}H NMR** (500 MHz, $CDCl_3$) δ 7.47 – 7.43 (m, 2H), 7.42 – 7.38 (m, 2H), 7.37 – 7.26 (m, 5H), 7.25 – 7.19 (m, 3H), 7.18 – 7.10 (m, 2H), 7.04 – 6.99 (m, 1H), 3.93 (d, *J* = 13.8, 1H), 3.85 (dd, *J* = 13.0 Hz, 1H), 3.60 – 3.53 (m, 0.5H), 3.48 – 3.44 (m, 1H), 3.44 – 3.40 (m, 1H), 3.24 – 3.19 (m, 0.5H), 3.16 – 3.07 (m, 1H), 2.49 – 2.46 (m, 0.5H), 2.40 - 2.37 (m, 0.5H), 2.12 – 1.99 (m, 1H), 1.89 -1.79 (m, 0.5H), 0.91 – 0.84 (m, 3.5H); **^{13}C NMR** (126 MHz, $CDCl_3$) δ 141.2, 140.9, 139.5, 139.4, 129.2, 129.2, 129.0, 128.9, 128.4, 128.3, 128.2, 128.1, 127.0, 126.9, 125.8, 125.7, 81.0, 80.6, 74.2, 73.8, 55.2, 54.9, 40.9, 39.7, 38.1, 37.5, 17.0, 16.1; **IR** (cm^{-1}): 3297, 308, 296, 1494, 1452, 743, 696; **[α]^{20}D** = -83.60 (c = 0.1, $CHCl_3$); **HRMS**: (ESI-TOF) calculated for $C_{26}H_{27}N$ $[M + H]^+$ 354.2216, found 354.2213.

(1-Adamantyl)dimethylamine [36]

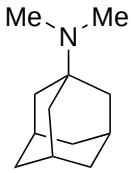

1-Adamantylamine (600 mg, 4 mmol, 1 equiv.) was added to a round-bottomed flask. Formaldehyde (0.40 mL, 4 mmol, 1 equiv.), formic acid (0.60 mL, 16 mmol, 4 equiv.), H_2O (3 mL) were added and the reaction was heated to 120 °C for 24 h. The reaction was allowed to cool to rt and was quenched with 2M NaOH (3 mL) until pH 11. The reaction mixture was extracted with Et_2O (3 x 10 mL), dried with $MgSO_4$, was filtered and concentrated *in vacuo* to give a colourless oil (200 mg, 28% yield)**. ^{1}H NMR** (300 MHz, $CDCl_3$) δ 2.20 (s, 6H), 2.02 (d, *J* = 4.7 Hz, 3H), 1.68 – 1.48 (m, 12H). All physical data were in agreement with literature values

Tert-butyl adamantan-1-yl-carbamate **31**[37]

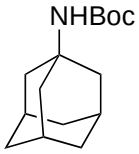

1-Adamantylamine (900 mg, 6.3 mmol, 1 equiv.) was added to a flame-dried Schlenk flask. Triethylamine (2.0 mL, 12.6 mmol, 2 equiv.) and di-*tert*-butyl decarbonate (2.00 g, 9.45 mmol, 1.5 equiv.) were added and the reaction was stirred at room temperature for 48 h. The reaction was heated to 30 °C for 6 d as starting material was still present by TLC (stained with vanillin). The reaction was cooled to 0 °C and was quenched with H_2O (10 mL). The phases were separated and the aqueous phase was extracted with CH_2Cl_2 (3 x 10 mL). The organics were combined, were washed with brine (50 mL), were dried with $MgSO_4$ and were concentrated *in vacuo* to give the pure product (1.30 g, 87%) as white solid where no further purification was necessary. **^{1}H NMR** (500 MHz, $CDCl_3$) δ 4.35 (S, 1H), 2.04 (m, 3H), 1.90 (m, 6H), 1.64 (m, 6H), 1.41 (s, 9H). All characterisation data are in agreement with reported literature data.

2-Methylpentanoic acid **34** [38]

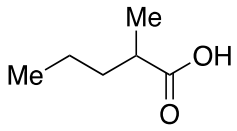

Sodium phosphate monobasic monohydrate (1.24 g, 8.98 mmol, 0.24 equiv.) was dissolved in H_2O (10 mL) and H_2O_2 (30% w/v) (3.8 mL, 43 mmol, 1.2 equiv.) was added. Acetonitrile (25 mL) was added followed by 2-methylpentanal (4.46 mL, 36 mmol, 1 equiv.). The reaction was the cooled to 0 °C. $NaClO_2$ (4.80 g, 53 mmol, 1.43 equiv.) was dissolved in H_2O (25 mL) and was added dropwise to the reaction mixture. The reaction was stirred at 0 °C for 3 h until completion (TLC). Sodium sulfite (700 mg, 5.55 mmol, 0.15 equiv.) was added to quench unreacted HOCl and H_2O_2.

The pH of the reaction mixture was adJusted to 9-10 with 2M NaOH. The reaction mixture was extracted with CH_2Cl_2 (3 x 100 mL), acidified to pH 1 with concentrated HCl and was extracted with CH_2Cl_2 (3 x 100 mL). The combined organics from the acidified extraction were combined, dried with magnesium sulfate, were filtered and concentrated *in vacuo* to give a crude yellow oil (3.87 g, 67%) which was used without purification. **^{1}H NMR** (500 MHz, $CDCl_3$) δ 2.52 – 2.44 (m, 1H), 1.72 – 1.63 (m, 1H), 1.47 – 1.30 (m, 3H), 1.18 (d, *J* = 7.0 Hz, 3H), 0.92 (t, *J* = 7.0 Hz, 3H); **^{13}C NMR** (126 MHz, $CDCl_3$) δ 183.3, 39.1, 35.7, 20.3, 16.8, 13.9. All characterisation data are in agreement with reported literature data.

2-Methylpentanoyl chloride **35**[39]

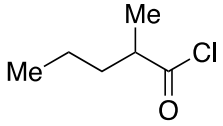

2-Methylpentanoic acid (3.87 g, 0.033 mol, 1 equiv.) was dissolved in CH_2Cl_2 (30 mL) and was cooled to 0 °C. Thionyl chloride (5.51 mL, 0.046 mol, 1.3 equiv.) was added dropwise followed by dimethylformamide (0.20 mL). The reaction was allowed to warm to room temperature and was stirred for 24 h. The organics were concentrated *in vacuo* to give the crude acid chloride as a brown oil which was used without purification. **^{1}H NMR** (400 MHz, $CDCl_3$) δ 2.88 (h, *J* = 7.1 Hz, 1H), 1.85 – 1.74 (m, 1H), 1.56 – 1.45 (m, 1H), 1.44 – 1.34 (m, 2H), 1.28 (d, *J* = 6.9 Hz, 3H)), 0.94 (t, *J* = 7.1 Hz, 3H); **^{13}C NMR** (101 MHz, $CDCl_3$)) δ 177.8, 51.2, 35.4, 19.9, 16.9, 13.8. All characterisation data are in agreement with reported literature data.

2-Phenylpropanoic acid [40]

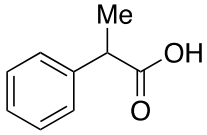

Sodium phosphate monobasic monohydrate (1.24 g, 8.98 mmol, 0.24 equiv.) was dissolved in H_2O (10 mL) and H_2O_2 (30% w/v) (3.80 mL, 43 mmol, 1.2 equiv.) was added. Acetonitrile (25 mL) was added followed by 2-phenylpropionaldehyde (5.0

mL, 37 mmol, 1 equiv.). The reaction was the cooled to 0 °C. $NaClO_2$ (4.81 g, 53 mmol, 1.43 equiv.) was dissolved in H_2O (25 mL) and was added dropwise to the reaction mixture. The reaction was stirred at 0 °C for 3 h until completion (TLC). Sodium sulfite (700 mg, 5.55 mmol, 0.15 equiv.) was added to quench unreacted HOCl and H_2O_2. The pH of the reaction mixture was adJusted to 9-10 with 2M NaOH. The reaction mixture was extracted with CH_2Cl_2 (3 x 100 mL), acidified to pH 1 with concentrated HCl and was extracted with CH_2Cl_2 (5 x 100 mL). The combined organics from the acidified extraction were combined, dried with magnesium sulfate, were filtered and concentrated *in vacuo* to give a crude yellow oil (4.33 g, 80%) which was used without purification. **^{1}H NMR** (500 MHz, $CDCl_3$) δ 7.35 – 7.30 (m, 4H), 7.28 – 7.24 (m, 1H), 3.73 (q, *J* = 7.2 Hz, 1H), 1.51 (d, *J* = 7.2 Hz, 3H). All characterisation data are in agreement with reported literature data.

2-Phenylpropanoyl chloride[31]

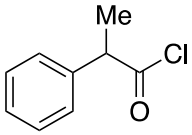

2-Phenylpropanoic acid (4.32 g, 0.028 mol, 1 equiv.) was dissolved in CH_2Cl_2 (30 mL) and was cooled to 0 °C. Thionyl chloride (8.40 mL, 0.043 mol, 1.5 equiv.) was added dropwise followed by dimethylformamide (0.20 mL). The reaction was allowed to warm to room temperature and was stirred for 24 h. The organics were concentrated *in vacuo* to give the crude acid chloride in a quantitative yield which was used without purification. **^{1}H NMR** (300 MHz, $CDCl_3$) δ 7.43 – 7.24 (m, 5H), 4.12 (q, *J* = 7.1 Hz, 1H), 1.60 (d, *J* = 7.1 Hz, 3H). All characterisation data are in agreement with reported literature data.

(*S*)-2-Amino-3-phenylpropan-1-ol **36**[41]

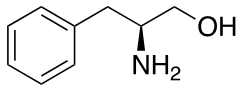

Lithium aluminium hydride pellets (6.0 g, 0.158 mol, 6 equiv.) were dissolved in THF (100 mL) at 0 °C. (*L*)-Phenylalanine (5.12 g, 31 mmol, 1 equiv.) was added in portions over 1 h. The reaction was heated at reflux for 3 h. The reaction was then cooled to 0 °C and was slowly quenched with H_2O (50 mL) until the evolution of gas ceased. The phases were separated and the aqueous phase was extracted with EtOAc (100 mL). The organics were combined, dried with magnesium sulfate, were filtered and concentrated *in vacuo* to give a crude light-yellow solid (2.60 g, 56%) which was used without purification. **^{1}H NMR** (300 MHz, $CDCl_3$) δ 7.36 – 7.14 (m, 5H), 3.63 (dd, *J* = 10.7, 3.8 Hz, 1H), 3.39 (dd, *J* = 10.7, 7.2 Hz, 1H), 3.12 (dddd, *J* = 8.9, 7.2, 5.2, 3.8 Hz, 1H), 2.79 (dd, *J* = 13.5, 5.2 Hz, 1H), 2.52 (dd, *J* = 13.5, 8.9 Hz, 1H), 2.09 (S, br, NH_2, 2H). All characterisation data are in agreement with reported literature data.

(*S*)-(1-Hydroxy-3-phenylpropan-2-yl) carbamate **37**[42]

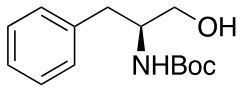

(*S*)-2-Amino-3-phenylpropan-1-ol (2.60 g, 17.2 mmol, 1 equiv.) was dissolved in CH_2Cl_2 (20 mL) and was cooled to 0 °C. Triethylamine (2.60 mL, 18.06 mmol, 1.05 equiv.) was added followed by di-tert-butyl decarbonate (4.01 g, 18.4 mmol, 1.07 equiv.). The mixture was stirred at room temperature for 24 h. The reaction was quenched with H_2O (20 mL), extracted with CH_2Cl_2 (3 x 20 mL), washed with brine (50 mL) and dried with magnesium sulfate. The solvent was removed under reduced pressure to give crude light-yellow solid (3.65 g, 84%) which was used without further purification. **^{1}H NMR** (500 MHz, $CDCl_3$) δ 7.32 – 7.27 (m, 2H), 7.24 – 7.17 (m, 4H), 4.83 (s, 1H), 3.86 (s, 1H), 3.64 (dd, *J* = 11.0, 4.0 Hz, 1H), 3.54 (dd, *J* = 11.0, 5.3 Hz, 1H), 2.88 – 2.78 (m, 2H), 2.58 – 2.42 (m, 2H), 1.41 (s, 9H). All characterisation data are in

agreement with reported literature data.

(*S*)-4-Benzyloxazolidin-2-one **38**[43]

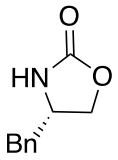

Boc-protected (L)-phenylalaninol **37** (3.65 g, 0.0145 mol, 1 equiv.) was dissolved in THF (15 mL) and was cooled to 0 °C. Thionyl chloride (8.50 mL, 0.12 mol, 8 equiv.) was added in a dropwise manner and the mixture was stirred at room temperature for 30 h. The volatiles were removed under reduced pressure. The resulting organic residue was dissolved in Et_2O (75 mL), was washed with H_2O (3 x 50 mL), washed with brine (50 mL), dried with magnesium sulfate and was concentrated *in vacuo* to give a crude brown residue. The product was purified by flash column chromatography (25% to 50% EtOAc/cyclohexane) to give (*S*)-4-benzyloxazolidin-2-one **38** (0.99 g, 39%) as a white solid. $\mathbf{R_f}$ = (0.3 in 50% EtOAc/cyclohexane); ^{1}**H NMR** (400 MHz, $CDCl_3$) δ 7.37 – 7.31 (m, 2H), 7.30 – 7.25 (m, 1H), 7.20 – 7.16 (m, 2H), 5.63 (s, 1H), 4.45 (dd, *J* = 8.5, 7.9 Hz, 1H), 4.18 – 4.05 (m, 2H), 2.88 (d, *J* = 6.8 Hz, 2H). All characterisation data are in agreement with reported literature data.

References

(1) Clayden, J.; Greeves, N.; Warren, S. *Organic Chemistry*, 2nd Ed.; Oxford; New York, Oxford University Press, 2012.

(2) Akiba, K.; Sakurai, Y.; Wada, M. *Tetrahedron Lett.* **1984**, *25* (10), 1083–1084.

(3) Suzuki, H.; Shimokawa, K.; Shiraishi, Y.; Uno, H. *Chem. Soc. Japan* **1988**, *21* (1), 729–732.

(4) Aubrecht, K. B.; Winemiller, M. D.; Collum, D. B. *J. Am. Chem. Soc.* **2000**, *122* (45), 11084–11089.

(5) Peshkov, V. A.; Pereshivko, O. P.; Van Der Eycken, E. V. *Chem. Soc. Rev.* **2012**, *41* (10), 3790–3807.

(6) McNally, J. J.; Youngman, M. A.; Dax, S. L. *Tetrahedron Lett.* **1998**, *39* (9), 967–970.

(7) Dyatkin, A. B.; Rivero, R. A. *Tetrahedron Lett.* **1998**, *39* (22), 3647–3650.

(8) Fischer, C.; Carreira, E. M. *Org. Lett.* **2001**, *3* (26), 4319–4321.

(9) Li, C. J.; Wei, C. *Chem. Commun.* **2002**, *2* (3), 268–269.

(10) Wei, C.; Li, Z.; Li, C. *J. Org. Lett.* **2003**, *5* (23), 4473–4475.

(11) Wei, C.; Li, C. *J. Am. Chem. Soc.* **2002**, *124* (I), 5638–5639.

(12) Yao, X.; Li, C. *J. Met. React. Water* **2013**, *43* (4), 87–108.

(13) Rokade, B. V.; Barker, J.; Guiry, P. J. *Chem. Soc. Rev.* **2019**, *48* (18), 4766–4790.

(14) Gommermann, N.; Koradin, C.; Polborn, K.; Knochel, P. *Angew. Chemie - Int. Ed.* **2003**, *42* (46), 5763–5766.

(15) Koradin, C.; Polborn, K.; Knochel, P. *Angew. Chemie-Int. Ed.* **2002**, *41* (14), 2535-+.

(16) Dube, H.; Gommermann, N.; Knochel, P. *Synthesis.* **2004**, *4* (12), 2015–2025.

(17) Gommermann, N.; Gehrig, A.; Knochel, P. *Synlett* **2005**, *4* (18), 2796–2798.

(18) Gommermann, N.; Knochel, P. *Tetrahedron* **2005**, *61* (48), 11418–11426.

(19) Rokade, B. V.; Guiry, P. *J. ACS Catal.* **2017**, *7* (4), 2334–2338.

(20) Rokade, B. V.; Guiry, P. J. *J. Org. Chem.* **2019**, *84* (9), 5763–5772.

(21) Eames, J. *Angew. Chemie - Int. Ed.* **2000**, *39*, 885–888.

(22) Martin, V. S.; Woodard, S. S.; Katsuki, T.; Yamada, Y.; Ikeda, M.; Sharpless, K. B. *J. Am. Chem. Soc.* **1981**, *103* (20), 6237–6240.

(23) Gao, Y.; Hanson, R. M.; Janice, M. K.; Ko, S. Y.; Masamune, H.; B., S. K. *J. Am. Chem. Soc.* **1987**, *109* (19), 5765–5780.

(24) Kitano, Y.; Matsumoto, T.; Sato, F. *Tetrahedron* **1988**, *44* (13), 4073–4086.

(25) Doyle, M. P.; Dyatkin, A. B.; Kalinin, A. V.; Ruppar, D. A.; Martin, S. F.; Spaller, M. R.; Liras, S. *J. Am. Chem. Soc.* **1995**, *117* (44), 11021–11022.

(26) Huerta, F. F.; Minidis, A. B. E.; Bäckvall, J. E. *Chem. Soc. Rev.* **2001**, *30* (6), 321–331.

(27) Chen, Z.; Aota, Y.; Nguyen, H. M. H.; Dong, V. M. *Angew. Chemie - Int. Ed.* **2019**, *58* (14), 4705–4709.

(28) Trost, B. M.; Patterson, D. E.; Hembre, E. J. *J. Am. Chem. Soc.* **1999**, *121* (46), 10834–10835.

(29) Trost, B. M.; Toste, F. D. *J. Am. Chem. Soc.* **1999**, *121* (14), 3543–3544.

(30) Dhanasekaran, S.; Kannaujiya, V. K.; Biswas, R. G.; Singh, V. K. *J. Org. Chem.* **2019**, *84* (6), 3275–3292.

(31) Chavda, S.; Coulbeck, E.; Coumbarides, G. S.; Dingjan, M.; Eames, J.; Ghilagaber, S.; Yohannes, Y. *Tetrahedron Asymmetry* **2006**, *17* (24), 3386–3399.

(32) Malkov, A. V.; Gouriou, L.; Lloyd-Jones, G. C.; Starý, I.; Langer, V.; Spoor, P.; Vinader, V.; Kočovský, P. *Chem. - A Eur. J.* **2006**, *12* (26), 6910–6929.

(33) Franzoni, I.; Guénée, L.; Mazet, C. *Chem. Sci.* **2013**, *4* (6), 2619–2624.

(34) Yang, K.; Li, Q.; Liu, Y.; Li, G.; Ge, H. *J. Am. Chem. Soc.* **2016**, *138* (39), 12775–12778.

(35) Gommermann, N.; Knochel, P. *Chem. - A Eur. J.* **2006**, *12* (16), 4380–4392.

(36) Toyooka, G.; Tuji, A.; Fujita, K. I. *Synth.* **2018**, *50* (23), 4617–4626.

(37) Hyodo, K.; Hasegawa, G.; Maki, H.; Uchida, K. *Org. Lett.* **2019**, *21* (8), 2818–2822.

(38) Villano, R.; Acocella, M. R.; Scettri, A. *Tetrahedron Lett.* **2014**, *55* (15), 2442–2445.

(39) Derivatives, A. **1981**, *15* (1), 22–24.

(40) Ebbers, E. J.; Ariaans, G. J. A.; Bruggink, A.; Zwanenburg, B. *Tetrahedron Asymmetry* **1999**, *10* (19), 3701–3718.

(41) Campbell, C. D.; Concellón, C.; Smith, A. D. *Tetrahedron Asymmetry* **2011**, *22*

(7), 797–811.

(42) Kaur, P.; Chamberlin, A. R.; Poulos, T. L.; Sevrioukova, I. F. *J. Med. Chem.* **2016**, *59* (9), 4210–4220.

(43) Hatano, M.; Yamashita, K.; Ishihara, K. *Org. Lett.* **2015**, *17* (10), 2412–2415.

Chapter 4: Heteroatom-directed Cu-catalysed Asymmetric Borylation of Heteroaryl-substituted Alkenes

Introduction

Miyaura-Borylation Reaction

The transition metal-catalysed borylation of organic compounds has seen significant advances in recent years.[1,2,3] Organoboron functional groups serve as valuable handles for a wide range of well described synthetic transformations.[4] In 1995, Miyaura reported the first procedure for the borylation of haloarenes to synthesise aryl-boronic ester products of type **1** (**Scheme 118**).[5] The system employed a Pd catalyst and relied on the *J*udicious choice of base. Potassium acetate facilitated the desired transformation in mostly excellent yields, while stronger bases such as potassium carbonate led to the borylated products of type **1** reacting with haloarene starting material in a Suzuki reaction to form the undesired bi-aryl products. The methodology boasted wide functional group compatibility including nitro, cyano, ester and carbonyl group tolerance.

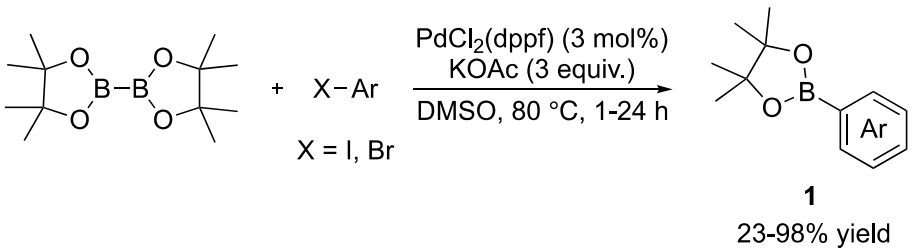

***Scheme 118**: First reported of metal-catalysed borylation of haloarenes*[5]

The catalytic cycle for the Pd-catalysed Miyaura borylation of haloarenes (**Scheme 119**) has as its first step the oxidative addition of the Pd^0 catalyst into the arene-halogen bond furnishing the Pd^{II} complex **2**. Acetate anion displacement of the halogen from the Pd^{II} species **2** followed by transmetallation with B_2Pin_2 **3** leads to the formation of the borylated Pd^{II} species **4**. Subsequent reductive elimination released the desired borylated arene **5** and regenerates the Pd^0 catalyst for further turn-over of the system.

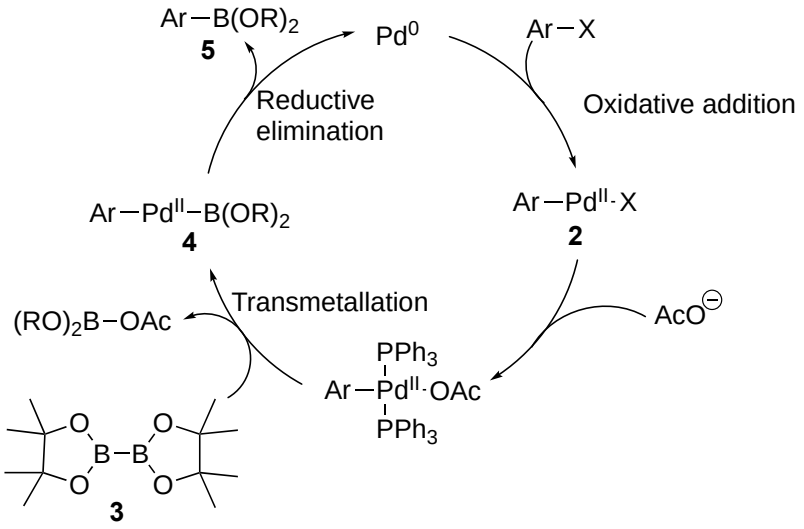

***Scheme 119**: Catalytic cycle for the Pd-catalysed Miyaura borylation of haloarenes*[6]

The synthetic utility of the boronic ester handle, readily installed by the methodology first reported by Miyaura, is demonstrated in **Scheme 120**. Treatment of arylboronic esters with a Cu catalyst and potassium iodide or bromide represents one well reported methodology for the transformation of boronic esters to the corresponding organohalide.[7] The lithiation of methoxyamine followed by introduction of the corresponding aryl pinacol borane represents one strategy for the amination of aryl boronates.[8] A variety of oxidants can furnish the corresponding alcohol from the boronic acids and esters, including hydrogen peroxide, *m*-CPBA, and *tert*-butyl hydroperoxide.[9,10] The utility of such aryl boronic acids and esters in Suzuki-Miyaura couplings is extensively documented in the literature.[11,12,13] This schematic of transformations is by no means exhaustive, with other transformations such as the cyanation of arenes *via* the corresponding aryl boronic ester also being known.[14]

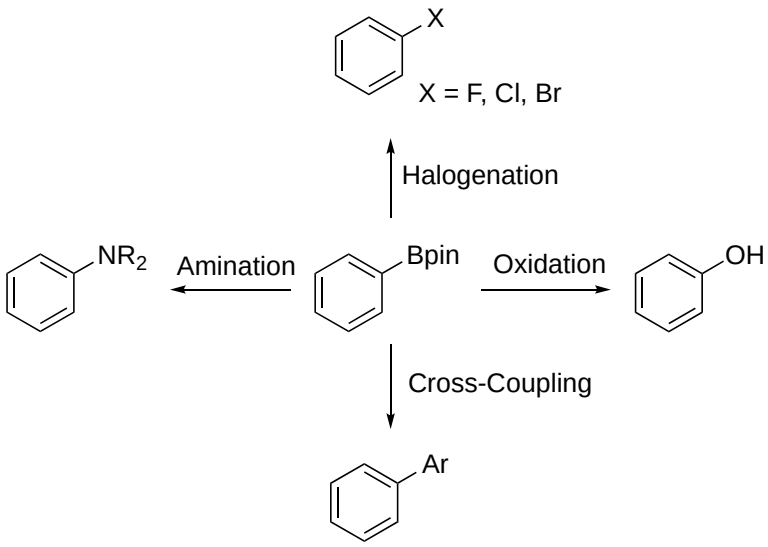

***Scheme 120**: Examples of possible synthetic transformations with boron as a synthetic handle*[15]

Further developments in the Miyaura borylation reaction led to the compatibility of non-halogenated substrates in updated methodologies. This meant that previously required halogen synthetic handles were no longer required for the installation of the organoboron functional group. The C-H activation borylation reaction represents a major advancement as it offers a viable method for late-stage functionalisation of organic compounds and is therefore particularly attractive towards medicinal and material applications.[15] The compatibility of C-H borylation protocols with a wide variety of existing functional groups within a molecule further strengthens its potential use in the late-stage functionalisation of complex organic molecules. The area has expanded extensively in recent years, with protocols in catalytic C-H borylation reactions of arenes and heteroarenes being reported with Fe, Co, Ni, Zn, Ru, Rh, Pt, Ir and Cu based catalysts (**Scheme 121**).[14]

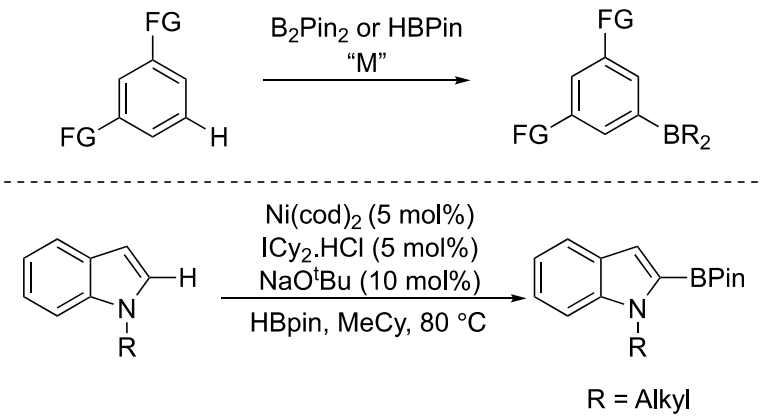

***Scheme 121**: Early examples of metal-catalysed C-H borylation reactions*[14]

Copper-catalysed borylation of Alkene

An early example of the Cu-catalysed addition of boron to aryl alkenes was reported by Hoveyda in 2009 using the copper NHC catalyst **6** (**Scheme 122**).[16] The protocol utilised exceptionally low catalyst loadings of just 0.5 mol% and offered great site selectivities of >98:<2. Importantly, it offered a viable alternative to Rh- and Ir-based catalysts already known in the literature at the time.[17,18]. Sterically hindered olefins, substituted aryl alkenes, indene, dihydronaphthalene, allylic esters, allylic ethers and allylic alcohols were well tolerated with yields ranging from 41-97% in reaction times of 10 min to 24 h.

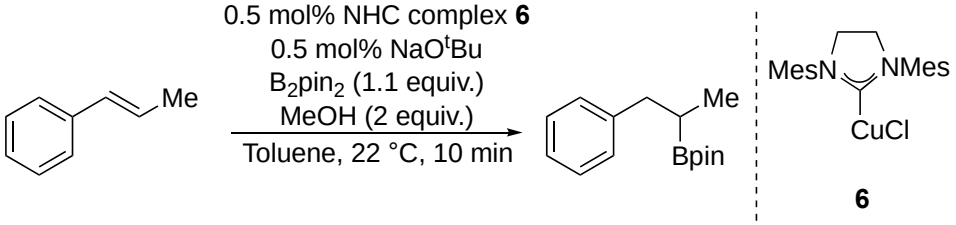

***Scheme 122**: Cu-NHC complex **6**-catalysed boron additions to aryl-substituted alkenes*

By employing chiral NHC-catalyst **7**, Hoveyda could also achieve the same catalytic transformation in an enantioselective fashion (**Scheme 123**).[16] High enantioselectivities were achieved for the reaction, but the reaction had to be cooled to -50 °C and was carried out over 48 h. Nonetheless, this represented a highly sought after advancement in the field as it moved from expensive Rh- and Ir-catalysed systems in favour of a cheaper and more readily available Cu-based system.

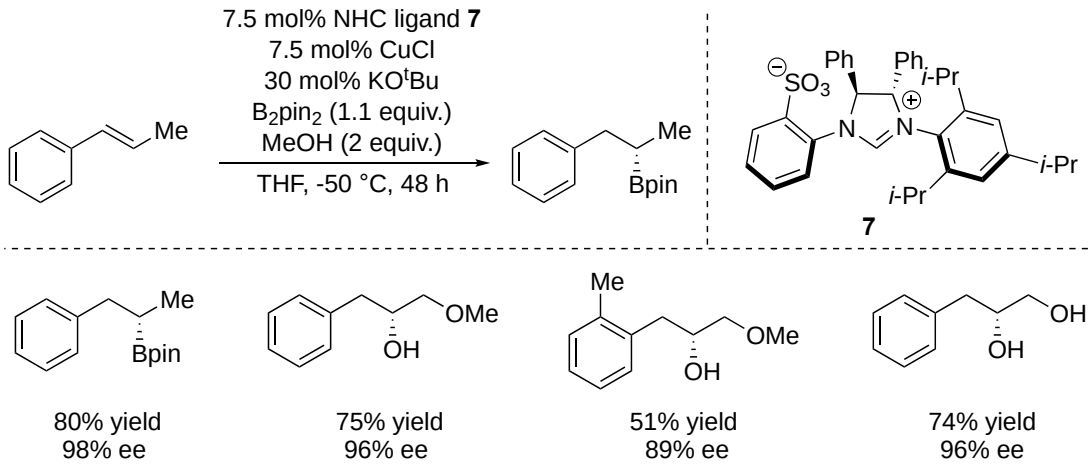

***Scheme 123**: Enantioselective boron addition to aryl-substituted alkenes using chiral NHC ligand and Cu catalyst*[16]

Synthetic Transformations Using Enantioenriched Organoboron Compounds

A notable benefit of the development of enantioselective borylation reactions is the subsequent array of stereoretentive and stereoinverting reactions that can be performed with minimal enantioerosion. An informative depiction of such transformations was reported by Aggarwal in a 2017 review on the topic (**Figure 24**).[19] The development of such stereoretentive and stereoinverting reactions has renewed efforts towards investigating novel enantioselective borylation protocols for new substrates.

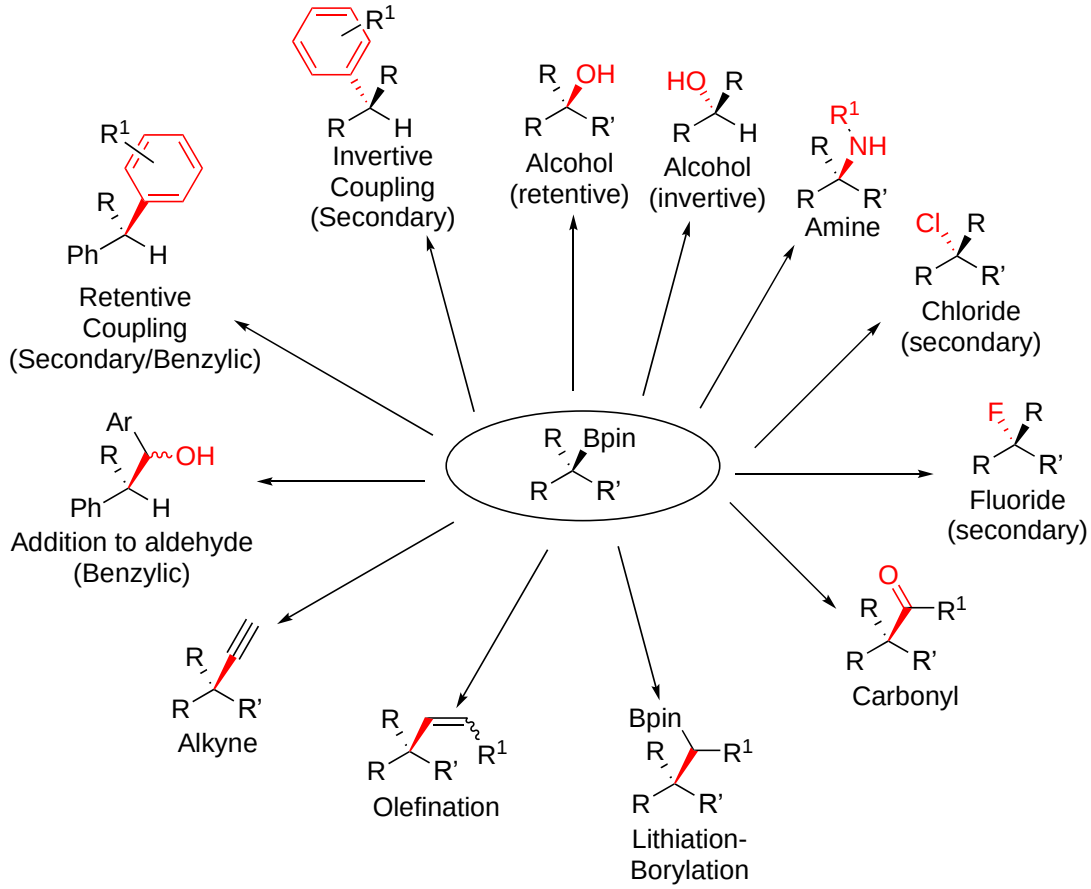

***Figure 24**: Schematic representation of possible transformation of enantioenriched boronic esters*[4]

Asymmetric Heteroatom-Directed Borylations Reactions

In 2017, Meng described a Cu-catalysed enantioselective boron addition to *N*-heteroaryl-substituted alkenes (**Scheme 124**).[20] The system uses a Cu catalyst and bis-phosphine ligand **8** for the enantioselective addition of Bpin group to the alkene. A wide variety of pyridyl, quinoline, isoquinoline, pyrimidine, triazine and benzothiazole-substituted alkenes were compatible with the protocol, forming the borylated products which were oxidised before isolating the corresponding alcohols. The protocol was successful when alkenes bearing aliphatic substituents α to the newly formed stereocentre were used. However, bis-aryl 1,2-disubstituted alkenes suffered from low yields (32-57%) and lower enantioselectivities (70-82%) with higher 7.5 mol% catalyst loadings over 14 h reaction times.

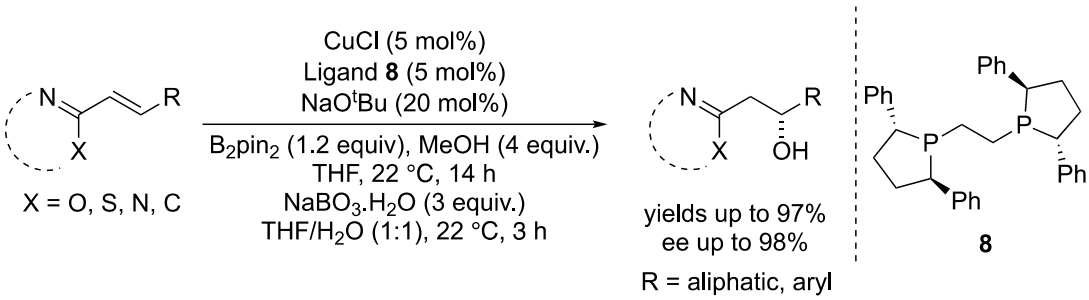

***Scheme 124**: Cu-catalysed enantioselective boron addition to N-heteroaryl-substituted alkenes*[20]

In order to understand the directing nature of the heteroatoms in the aryl groups bound to the alkenes, Meng conducted a series of investigative experiments to understand their role (**Scheme 125**).[20] The absence of a heteroatom in the phenyl-substituted alkene led to the formation of **9** in 55% yield and 74% ee. In contrast, the corresponding 2-pyridyl product **10** was formed in a 86% yield and 96% ee. The 4-pyridyl product **11** was furnished in a much lower yield (41%) and ee (20%) and the 3-pyridyl product **12** showed less than <2% conversion by ^{1}H NMR spectroscopy. From these observations, the authors proposed that the identity of the heteroatom and its location within the heterocycle played key roles in both substrate reactivity and enantioselectivity. They postulated that possible N atom co-ordination to the Lewis acidic metal would enhance the electrophilicity of the β-carbon, giving a more organised transition state and better enantioselectivity.

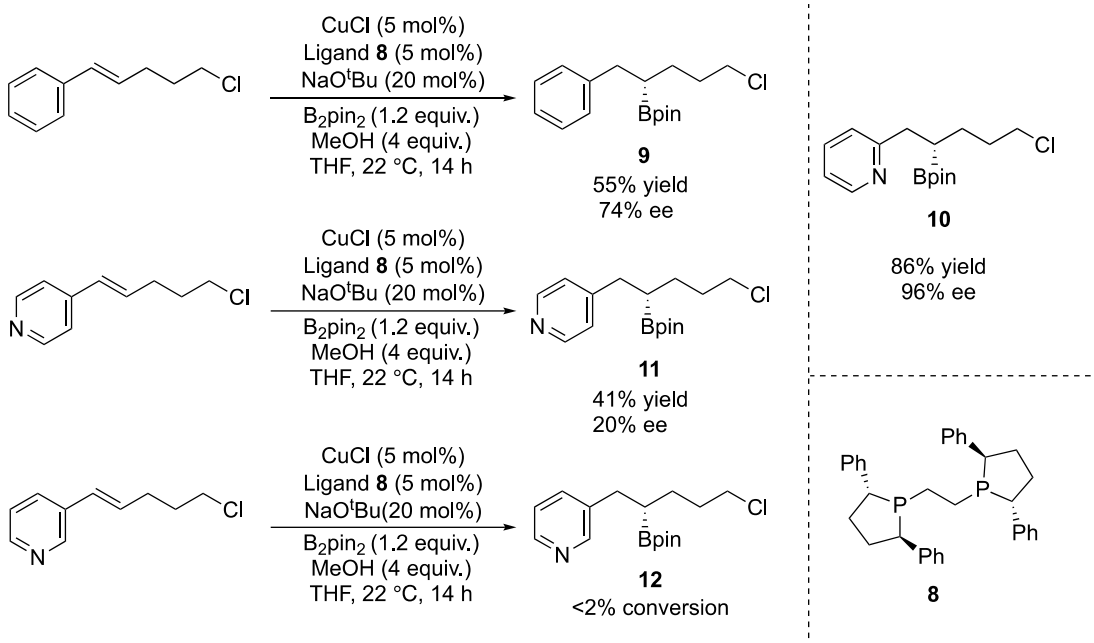

***Scheme 125**: Investigation into role of heteroatom co-ordination during enantioselective boron addition*[20]

The catalytic cycle for the transformation proposed by Meng (**Scheme 126**)[20] shows the Cu-Bpin species being generated by a reaction between the Cu-alkoxide with B_2pin_2, which subsequently undergoes *syn*-addition to the *N*-heteroaryl substrate. This generates an organocopper intermediate which undergoes protonation to release the borylated product and regenerates the Cu-alkoxide catalyst.

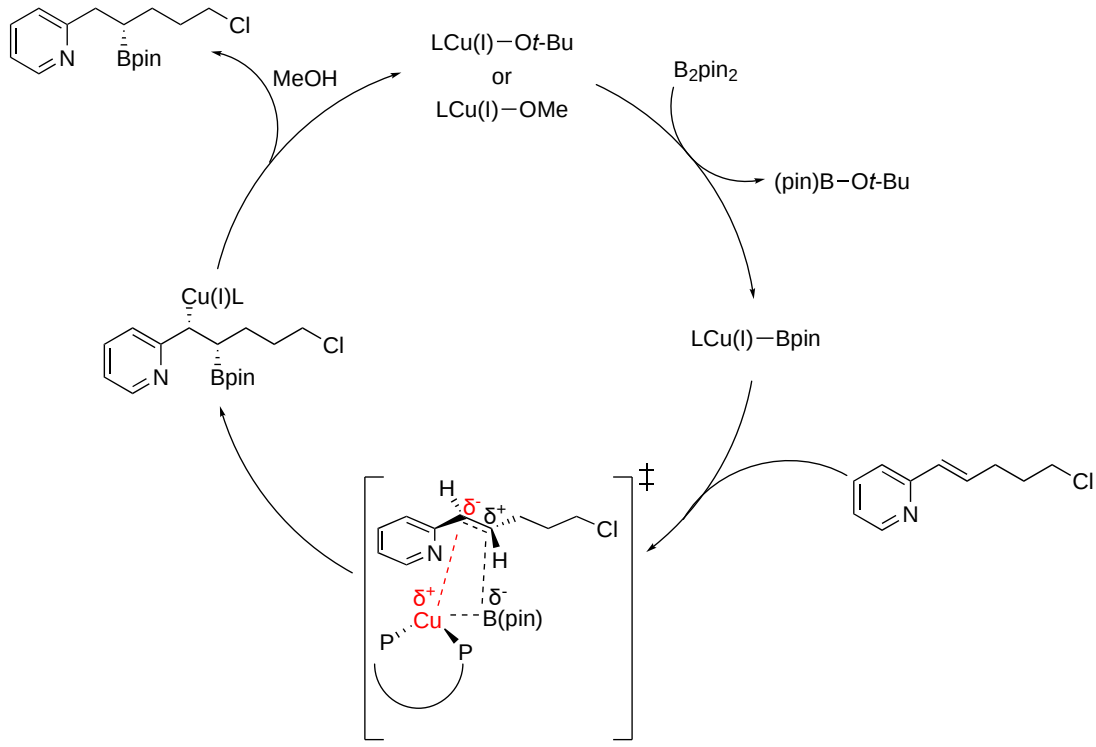

***Scheme 126**: Proposed catalytic cycle for Cu-catalysed enantioselective boron addition by Meng*

In 2019, Reyes described the Ir-catalysed asymmetric borylation of unactivated methylene C(sp^3)-H bonds with the use of chiral phosphite **13** (**Scheme 127**). The methodology asymmetrically installed a Bpin group on various alkane chains branched from heteroaryl substrates, which were subsequently oxidised to the corresponding alcohols through the use of sodium perborate. The product **14** is the only enantioenriched benzoxazole product of this type synthesised in the literature to the best of our knowledge.

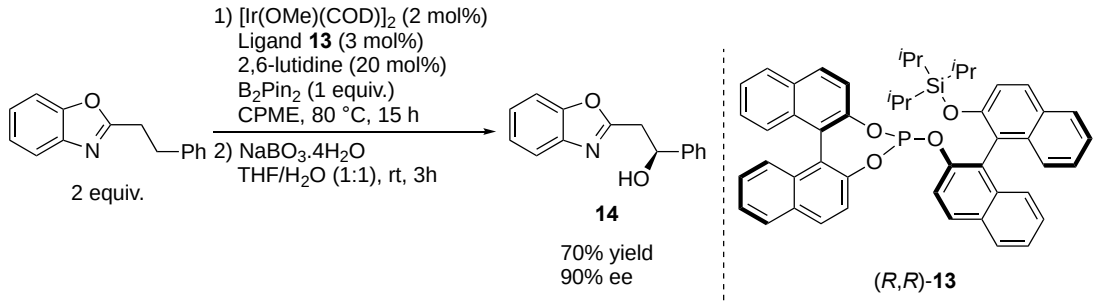

***Scheme 127**: Ir-catalysed asymmetric borylation of unactivated methylene C(sp^3)-H bonds*[21]

Project Aim

To the best of our knowledge, there are no racemic or asymmetric protocols for the installation of any boron species into benzoxazole substrates of type **15** (**Scheme 128**). There are also no known methodologies reported for access to enantioenriched benzoxazole alcohols of type **16.** Asymmetric borylation strategies for quinoline substrates of type **17** are also absent from the literature to the best of our knowledge. The corresponding alcohol of quinoline-organoborane **18** has been accessed *via* an asymmetric enzymatic reduction of 1-aryl-2-(azaaryl)ethanones with ketoreductases and *via* kinetic resolution of the racemic alcohol.[22,23]

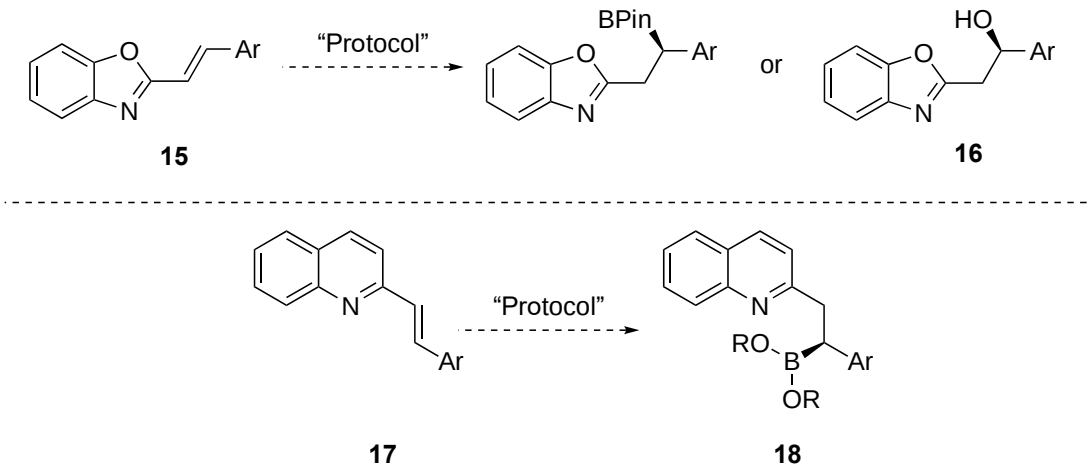

Scheme 128**: Lacking protocol for the achiral or chiral installation of boronic acids/esters into alkenes **15** or **17

The aim of this project was to devise a general novel protocol for the asymmetric hetereoatom-directed Cu-catalysed borylation of benzoxazole and quinolone-substituted aryl alkenes. The P,N ligands synthesised in earlier projects would be applied in the asymmetric borylation reactions, given the proven track record of UCDPhim type ligands and other P,N ligands in Cu-catalysed enantioselective reactions.[24,25, 26,27]

Results and Discussion

Reaction Optimisation

Taking inspiration from the work of Meng, we decided to investigate the application of P,N ligands for the Cu-catalysed borylation of alkenyl-benzoxazole substrates of type **19** (**Scheme 129**). The model substrate was synthesised by the protocol described by Ivanov and was isolated in 25% yield after purification by recrystallisation from ethanol.[28]

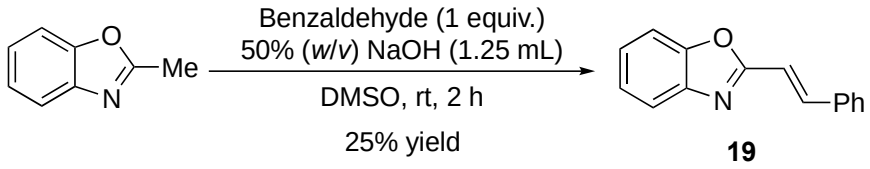

***Scheme 129**: Synthesis of model substrate (E)-2-styrylbenzo[d]oxazole*[28]

Preliminary racemic studies on the substrate indicated that the borylated products were unstable under aerobic conditions and also degraded on attempts to purify them *via* flash chromatography on silica gel. Therefore, it was decided that the crude products would be oxidised using sodium perborate monohydrate, which would furnish the corresponding alcohols.

The first step in the optimisation of the asymmetric catalytic reaction was to examine the ligands prepared previously (**Table 10**). *N*-Aryl imidazoline ligands **L1-L3** were screened and gratifyingly furnished the desired alcohol in moderate to good yields (53-70%). However, the enantioselectivities achieved with ligands **L1-L3** were poor (3-33% ee). (*S*)-*tert*-Butyl PHOX **L4** was more successful, giving the product in a higher yield (78%) and moderate enantioselectivity (45% ee). Monitoring the progress of the reaction proved difficult as the starting alkene substrate and borylated intermediate exhibited the same retention factor by TLC. Therefore, a test reaction was conducted, where the reaction was worked up after 1 h and was oxidised using the standard protocol (**entry 4, Table 10**). To our delight, **L4** with CuCl in 5 mol% loading led to the

isolation of the alcohol product in an 86% isolated yield after Just 1 hour, with a similar enantioselectivity of 41% ee. This was an encouraging result as the protocol reported by Meng for alkenylpyridine substrates yielded products in 32%-57% yields using 7.5 mol% catalysts over 18 h.[20] As such, this surprising result with respect to reactivity led to **L4** being chosen as the ligand to conduct further reaction optimisation upon.

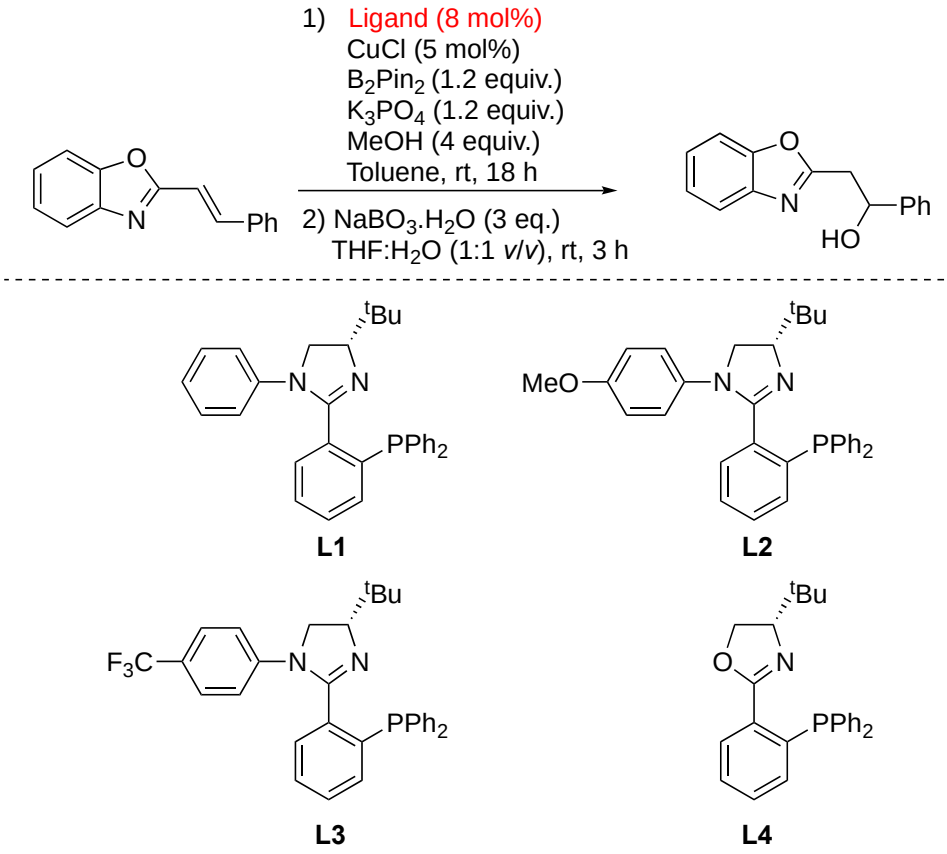

***Table 10**: Ligand screen in asymmetric borylation of model substrate*

Entry	Ligand	Time	Yield %[a]	Ee%[b]
1	**L1**	**18h**	**70**	**33**
2	**L2**	**18h**	**68**	**3**
3	**L3**	**18h**	**53**	**27**
4	**L4**	**18h**	**78**	**45**
5	**L4**	**1h**	**86**	**41**

[a]Isolated yields after purification

[b]enantiomeric excess determined by separation on chiral UPC[2]

Solvents were subsequently screened to probe their effect on the yield and enantioselectivity on the model reaction (**Table 11**). The benchmark for the reaction was set by toluene from the ligand screen (**entry 1**, 86% yield and 40% ee). Ethereal solvents were screened first (**entries 2-4**). While exhibiting slightly reduced reactivity, the use of diethyl ether led to the best enantioselectivity to date in our investigation (55% ee). Surprisingly, isopropanol was compatible with the protocol, showing equivalent reactivity and enantioselectivity to ethereal solvents (**entry 5**). Dimethylformamide furnished the product in the highest enantioselectivity (68% ee), but in a disappointingly low yield (20%). Extension of the reaction time to 18 h and increasing the equivalents of base did not change the yield. Therefore, it was not considered as a viable solvent for the reaction. Dimethylacetamide was more reactive towards product formation but at the expense of enantioselectivity (**entry 7**). Other reported solvents in borylation reactions furnished the product in poorer enantioselectivities (**entries 8-10**). As such, diethyl ether was chosen as the optimum solvent when both reactivity and enantioselectivity were considered.

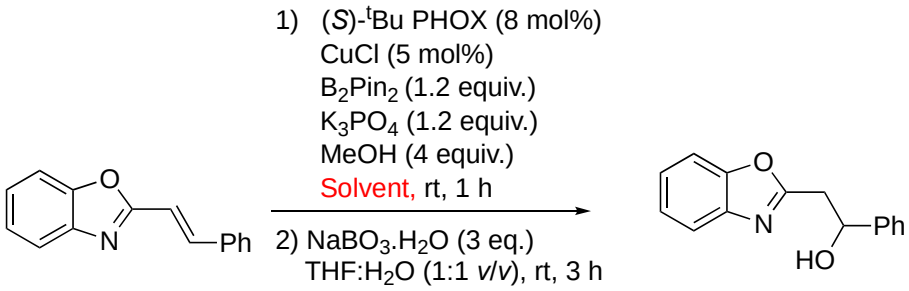

***Table 11**: Solvent screen for asymmetric borylation reaction*

Entry	Solvent	Yield%[a]	Ee%[b]
1	**Toluene**	**86**	**41**
2	**THF**	**77**	**42**
3	**Dioxane**	**83**	**43**
4	**Et_2O**	**70**	**55**
5	**iPrOH**	**81**	**47**
6[c]	**DMF**	**20**	**68**
7	**DMA**	**77**	**40**
8	**DME**	**64**	**34**
9	**CH_3Cl**	**55**	**30**
10	**MeCN**	**85**	**36**

[a]Isolated yields after purification

[b]enantiomeric excess determined by separation on chiral UPC[2]

[c] Reaction time was extended to 18 h, 3 equiv. Of K_3PO_4 was used with no change in yield

An evaluation of Cu salts was conducted for the purpose of probing their effect on yield and enantioselectivity in the model reaction (**Table 12**). Both Cu(I) and Cu(II) salts were successful in the protocol, with Cu(I) tetrakis-acetonitrile complexes (**entries 6-7**) proving the best in terms of balancing reactivity with enantioselectivity. Cu(I) Tetrakis-acetonitrile tetrafluoroborate was chosen as the best catalyst to continue reaction optimisation.

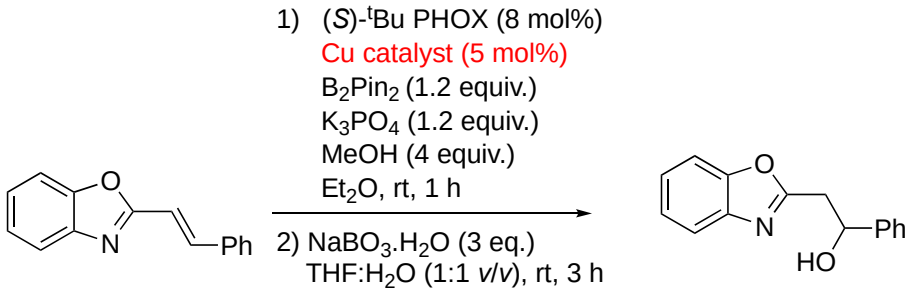

***Table 12**: Evaluation of Cu salts in the enantioselective model reaction*

Entry	Cu Source	Yield%[a]	Ee%[b]
1	**CuCl**	**70**	**55**
2	**CuBr**	**83**	**44**
3	**CuI**	**62**	**34**
4	**CuOAc**	**57**	**57**
5	**$Cu(OTf).C_6H_6$**	**87**	**45**
6	**$Cu(MeCN)_4BF_4$**	**79**	**56**
7	**$Cu(MeCN)_4PF_6$**	**94**	**49**
8	**$CuBr.SMe_2$**	**69**	**40**
9	**CuTc**	**83**	**30**
10	**$Cu(OAc)_2$**	**64**	**40**
11	**$Cu(OTf)_2$**	**75**	**45**

[a]Isolated yields after purification

[b]enantiomeric excess determined by separation on chiral UPC[2]

Alcohol additives were examined in the enantioselective model reaction after the best Cu catalyst was identified (**Table 13**). The equivalents of the alcohol additive were first investigated. It is worth nothing that all alcohols were dried for 48 h over 3Å molecular sieves prior to their use in catalysis. Firstly, the amount of methanol was reduced from four to two equivalents (**entries 1-2**). The reduction in equivalents of methanol increased the yield from 79% to 91%. Ethanol and iso-propanol had negative effects on both yield and enantioselectivity (**entries 3-4**), and as such other analogues of these alcohols such as hexafluoro-2-propanol and trifluoroethanol were not considered.

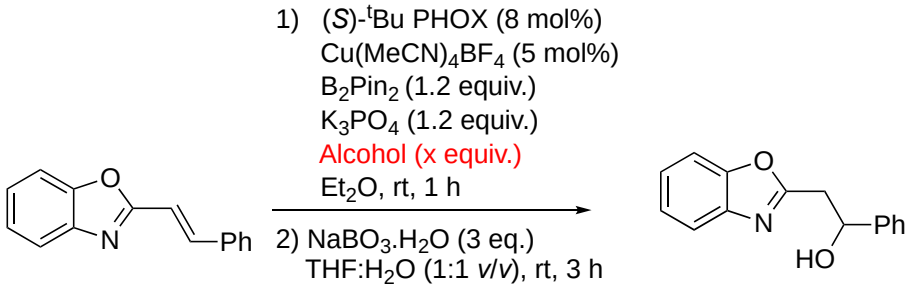

***Table 13**: Screening of alcohol additives in enantioselective model reaction*

Entry	Alcohol	Yield%[a]	Ee%[b]
1	**MeOH (4 eq.)**	**79**	**56**
2	**MeOH (2 eq.)**	**91**	**52**
3	**EtOH (2 eq.)**	**86**	**46**
4	**iPrOH (2 eq.)**	**77**	**38**

[a]Isolated yields after purification

[b]enantiomeric excess determined by separation on chiral UPC^2

The role of the base was then examined (**Table 14**). **Entry 1** represents the best conditions for the model reaction to date and serves as a point of comparison with other bases. All bases were dried under vacuum prior to their use in catalysis. Potassium pivalate increased the enantioselectivity of the reaction by approximately 10% ee, however the yields were poor in reaction time of 1 hour (**entry 2**). Extension of the reaction time to 17 h marginally increased the yield of the reaction to 32% (**entry 3**). The marked decreased reactivity of the system with potassium pivolate precluded its use as a viable base in the reaction. Potassium 2-ethylhexanoate (**entry 4**) has seen recent success in Miyaura borylation reactions with B_2Pin_2,[29] but unfortunately only yielded the product in a 23% yield with an enantioselectivity of 58% ee. Alkoxide bases (**entries 5-7**) showed increased reactivity, however the enantioselectivity was not improved (highest ee of 40%). Carbonate bases (**entry 8** and **entry 9**) furnished the product in high yields (up to 85%) but with lower enantioselectivity (33% and 39% ee). Potassium acetate (**entry 10**) was employed to

evaluate the suitability of acetate bases in the reaction, giving a yield of 39% and an ee of 55%. Further acetate bases were not probed based on the outcome of this result and potassium phosphate tribasic was kept as the optimised base for the reaction.

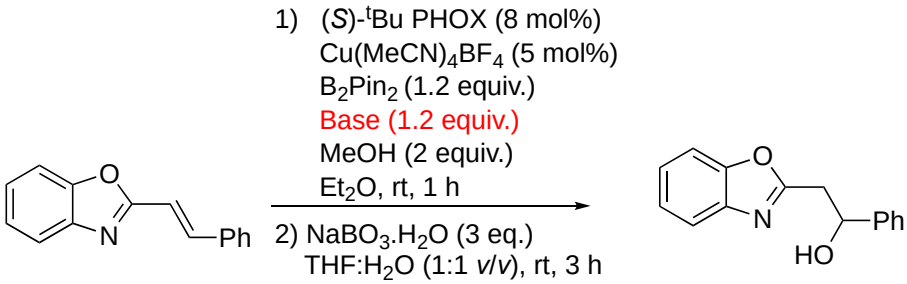

***Table 14**: Base screen in the enantioselective model reaction*

Entry	Time	Base	Yield%[a]	Ee%[b]
1	**1 h/3 h**	**K_3PO_4 (1.2 eq.)**	**91**	**52**
2	**1 h/3 h**	**Potassium Pivalate (1.2 eq.)**	**23**	**63**
3	**17 h/3 h**	**Potassium Pivalate (1.2 eq.)**	**32**	**61**
4	**1 h/3 h**	**Potassium 2-ethylhexanoate (1.2 eq)**	**23**	**58**
5	**1 h/3 h**	**NaO^tBu (1.2 eq.)**	**85**	**30**
6	**1 h/3 h**	**KO^tBu (1.2 eq.)**	**n/a**	**n/a**
7	**1 h/3 h**	**LiOMe (1.2 eq.)**	**70**	**40**
8	**1 h/3 h**	**Cs_2CO_3 (1.2 eq.)**	**83**	**33**

9	**1 h/3 h**	**K_2CO_3 (1.2 eq.)**	**85**	**39**
10	**1 h/3 h**	**KOAc (1.2 eq.)**	**36**	**55**

[a]Isolated yields after purification

[b]enantiomeric excess determined by separation on chiral UPC[2]

Reaction concentration, temperature and equivalents of B_2Pin_2 were next evaluated (**Table 15**). For the purpose of clarity, the optimised result to date is shown in bold at the top of the table. A reduction in temperature to -30 °C (**entry 1**) led to a decrease in product formation and did not affect enantioselectivity. A decrease in reaction concentration (**entry 2**) was examined, which led to a minor decrease in yield and enantioselectivity. Increasing the equivalents of B_2Pin_2 has been shown in the literature to increase enantioselectivity of other catalytic protocols, however in this system a reduction in enantioselectivity was observed when two equivalents of B_2Pin_2 were employed.[30]

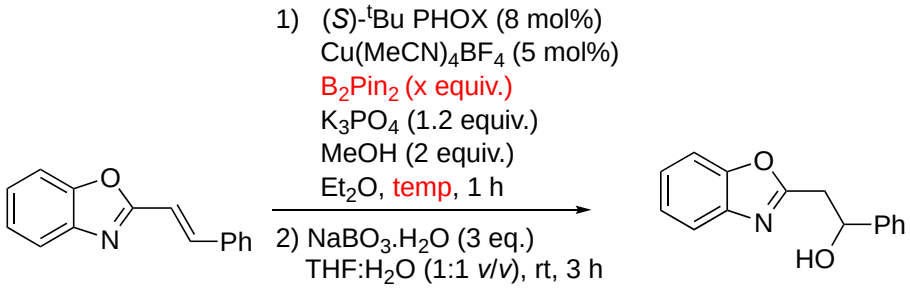

***Table 15**: Optimisation of temperature, concentration and B_2Pin_2 equivalents*

Entry	Temp (Conc)	Time	B_2Pin_2	Yield%[a]	Ee%[b]
Best	**rt (0.1 M)**	**1 h/3 h**	**1.2 eq.**	**91**	**52**
1	**-30 °C (0.1 M)**	**18 h/3 h**	**1.2 eq.**	**67**	**52**
2	**rt (0.05 M)**	**1 h/3 h**	**1.2 eq.**	**83**	**42**
3	**rt (0.1 M)**	**1 h/3 h**	**2 eq.**	**91**	**38**

[a]Isolated yields after purification

[b]enantiomeric excess determined by separation on chiral UPC[2]

The loadings of catalyst and base were subsequently investigated (**Table 16**). Sub-stoichiometric amounts of base improved the yield of the reaction but lowered the enantioselectivity by 9% (**entry 1**). Increasing or decreasing the catalyst loading from the standard 5 mol% led to minor decreases in enantioselectivity (**entry 2** and **entry 3**).

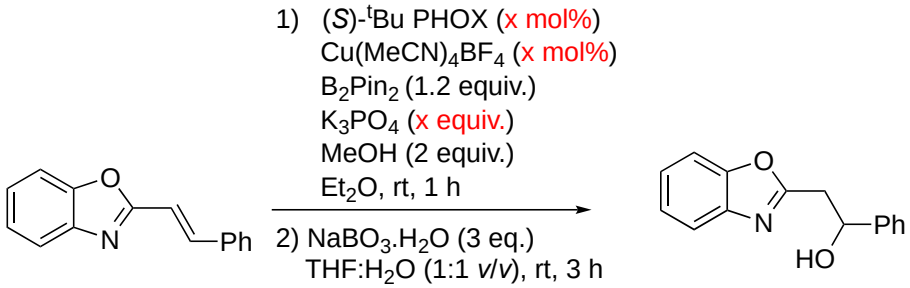

***Table 16**: Optimisation of catalyst and base loading*

Entry	Cat. Loading (mol %)	Base	Yield%[a]	Ee%[b]
1	**5 (std.)**	**K_3PO_4 (20 mol%)**	**96**	**43**
2	**2.5**	**K_3PO_4 (1.2 eq.)**	**96**	**42**
3	**10**	**K_3PO_4 (1.2 eq.)**	**77**	**49**

[a]Isolated yields after purification

[b]enantiomeric excess determined by separation on chiral UPC[2]

The commercially available axially chiral P,N ligand PINAP became available at this point in the project after supply issues from the manufacturer. After repeated experiments, the ligand gave an isolated yield of 86% and an enantioselectivity of 53% ee. PINAP was subsequently chosen as the optimal ligand, and was employed in the substrate scope to determine the robustness of the protocol.

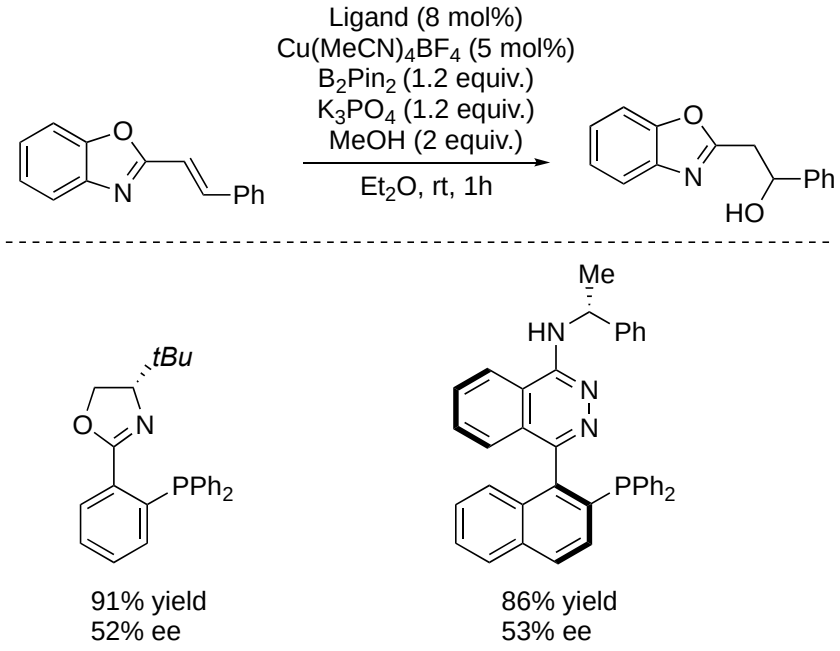

***Scheme 130**: Use of PINAP ligand in asymmetric borylation protocol*

Synthesis of Substrates

A variety of aryl-substituted benzoxazole substrates were synthesised as per the protocol described by Dryanska.[28] 2-Methylbenzoxazole and the corresponding aryl aldehyde were stirred at room temperature in DMSO open to air, before being treated with a 50% *w*/*v* aqueous solution of NaOH. After 1-3h, the reaction mixture was poured into water and was cooled to 4 °C. The resulting solid was isolated by vacuum filtration and was recrystallised from boiling ethanol to yield the pure substrates in 25-53% yields (**Scheme 131**). *o*-Tolyl-substituted benzoxazole **20** and the ferrocenyl-substituted benzaoxazole **21** were gifts synthesised by a previous group member, Dr. Bali Rokade.

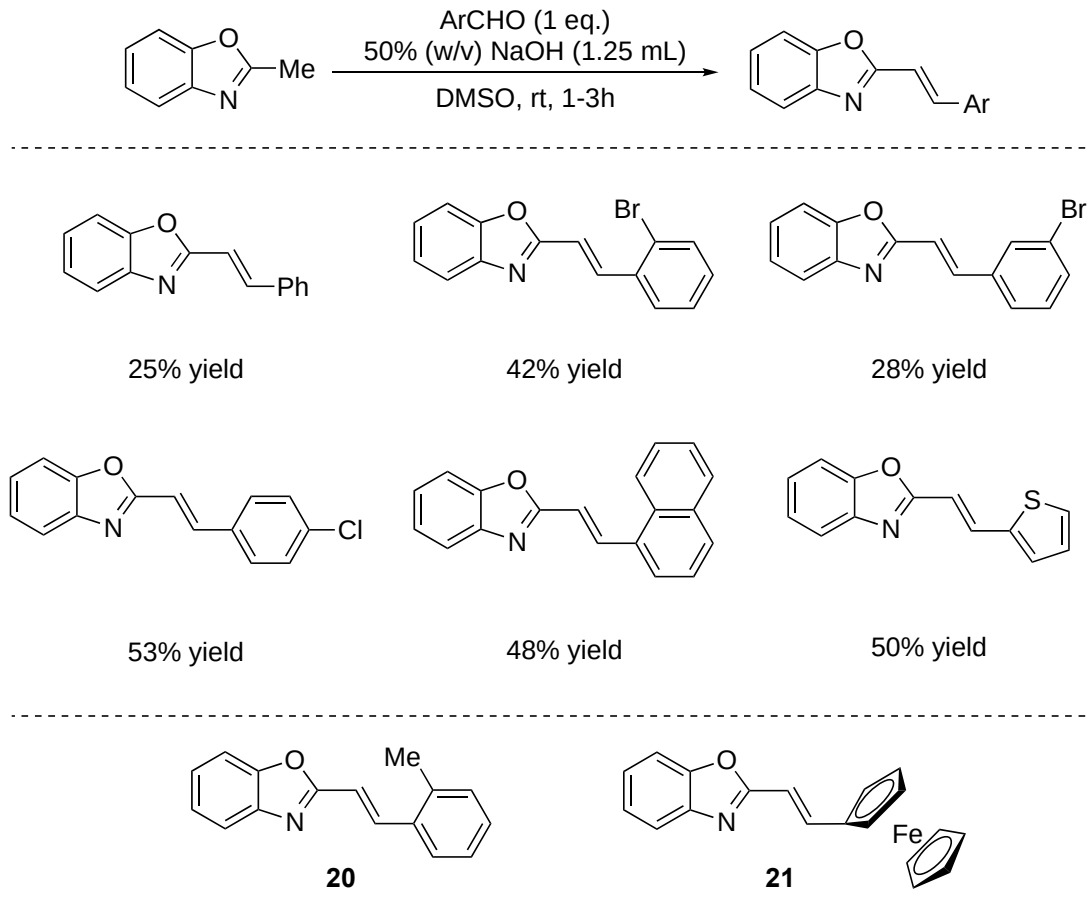

***Scheme 131**: Synthesis of aryl-substituted alkenyl-benzoxazoles*

Pi reported a system for the Fe-catalysed C(sp)^3-H functionalisation of methyl azaarenes (**Scheme 132**).[31] 2-Methylquinoline and the corresponding aryl aldehydes were refluxed in toluene in the presence of a catalytic amount Fe(II) acetate and trifluoroacetic acid. After 18h, the reaction mixtures were filtered through celite, concentrated *in vacuo* and were purified by column chromatography to yield the desired aryl-substituted alkenyl-quinolines in yields from 51% to 90%.

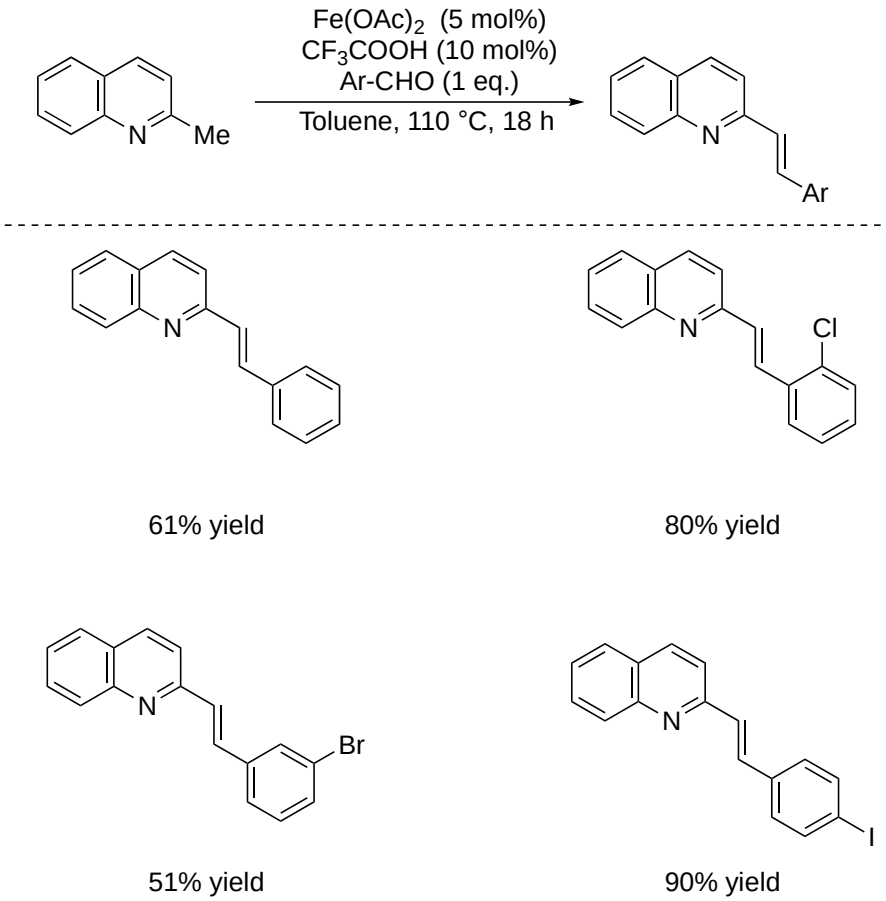

***Scheme 132**: Synthesis of aryl-substituted alkenyl quinolines*

A styrylpyridine substrate **22** was synthesised *via* a Pd-catalysed cross coupling in an 80% yield, using conditions optimised within the Guiry group in the synthesis of lipoxins (**Scheme 133**).

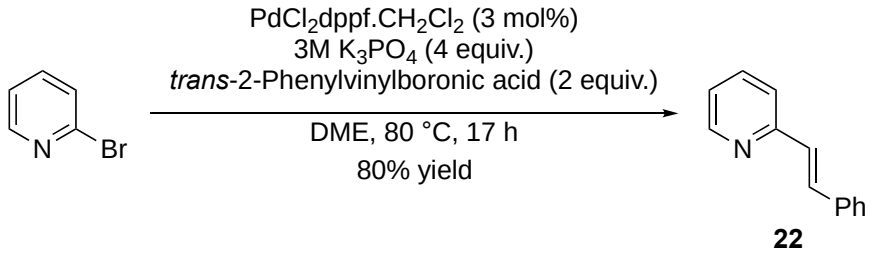

22

***Scheme 133**: Synthesis of (E)-2-styrylpyridine*

Substrate Scope

The racemic catalysis for this project was conducted under similar conditions to the asymmetric conditions but using toluene as the solvent and tricyclohexylphosphine as the achiral ligand. The quality of the tricyclohexylphosphine ligand was of utmost importance, as its rapid oxidation in air greatly diminished its reactivity. It was later found that taking the optimised asymmetric conditions and using 1,1'-bis(diphenylphosphino)ferrocene as the ligand reliably furnished the racemic product.

With the substrates and racemic products in hand, the asymmetric substrate scope of this project was conducted. Benzoxazole substrates were first examined and the results (**Scheme 134**) show that the phenyl-substituted product **14** under the optimised conditions was isolated in a high yield of 88% and a moderate enantioselectivity of 53% ee. To our delight, substitution on the aryl ring furnished products with higher levels of enantioselectivity compared to the phenyl-substituted product. *Ortho*-bromo and *ortho*-methyl substituted products **23** and **24** were accessed in 83% and 63% yields and with 76% and 73% ee, respectively. *Meta*-bromo product **25** was also tolerated in the protocol, with a 71% yield and 69% ee being obtained. The *para*-chloro derivative **26** showed similar reactivity to the model product, but again with a higher enantioselectivity of 74% ee. The naphthalene-substituted product **27** proved to be less reactive compared to the model product **22**, and was accessed in a similar level of enantioselectivity of 56% ee. The heteroaryl-thiophene substituted product **28** was amenable to the protocol, with the enantioselectivity on par with the other functionalised aryl products (75% ee). Curiously, although the ferrocene-substituted product **29** was synthesised racemically, it proved incompatible with the asymmetric methodology as only starting material was recovered. The optical rotation of these compounds was compared to the known product (**Scheme 127**), which was synthesised *via* Iridium C-H activation chemistry, and was used to tentatively assign the absolute configuration of the products in the absence of X-ray data.

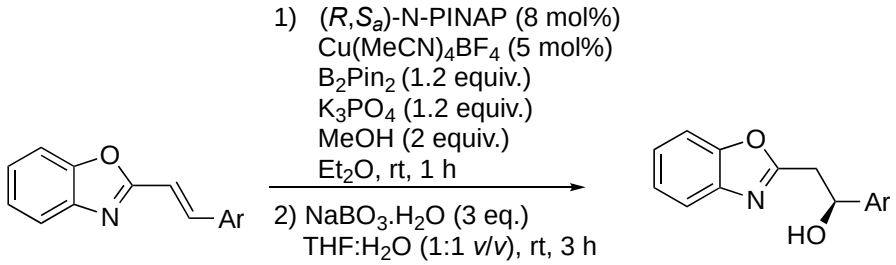

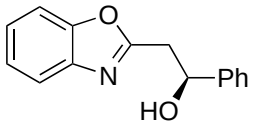

14

88% yield
53% ee

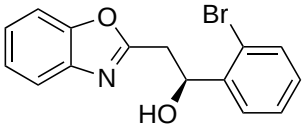

23

83% yield
76% ee

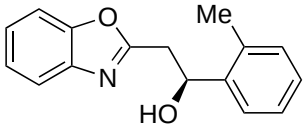

24

63% yield
73% ee

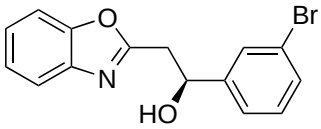

25

71% yield
69% ee

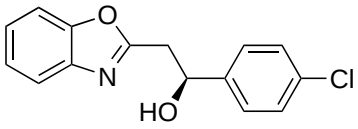

26

86% yield
74% ee

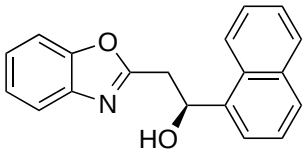

27

71% yield
56% ee

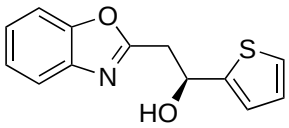

28

59% yield
75% ee

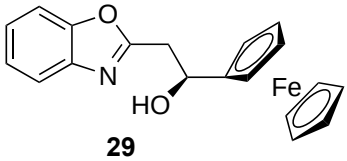

29

yield = n/a%

Scheme 134*: Substrate scope of alkenyl-substituted benzoxazoles in catalytic asymmetric borylation*

All yields quoted are isolated after column chromatography. Enantiomeric excesses were determined by chiral UHPLC.

The protocol was next applied to the previously synthesised aryl-substituted alkenyl-quinoline substrates (**Scheme 135**). The phenyl-substituted product **30** was first subjected to the optimised conditions used for the alkenyl-substituted benzoxazole products. Disappointingly, product **30** was only isolated in a 14% yield after 1 h. The reaction time was extended to 18 h, after which **30** was synthesised in a satisfactory 88% yield and in a moderate enantioselectivity of 53% ee.

To our disappointment, phenyl rings bearing substituted in the *ortho*-, *meta*-, and *para*-positions resulted in an inseparable mixture of two products (95% major product and 5% side product). Analysis of the NMR data suggests that the 5% side product is the other regioisomer of the alcohol product, where the initial borylation occurred at the α-position of the alkene. Synthesis of this α-regioisomer would be required to confirm this hypothesis, as they are also novel compounds with no reported literature data. Representative ^{1}H and ^{13}C NMR spectra of product **31** are shown in **Figure 25** and **Figure 26**, respectively. An extra set of aliphatic protons in the ^{1}H NMR spectrum (annotated with black arrows) and an extra set of aliphatic carbons (methylene and alcohol substituted – annotated with black arrows) in the ^{13}C NMR spectrum support the hypothesis of the other inseparable regio-isomer being present after purification after column chromatography. TLC analysis of the purified product shows only one spot under visualisation with a UV lamp.

The yield of the products **31**, **32**, and **33** could therefore not be recorded. However, the presence of the asymmetric product was supported by NMR comparison with the pure racemic sample and also by HRMS. The enantioselectivities were determined by comparison with the corresponding accessible pure racemic compounds using chiral UHPLC. The enantioselectivities of **31**, **32**, and **33** range from 52-62% (**Scheme 135**). Further work including further ligand screening could make substituted quinoline substrates compatible with the protocol. The absolute configuration of the products was deduced by inference from product **14** (**Scheme 134**).

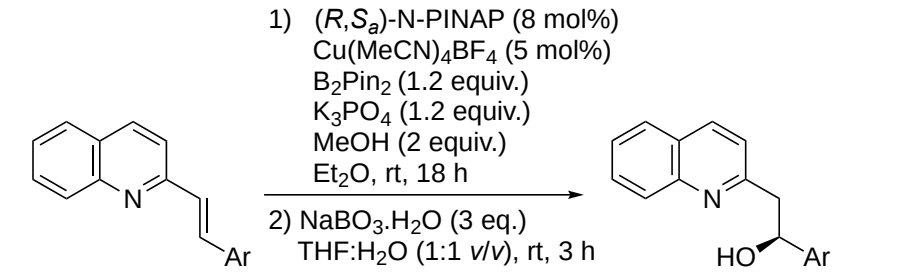

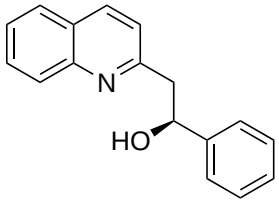

30

88% yield
53% ee

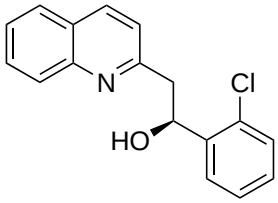

31

n/a% yield
62% ee

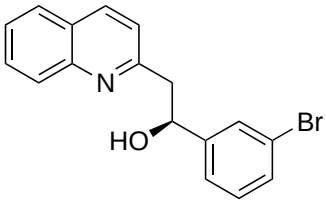

32

n/a% yield
52% ee

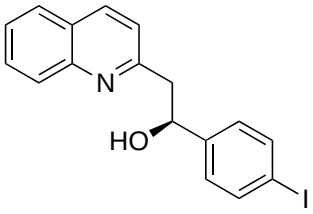

33

n/a% yield
59% ee

Scheme 135*: Substrate scope of alkenyl-substituted quinolines in catalytic asymmetric borylation*

All yields quoted are isolated after column chromatography. Enantiomeric excesses were determined by chiral UHPLC.

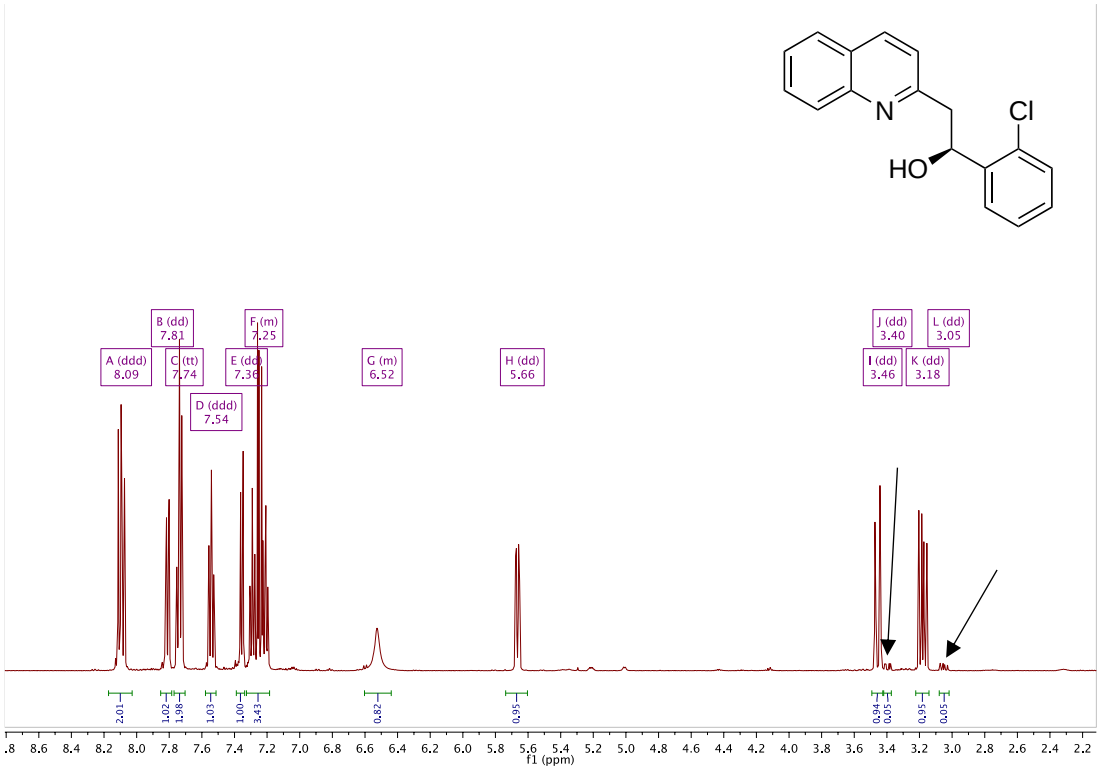

***Figure 25**: [1]H NMR of product **31**, showing presence of a suspected regioisomer*

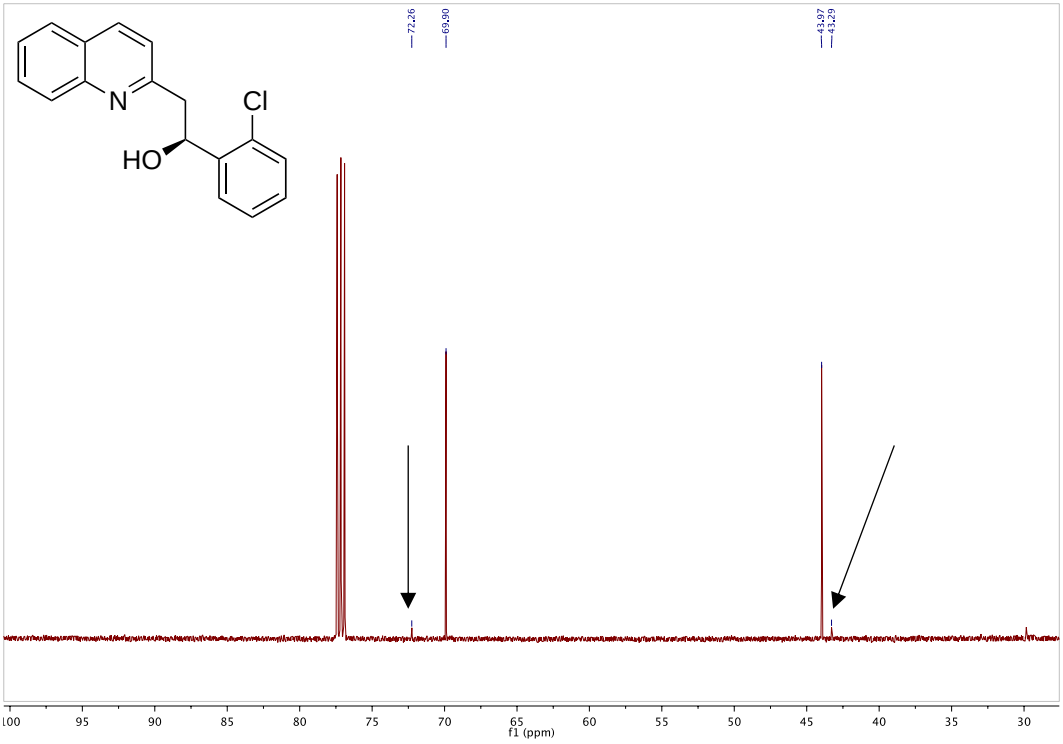

***Figure 26**: [13]C NMR of product **31**, showing presence of a suspected regioisomer*

The compatibility of styryl-pyridine substrates was probed (**Scheme 136**). Unfortunately, the pyridine product **34** also appears to be a mixture of regioisomers by NMR spectral analysis. The enantioselectivity of the product was also poor, with an ee of only 9% achieved. An initial comparison between pyridyl product **34** and the quinoline product **30** (**Scheme 136**) would suggest that sterically larger heteroaryl groups are required for higher enantioselectivities, however further work is required to gather more evidence to support this observation.

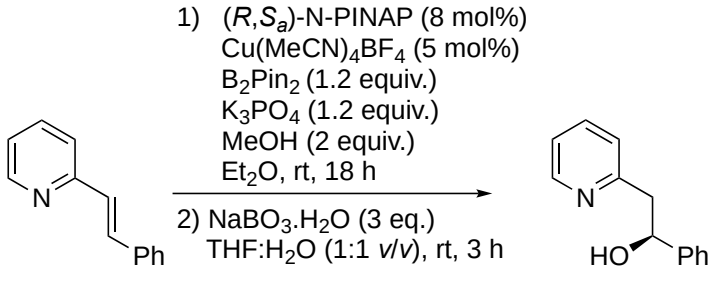

34

n/a% yield
9% ee

***Scheme 136**: Application of styryl-pyridine substrate in catalytic asymmetric borylation*

A catalytic cycle for the asymmetric formation of the benzoxazole type products is proposed below (**Scheme 137**), based on the worked reported by Meng.[20] The Cu(I)-Bpin species is generated from the reaction of Cu(I)-OMe and $B_2(pin)_2$. The Cu(I)-Bpin intermediate undergoes *syn*-addition with the benzoxazole substrate to give the organocopper intermediate **35**. The organocopper intermediate reacts with methanol to furnish the enantioenriched organoboron product and regenerates the Cu(I)-OMe species which can re-enter the catalytic cycle.

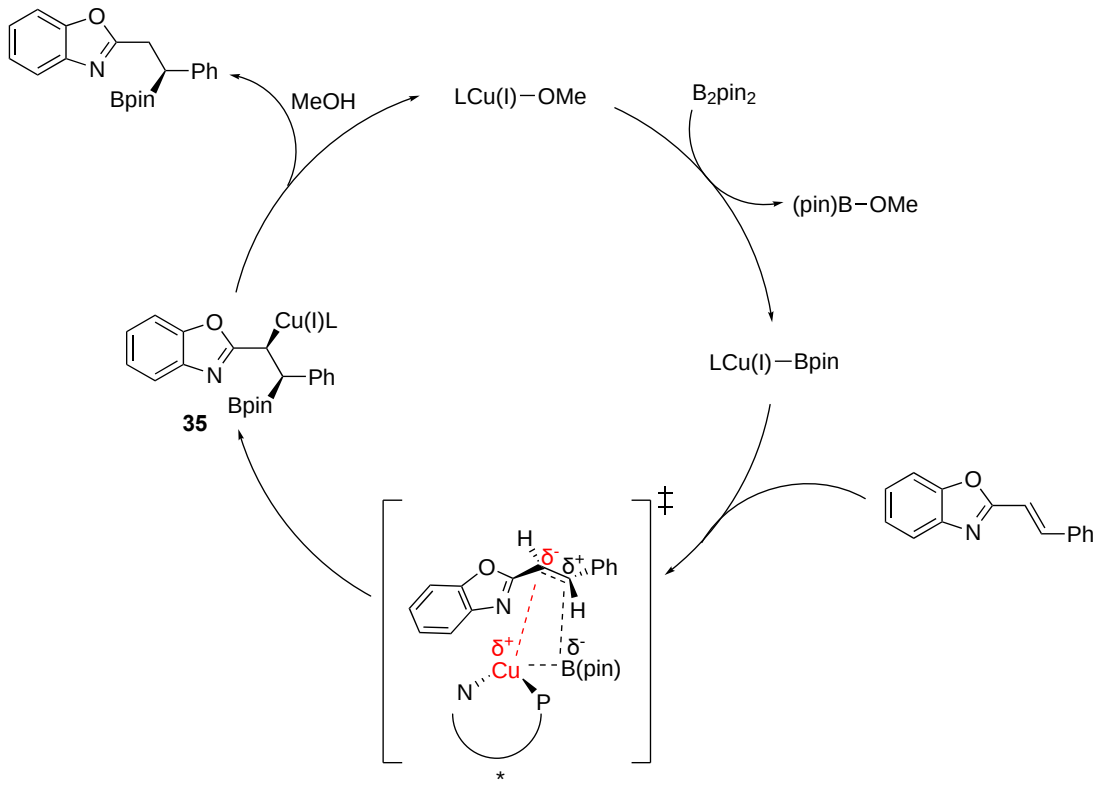

***Scheme 137**: Proposed catalytic cycle for the formation of enantioenriched benzoxazole products*

Conclusions and Future Work

In conclusion, a novel protocol was developed for the successful catalytic asymmetric borylation of alkenyl-substituted benzoxazoles (**Scheme 131**). These novel products were isolated as the corresponding alcohols, as isolation of the organoboron compounds proved unsuccessful by column chromatography. The protocol was also applied to quinolone- and pyridine-based substrates. Further expansion of the substrate scope beyond the twelve preliminary examples was not possible during the current study due to time constraints.

Further expansion of substrate scope to include more electronically varied alkenyl-substituted benzoxazoles would serve to demonstrate the robustness of the methodology. The substrate scope could be further broadened to include aliphatic groups on the alkene moiety as well as extended to benzimidazoles and benzothiazoles (**Scheme 138**). The current substrate scope was focussed on halogenated substituents as they serve as valuable synthetic handles for subsequent cross coupling reactions and other synthetic transformations.

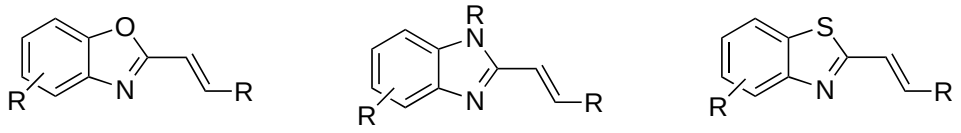

***Scheme 138**: Candidates for further extending the substrate scope of the novel methodology*

In 2015, Liang reported a $BF_3.Et_2O$ mediated C_{sp}-C_{sp2} cleavage of 2-propynolphenols towards accessing C2-alkenylated benzoxazoles of type **36** (**Scheme 139**).[32] These tri-substituted alkenyl substrates could be employed in the protocol developed in this project to probe the potential for the asymmetric formation of products bearing quaternary stereocentres.

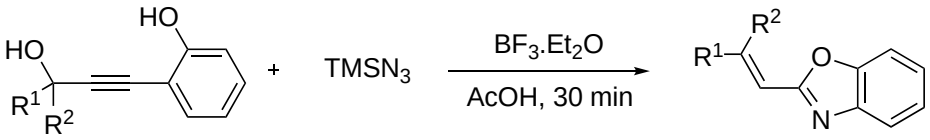

36

Scheme 139*: Synthesis of substrates to give quaternary chiral centres in asymmetric borylation protocol*

Further derivatisation of the useful organoboron intermediate in future work would demonstrate the versatility of the synthetic handle. Potential future transformations that would warrant investigation include stereoretentive cross-couplings, fluorinations, alkynylations, and aminations (**Scheme 140**).[4,33,34,8] Examining the enantiomeric excess of these products would be important due to the nature of the acidic benzylic stereocentre, which could potentially racemise under the reaction conditions described in **Scheme 140**.

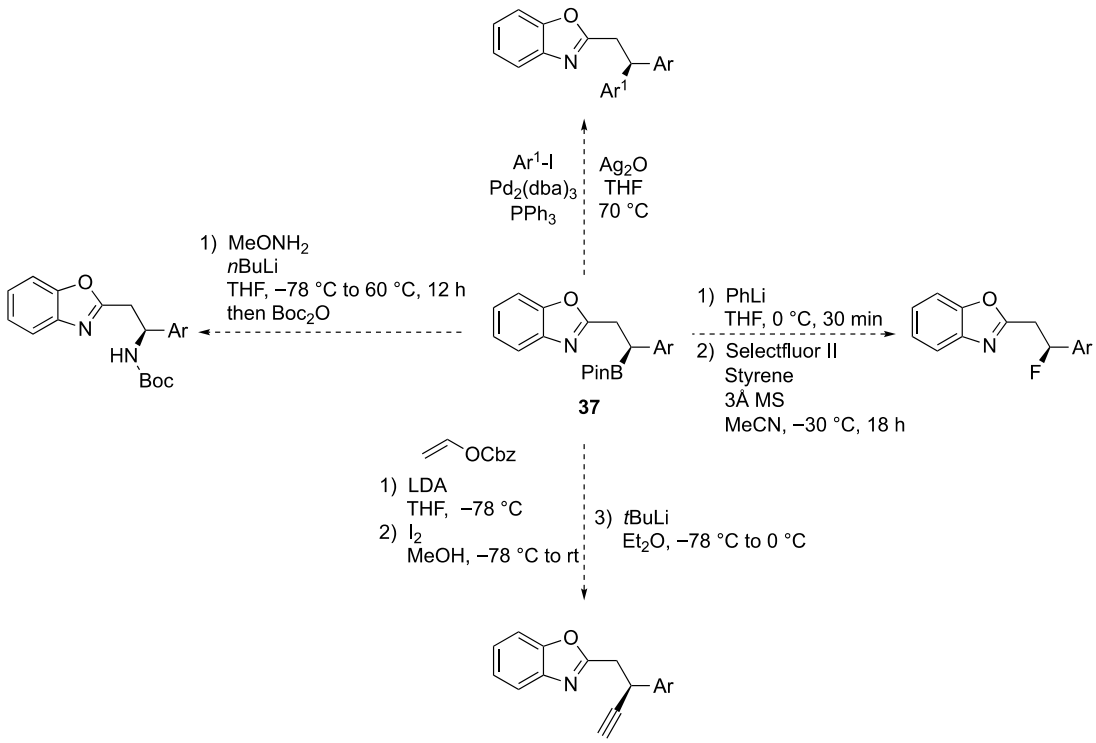

Scheme 140**: Future possible transformations of novel organoboron intermediate **37

Experimental

All chemicals were purchased from Sigma-Aldrich, Acros, or Fluorochem unless otherwise stated. Dry solvents were obtained from a Puresol Grubbs solvent system and were dried using 3Å molecular sieves unless otherwise stated. All of the solvents were reagent grade and were used as received. Column chromatography was performed on Davilsil LC60A 40-63 micron silica gel. Thin-layer chromatography (TLC) was performed on aluminium-backed sheets purchased from Merck pre-coated with silica 60 F254. All reactions were performed under an atmosphere of N_2 and in flame-dried glassware unless otherwise stated. The Varian 300 MHz, 400 MHz and 500 MHz NMR instruments were used for the recording of ^{1}H NMR and ^{13}C NMR spectra. Deuterated chloroform was used as the solvent for recording NMR spectra unless otherwise state, the chemical shifts (δ) are given in parts per million and the coupling constants (*J*) are given in absolute values expressed in Hz. Supercritical fluid chromatography (SFC) was performed on a Waters Acquity UPC2 ® instrument with Chiralpak ® IA3, IB3, IC3 and ID3 columns. UHPLC was performed using Shimadzu Nexera series instrument with CHIRALCEL®OD-3 and O*J*-3 columns (4.6 mm Ø x 250 mm, Daicel Chemical Industries). Optical rotation measurements were recorded using a Schmidt-Haensch Unipol L2000 polarimeter at 589 nm and are quoted in units of deg dm^{-1} cm^3 g^{-1} (concentration c is given in g/100 mL). Bis(pinacolato)diboron was recrystallised from hot pentane and was stored under vacuum prior to use. CuCl was purified prior to use by dissolving in concentrated aqueous HCl, followed by precipitation with H_2O. The filtered solid was washed with ethanol and diethyl ether before storing under vacuum for 16 h prior to use. All bases used were stored under vacuum prior to their use in catalysis.

General procedure 1 for the synthesis of alkenyl-benzoxazole substrates (GP1)[28]

A 50 mL round-bottomed flask was charged with 2-methylbenzoxazole (0.59 mL, 5 mmol, 1.equiv.) followed by DMSO (5 mL) and was stirred at room temperature. The corresponding arylaldehyde (5 mmol, 1.equiv.) was added, followed by 50% (*w*/*v*) aqueous NaOH solution (1.25 mL, 15.63 mmol, 15.63 equiv.). The reaction was stirred at room temperature for 1-3 h. The reaction mixture was poured into H_2O (200 mL) and was cooled to 4 °C for 18 h. The resulting precipitate was isolated *via* vacuum filtration and was dried under vacuum. The crude solid was recrystallised from hot ethanol to yield the title compound, which was isolated *via* vacuum filtration.

(*E*)-2-Styrylbenzo[*d*]oxazole[35]

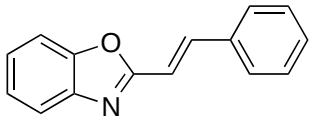

A 250 mL round-bottomed flask was charged with 2-methylbenzoxazole (2.66 g, 2.37 mL, 20 mmol, 1.equiv.) followed by DMSO (20 mL) and was stirred at room temperature. Benzaldehyde (2.12 g, 2.03 mL, 20 mmol) was added, followed by 50% (*w*/*v*) NaOH solution (6.25 mL). The reaction was stirred at room temperature for 2h. The reaction mixture was poured into H_2O (1000 mL) and was chilled at 4 °C for 18h. The resulting precipitate was isolated *via* vacuum filtration and was dried under vacuum. The crude solid was recrystallised from hot ethanol to yield the title compound, which was isolated *via* vacuum filtration as a white solid (1.10 g, 25% yield).**^{1}H NMR** (500 MHz, $CDCl_3$) δ 7.80 (d, *J* = 16.4 Hz, 1H), 7.75 – 7.70 (m, 1H), 7.63 – 7.57 (m, 2H), 7.55 – 7.50 (m, 1H), 7.46 – 7.31 (m, 5H), 7.08 (d, *J* = 16.4 Hz, 1H);**^{13}C NMR** (126 MHz, $CDCl_3$) δ 162.9, 150.5, 142.3, 139.6, 135.3, 129.9, 129.1, 127.7, 125.3, 124.6, 120.0, 114.1, 110.4. All characterisation data are in agreement with reported literature data.

(*E*)-2-(2-Bromostyryl)benzo[*d*]oxazole

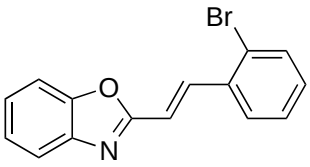

The title compound was synthesised *via* **GP1** and was isolated as a white solid (637 mg, 42% yield). **Melting point:** 119 – 120 °C; **^{1}H NMR** (500 MHz, $CDCl_3$) δ 8.12 (d, *J* = 16.3 Hz, 1H), 7.76 – 7.50 (m, 3H), 7.40 -7.27 (m, 3H), 7.19 (t, *J* = 7.7 Hz, 1H), 7.02 (d, *J* = 16.3 Hz, 1H); **^{13}C NMR** (126 MHz, $CDCl_3$) δ 162.3, 150.5, 142.3, 137.7, 135.1, 133.5, 130.8, 127.9, 127.3, 125.6, 125.1, 124.7, 120.1, 116.7, 110.6; **IR** ν(cm^{-1}): 1814, 1637, 1594, 1560, 760, 544; **HRMS**: (ESI-TOF) calculated for $C_{15}H_{10}BrNO$ $[M + H]^+$ 300.0021 found 300.0019.

(*E*)-2-(2-Methylstyryl)benzo[*d*]oxazole[35]

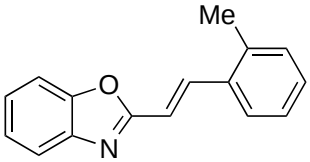

The title compound was received as a gift from Dr. Balaji Rokade. The synthesis of the title compound is reported using **GP1**. **^{1}H NMR** (500 MHz, $CDCl_3$) δ 8.06 (d, *J* = 16.2 Hz, 1H), 7.77 – 7.70 (m, 1H), 7.66 (dd, *J* = 7.2, 1.9 Hz, 1H), 7.57 – 7.51 (m, 1H), 7.37 – 7.31 (m, 2H), 7.31 – 7.21 (m, 3H), 7.01 (d, *J* = 16.2 Hz, 1H), 2.52 (s, 3H); **^{13}C NMR** (126 MHz, $CDCl_3$) δ 162.9, 150.4, 142.2, 137.2, 137.04, 134.1, 130.8, 129.6, 126.5, 125.9, 125.2, 124.5, 119.9, 115.0, , 110.3, 19.9. All characterisation data are in agreement with reported literature data.

(*E*)-2-(Ferroceneyl)vinyl)benzo[*d*]oxazole

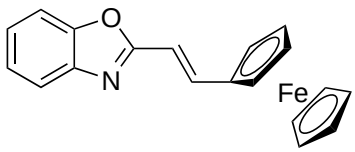

The title compound was received as a gift from Dr. Balaji Rokade. The synthesis of the title compound is reported using **GP1**. **Melting point:** 151 – 153; **^{1}H NMR** (500 MHz, $CDCl_3$) δ 7.72 – 7.61 (m, 2H), 7.53 - 7.47 (m, 1H), 7.36 – 7.27 (m, 2H), 6.66 (d, *J* = 16.0 Hz, 1H), 4.60 – 4.40 (m, 4H), 4.18 (s, 5H);**^{13}C NMR** (126 MHz, $CDCl_3$) δ 163.4, 150.4, 142.5, 140.36, 124.8, 124.5, 119.6, 110.8, 110.2, 80.1, 70.8, 69.8, 68.2; **IR** ν(cm^{-1}): 1780, 1683, 1595, 1449, 762, 595. °C; **HRMS**: (ESI-TOF) calculated for $C_{19}H_{15}FeNO$ $[M + H]^+$ 329.0492 found 329.0498.

(*E*)-2-(2-(Thiophen-2-yl)vinyl)benzo[*d*]oxazole[35]

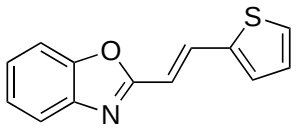

The title compound was synthesised *via* **GP1** and was isolated as a yellow solid (572 mg, 50% yield). **^{1}H NMR** (500 MHz, $CDCl_3$) δ 7.85 (d, *J* = 16.0 Hz, 1H), 7.73 – 7.64 (m, 1H), 7.51 – 7.44 (m, 1H), 7.35 – 7.26 (m, 3H), 7.26 – 7.20 (m, 1H), 7.03 (dd, *J* = 5.1, 3.6 Hz, 1H), 6.84 (d, *J* = 16.0 Hz, 1H);**^{13}C NMR** (126 MHz, $CDCl_3$) δ 162.5, 150.4, 142.3, 140.5, 132.0, 129.7, 128.1, 127.7, 125.1, 124.5, 119.8, 112.9, 110.3. All characterisation data are in agreement with reported literature data.

(*E*)-2-(2-(Naphthalen-1-yl)vinyl)benzo[*d*]oxazole[36]

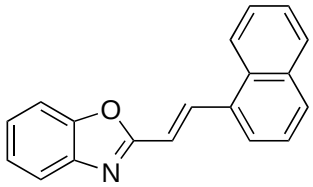

The title compound was synthesised *via* **GP1** and was isolated as a yellow solid (654 mg, 48% yield).**^{1}H NMR** (500 MHz, $CDCl_3$) δ 8.61 (d, *J* = 16.1 Hz, 1H), 8.30 (dd, *J* = 8.4, 1.2 Hz, 1H), 7.89 (dd, *J* = 8.4, 1.7 Hz, 2H), 7.85 (d, *J* = 7.2, 1H), 7.81 – 7.75 (m, 1H), 7.63 – 7.49 (m, 4H), 7.41 – 7.32 (m, 2H), 7.18 (d, *J* = 16.1 Hz, 1H); **^{13}C NMR** (126 MHz, $CDCl_3$) δ 162.9, 150.5, 142.3, 136.3, 133.8, 132.5, 131.4, 130.2, 128.9, 126.9, 126.3, 125.7, 125.4, 124.7, 124.5, 123.5, 120.1, 116.5, 110.5 . All characterisation data are in agreement with reported literature data.

(*E*)-2-(3-Bromostyryl)benzo[*d*]oxazole

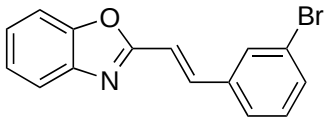

The title compound was synthesised *via* **GP1** and was isolated as a white solid (413 mg, 28% yield). **Melting point:** 116 – 118 °C; **^{1}H NMR** (400 MHz, $CDCl_3$) δ 7.76 – 7.64 (m, 3H), 7.56 – 7.46 (m, 3H), 7.38 – 7.30 (m, 2H), 7.30 – 7.24 (m, 1H), 7.05 (d, *J* = 16.3 Hz, 1H); **^{13}C NMR** (101 MHz, $CDCl_3$) δ 162.3, 150.6, 142.2, 137.8, 137.4, 132.6, 130.6, 130.5, 126.2, 125.6, 124.7, 123.2, 120.2, 115.5, 110.5; **IR** ν(cm^{-1}): 1808, 1767, 1586, 1540, 778, 574; **HRMS**: (ESI-TOF) calculated for $C_{15}H_{10}BrNO_2$ $[M + H]^+$ 300.0019 found 300.0020**.**

(*E*)-2-(4-Chlorostyryl)benzo[*d*]oxazole[36]

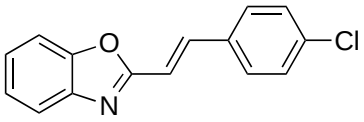

The title compound was synthesised *via* **GP1** and was isolated as a white solid (682 mg, 53% yield). **^{1}H NMR** (500 MHz, $CDCl_3$) δ 7.75 – 7.68 (m, 2H), 7.54 – 7.47 (m, 3H), 7.41 – 7.30 (m, 4H), 7.03 (d, *J* = 16.3 Hz, 1H); **^{13}C NMR** (126 MHz, $CDCl_3$) δ 162.4, 150.4, 142.2, 137.9, 135.6, 133.6, 129.2, 128.7, 128.6, 125.4, 124.6, 112.0, 114.5, 110.3. All characterisation data are in agreement with reported literature data.

General procedure 2 for the synthesis of alkenyl-quinoline substrates (GP2)[31]

A 25 mL Schlenk flask was flame-dried and backfilled under a nitrogen atmosphere. $Fe(OAc)_2$ (21 mg, 0.12 mmol, 10 mol%) was added followed by anhydrous toluene (6 mL). 2-Methylquinoline (0.33 mL, 2.4 mmol, 0.83 equiv.) was added followed by the corresponding arylaldehyde (2.88 mmol, 1 equiv.) and trifluoroacetic acid (18 µL, 0.24 mmol, 20 mol%). The reaction was stirred at 100 °C for 18 h and was then concentrated *in vacuo* in a fumehood to yield the crude reaction mixture. The reaction mixture was purified using flash column chromatography with silica gel to yield the target compound.

(*E*)-2-Styrylquinoline[37]

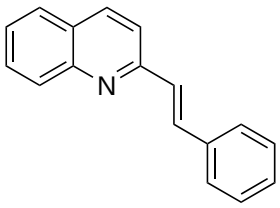

The title compound was synthesised *via* **GP2** and was isolated by column chromatography as a white solid (342 mg, 61% yield). $\mathbf{R_f}$ = 0.38 in 10% EtOAc/cyclohexane; **^{1}H NMR** (500 MHz, $CDCl_3$) δ 8.14 – 8.06 (m, 2H), 7.76 (d, *J* = 8.2, 1H), 7.74 – 7.61 (m, 5H), 7.51 – 7.47 (m, 1H), 7.44 – 7.38 (m, 3H), 7.36 – 7.30 (m, 1H); **^{13}C NMR** (126 MHz, $CDCl_3$) δ 156.1, 148.3, 136.6, 136.4, 134.52, 129.8, 129.3, 129.1, 128.9, 128.7, 127.6, 127.4, 127.4, 126.2, 119.3. All characterisation data are in agreement with reported literature data.

(*E*)-2-(2-Chlorostyryl)quinoline[37]

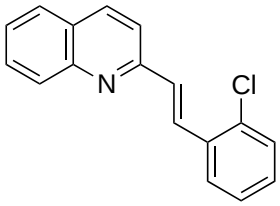

The title compound was synthesised *via* **GP2** and was isolated by column chromatography as a white solid (506 mg, 80% yield). $\mathbf{R_f}$ = 0.28 in 10% EtOAc/cyclohexane; **^{1}H NMR** (500 MHz, $CDCl_3$) δ 8.13 – 7.98 (m, 3H), 7.84 – 7.65 (m, 4H), 7.51 – 7.45 (m, 1H), 7.43 – 7.34 (m, 2H), 7.31 – 7.19 (m, 2H); **^{13}C NMR** (126 MHz, $CDCl_3$) δ 155.8, 148.3, 136.4, 134.7, 134.1, 131.8, 130.3, 130.0, 129.8, 129.5, 129.4, 127.6, 127.5, 127.1, 127.0, 126.5, 119.0. All characterisation data are in agreement with reported literature data.

(*E*)-2-(3-Bromostyryl)quinoline[36]

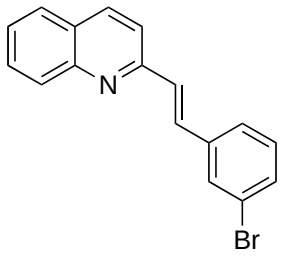

The title compound was synthesised *via* **GP2** and was isolated by column chromatography as a white solid (396 mg, 51% yield). $\mathbf{R_f}$ = 0.28 in 5% EtOAc/cyclohexane; **^{1}H NMR** (400 MHz, $CDCl_3$) δ 8.11 – 8.04 (m, 2H), 7.79 – 7.73 (m, 2H), 7.69 (ddd, *J* = 8.4, 6.9, 1.5 Hz, 1H), 7.62 – 7.54 (m, 2H), 7.53 – 7.45 (m, 2H), 7.41 (ddd, *J* = 7.9, 2.0, 1.0 Hz, 1H), 7.35 (d, *J* = 16.3 Hz, 1H), 7.22 (t, *J* = 7.9 Hz, 1H);**^{13}C NMR** (101 MHz, $CDCl_3$) δ 155.4, 148.3, 138.8, 136.5, 132.7, 131.4, 130.4, 130.1, 129.9, 129.4, 127.6, 127.5, 126.5, 125.9, 123.1, 119.5. All characterisation data are in agreement with reported literature data.

(*E*)-2-(4-Iodostyryl)quinoline[36]

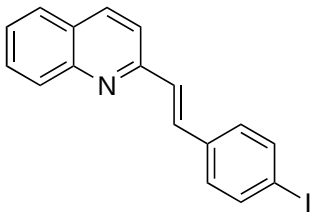

The title compound was synthesised *via* **GP2** and was isolated by column chromatography as a white solid (777 mg, 90% yield). $\mathbf{R_f}$ = 0.27 in 5% EtOAc/cyclohexane; **^{1}H NMR** (500 MHz, $CDCl_3$) δ 8.12 (d, *J* = 8.6 Hz, 1H), 8.07 (d, *J* = 8.6 Hz, 1H), 7.81 – 7.68 (m, 4H), 7.65 – 7.57 (m, 2H), 7.53 – 7.48 (m, 1H), 7.42 – 7.33 (m, 3H);**^{13}C NMR** (126 MHz, $CDCl_3$) δ 155.7, 148.4, 138.1, 136.6, 136.2, 133.3, 129.9, 129.4, 129.0, 127.7, 127.6, 126.5, 119.5, 94.3. All characterisation data are in agreement with reported literature data.

(*E*)-2-Styrylpyridine[38]

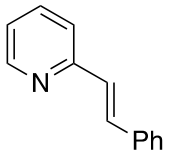

$PdCl_2dppf.CH_2Cl_2$ (40 mg, 0.05 mmol, 3 mol%) was added to a flame-dried Schlenk flask under N_2. DME (10 mL) was added, followed by 2-bromopyridine (237 mg, 0.14 mL, 1.5 mmol, 1 equiv.) and *trans*-2-phenylvinylboronic acid (444 mg, 3 mmol, 2 equiv.). An aqueous solution of K_3PO_4 (2 ml, 3 M, 6 mmol, 4 equiv.) was added and the reaction was heated to 80 °C for 17 h. The reaction mixture was filtered through celite and was concentrated *in vacuo*. The crude reaction mixture was purified by flash column chromatography (5% to 20% EtOAc/cyclohexane) to afford the product as an off white solid (217 mg, 80%). $\mathbf{R_f}$ = 0.3 in 20% EtOAc/cyclohexane; **^{1}H NMR** (400 MHz, $CDCl_3$) δ 8.60 (ddd, *J* = 4.8, 1.9, 0.9 Hz, 1H), 7.69 – 7.54 (m, 5H), 7.43 – 7.33 (m, 4H), 7.32 – 7.23 (m, 1H), 7.22 – 7.09 (m, 2H); **^{13}C NMR** (101 MHz, $CDCl_3$) δ 155.7, 149.8, 136.8, 136.6, 132.8, 128.8, 128.4, 128.1, 127.2, 122.20, 122.16. All characterisation data are in agreement with reported literature data.

Asymmetric catalysis -General procedure 3 (GP3)

The enantioenriched products were synthesised as per the following procedure. (*R*,S_a)-N-PINAP (8.96 mg, 0.016 mmol, 8 mol%) and $Cu(MeCN)_4BF_4$ (3.14 mg, 0.01 mmol, 5 mol%) were added to a flame-dried 10 mL Schlenk flask under a nitrogen atmosphere. Anhydrous toluene (1 mL) was added and the reaction was stirred for 20 min at room temperature. B_2Pin_2 (61 mg, 0.24 mmol, 1.2 equiv.) was added, followed by K_3PO_4 (51 mg, 0.24 mmol, 1.2 equiv.). Substrate (0.2 mmol, 1 equiv.) was added followed by anhydrous toluene (1 mL). Anhydrous methanol (16 µL, 0.4 mmol, 2 equiv.) was added and the reaction was stirred at room temperature for 1 h. The reaction mixture was filtered through a small pad of Celite® using CH_2Cl_2 and was concentrated *in vacuo*.

The reaction mixture was transferred into a screw-cap vial using THF (1 mL) and sodium perborate monohydrate (60 mg, 0.6 mmol, 3 equiv.) was added. H_2O (1 mL) was added and the reaction was stirred vigorously for 2 h. The reaction mixture was diluted with H_2O (5 mL) and was transferred to a separatory funnel. The screw-cap vial was washed with CH_2Cl_2 (5 mL) and the organic washings were transferred to the separatory funnel. The organic phase was separated and the aqueous phase was extracted with CH_2Cl_2 (2 x 5mL). The combined organic phases were dried using sodium sulfate, was filtered and concentrated *in vacuo*. The crude product was purified by flash column chromatography (5% EtOAc/cyclohexane to 30% EtOAc/cyclohexane) to afford the product.

(*R*)-2-(Benzo[*d*]oxazol-2-yl)-1-phenylethan-1-ol **22**

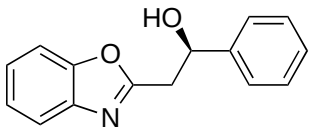

The title compound was synthesised as per general procedure 3 (**GP3**) and was isolated as a white crystalline solid (42 mg, 88% yield) after purification by column chromatography on silica gel. **Melting point:** 167 – 169 °C; $\mathbf{R_f}$ = 0.33 in 30% EtOAc/cyclohexane; **^{1}H NMR** (400 MHz, $CDCl_3$) δ 7.73 – 7.65 (m, 1H), 7.54 – 7.44 (m, 3H), 7.43 – 7.29 (m, 5H), 5.43 – 5.28 (m, 1H), 3.90 (dd, *J* = 6.1, 3.2 Hz, 1H), 3.38 – 3.25 (m, 2H); **^{13}C NMR** (101 MHz, $CDCl_3$) δ 164.9, 150.7, 142.6, 141.0, 128.80, 128.1, 125.9, 125.0, 124.5, 119.8, 110.6, 71.4, 38.2; **IR** ν(cm^{-1}): 3252, 3054, 3026, 1609, 1565, 759, 543; **[α]^{20}D** = +5.19 (c = 0.1, $CHCl_3$); **HRMS**: (ESI-TOF) calculated for $C_{15}H_{13}NO_2$ $[M + H]^+$ 240.1019 found 240.1022.

The enantioselectivity (53% ee) was determined by chiral UHPLC analysis of the title compound [CHIRALCEL®OD-3 column, 4.6 mm Ø x 250 mm, Daicel Chemical Industries], heptane/2-propanol = 97:3, 1.0 mL/min, 40 °C column temperature, 190 nm UV. Retention time = 14.21 min (*S*), 16.15 min (*R*).

(*R*)-2-(Benzo[*d*]oxazol-2-yl)-1-(2-bromophenyl)ethan-1-ol **23**

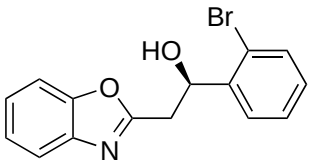

The title compound was synthesised as per general procedure 3 (**GP3**) and was isolated as a white crystalline solid (53 mg, 83% yield) after purification by column chromatography on silica gel. **Melting point:** 103 – 105 °C; $\mathbf{R_f}$ = 0.45 in 30% EtOAc/cyclohexane; **^{1}H NMR** (400 MHz, $CDCl_3$) δ 7.72 (t, *J* = 7.7 Hz, 2H), 7.61 – 7.45 (m, 2H), 7.44 – 7.29 (m, 3H), 7.18 (t, *J* = 7.7 Hz, 1H), 5.66 (d, *J* = 9.5 Hz, 1H), 4.28 –

4.21 (m, 1H), 3.54 – 3.41 (m, 1H), 3.14 (dd, *J* = 16.4, 9.6 Hz, 1H); **^{13}C NMR** (101 MHz, $CDCl_3$) δ 164.8, 150.7, 141.6, 140.9, 132.9, 129.4, 128.1, 127.5, 125.1, 124.6, 121.7, 119.8, 110.7, 70.2, 36.4; **IR** ν(cm^{-1}): 3263, 3063, 2918, 1610, 1572, 760, 692; **[α]^{20}D** = +6.10 (c = 0.25, $CHCl_3$); **HRMS**: (ESI-TOF) calculated for $C_{15}H_{12}BrNO_2$ $[M + H]^+$ 318.0128 found 318.0128.

The enantioselectivity (76% ee) was determined by chiral UHPLC analysis of the title compound [CHIRALCEL®OD-3 column, 4.6 mm Ø x 250 mm, Daicel Chemical Industries], heptane/2-propanol = 97:3, 1.0 mL/min, 40 °C column temperature, 190 nm UV. Retention time = 9.32 min (*S*), 10.77 min (*R*).

(*R*)-2-(Benzo[*d*]oxazol-2-yl)-1-(*o*-tolyl)ethan-1-ol **24**

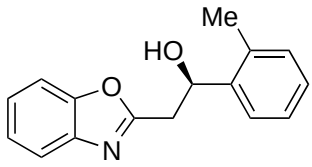

The title compound was synthesised as per general procedure 3 (**GP3**) and was isolated as a white crystalline solid (32 mg, 63% yield) after purification by column chromatography on silica gel. **Melting point:** 107 – 109 °C; **R_f** = 0.40 in 30% EtOAc/cyclohexane; **^{1}H NMR** (500 MHz, $CDCl_3$) δ 7.74 – 7.68 (m, 1H), 7.62 (dd, *J* = 7.7, 1.5 Hz, 1H), 7.55 – 7.49 (m, 1H), 7.37 – 7.31 (m, 2H), 7.28 (dd, *J* = 7.4, 1.5 Hz, 1H), 7.23 (td, *J* = 7.4, 1.5 Hz, 1H), 7.20 – 7.15 (m, 1H), 5.58 (dt, *J* = 8.8, 3.4 Hz, 1H), 3.74 (dd, *J* = 6.5, 3.1 Hz, 1H), 3.33 – 3.21 (m, 2H), 2.42 (s, 3H); **^{13}C NMR** (126 MHz, $CDCl_3$) δ 165.1, 150.7, 141.0, 140.6, 134.5, 130.7, 127.9, 126.7, 125.4, 125.0, 124.6, 119.8, 110.7, 68.0, 37.0, 19.2; **IR** ν(cm^{-1}): 3285, 3053, 3025, 1608, 1562, 796, 552; **[α]^{20}D** = +4.87 (c = 0.1, $CHCl_3$) **HRMS**: (ESI-TOF) calculated for $C_{16}H_{15}NO_2$ $[M + H]^+$ 254.1176 found 254.1179.

The enantioselectivity (73% ee) was determined by chiral UHPLC analysis of the title compound [CHIRALCEL®OD-3 column, 4.6 mm Ø x 250 mm, Daicel Chemical Industries], heptane/2-propanol = 98:2, 1.0 mL/min, 40 °C column temperature, 190 nm UV). Retention time = 16.05 min (*S*), 17.13 min (*R*).

(*R*)-2-(Benzo[*d*]oxazol-2-yl)-1-(3-bromophenyl)ethan-1-ol **25**

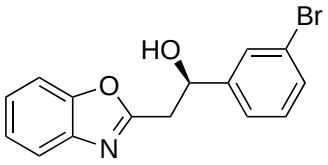

The title compound was synthesised as per general procedure 3 (**GP3**) and was isolated as a white crystalline solid (45 mg, 71% yield) after purification by column chromatography on silica gel. **Melting point:** 119 – 121 °C; $\mathbf{R_f}$ = 0.44 in 30% EtOAc/cyclohexane; **^{1}H NMR** (400 MHz, $CDCl_3$) δ 7.72 – 7.62 (m, 2H), 7.54 – 7.46 (m, 1H), 7.46 – 7.41 (m, 1H), 7.40 – 7.29 (m, 3H), 7.27 – 7.20 (m, 1H), 5.37 – 5.27 (m, 1H), 4.21 – 4.10 (m, 1H), 3.33 – 3.22 (m, 2H);**^{13}C NMR** (101 MHz, $CDCl_3$) δ 164.6, 150.6, 144.9, 140.8, 131.2, 130.4, 129.1, 125.2, 124.7, 124.5, 122.9, 119.8, 110.7, 70.5, 38.1; **IR** ν(cm^{-1}): 3252, 3053, 2923, 1609, 1592, 760, 698; **$[\alpha]^{20}D$** = +7.76 (c = 0.26, $CHCl_3$); **HRMS**: (ESI-TOF) calculated for $C_{15}H_{12}BrNO_2$ $[M + H]^+$ 318.0124 found 318.0126.

The enantioselectivity (69% ee) was determined by chiral UHPLC analysis of the title compound [CHIRALCEL®OD-3 column, 4.6 mm Ø x 250 mm, Daicel Chemical Industries], heptane/2-propanol = 98:2, 1.0 mL/min, 40 °C column temperature, 190 nm UV). Retention time = 20.98 min (*S*), 22.52 min (*R*).

(*R*)-2-(Benzo[*d*]oxazol-2-yl)-1-(4-chlorophenyl)ethan-1-ol **26**

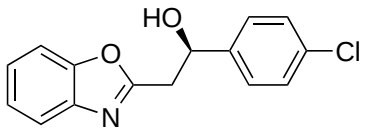

The title compound was synthesised as per general procedure 3 (**GP3**) and was isolated as a white crystalline solid (47 mg, 86% yield) after purification by column chromatography on silica gel. **Melting point:** 171 – 173 °C; $\mathbf{R_f}$ = 0.32 in 30% EtOAc/cyclohexane; **^{1}H NMR** (400 MHz, $CDCl_3$) δ 7.71 – 7.64 (m, 1H), 7.53 – 7.48 (m, 1H), 7.43 – 7.30 (m, 6H), 5.36 – 5.30 (m, 1H), 4.11 – 4.04 (m, 1H), 3.28 (d, *J* = 6.4 Hz, 2H); **^{13}C NMR** (101 MHz, $CDCl_3$) δ 164.6, 150.6, 141.1, 140.8, 133.8, 128.9, 127.3, 125.1, 124.6, 119.8, 110.7, 70.6, 38.1; **IR** ν(cm^{-1}): 3251, 3097, 3057, 1607, 1565, 760, 540; **$[\alpha]^{20}$D** = +5.55 (c = 0.16, $CHCl_3$); **HRMS**: (ESI-TOF) calculated for $C_{15}H_{12}ClNO_2$ $[M + H]^+$ 274.0629 found 274.0632.

The enantioselectivity (74% ee) was determined by chiral UHPLC analysis of the title compound [CHIRALCEL®OD-3 column, 4.6 mm Ø x 250 mm, Daicel Chemical Industries], heptane/2-propanol = 97:3, 1.0 mL/min, 40 °C column temperature, 190 nm UV). Retention time = 15.93 min (*S*), 17.17 min (*R*).

(*R*)-2-(Benzo[*d*]oxazol-2-yl)-1-(thiophen-2-yl)ethan-1-ol **27**

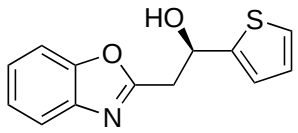

The title compound was synthesised as per general procedure 3 (**GP3**) and was isolated as a yellow solid (29 mg, 59% yield) after purification by column chromatography on silica gel. **Melting point:** 118 – 120 °C; $\mathbf{R_f}$ = 0.30 in 30% EtOAc/cyclohexane; **^{1}H NMR** (500 MHz, $CDCl_3$) δ 7.74 – 7.65 (m, 1H), 7.58 – 7.47 (m, 1H), 7.36 – 7.31 (m, 2H), 7.29 – 7.26 (m, 1H), 7.07 – 7.04 (m, 1H), 7.00 – 6.96 (dd, *J* = 5.0, 3.5 Hz, 1H), 5.66 – 5.56 (m, 1H), 4.16 -4.12 (m, 1H), 3.53 – 3.37 (m, 2H); **^{13}C NMR** (126 MHz, $CDCl_3$) δ 164.3, 150.6, 146.3, 140.9, 126.9, 125.1, 125.1, 124.6, 124.0, 119.9, 110.7, 67.6, 38.1; **IR** ν(cm^{-1}): 3221, 3069, 2922, 1610, 1566, 780, 590; **[α]^{20}D** = +3.63 (c = 0.19, $CHCl_3$); **HRMS**: (ESI-TOF) calculated for $C_{13}H_{11}NO_2S$ $[M + H]^+$ 246.0583 found 246.0584.

The enantioselectivity (75% ee) was determined by chiral UHPLC analysis of the title compound [CHIRALCEL®OD-3 column, 4.6 mm Ø x 250 mm, Daicel Chemical Industries], heptane/2-propanol = 99:1, 1.0 mL/min, 40 °C column temperature, 190 nm UV). Retention time = 39.99 min (*S*), 42.63 min (*R*).

(*R*)-2-(Benzo[*d*]oxazol-2-yl)-1-(naphthalen-1-yl)ethan-1-ol **28**

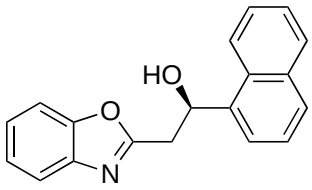

The title compound was synthesised as per general procedure 3 (**GP3**) and was isolated as an off white wax (41 mg, 71% yield) after purification by column chromatography on silica gel. $\mathbf{R_f}$ = 0.38 in 30% EtOAc/cyclohexane; **^{1}H NMR** (500 MHz, $CDCl_3$) δ 8.17 (dd, *J* = 8.6, 1.2 Hz, 1H), 7.93 – 7.88 (m, 1H), 7.85 – 7.81 (m, 2H), 7.78 – 7.72 (m, 1H), 7.59 – 7.48 (m, 4H), 7.40 – 7.32 (m, 2H), 6.17 – 6.13 (m, 1H), 3.98 – 3.95 (m, 1H), 3.53 (dd, *J* = 16.5, 3.0 Hz, 1H), 3.43 (dd, *J* = 16.5, 9.8 Hz, 1H); **^{13}C NMR** (126 MHz, $CDCl_3$) δ 165.2, 150.8, 141.1, 138.1, 134.0, 130.2, 129.2, 128.6, 126.6, 125.8, 125.7, 125.1, 124.6, 123.2, 122.9, 119.9, 110.7, 68.4, 37.6; **IR** ν(cm^{-1}): 3280, 3050, 2924, 1611, 1569, 796, 565; **[α]^{20}D** = +3.07 (c = 0.16, $CHCl_3$); **HRMS**: (ESI-TOF) calculated for $C_{19}H_{15}NO_2$ $[M + H]^+$ 290.1176 found 290.1180.

The enantioselectivity (56% ee) was determined by chiral UHPLC analysis of the title compound [CHIRALCEL®O*J*-3 column, 4.6 mm Ø x 250 mm, Daicel Chemical Industries], heptane/2-propanol = 97:3, 1.0 mL/min, 40 °C column temperature, 190 nm UV). Retention time = 27.49 min (*S*), 35.86 min (*R*).

1-Phenyl-2-(quinolin-2-yl)ethan-1-ol **30**

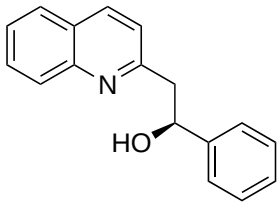

The title compound was synthesised as per general procedure 3 (**GP3**) but the reaction time was extended to 18 h. The compound was isolated as an off white solid (19 mg, 38% yield) after purification by column chromatography on silica gel. **Melting point:** 122 – 124 °C; $\mathbf{R_f}$ = 0.15 in 20% EtOAc/cyclohexane; **^{1}H NMR** (400 MHz, $CDCl_3$) δ 8.09 (t, *J* = 9.1 Hz, 2H), 7.87 – 7.66 (m, 2H), 7.42 (s, 1H), 7.42 – 7.16 (m, 4H), 6.18 (s, 1H), 5.33 (dd, *J* = 8.1, 4.1 Hz, 1H), 3.42 – 3.24 (m, 2H); **^{13}C NMR** (101 MHz, $CDCl_3$) δ 160.55, 147.04, 143.95, 136.84, 129.84, 128.73, 128.36, 127.59, 127.31, 126.87, 126.24, 125.89, 122.09, 72.97, 46.10; **IR** ν(cm^{-1}): 3196, 3055, 3040, 1615, 1598, 784, 590; **[α]^{20}D** = +18.91 (c = 0.1, $CHCl_3$); **HRMS**: (ESI-TOF) calculated for $C_{17}H_{15}NO$ $[M + H]^+$ 250.1226 found 250.1226.

The enantioselectivity (51% ee) was determined by chiral UHPLC analysis of the title compound [CHIRALCEL®OD-3 column, 4.6 mm Ø x 250 mm, Daicel Chemical Industries], heptane/2-propanol = 97:3, 1.0 mL/min, 40 °C column temperature, 190 nm UV). Retention time = 16.22 min (*S*), 21.78 min (*R*).

Racemic catalysis – General procedure 4 (GP4)

Tricyclohexylphosphine (24 mg, 0.08 mmol, 40 mol%) and CuCl (8 mg, 0.08 mmol, 40 mol%) were added to a flame-dried 10 mL Schlenk flask under a nitrogen atmosphere. Anhydrous toluene (1 mL) was added and the reaction was stirred for 20 min at room temperature. B_2Pin_2 (61 mg, 0.24 mmol, 1.2 equiv.) was added followed by K_3PO_4 (51 mg, 0.24 mmol, 1.2 equiv.). Alkenyl-substrate (0.2 mmol, 1 equiv.) was added followed by anhydrous toluene (1 mL). Anhydrous methanol (32 µL, 0.8 mmol, 4 equiv.) was added and the reaction was stirred at room temperature for 18 h. The reaction mixture was filtered through a small pad of Celite® using CH_2Cl_2 and was concentrated *in vacuo*.

The reaction mixture was transferred into a screw-cap vial using THF (1 mL) and sodium perborate monohydrate (80 mg, 0.8 mmol, 4 equiv.) was added. H_2O (1 mL) was added and the reaction was stirred vigorously for 3 h. The reaction mixture was diluted with H_2O (5 mL) and was transferred to a separatory funnel. The screw-cap vial was washed with CH_2Cl_2 (5 mL) and the organic washings were transferred to the separatory funnel. The organic phase was separated and the aqueous phase was extracted with CH_2Cl_2 (2 x 5 mL). The combined organic phases were dried using sodium sulfate, filtered and concentrated *in vacuo*. The crude product was purified by flash column chromatography (5% EtOAc/cyclohexane to 30% EtOAc/cyclohexane) to give the product.

N.B: The quality of PCy_3 ligand is very important – it is prone rapid oxidation which inhibits the reaction. The racemic reaction can also be successfully conducted using dppf (1,1'-bis(diphenylphosphino)ferrocene (20 mol%), $Cu(MeCN)_4BF_4$ (20 mol%) in Et_2O (0.1 M).

1-(2-Chlorophenyl)-2-(quinolin-2-yl)ethan-1-ol

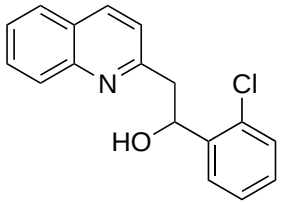

The title compound was synthesised as per general procedure 4 (**GP4**) and was isolated as a white solid (29 mg, 51% yield) after purification by column chromatography on silica gel. **Melting point:** 123 – 125 °C; $\mathbf{R_f}$ = 0.56 in 30% EtOAc/cyclohexane; **^{1}H NMR** (400 MHz, $CDCl_3$) δ 8.08 (dd, *J* = 8.5, 6.0 Hz, 2H), 7.82 – 7.69 (m, 3H), 7.56 – 7.49 (m, 1H), 7.38 – 7.16 (m, 4H), 5.66 (dd, *J* = 9.1, 2.5 Hz, 1H), n$CDCl_3$) δ 160.6, 147.1, 141.4, 137.1, 131.5, 130.0, 129.3, 128.8, 128.4, 127.8, 127.7, 127.2, 127.1, 126.4, 122.1, 69.9, 44.0; **IR** ν(cm^{-1}): 3125, 3065, 1918, 1618, 1598, 785, 558; **HRMS**: (ESI-TOF) calculated for $C_{17}H_{14}ClNO$ $[M + H]^+$ 284.0837 found 284.0838.

An asymmetric sample was prepared using general procedure 3 (**GP3**), which contained an-inseparable impurity. The presence of the enantioenriched product was confirmed by NMR and HRMS analysis. The enantioselectivity was determined by UHPLC comparison with a fully characterised racemic sample. Yield, IR, melting point and optical data for the asymmetric sample were not quoted due the inseparable product being present.

The enantioselectivity (62% ee) was determined by chiral UHPLC analysis of the title compound [CHIRALCEL®OD-3 column, 4.6 mm Ø x 250 mm, Daicel Chemical Industries], heptane/2-propanol = 97:3, 1.0 mL/min, 40 °C column temperature, 190 nm UV). Retention time = 11.39 min (*S*), 17.37 min (*R*).

1-(3-Bromophenyl)-2-(quinolin-2-yl)ethan-1-ol

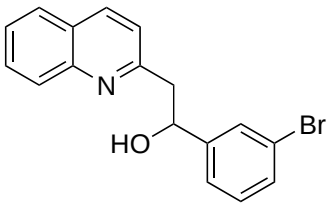

The title compound was synthesised as per general procedure 4 (**GP4**) and was isolated as a white solid (9 mg, 13% yield) after purification by column chromatography on silica gel. **Melting point:** 123 – 125 °C; $\mathbf{R_f}$ = 0.25 in 20% EtOAc/cyclohexane; **^{1}H NMR** (400 MHz, $CDCl_3$) δ 8.09 (dd, *J* = 20.7, 8.4 Hz, 2H), 7.87 – 7.64 (m, 3H), 7.59 – 7.50 (ddd, *J* = 8.1, 6.9, 1.2 Hz, 1H), 7.40 (dt, *J* = 7.9, 1.9 Hz, 2H), 7.31 – 7.17 (m, 2H), 6.40 (s, 1H), 5.30 (t, *J* = 6.1 Hz, 1H), 3.29 (d, *J* = 6.1 Hz, 2H); **^{13}C NMR** (101 MHz, $CDCl_3$) δ 160.3, 147.1, 146.5, 137.2, 130.5, 130.1, 129.3, 128.9, 127.8, 127.1, 126.5, 124.7,122.7, 122.1, 72.4, 45.9; **IR** ν(cm^{-1}): 3058, 1854, 1736, 1616, 1594, 780, 572; **HRMS**: (ESI-TOF) calculated for $C_{17}H_{14}BrNO$ $[M + H]^+$ 328.0332 found 328.0328.

An asymmetric sample was prepared using general procedure 3 (**GP3**), which contained an-inseparable impurity. The presence of the enantioenriched product was confirmed by NMR and HRMS analysis. The enantioselectivity was determined by UHPLC comparison with a fully characterised racemic sample. Yield, IR, melting point and optical data for the asymmetric sample were not quoted due the inseparable product being present.

The enantioselectivity (52% ee) was determined by chiral UHPLC analysis of the title compound [CHIRALCEL®OD-3 column, 4.6 mm Ø x 250 mm, Daicel Chemical Industries], heptane/2-propanol = 97:3, 1.0 mL/min, 40 °C column temperature, 190 nm UV). Retention time = 15.29 min (*S*), 23.55 min (*R*).

1-(4-Iodophenyl)-2-(quinolin-2-yl)ethan-1-ol

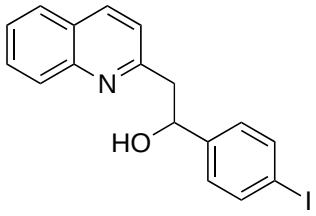

The title compound was synthesised as per general procedure 4 (**GP4**) and was isolated as a white solid (3 mg, 4% yield) after purification by column chromatography on silica gel. **Melting point:** 123 – 125 °C; $\mathbf{R_f}$ = 0.25 in 20% EtOAc/cyclohexane; **^{1}H NMR** (400 MHz, $CDCl_3$) δ 8.14 – 8.01 (m, 2H), 7.85 – 7.64 (m, 4H), 7.54 (ddd, *J* = 8.1, 6.9, 1.2 Hz, 1H), 7.31 – 7.17 (m, 3H), 6.36 (s, 1H), 5.34 – 5.21 (m, 1H), 3.34 – 3.20 (m, 2H); **^{13}C NMR** (101 MHz, $CDCl_3$) δ 160.3, 147.1, 143.9, 137.5, 137.1, 130.1, 128.8, 128.1, 127.8, 127.0, 126.5, 122.2, 92.7, 72.6, 45.9; **IR** ν(cm^{-1}): 3114, 2920, 2849, 1619, 1599, 786, 553; **HRMS**: (ESI-TOF) calculated for $C_{17}H_{14}INO$ $[M + H]^+$ 376.0193 found 376.0187.

An asymmetric sample was prepared using general procedure 3 (**GP3**), which contained an-inseparable impurity. The presence of the enantioenriched product was confirmed by NMR and HRMS analysis. The enantioselectivity was determined by UHPLC comparison with a fully characterised racemic sample. Yield, IR, melting point and optical data for the asymmetric sample were not quoted due the inseparable product being present.

The enantioselectivity (59% ee) was determined by chiral UHPLC analysis of the title compound [CHIRALCEL®OD-3 column, 4.6 mm Ø x 250 mm, Daicel Chemical Industries], heptane/2-propanol = 97:3, 1.0 mL/min, 40 °C column temperature, 190 nm UV). Retention time = 20.11 min (*S*), 26.57 min (*R*).

1-Phenyl-2-(pyridin-2-yl)ethan-1-ol[23]

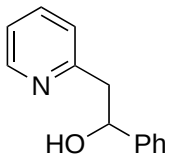

The title compound was synthesised as per general procedure 4 (**GP4**) and was isolated as a white solid (15 mg, 37% yield) after purification by column chromatography on silica gel. **Melting point:** 106 – 108 °C; $\mathbf{R_f}$ = 0.5 in 40% EtOAc/cyclohexane; **^{1}H NMR** (400 MHz, $CDCl_3$) δ 8.59 – 8.45 (m, 1H), 7.60 (td, *J* = 7.7, 1.8 Hz, 1H), 7.45 – 7.38 (m, 2H), 7.37 – 7.29 (m, 2H), 7.29 – 7.21 (m, 2H), 7.21 – 7.13 (m, 1H), 7.09 (d, *J* = 7.8 Hz, 1H), 5.68 (s, 1H), 5.15 (dd, *J* = 8.2, 4.0 Hz, 1H), 3.21 – 3.02 (m, 2H);**^{13}C NMR** (101 MHz, $CDCl_3$) δ 159.9, 148.7, 144.2, 137.0, 128.4, 127.4, 126.0, 123.9, 121.9, 73.5, 45.8; **IR** ν(cm^{-1}): 3175, 3059, 1881, 1808, 1593, 756, 584; **HRMS**: (ESI-TOF) calculated for $C_{13}H_{13}NO$ $[M + H]^+$ 200.1070 found 200.1072. All characterisation data are in agreement with reported literature data.

An asymmetric sample was prepared using general procedure 3 (**GP3**), which contained an-inseparable impurity. The presence of the enantioenriched product was confirmed by NMR and HRMS analysis. The enantioselectivity was determined by UHPLC comparison with a fully characterised racemic sample. Yield, IR, melting point and optical data for the asymmetric sample were not quoted due the inseparable product being present.

The enantioselectivity (9% ee) was determined by chiral UHPLC analysis of the title compound [CHIRALCEL®OD-3 column, 4.6 mm Ø x 250 mm, Daicel Chemical Industries], heptane/2-propanol = 97:3, 1.0 mL/min, 40 °C column temperature, 190 nm UV). Retention time = 15.77 min (*S*), 25.39 min (*R*).

2-(Benzo[*d*]oxazol-2-yl)-1-ferrocenylethan-1-ol

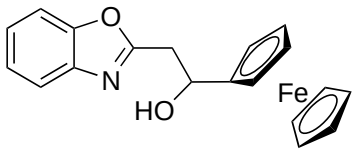

The title compound was synthesised as per general procedure 4 (**GP4**) and the compound was isolated as a brown solid (52 mg, 75% yield) after purification by column chromatography on silica gel. **Melting point:** 117 – 119 °C; $\mathbf{R_f}$ = 0.52 in 40% EtOAc/cyclohexane; **^{1}H NMR** (400 MHz, $CDCl_3$) δ 7.72 – 7.64 (m, 1H), 7.53 – 7.45 (m, 1H), 7.36 – 7.26 (m, 2H), 5.09 – 5.01 (m, 1H), 4.32 (s, 1H), 4.26 – 4.12 (m, 8H), 3.38 – 3.24 (m, 2H); **^{13}C NMR** (101 MHz, $CDCl_3$) δ 164.9, 150.7, 141.2, 124.8, 124.4, 119.8, 110.6, 91.7, 68.7, 68.4, 68.3, 67.6, 66.7, 66.2, 37.5; **IR** ν(cm^{-1}): 3286, 3098, 1644, 1613, 1572, 798, 577; **HRMS**: (ESI-TOF) calculated for $C_{19}H_{17}FeNO_2$ $[M + H]^+$ 347.0603 found 347.0602.

References

(1) Hu, J.; Ferger, M.; Shi, Z.; Marder, T. B. *Chem. Soc. Rev.* **2021**, 13129–13188.

(2) Ishiyama, T.; Miyaura, N. *J. Organomet. Chem.* **2003**, *680* (1–2), 3–11.

(3) Chow, W. K.; Yuen, O. Y.; Choy, P. Y.; So, C. M.; Lau, C. P.; Wong, W. T.; Kwong, F. Y. *RSC Adv.* **2013**, *3* (31), 12518–12539.

(4) Sandford, C.; Aggarwal, V. K. *Chem. Commun.* **2017**, *53* (40), 5481–5494.

(5) Chen, H.; Schlecht, S.; Semple, T. C.; Hartwig, J. F. *Science (80-.).* **2000**, *287* (5460), 1995–1997.

(6) Ishiyama, T.; Murata, M.; Miyaura, N. *J. Org. Chem.* **1995**, *60* (23), 7508–7510.

(7) Zhang, G.; Lv, G.; Li, L.; Chen, F.; Cheng, J. *Tetrahedron Lett.* **2011**, *52* (16), 1993–1995.

(8) Mlynarski, S. N.; Karns, A. S.; Morken, J. P. *J. Am. Chem. Soc.* **2012**, *134* (40), 16449–16451.

(9) Wagh, R. B.; Nagarkar, J. M. *Tetrahedron Lett.* **2017**, *58* (48), 4572–4575.

(10) Webb, K. S.; Levy, D. *Tetrahedron Lett.* **1995**, *36* (29), 5117–5118.

(11) Martin, R.; Buchwald, L., S. *Acc. Chem. Res.* **2008**, *41* (11), 1461–1473.

(12) Taheri Kal Koshvandi, A.; Heravi, M. M.; Momeni, T. *Appl. Organomet. Chem.* **2018**, *32* (3), 1–59.

(13) Kotha, S.; Lahiri, K.; Kashinath, D. *Tetrahedron* **2002**, *58* (48), 9633–9695.

(14) Xu, L.; Wang, G.; Zhang, S.; Wang, H.; Wang, L.; Liu, L.; Jiao, J.; Li, P. *Tetrahedron* **2017**, *73* (51), 7123–7157.

(15) Hartwig, J. F. *Acc. Chem. Res.* **2012**, *45* (6), 864–873.

(16) Lee, Y.; Hoveyda, A. H. *J. Am. Chem. Soc.* **2009**, *131* (9), 3160–3161.

(17) Azzena, U.; Pisano, L.; Antonello, S.; Maran, F. *J. Org. Chem.* **2009**, *74* (21), 8064–8070.

(18) Doucet, H.; Fernandez, E.; Layzell, T. P.; Brown, J. M. *Chem. - A Eur. J.* **1999**, *5* (4), 1320–1330.

(19) Pattison, G.; Piraux, G.; Lam, H. W. *J. Am. Chem. Soc.* **2010**, *132* (41), 14373–14375.

(20) Wen, L.; Yue, Z.; Zhang, H.; Chong, Q.; Meng, F. *Org. Lett.* **2017**, *19* (24), 6610–

6613.

(21) Reyes, R. L.; Iwai, T.; Maeda, S.; Sawamura, M. *J. Am. Chem. Soc.* **2019**, *141* (17), 6817–6821.

(22) Liz, R.; Liardo, E.; Rebolledo, F. *Org. Biomol. Chem.* **2019**, *17* (35), 8214–8220.

(23) Rendler, S.; Plefka, O.; Karatas, B.; Auer, G.; Fröhlich, R.; Mück-Lichtenfeld, C.; Grimme, S.; Oestreich, M. *Chem. - A Eur. J.* **2008**, *14* (36), 11512–11528.

(24) Rokade, B. V.; Guiry, P. J. *ACS Catal.* **2017**, *7* (4), 2334–2338.

(25) Rokade, B. V.; Guiry, P. J. *J. Org. Chem.* **2019**, *84* (9), 5763–5772.

(26) Fleming, W. J.; Müller-Bunz, H.; Lillo, V.; Fernández, E.; Guiry, P. J. *Org. Biomol. Chem.* **2009**, *7* (12), 2520–2524.

(27) Valk, J. M.; Whitlock, G. A.; Layzell, T. P.; Brown, J. M. *Tetrahedron: Asymmetry* **1995**, *6* (10), 2593–2596.

(28) Dryanska, V.; Ivanov, C. *Synthesis (Stuttg).* **1976**, *1976* (01), 37–38.

(29) Barroso, S.; Joksch, M.; Puylaert, P.; Tin, S.; Bell, S. J.; Donnellan, L.; Duguid, S.; Muir, C.; Zhao, P.; Farina, V.; Tran, D. N.; De Vries, J. G. *J. Org. Chem.* **2021**, *86* (1), 103–109.

(30) Dahiya, G.; Pappoppula, M.; Aponick, A. *Angew. Chemie - Int. Ed.* **2021**, *60* (36), 19604–19608.

(31) Pi, D.; Jiang, K.; Zhou, H.; Sui, Y.; Uozumi, Y.; Zou, K. *RSC Adv.* **2014**, *4* (101), 57875–57884.

(32) Song, X. R.; Qiu, Y. F.; Song, B.; Hao, X. H.; Han, Y. P.; Gao, P.; Liu, X. Y.; Liang, Y. M. *J. Org. Chem.* **2015**, *80* (4), 2263–2271.

(33) Sandford, C.; Rasappan, R.; Aggarwal, V. K. *J. Am. Chem. Soc.* **2015**, *137* (32), 10100–10103.

(34) Wang, Y.; Noble, A.; Myers, E. L.; Aggarwal, V. K. *Angew. Chemie - Int. Ed.* **2016**, *55* (13), 4270–4274.

(35) Meng, L.; Kamada, Y.; Muto, K.; Yamaguchi, J.; Itami, K. *Angew. Chemie - Int. Ed.* **2013**, *52* (38), 10048–10051.

(36) Szappanos; Mándi, A.; Gulácsi, K.; Lisztes, E.; István Tóth, B.; Bíró, T.; Kónya-Ábrahám, A.; Kiss-Szikszai, A.; Bényei, A.; Antus, S.; Kurtán, T. *Biomolecules* **2020**, *10* (10), 1–42.

(37) Liang, E.; Wang, J.; Wu, Y.; Huang, L.; Yao, X.; Tang, X. *Adv. Synth. Catal.* **2019**,

361 (15), 3619–3623.

(38) Cívicos, J. F.; Alonso, D. A.; Nájera, C. *Adv. Synth. Catal.* **2012**, *354* (14–15), 2771–2776.

Appendix

Chapter 2 Appendix: Synthesis of P,N ligands

Compound **52**

^{1}H NMR (400 MHz, DMSO-d_6)

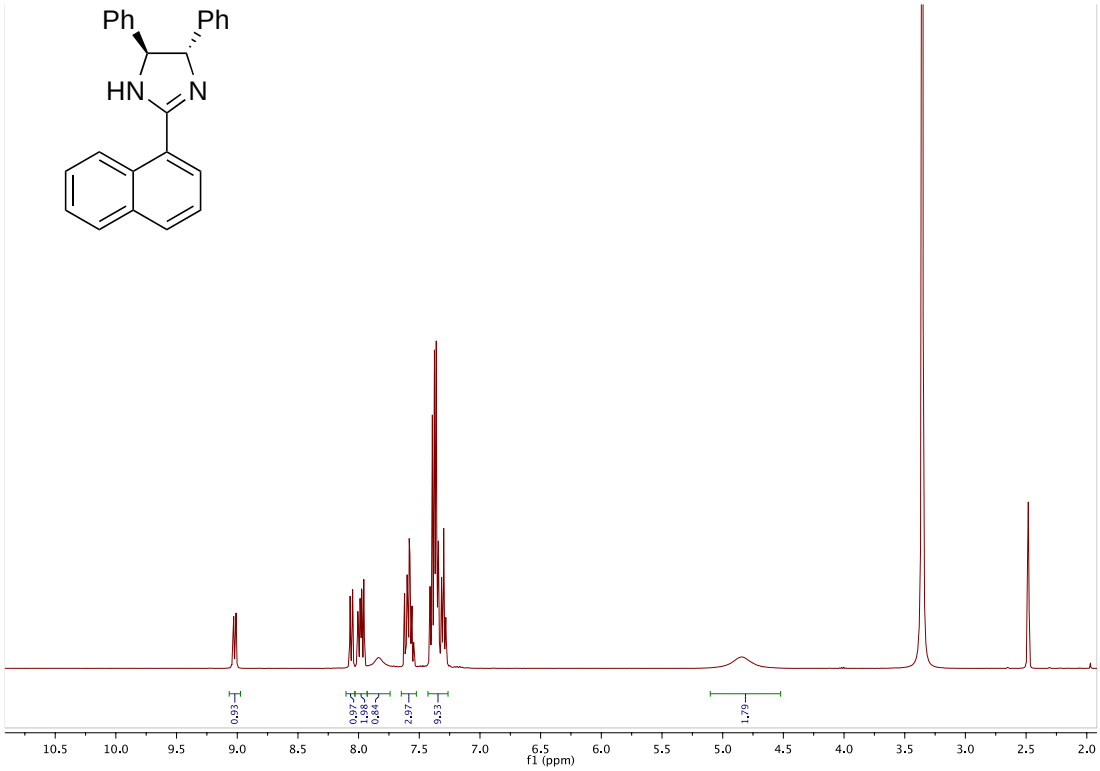

^{13}C NMR (101 MHz, DMSO-d_6)

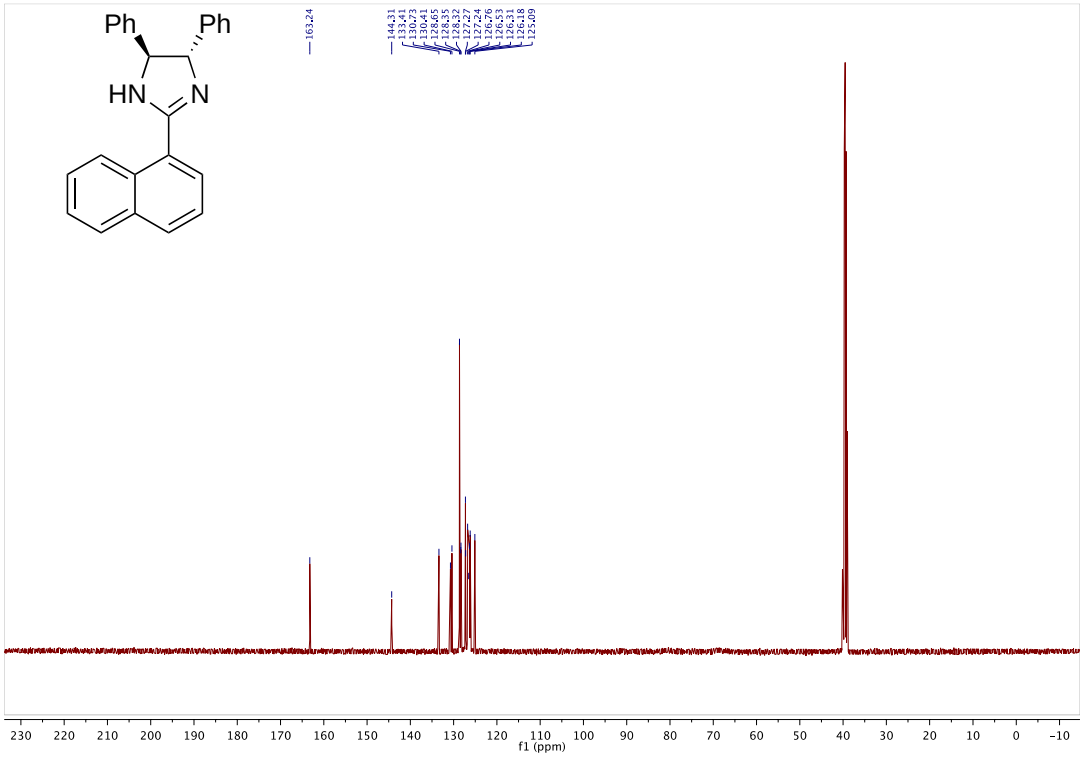

Compound **51**

^{1}H NMR (400 MHz, $CDCl_3$)

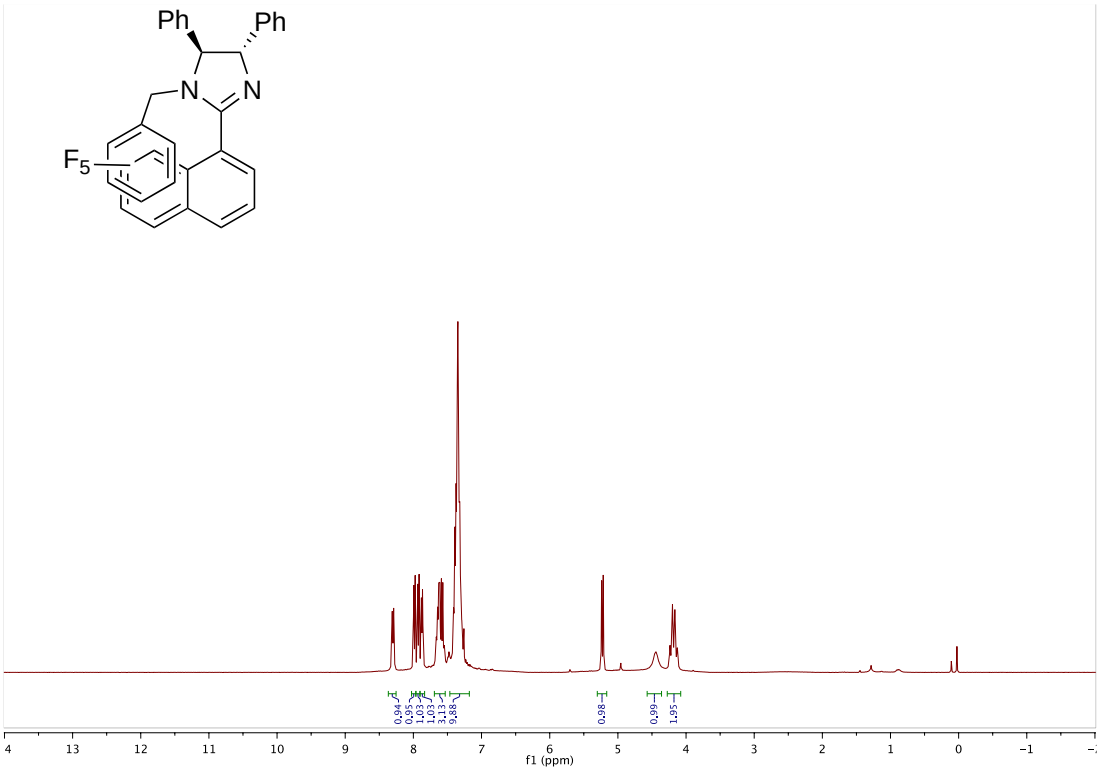

^{13}C NMR (400 MHz, $CDCl_3$)

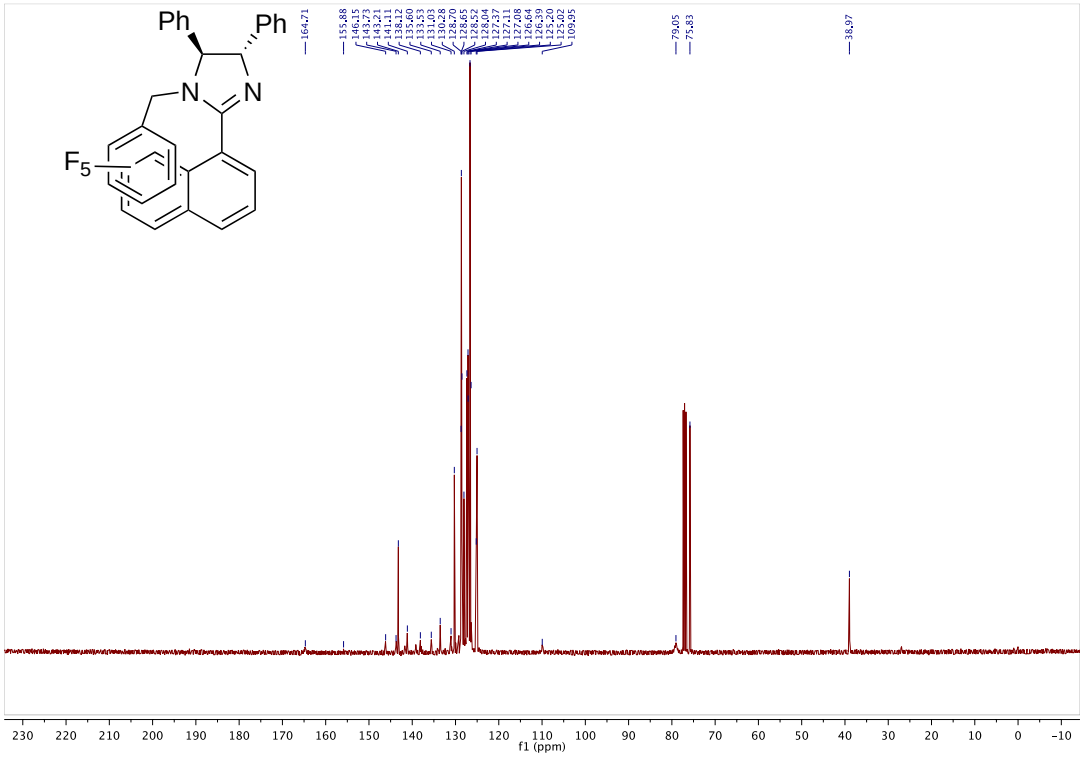

Compound **51**

^{19}F NMR (400 MHz, $CDCl_3$)

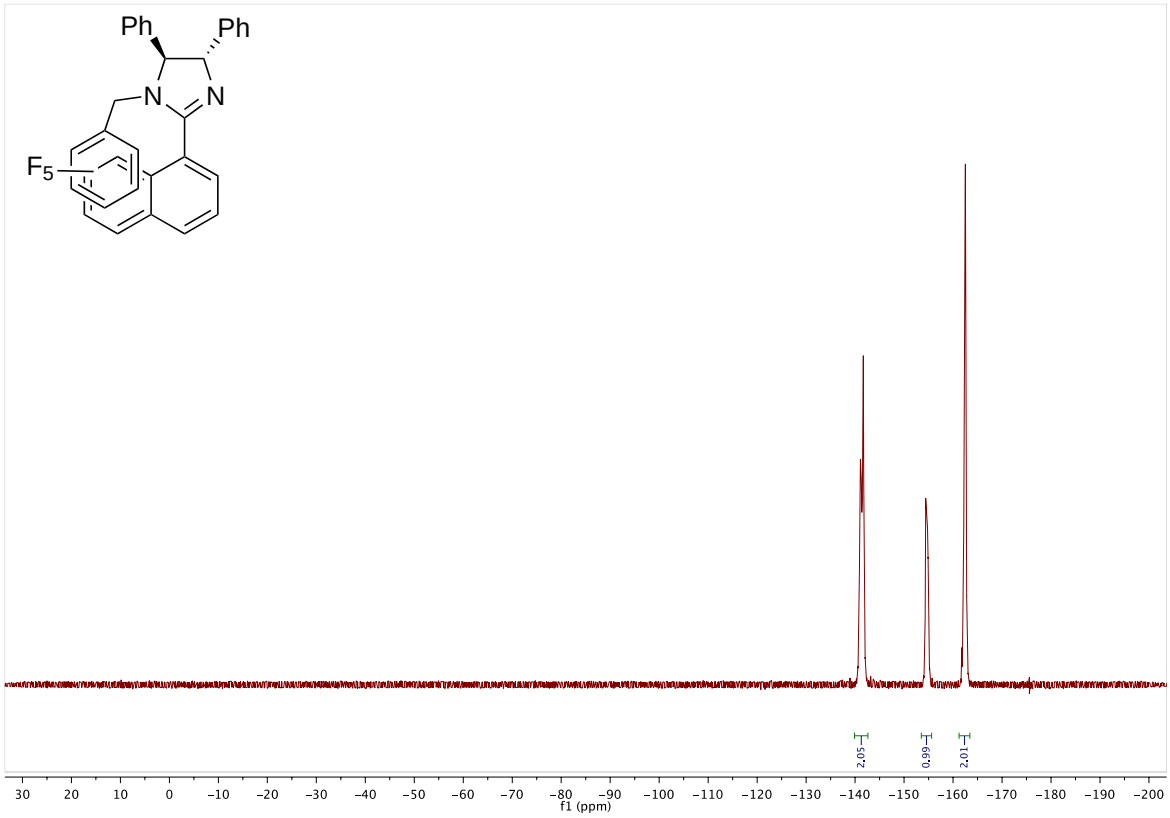

Compound **56**

^{1}H NMR (400 MHz, $CDCl_3$)

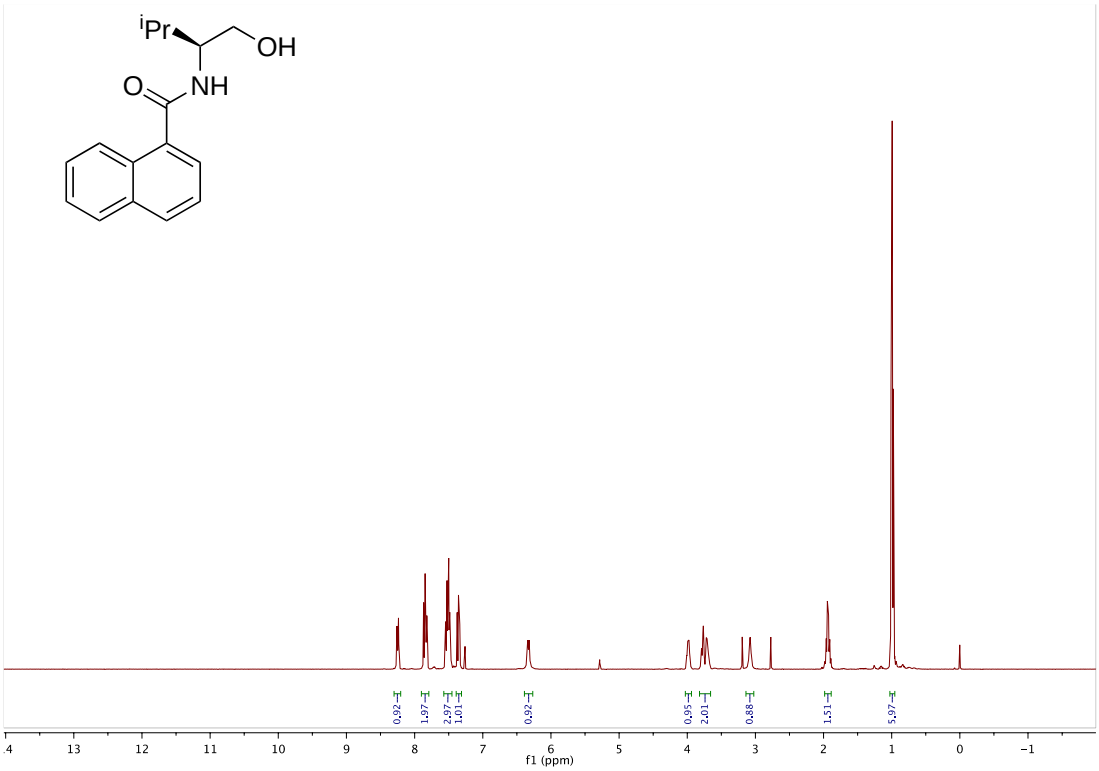

^{13}C NMR (101 MHz, $CDCl_3$)

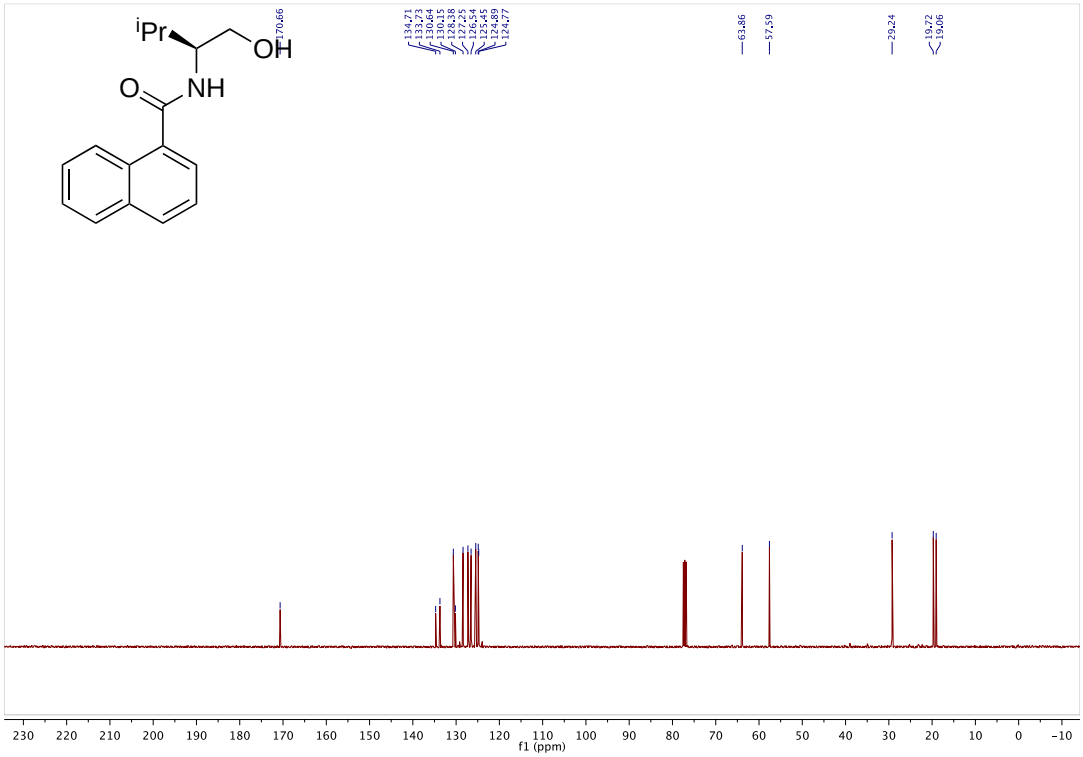

Compound **57**

^{1}H NMR (400 MHz, $CDCl_3$)

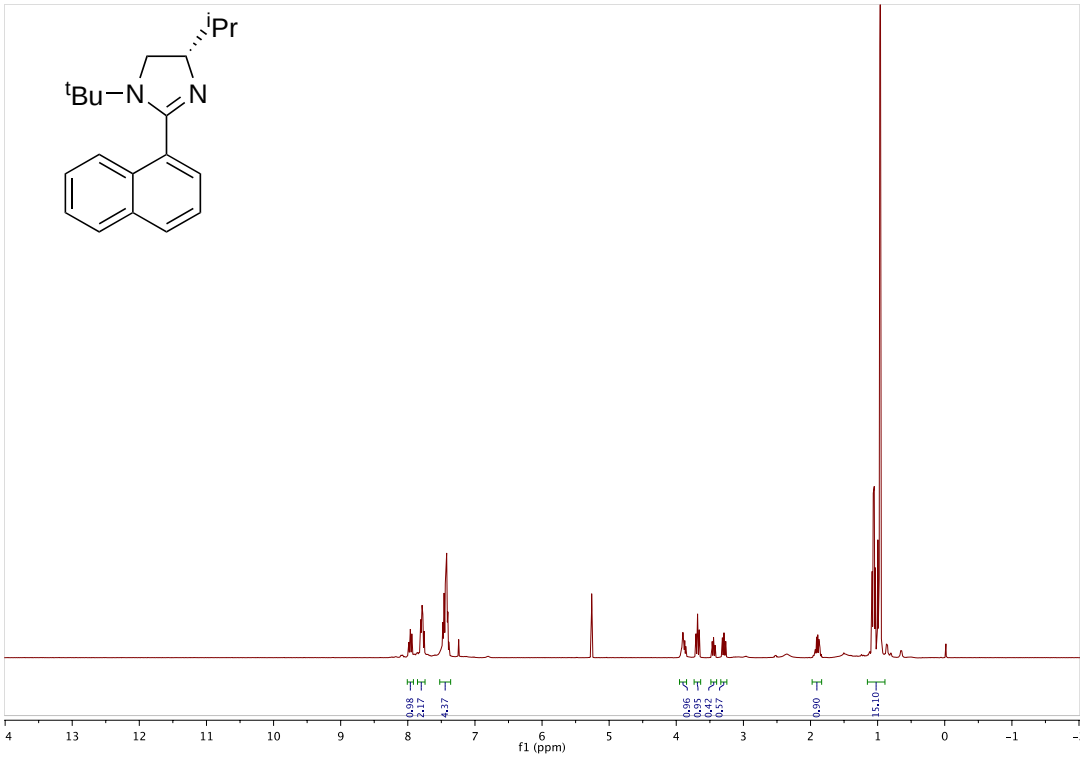

^{13}C NMR (101 MHz, $CDCl_3$)

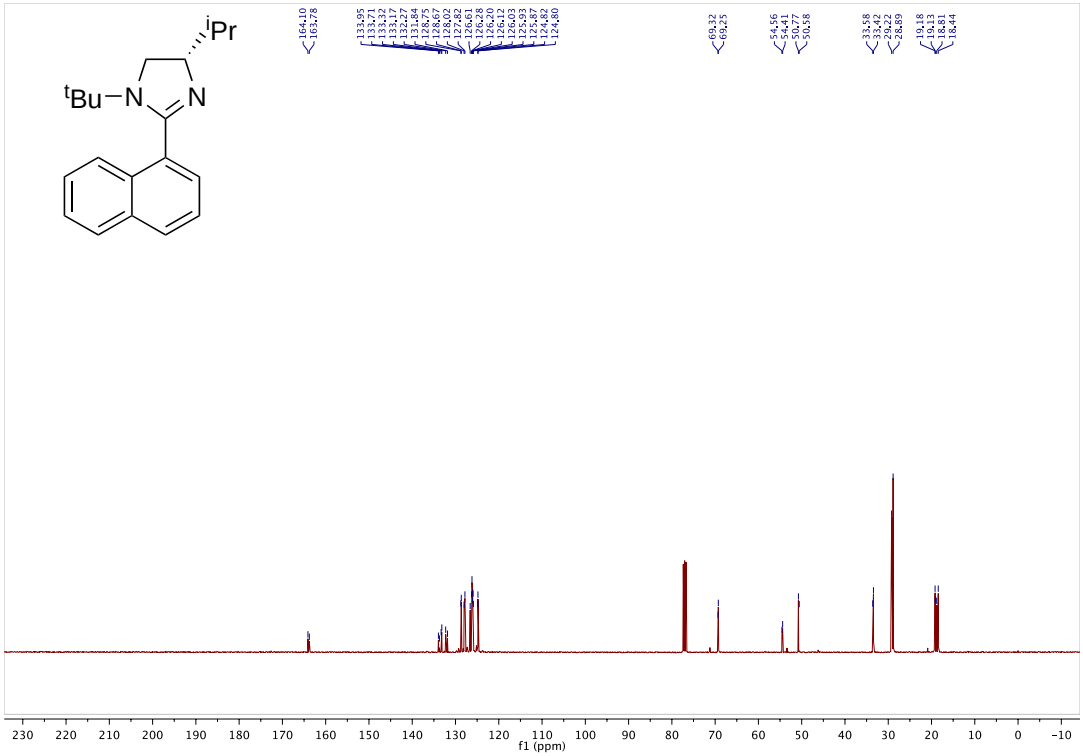

Compound **58**

^{1}H NMR (400 MHz, $CDCl_3$)

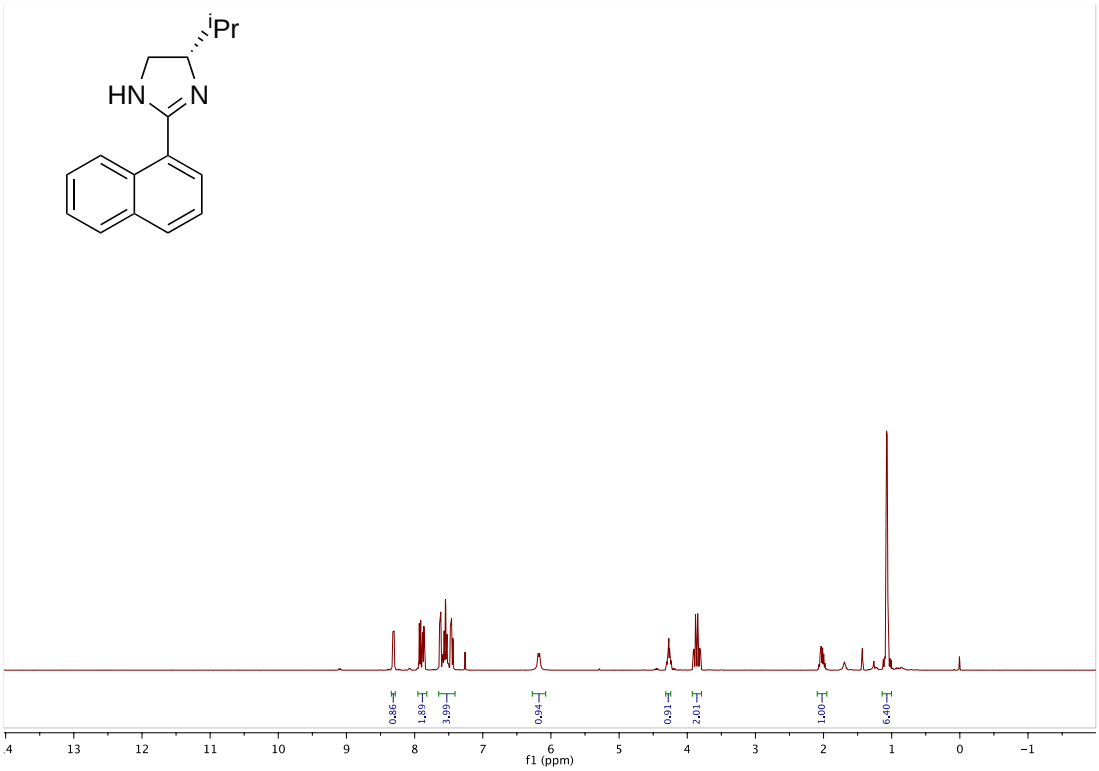

^{13}C NMR (101 MHz, $CDCl_3$)

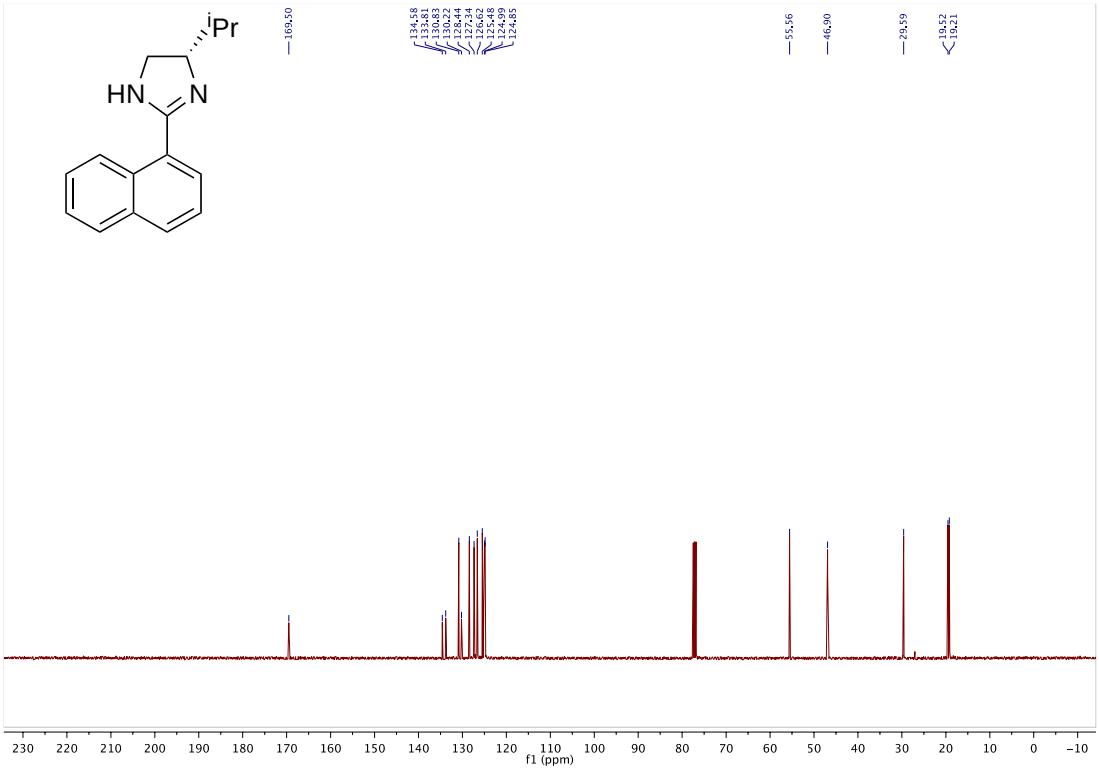

Compound **59**

^{1}H NMR (400 MHz, $CDCl_3$)

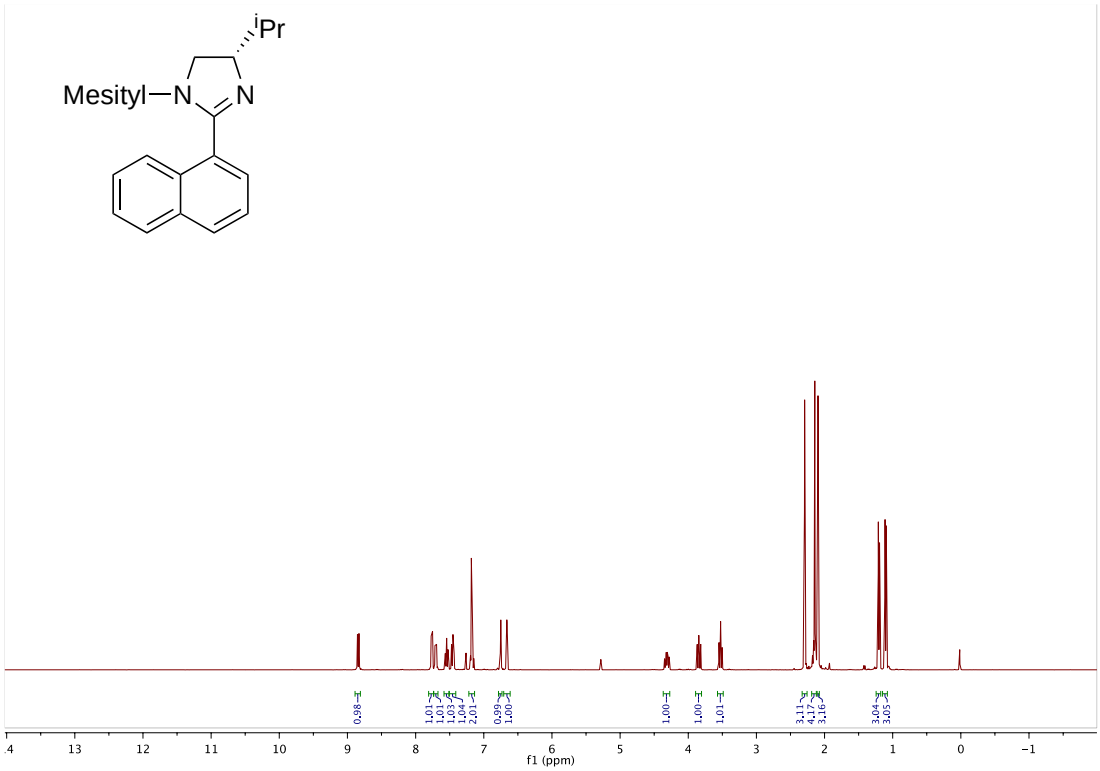

^{13}C NMR (101 MHz, $CDCl_3$)

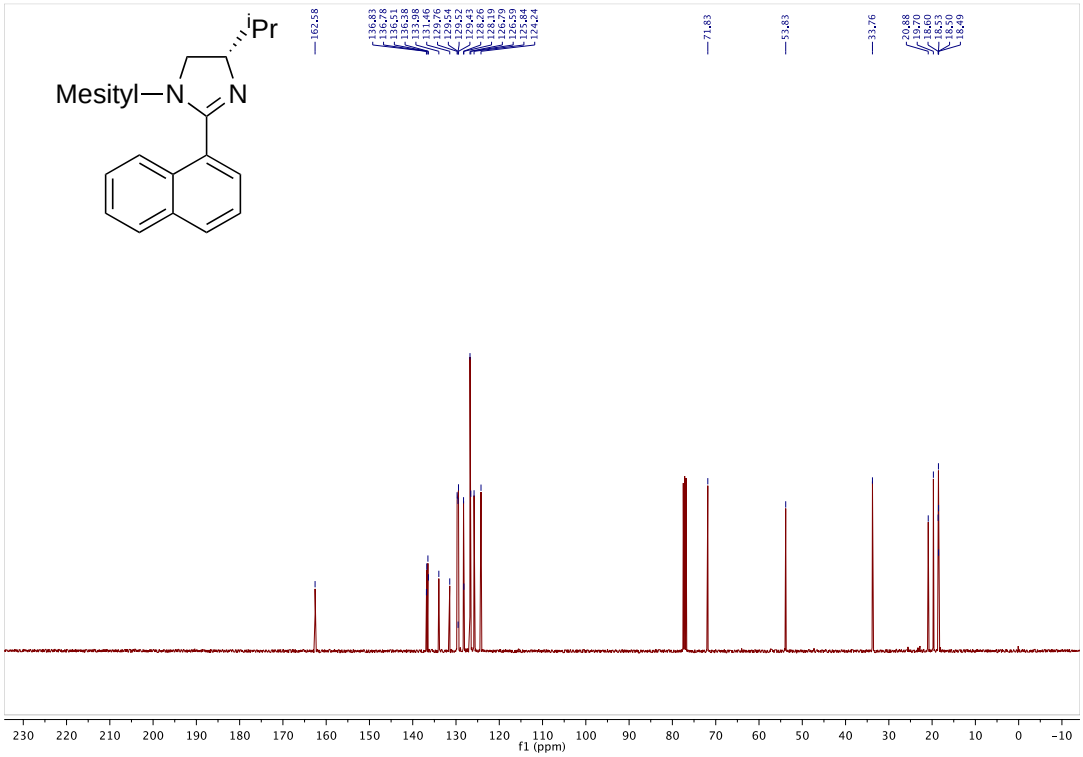

Compound **73**

^{1}H NMR (500 MHz, $CDCl_3$)

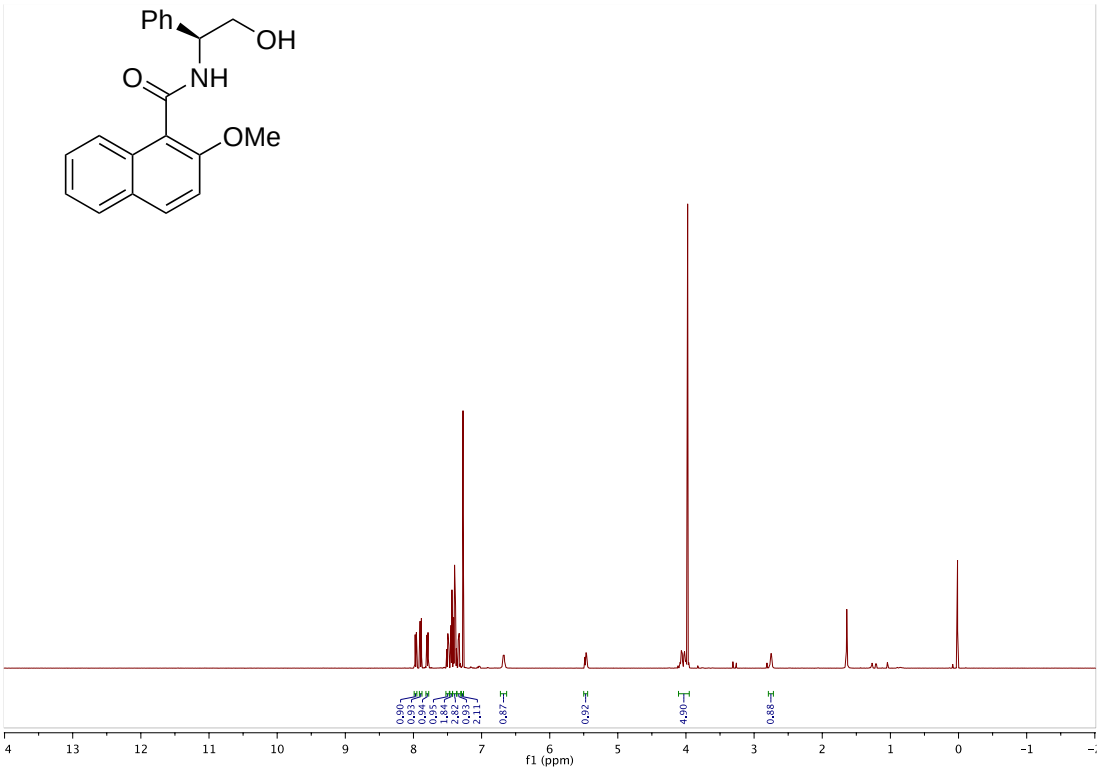

^{13}C NMR (126 MHz, $CDCl_3$)

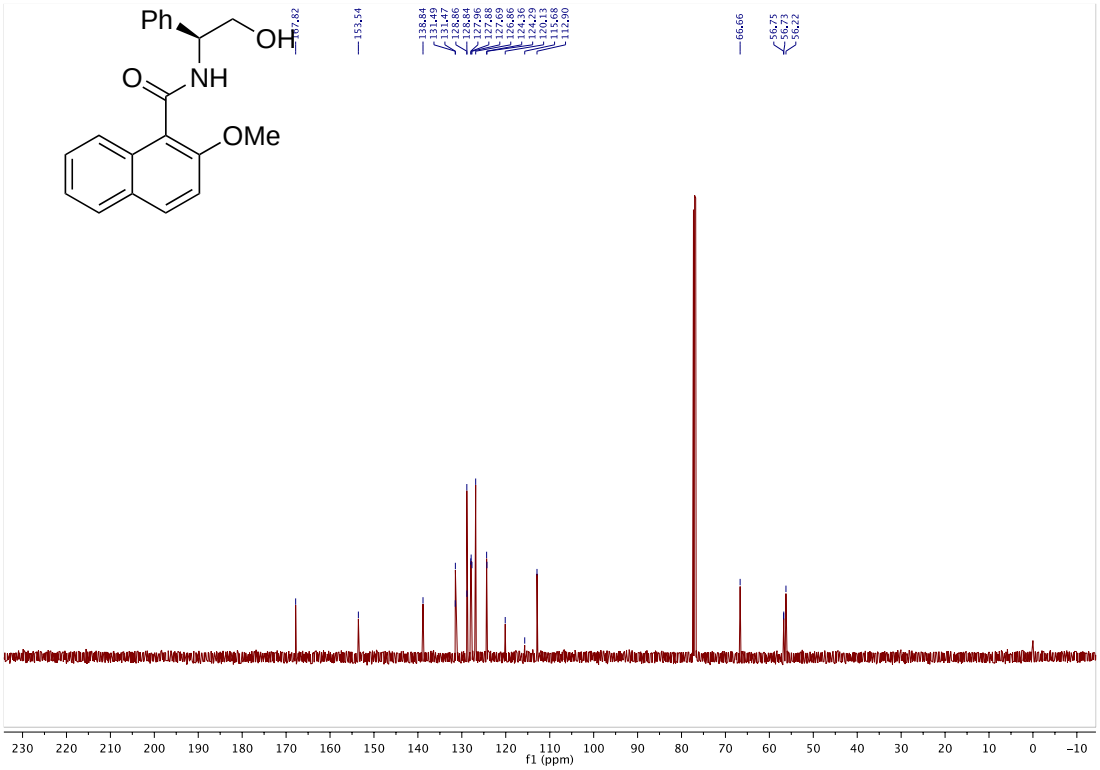

^{1}H NMR (500 MHz, $CDCl_3$)

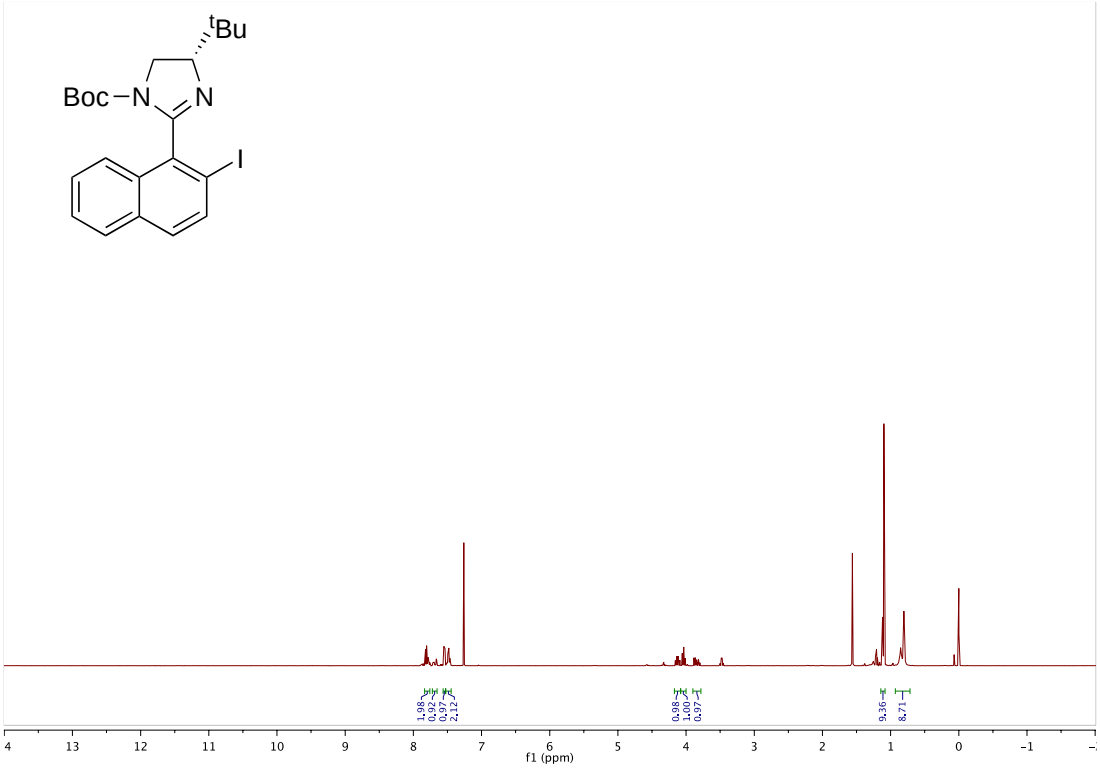

^{13}C NMR (126 MHz, $CDCl_3$)

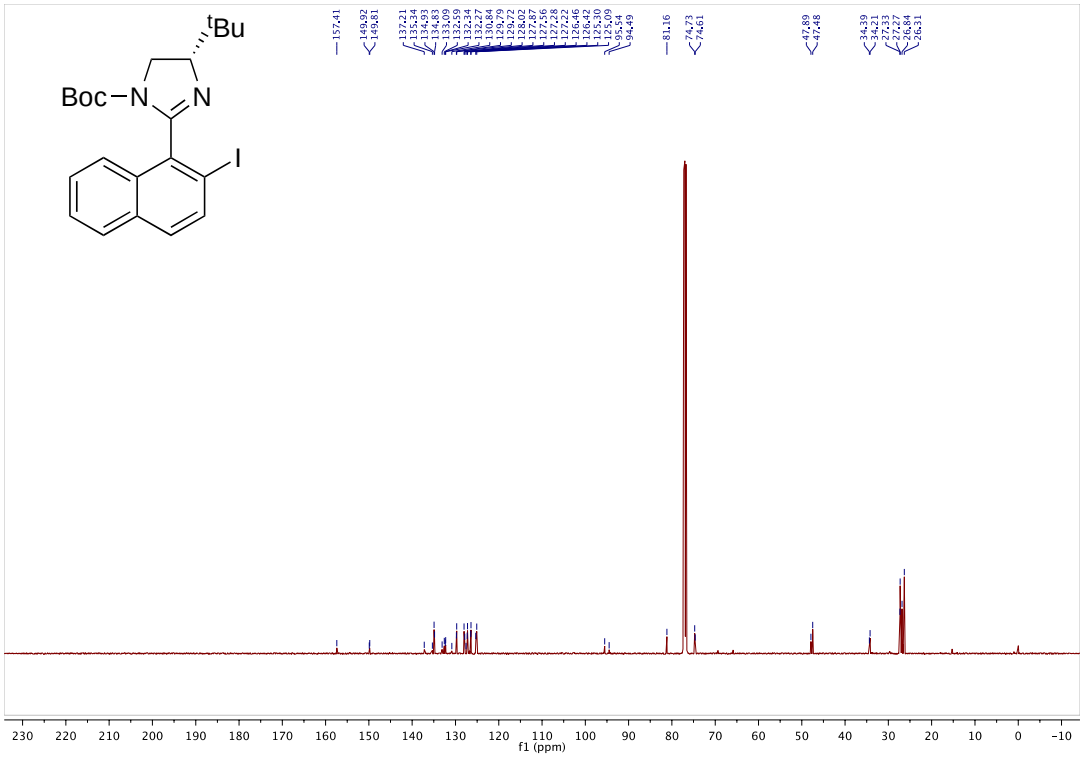

^{1}H NMR (500 MHz, $CDCl_3$)

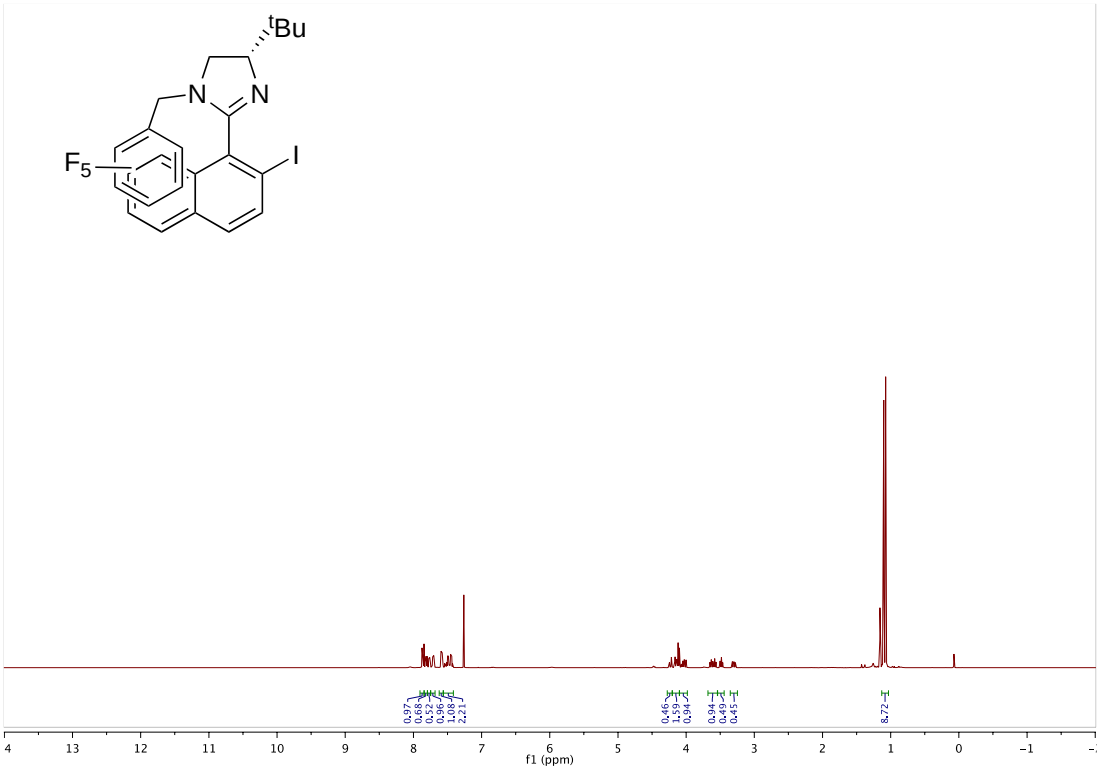

^{13}C NMR (126 MHz, $CDCl_3$)

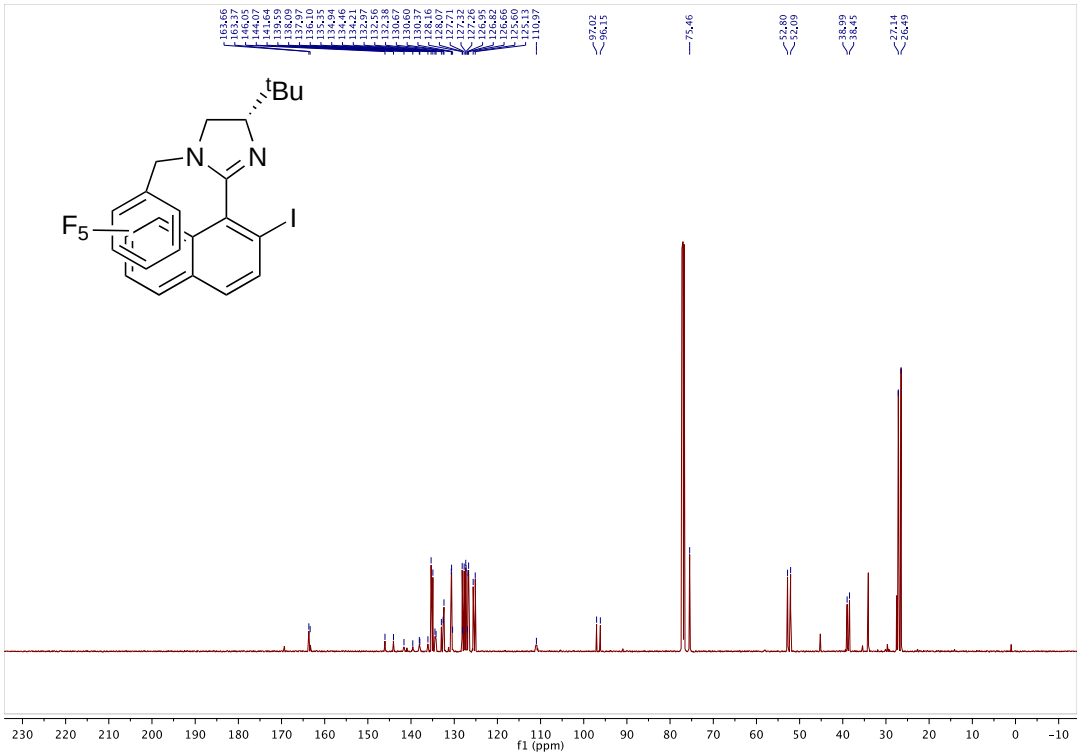

^{19}F NMR (376 MHz, $CDCl_3$)

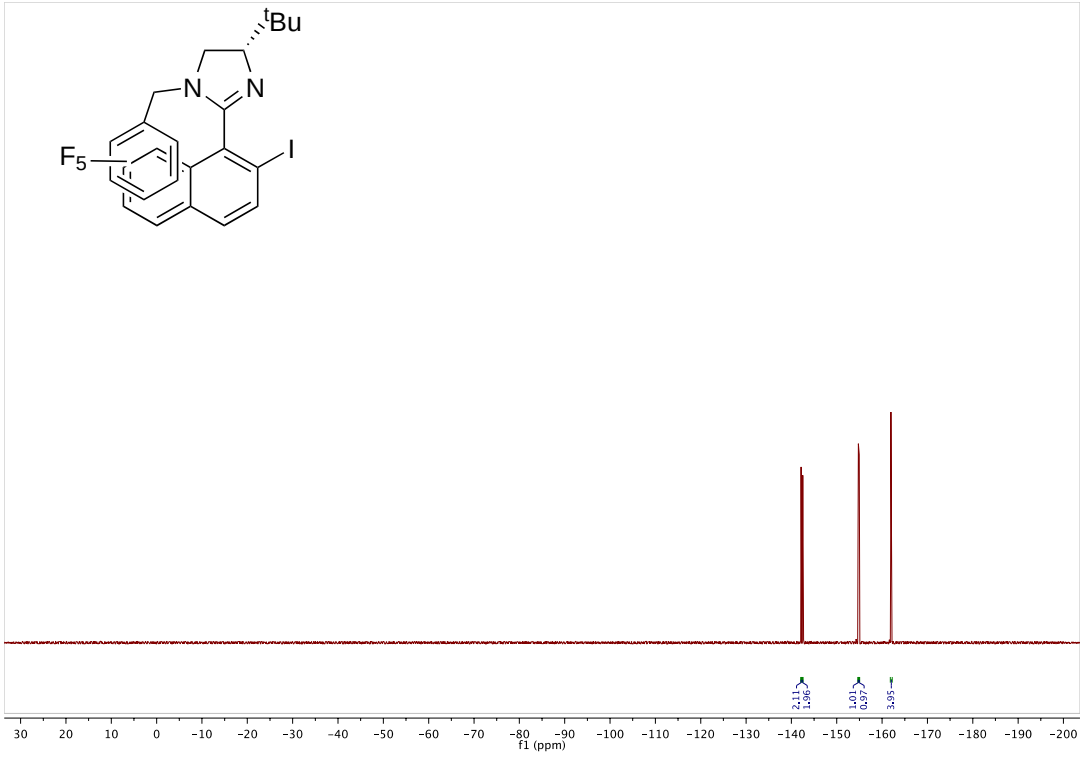

^{1}H NMR (400 MHz, $CDCl_3$)

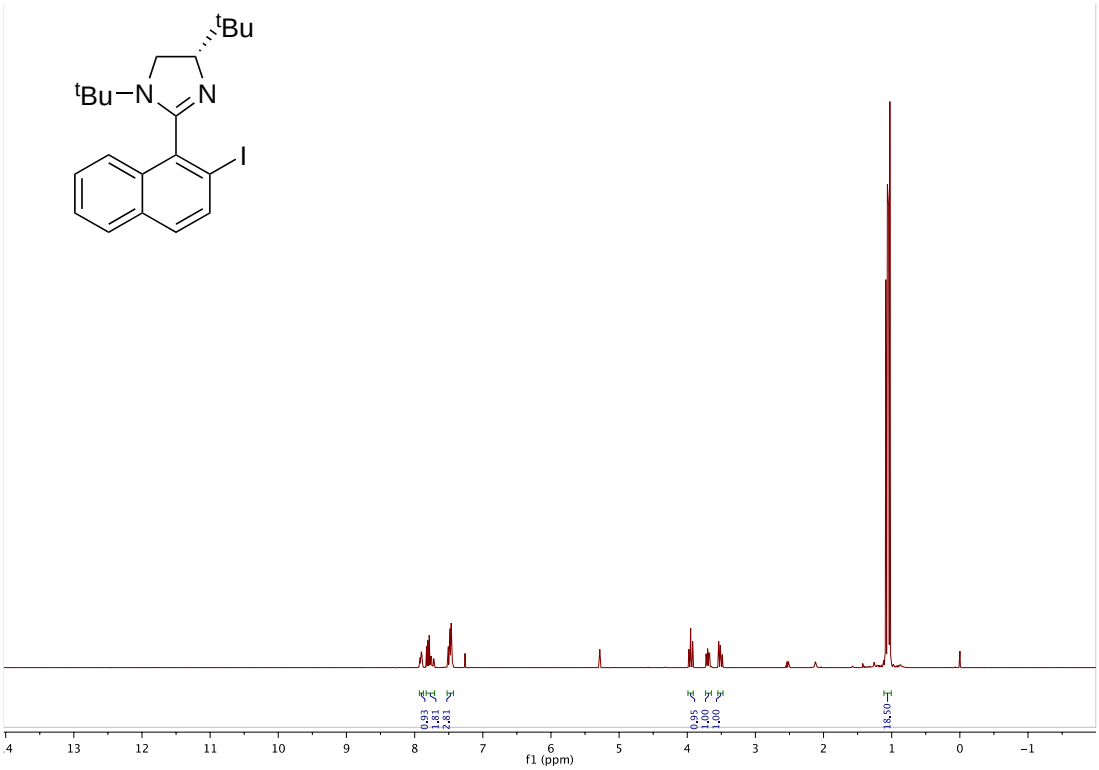

^{13}C NMR (101 MHz, $CDCl_3$)

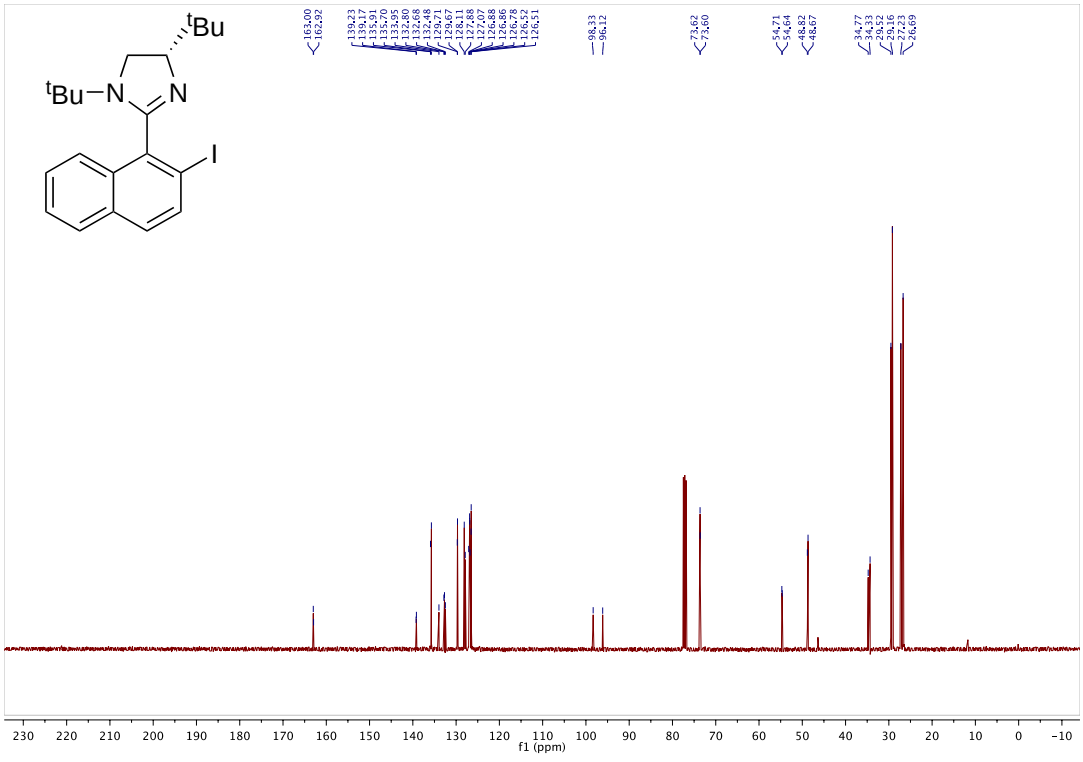

^{1}H NMR (400 MHZ, $CDCl_3$)

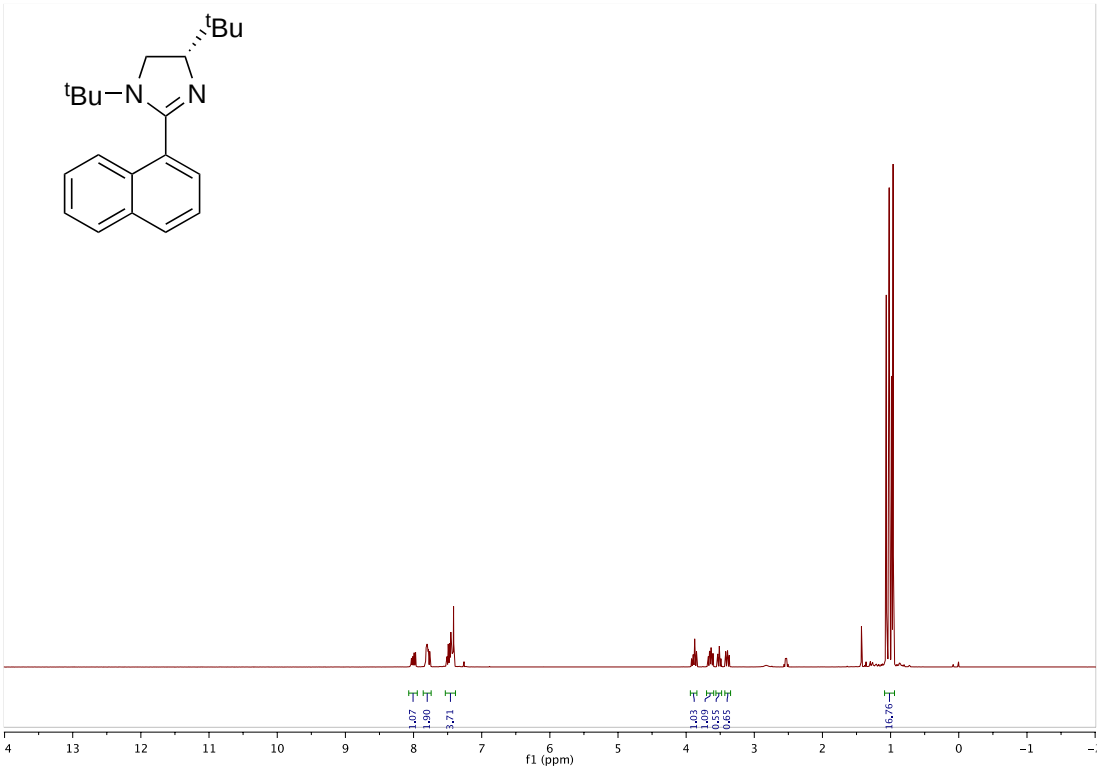

^{13}C NMR (101 MHZ, $CDCl_3$)

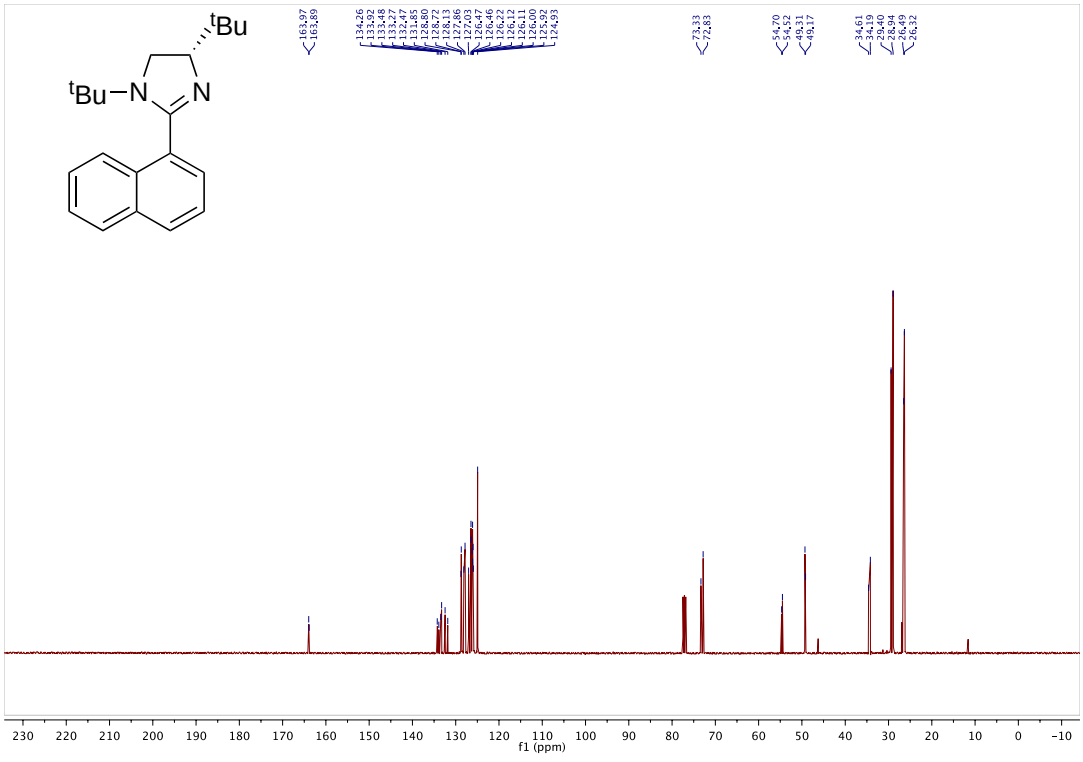

^{1}H NMR (400 MHz, $CDCl_3$)

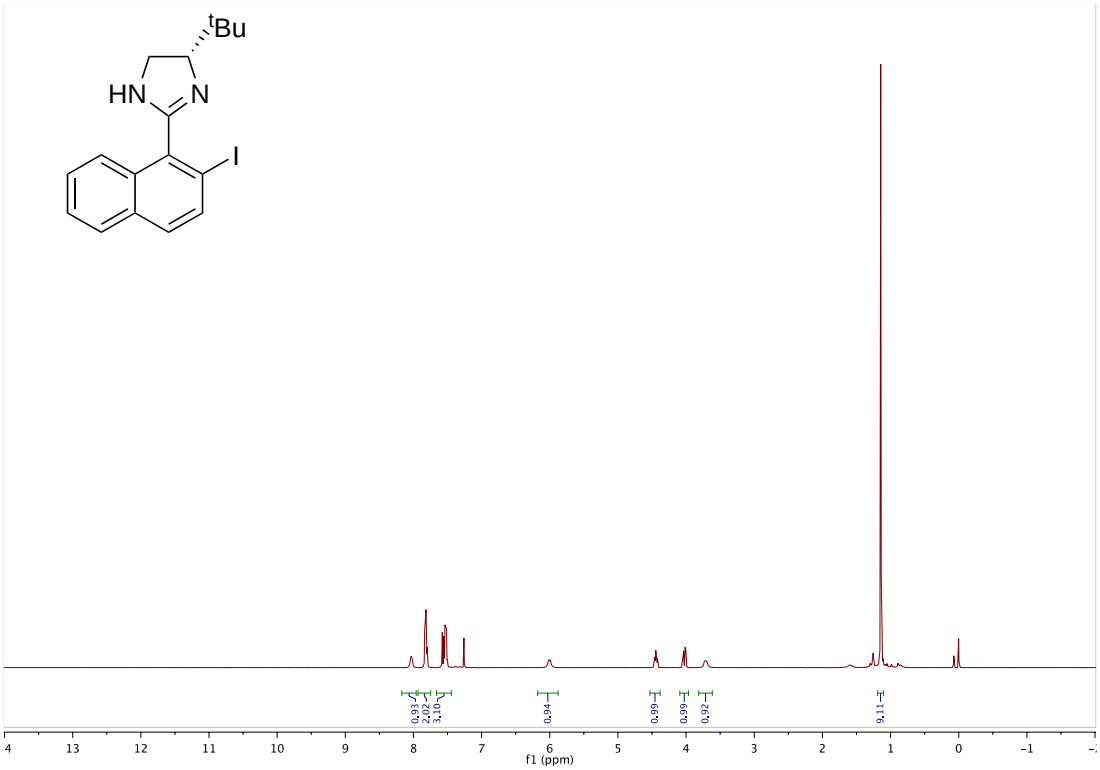

^{13}C NMR (101 MHz, $CDCl_3$)

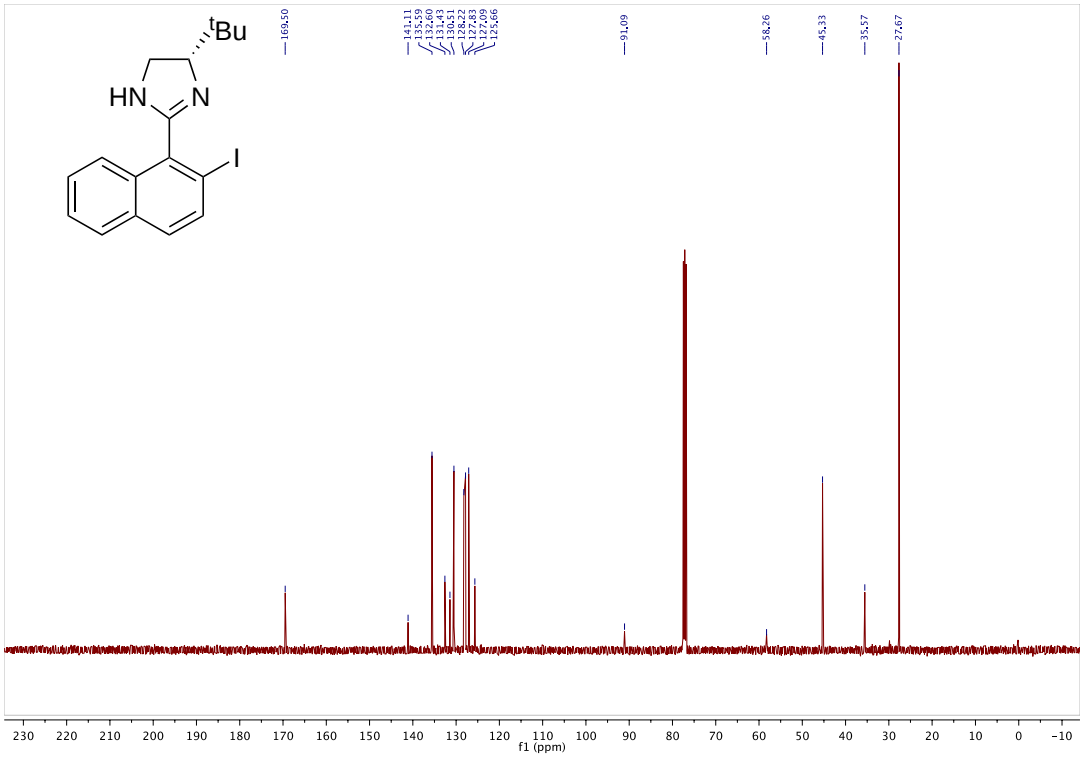

^{1}H NMR (400 MHz, $CDCl_3$)

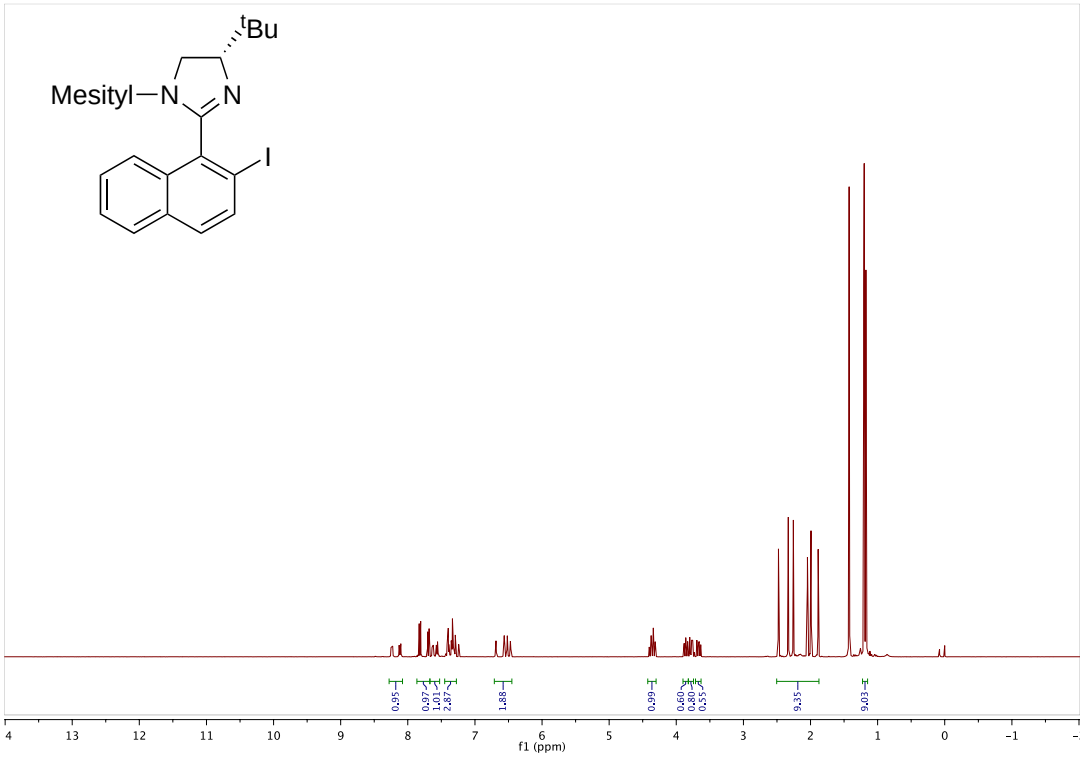

^{13}C NMR (101 MHz, $CDCl_3$)

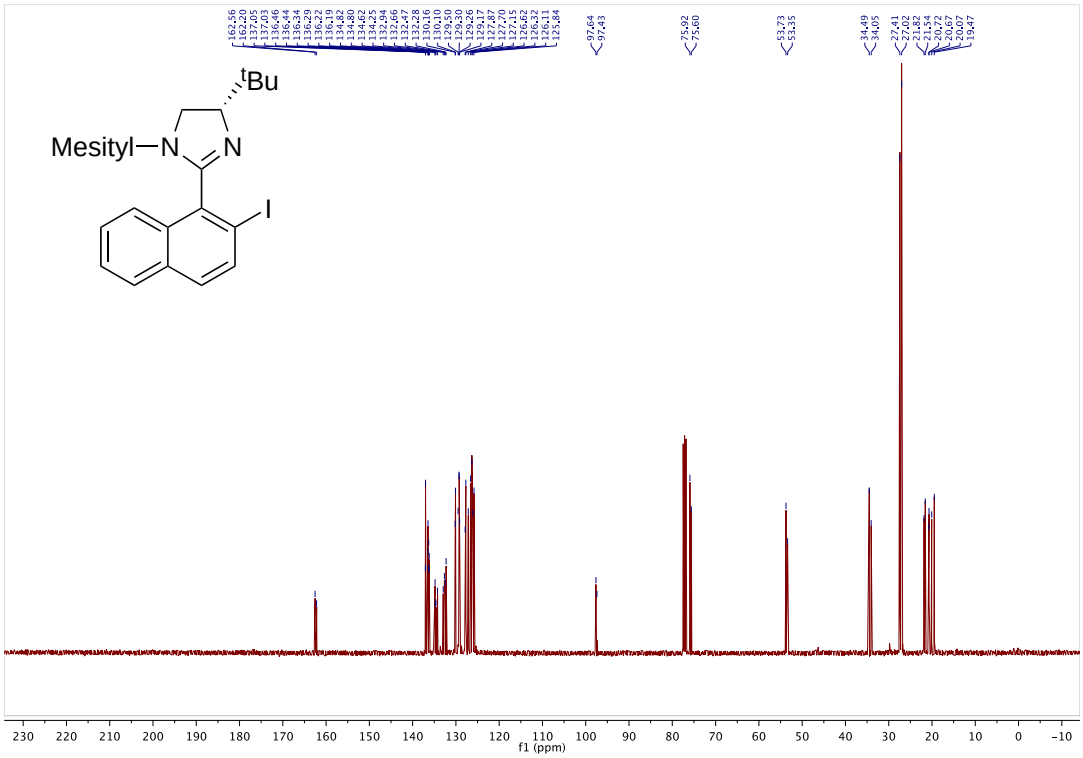

^{1}H NMR (400 MHz, $CDCl_3$)

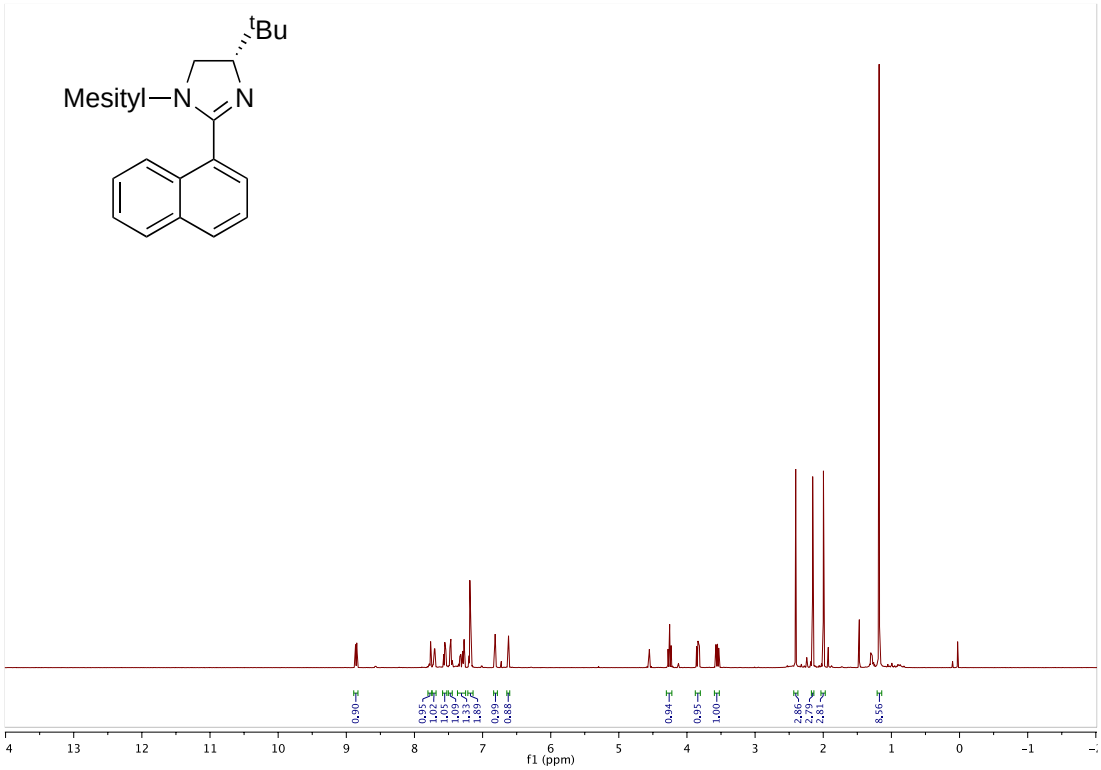

^{13}C NMR (101 MHz, $CDCl_3$)

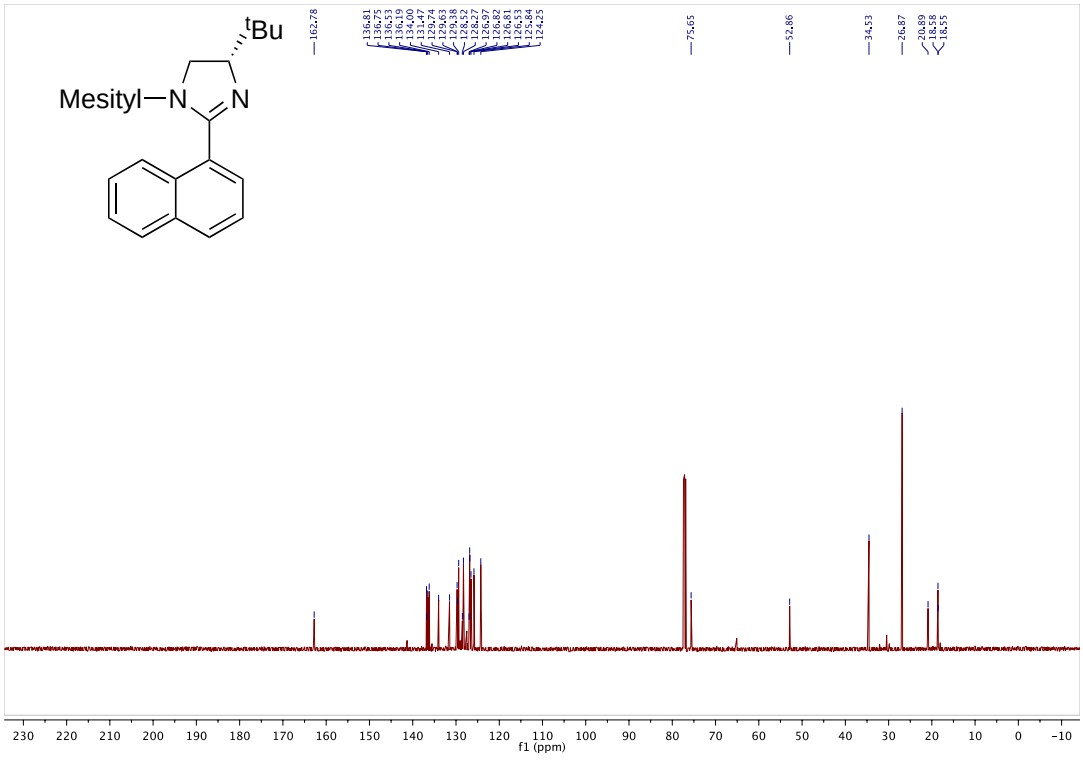

^{1}H NMR (400 MHz, $CDCl_3$)

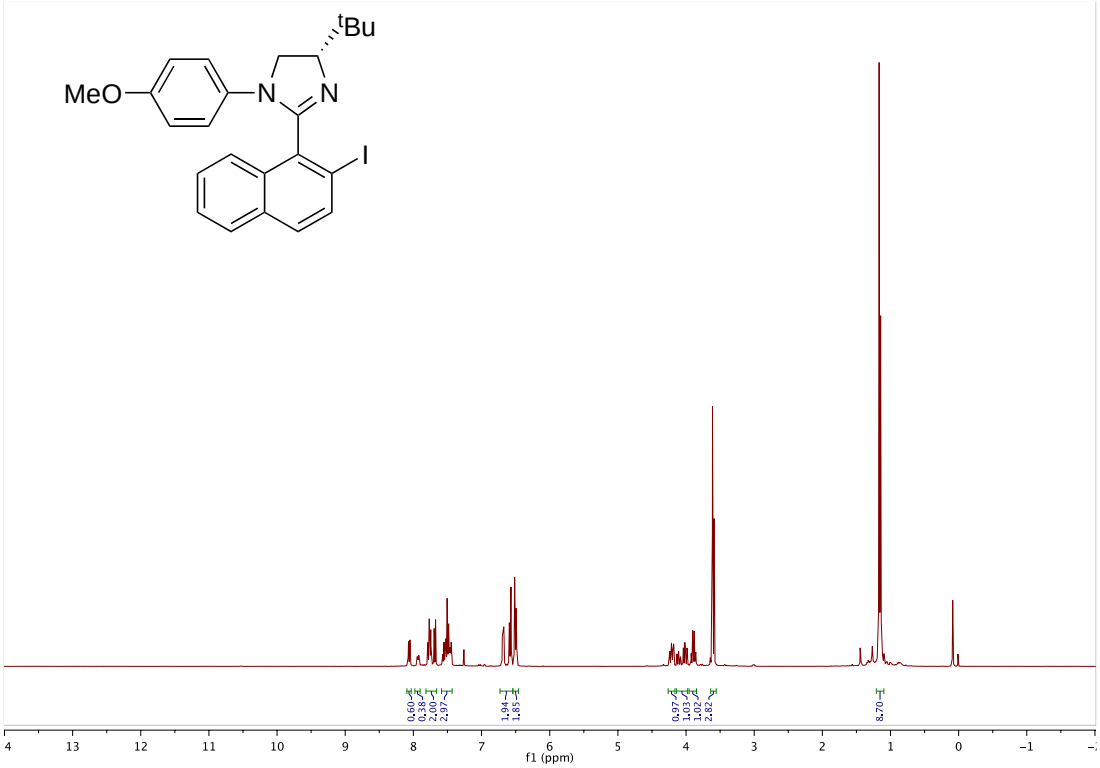

^{13}C NMR (101 MHz, $CDCl_3$)

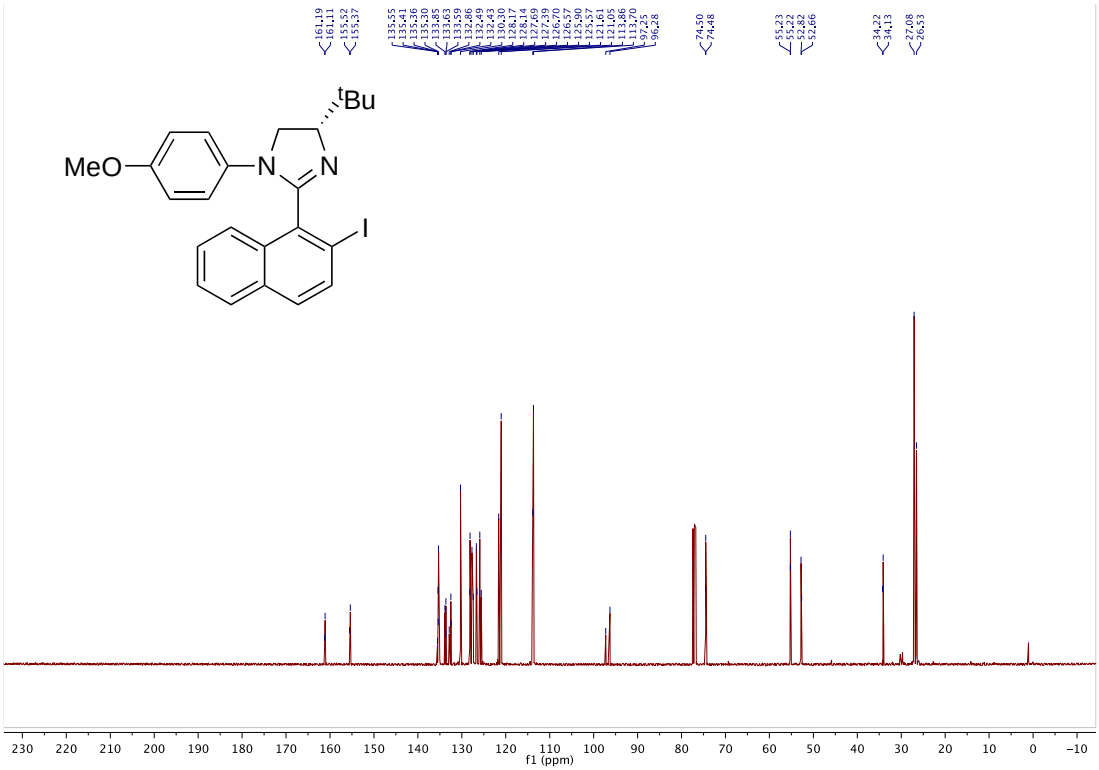

^{1}H NMR (500 MHz, $CDCl_3$)

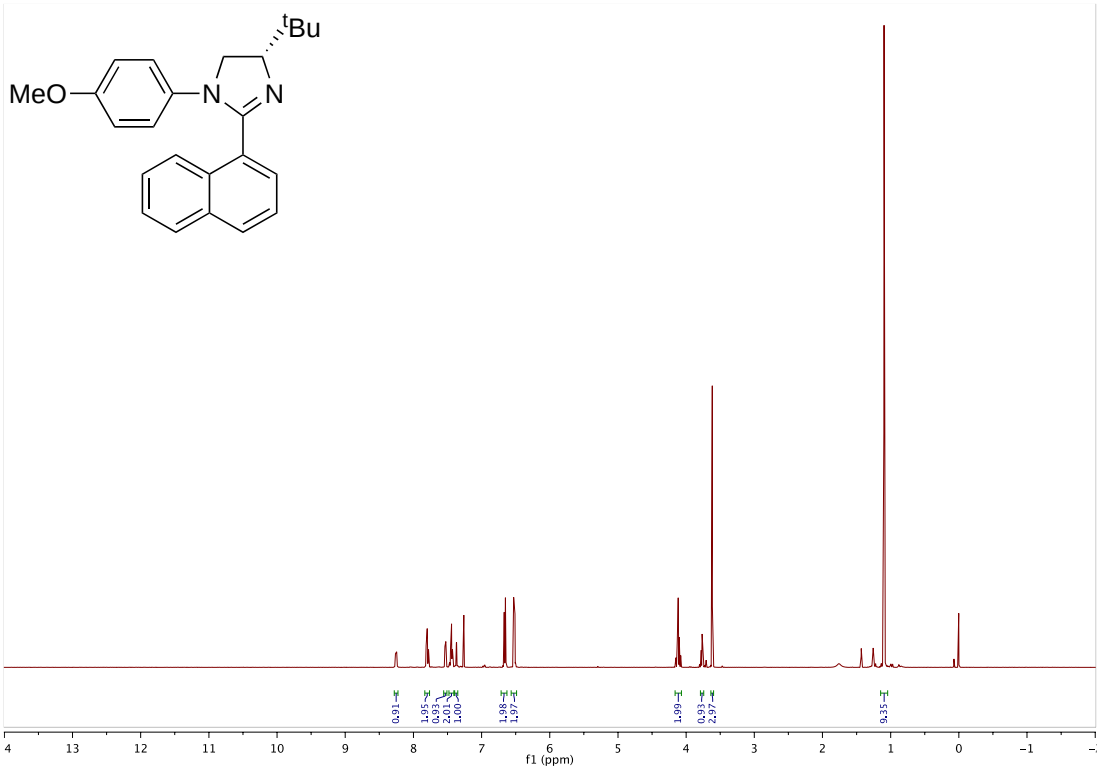

^{13}C NMR (126 MHz, $CDCl_3$)

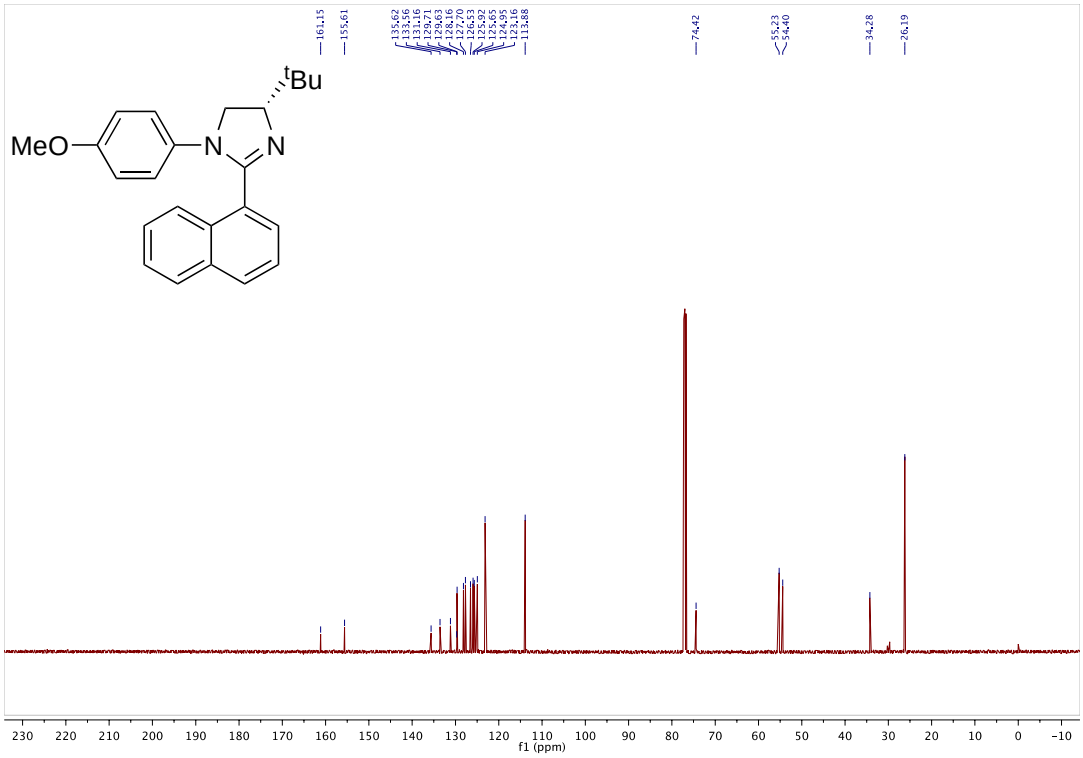

Compound **87**

^{1}H NMR (600 MHz, $CDCl_3$)

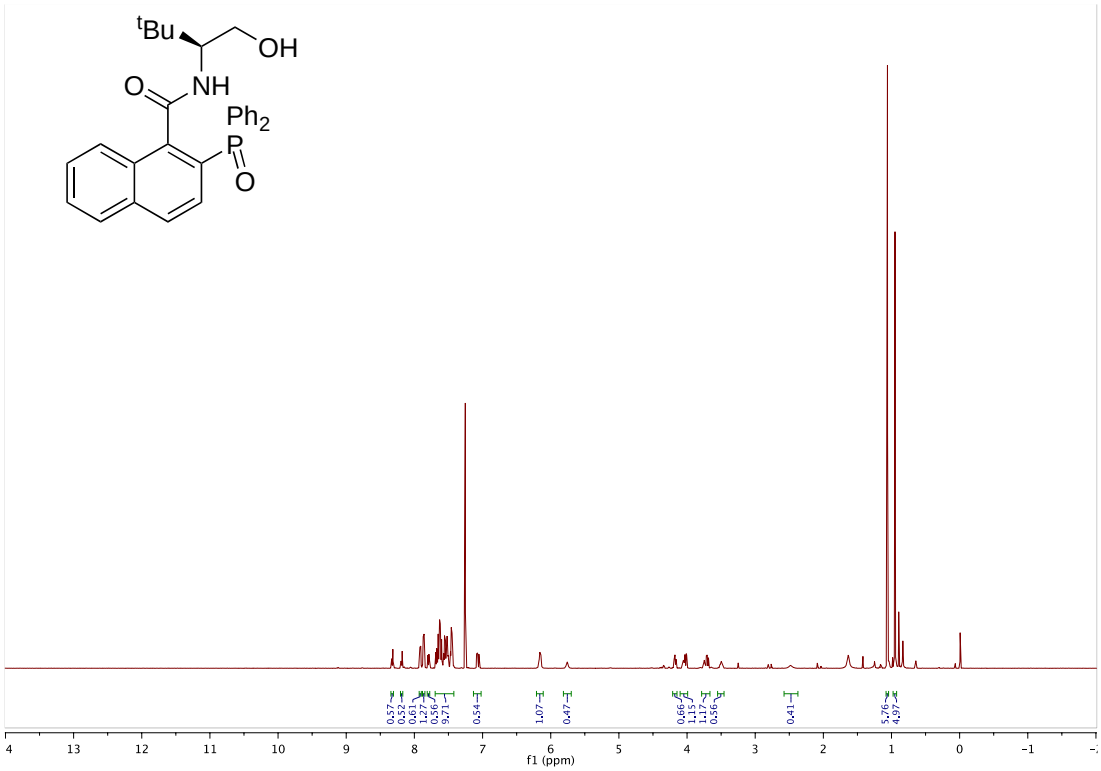

^{13}C NMR (151 MHz, $CDCl_3$) (Phosphorus decoupled)

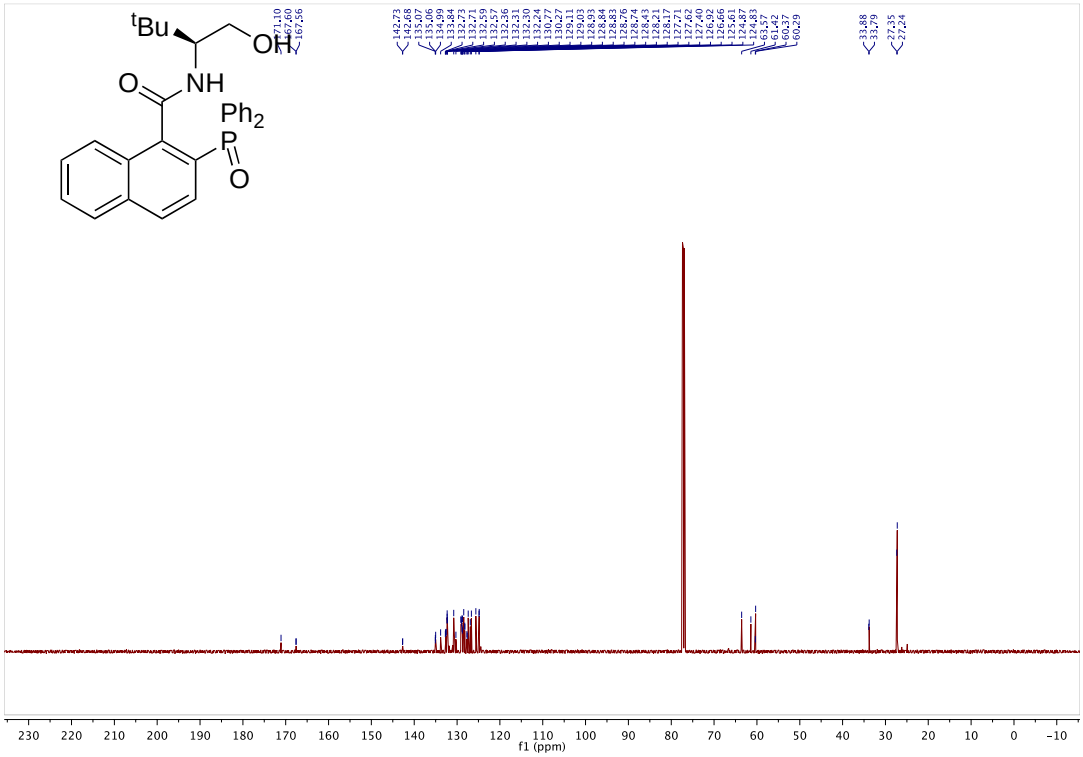

^{31}P NMR (243 MHz, $CDCl_3$)

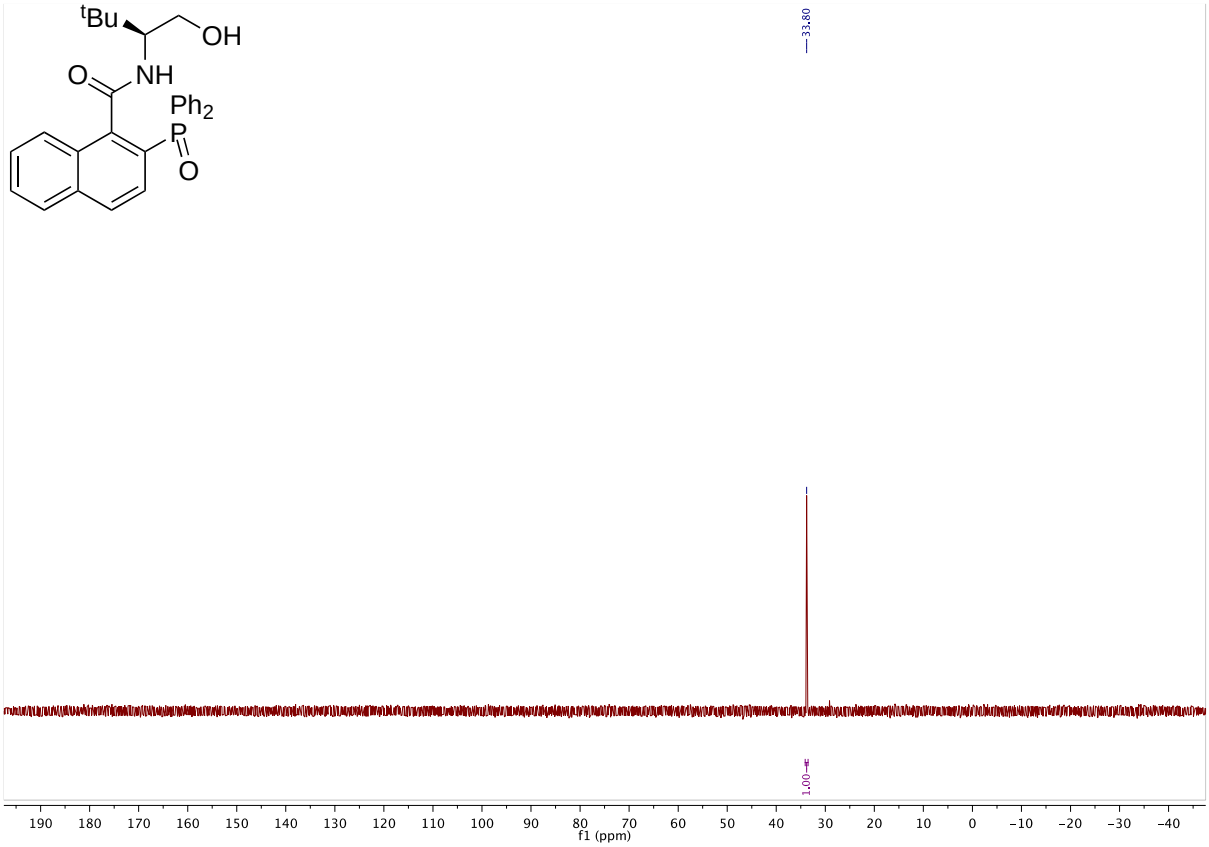

Compound **89**

^{1}H NMR (600 MHz, $CDCl_3$)

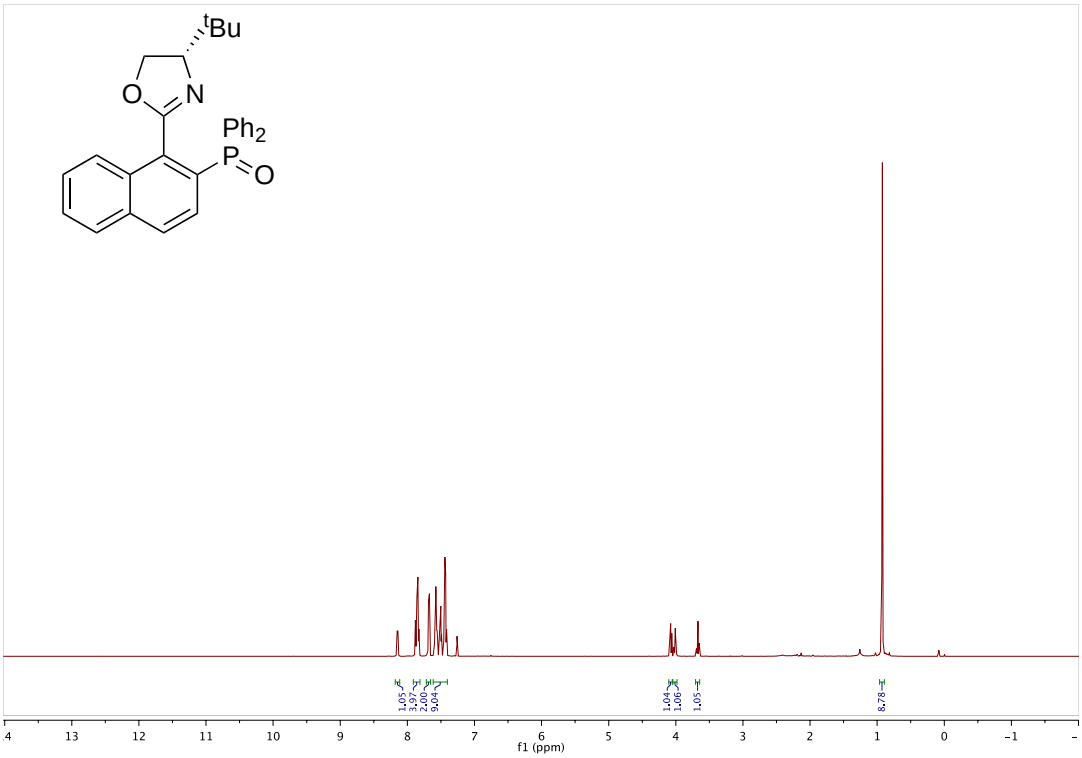

^{13}C NMR (151 MHz, $CDCl_3$)

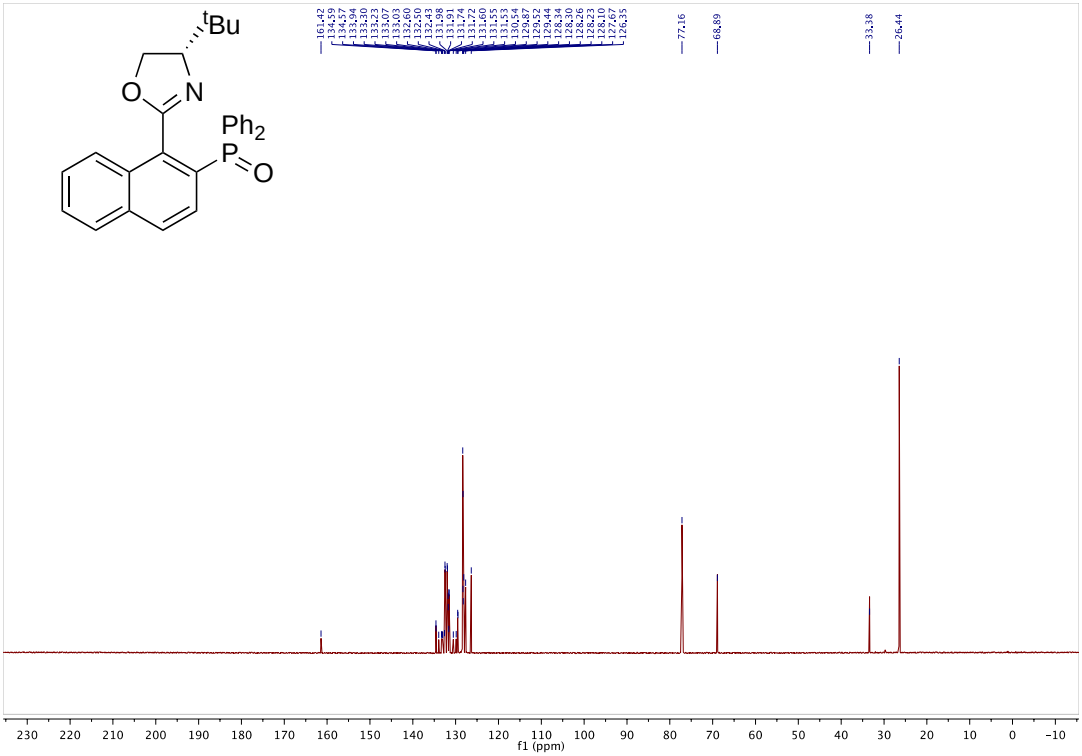

^{31}P NMR ($CDCl_3$, 243 MHz)

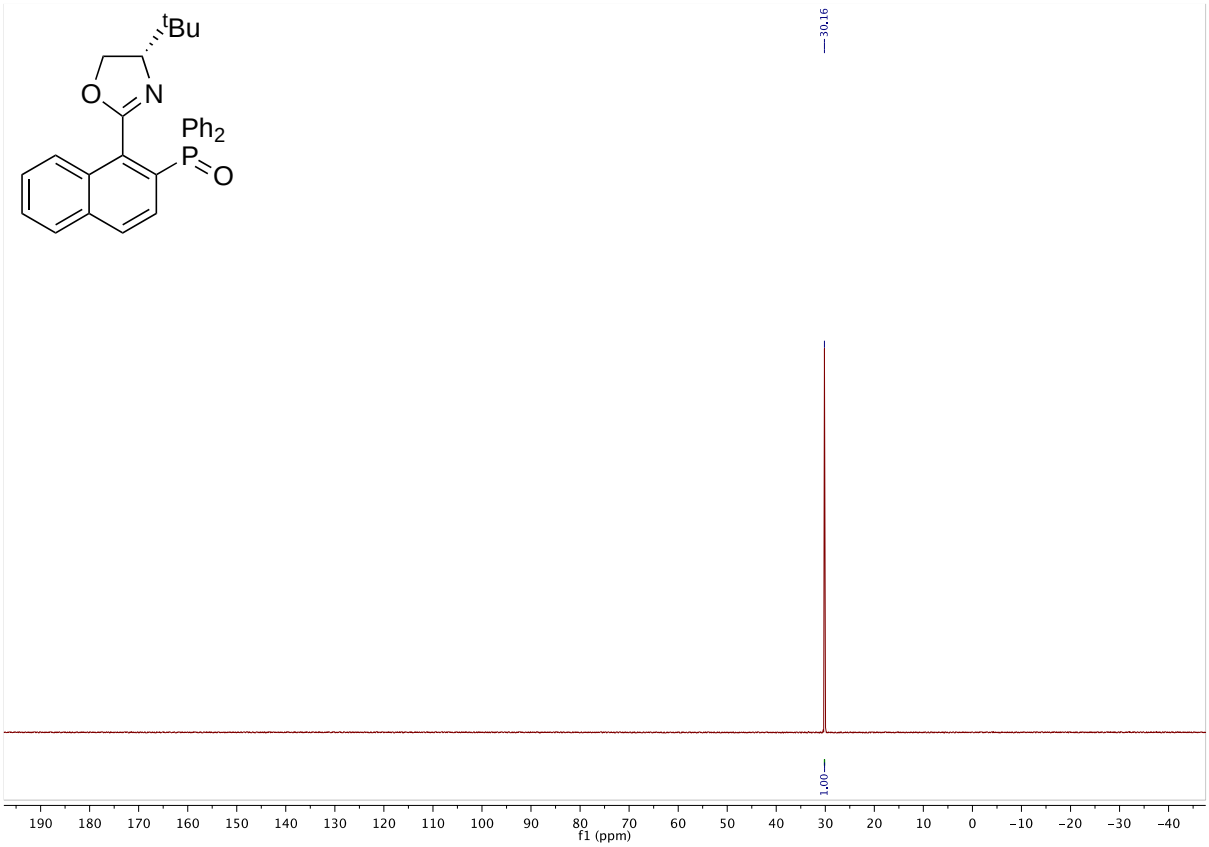

^{1}H NMR (500 MHz, $CDCl_3$)

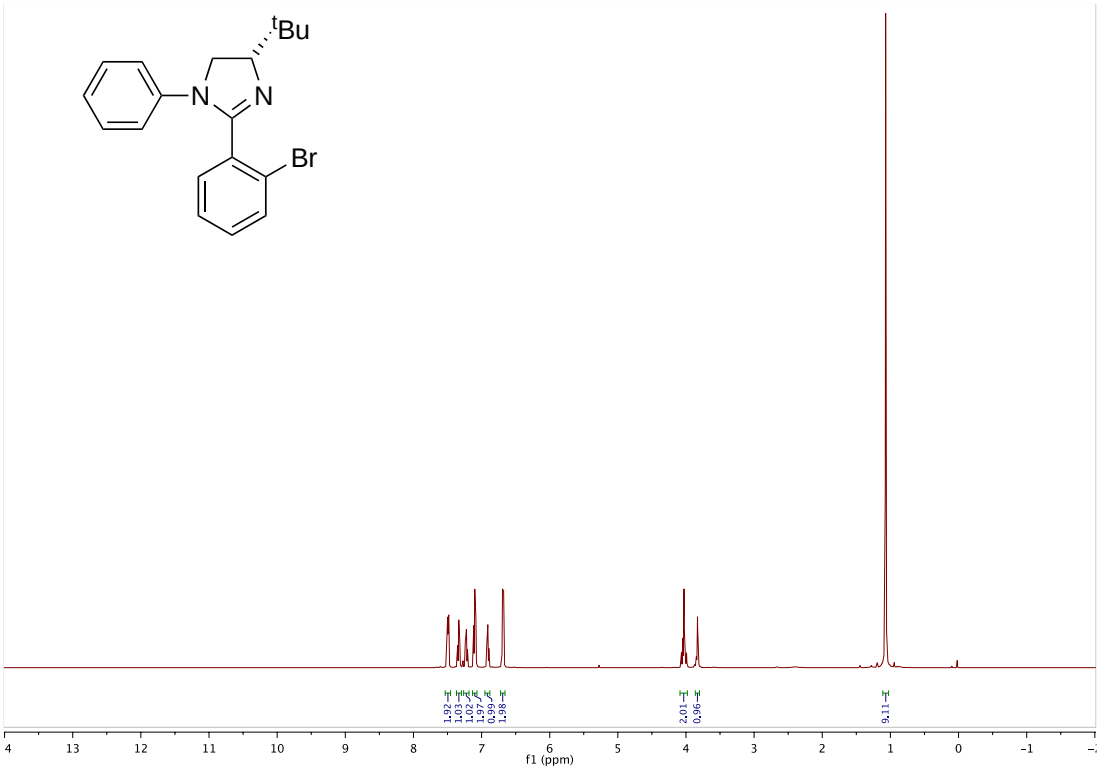

^{13}C NMR (126 MHz, CDC_3)

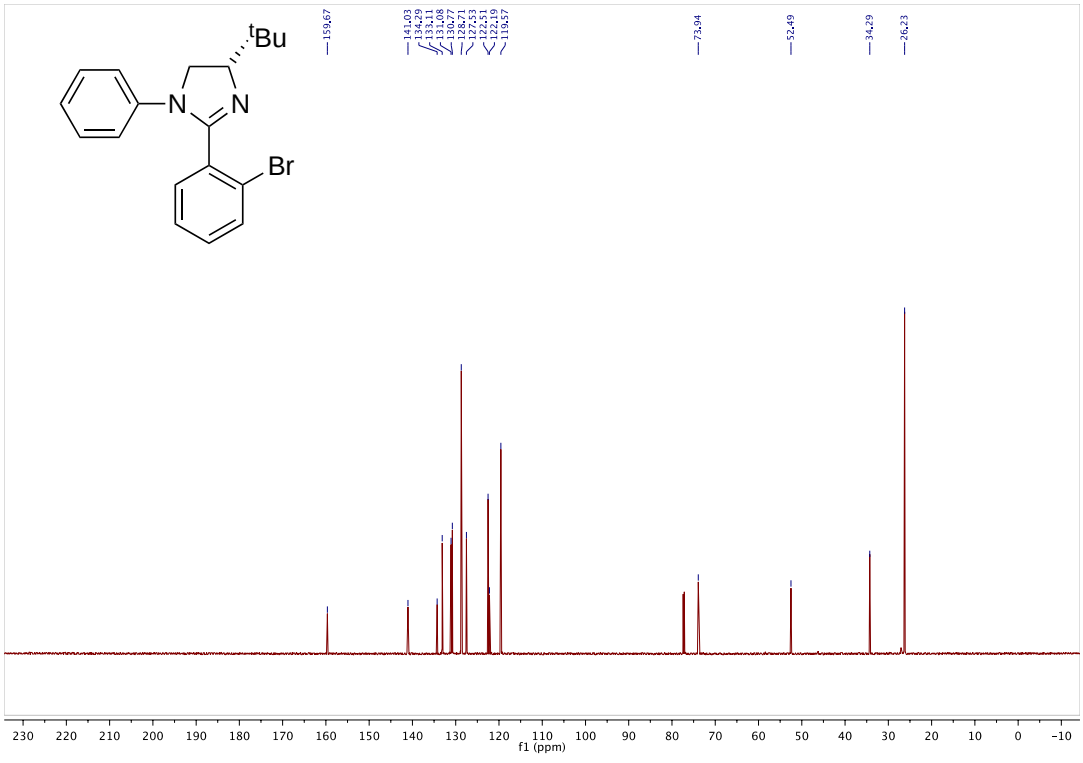

^{1}H NMR (400 MHz, $CDCl_3$)

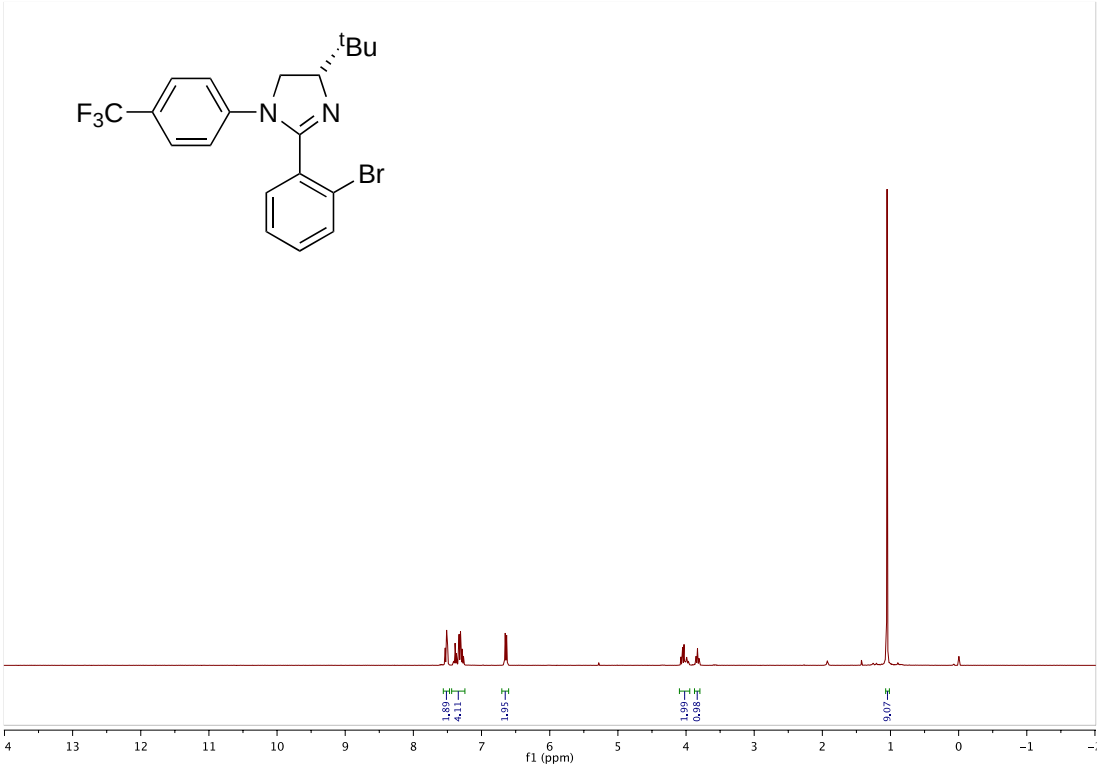

^{13}C NMR (101 MHz, $CDCl_3$)

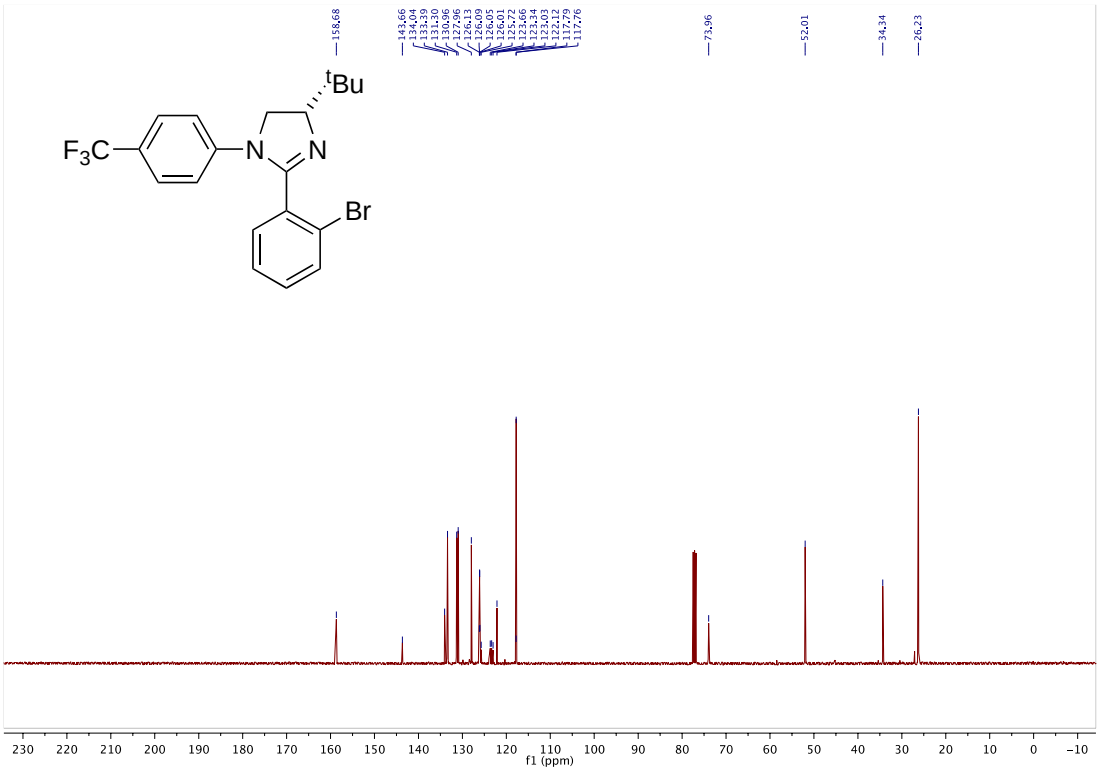

^{19}F NMR (376 MHz, $CDCl_3$)

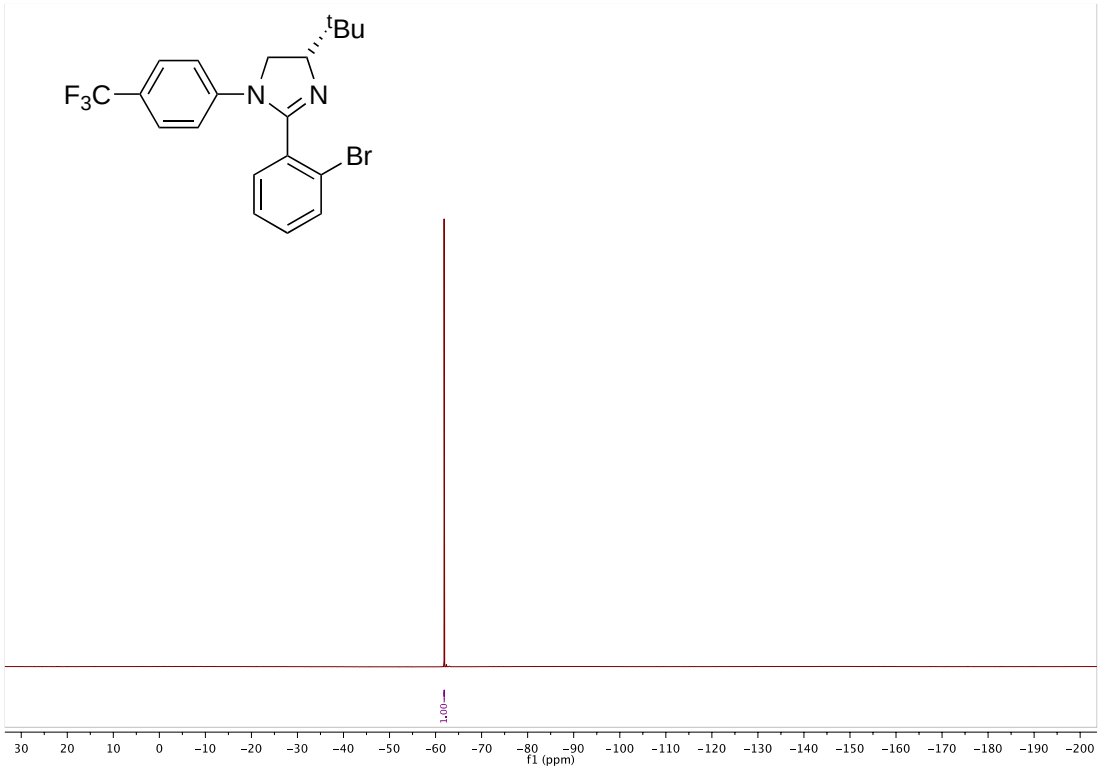

^{1}H NMR (400 MHz, $CDCl_3$)

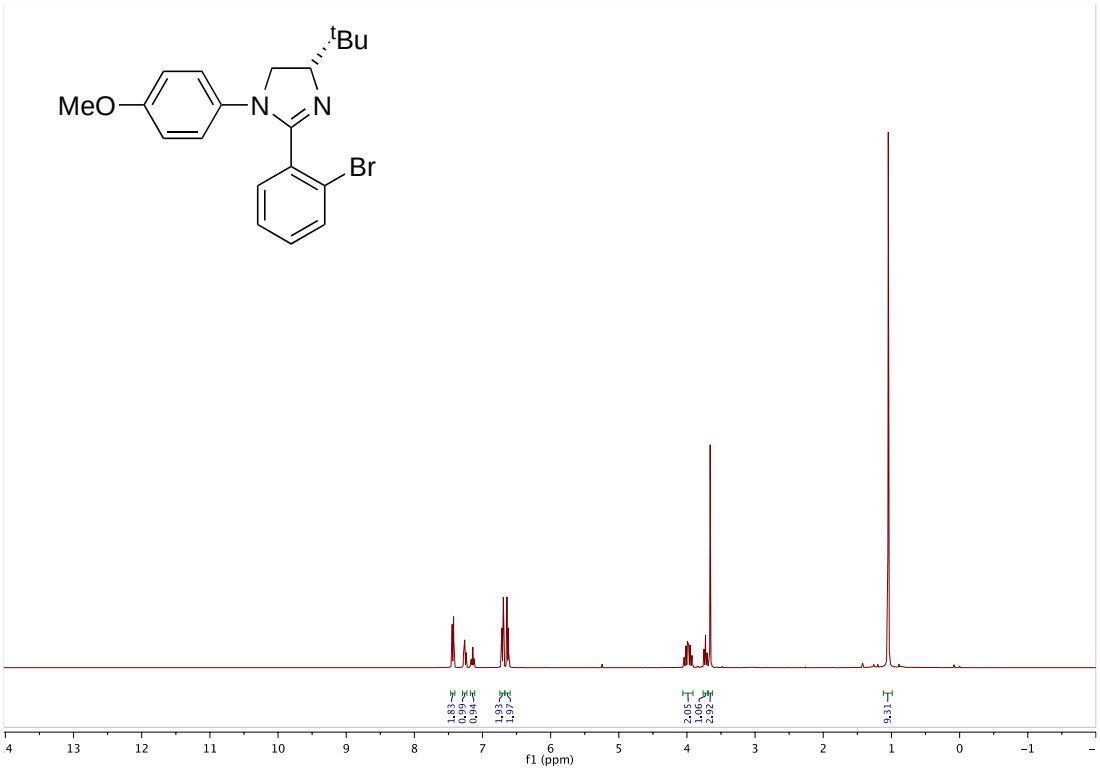

^{13}C NMR (101 MHz, $CDCl_3$)

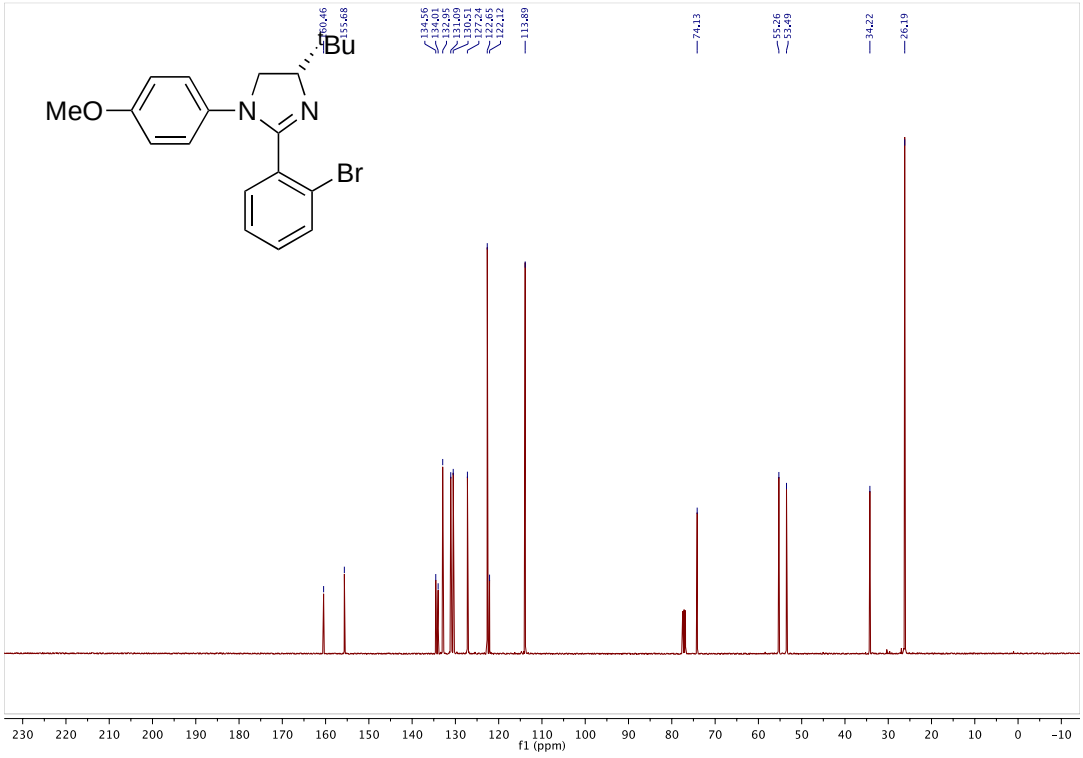

X-Ray Crystallographic Structure and Information for 2-Iodo-1-naphthoic acid

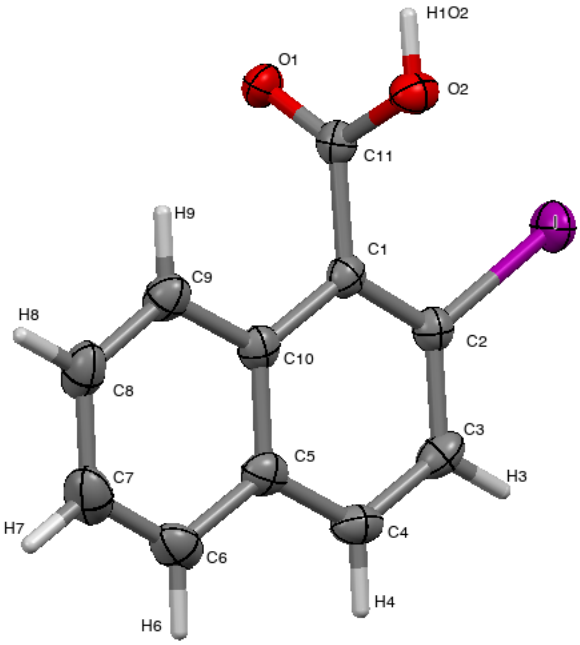

Identification code: gui177

Empirical formula: $C_{11}H_7IO_2$

Formula weight: 298.07

Temperature: 100(2) K

Wavelength: 1.54184 Å

Crystal system: Tetragonal

Space group: $I4_1/a$ (#88)

Unit cell dimensions: a = 20.18990(4) Å α= 90°. b = 20.1890(4) Å β= 90°

c = 9.9058(3) Å γ = 90°.

Volume: 4037.56 Å3

Z: 16

Density (calculated) 1.961 Mg/m^3

Absorption coefficient: 24/689 mm^{-1}

F(000): 2272

Crystal size: 0.284 x 0.228 x 0.065 mm^3

Theta range for data collection: 4.380 to 76.818°.

Index ranges: –25<=h<=24, –24<=k<=24, –12<=l<=12

Reflections collected: 13890

Independent reflections 2117 [R(int) = 0.0439]

Completeness to theta: 69.684° 100 %

Absorption correction: Gaussian

Max. and min. transmission: 0.393 and 0.063

Refinement method: Full–matrix least–squares on F^2

Data / restraints / parameters: 2117 / 0 / 130

Goodness–of–fit on F^2: 1.085

Final R indices [I>2sigma(I)]: R1 = 0.0243, wR2 = 0.0607

R indices (all data): R1 = 0.0260, wR2 = 0.0617

Extinction coefficient n/a

Largest diff. peak and hole: 0.492 and –0.588 e.$Å^{-3}$

Table 2. Atomic coordinates (x 10^4) and equivalent isotropic displacement parameters ($Å^2$x 10^3) for *J*B3.21. U(eq) is defined as one third of the trace of the orthogonalized U^{iJ} tensor.

Atom	x	y	z	U(eq)
C(1)	5860(1)	4418(1)	5290(3)	22(1)
C(11)	6360(1)	4689(1)	6255(3)	22(1)
O(1)	6938(1)	4507(1)	6263(2)	27(1)
O(2)	6131(1)	5138(1)	7081(2)	28(1)
C(2)	5408(1)	3951(1)	5700(3)	24(1)
I	5424(1)	3575(1)	7676(1)	32(1)
C(3)	4950(2)	3668(2)	4793(3)	28(1)
C(4)	4966(2)	3855(2)	3469(3)	29(1)
C(5)	5424(1)	4330(2)	2992(3)	26(1)
C(6)	5447(2)	4520(2)	1608(3)	34(1)
C(7)	5894(2)	4976(2)	1177(3)	40(1)
C(8)	6341(2)	5269(2)	2090(4)	37(1)
C(9)	6333(2)	5100(2)	3430(3)	30(1)

C(10)	5876(1)	4622(1)	3912(3)	24(1)

Table 3. Bond lengths [Å] and angles [°] for *J*B3.21.

C(1)–C(2)	1.372(4)
C(1)–C(10)	1.427(4)
C(1)–C(11)	1.495(4)
C(11)–O(1)	1.222(4)
C(11)–O(2)	1.306(3)
O(2)–H(1O2)	0.85(5)
C(2)–C(3)	1.410(4)
C(2)–I	2.100(3)
C(3)–C(4)	1.365(5)
C(3)–H(3)	0.9500
C(4)–C(5)	1.415(5)
C(4)–H(4)	0.9500
C(5)–C(10)	1.418(4)
C(5)–C(6)	1.424(4)
C(6)–C(7)	1.359(5)
C(6)–H(6)	0.9500
C(7)–C(8)	1.408(5)
C(7)–H(7)	0.9500
C(8)–C(9)	1.370(5)
C(8)–H(8)	0.9500
C(9)–C(10)	1.418(4)
C(9)–H(9)	0.9500
C(2)–C(1)–C(10)	119.8(3)
C(2)–C(1)–C(11)	120.8(3)
C(10)–C(1)–C(11)	119.3(2)
O(1)–C(11)–O(2)	122.9(3)
O(1)–C(11)–C(1)	122.5(3)
O(2)–C(11)–C(1)	114.5(2)
C(11)–O(2)–H(1O2)	114(3)
C(1)–C(2)–C(3)	121.7(3)

C(1)–C(2)–I	120.9(2)
C(3)–C(2)–I	117.2(2)
C(4)–C(3)–C(2)	119.1(3)
C(4)–C(3)–H(3)	120.5
C(2)–C(3)–H(3)	120.5
C(3)–C(4)–C(5)	121.5(3)
C(3)–C(4)–H(4)	119.2
C(5)–C(4)–H(4)	119.2
C(4)–C(5)–C(10)	119.2(3)
C(4)–C(5)–C(6)	121.6(3)
C(10)–C(5)–C(6)	119.1(3)
C(7)–C(6)–C(5)	120.3(3)
C(7)–C(6)–H(6)	119.8
C(5)–C(6)–H(6)	119.8
C(6)–C(7)–C(8)	120.6(3)
C(6)–C(7)–H(7)	119.7
C(8)–C(7)–H(7)	119.7
C(9)–C(8)–C(7)	120.7(3)
C(9)–C(8)–H(8)	119.7
C(7)–C(8)–H(8)	119.7
C(8)–C(9)–C(10)	120.2(3)
C(8)–C(9)–H(9)	119.9
C(10)–C(9)–H(9)	119.9
C(5)–C(10)–C(9)	119.0(3)
C(5)–C(10)–C(1)	118.7(3)
C(9)–C(10)–C(1)	122.3(3)

Chapter 3 Appendix: Towards a Dynamic Kinetic Resolution System for A3 Coupling Reactions

Compound **19**

^{1}H NMR (500 MHz, $CDCl_3$)

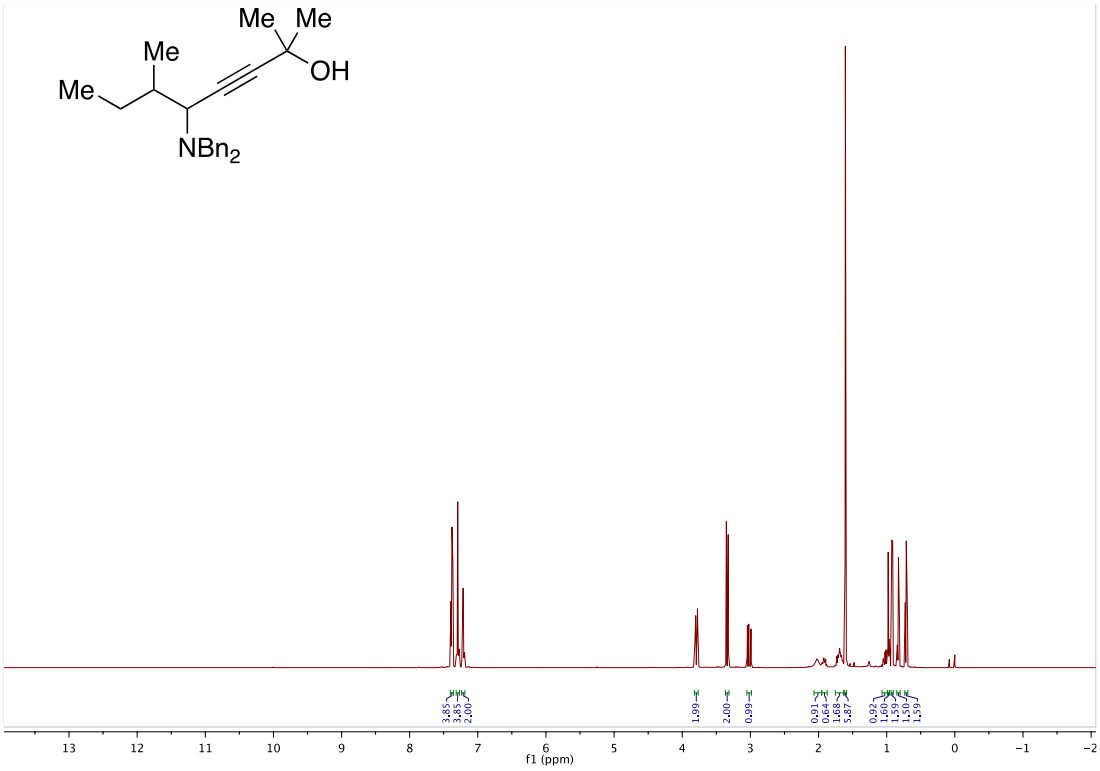

^{13}C NMR (126 MHz, $CDCl_3$)

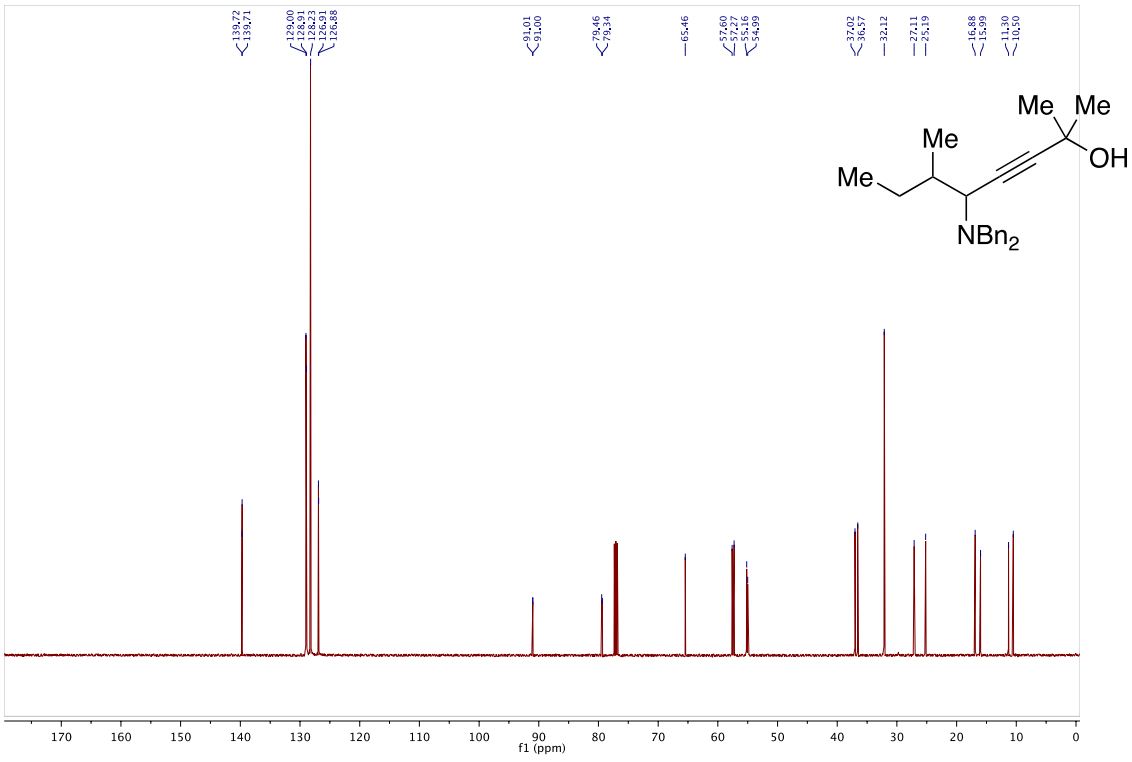

Compound **20**

^{1}H NMR (400 MHz, $CDCl_3$)

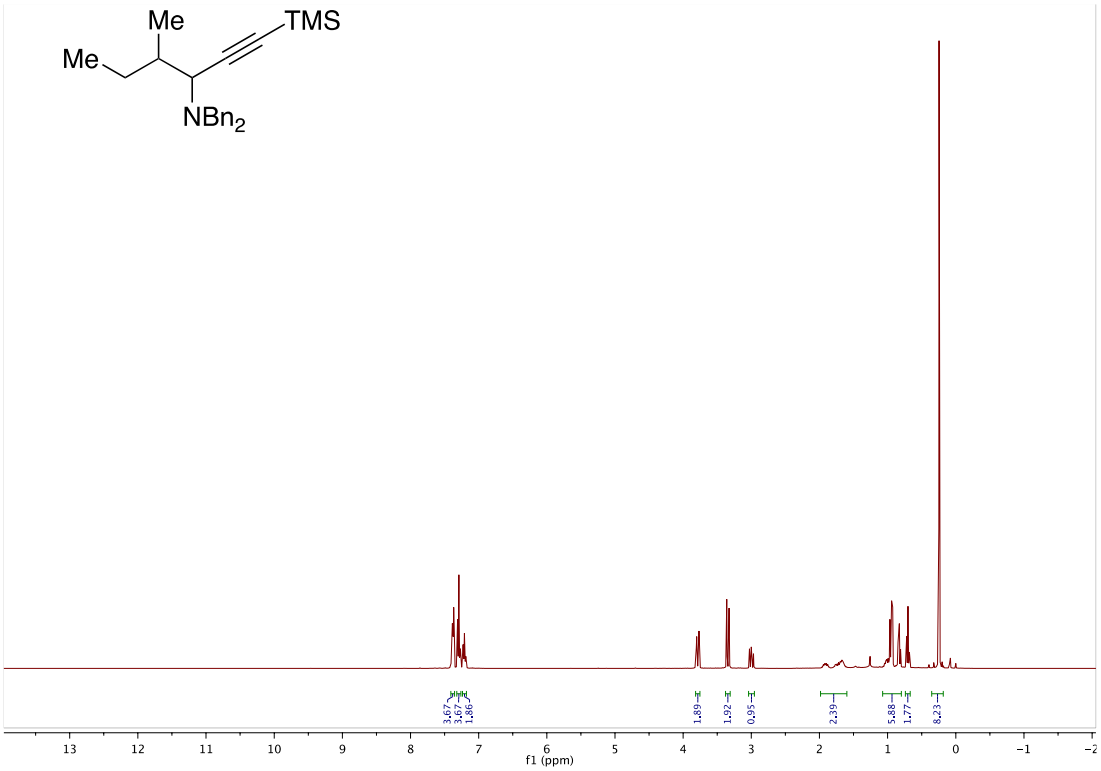

^{13}C NMR (101 MHz, $CDCl_3$)

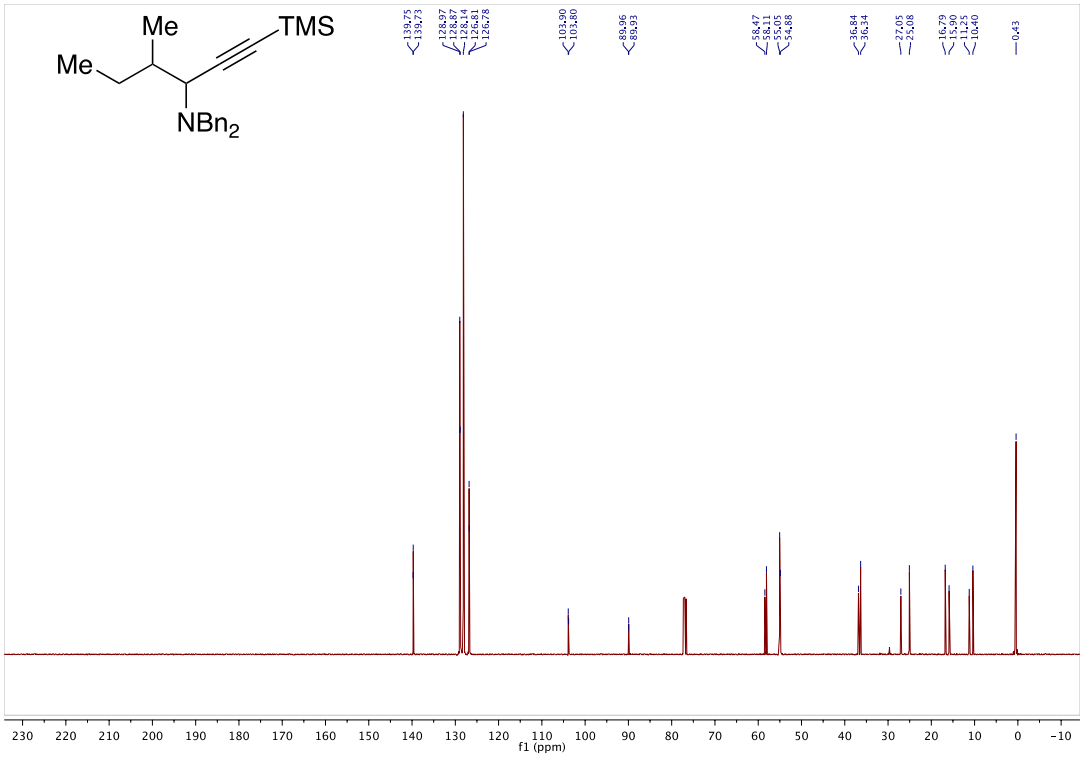

^{1}H NMR (500 MHz, $CDCl_3$)

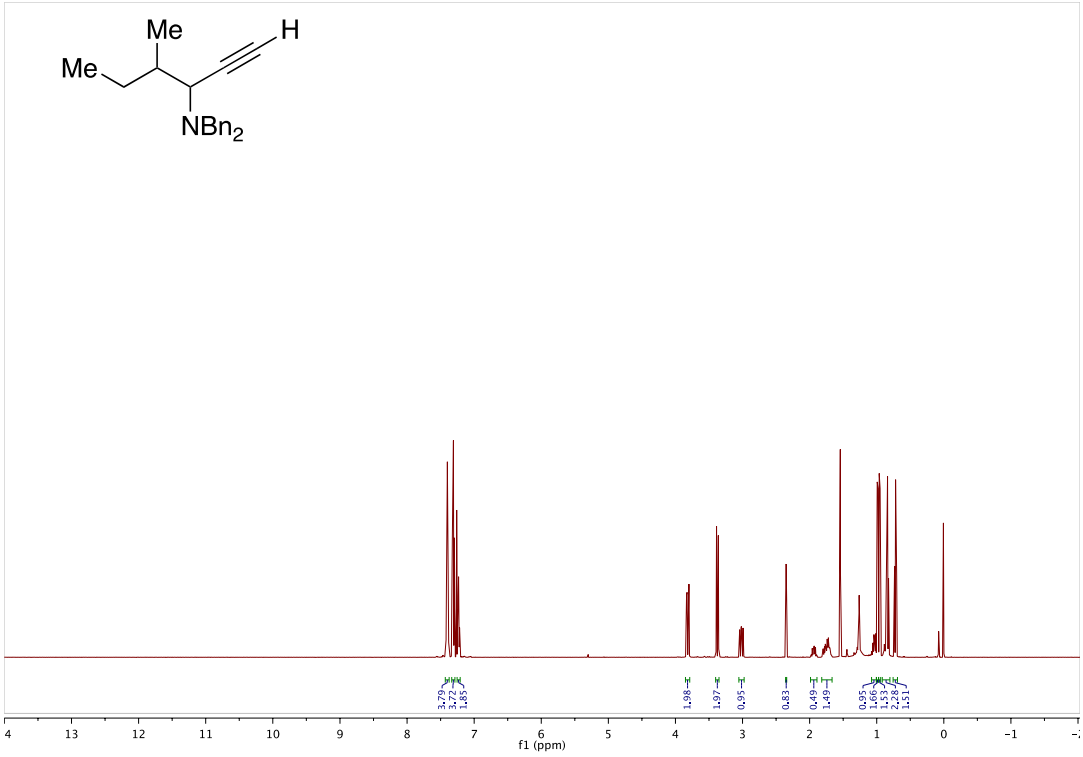

^{13}C NMR (126 MHz, $CDCl_3$)

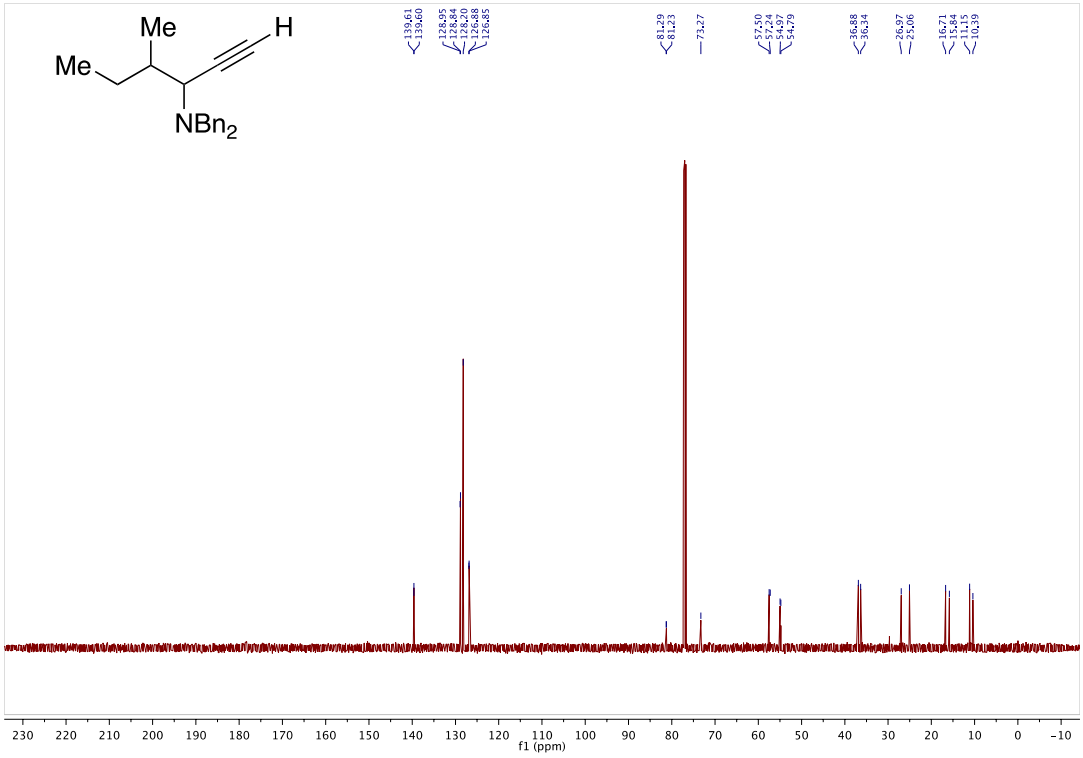

^{1}H NMR (500 MHz, $CDCl_3$)

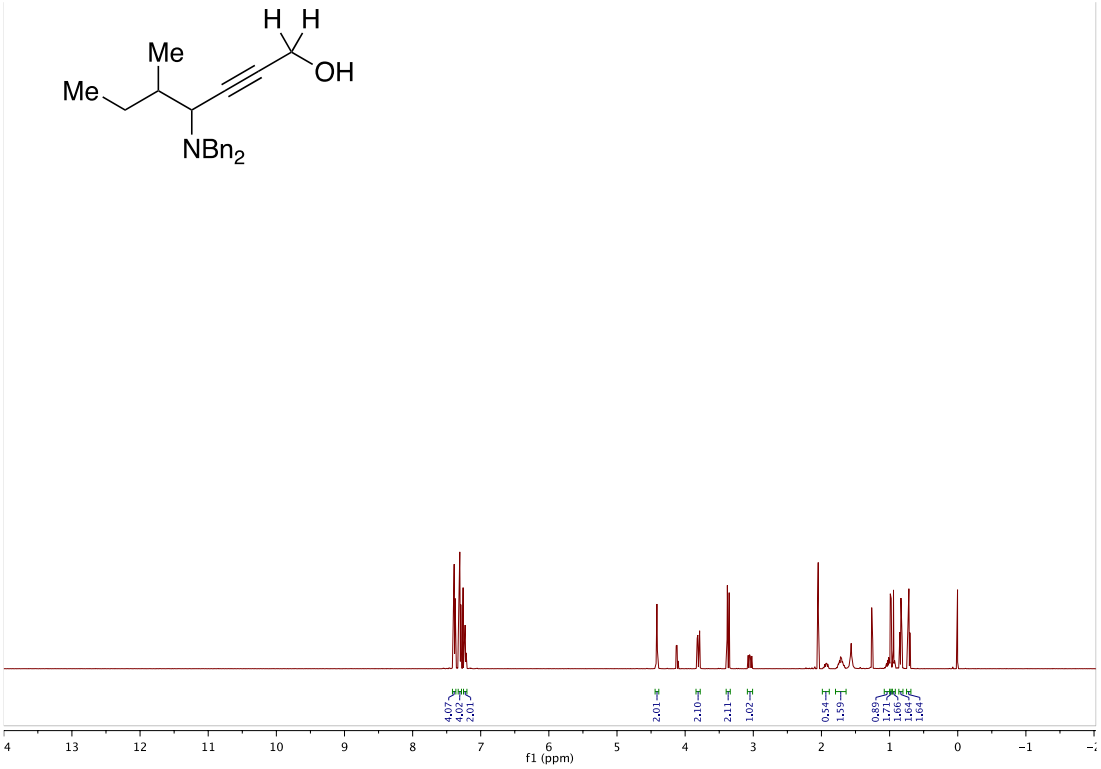

^{13}C NMR (126 MHz, $CDCl_3$)

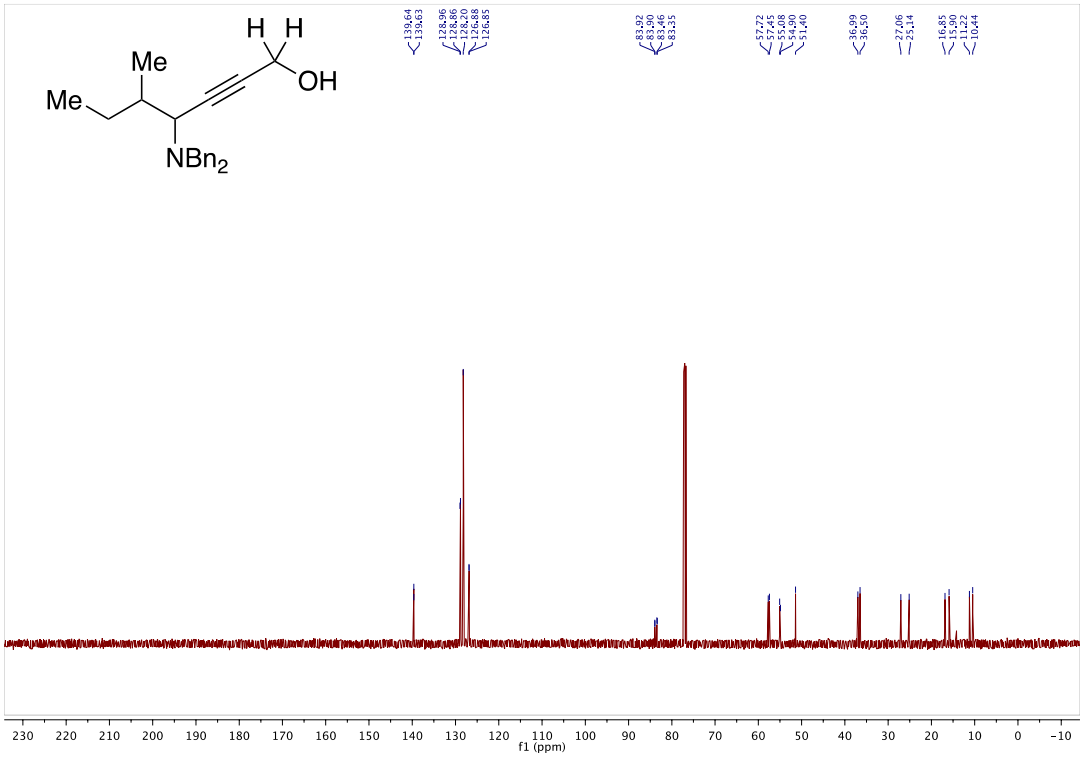

^{1}H NMR (500 MHz, $CDCl_3$)

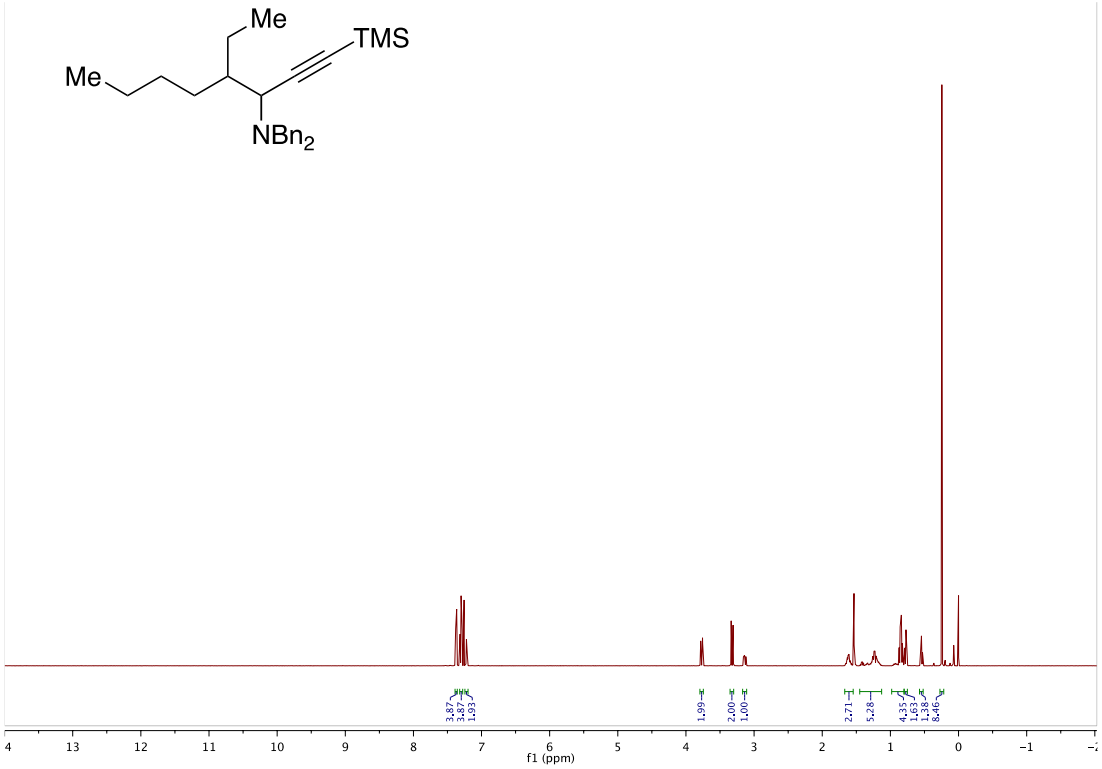

^{13}C NMR (126 MHz, $CDCl_3$)

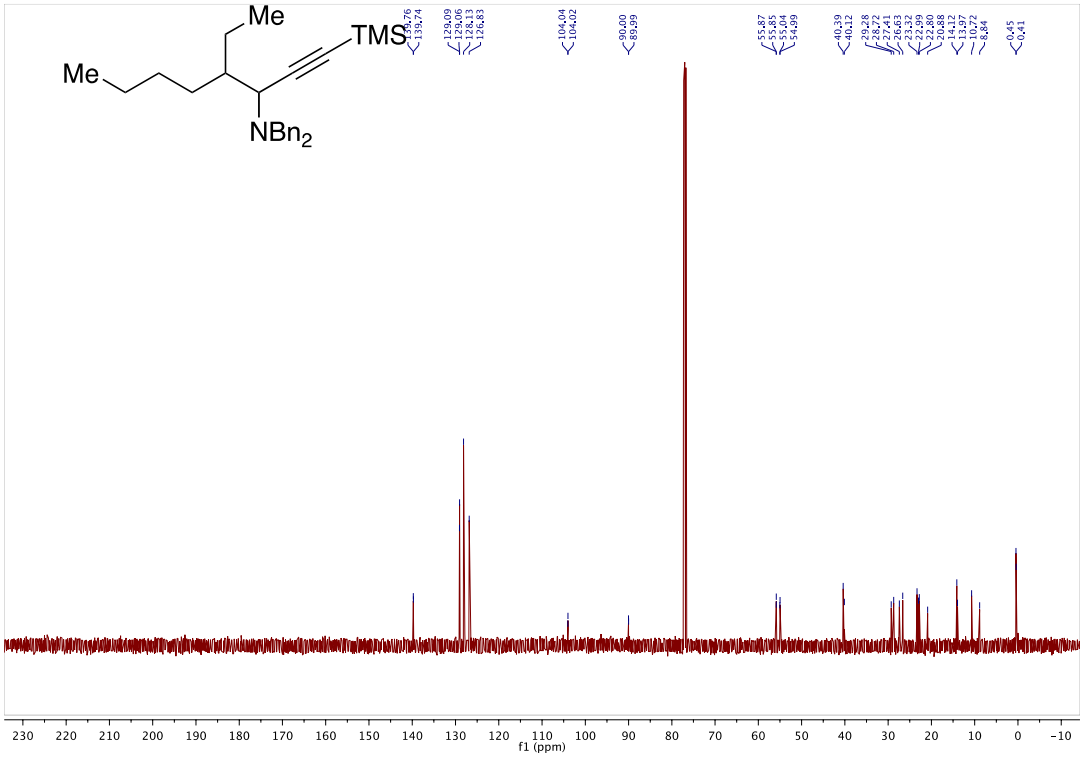

^{1}H NMR (500 MHz, $CDCl_3$)

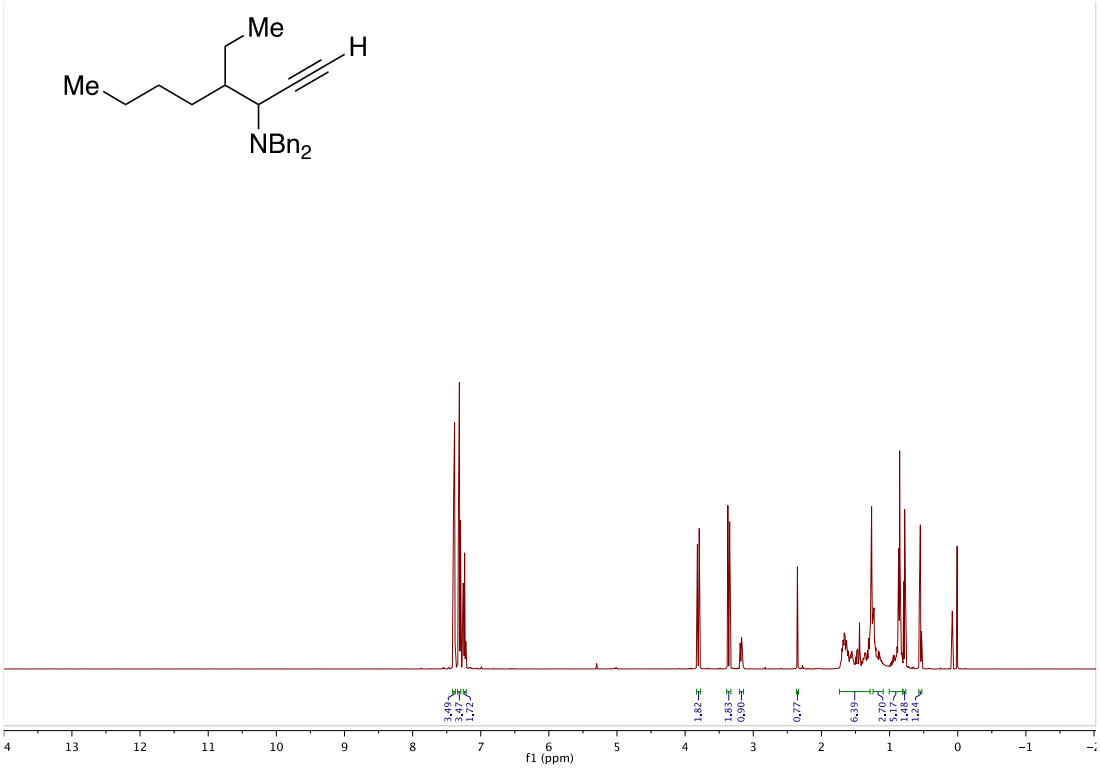

^{13}C NMR (126 MHz, $CDCl_3$)

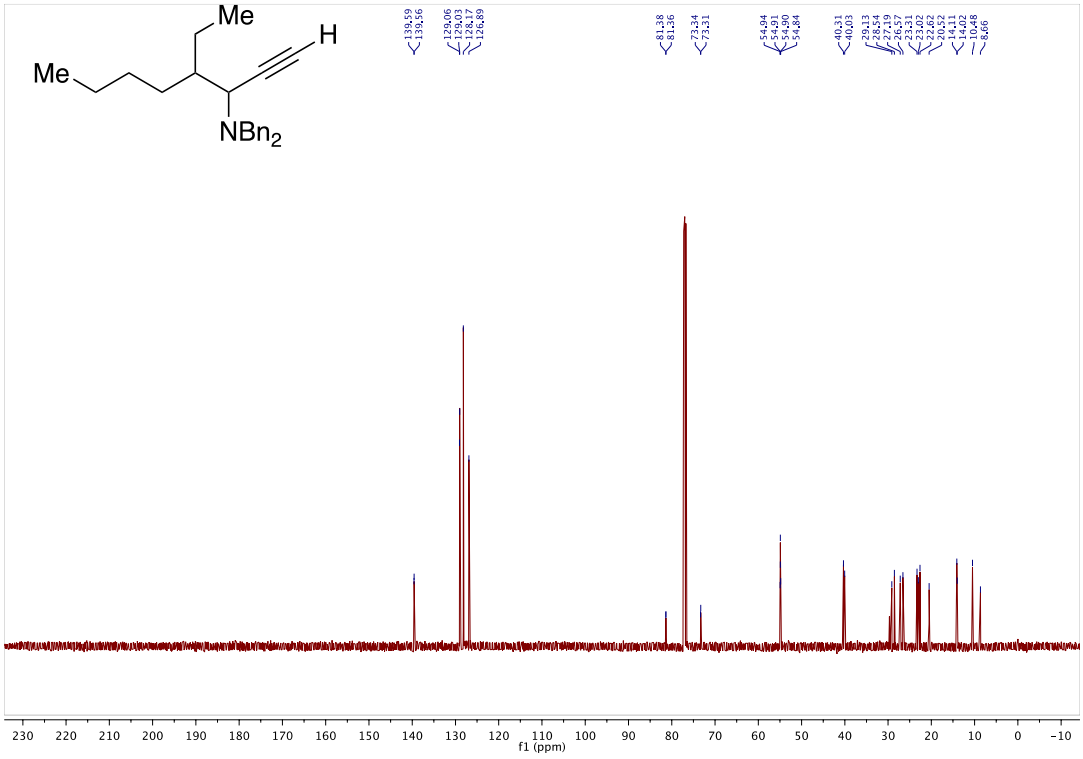

^{1}H NMR (500 MHz, $CDCl_3$)

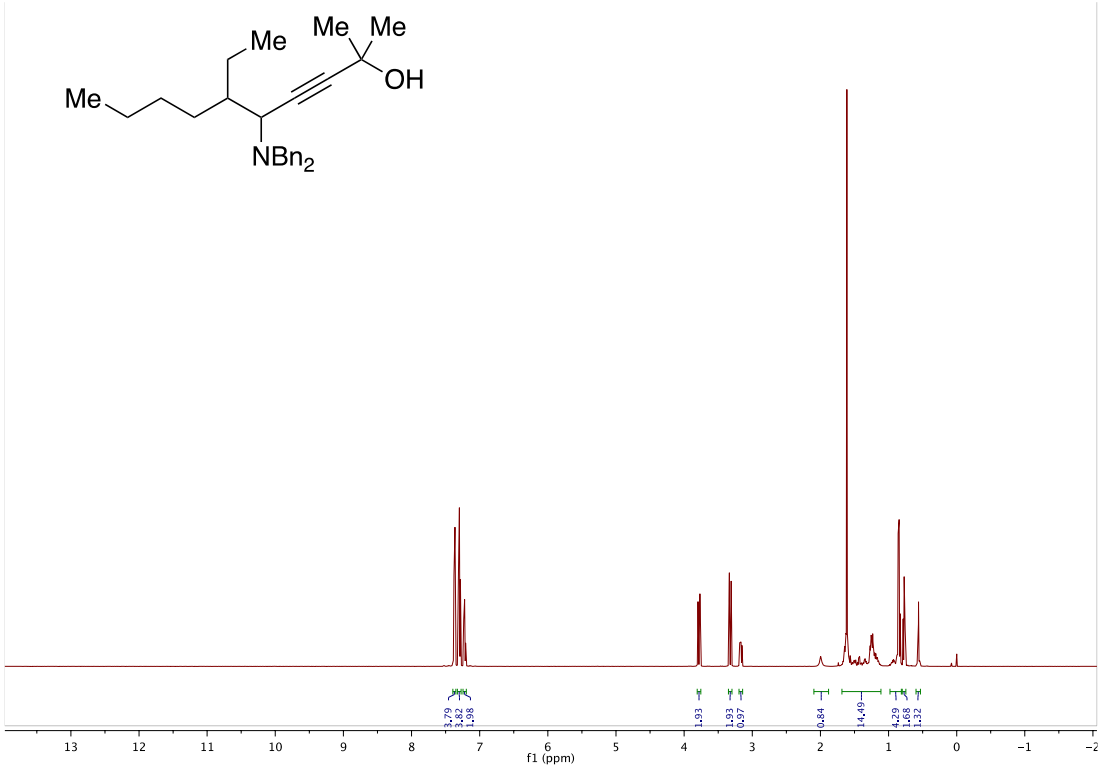

^{13}C NMR (126 MHz, $CDCl_3$)

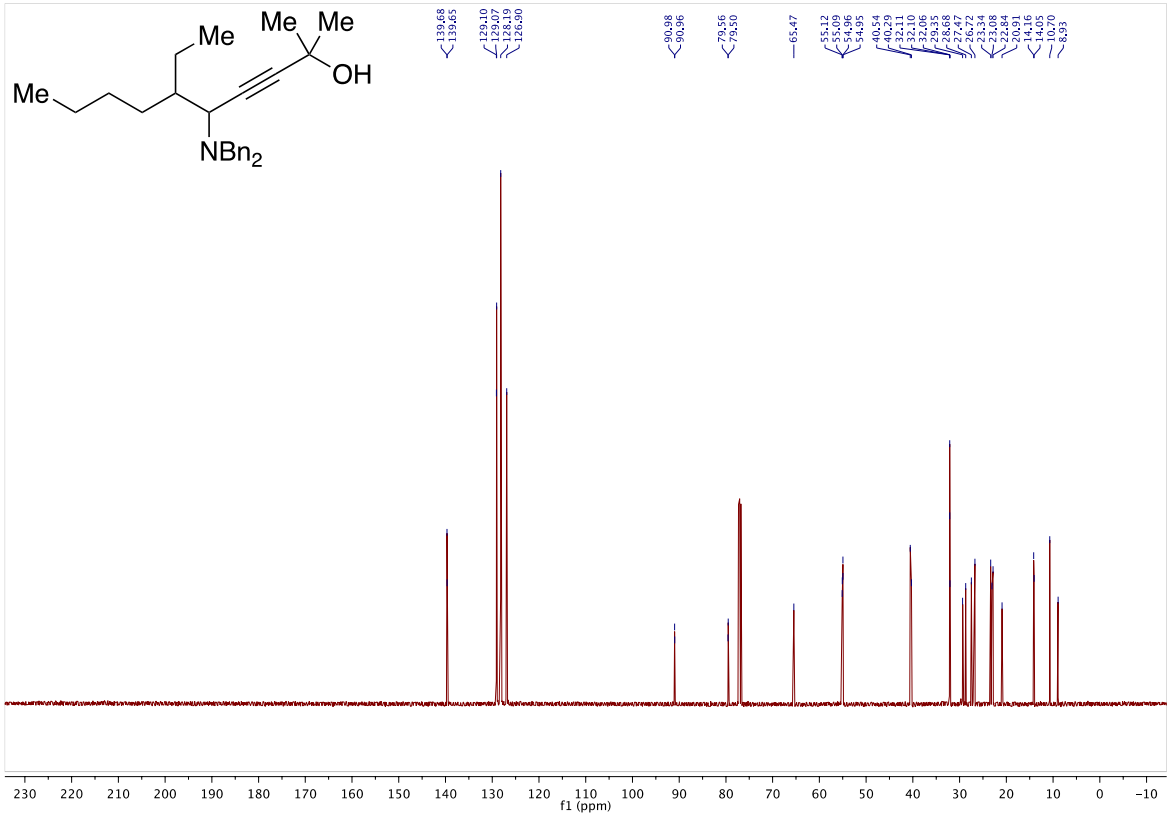

Compound **23**

^{1}H NMR (400 MHz, $CDCl_3$)

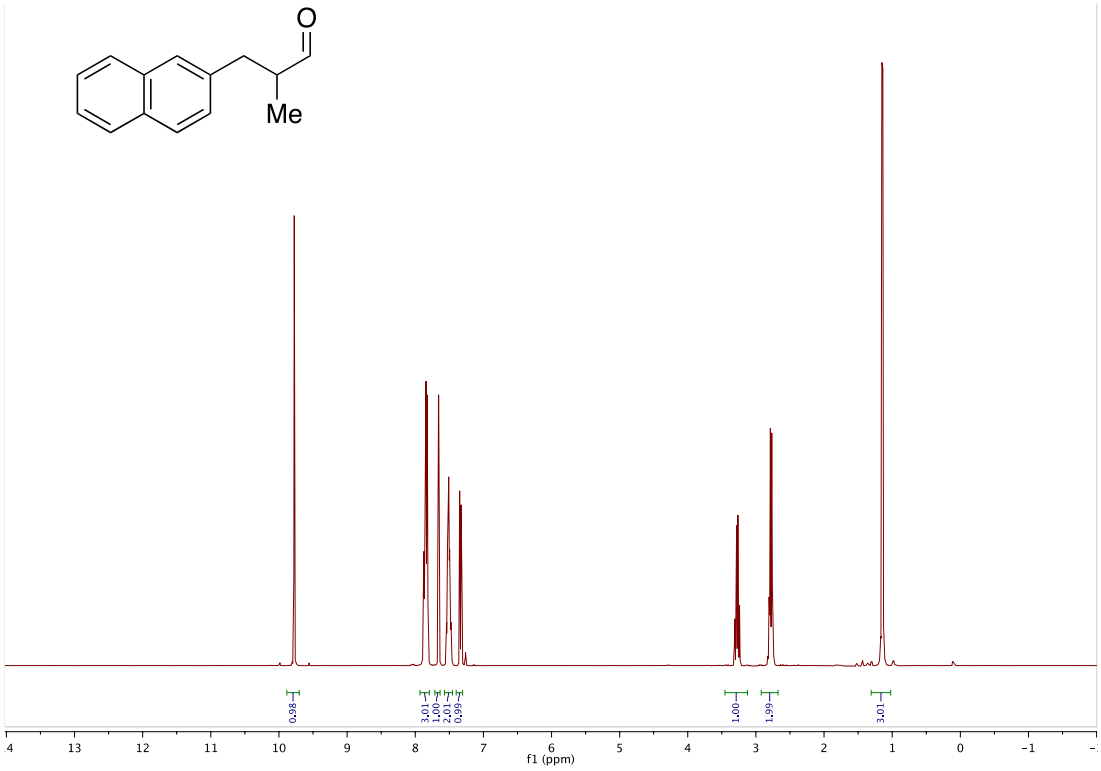

^{13}C NMR (101 MHz, $CDCl_3$)

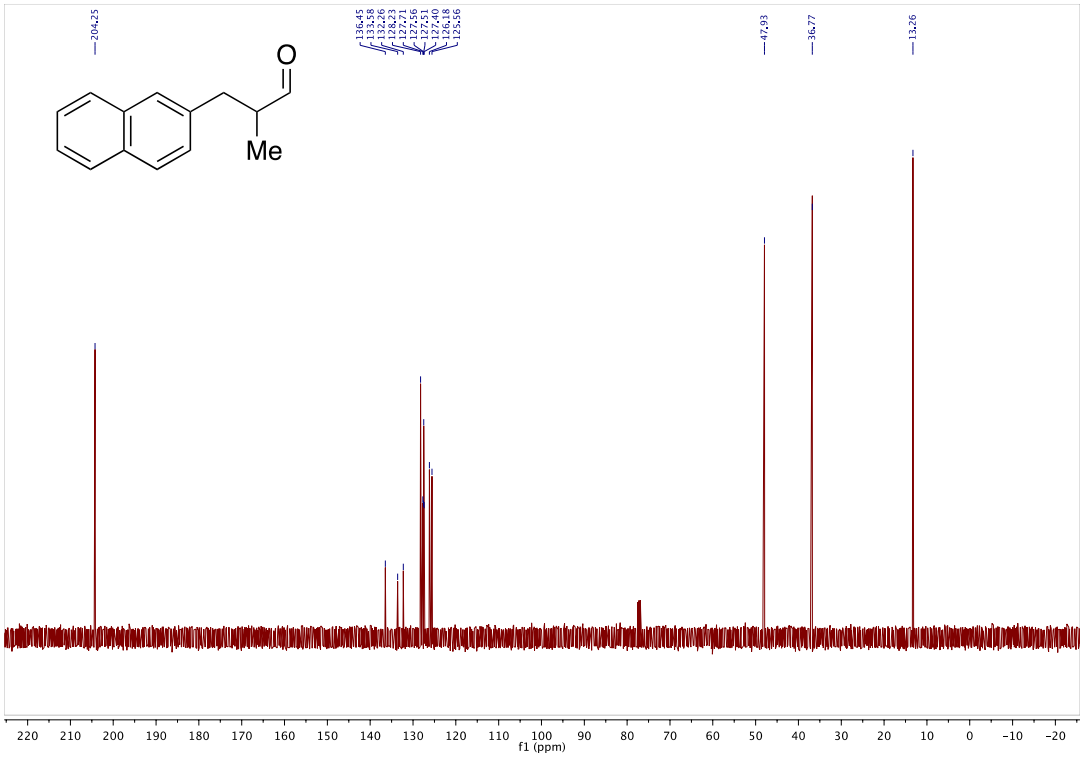

Compound **23**

^{1}H NMR (500 MHz, $CDCl_3$)

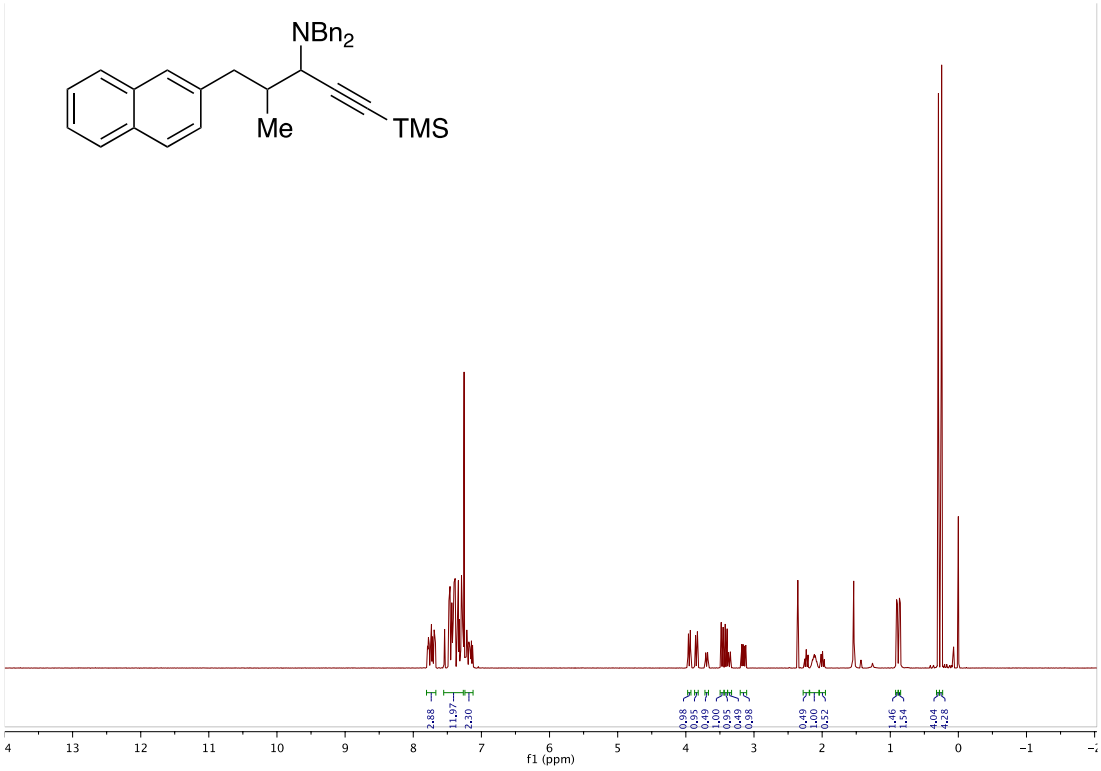

^{13}C NMR (126 MHz, $CDCl_3$)

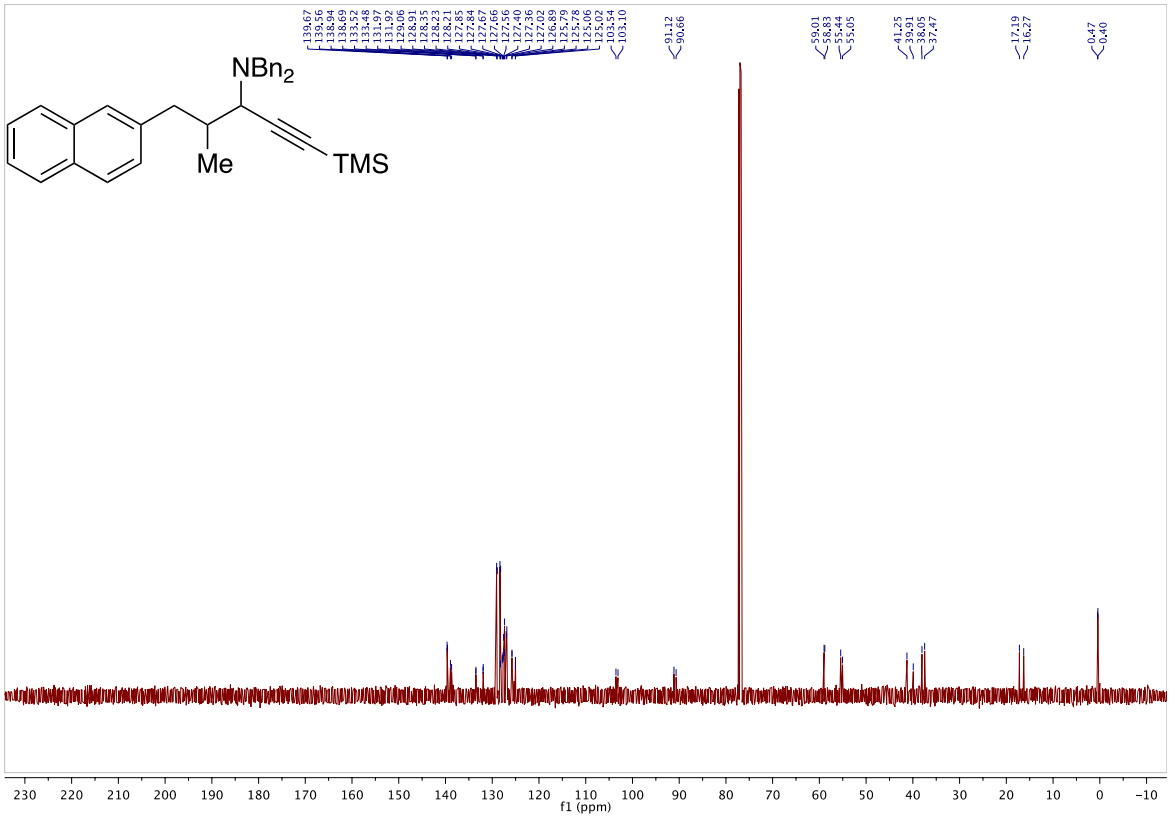

^{1}H NMR (500 MHz, $CDCl_3$)

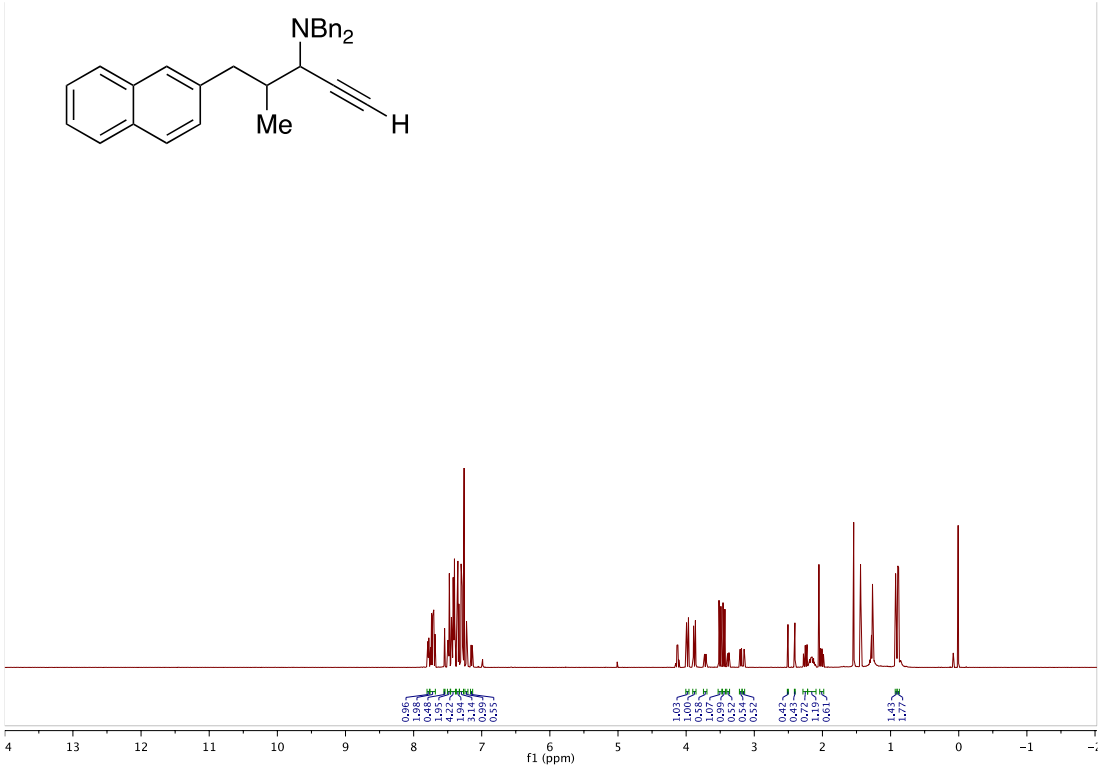

^{13}C NMR (126 MHz, $CDCl_3$)

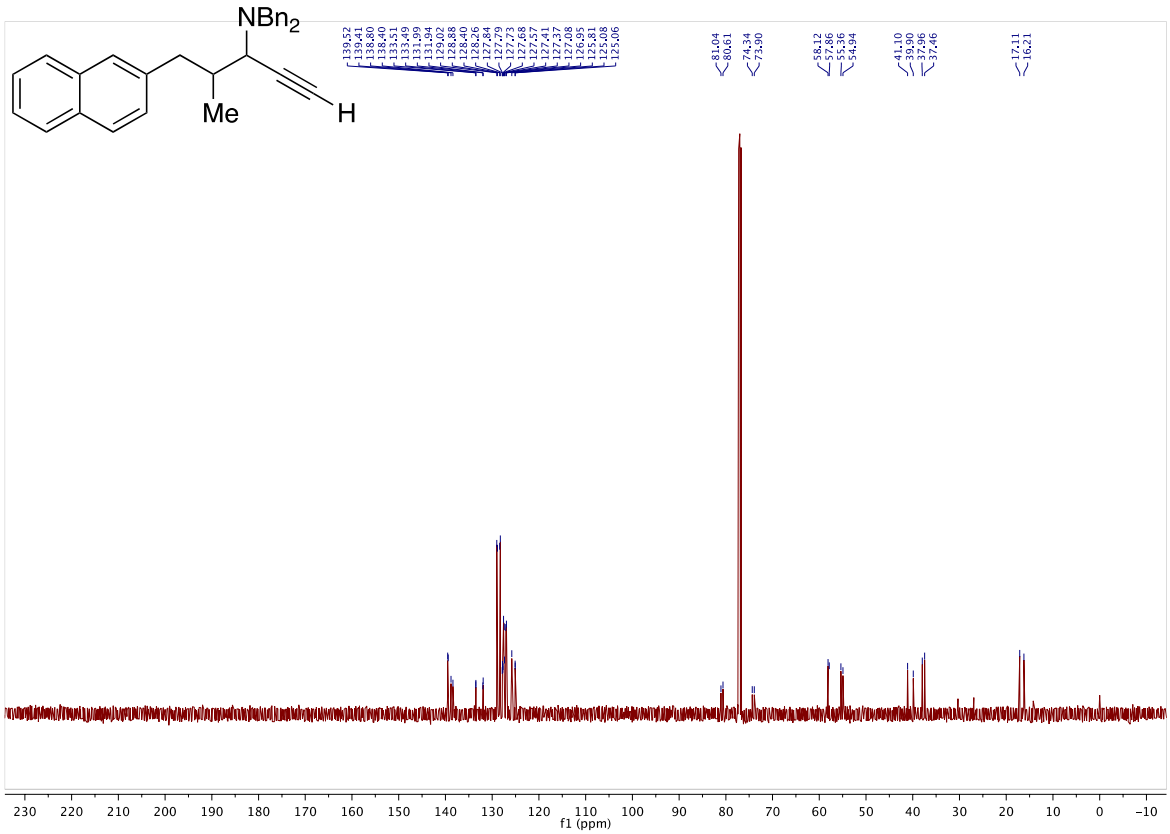

^{1}H NMR (500 MHz, $CDCl_3$)

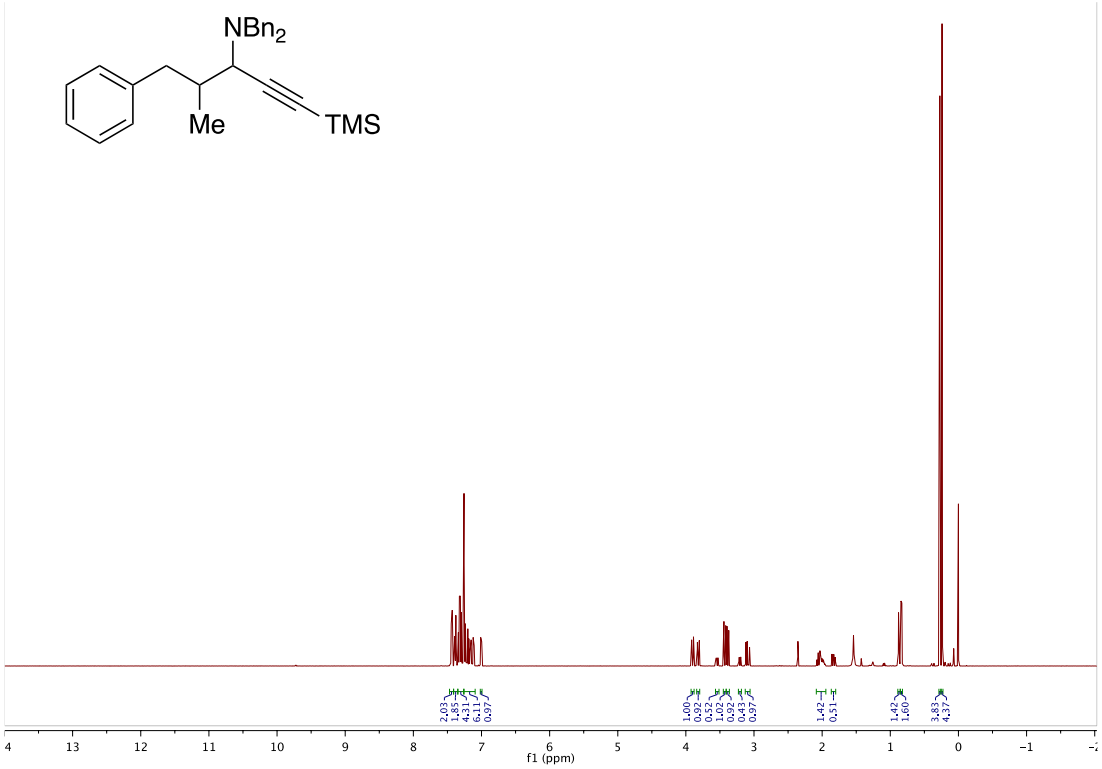

^{13}C NMR (126 MHz, $CDCl_3$)

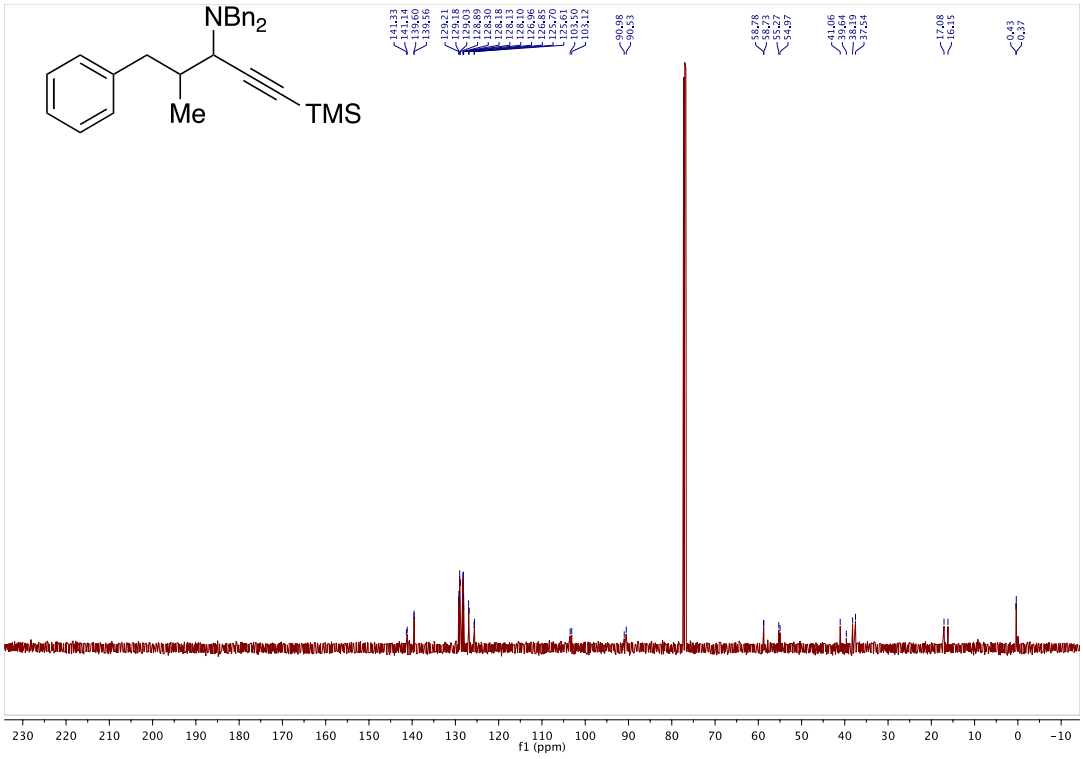

^{1}H NMR (500 MHz, $CDCl_3$)

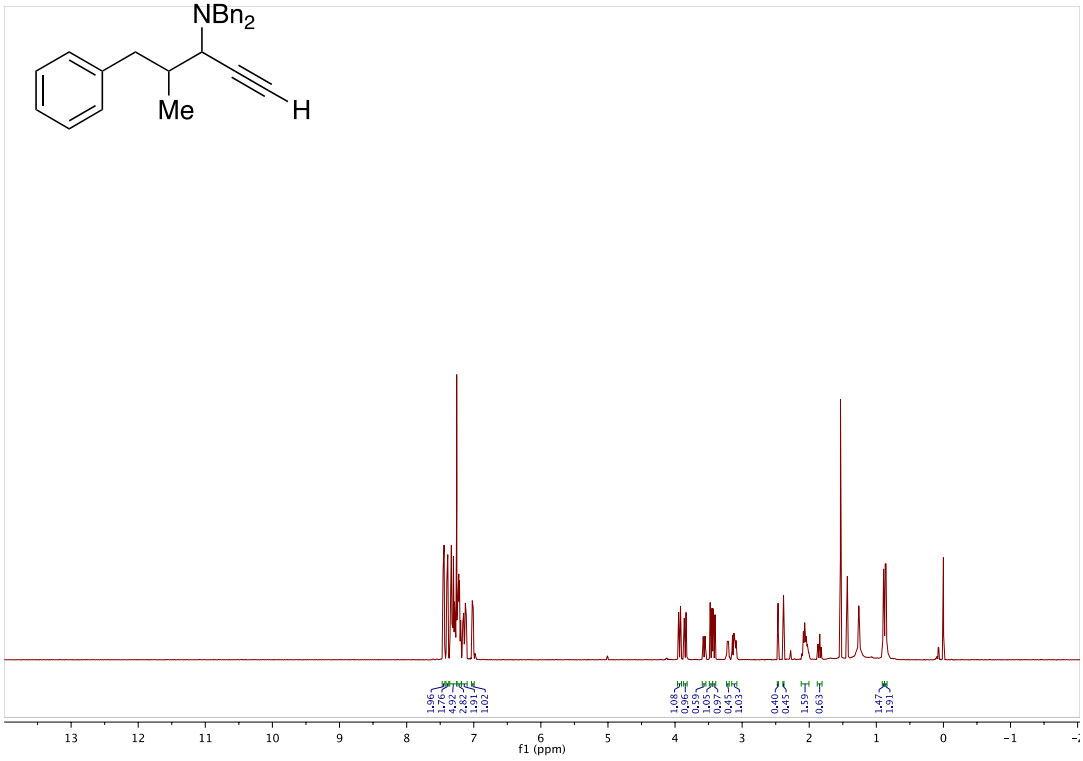

^{13}C NMR (126 MHz, $CDCl_3$)

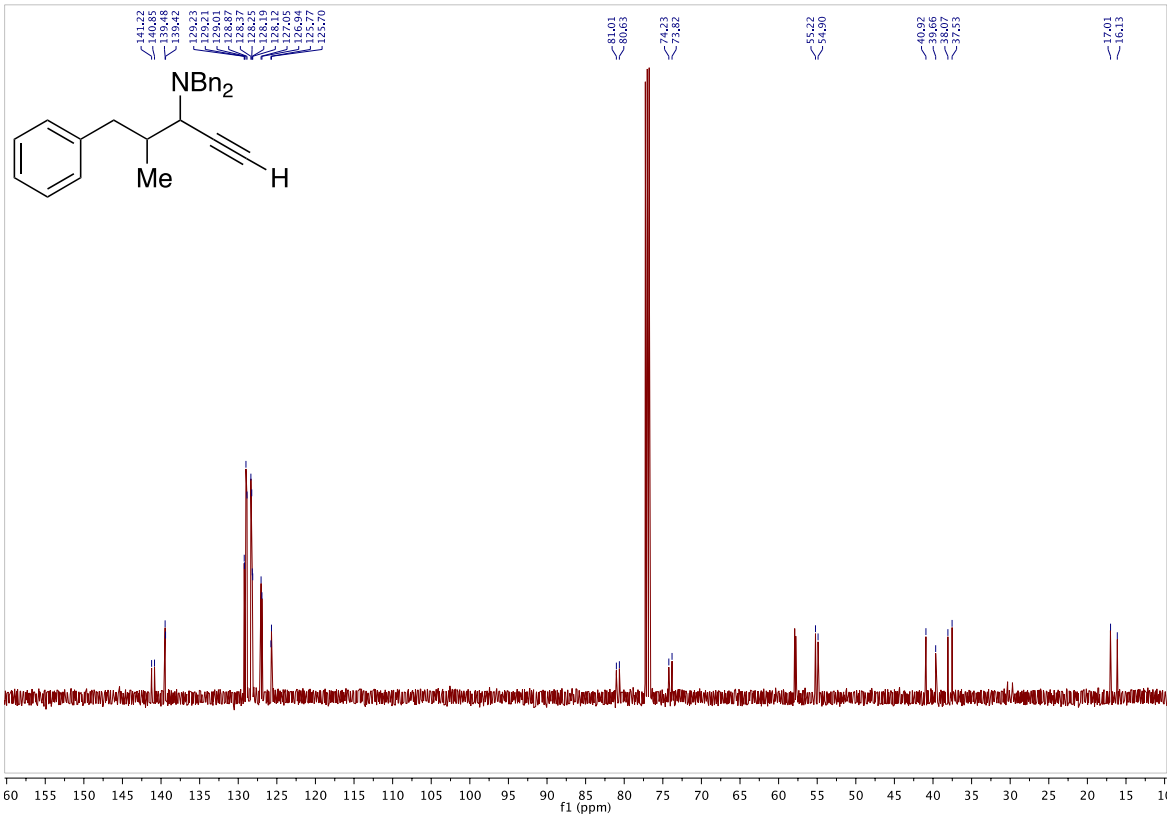

Chapter 4 Appendix: Heteroatom-directed Cu-catalysed Asymmetric Borylation of Heteroaryl-substituted Alkenes

^{1}H NMR (500 MHz, $CDCl_3$)

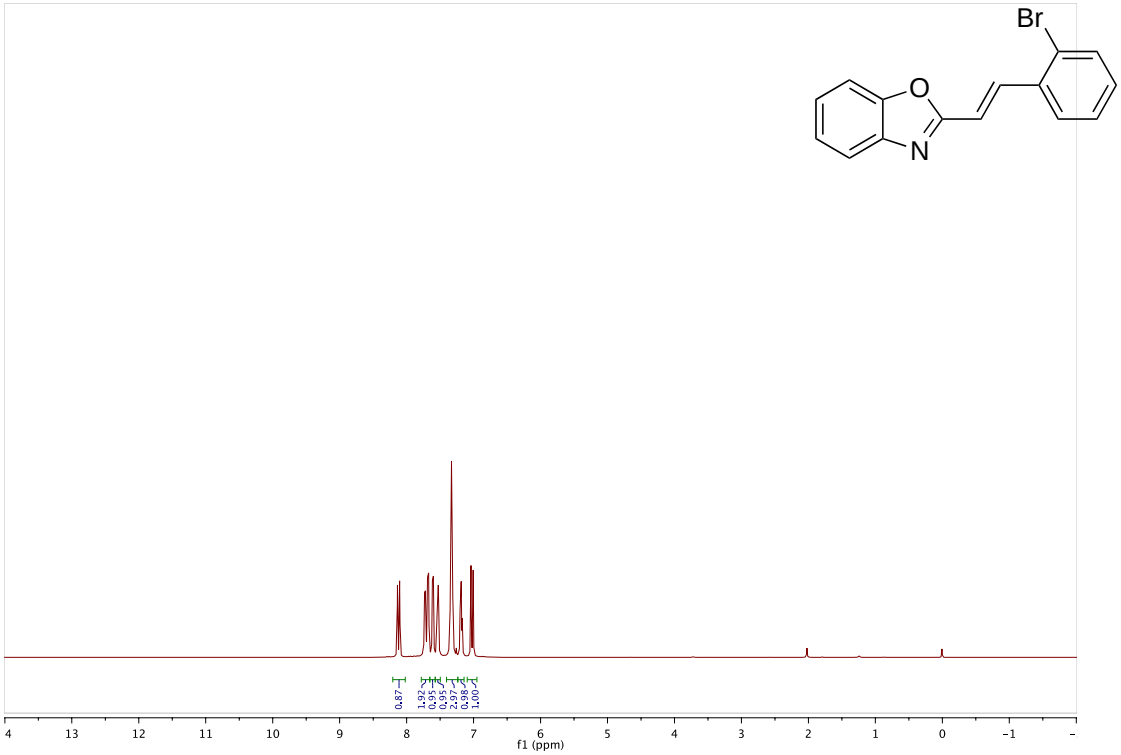

^{3}C NMR (126 MHz, $CDCl_3$)

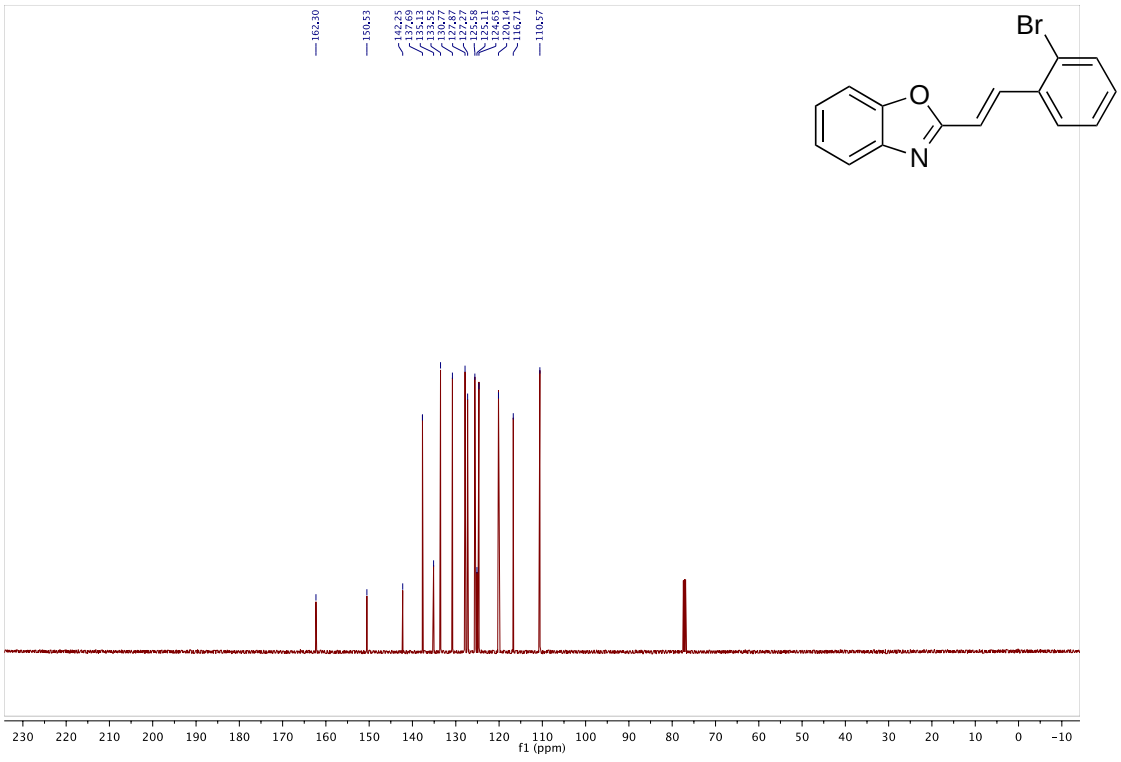

^{1}H NMR (500 MHz, $CDCl_3$)

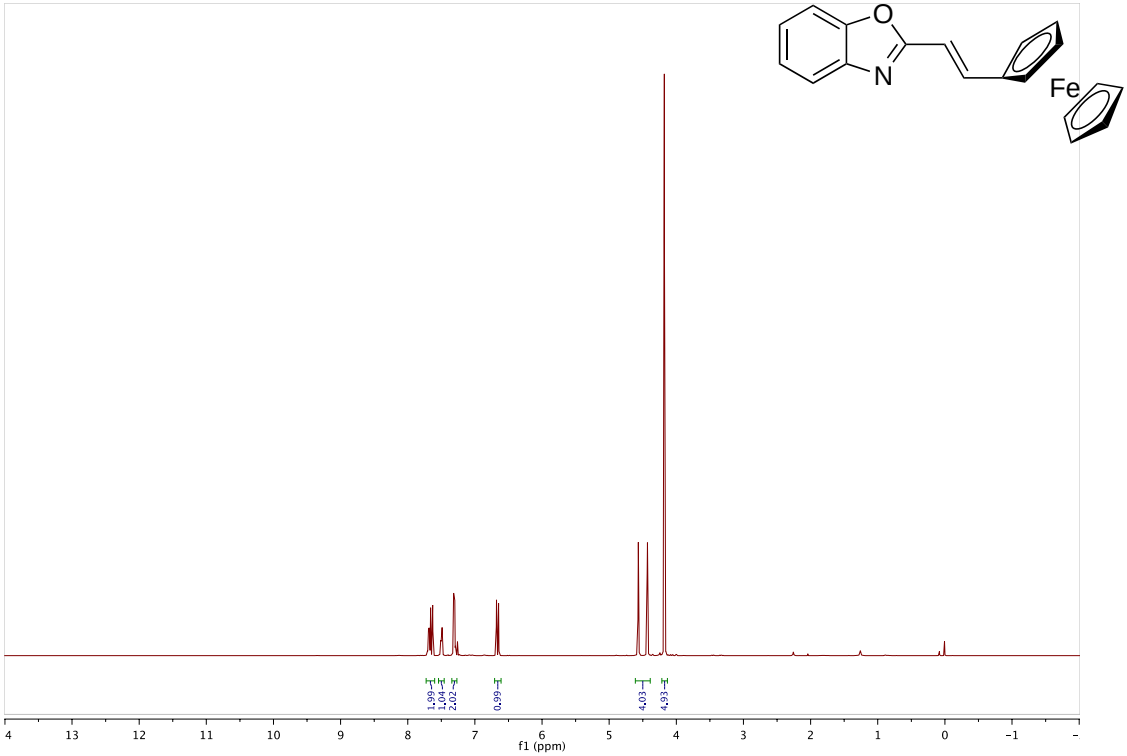

^{13}C NMR (126 MHz, $CDCl_3$)

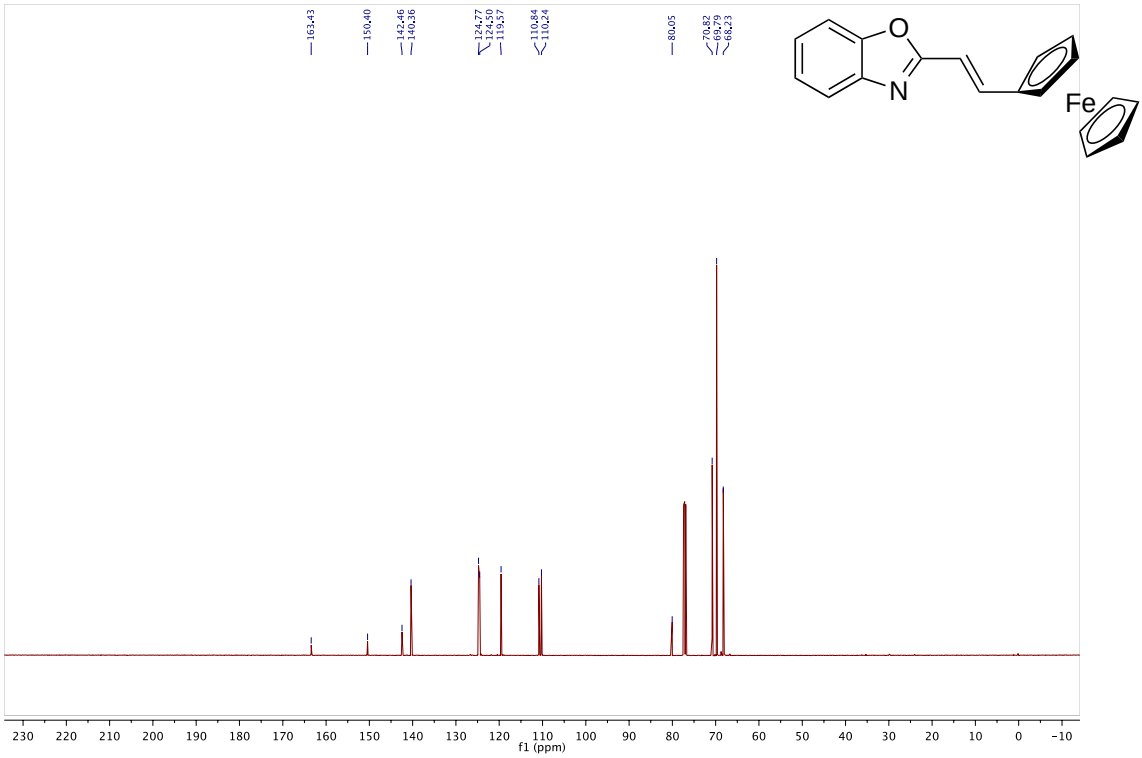

^{1}H NMR (400 MHz, $CDCl_3$)

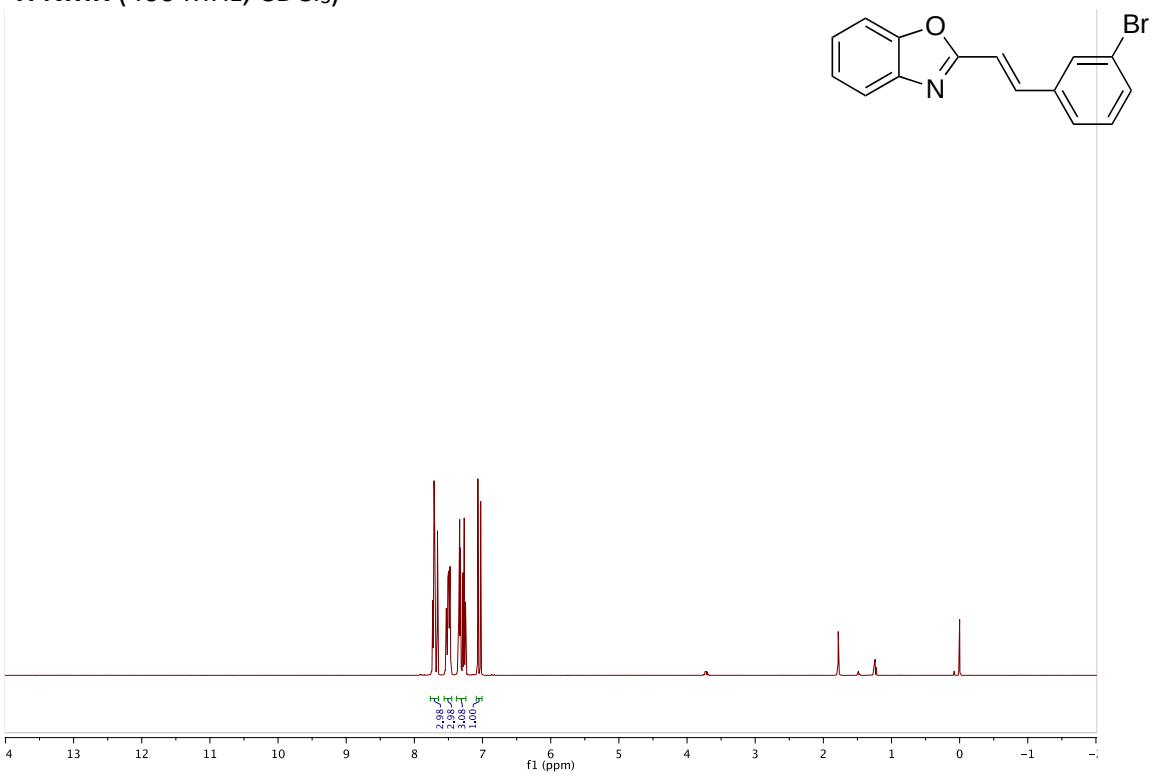

^{3}C NMR (101 MHz, $CDCl_3$)

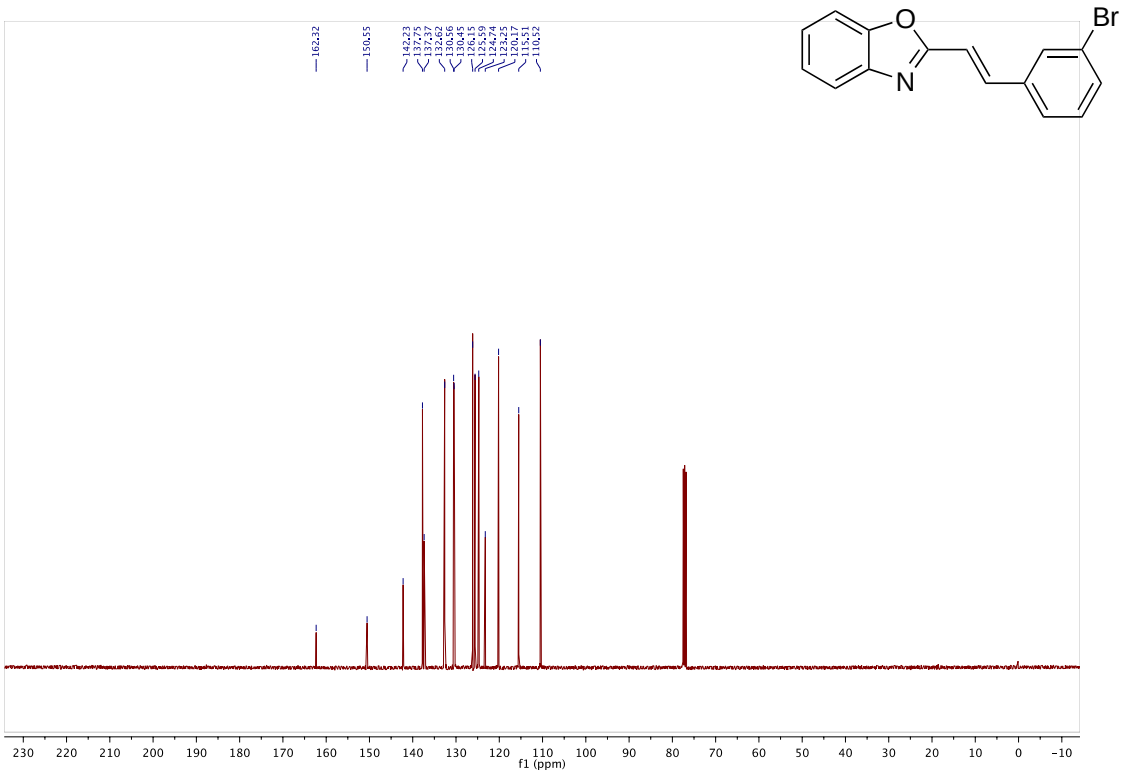

Compound **22**

^{1}H NMR (400 MHz, $CDCl_3$)

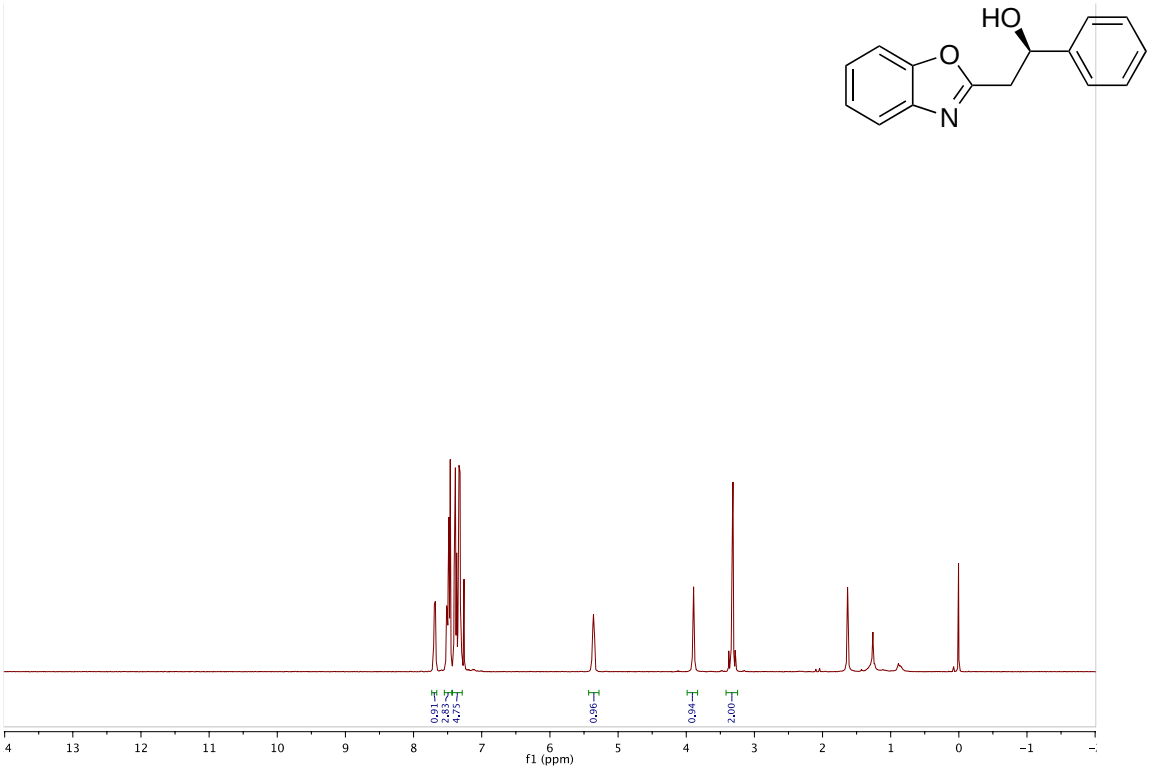

^{13}C NMR (101 MHz, $CDCl_3$)

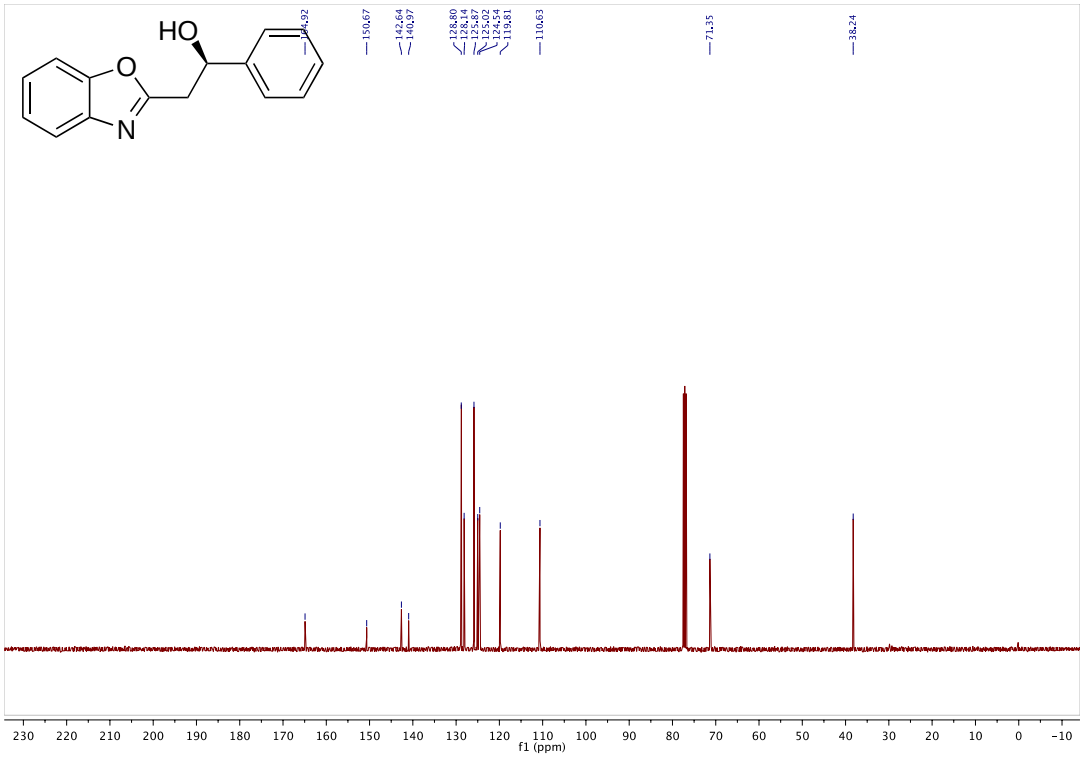

Compound **23**

^{1}H NMR (400 MHz, $CDCl_3$)

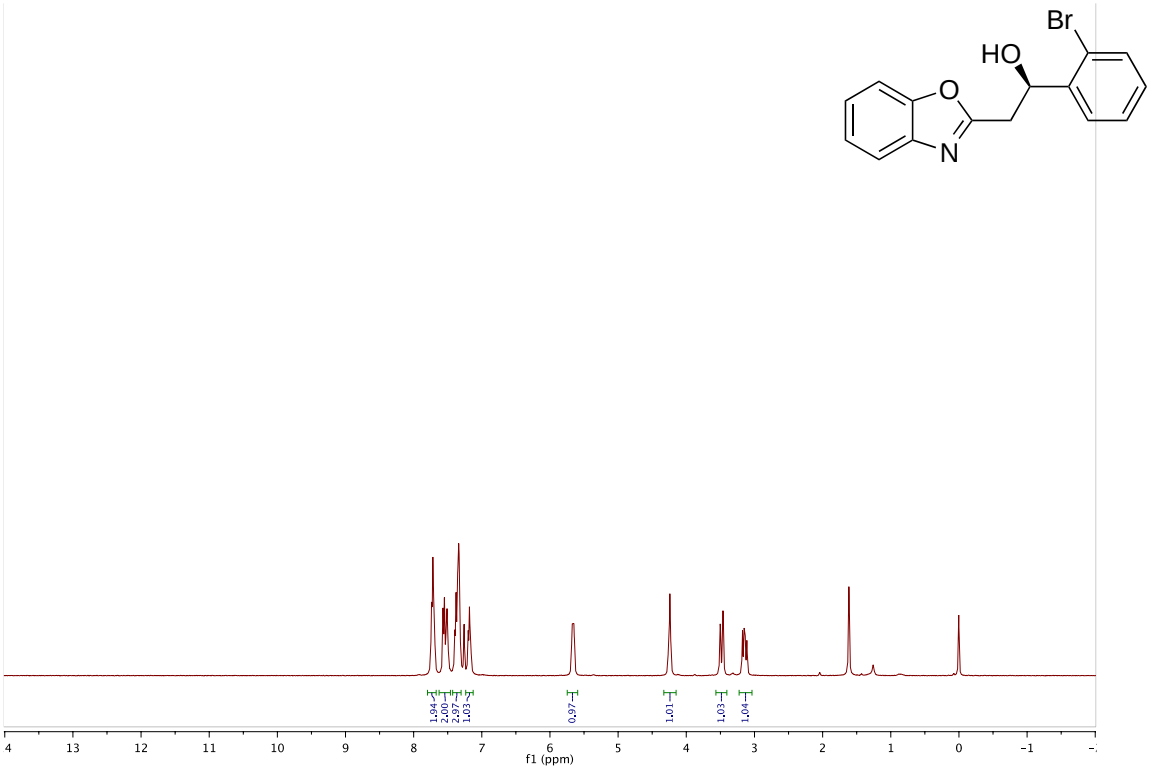

^{13}C NMR (101 MHz, $CDCl_3$)

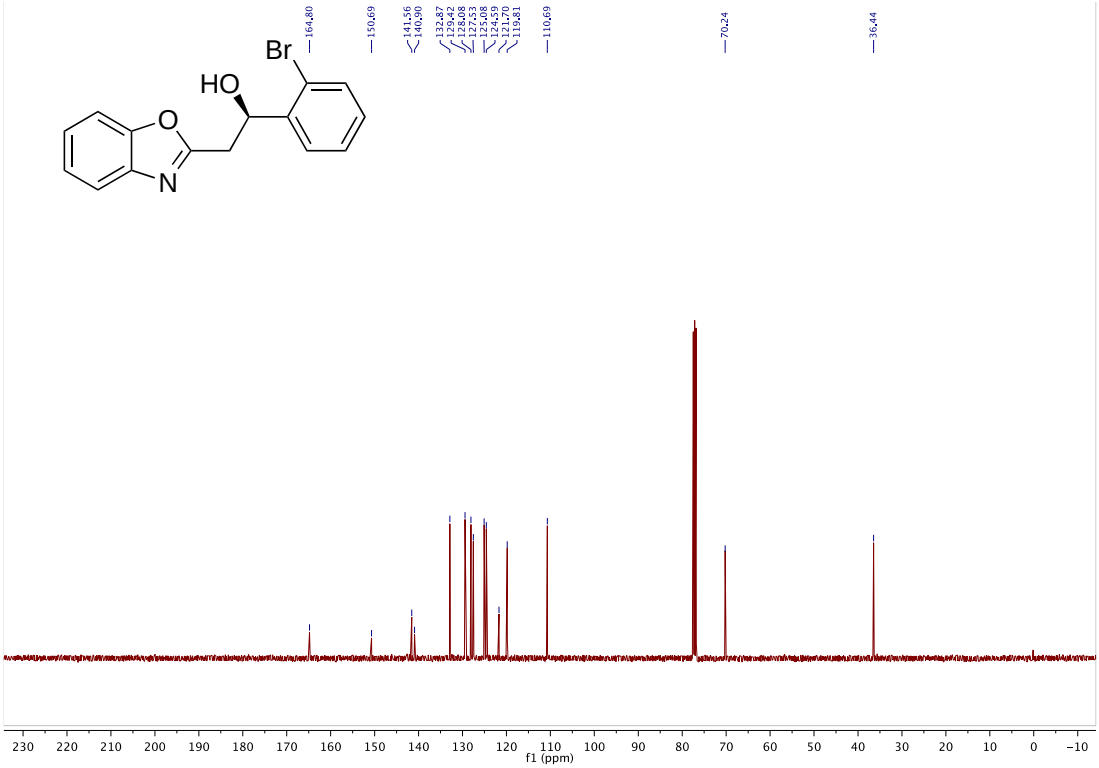

Compound **24**

^{1}H NMR (500 MHz, $CDCl_3$)

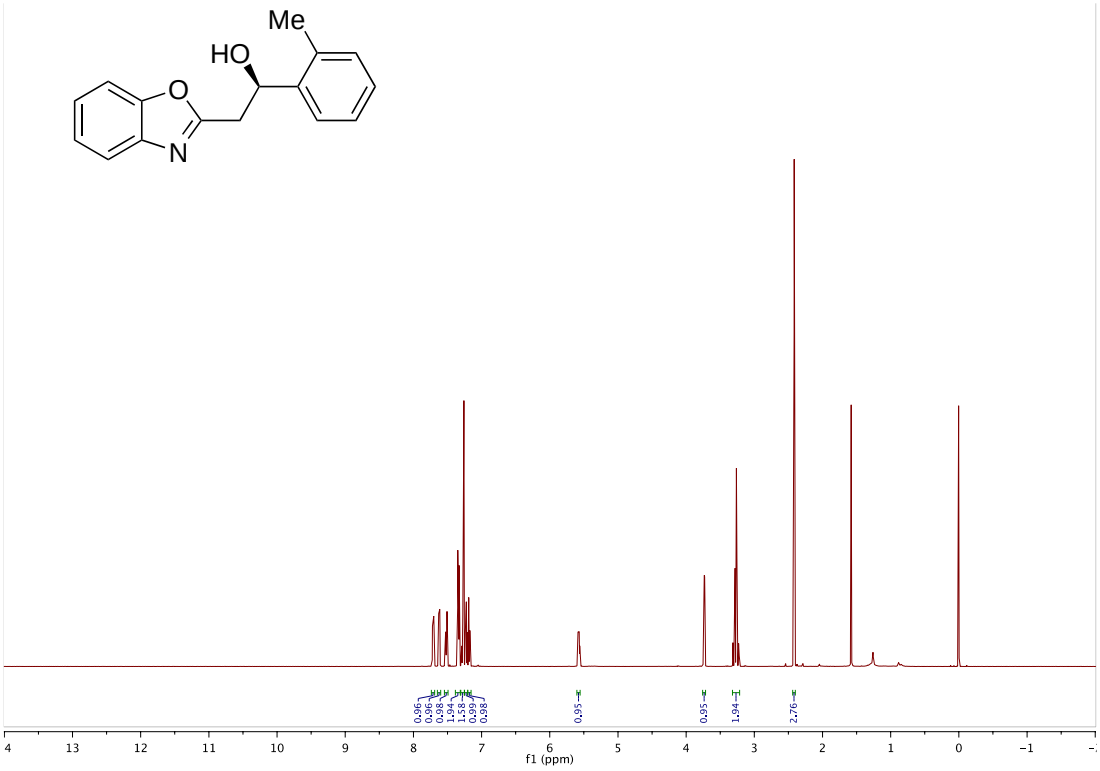

^{13}C NMR (126 MHz, $CDCl_3$)

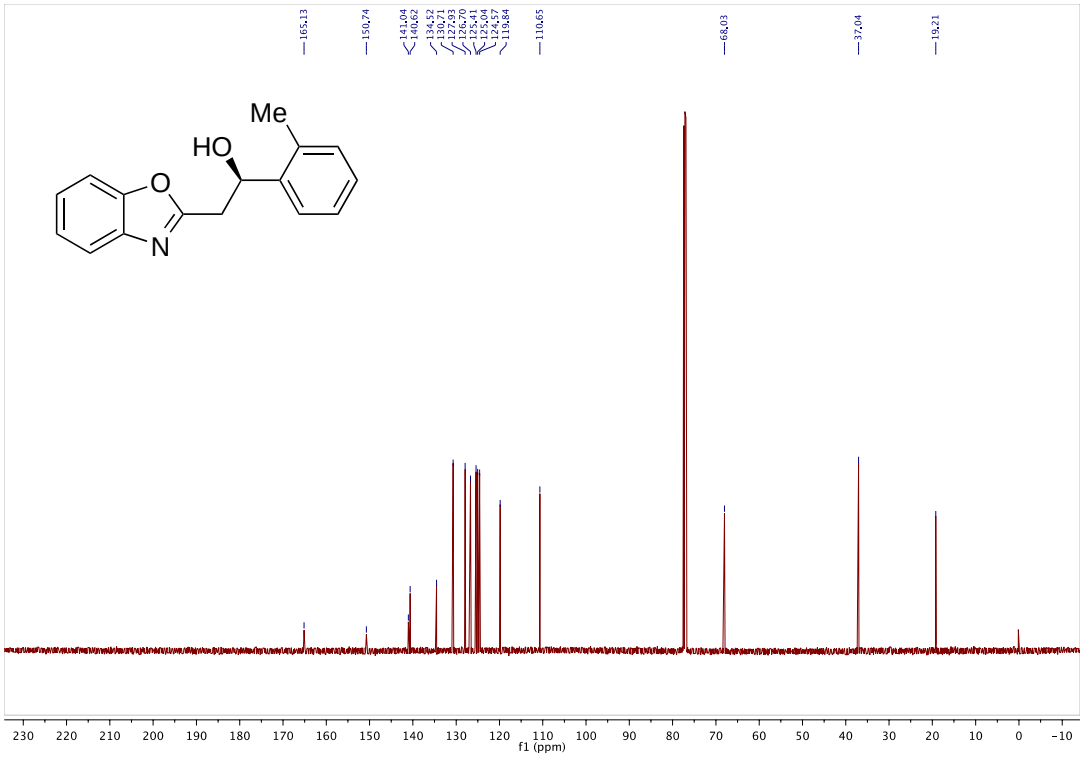

Compound **25**

^{1}H NMR (400 MHz, $CDCl_3$)

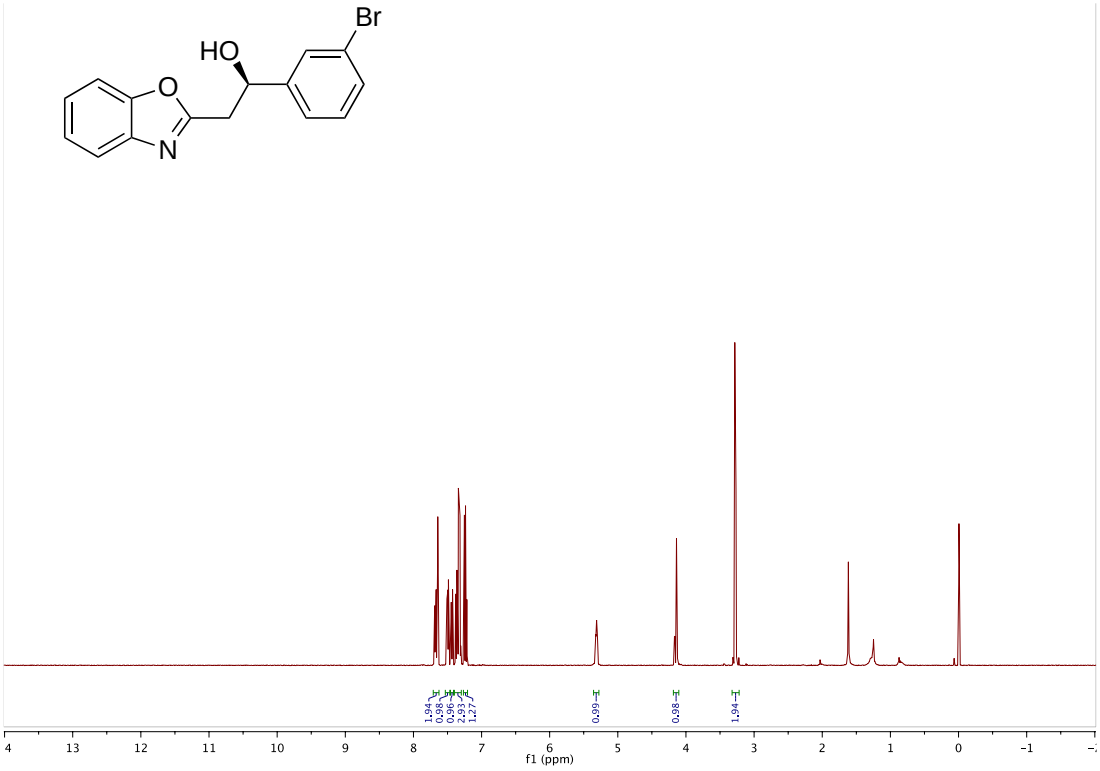

^{13}C NMR (101 MHz, $CDCl_3$)

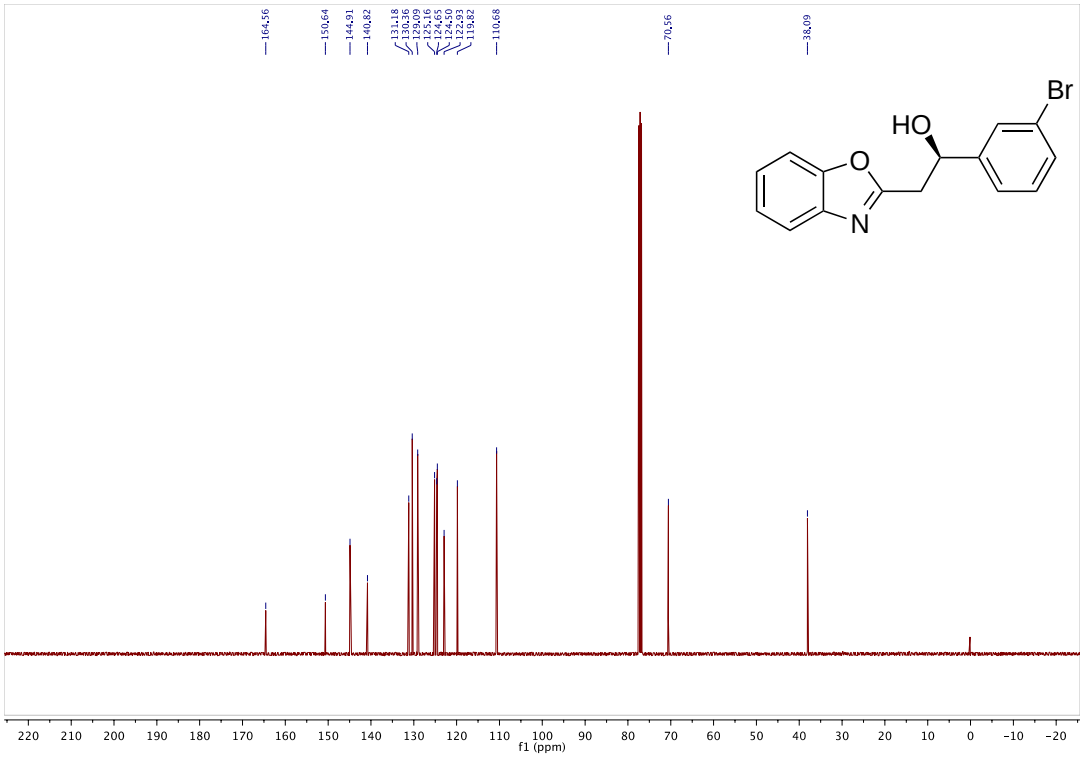

Compound **26**

^{1}H NMR (400 MHz, $CDCl_3$)

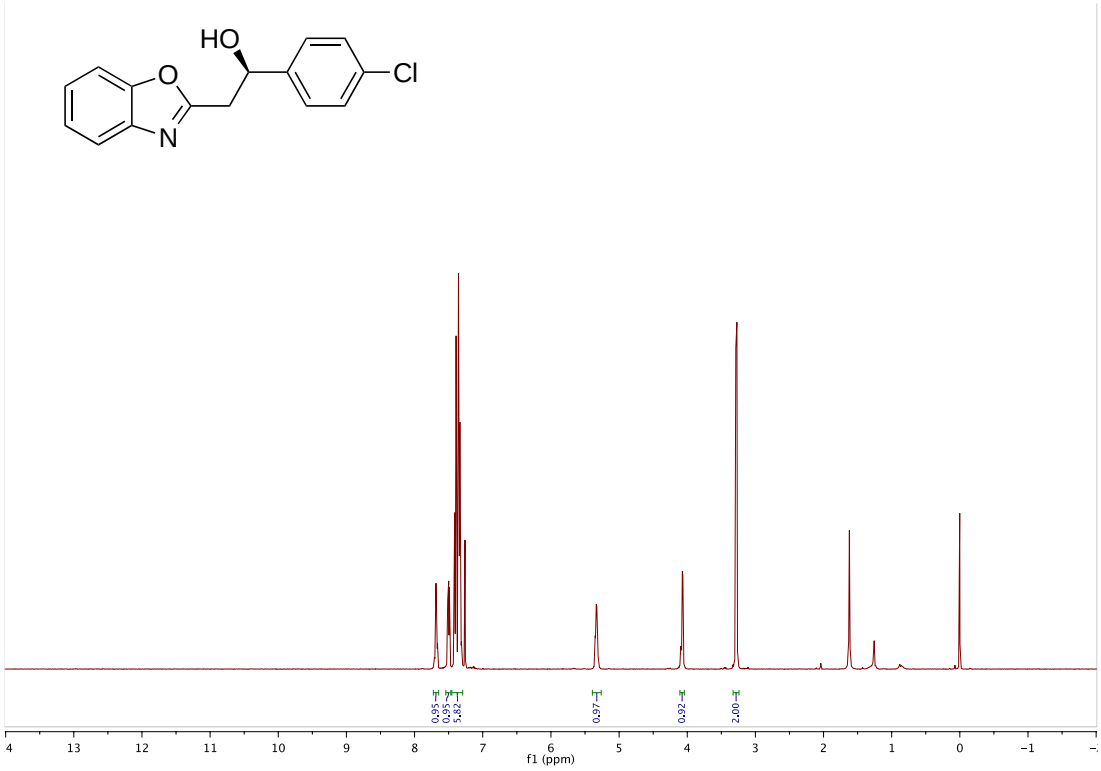

^{13}C NMR (101 MHz, $CDCl_3$)

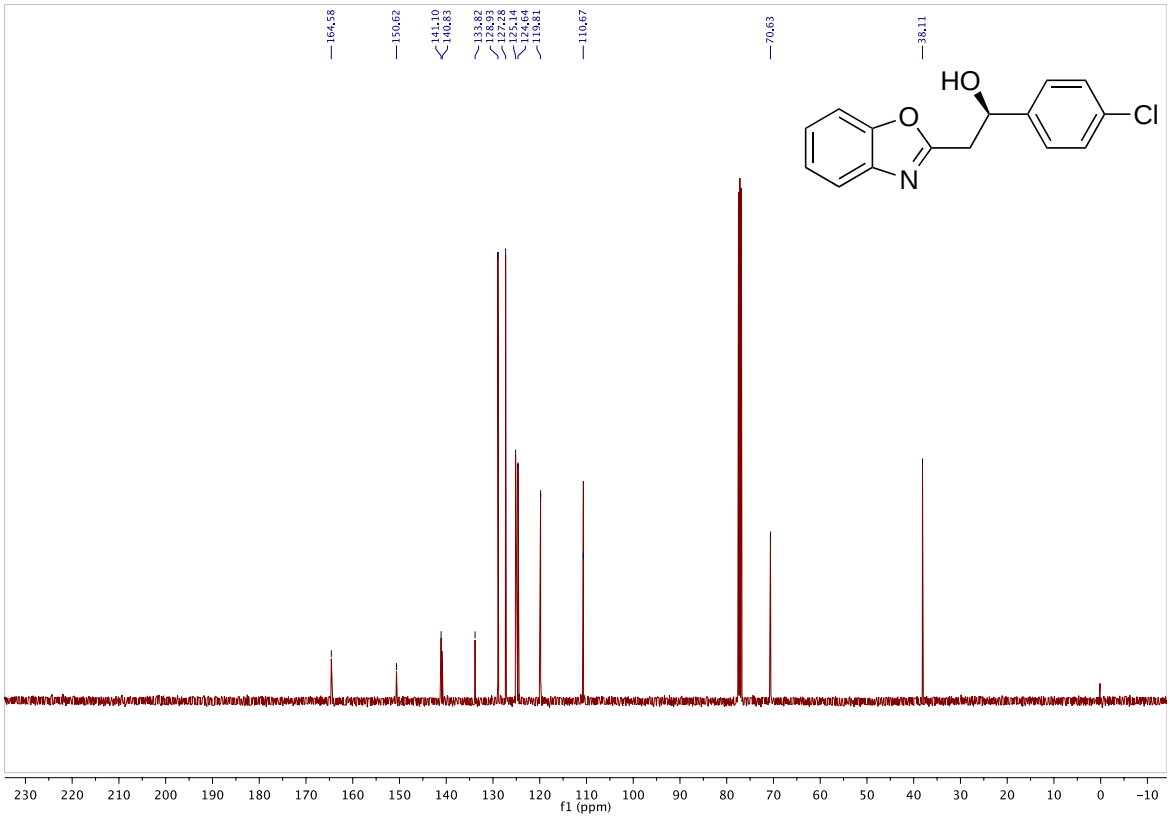

Compound **27**

^{1}H NMR (500 MHz, $CDCl_3$)

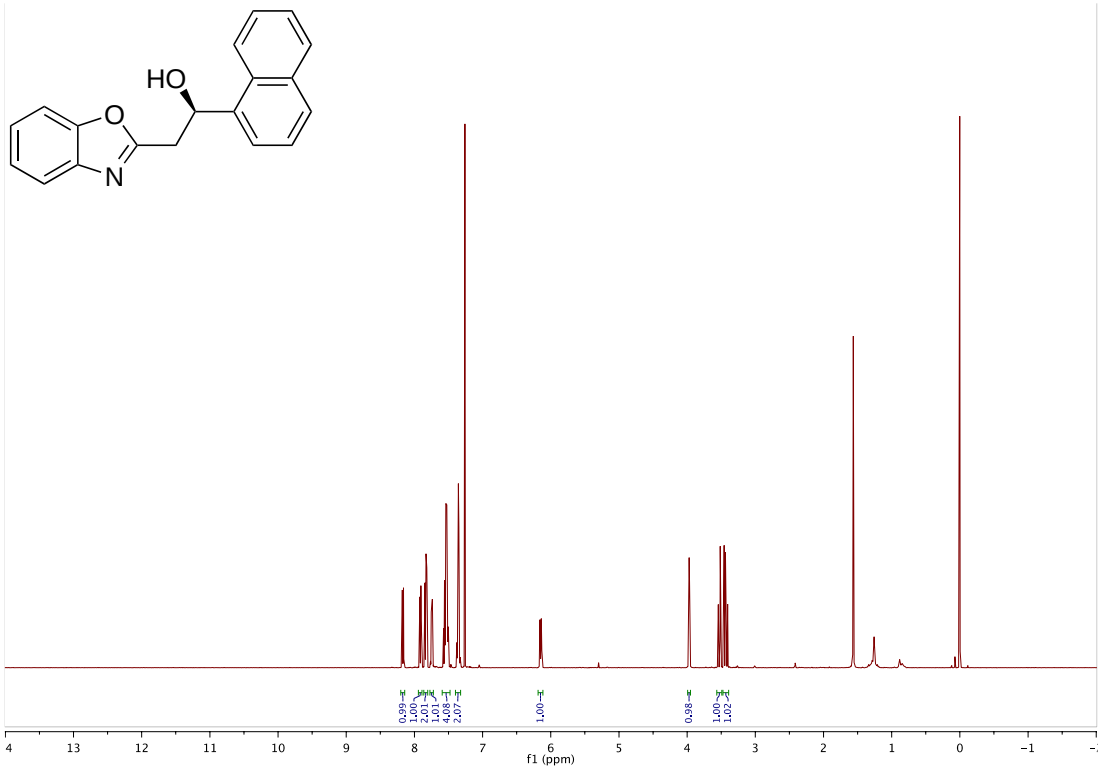

^{13}C NMR (126 MHz, $CDCl_3$)

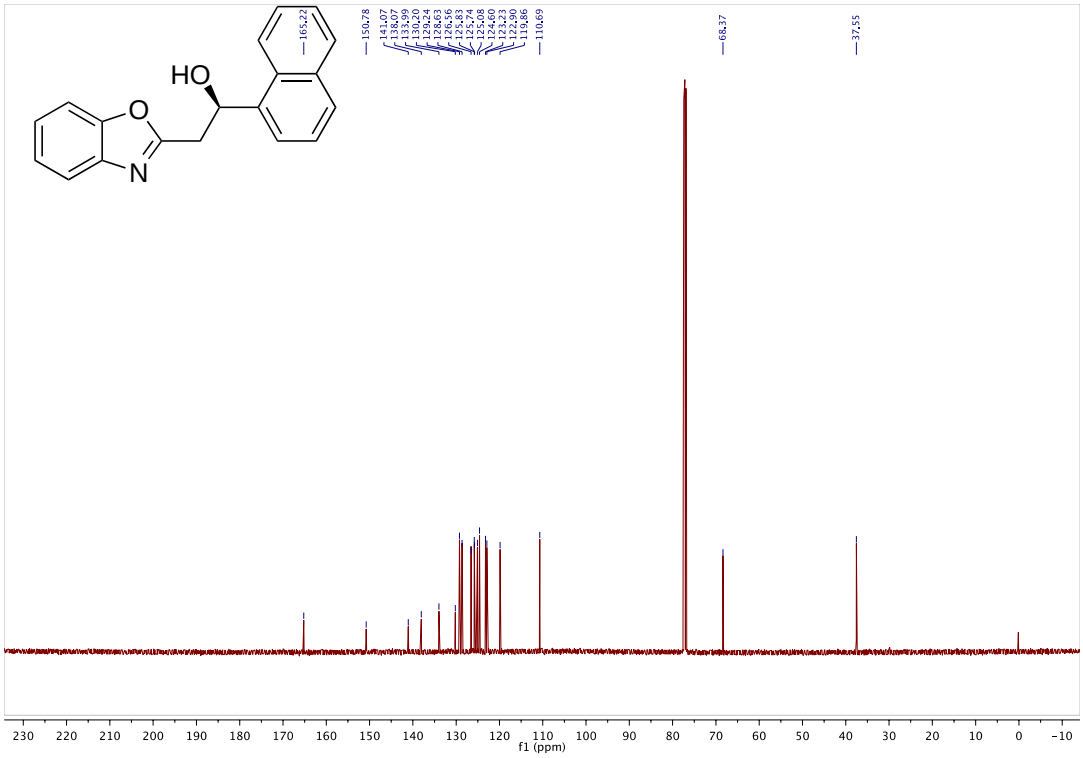

Compound **28**

^{1}H NMR (500 MHz, $CDCl_3$)

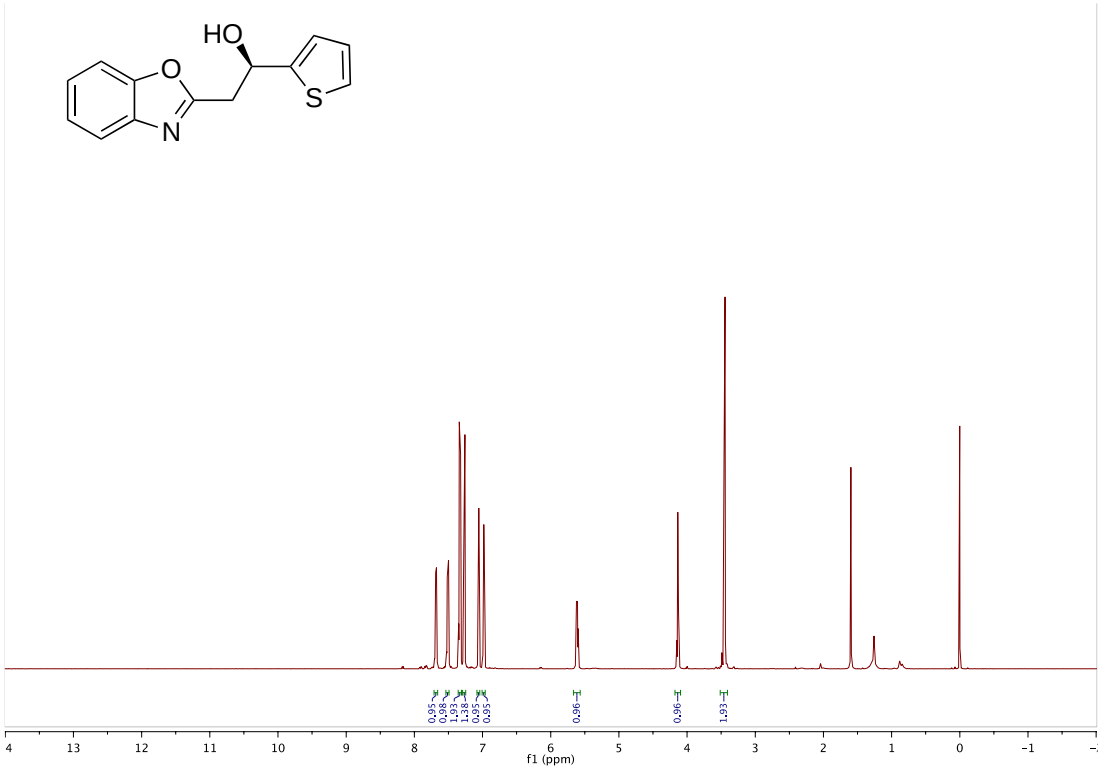

^{13}C NMR (126 MHz, $CDCl_3$)

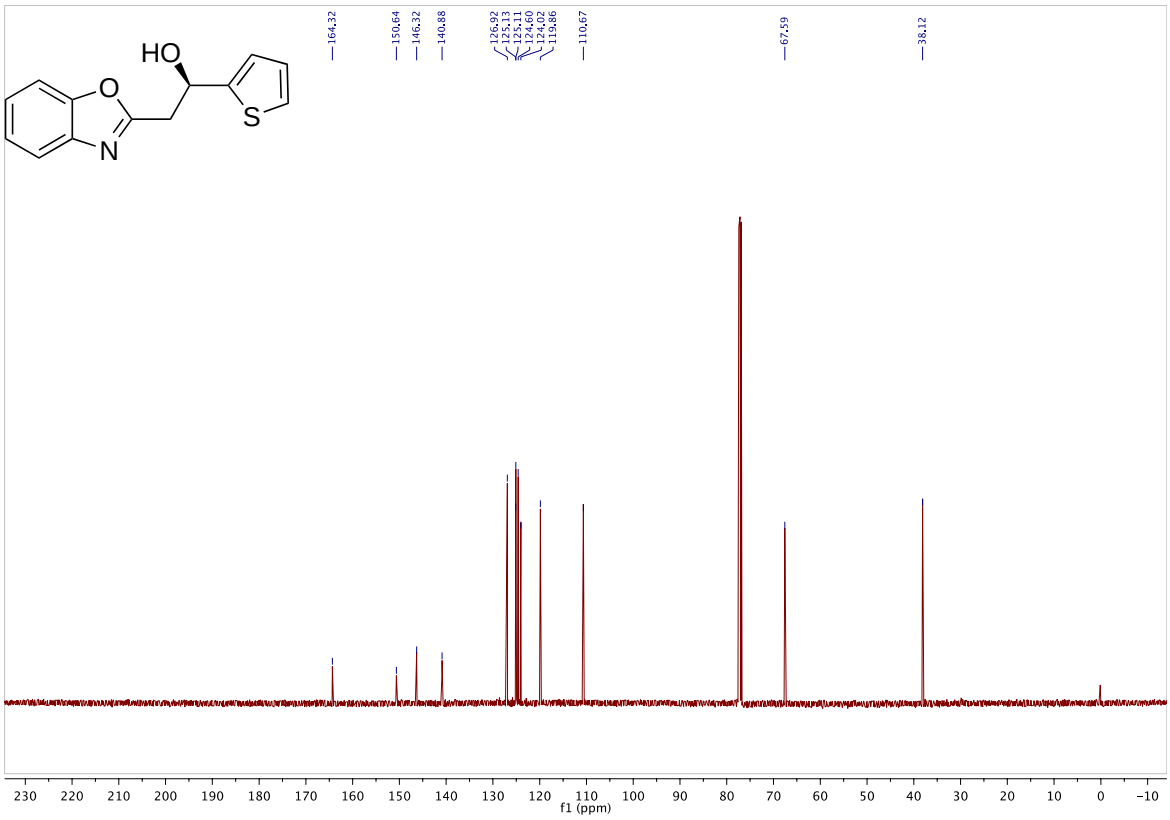

Compound **30**

^{1}H NMR (400 MHz, $CDCl_3$)

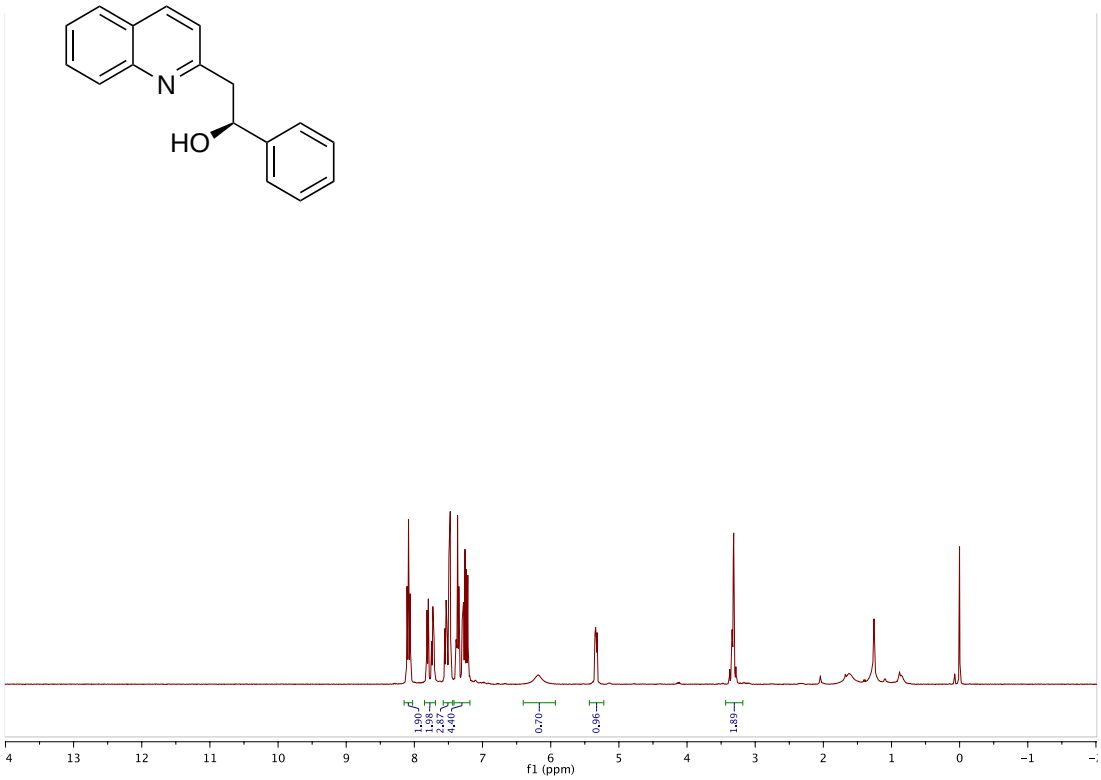

^{13}C NMR (101 MHz, $CDCl_3$)

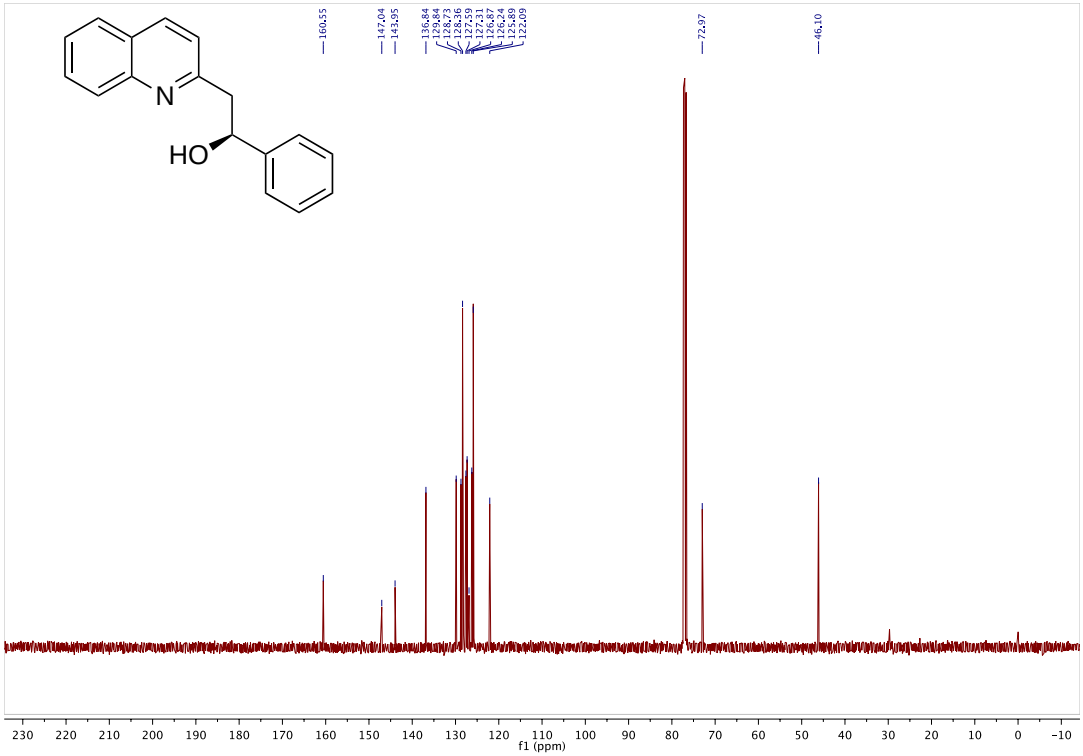

^{1}H NMR (400 MHz, $CDCl_3$)

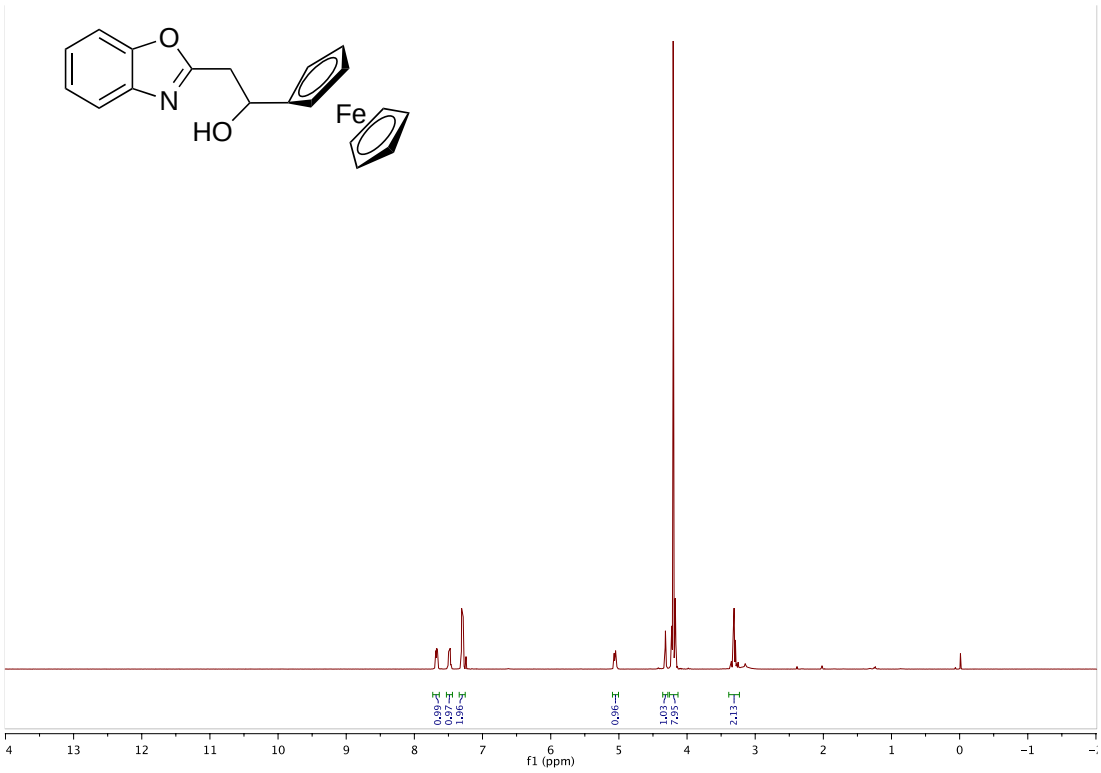

^{13}C NMR (101 MHz, $CDCl_3$)

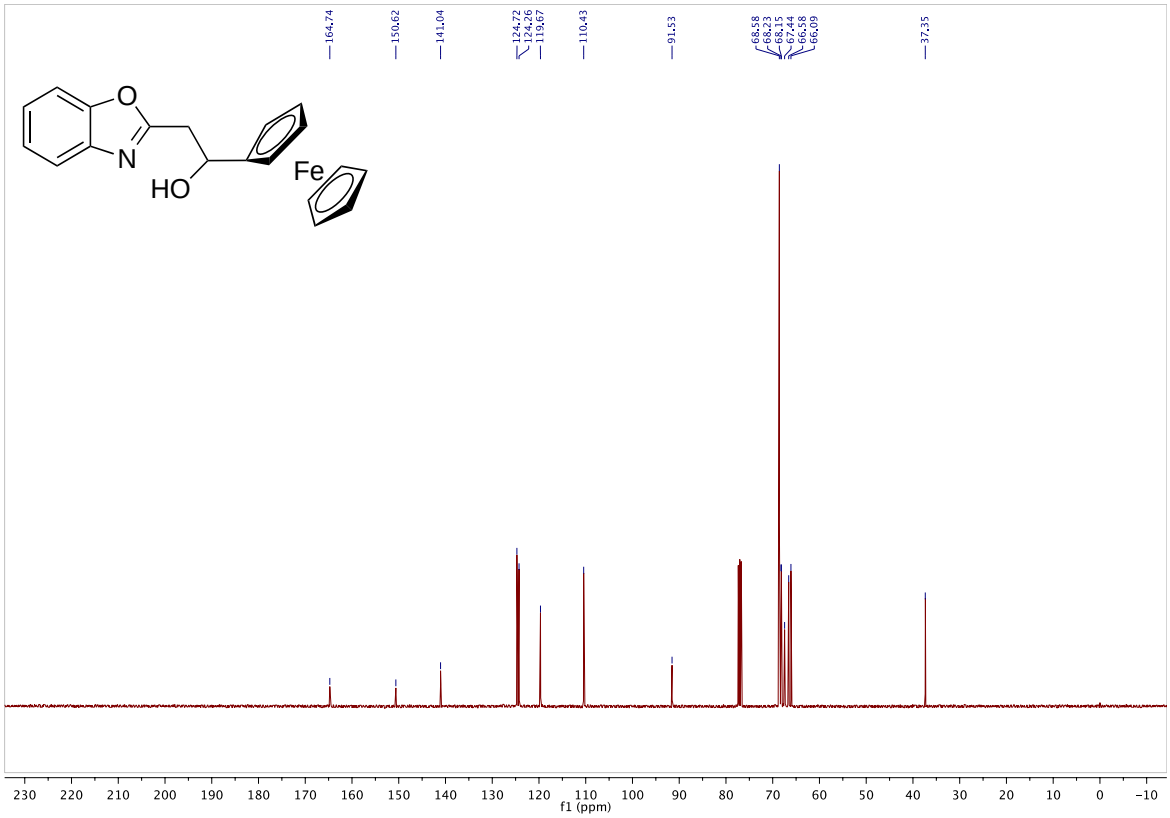

UHPLC Chromatograms

Compound **22**

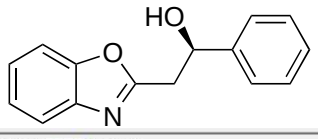

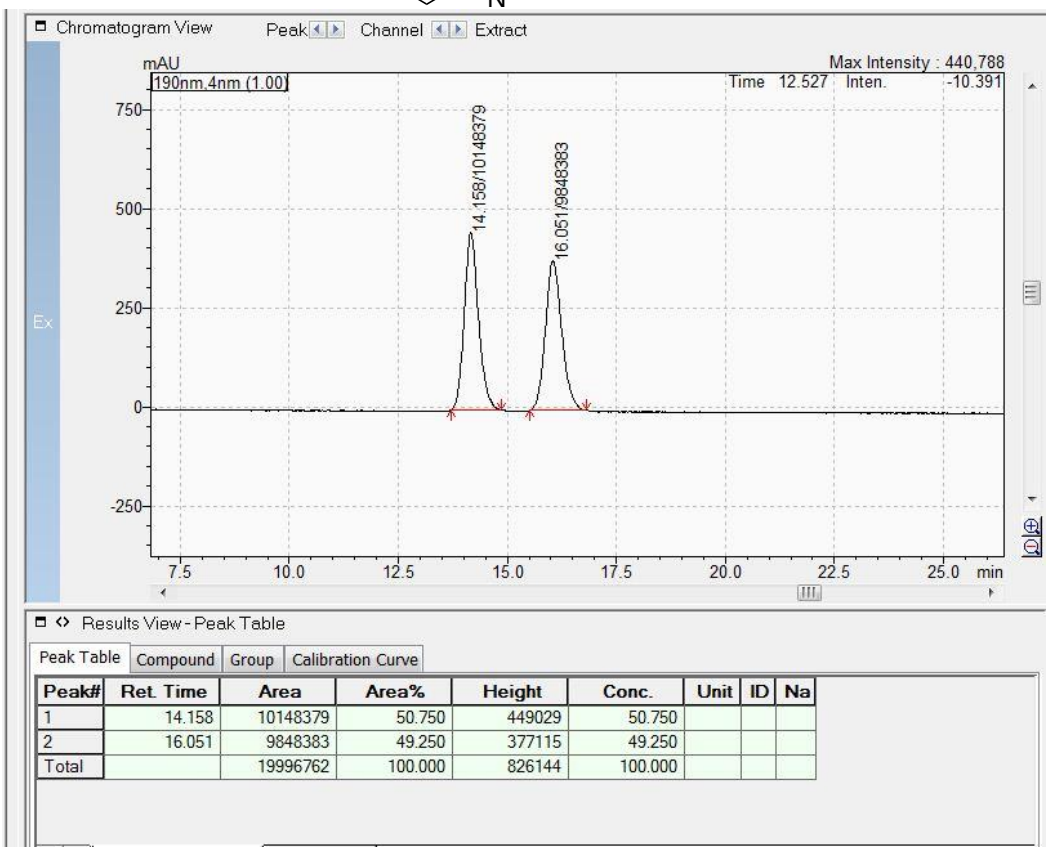

Peak#	Ret. Time	Area	Area%	Height	Conc.	Unit	ID	Na
1	14.158	10148379	50.750	449029	50.750			
2	16.051	9848383	49.250	377115	49.250			
Total		19996762	100.000	826144	100.000			

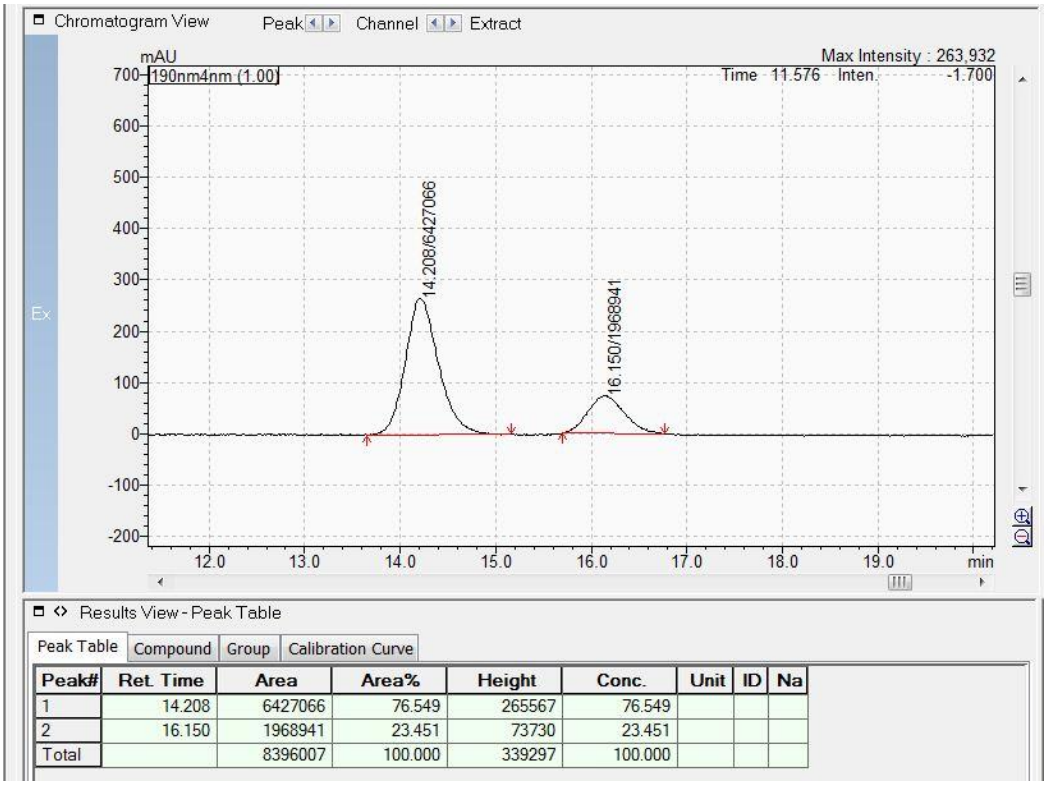

Peak#	Ret. Time	Area	Area%	Height	Conc.	Unit	ID	Na
1	14.208	6427066	76.549	265567	76.549			
2	16.150	1968941	23.451	73730	23.451			
Total		8396007	100.000	339297	100.000			

Compound **23**

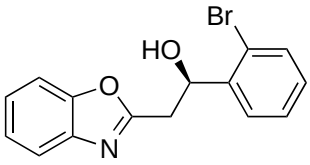

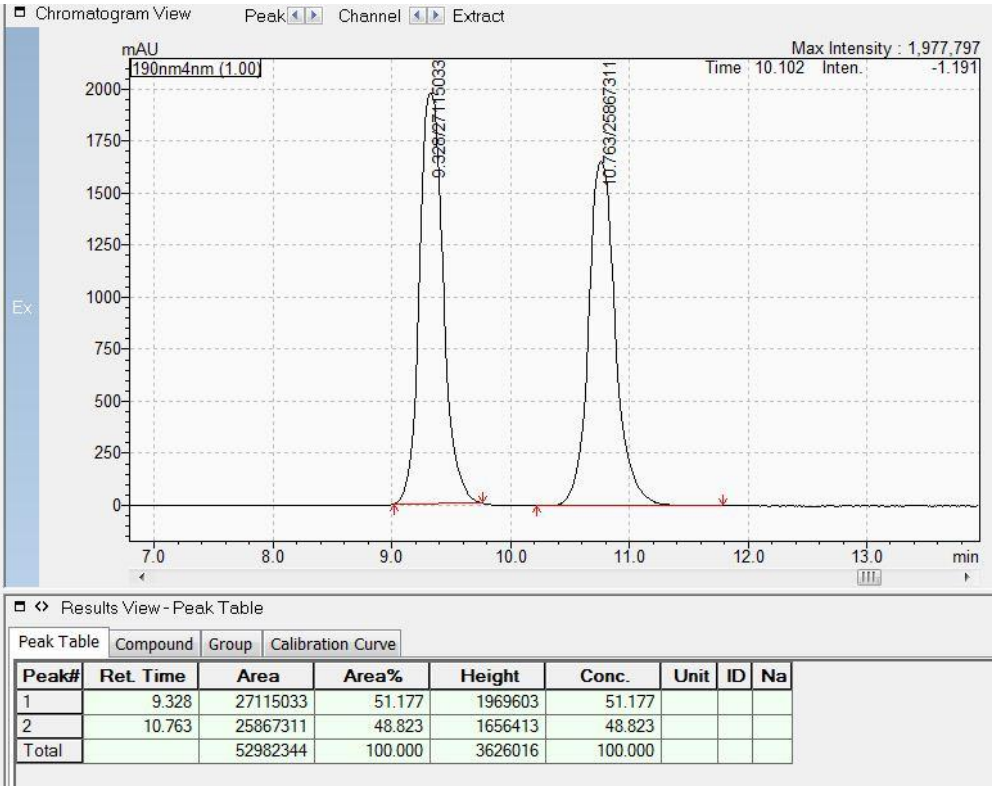

Results View - Peak Table

Peak Table | Compound | Group | Calibration Curve

Peak#	Ret. Time	Area	Area%	Height	Conc.	Unit	ID	Na
1	9.328	27115033	51.177	1969603	51.177			
2	10.763	25867311	48.823	1656413	48.823			
Total		52982344	100.000	3626016	100.000			

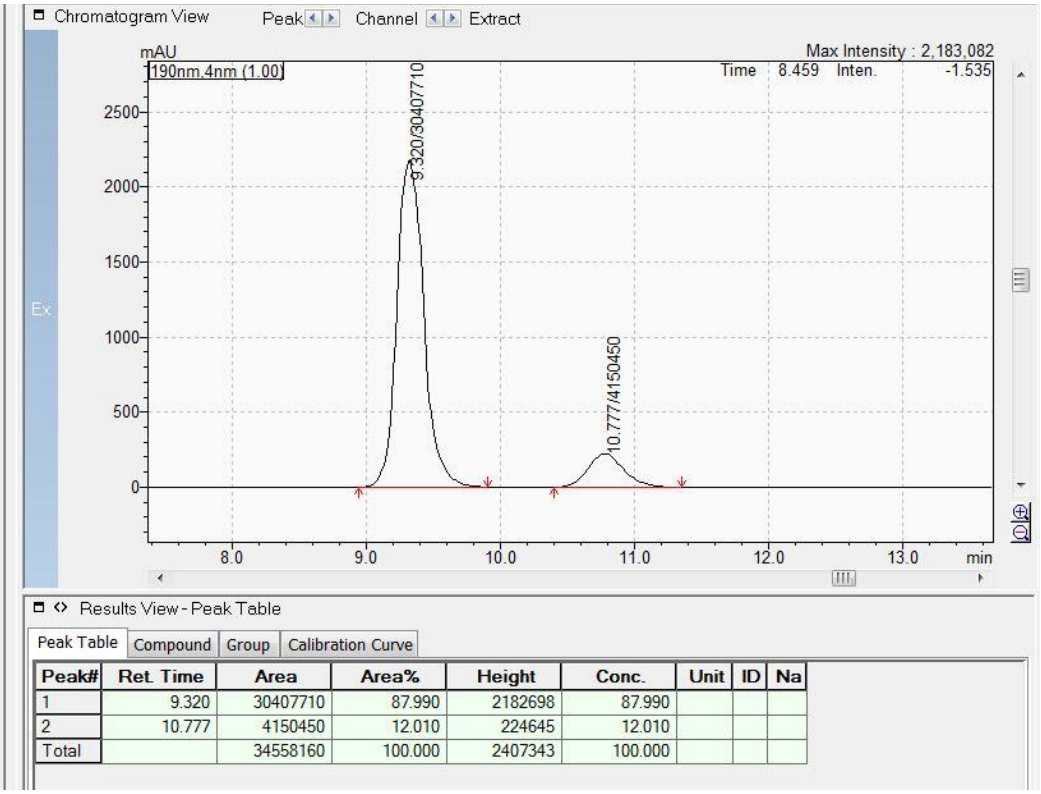

Results View - Peak Table

Peak Table | Compound | Group | Calibration Curve

Peak#	Ret. Time	Area	Area%	Height	Conc.	Unit	ID	Na
1	9.320	30407710	87.990	2182698	87.990			
2	10.777	4150450	12.010	224645	12.010			
Total		34558160	100.000	2407343	100.000			

Compound **24**

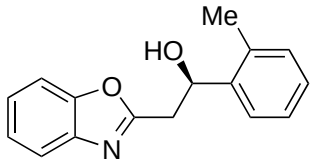

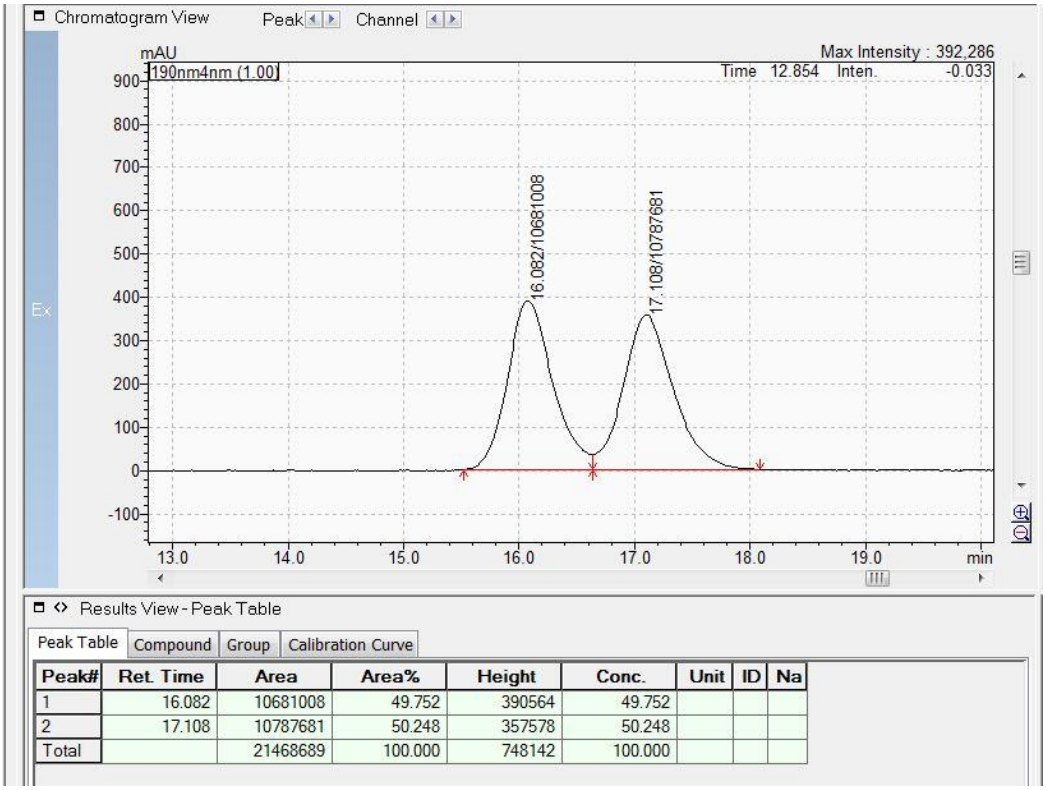

Results View - Peak Table

Peak Table | Compound | Group | Calibration Curve

Peak#	Ret. Time	Area	Area%	Height	Conc.	Unit	ID	Na
1	16.082	10681008	49.752	390564	49.752			
2	17.108	10787681	50.248	357578	50.248			
Total		21468689	100.000	748142	100.000			

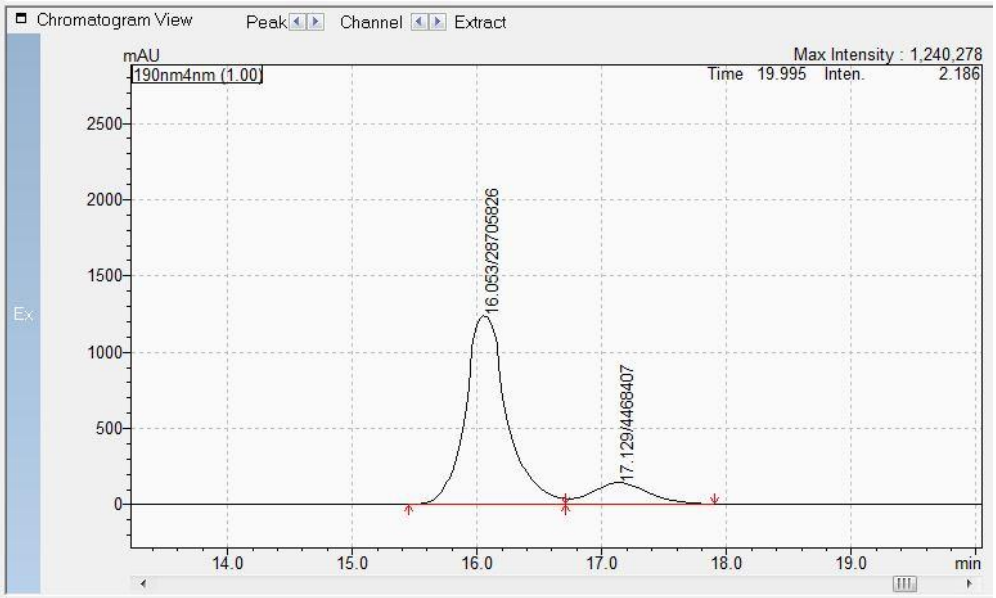

Results View - Peak Table

Peak Table | Compound | Group | Calibration Curve

Peak#	Ret. Time	Area	Area%	Height	Conc.	Unit	ID	Na
1	16.053	28705826	86.530	1236325	86.530			
2	17.129	4468407	13.470	141382	13.470			
Total		33174234	100.000	1377707	100.000			

Compound **25**

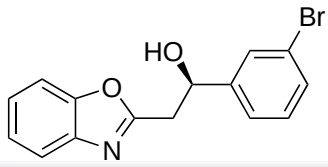

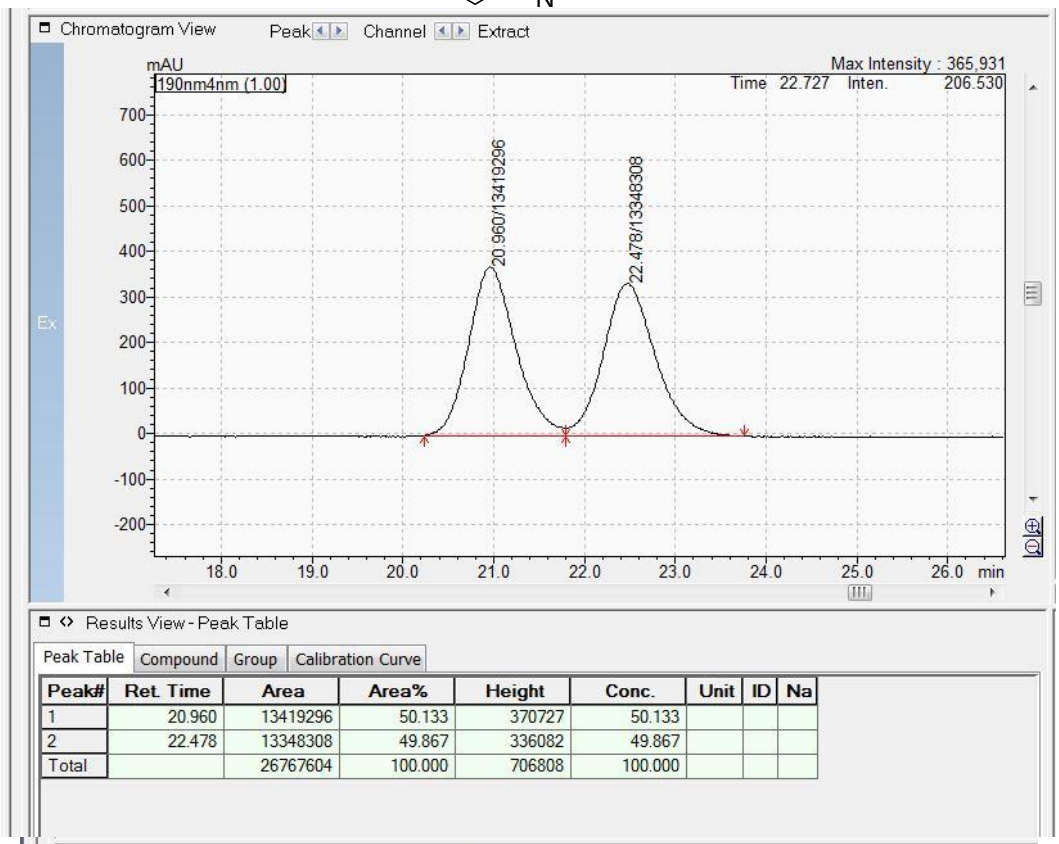

Results View - Peak Table

Peak Table | Compound | Group | Calibration Curve

Peak#	Ret. Time	Area	Area%	Height	Conc.	Unit	ID	Na
1	20.960	13419296	50.133	370727	50.133			
2	22.478	13348308	49.867	336082	49.867			
Total		26767604	100.000	706808	100.000			

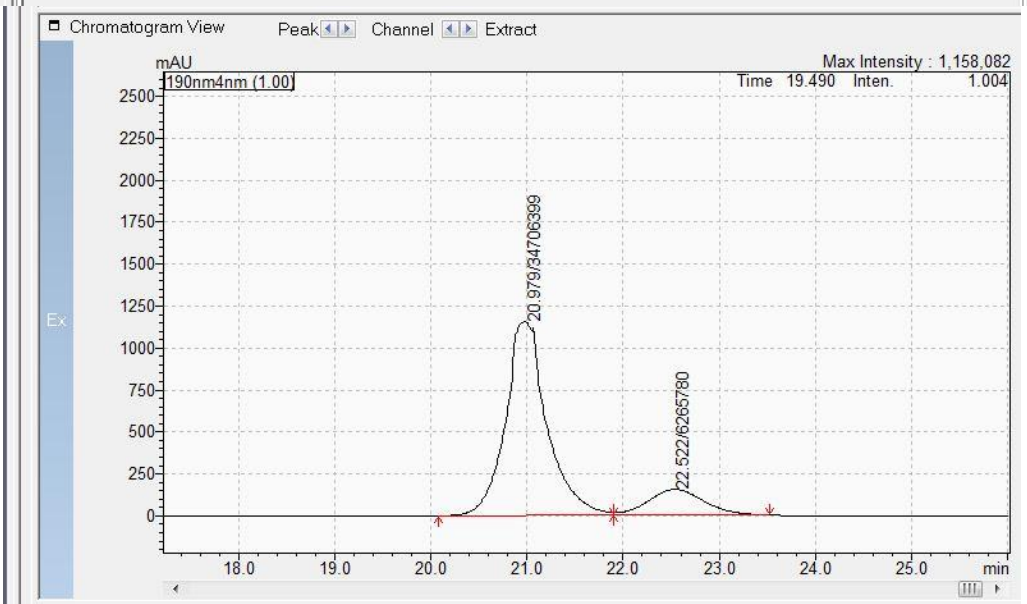

Results View - Peak Table

Peak Table | Compound | Group | Calibration Curve

Peak#	Ret. Time	Area	Area%	Height	Conc.	Unit	ID	Na
1	20.979	34706399	84.707	1155998	84.707			
2	22.522	6265780	15.293	154325	15.293			
Total		40972179	100.000	1310322	100.000			

Compound **26**

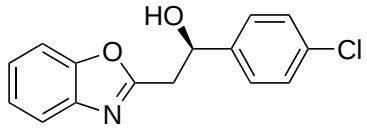

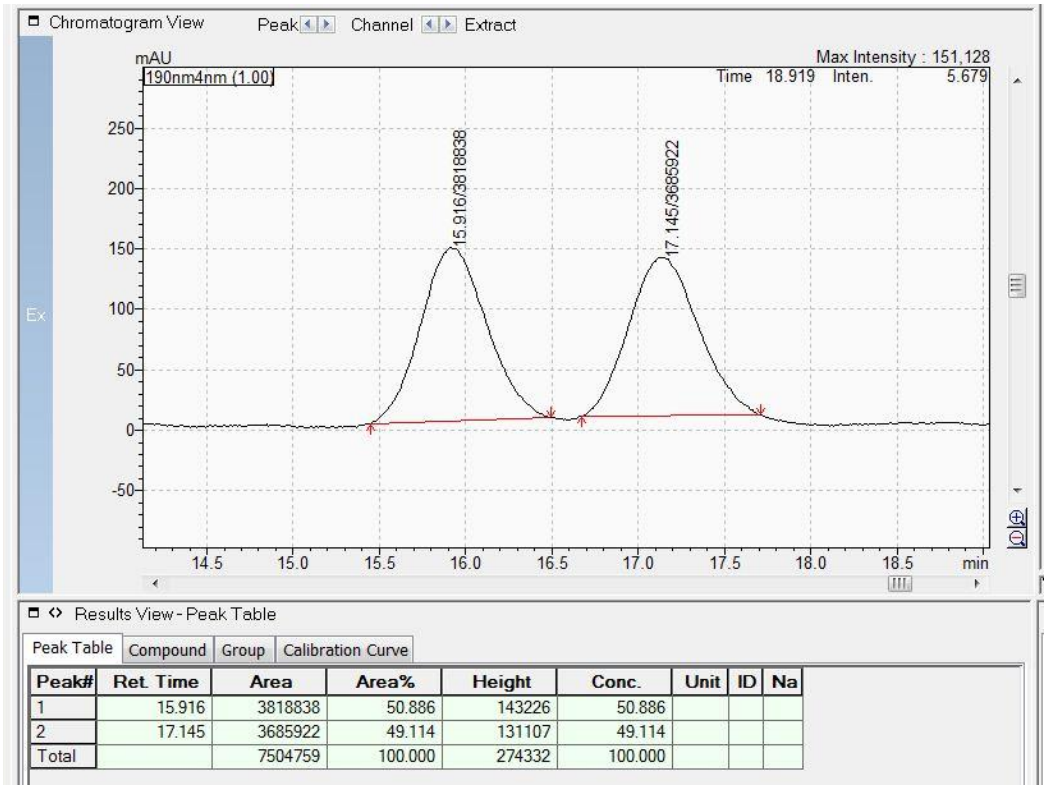

Peak#	Ret. Time	Area	Area%	Height	Conc.	Unit	ID	Na
1	15.916	3818838	50.886	143226	50.886			
2	17.145	3685922	49.114	131107	49.114			
Total		7504759	100.000	274332	100.000			

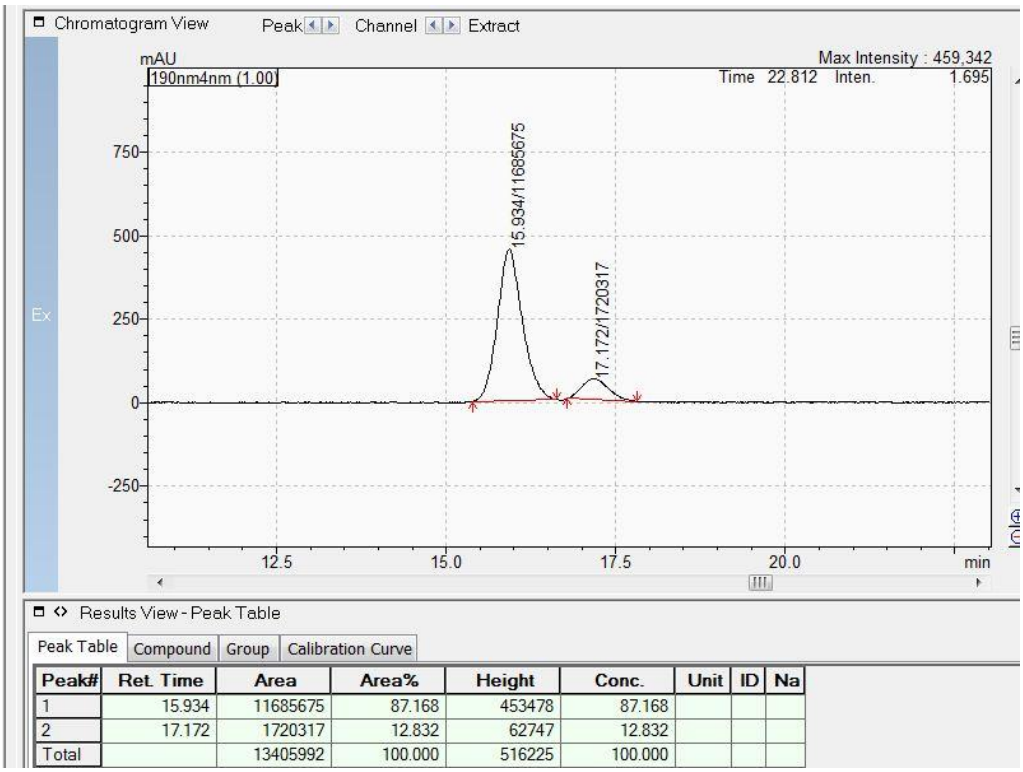

Peak#	Ret. Time	Area	Area%	Height	Conc.	Unit	ID	Na
1	15.934	11685675	87.168	453478	87.168			
2	17.172	1720317	12.832	62747	12.832			
Total		13405992	100.000	516225	100.000			

Compound **27**

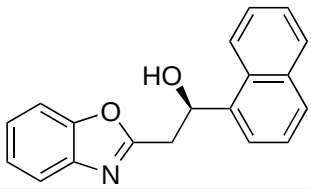

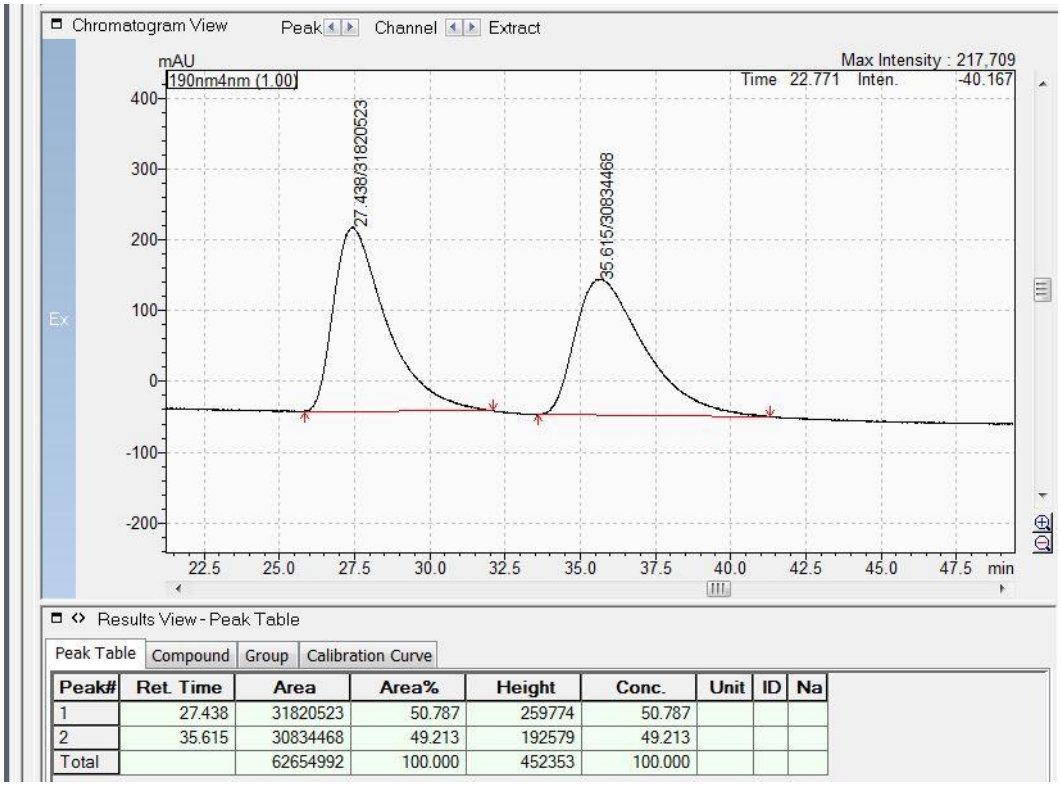

Results View - Peak Table

Peak Table | Compound | Group | Calibration Curve

Peak#	Ret. Time	Area	Area%	Height	Conc.	Unit	ID	Na
1	27.438	31820523	50.787	259774	50.787			
2	35.615	30834468	49.213	192579	49.213			
Total		62654992	100.000	452353	100.000			

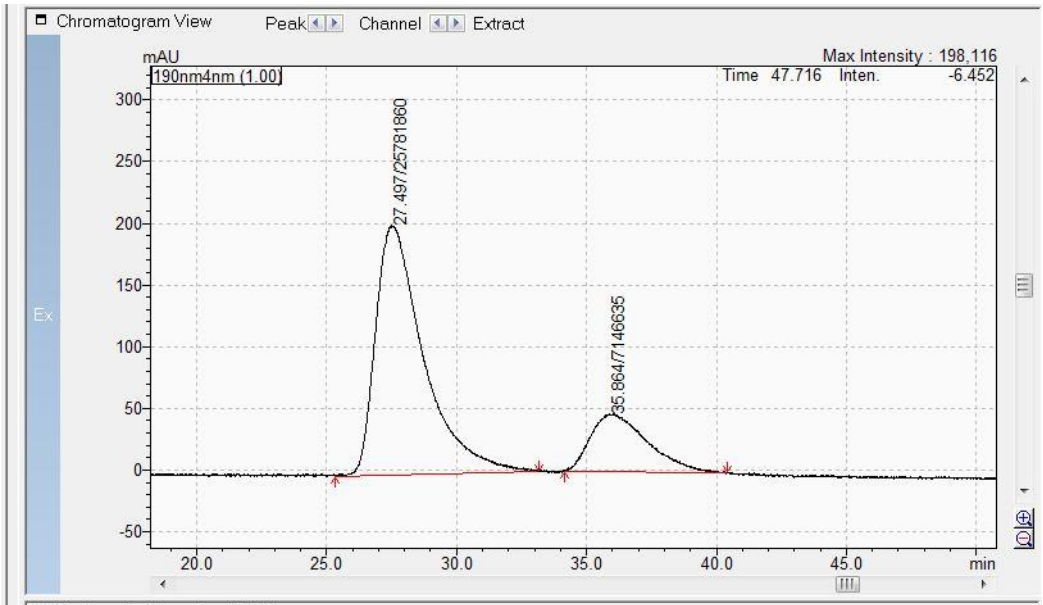

Results View - Peak Table

Peak Table | Compound | Group | Calibration Curve

Peak#	Ret. Time	Area	Area%	Height	Conc.	Unit	ID	Na
1	27.497	25781860	78.297	201915	78.297			
2	35.864	7146635	21.703	46913	21.703			
Total		32928495	100.000	248828	100.000			

Compound **28**

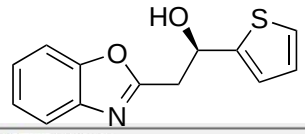

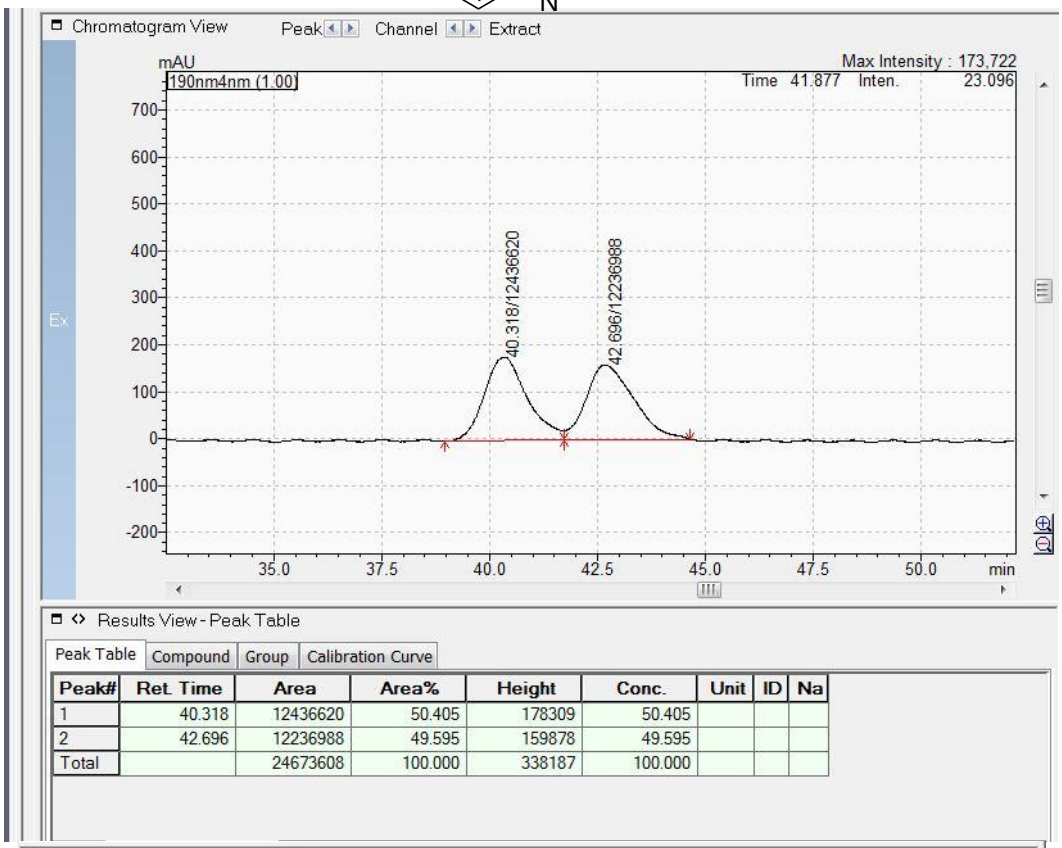

Peak#	Ret. Time	Area	Area%	Height	Conc.	Unit	ID	Na
1	40.318	12436620	50.405	178309	50.405			
2	42.696	12236988	49.595	159878	49.595			
Total		24673608	100.000	338187	100.000			

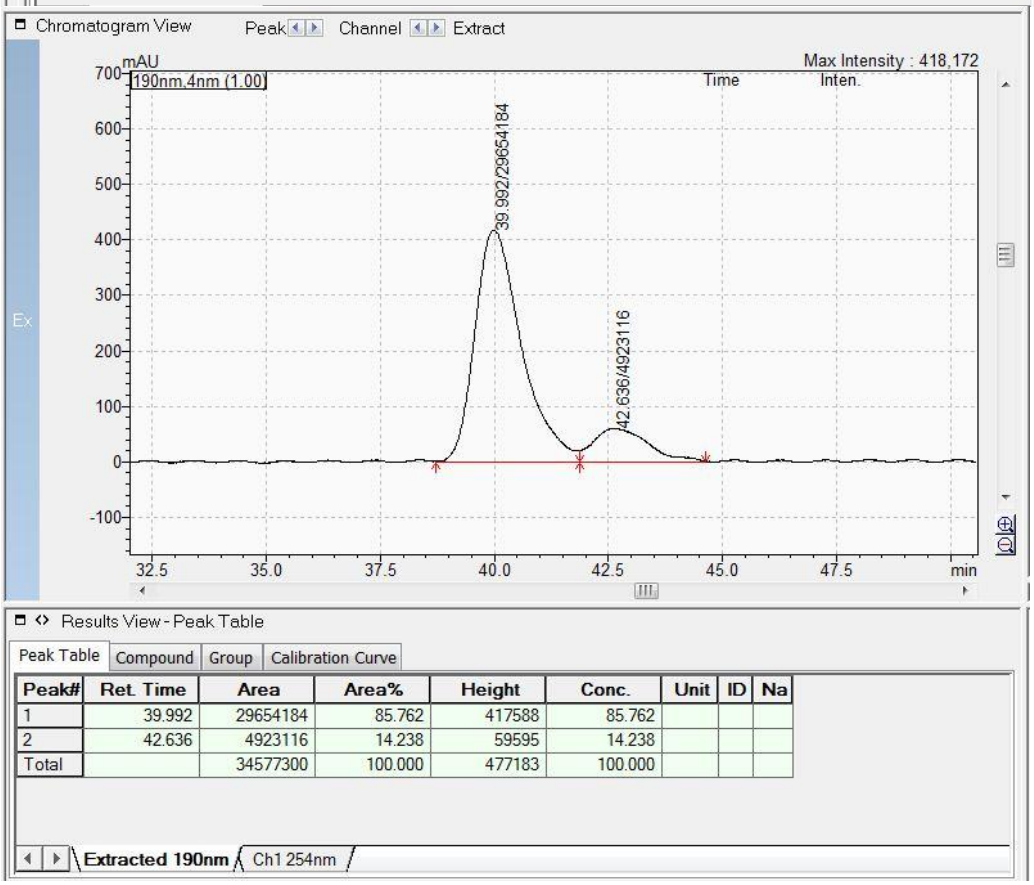

Peak#	Ret. Time	Area	Area%	Height	Conc.	Unit	ID	Na
1	39.992	29654184	85.762	417588	85.762			
2	42.636	4923116	14.238	59595	14.238			
Total		34577300	100.000	477183	100.000			

Compound **30**

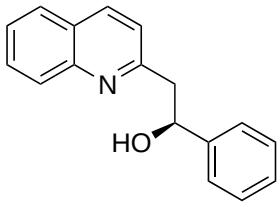

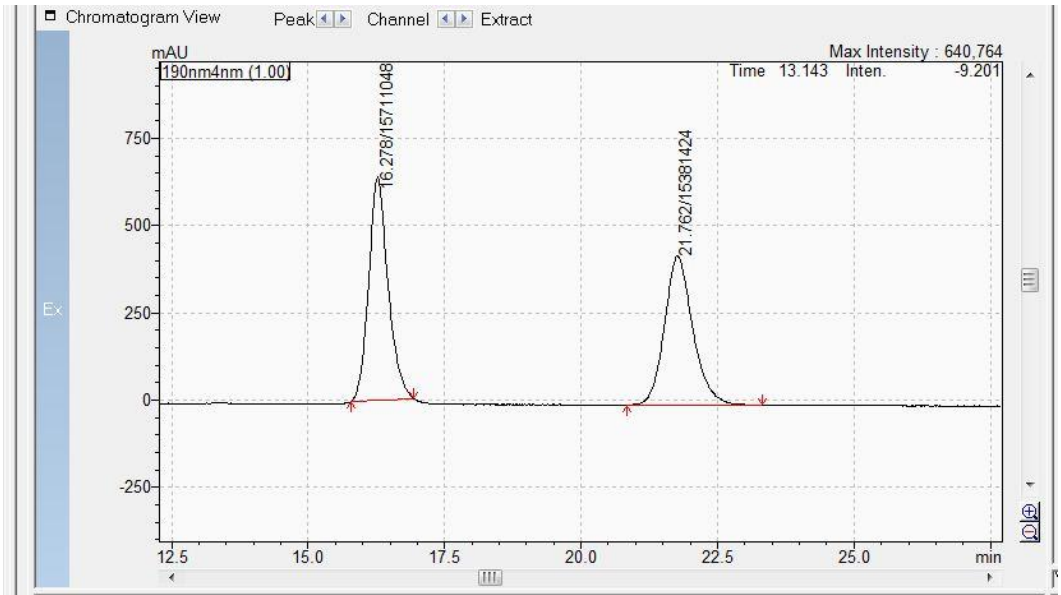

Results View - Peak Table

Peak Table | Compound | Group | Calibration Curve

Peak#	Ret. Time	Area	Area%	Height	Conc.	Unit	ID	Na
1	16.278	15711048	50.530	639972	50.530			
2	21.762	15381424	49.470	426317	49.470			
Total		31092472	100.000	1066290	100.000			

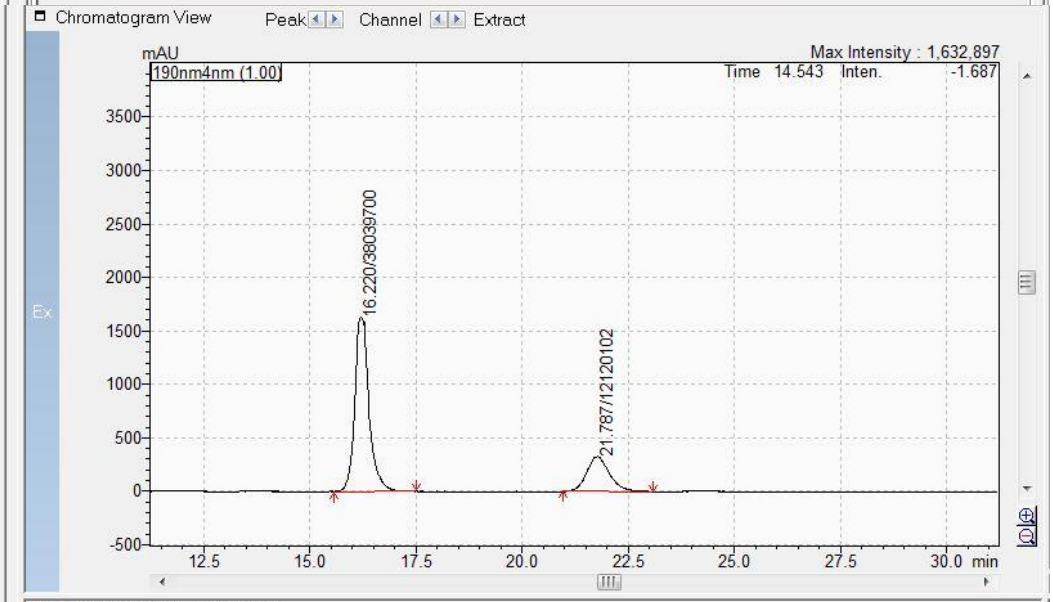

Results View - Peak Table

Peak Table | Compound | Group | Calibration Curve

Peak#	Ret. Time	Area	Area%	Height	Conc.	Unit	ID	Na
1	16.220	38039700	75.837	1633621	75.837			
2	21.787	12120102	24.163	325950	24.163			
Total		50159802	100.000	1959571	100.000			

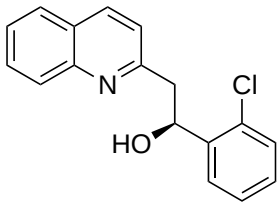

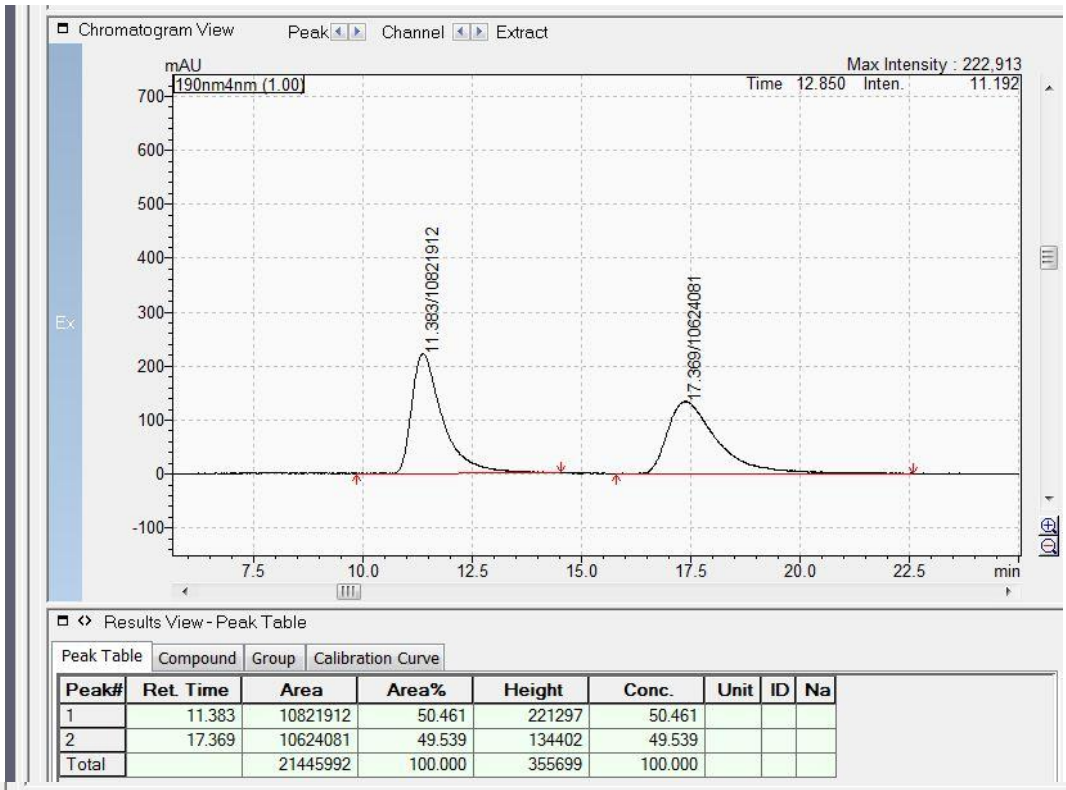

Results View - Peak Table

Peak Table | Compound | Group | Calibration Curve

Peak#	Ret. Time	Area	Area%	Height	Conc.	Unit	ID	Na
1	11.383	10821912	50.461	221297	50.461			
2	17.369	10624081	49.539	134402	49.539			
Total		21445992	100.000	355699	100.000			

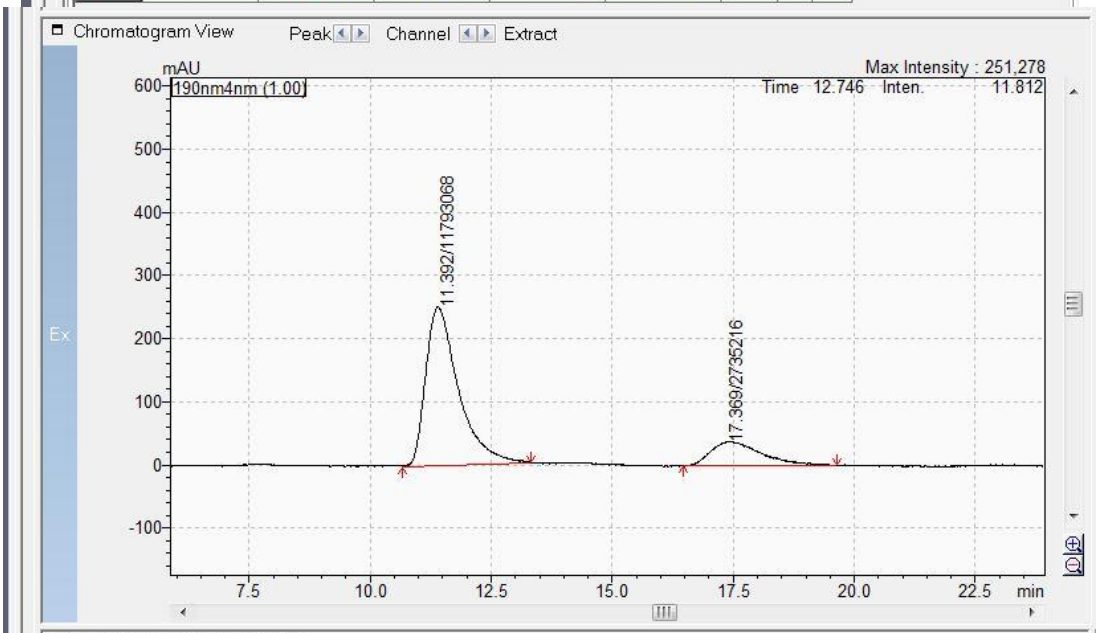

Results View - Peak Table

Peak Table | Compound | Group | Calibration Curve

Peak#	Ret. Time	Area	Area%	Height	Conc.	Unit	ID	Na
1	11.392	11793068	81.173	251815	81.173			
2	17.369	2735216	18.827	37803	18.827			
Total		14528284	100.000	289619	100.000			

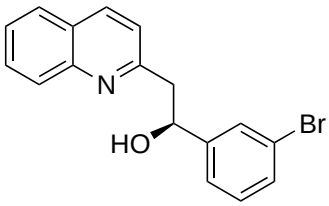

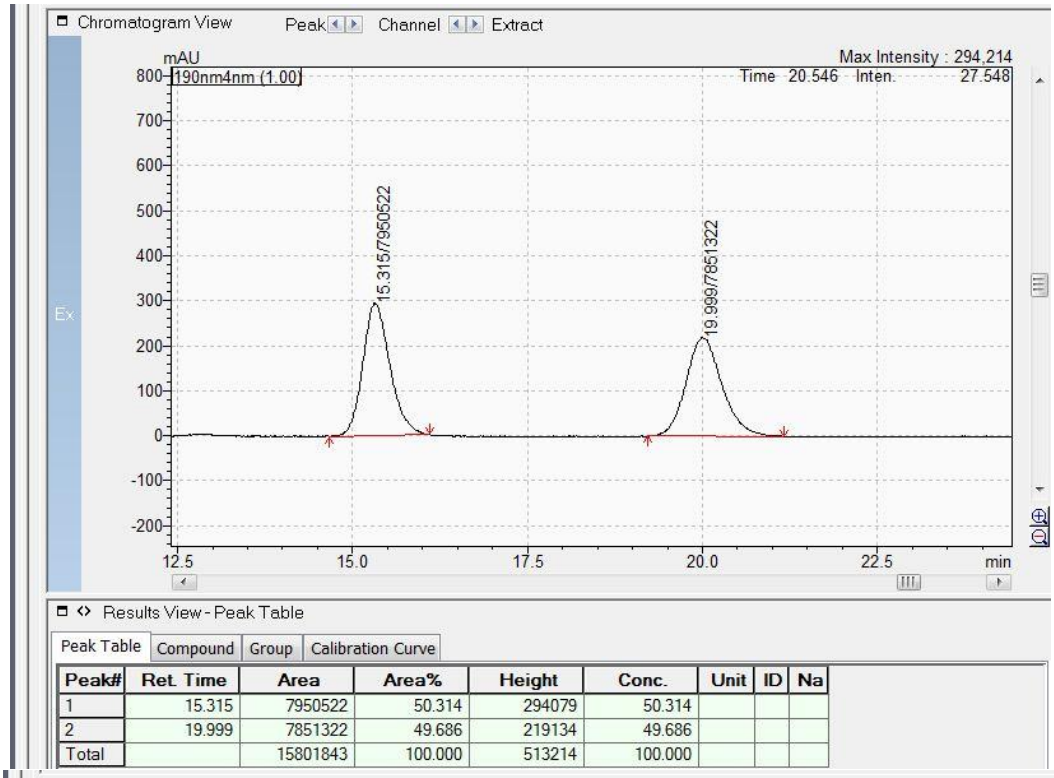

Results View - Peak Table

Peak Table | Compound | Group | Calibration Curve

Peak#	Ret. Time	Area	Area%	Height	Conc.	Unit	ID	Na
1	15.315	7950522	50.314	294079	50.314			
2	19.999	7851322	49.686	219134	49.686			
Total		15801843	100.000	513214	100.000			

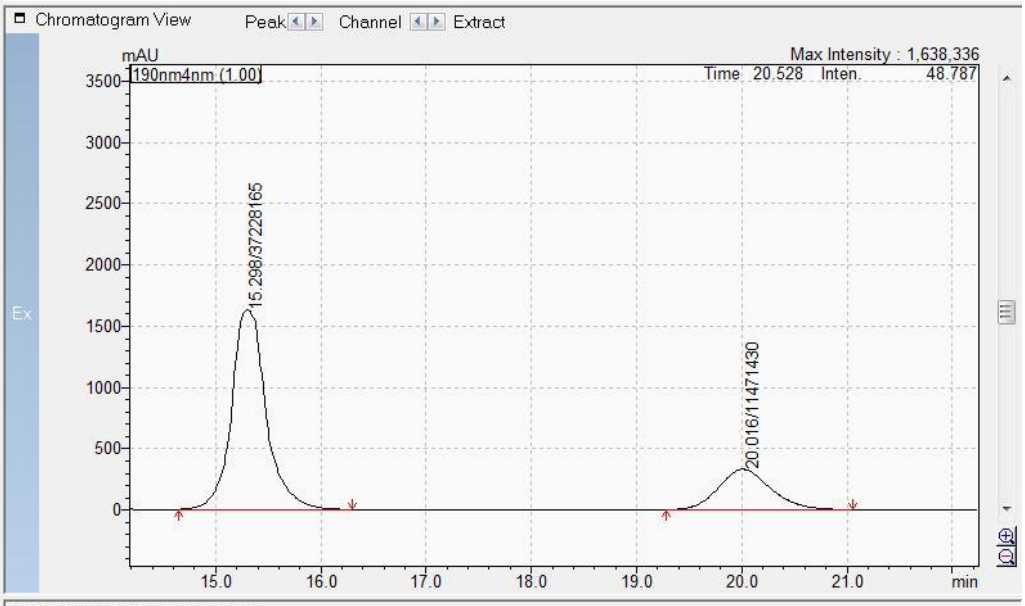

Results View - Peak Table

Peak Table | Compound | Group | Calibration Curve

Peak#	Ret. Time	Area	Area%	Height	Conc.	Unit	ID	Na
1	15.298	37228165	76.445	1633304	76.445			
2	20.016	11471430	23.555	332082	23.555			
Total		48699596	100.000	1965386	100.000			

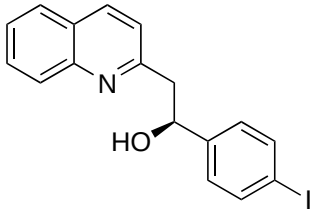

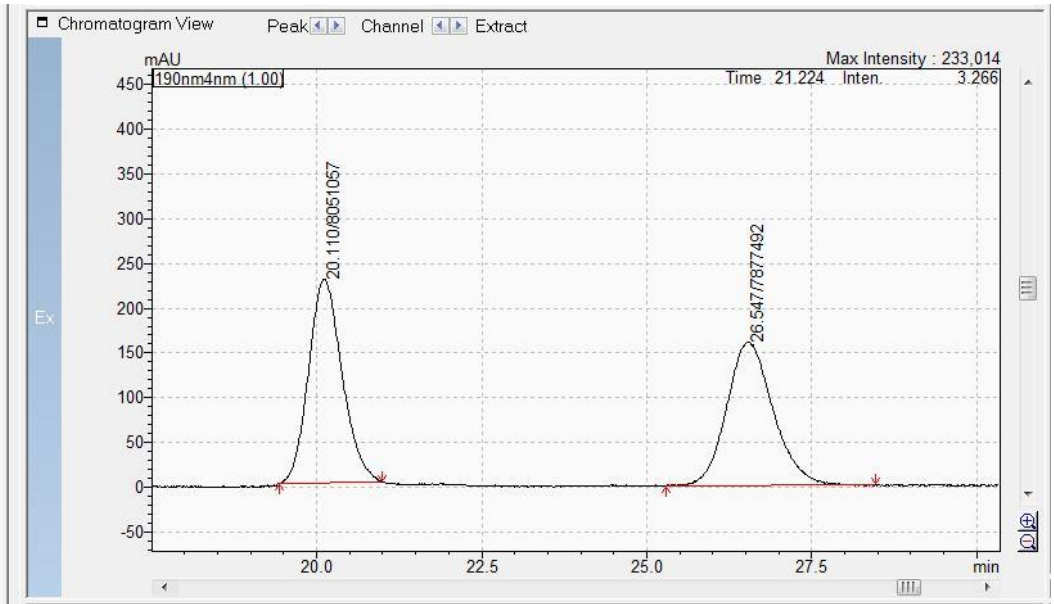

Results View - Peak Table

Peak Table | Compound | Group | Calibration Curve

Peak#	Ret. Time	Area	Area%	Height	Conc.	Unit	ID	Na
1	20.110	8051057	50.545	228187	50.545			
2	26.547	7877492	49.455	160680	49.455			
Total		15928549	100.000	388867	100.000			

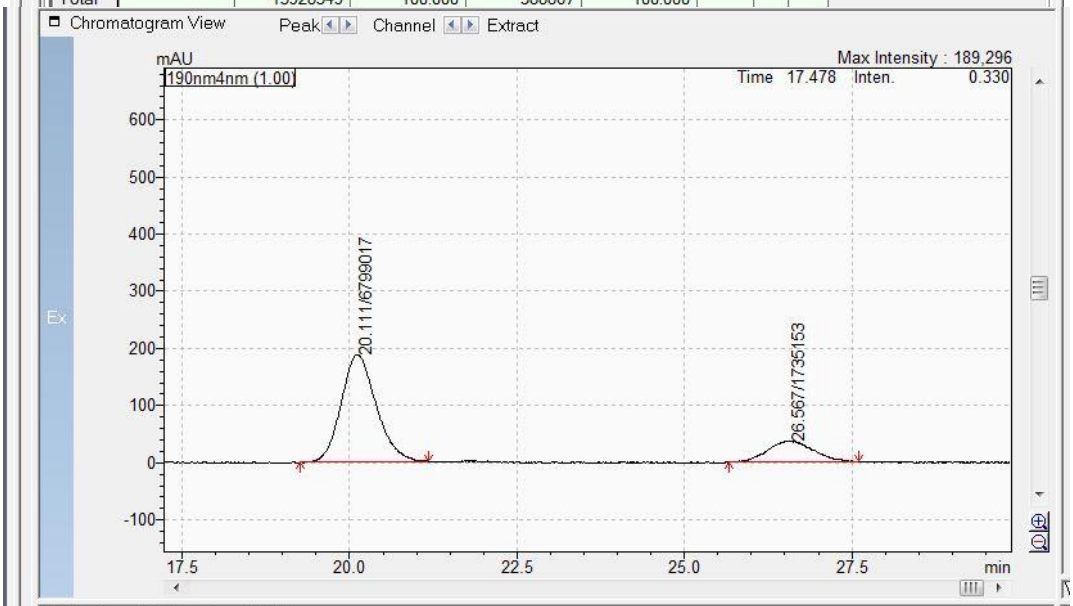

Results View - Peak Table

Peak Table | Compound | Group | Calibration Curve

Peak#	Ret. Time	Area	Area%	Height	Conc.	Unit	ID	Na
1	20.111	6799017	79.668	187608	79.668			
2	26.567	1735153	20.332	37056	20.332			
Total		8534171	100.000	224664	100.000			

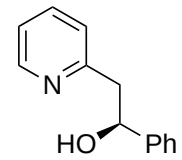

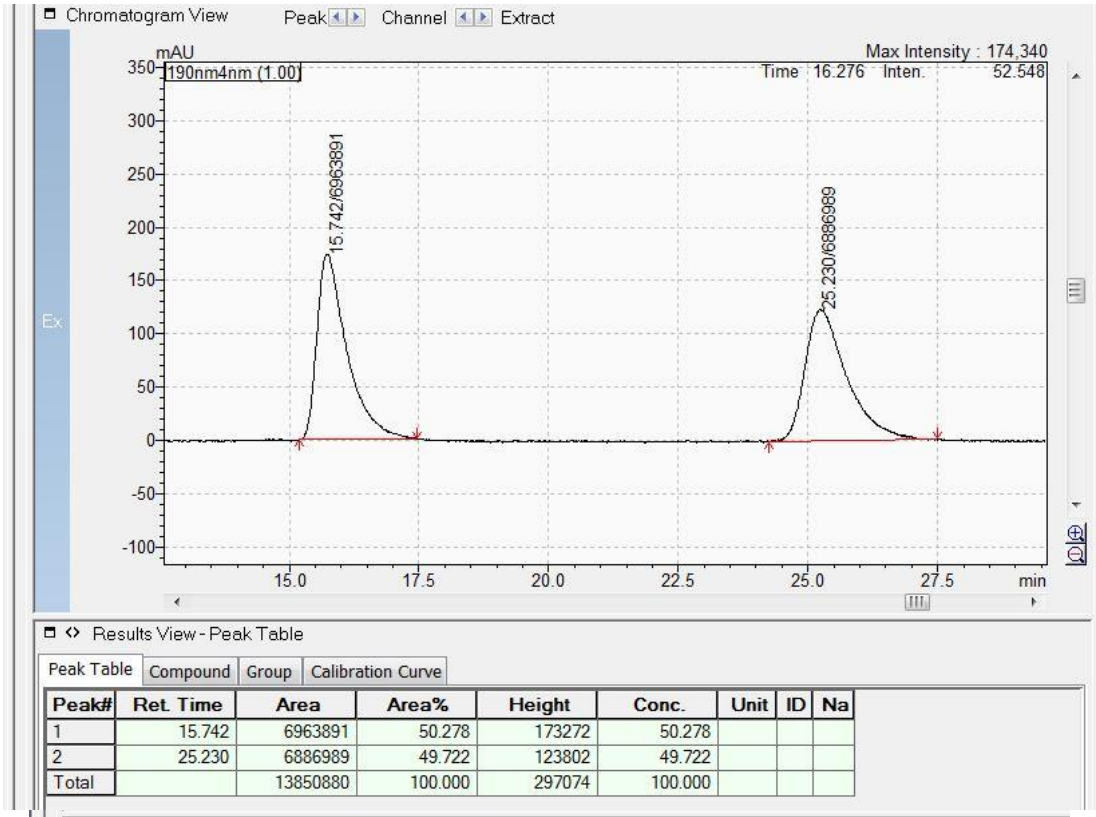

Results View - Peak Table

Peak Table | Compound | Group | Calibration Curve

Peak#	Ret. Time	Area	Area%	Height	Conc.	Unit	ID	Na
1	15.742	6963891	50.278	173272	50.278			
2	25.230	6886989	49.722	123802	49.722			
Total		13850880	100.000	297074	100.000			

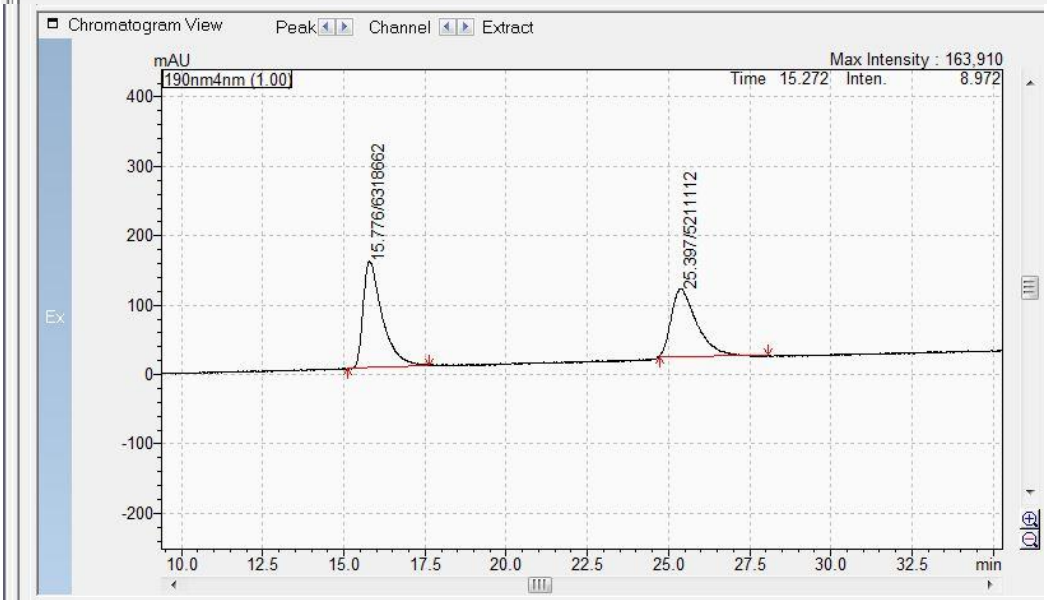

Results View - Peak Table

Peak Table | Compound | Group | Calibration Curve

Peak#	Ret. Time	Area	Area%	Height	Conc.	Unit	ID	Na
1	15.776	6318662	54.803	154275	54.803			
2	25.397	5211112	45.197	97299	45.197			
Total		11529774	100.000	251574	100.000			